FINAL REPORT

The Role of Trace Elements in Tin Whisker Growth

SERDP Project WP-1751

SEPTEMBER 2013

Jean A. Nielsen
Thomas A. Woodrow
Boeing Research and Technology
The Boeing Company

Distribution Statement A
This document has been cleared for public release

SERDP
DOD ▪ EPA ▪ DOE

REPORT DOCUMENTATION PAGE

Form Approved
OMB No. 0704-0188

Public reporting burden for this collection of information is estimated to average 1 hour per response, including the time for reviewing instructions, searching existing data sources, gathering and maintaining the data needed, and completing and reviewing this collection of information. Send comments regarding this burden estimate or any other aspect of this collection of information, including suggestions for reducing this burden to Department of Defense, Washington Headquarters Services, Directorate for Information Operations and Reports (0704-0188), 1215 Jefferson Davis Highway, Suite 1204, Arlington, VA 22202-4302. Respondents should be aware that notwithstanding any other provision of law, no person shall be subject to any penalty for failing to comply with a collection of information if it does not display a currently valid OMB control number. **PLEASE DO NOT RETURN YOUR FORM TO THE ABOVE ADDRESS.**

1. REPORT DATE *(DD-MM-YYYY)* 09-22-2013	**2. REPORT TYPE** Final	**3. DATES COVERED** (From - To) April 2010 - Sept 2013
4. TITLE AND SUBTITLE The Role of Trace Elements in Tin Whisker Growth		**5a. CONTRACT NUMBER** W912HQ-10-C-0022
		5b. GRANT NUMBER
		5c. PROGRAM ELEMENT NUMBER
6. AUTHOR(S) Nielsen, Jean A. and Woodrow, Thomas A.		**5d. PROJECT NUMBER** WP-1751
		5e. TASK NUMBER
		5f. WORK UNIT NUMBER
7. PERFORMING ORGANIZATION NAME(S) AND ADDRESS(ES) Boeing Research and Technology The Boeing Company PO Box 3707 Seattle, WA 98124-2207		**8. PERFORMING ORGANIZATION REPORT NUMBER**
9. SPONSORING / MONITORING AGENCY NAME(S) AND ADDRESS(ES) Strategic Environmental Research and Development Program 4800 Mark Center Dr.,Suite 17D08 Alexandria, VA 22203		**10. SPONSOR/MONITOR'S ACRONYM(S)** SERDP
		11. SPONSOR/MONITOR'S REPORT NUMBER(S)

12. DISTRIBUTION / AVAILABILITY STATEMENT

13. SUPPLEMENTARY NOTES

14. ABSTRACT

The focus of this project was to investigate six elements, other than lead, that when added to tin in small amounts had been reported to greatly reduce or eliminate the formation of tin whiskers. Tin whiskers are conductive, filamentary growths that can form on the surface of plated tin films. The whiskers can lead to electronic failures due to electrical shorting and plasma events; risks unacceptable for high reliability electronics. Plating methods were developed for doping tin plated films with nickel, cobalt, antimony, gold, germanium, and copper. In addition, a thin film of gold was deposited after plating pure tin to determine if it could suppress whisker formation. The effectiveness of the dopants was determined by aging the films in an elevated temperature/humidity environment known to accelerate whisker growth and then quantifying whisker growth using optical and scanning electron microscopy. Focused ion beam and electron backscatter diffraction analysis was performed to determine if any correlation between morphological and crystallographic properties of the films and the

15. SUBJECT TERMS

Tin whiskers, lead free, doped tin, whisker mitigation

16. SECURITY CLASSIFICATION OF:			**17. LIMITATION OF ABSTRACT**	**18. NUMBER OF PAGES**	**19a. NAME OF RESPONSIBLE PERSON**
a. REPORT	**b. ABSTRACT**	**c. THIS PAGE**			**19b. TELEPHONE NUMBER** (include area code)

Standard Form 298 (Rev. 8-98)
Prescribed by ANSI Std. Z39.18

This report was prepared under contract to the Department of Defense Strategic Environmental Research and Development Program (SERDP). The publication of this report does not indicate endorsement by the Department of Defense, nor should the contents be construed as reflecting the official policy or position of the Department of Defense. Reference herein to any specific commercial product, process, or service by trade name, trademark, manufacturer, or otherwise, does not necessarily constitute or imply its endorsement, recommendation, or favoring by the Department of Defense.

LIST OF ACRONYMS

COTS – Commercial-Off-The-Shelf
CSL – Coincident Site Lattice
CSLB – Coincident Site Lattice Boundary
DI – Deionized
EBM – Environmentally Benign Manufacturing
EBSD – Electron Backscatter Diffraction
EDX – Energy Dispersive X-Ray Spectrometry
FIB – Focused Ion Beam
HAGD - High Angle Grain boundary
ICP – Inductively Coupled Plasma
IPF – Inverse Pole Figure
LAGD - Low Angle Grain boundary
MODF – Misorientation Distribution Function
ND – Normal Direction
RD – Reference Direction
SEM – Scanning Electron Microscopy (Microscope)
STEM – Scanning Transmission Electron Microscopy (Microscope)
TD – Transverse Direction
TIR - Total Indicator Reading

LIST OF KEYWORDS

tin, whisker (crystal), doped tin, plating, lead free

LIST OF FIGURES

Figure 1.	Technical approach flowchart	5
Figure 2.	Flowchart of SnNi electroplating development	8
Figure 3.	Formulation of Pure Sn Electroplating Solution	9
Figure 4.	Formulation of SnPb Electroplating Solution	10
Figure 5.	Formulation of SnCu Electroplating Solution	11
Figure 6.	Formulation of SnNi Electroplating Solution	12
Figure 7.	Formulation of SnCo Electroplating Solution	13
Figure 8.	Formulation of SnSb Electroplating Solution	14
Figure 9.	Formulation of SnGe Electroplating Solution	15
Figure 10.	Formulation of SnAu Electroplating Solution	16
Figure 11.	Chart of average number of whiskers/cm^2 at 8,000 hours	21
Figure 12.	Chart of average number of whiskers/cm^2 at 12,000 hours	21
Figure 13.	SEM images of particles that precipitated out of the SnGe film after 8,000 hours of aging	22
Figure 14.	SEM images of particles on SnAu (left) and Sn/Au (right) films after 8,000 hours of aging	22
Figure 15.	SEM image of particulates in SnCu matrix after aging 8,000 hours (left) and on SnCu surface after 12,000 hours aging (right)	23
Figure 16.	Drawing of pure tin plated area on coupons 62, 63, and 64	25
Figure 17.	Drawing of pure tin plated area on coupons 67, 68, and 69	25
Figure 18.	SEM images of Sn grain structure after 12,000 hours of aging	26
Figure 19.	SEM images of the Sn grain structure after 12,000 hours of aging	26
Figure 20.	SEM images of nodules on Sn coupons after 8,000 hours aging	26
Figure 21.	SEM images of whiskers on Sn coupons after 8,000 hours aging	27
Figure 22.	SEM images of Sn whiskers on pure Sn coupons after12,000 hours aging	27

Figure 23.	SEM image of a long whisker on the Sn/Au sample at the interface of the pure Sn and Au sputtered Sn areas after 8,000 hours of aging	29
Figure 24.	SEM image of the Sn/Au and Pure Sn interface after 8,000 hours of aging	29
Figure 25.	SEM image of intermetallic formation on the surface of the Sn/Au samples after 8,000 hours of aging	30
Figure 26.	SEM image of whiskers forming under flakes of contamination on Sn/Au samples after 12,000 hours of aging	30
Figure 27.	SEM image of a nodule forming under a flake of contamination on Sn/Au sample after 12,000 hours of aging	31
Figure 28.	SEM image of Sn/Au grain structure after 12,000 hours of aging	31
Figure 29.	SEM image of Sn/Au grain structure after 12,000 hours of aging	32
Figure 30.	SEM image of whiskers on the Sn/Au film after 12,000 hours of aging	32
Figure 31.	SEM Image of defect on Sn3.1%Pb film immediately after plating	33
Figure 32.	SEM image of SnPb grain structure after 12,000 hours of aging	34
Figure 33.	SEM image of SnPb grain structure after 12,000 hours of aging	34
Figure 34.	SEM image of (left) multifaceted filamentary growth and (right) “typical” whisker on SnPb film	35
Figure 35.	SEM image of whiskers on SnPb film after 8,000 hours of aging	35
Figure 36.	SEM image of whiskers on SnSb films after 8,000 hours (left) and 12,000 hours (right) of aging	35
Figure 37.	SEM image of whiskers on SnPb films after 12,000 hours of aging	36
Figure 38.	SEM image of SnCu typical grain structure after 12,000 hours of aging	37
Figure 39.	SEM image of SnCu typical grain structure after 12,000 hours of aging	37
Figure 40.	SEM image of particulates in SnCu matrix after aging 8,000 hours (left) and on SnCu surface after 12,000 hours aging (right)	38

Figure 41. SEM image of particulates in SnCu matrix after aging 8,000 hours (left) and on SnCu surface after 12,000 hours aging (right) 38

Figure 42. SEM image of whiskers on SnCu film after 8,000 hours of aging 39

Figure 43. SEM image of whisker (left) and irregular eruption (right) on SnCu film after 8,000 hours of aging 39

Figure 44. SEM image of whiskers on SnCu film after 8,000 hours of aging 39

Figure 45. SEM image of SnNi typical grain structure after 12,000 hours of aging 41

Figure 46. SEM image of SnNi typical grain structure after 12,000 hours of aging 41

Figure 47. SEM image of SnNi typical grain structure after 12,000 hours of aging 41

Figure 48. SEM image of whiskers on SnCu film after 8,000 hours of aging 42

Figure 49. SEM image of whiskers on SnCu film after 8,000 hours of aging 42

Figure 50. SEM image of whiskers on SnCu film after 12,000 hours of aging 42

Figure 51. SEM image of SnCo typical grain structure after 12,000 hours of aging 44

Figure 52. SEM image of SnCo typical grain structure after 12,000 hours of aging 44

Figure 53. SEM image of SnCo typical grain structure after 12,000 hours of aging 44

Figure 54. SEM image of whiskers on SnCo film after 8,000 hours of aging 45

Figure 55. SEM image of whiskers on SnCo film after 8,000 hours of aging 45

Figure 56. SEM image of SnSb typical grain structure after 12,000 hours of aging 47

Figure 57. SEM image of SnSb grain structure after 12,000 hours of aging 47

Figure 58. SEM image of SnSb grain structure after aging 8,000 hours 48

Figure 59. SEM image of SnSb grain structure after aging 12,000 hours 48

Figure 60. SEM image of SnSb hillock (left) and delamination in SnSb film (right) 48

Figure 61. SEM image of whiskers in SnSb film with a multigrain structure after 8,000 hours of aging 49

Figure 62. SEM image of whiskers in SnSb film after 12,000 hours of aging 49

Figure 63. SEM image of whiskers on SnSb film after 12,000 hours of aging 50

Figure 64. Ion image of SnGe film taken by Evans Analytical Group prior to aging 50

Figure 65. SEM image of SnGe typical grain structure after 12,000 hours of aging 51

Figure 66. SEM image of SnGe typical grain structure after 12,000 hours of aging 51

Figure 67. SEM image of SnGe grain structure at 12,000 hours of aging 52

Figure 68. SEM image of whiskers on SnGe film after 8,000 hours of aging 53

Figure 69. SEM images of whiskers on SnGe film after 12,000 hours of aging 53

Figure 70. SEM image of SnAu typical grain structure after 12,000 hours of aging 55

Figure 71. SEM image of SnAu typical grain structure after 12,000 hours of aging 55

Figure 72: SEM image showing formation of intermetallics on the surface of the SnAu film at 8,000 hours aging and at 12,000 hours aging 55

Figure 73: SEM image showing formation of intermetallics on the surface of the SnAu film after 12,000 hours aging 56

Figure 74. Electron image of particles on SnAu film (left) and EDX Sn scan (right) after 8,000 hours of aging 56

Figure 75. EDX Au scan (left) and EDX Cu Scan (right) after 8,000 hours of aging 57

Figure 76. SEM image of whiskers on SnAu film after 12,000 hours of aging 57

Figure 77. SEM images of a whisker on the Sn sample at 8,000 hours (left) and 12,000 hours (right) 58

Figure 78. SEM images of a whisker on the Sn sample at 8,000 hours (left) and 12,000 hours (right) 59

Figure 79. SEM images of a whisker on the Sn sample at 8,000 hours (left) and 12,000 hours (right) 59

Figure 80. SEM images of a whisker on the Sn sample at 8,000 hours (left) and 12,000 hours (right) 59

Figure 81. SEM images of a whisker on the Sn/Au sample at 8,000 hours (left) and 12,000 hours (right) 60

Figure 82. Focused ion beam microsection of tin plated on copper 61

Figure 83. FIB micro-section of Sn plated film taken after electroplating; note the columnar grain structure and the SnCu intermetallic formation 62

Figure 84. FIB micro-section of SnCo plated film taken after electroplating; note the columnar and equiaxial grains 62

Figure 85. FIB micro-section of SnNi plated film taken after electroplating; note that the SnCu intermetallic completely surrounding some Sn grains 63

Figure 86. FIB micro-section of SnAu plated film prior to aging 64

Figure 87. FIB micro-section of the root of a SnAu whisker after 12,000 hours of aging 64

Figure 88. FIB micro-section of a whisker on the SnAu film after 12,000 hours aging 65

Figure 89. FIB micro-section of the root of a whisker on a pure Sn plated film after 8,000 hours of aging 66

Figure 90. FIB microsection of the root of a whisker on a SnPb plated film after 8,000 hours of aging 66

Figure 91. FIB micro-section of the root of a whisker on a SnCu plated film after 8,000 hours of aging 67

Figure 92. FIB micro-section of the root of a whisker on a SnNi plated film after 8,000 hours of aging 67

Figure 93. FIB micro-section of bulk Sn plated film capped with 53nm of Au after 12,000 hours of aging 68

Figure 94. EBSD measurements on a bright tin plating. Inverse pole figures are shown for the normal (ND), reference (RD), and transverse (TD) directions. The tin plating has a strong 113 orientation in the normal direction. 69

Figure 95. (a) SnPb film as plated (b) SnPb film after polishing 71

Figure 96. (a) SnCu film as plated (b) SnCu film after polishing 71

Figure 97. Whisker density after 8,000 hours aging versus post plating grain size 72

Figure 98. Whisker density after 12,000 hours aging versus post plating grain size 73

Figure 99. Phase ID map of tin and copper tin on the SnAu film taken after 12,000 hours of aging 74

Figure 100. Crystal direction map showing <111> crystal direction in ND direction 20 degree tolerance for SnCo film (left) pre-aging and (right) after 8,000 hours aging 76

Figure 101. Crystal direction map showing <111> crystal direction in ND direction 20 degree tolerance for SnNi film (left) pre-aging and (right) after 8,000 hours aging 76

Figure 102. Crystal direction map showing <111> crystal direction in ND direction 20 degree tolerance for SnGe film (left) pre-aging and (right) after 12,000 hours aging 77

Figure 103. Crystal direction map showing <111> crystal direction in ND direction 20 degree tolerance for Sn film (left) pre-aging and (right) after 8,000 hours aging 77

Figure 104. Percentage of grains that have CSL Boundaries after plating 81

Figure 105. Percentage of grains that have CSL Boundaries after aging 82

Figure 106. Misorientation Angle Distribution prior to aging for SnAu 83

Figure 107. Misorientation Angle Distribution prior to aging for SnGe 84

Figure 108. Misorientation angle distribution for all films prior to aging 85

Figure 109. Misorientation angle distribution for all films post-aging 86

Figure 110. MODF Plot of pure Sn prior to aging 87

Figure 111. MODF Plot of SnGe prior to aging 87

Figure 112. MODF maximum intensity vs. whisker density post aging 88

Figure 113. EBSD crystal direction map of SnSb prior to aging; blue grains indicate C-direction normal to the substrate, red indicates grains in plane (15 degree tolerance) 89

LIST OF TABLES

Table 1. ICP analysis results for weight percent of dopants 18

Table 2: Profilometer measurement averages of film roughness as plated and after aging 19

Table 3. Average number of whiskers/cm^2 on pure Sn films at 8,000 hours 24

Table 4. Average number of whiskers/cm^2 on pure Sn films at 12,000 hours 24

Table 5. Average number of whiskers/cm^2 on Sn/Au films at 8,000 hours 28

Table 6. Average number of whiskers/cm^2 on Sn/Au films at 12,000 hours 28

Table 7. Average number of whiskers/cm^2 on SnPb films at 8,000 hours 33

Table 8. Average number of whiskers/cm^2 on SnPb films at 12,000 hours 34

Table 9. Average number of whiskers/cm^2 on SnCu films at 8,000 hours 36

Table 10. Average number of whiskers/cm^2 on SnCu films at 12,000 hours 36

Table 11. Average number of whiskers/cm^2 on SnNi films at 8,000 hours 40

Table 12. Average number of whiskers/cm^2 on SnNi films at 12,000 hours 40

Table 13. Average number of whiskers/cm^2 on SnCo films at 8,000 hours 43

Table 14. Average number of whiskers/cm^2 on SnCo films at 12,000 hours 43

Table 15. Average number of whiskers/cm^2 on SnSb films at 8,000 hours 46

Table 16. Average number of whiskers/cm^2 on SnSb films at 12,000 hours 46

Table 17. Average number of whiskers/cm^2 on SnGe films at 8,000 hours 52

Table 18. Average number of whiskers/cm^2 on SnGe films at 12,000 hours 52

Table 19. Average number of whiskers/cm^2 on SnAu films at 8,000 hours 54

Table 20. Average number of whiskers/cm^2 on SnAu films at 12,000 hours 54

Table 21. Percentage of Grains Indexed by EBSD before and after polishing of films 70

Table 22. Grain size measurements from EBSD post plating and post aging 73

Table 23. Primary Crystallographic Textures of the Plated Films 75

Table 24. Grain Boundary Character of the Plated Films 79

Table 25. EBSD crystal direction data for c-Direction aligned grains normal to the plane of the substrate and in the plane of the substrate 90

ACKNOWLEDGEMENTS

Several people made significant contributions to the efforts documented in this report. Primarily I want to thank Tom Woodrow started this project, but retired before seeing its completion. Thanks to Ron Witt of EBSD Analytical, Inc. for conducting the EBSD analyses for this project. Thanks to Mario Sandoval, John Moskito, and Hong Qi of Evans Analytical Group for doing the FIB microsections and Auger analyses. Thanks to Eric Bleckwehl of Boeing for doing the ICP analyses of the plated films. Thanks to Chris Meyer of Boeing for his very helpful discussions on EBSD and FIB. Thanks to Minas Tanielian of Boeing for his helpful discussions and insights.

A special thanks to Bruce Sartwell and Robin Nissan of SERDP for funding and supporting this project. We would also like to thank the support of Jeff Houff, Matthew Penning, and Caitlin Rohan throughout this project.

TABLE OF CONTENTS

LIST OF ACRONYMS iv
LIST OF KEYWORDS iv
LIST OF FIGURES v
LIST OF TABLES xii
ACKNOWLEDGEMENTS xiii
TABLE OF CONTENTS xiv

1.0 ABSTRACT 1

2.0 OBJECTIVES 3

3.0 BACKGROUND 4

4.0 MATERIALS AND METHODS 5
4.1 Technical Approach 5
4.1.1 Method for Producing Doped Tin Electroplates 6
4.1.2 Electroplating of the Pure Tin Sample (Sn) 9
4.1.3 Electroplating of Tin Doped with 3.1% Lead (SnPb) 10
4.1.4 Electroplating of the Doped with 2.1% Copper (SnCu) 11
4.1.5 Electroplating of Tin Doped with 3.0% Nickel (SnNi) 12
4.1.6 Electroplating of Tin Doped with 0.95% Cobalt (SnCo) 13
4.1.7 Electroplating of Tin Doped with 2.4% Antimony (SnSb) 14
4.1.8 Electroplating of Tin Doped with 1.1% Germanium (SnGe) 15
4.1.9 Electroplating of Tin Doped with 1.3% Gold (SnAu) 16
4.2.0 Sputter Deposition of Gold Cap Layer onto Pure Tin Plating (Sn/Au) 17

5.0 RESULTS AND DISCUSSION

5.1 Inductively Coupled Plasma (ICP) Analysis of Films 18

5.2 Profilometer Measurements of Film Roughness 19

5.3 Temperature/Humidity Aging of the Test Coupons 20

5.4 Qualitative and Quantitative Inspection of Test Coupons 20
5.4.1 Inspection of Pure Tin Samples 24
5.4.2 Inspection of Tin with 53nm Sputter Gold Cap (Sn/Au) Films 27
5.4.3 Inspection of Tin with 3.1% Lead (SnPb) Films 32
5.4.4 Inspection of Tin with 2.1% Copper (SnCu) Films 36
5.4.5 Inspection of Tin with 3.0% Nickel (SnNi) Films 40
5.4.6 Inspection of Tin with 0.95% Cobalt (SnCo) Films 43
5.4.7 Inspection of Tin with 2.4% Antimony (SnSb) Films 46

5.4.8 Inspection of Tin with 1.1% Germanium (SnGe) Films 50
5.4.9 Inspection of Tin with 1.3% Gold (SnAu) Films 54
5.4.10 Influence of Inspection on Whisker Growth and Development 58

5.5 Focused Ion Beam (FIB) Analysis 61

5.6 Electron Backscatter Diffraction (EBSD) Analysis 69
5.6.1 Grain Size 72
5.6.2 Crystallographic Texture 75
5.6.3 Grain Boundary Types Present in the Plated Films 78
5.6.4 Misorientation Angle Distribution 83
5.6.5 Misorientation Distribution Function (MODF) Plots 87
5.6.6 Stiffness vs. Crystallographic Orientation 88

6.0 CONCLUSIONS AND IMPLICATIONS FOR FUTURE RESEARCH/IMPLEMENTATION 90
6.1 Conclusions and Observations 90
6.2 Implication for Future Research 91

7.0 LITERATURE CITED 92

APPENDICES

Appendix A: FIB Microsections and Ion Images of Pure Sn Plating 94
Appendix B: FIB Microsections and Ion Images of SnPb Plating 101
Appendix C: FIB Microsections and Ion Images of SnCu Plating 110
Appendix D: FIB Microsections and Ion Images of SnNi Plating 117
Appendix E: FIB Microsections and Ion Images of SnCo Plating 124
Appendix F: FIB Microsections and Ion Images of SnSb Plating 130
Appendix G: FIB Microsections and Ion Images of SnGe Plating 138
Appendix H: FIB Microsections and Ion Images of SnAu Plating 146
Appendix I: FIB Microsections and Ion Images of Pure Sn with Au thin film cap (Sn/Au) 154
Appendix J: EBSD Data for Pure Tin Plating 160
Appendix K: EBSD Data for SnPb Plating 174
Appendix L: EBSD Data for SnCu Plating 188
Appendix M: EBSD Data for SnNi Plating 202
Appendix N: EBSD Data for SnCo Plating 216
Appendix O: EBSD Data for SnSb Plating 230
Appendix P: EBSD Data for SnGe Plating 244
Appendix Q: EBSD Data for SnAu Plating 258
Appendix R: EBSD Data for Pure Sn prior to aging compared with Au thin film cap (Sn/Au) after aging 273

1.0 ABSTRACT

Tin whiskers are conductive, filamentary growths that can form on the surface of plated tin and tin solders. Tin whiskers can lead to electronic failures, due to electrical shorting and plasma events; risks unacceptable for high reliability electronics. It has been known for decades that the addition of lead to tin plated films greatly reduces or eliminates whisker formation and growth, although the mechanism by which lead prevents whisker formation is not fully understood. Environmental legislation passed in Japan and Europe, including the Restriction of Hazardous Substances Directive, has driven the increased use of lead-free solders and plated films, particularly the use of pure tin. Even though such legislation has yet to be adopted in the United States, many companies are already switching to lead-free solders and plated films in order to remain competitive in the European and Asian markets. As more companies switch to lead-free products it will become increasingly difficult for aerospace and military programs to procure electronics made with tin-lead surface finishes.

Boeing had identified six elements, in addition to elemental lead, that when added to tin in trace amounts were thought to have the ability to greatly reduce or eliminate the formation of tin whiskers. The objective of this study was to quantify the effectiveness of these alternative elements: germanium, nickel, cobalt, copper, antimony, and gold. During this study, electrochemical methods for incorporating these candidate elements into the tin films were evaluated. We concluded that for some of these elements electrochemical co-deposition of the element and tin may not be practical or even possible. For those elements, the effectiveness of thin layers deposited over the tin electroplated films was evaluated.

Samples were analyzed before and after aging in an environmental chamber to accelerate whisker growth. To determine the effectiveness of whisker suppression, three samples from each plated film group were inspected both with optical and scanning electron microscopy. The samples were inspected prior to aging, at 4,000 hours and at 8,000 hours. Samples that had low whisker counts at 8,000 hours were returned to the environmental chamber for an additional 4,000 hours of aging. In addition, data was collected to determine if morphological and crystallographic changes of the films could be correlated with whisker growth or suppression. Electron backscatter diffraction analysis was performed by EBSD Analytical and focused ion beam analysis was performed by Evans Analytical Group.

During this study, we searched the technical literature to determine if methods for electroplating these doped-tin films already existed or if existing techniques could be modified. For films for which no method could be found, Boeing developed the needed techniques. Tin films doped with each of these elements to a weight percent of 1-3% were successfully plated. In addition, a thin film layer of gold was sputtered over the surface of pure plated tin and was evaluated for whisker suppression. In order to have a baseline, pure tin samples and lead-doped tin samples were also plated and analyzed.

The method used for plating the pure tin samples was a technique known to generate low whisker density. Even so, three of the elements investigated in this study; gold, germanium, and antimony, showed substantially lower whisker growth than the pure tin samples. Gold was effective both when added as a dopant to the electroplated film and when applied as a sputtered thin film layer. Not all of the dopants were successful in suppressing whisker growth; most notably the nickel- and cobalt-doped films had whisker densities substantially higher than the pure tin baseline. Interestingly, the lead-doped tin film had higher whisker density than the pure tin samples, although it should be noted that the weight percent of lead used in this study is substantially lower than most lead-tin solders or plated films.

It was also observed during the scanning electron microscope inspection, that on the gold-doped and germanium-doped films, intermetallics or elemental gold and germanium precipitated out as fine particles leaving small nano-pores in the films. Although there were no obvious precipitates noted on the surface of the antimony-doped film, the film was very porous. Whether this change in porosity affected the whisker formation will require additional research.

The results from the morphological and crystallographic data were less clear. The electron backscatter diffraction analysis did show a general trend that indicated the lower the pole figure maximum intensity (the more random the texture), the more likely a film was to form whiskers.

Finding alternatives to pure tin for lead-free plating and solder is critical. Although strategies have been identified to reduce the chance of growing whiskers, none have been 100% effective. The use of conformal coatings, altering current density during plating, the use of barrier layers between the substrate and the plated film, regulating the film thickness and texture have all had unsatisfactory results. On the other hand, there is an undeniable shift to lead-free electronics. The benefits of using tin-based solders - low melting point, high electrical conductivity, good corrosion resistance, and good solderability - make it attractive for use in many consumer electronics. Regardless of whether it is driven by environmental stewardship, a desire to be responsive to global regulations, or the need to remain competitive in a world market, the proliferation of lead-free tin electronics will continue.

Since it will become increasingly more difficult and expensive in the future to obtain tin-lead components for high-reliability systems, such as military and aerospace platforms, it is important that effective and low cost strategies for controlling tin whisker risks be developed to ensure the reliability of military/aerospace hardware in the field.

2.0 OBJECTIVES

The main objective of this study was to investigate the claim made by S.M. Arnold of Bell Labs over four decades ago [1] that six elements (Cu, Ni, Co, Sb, Ge, Au) other than lead can suppress tin whisker growth.

The goals of the study were:

1. To develop plating methods for doping tin plated films with the six elements identified by Arnold as tin whisker mitigators, i.e., Cu, Ni, Co, Sb, Ge and Au. The target concentration for the dopants will be 1 to 3 percent by weight. The plated films needed to be relatively flat and free from nodules and dendrites.

2. To evaluate a thin film of Au over a pure tin plating as a tin whisker mitigators. Literature data suggests that thin metallic films applied over tin electroplated films can suppress whisker growth [1, 2].

3. To determine the effectiveness of the dopants by aging the doped tin electroplated films in an elevated temperature/humidity environment known to accelerate whisker growth [3] and then quantifying whisker growth using light and scanning electron microscopy.

4. To attempt to correlate any observed whisker mitigation with the morphological and crystallographic properties of the doped electroplated films. Morphological data will be collected using focused ion beam (FIB) microsections which will show the grain structure within the electroplated films. Electron backscatter diffraction (EBSD) data will be collected on the doped electroplated films which will reveal the average grain size; preferred crystallographic textures; and misorientation relationships between the grains in the electroplated films.

3.0 BACKGROUND

Conversion to lead-free electronics is underway as most industrialized nations including the United States, Europe, and Japan move toward more Environmentally Benign Manufacturing (EBM). Whether this shift toward EBM, including lead-free electronics, is driven by environmental stewardship, a desire to be responsive to global regulations, or the need to remain competitive in a world market, the proliferation of lead-free tin electronics will continue [4]. This will undoubtedly lead to an increase in reliability issues, primarily shorting in electronic circuits, due to the formation of tin whiskers on lead-free tin surfaces and the constant trend of shrinking circuit geometries.

These types of failures have already cost individual programs many millions of dollars and have caused significant customer dissatisfaction [5]. However, the benefits of tin use, low melting point, high electrical conductivity, good corrosion resistance, and good solderability make it attractive for use in electronics. However, without the addition of lead, the spontaneous growth of conductive tin whiskers will continue to be an issue with the use of pure tin.

Although strategies have been identified to reduce the chance of growing whiskers, none have been 100% effective. The use of conformal coatings, altering current density during plating, the use of barrier layers between the substrate and the plated film, regulating the film thickness and texture have all shown disappointing results [6]. Even so, the use of lead-free tin in consumer products is increasing and progressively more commercial-off-the-shelf (COTS) components are only available with the lead-free option. Since it will become increasingly more difficult and expensive in the future to obtain SnPb components for high-reliability systems, such as military and aerospace platforms, it is important that effective and low cost strategies for controlling tin whisker risks be developed to ensure the reliability of military/aerospace hardware in the field.

4.0 MATERIALS AND METHODS

4.1 Technical Approach

Determining a method for electroplating the doped films was the primary goal of the first part of this program. Coupons from each plating were sent for inductively coupled plasma (ICP) analysis. Once the dopant level was confirmed, additional coupons were sent for electron backscatter diffraction (EBSD) and focused ion beam (FIB) analyses. Three coupons from each plating were aged for 8,000 hours. Coupons with little to no whisker growth were aged an additional 4,000 hours for a total of 12,000 hours.

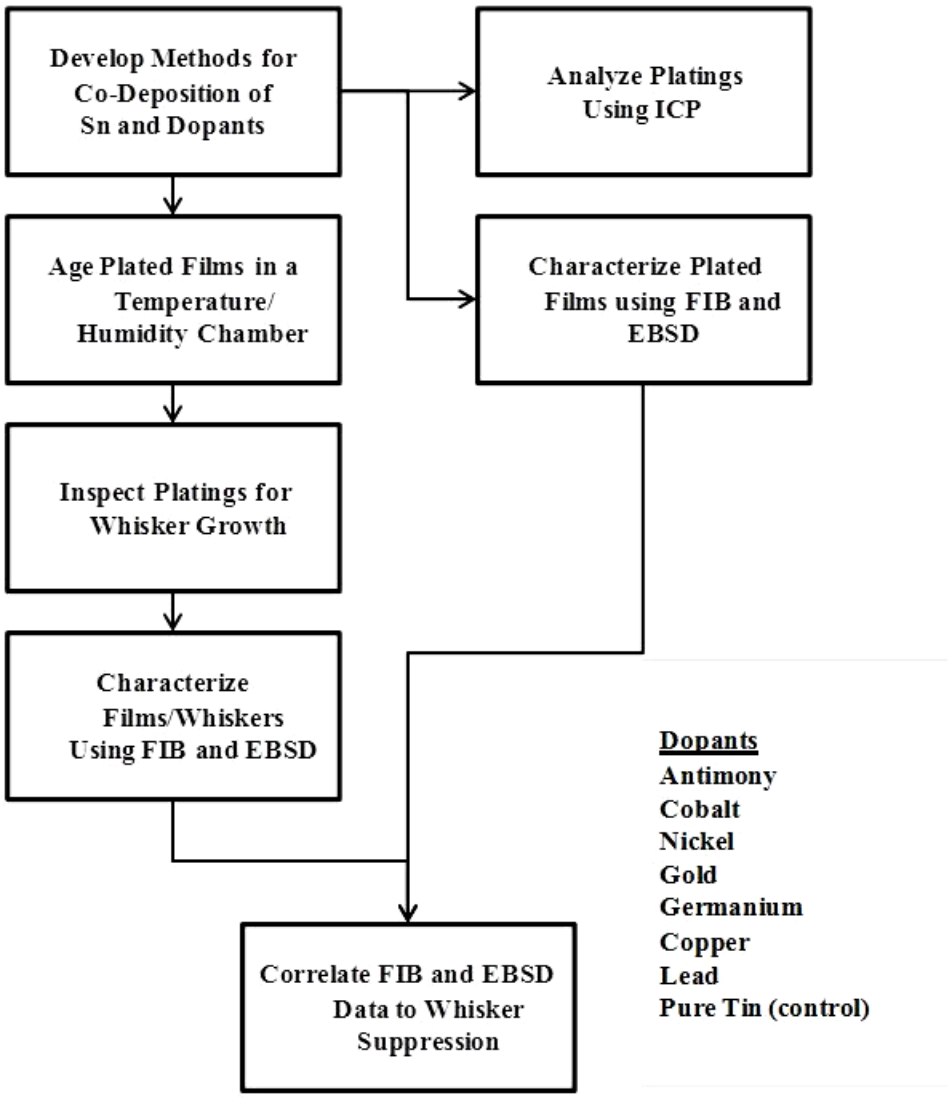

Figure 1. Technical approach flowchart

4.1.1 Method for Producing Doped Tin Electroplates

Electroplating methods were developed for doping tin plated films with the six elements identified by Arnold as tin whisker mitigators, i.e., Cu, Ni, Co, Sb, Ge and Au. The electroplated films used in this study were deposited on Copper 110 material, a 99.9% pure copper. The material was cut into coupons approximately 1cm by 2.54cm x 0.041cm. The coupons were cleaned with detergent and dipped into a 10% sulfuric acid solution for 15 seconds to remove any native oxide growth on the surface. SM80 Red Platers film tape was used to mask each coupon so that approximately 1cm x 1cm area was plated.

The anodes used during electroplating were always $2cm^2$, twice the area of a single copper cathode. Pure tin anodes were used for the electroplating of Sn and SnGe. A pure Ni anode was used for the electroplating of SnNi and a pure Co anode was used for the electroplating of SnCo.

For the electroplating of SnPb, SnCu, and SnSb, anodes made from alloys of Sn and the appropriate dopant were used. These anodes were fabricated by placing the desired ratios of Sn metal (99.9%, Aldrich) and dopant into a glazed crucible and then covering them with a flux (Kester 197 Type RMA) to prevent oxidation of the metals. The purity of the Pb, Cu, and Sb used to fabricate the anodes was 99.0+%, 99.5%, and 99.5%, respectively. The crucible was then heated in a controlled bath to 340 degrees C and the contents of the crucible were stirred with a glass rod until all of the dopant appeared to dissolve in the molten Sn. The bolus of alloy was then cleaned well with water and acetone and formed into a flat sheet of the appropriate dimensions. Each alloy used to fabricate the anodes was dissolved in mixed acids and analyzed by Inductively Coupled Plasma (ICP) to verify its composition. The inductively coupled plasma ionizes the sample, then mass spectrometry is used determine the elemental composition [7].

The coupons were electroplated using a HP6033A DC power supply in series with a Keithley 175 Autoranging Multimeter for monitoring amperage. If necessary, the amperage used during the electroplating was adjusted manually to maintain a constant current density. One specimen at a time was plated with the exception of SnSb and SnGe that were plated two at a time.
In theory, two metals with different electromotive potentials cannot be practically plated at the same time. For example:

> The deposition of alloys by simple DC methods can only be accomplished when the deposition potential for each of the components are approximately the same. The standard reduction potentials for Mn^{+2} and Co^{+2} are -1.180V and - 0.277V respectively, and the standard reduction potentials for Ni^{+2} and Fe^{+2} are -0.250V and -0.440V respectively. The larger difference in standard reduction potential for the Mn/Co suggests that this alloy may be more difficult to deposit in a controlled fashion. For instance, estimation of the concentrations necessary to bring the deposition potentials to equal levels for Mn^{+2} and Co^{+2} done using the Nernst

equation and assuming dilute solutions (so that concentration can be used instead of activity) shows that the Co^{+2} concentration would need to be approximately 30 orders of magnitude more dilute than the Mn+2 ion concentration [8].

This limitation is usually overcome by chemically complexing one or both metals which effectively brings their electromotive potentials closer together and allows them both to be plated at the same time to form an alloy. Finding an appropriate complexing agent for a given plating system is often not straightforward, however.

The electromotive forces for some metals vs. a standard hydrogen electrode are given in Table 3. Not shown in the table are Sb (+0.15) and Ge (-0.25 vs. a standard calomel electrode [9]).

For this study, a literature search was conducted for plating methods for producing each doped Sn alloy. Often a plating method could be found in the literature for a given alloy (e.g., SnNi) but the alloy produced by that method usually had a different stoichiometry than the one desired for this study. This required that each published plating method be modified to produce an alloy with the desired amount of dopant (i.e., 1-3%). Modification of the published plating method was often not straightforward since the degree of doping is determined by a complex interaction of variables including dopant concentration in the electrolyte, temperature, pH, plating additives, and current density used during plating.

An example of this modification procedure is shown in Figure 2 for the development of a suitable plating process for Sn3.0%Ni. The amount of Ni in the doped Sn plating was highly dependent upon temperature and the concentration of leveling additive added to the plating bath.

No suitable process was found in the literature for SnGe so the process had to be developed from scratch.

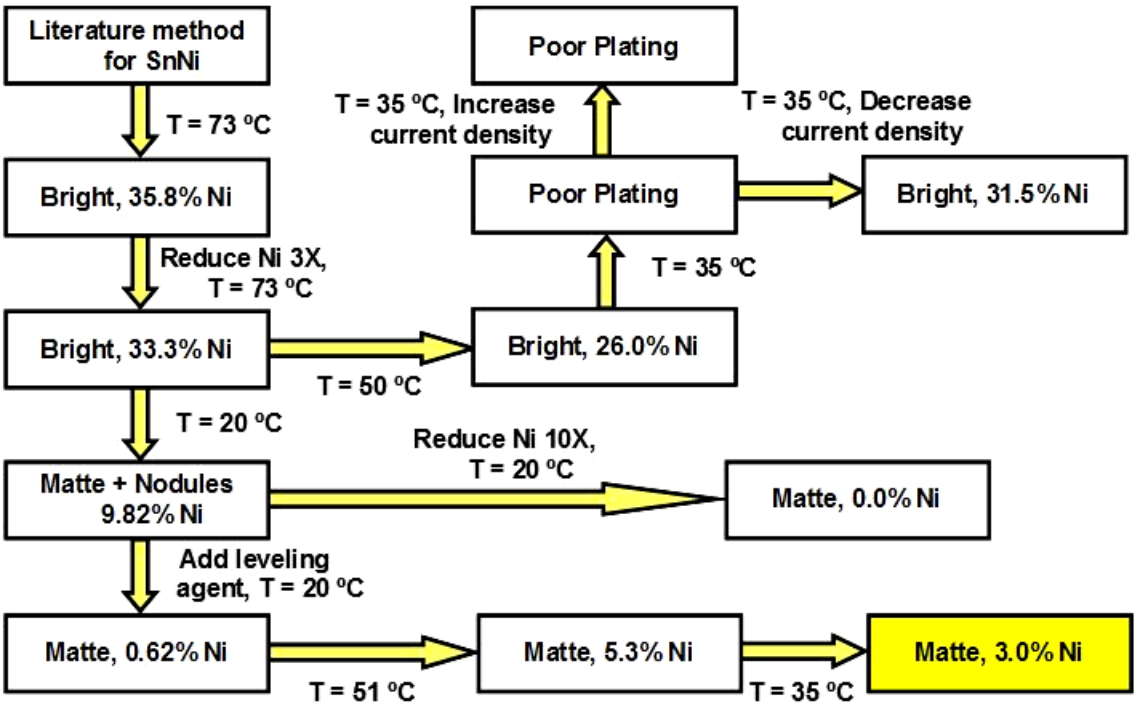

Figure 2. Flowchart of SnNi electroplating development

4.1.2 Electroplating of the Pure Tin Sample (Sn)

The electroplating of the pure tin sample was achieved using a method developed by Yun Zhang [10]. Plating was conducted using 30ml of the above electrolyte solution held at 50°C in a 50 milliliter glass beaker while stirring. The anode was constructed from 99.998% tin sheet (Aldrich). Plating was performed at 0.045V and 10.9 milliamps for 8 minutes to yield a gray satin film.

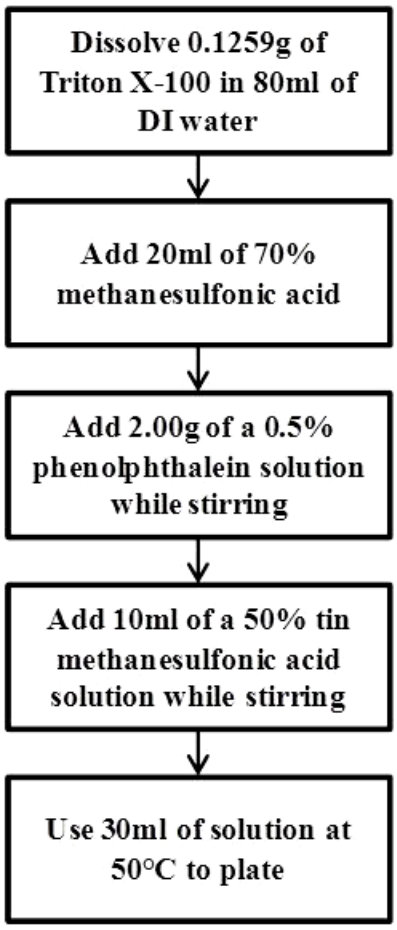

Figure 3. Formulation of Pure Sn Electroplating Solution

4.1.3 Electroplating of Tin Doped with 3.1% Lead (SnPb)

The lead-doped tin was achieved using a modified version of the method developed by Yun Zhang [10]. Plating was conducted using the above electrolyte solution held at 20°C in a 50 milliliter glass beaker while stirring. The anode was constructed from SnPb sheet containing 3.5%Pb. Plating was performed at 0.250V and 3.0 milliamps for 18 minutes to yield a light gray matte film.

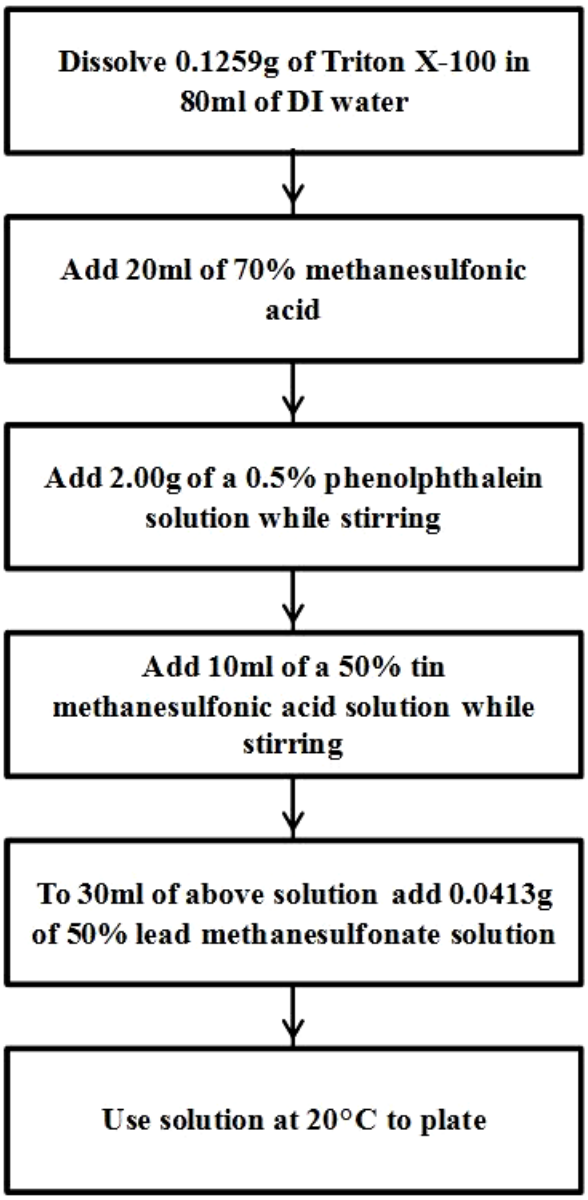

Figure 4. Formulation of SnPb Electroplating Solution

4.1.4 Electroplating of the Doped with 2.1% Copper (SnCu)

The copper-doped tin was achieved using a modified version of the method developed by Oscar Khaselev [11]. Plating was conducted using the above electrolyte solution held at 20°C in a 50 milliliter glass beaker while stirring. The anode was constructed from SnCu sheet containing 4.4% Cu and was cleaned with 1200 grit silicon carbide paper before each sample was plated. Plating was performed as 0.220V and 21.2 milliamps for 4 minutes to yield a light gray matte film.

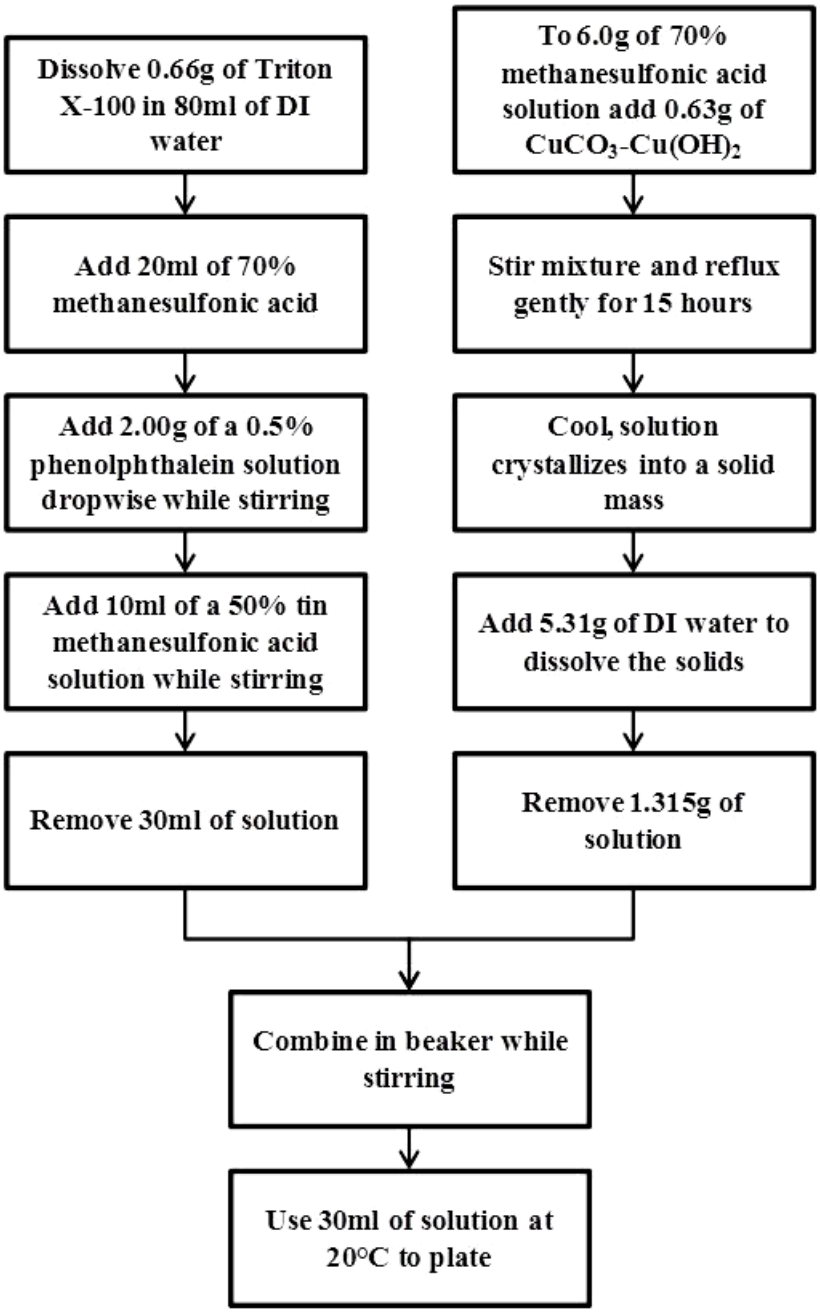

Figure 5. Formulation of SnCu Electroplating Solution

4.1.5 Electroplating of Tin Doped with 3.0% Nickel (SnNi)

The nickel-doped tin was achieved using a modified version of the method developed by Horst Dillenberg [12]. Plating was conducted using 30 milliliters of the above electrolyte solution held at 35°C in a 50 milliliter glass beaker while stirring (Note: the electrolyte may attack the glass beaker upon prolonged exposure). The anode was constructed of a Ni sheet (99.98%, Aldrich). Plating was done at 1.31 V and 8.4 milliamps for 8 minutes to yield a light gray matte film. The anode was cleaned using 1200 grit silicon carbide paper before each sample was plated.

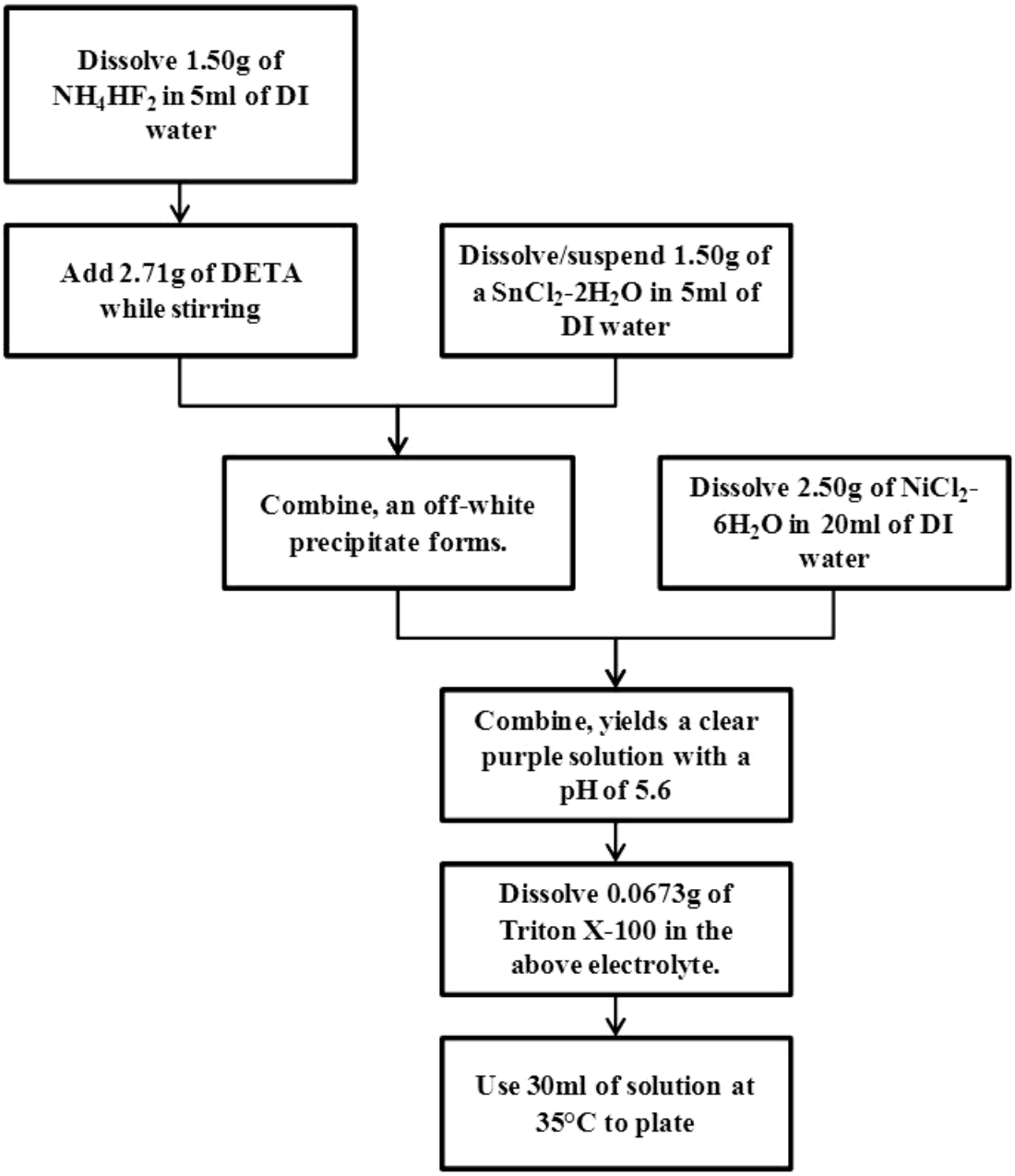

Figure 6. Formulation of SnNi Electroplating Solution

4.1.6 Electroplating of Tin Doped with 0.95% Cobalt (SnCo)

The cobalt-doped tin was achieved using a modified version of the method developed by Horst Dillenberg [12]. Plating was conducted using 30 milliliters of the above electrolyte solution held at 65°C in a 50 milliliter Fluoroware® beaker while stirring (Note: the electrolyte may attack the glass beaker upon prolonged exposure). The anode was constructed from a Co sheet (99.95%, Aldrich). Plating was done at 0.440 V and 10 milliamps for 8 minutes to yield a light gray matte plating. The anode was cleaned using 500 grit Silicon carbide paper before each sample was plated.

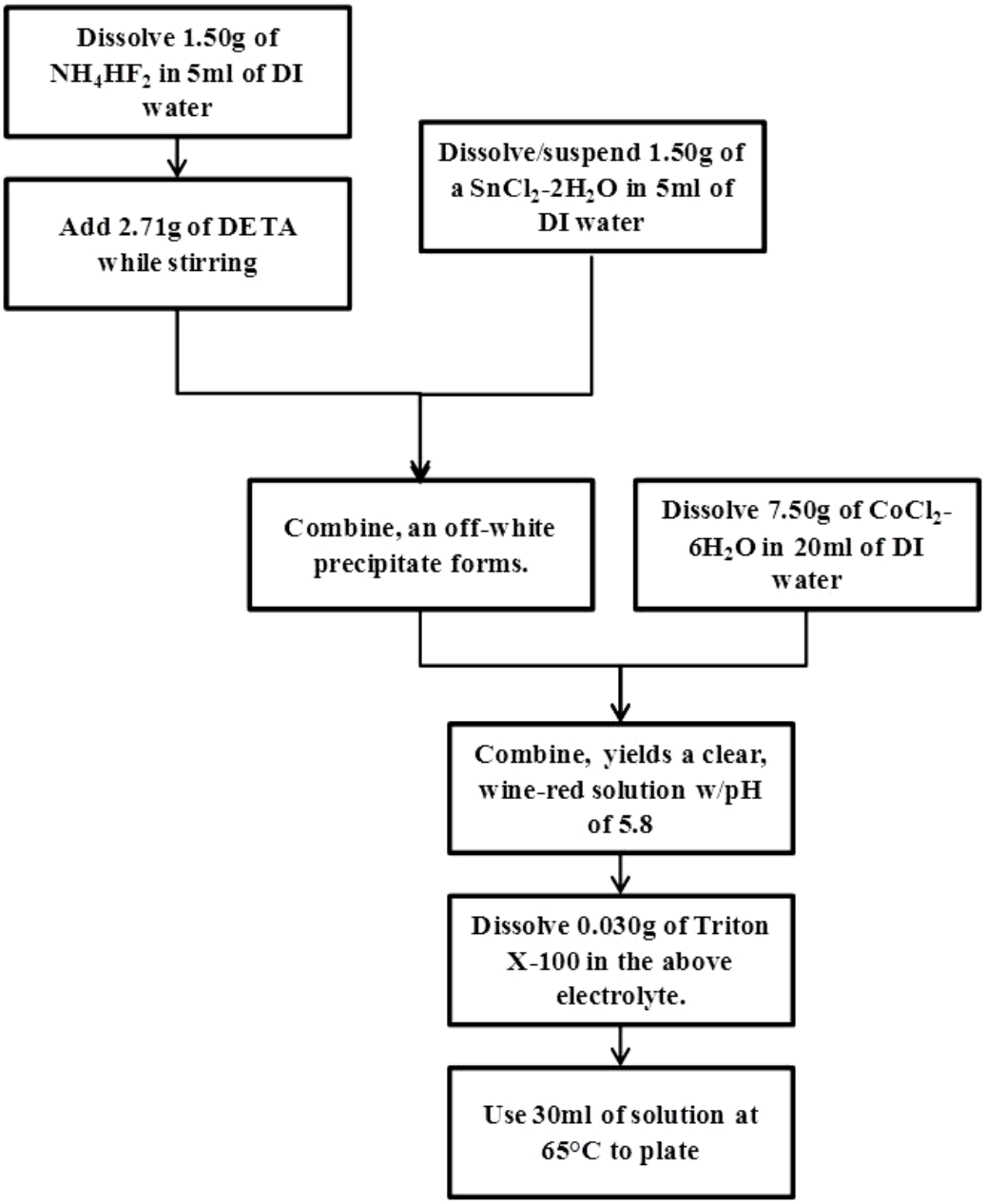

Figure 7. Formulation of SnCo Electroplating Solution

4.1.7 Electroplating of Tin Doped with 2.4% Antimony (SnSb)

The antimony-doped tin was achieved using a modified version of the method developed by G.I. Medvedev [13]. Plating was immediately conducted using 30 milliliters of the above electrolyte solution held at 71°C in a 50 milliliter glass beaker while stirring. The anode was constructed from SnSb sheet (17.9% antimony). Two coupons were plated at a time (total surface area = 2 cm^2). Plating was done at 0.175 V and 22 milliamps for 6 minutes to yield a gray matte plating. The SnSb anode was cleaned using 500 grit Silicon carbide paper before each set of samples was plated.

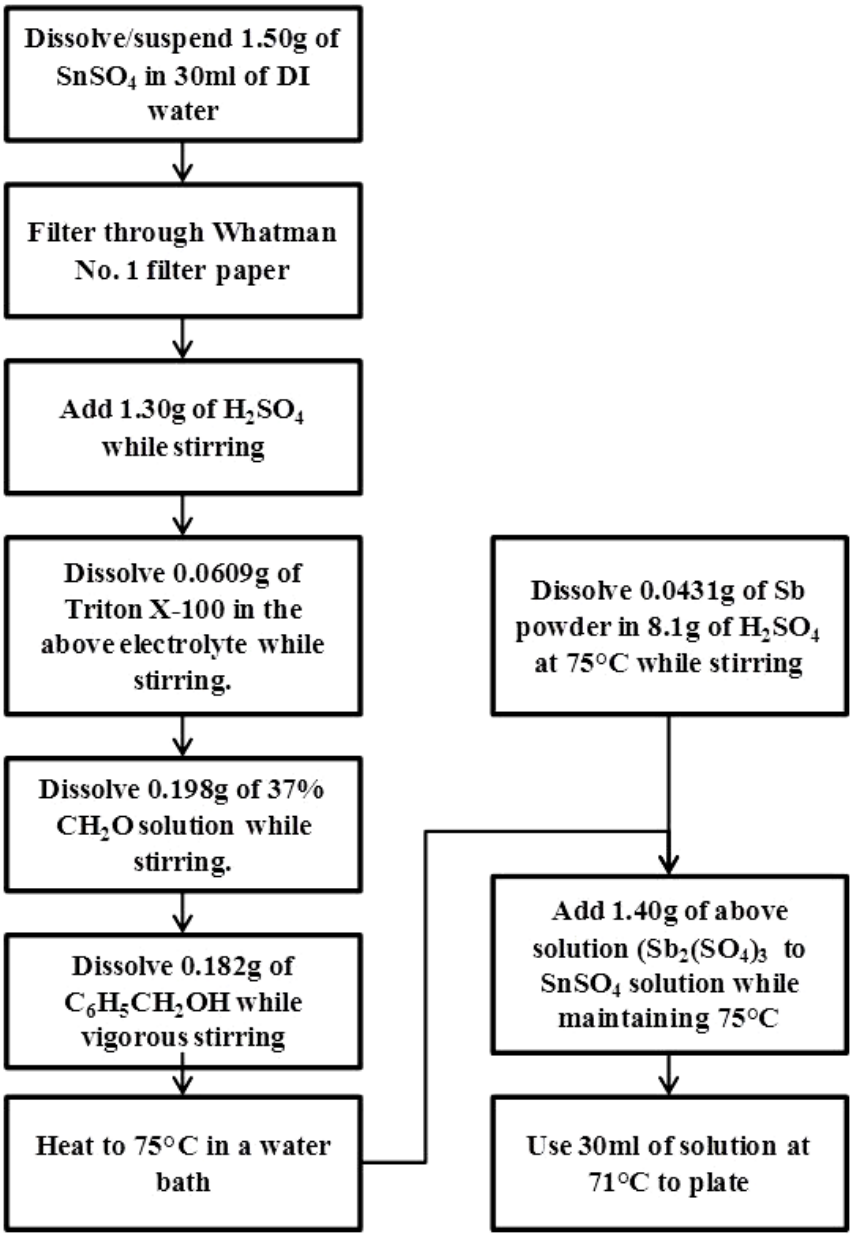

Figure 8. Formulation of SnSb Electroplating Solution

4.1.8 Electroplating of Tin Doped with 1.1% Germanium (SnGe)

Since no prior art could be found on the electroplating of germanium-doped tin film, the following process was developed at Boeing. Plating was conducted using 30 milliliters of the above electrolyte solution at 18°C in a 50 milliliter glass beaker while stirring. The anode was constructed from tin sheet (99.998%, Aldrich). Two coupons were plated at a time (total surface area = 2 cm^2). Plating was done at 0.995 V and 14 milliamps for 8 minutes to yield a light gray matte plating. The Sn anode was cleaned using 500 grit Silicon carbide paper before each set of samples was plated.

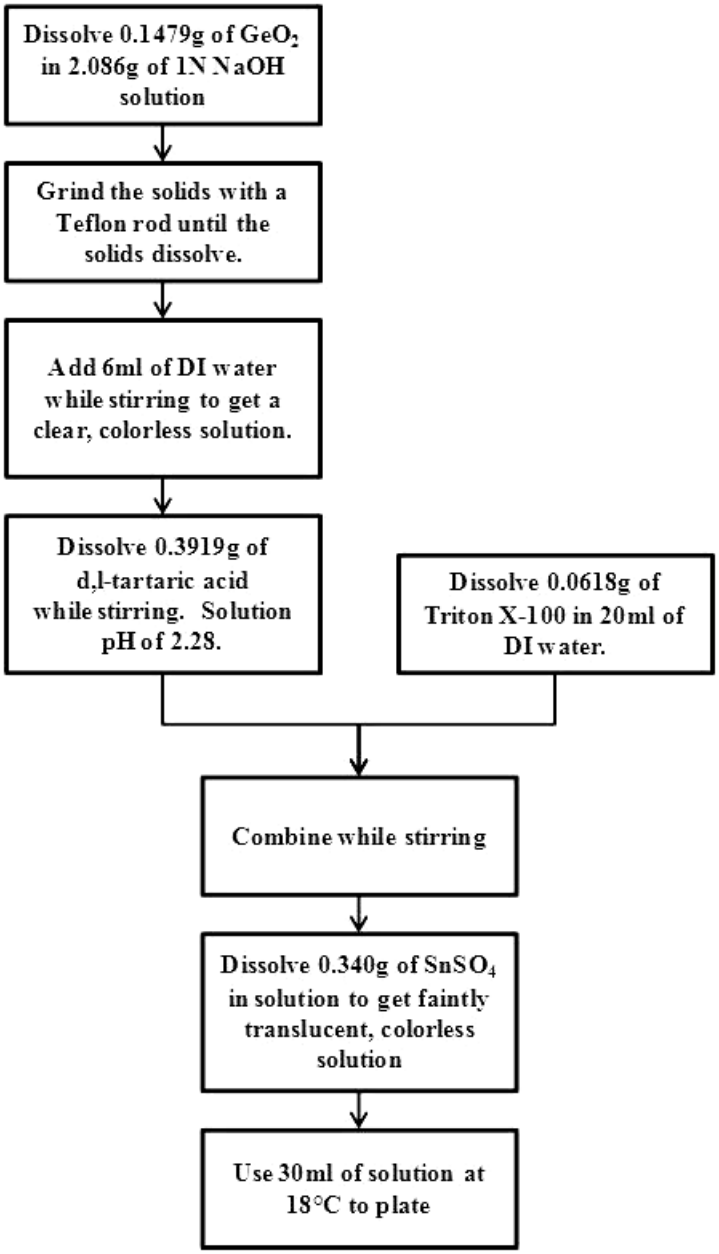

Figure 9. Formulation of SnGe Electroplating Solution

4.1.9 Electroplating of Tin Doped with 1.3% Gold (SnAu)

The gold-doped tin was achieved using a modified version of the method developed by Zhang and Ivey [14]. Plating was conducted using 30 milliliters of the above electrolyte solution at 69°C in a 50 milliliter glass beaker while stirring. The anode was constructed from tin sheet (99.998%, Aldrich). One coupon was plated at a time and fresh electrolyte was used for each sample plated. Plating was done at 0.500 V and 2.2 milliamps for 25 minutes to yield a light-gray satin matte plating. The cathode was gently wiped every 5 minutes during the plating with a Q-tip to removed fine particulates and gas bubbles. The Sn anode was cleaned using 500 grit Silicon carbide paper before each sample was plated.

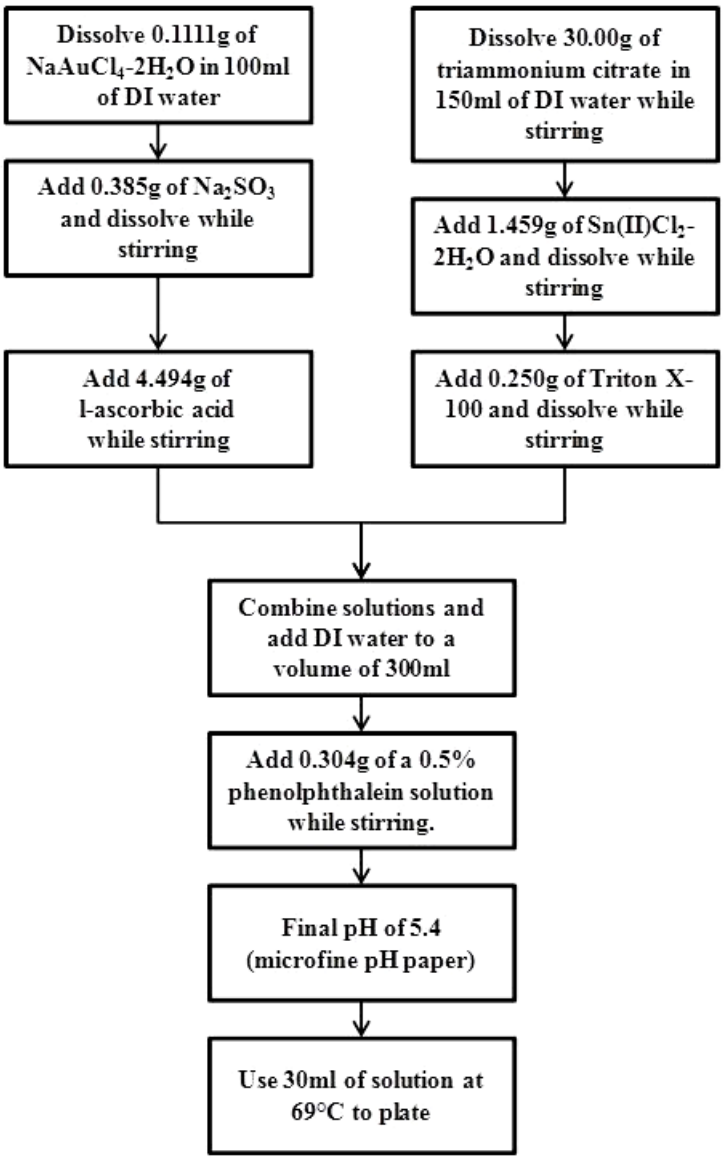

Figure 10. Formulation of SnAu Electroplating Solution

Fresh electrolyte was required for each sample since the stability of the plating bath during plating was poor. It is believed that the sodium sulfite was electrochemically reduced to hydrogen sulfide which then caused a black precipitate (presumably tin sulfide) to form.

4.1.10 Sputter Deposition of Gold Cap Layer onto Pure Tin Plating

Three coupons electroplated with pure Sn, as described in section 4.1.1, were used for the sputtered thin film gold experiment. All three coupons were loaded into a CVC 611 magnetron sputtering system with a hard mask placed over half of the coupon. This allowed for a direct comparison between pure tin and tin capped with a thin gold layer.

The gold sputtering parameters were as follows:

Chamber Base Pressure:	3.2×10^{-8} torr
Current:	2.0 amps
Pressure:	12.0 mtorr
Power:	1.00kW
Voltage:	500 volts
Pre-sputter time:	5 minutes
Deposition time:	1 minute
Final Thickness Avg.:	53.1nm

A thickness monitor sample was also loaded along with the coupons and the gold thickness was measured using an Alphastep 200 profilometer. The thickness ranged from 51.0nm to 56.5nm.

5.0 Results and Discussion

5.1 Inductively Coupled Plasma (ICP) Analysis of Films

In order to verify the percentage of dopant and the consistency of the plating process, the first and last specimens of each set of plated coupons were analyzed by inductively coupled plasma analysis (ICP). ICP is a method of quantitatively measuring the elemental content of a material and the results have an accuracy of better than 0.1 weight percent.

The plated films were etched off the copper coupons using 8 milliliters of 1:1 nitric acid plus 4 milliliters of concentrated hydrochloric acid in a small beaker. In all cases, the plated Sn films were gray in color and contrasted with the copper substrates, so the samples were etched until visibly clear, plus a 20% over etch by time. There was attack of the copper coupons during the nitric/hydrochloric solution, however since the copper coupons were 99.9% pure any trace elements in this slight over etch would be negligible. The solution was then transferred to a 100 ml volumetric flask, diluted to volume with DI water, and analyzed for the elements of interest using the ICP spectrometer.

Copper substrates could not be used for the ICP analysis on the SnCu plated films, since the copper from the substrate could not be distinguished from the copper dopant. Cold rolled carbon steel substrates were electroplated with SnCu and used for ICP analysis. Precision Brand low carbon C1008 cold rolled carbon steel was used because it had no trace copper in the composition.

The ICP results are shown in Table 1. The target concentration for the dopants was 1 to 3 percent by weight. The actual percentage of dopant ranged from a low of 0.9% for the SnCo to a high of 3.1% for the SnPb.

Plated Film	ICP Analysis		
	Dopant Weight % (1st Coupon)	Dopant Weight % (Last Coupon)	Average Dopant Weight %
SnPb	3.10%	3.10%	3.10%
SnCu	2.10%	2.10%	2.10%
SnNi	3.10%	3.00%	3.10%
SnCo	0.84%	0.95%	0.90%
SnSb	2.40%	2.20%	2.30%
SnGe	1.00%	1.10%	1.10%
SnAu	1.00%	1.30%	1.20%

Table 1. ICP analysis results for weight percent of dopants

5.2 Profilometer Measurements of Film Roughness

The average surface roughness (Ra) and the total indicator reading (TIR), also known as trough-to-peak roughness, of the plated films were measured using a KLA-Tencor Alpha-Step 200 profilometer with a 12.5µm stylus. The films were measured after electroplating and again after the aging in the temperature/humidity oven was completed.

Most of the films displayed an increase in the surface roughness after aging (Table 3). This is to be expected, given that most of the films formed nodules during the aging process. The SnNi and SnCo films had the largest increases in surface roughness and TIR, which corresponds with the highest whisker and nodule density seen in the post aging inspection. The SnAu film had no significant change in surface roughness, which was consistent with the low nodule and whisker formation seen at inspection. The Sn/Au and SnSb, which also had low nodule and whisker formation, showed a decrease in surface roughness.

Changes in surface morphology could be due to a number of factors including; whisker/nodule formation, recrystallization, new crystal growth, oxidation, and other factors. Since FIB analysis showed intermetallics frequently extended to the surface of the plated films, the changes in surface roughness will include the intermetallic grains as well as changes to the doped Sn plated films.

Plated Film	As Plated		Post-Aging	
	(ra) (nm)	(TIR) (nm)	(ra) (nm)	(TIR) (nm)
Sn	105	725	153	1073
Sn/Au			48	357
SnPb	120	720	175	785
SnCu	90	560	115	590
SnNi	80	575	577	2518
SnCo	90	490	310	1595
SnSb	520	2810	288	1570
SnGe	117	715	143	950
SnAu	60	330	63	358

Table 2: Profilometer measurement averages of film roughness as plated and after aging

5.3 Temperature/Humidity Aging of the Test Coupons

A Tabai Espec Corporation Platinous Lucifer Model PL-2G programmable temperature/humidity chamber was used in an effort to accelerate whisker formation and growth. After fabrication and initial inspection, three test coupons from each film were placed into an environmental chamber and subjected to a steady 50°C temperature and 50% relative humidity. These environmental conditions were identified in an earlier Boeing study as the best for growing whiskers rapidly [3].

5.4 Qualitative and Quantitative Inspection of Test Coupons

Once the fabrication of the test coupons was completed, they were inspected with both an optical microscope and a scanning electron microscope (SEM) to document grain structure and any defects seen immediately after plating. SEM inspection was performed on a Hitachi S4000 Field Emission SEM. Three coupons from each plating test were then placed in the environmental chamber to begin the aging process.

After 4,000 hours in the temperature/humidity chamber, a qualitative inspection of the coupons was performed. An optical microscope was used for the inspection and the presence or absence of whiskers and/or nodules was recorded and representative SEM images were taken, if appropriate. Whiskers are defined as filamentary growths, longer than 10 microns in length. They may be kinked, grow from nodules or hillocks, and have striations and/or rings [15].

Following 8,000 hours of aging in the temperature/humidity chamber, a quantitative assessment of the whisker densities and lengths was completed on all coupons including the baseline samples. Initially only a few mm^2 area of the coupons were to be inspected, but given that the whisker counts were extremely low on some of the samples (i.e., SnAu, Sn/Au, SnGe) and the density of the whisker growth varied widely across other samples, such as the SnNi, an $1cm^2$ area was inspected. The whisker count was recorded for a $1cm^2$ area on all samples, except for the Au capped pure Sn samples. Since only half of the plated Sn was sputtered with Au, only an area of slightly $>0.5cm^2$ per sample was available for inspection.

At this time, all samples with lower whisker density than the pure tin baseline samples were placed back into the environmental chamber for an additional 4,000 hours. On the specimens that showed a higher whisker density than the pure tin samples, one coupon was sent for FIB analysis and one coupon was sent for EBSD analysis. The remaining coupon was placed back into the environmental chamber for reference. At 12,000 hours, all coupons were removed from the chamber and a quantitative inspection was performed.

Whisker density and approximate whisker lengths were recorded for all whiskers greater than 10 microns in length. Exact measurements on all whiskers were not possible, due to varying angles, kinks, and bends. It would require multiple changes in SEM tilt and

rotation to get an exact measurement on every whisker that would be extremely time consuming, so the length of the whisker was estimated for most whiskers. All whiskers >50 microns were measured and care was taken to measure the longest whisker on each sample as accurately as possible. Representative SEM images of whiskers from each coupon were taken.

Average whisker density for each film at 8,000 hours is shown in Figure 11. Samples with low whisker counts were inspected again at 12,000 hours, shown in Figure 12. The Sn/Au, SnSb, SnGe, and SnAu all had whisker counts lower than the pure Sn at both 8,000 and 12,000 hours.

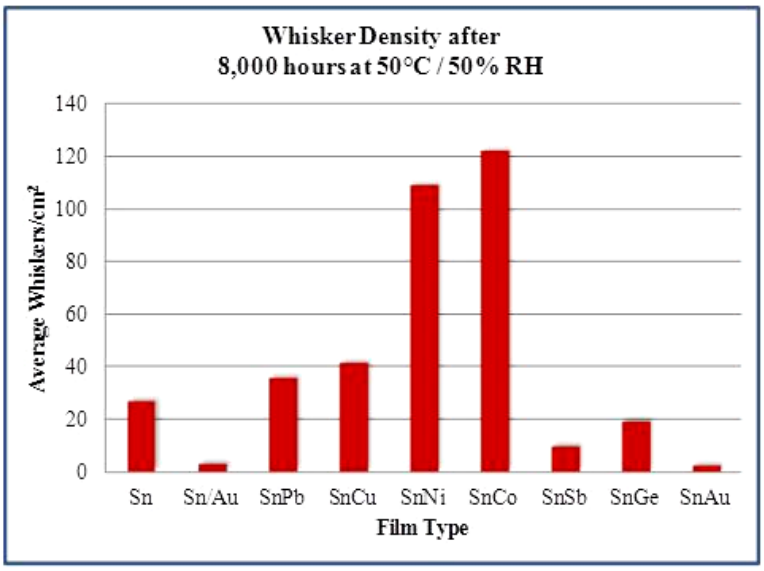

Figure 11. Chart of average number of whiskers/cm^2 at 8,000 hours

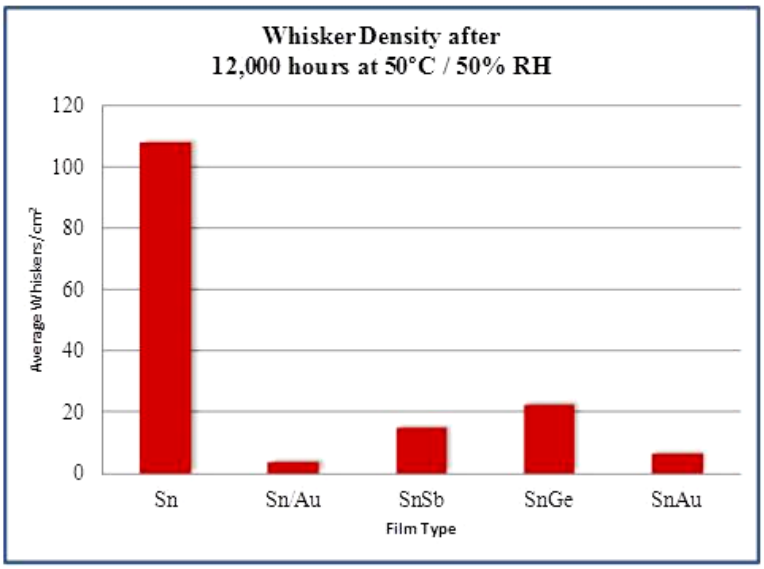

Figure 12. Chart of average number of whiskers/cm^2 at 12,000 hours

The presence of fine particles was observed on the surface of the Sn/Au, SnGe, and SnAu coupons during the first quantitative inspection at 8,000 hours. The particles had precipitated out of the tin matrix on the doped films (SnGe, SnAu), while on the Sn/Au they appeared to have formed at the surface. All three of these films had whisker counts lower than the baseline Sn samples.

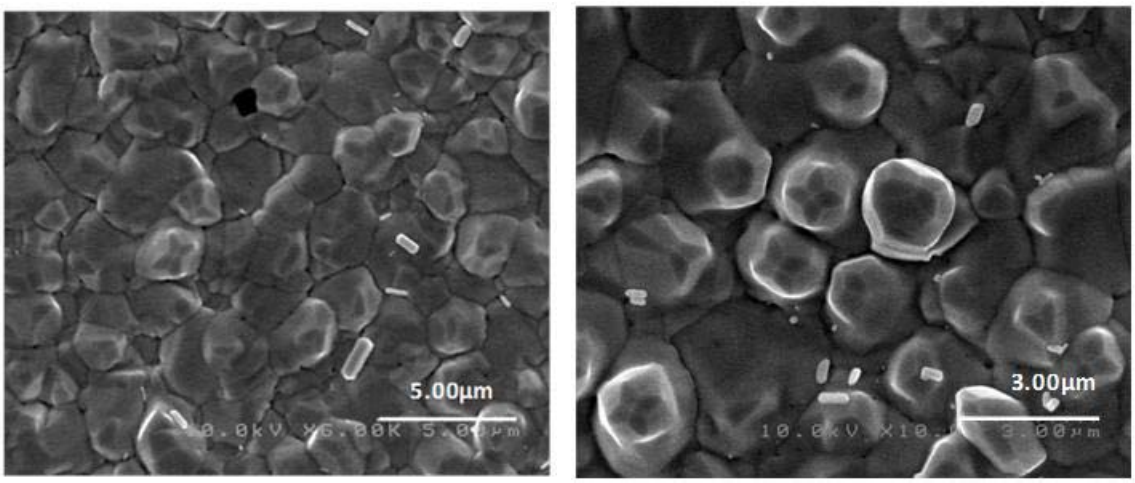

Figure 13. SEM images of particles that precipitated out of the SnGe film after 8,000 hours of aging

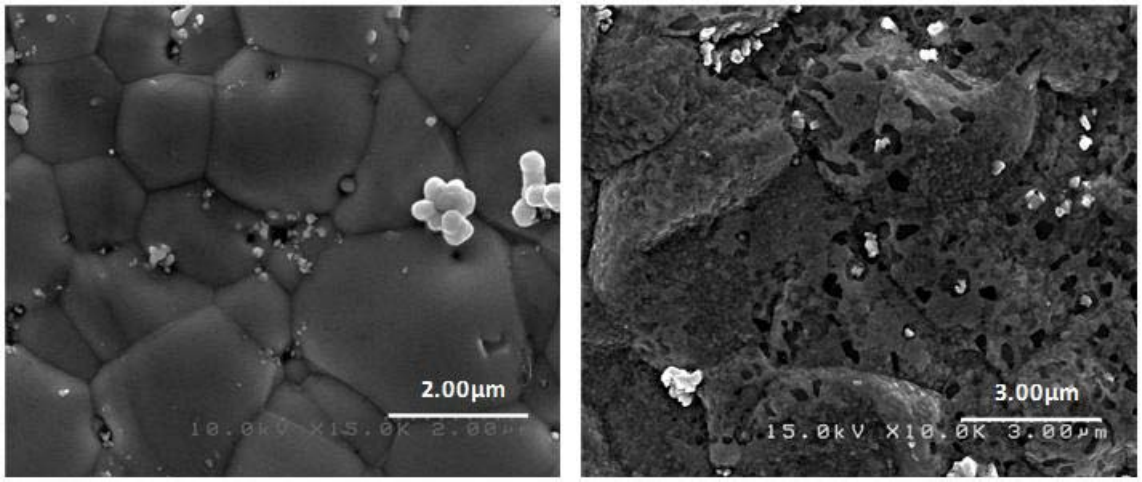

Figure 14. SEM images of particles on SnAu (left) and Sn/Au (right) films after 8,000 hours of aging

In comparison, the SnNi, SnCo, and SnCu films had the highest whisker counts in this study at 8,000 hours. Though these films had fine particles visible within the tin matrix under SEM inspection, they had not precipitated out. Since the whisker counts were

higher than the pure tin samples, coupons were pulled for FIB and EBSD analysis and only one coupon per film was returned to the environmental chamber. During the last 4,000 hours of aging, the particles on the SnCu film began to precipitate out as shown in Figure 15. The whisker formation on the SnCu film dropped off significantly, while the whisker count on SnCo increased 66% and SiNi increased 693%.

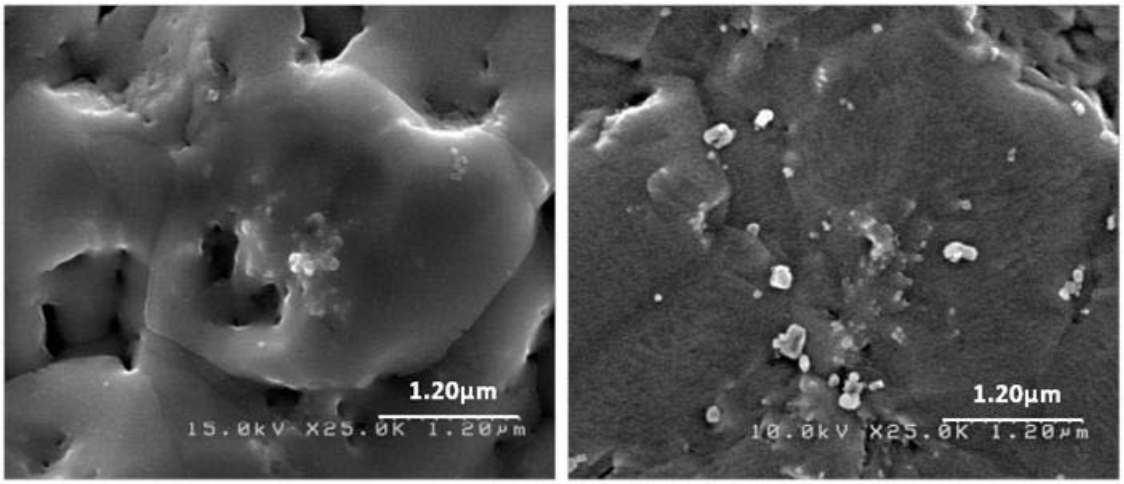

Figure 15. SEM image of particulates in SnCu matrix after aging 8,000 hours (left) and on SnCu surface after 12,000 hours aging (right)

None of these sub-micron particles were found in this study's SnPb film during SEM inspection. However, there have been studies that found Pb particles with a diameter of approximately 10nm in SnPb films with approximately 3.5% Pb. Scanning transmission electron microscopy (STEM) was used to identify the Pb particles on the films [16].

There were also no discernible particles found in the SnSb films, however, these films were extremely porous and small particles would have been difficult to differentiate from the pitted morphology.

Most of these particles are smaller than the resolution limits of the EBSD, EDX, and Auger spectroscopy, so the composition cannot be determined by these methods. Phase diagrams can be used to predict the plating compositions, but it should be noted that electroplating is capable of producing phases that are different from those reported in phase diagrams (metallurgical equilibrium conditions) [17]. In order to better determine how the dopants and/or intermetallics are distributed throughout the plating grains, careful transmission electron microscopy (TEM) studies will need to be done [16] but these studies are outside the scope of this program.

5.4.1 Inspection of Pure Tin Samples

The post plating inspection found all pure Sn coupons to be free of plating nodules, dendrites, and other plating artifacts. After 4,000 hours of aging in an environmental oven at 50°C and 50% relative humidity, qualitative inspection found some nodules and a few short whiskers. Inspection data from quantitative inspections can be found in Tables 3 & 4.

Film	Coupon Number	Inspection Area (cm^2)	Whisker Count at 8,000 hours					Longest Whisker
			10-20μm	21-30μm	31-40μm	41-50μm	>50μm	
Sn	67	0.5	13	0	0	0	0	< 20μm
	68	0.5	18	0	0	0	1	344μm
	69	0.5	15	0	0	0	2	118μm
	62	1	18	0	0	0	0	< 20μm
	63	1	8	0	0	0	0	< 20μm
	64	1	35	2	0	0	2	180
	Average Whiskers/cm^2		25.5	0.3	0.0	0.0	1.3	
	Total Average Number of Whiskers/cm^2 = 27							

Table 3. Average number of whiskers/cm^2 on pure Sn films at 8,000 hours

Film	Coupon Number	Inspection Area (cm^2)	Whisker Count at 12,000 hours					Longest Whisker
			10-20μm	21-30μm	31-40μm	41-50μm	>50μm	
Sn	67	0.5	40	6	0	0	2	304.8
	68	0.5	46	6	1	0	2	339.4
	69	0.5	59	6	0	0	1	112.3
	63	1	86	16	1	0	0	31.2
	Average Whiskers/cm^2		91.3	14.0	0.8	0.0	1.7	
	Total Average Number of Whiskers/cm^2 = 108							

Table 4. Average number of whiskers/cm^2 on pure Sn films at 12,000 hours

The inspection data for the pure tin includes coupons 62, 63, and 64 which had slightly greater than 1cm^2 area electroplated (Figure 16). It also includes the 0.5cm^2 area on coupons 67, 68, and 69 that was pure tin. The other 0.5cm^2 areas of these coupons were sputtered with Au (Figure 17).

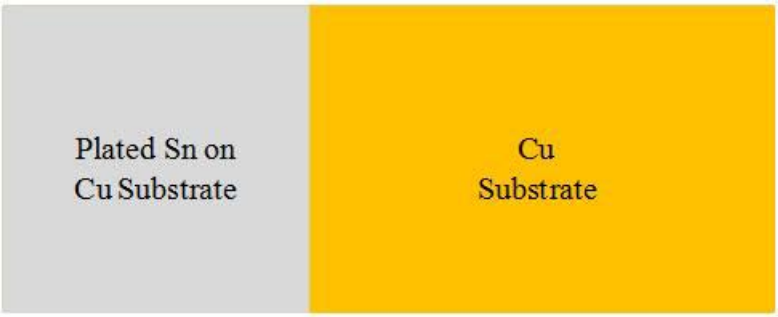

Figure 16. Drawing of pure tin plated area on coupons 62, 63, and 64

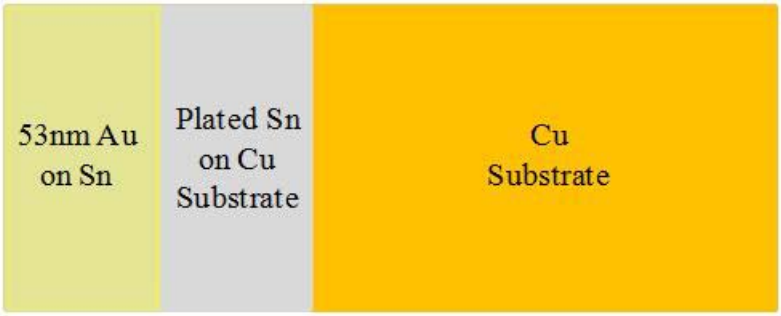

Figure 17. Drawing of pure tin plated area on coupons 67, 68, and 69

One coupon was randomly selected to continue aging to 12,000 hours. The other two samples were sent for EBSD and FIB analysis. Sample 63 had the lowest whisker count for a pure Sn coupon at 8,000 hours, but it increased to an average of 103 whiskers/cm^2 at 12,000 hours. The grain structure after 12,000 hours of aging was unremarkable with a grain size of approximately 3 microns (Figures 18-19). The tin whiskers and nodules that formed on the pure tin coupons were typical in diameter and shape to those found in literature [15, 18, 19] with no exceptional features (Figures 20-22).

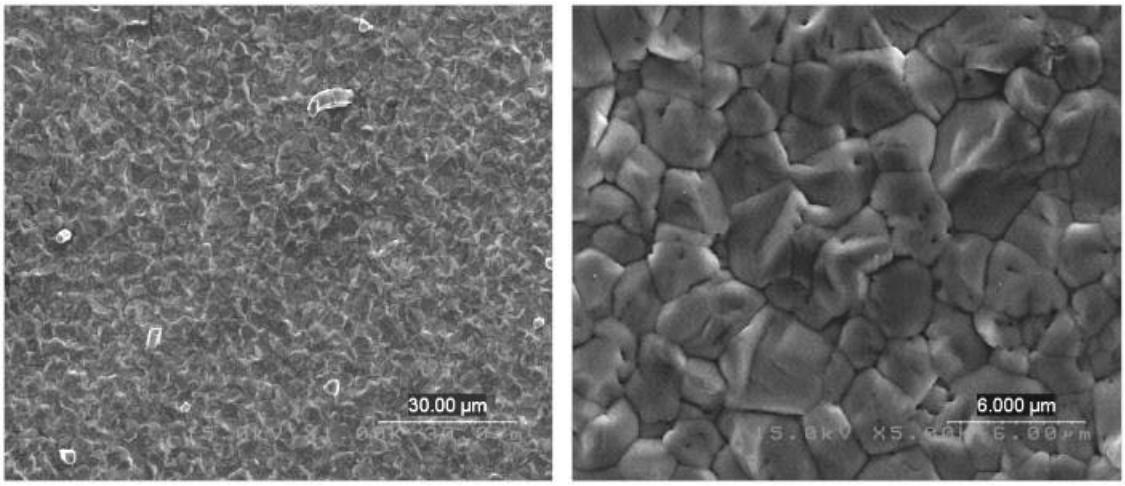

Figure 18. SEM images of Sn grain structure after 12,000 hours of aging

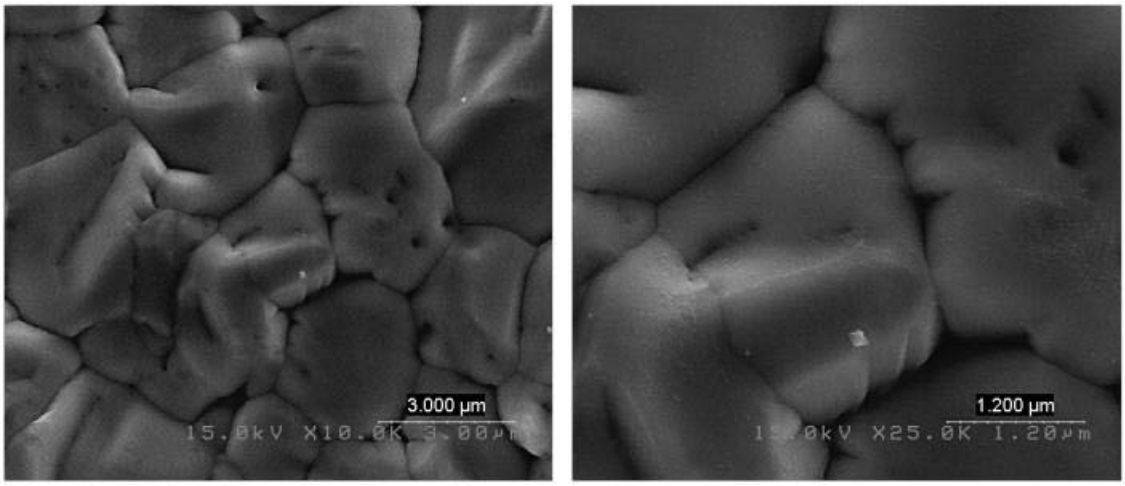

Figure 19. SEM images of the Sn grain structure after 12,000 hours of aging

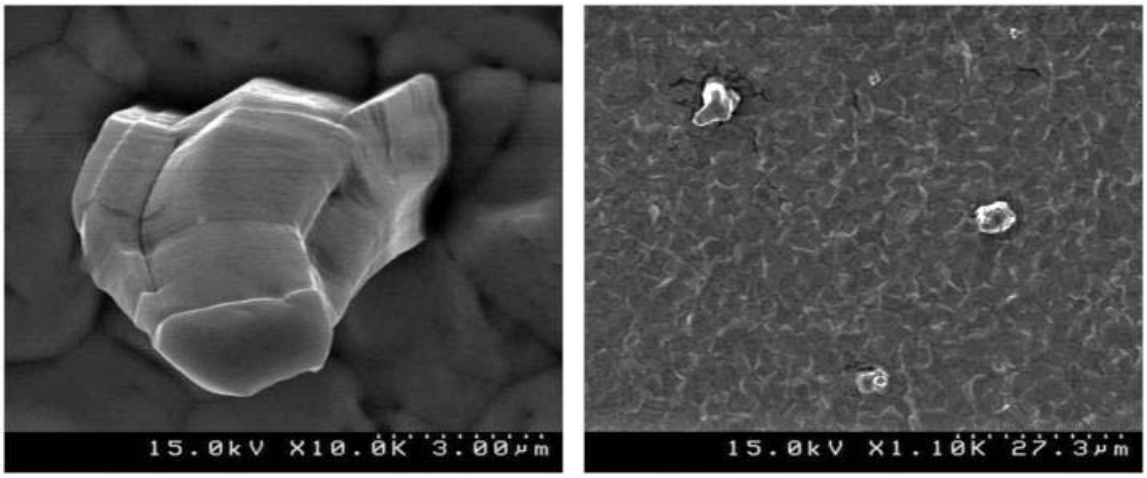

Figure 20. SEM images of nodules on Sn coupons after 8,000 hours aging

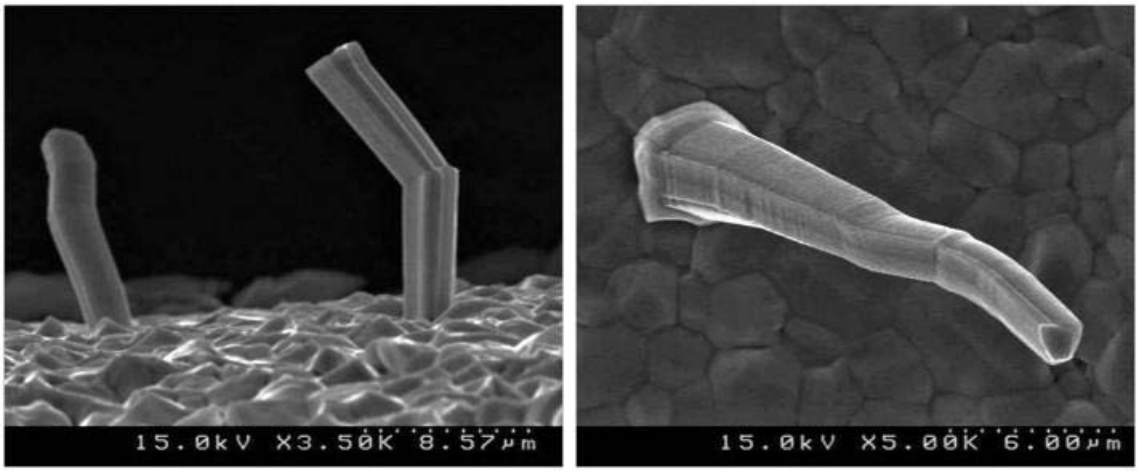

Figure 21. SEM images of whiskers on Sn coupons after 8,000 hours aging

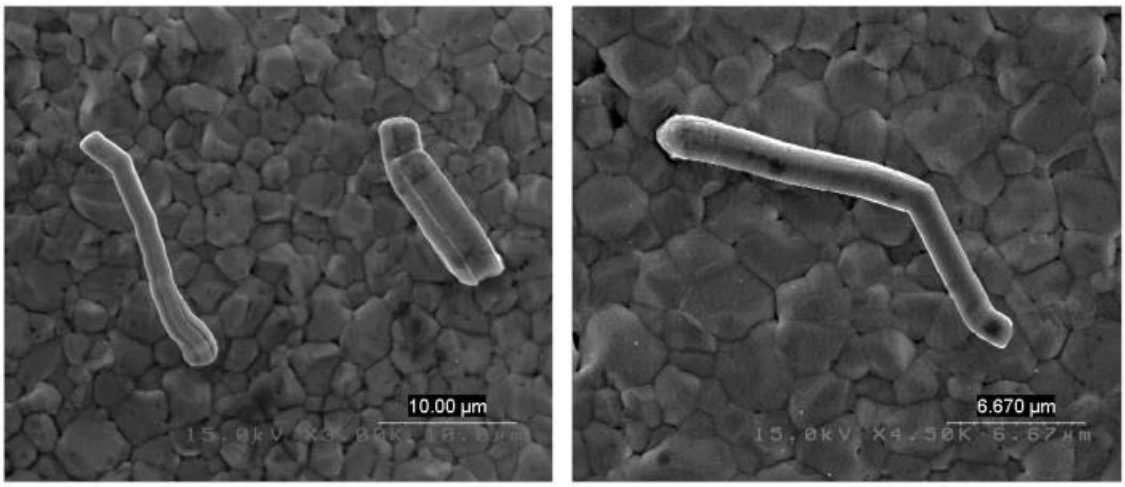

Figure 22. SEM images of Sn whiskers on pure Sn coupons after12,000 hours aging

5.4.2 Inspection of Tin with 53nm Sputter Gold Cap (Sn/Au) Films

Inspection of the pure tin film post plating showed that all coupons were free of plating nodules, dendrites, and other plating artifacts. After the gold was sputtered on half of the pure tin film (Figure 17), the sputtered areas appear gold when visually inspected, but no other differences were noted.

After 4,000 hours of aging the pure tin side of the coupons had numerous hillocks and some whiskers while the gold side had extremely few nodules and an average of one whisker. Visual inspection showed that the gold sputtered side had dulled and was now a silver-yellow. Inspection data from quantitative inspections can be found in Tables 5 & 6 for the Sn/Au film and in Tables 3 & 4 for the pure Sn half of the coupon.

Film	Part ID	Inspection Area (cm^2)	Whisker Count at 8,000 hours					Longest Whisker
			10-20μm	21-30μm	31-40μm	41-50μm	>50μm	
Sn/Au	67	0.5	1	0	0	0	0	< 20μm
	68	0.5	2	0	0	0	1	236μm
	69	0.5	1	0	0	0	0	< 20μm
	Average Whiskers/cm^2		2.7	0.0	0.0	0.0	0.7	
	Total Average Number of Whiskers/cm^2 = 3.3							

Table 5. Average number of whiskers/cm^2 on Sn/Au films at 8,000 hours

Film	Part ID	Inspection Area (cm^2)	Whisker Count at 12,000 hours					Longest Whisker
			10-20μm	21-30μm	31-40μm	41-50μm	>50μm	
Sn/Au	67	0.5	1	0	0	0	1	69.5
	68	0.5	2	0	0	0	1	236
	69	0.5	1	0	0	0	0	12.8
	Average Whiskers/cm^2		2.7	0.0	0.0	0.0	1.3	
	Total Average Number of Whiskers/cm^2 = 4							

Table 6. Average number of whiskers/cm^2 on Sn/Au films at 12,000 hours

At 8,000 hours of aging there was one long whisker on the Sn/Au film, but it was close to the interface of the sputtered/non-sputtered regions (Figure 23). It is possible that this area was partially shaded by the shadow mask used during sputtering, which lead to a thinner gold film or that stresses at this interface contributed to the whisker formation.

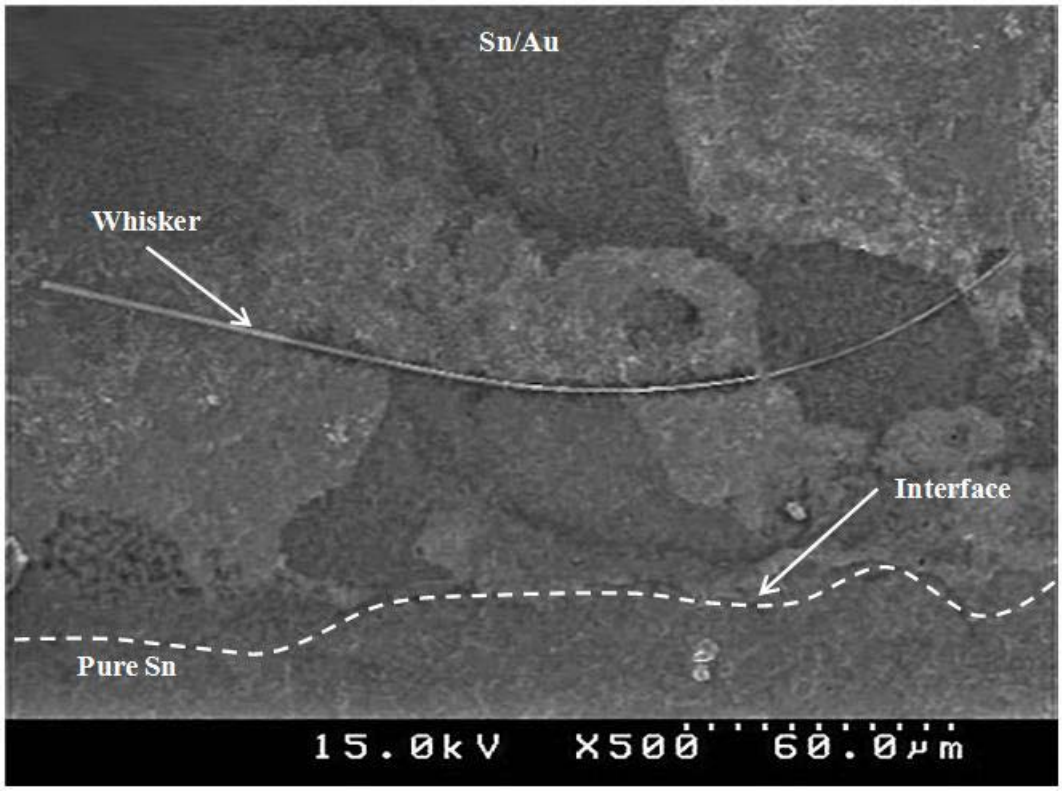

Figure 23. SEM image of a long whisker on the Sn/Au sample at the interface of the pure Sn and Au sputtered Sn areas after 8,000 hours of aging

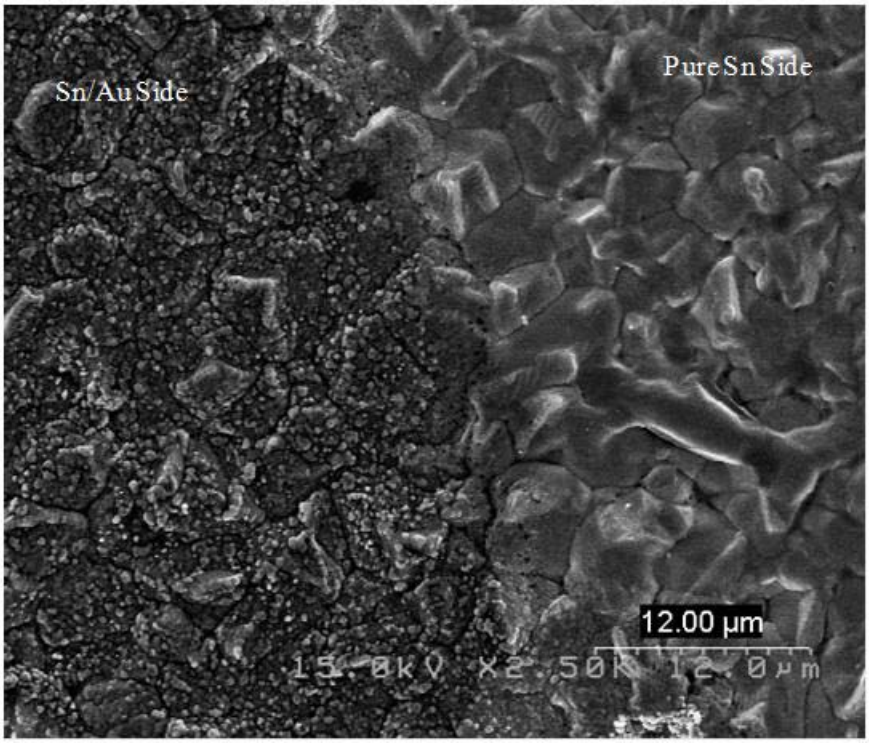

Figure 24. SEM image of the Sn/Au and Pure Sn interface after 8,000 hours of aging

It was also noted at 8,000 hours that clusters of particulates, likely SnAu intermetallics, had formed on the surface in the Sn/Au areas (Figure 25). There were also some random spots of organic debris on the surface of the Sn/Au side of the samples, possibly flakes of adhesive from the tape used to affix the shadow mask. These are noteworthy because they blocked the sputtered Au film from reaching the surface of the plated pure tin film and in several of these areas grew whiskers and nodules from under the flakes (Figure 26-27).

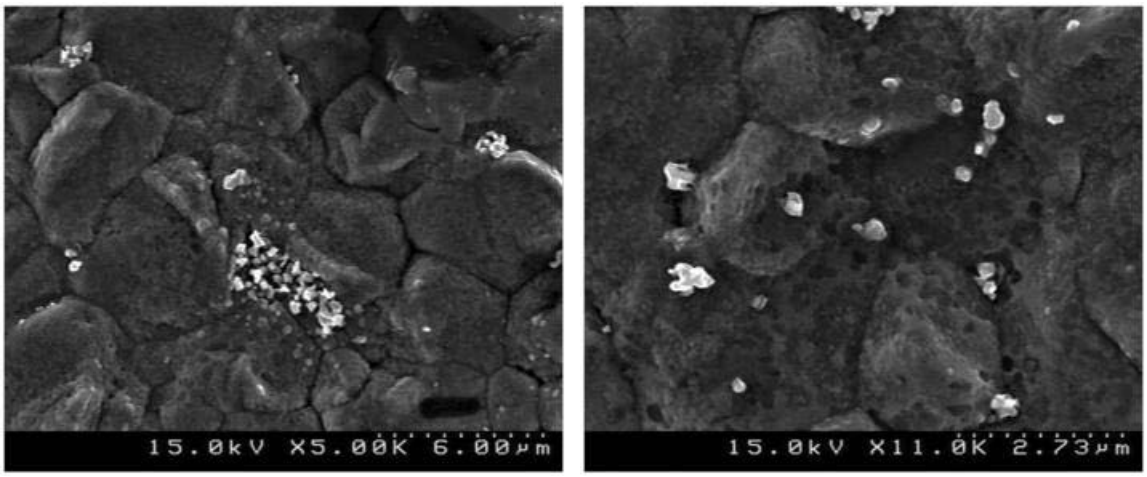

Figure 25. SEM image of intermetallic formation on the surface of the Sn/Au samples after 8,000 hours of aging

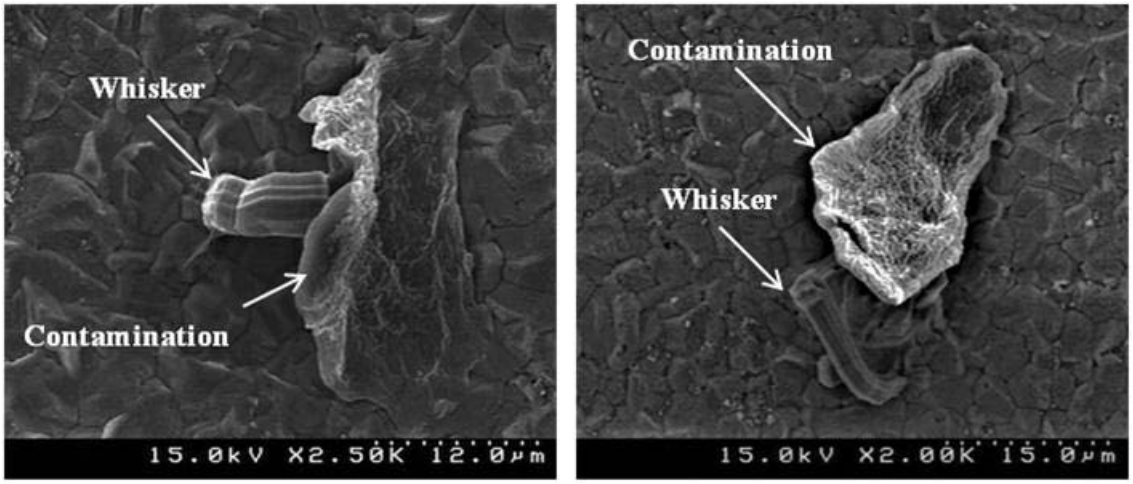

Figure 26. SEM image of whiskers forming under flakes of contamination on Sn/Au samples after 12,000 hours of aging

At 12,000 hours, on the Sn/Au side of the samples, two out of the three coupons had no increase in the number whiskers or any measurable change in their size. The third coupon only had one additional whisker, 69.5 microns in length. On all three of the Sn/Au samples, there were only two whiskers greater than 20 microns in length after 18

months of aging and both of these whiskers were close to the boundary between the sputtered gold film and gold-free areas.

By comparison, at 12,000 hours the pure tin films had an average of 113 whiskers/cm^2. The longest whisker had not increased in size during the last 4,000 hours of aging, but a second whisker >300 microns formed on the pure Sn side. The formation of intermetallics on the surface of the Sn/Au side of the coupons created an obvious difference between the pure Sn and the Sn/Au sides of the coupons with a clearly discernible interface (Figure 24). On all three Sn/Au samples there were only a very few short whiskers formed that did not appear to have any secondary causes such as proximity to the interface or contamination (Figure 30).

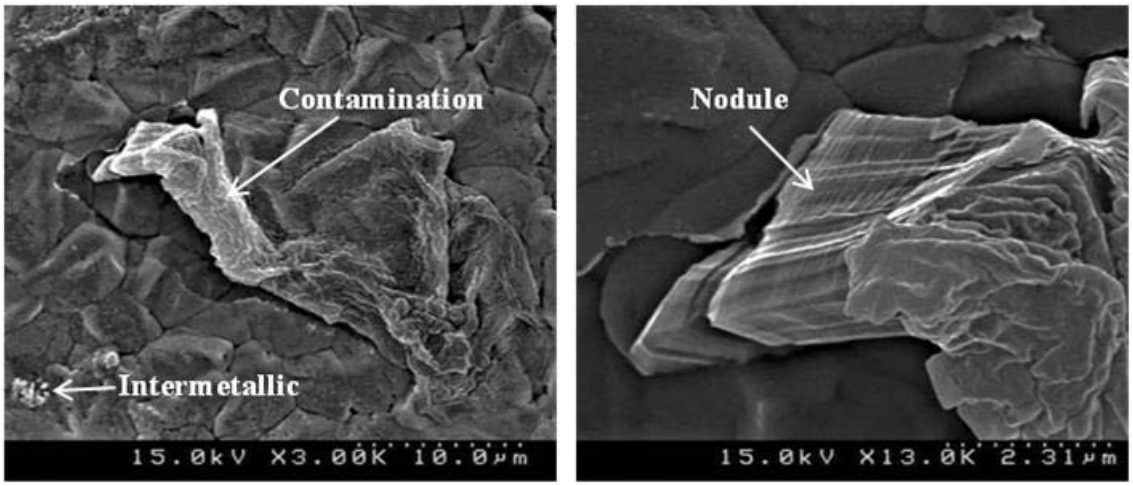

Figure 27. SEM image of a nodule forming under a flake of contamination on Sn/Au sample after 12,000 hours of aging

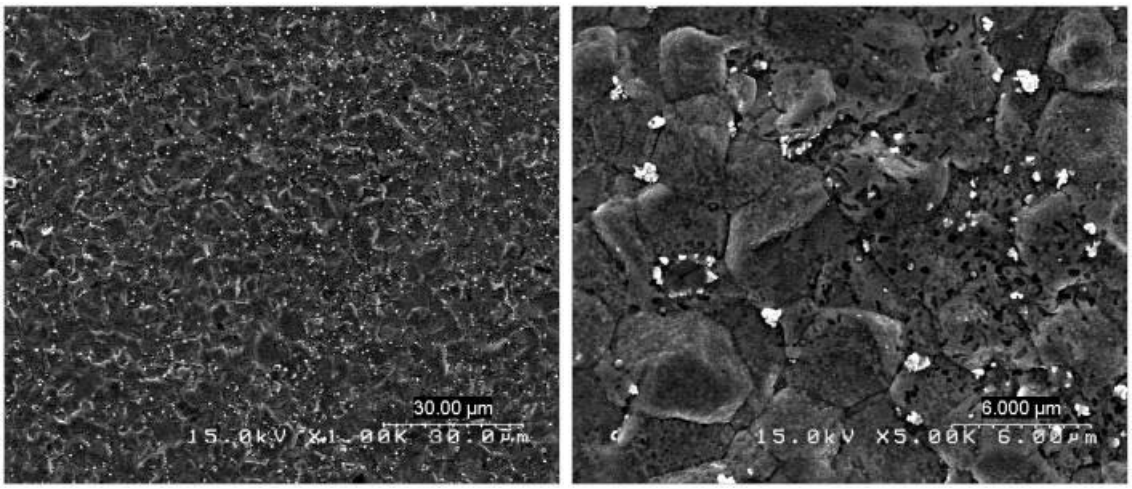

Figure 28. SEM image of Sn/Au grain structure after 12,000 hours of aging

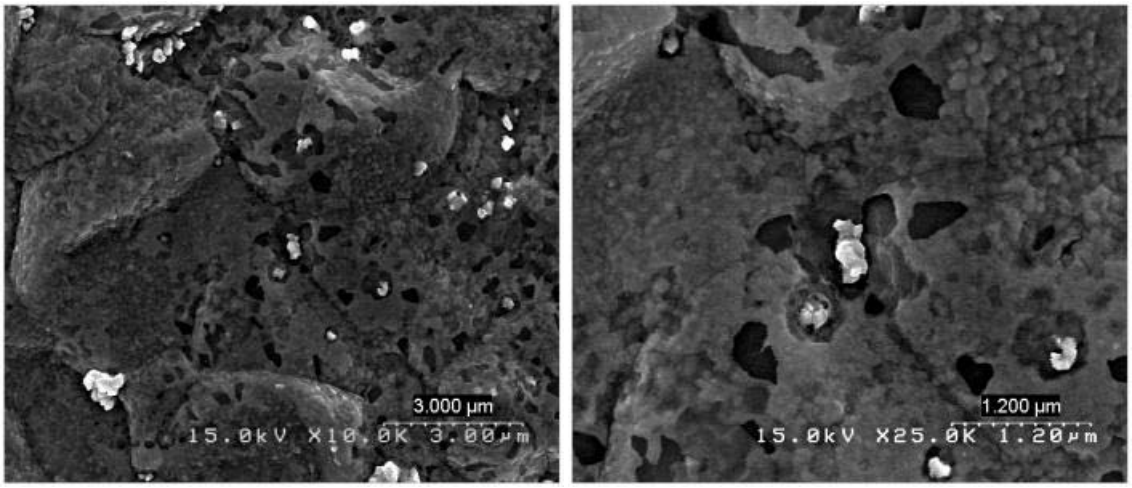

Figure 29. SEM image of Sn/Au grain structure after 12,000 hours of aging

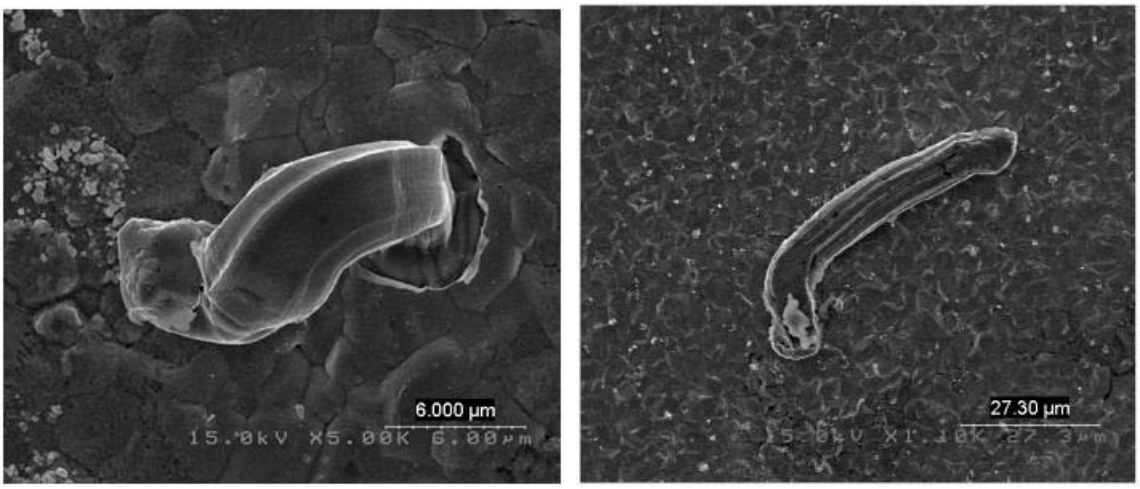

Figure 30. SEM image of whiskers on the Sn/Au film after 12,000 hours of aging

5.4.3 Inspection of Tin with 3.1% Lead (SnPb) Films

An initial optical microscope and scanning electron microscope inspection was performed on all coupons immediately after fabrication. Although every effort was made to produce a defect-free plated film, the SnPb films did exhibit some nodules and short filamentary growths (Figure 31).

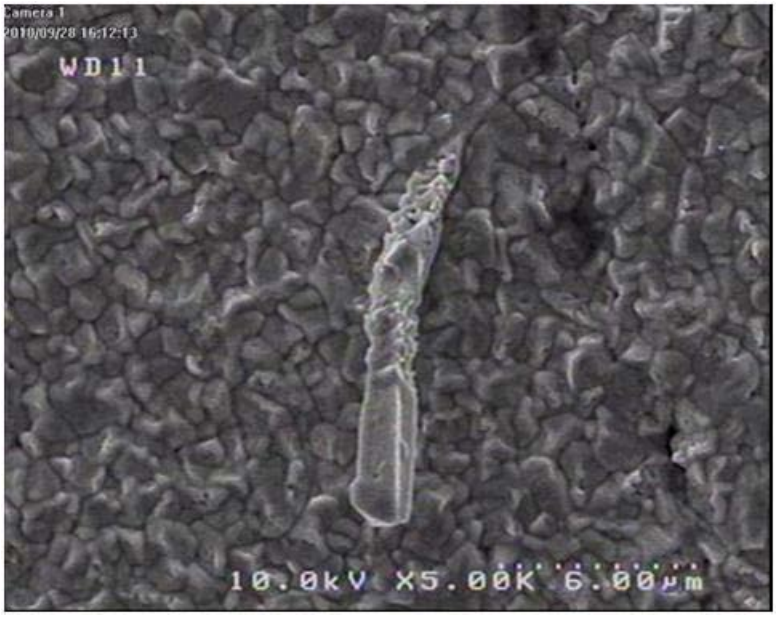

Figure 31. SEM Image of defect on Sn3.1%Pb film immediately after plating

Following approximately 4,000 hours of aging, the SnPb coupons were qualitatively inspected. Several nodules and long filamentary growths were noted. The vast majority of the whiskers appeared cubic with small protrusions off the sides of the whiskers (Figure 34, left). This multi-faceted appearance called into question whether they should be identified as dendrites rather than whiskers. Although not standard whisker formation (Figure 34, right), these filamentary growths also did not form into the characteristic fern-like structure that is typical of dendrites. Furthermore, they continued to grow and proliferate during the aging process. It was decided to include these filamentary growths in the whisker count since they protruded up from the surface and would have the same detrimental effect. It should be noted that approximately 90% of the whiskers on the SnPb film had this multifaceted morphology. The cause of the unusually high number of defects in the SnPb film has not been determined.

Inspection data from quantitative inspections can be found in Tables 7 & 8.

Film	Coupon Number	Inspection Area (cm^2)	Whisker Count at 8,000 hours					Longest Whisker
			10-20μm	21-30μm	31-40μm	41-50μm	>50μm	
SnPb	71	1	37	6	0	4	0	< 20μm
	72	1	30	5	2	0	2	116
	73	1	19	0	1	0	2	157
	Average Whiskers/cm^2		28.7	3.7	0.0	1.3	1.3	
	Total Average Number of Whiskers/cm^2 = 36							

Table 7. Average number of whiskers/cm^2 on SnPb films at 8,000 hours

Film	Coupon Number	Inspection Area (cm^2)	Whisker Count at 12,000 hours					Longest Whisker
			10-20μm	21-30μm	31-40μm	41-50μm	>50μm	
SnPb	71	1	78	44	19	9	4	123
	Total Average Number of Whiskers/cm^2 = 154							

Table 8. Average number of whiskers/cm^2 on SnPb films at 12,000 hours

The grain structure of the SnPb films was unremarkable with an average grain size of approximately 1.8 microns. The filamentary growths had a wide variety of shapes: zigzag patterns, multifaceted, as well as typical tin whisker form (Figures 35-37).

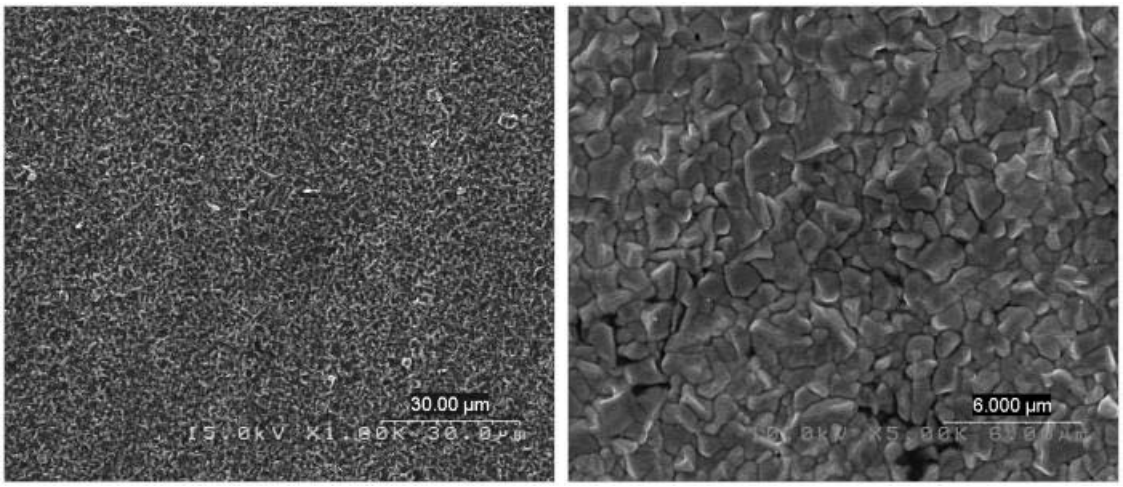

Figure 32. SEM image of SnPb grain structure after 12,000 hours of aging

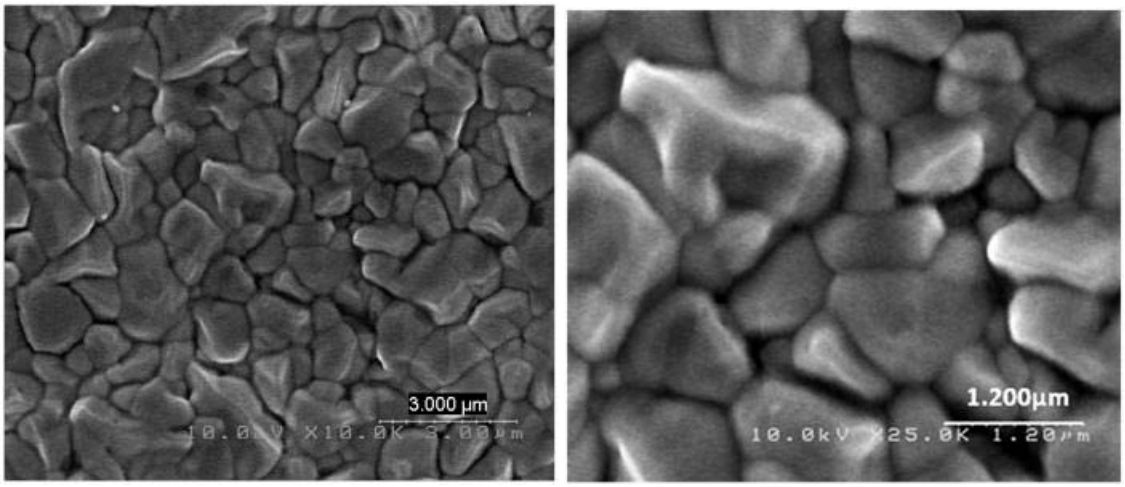

Figure 33. SEM image of SnPb grain structure after 12,000 hours of aging

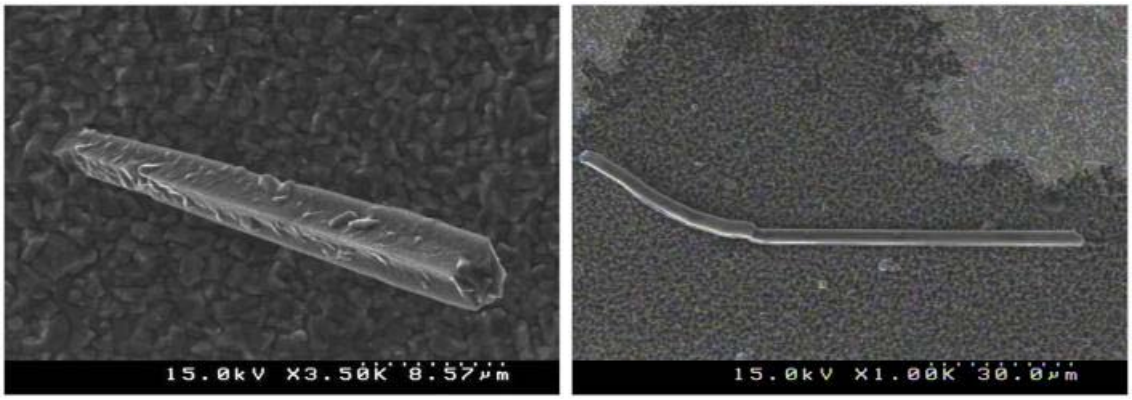

Figure 34. SEM image of (left) multifaceted filamentary growth and (right) “typical” whisker on SnPb film

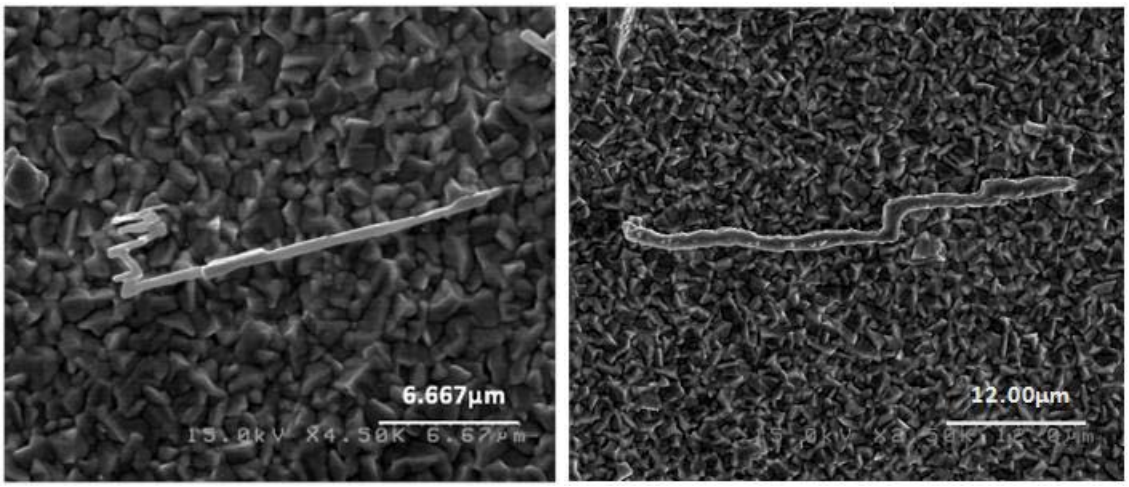

Figure 35. SEM image of whiskers on SnPb film after 8,000 hours of aging

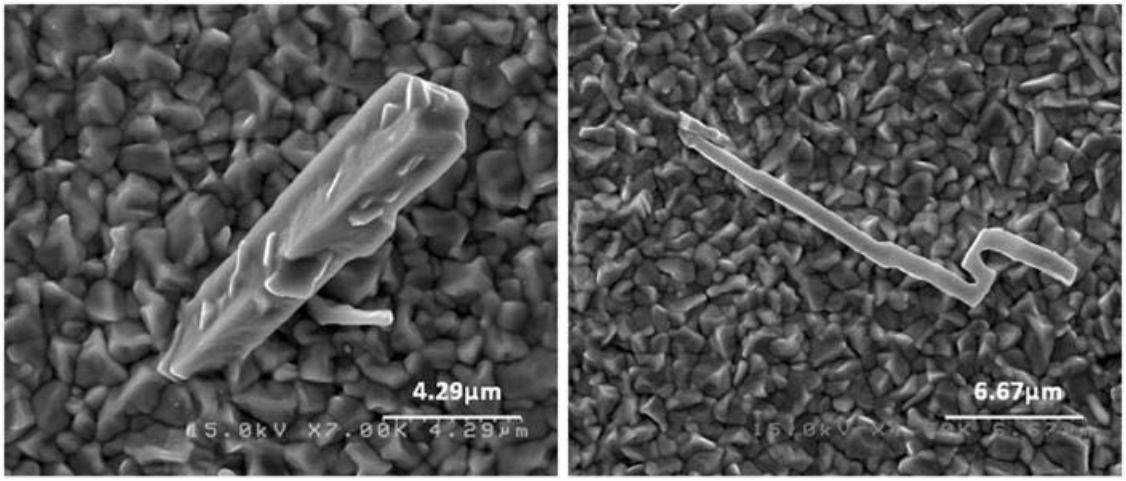

Figure 36. SEM image of whiskers on SnSb films after 8,000 hours (left) and 12,000 hours (right) of aging

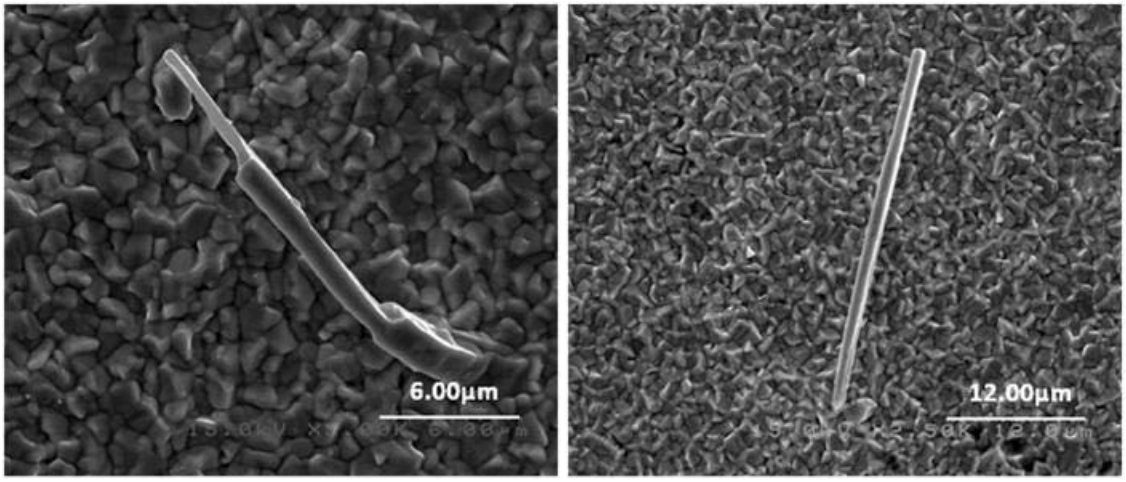

Figure 37. SEM image of whiskers on SnPb films after 12,000 hours of aging

5.4.4 Inspection of Tin with 2.1% Copper (SnCu) Films

Initial post plating inspection showed no noteworthy defects. Following 4,000 hours of aging, there were many nodules and whiskers of various sizes noted. Inspection data from quantitative inspections can be found in Tables 9 & 10. Typical grain structure for the SnCu films after 12,000 hours of aging are shown in Figures 38-39.

Film	Coupon Number	Inspection Area (cm^2)	Whisker Count at 8,000 hours					Longest Whisker
			10-20µm	21-30µm	31-40µm	41-50µm	>50µm	
SnCu	82	1	23	5	0	0	0	< 20µm
	83	1	29	3	0	0	1	259
	84	1	56	4	1	1	2	1740
	Average Whiskers/cm^2		36.0	4.0	0.0	0.3	1.0	
	Total Average Number of Whiskers/cm^2 = 42							

Table 9. Average number of whiskers/cm^2 on SnCu films at 8,000 hours

Film	Coupon Number	Inspection Area (cm^2)	Whisker Count at 12,000 hours					Longest Whisker
			10-20µm	21-30µm	31-40µm	41-50µm	>50µm	
SnCu	83	1	37	4	1	0	1	259
	Total Average Number of Whiskers/cm^2 = 43							

Table 10. Average number of whiskers/cm^2 on SnCu films at 12,000 hours

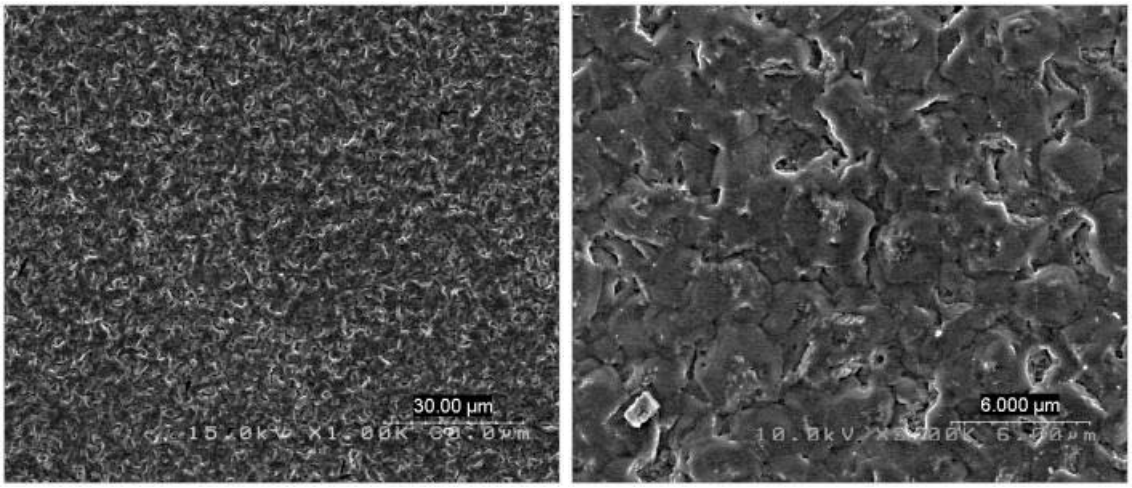

Figure 38. SEM image of SnCu typical grain structure after 12,000 hours of aging

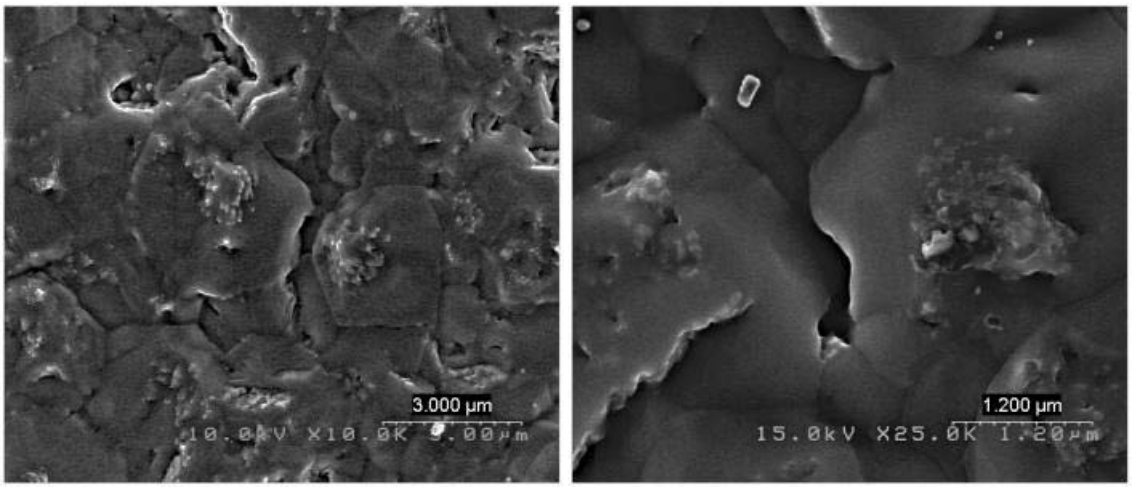

Figure 39. SEM image of SnCu typical grain structure after 12,000 hours of aging

Since the whisker count on the SnCu coupons was higher than the pure Sn coupons, the formal whisker count stopped at 8,000 hours and coupons were pulled for FIB and EBSD analysis. The last remaining coupon was returned to the environmental chamber for a total of 12,000 hours of aging. Although the whisker count on this coupon did increase, the growth rate did not accelerate between 8,000 and 12,000 hours as it did on other coupons with high whisker counts such as SnNi. It was also noted that at 12,000 hours of aging, particles that were noted in the SnCu film at 8,000 hours had begun to precipitate out of the film. As discussed earlier, this appears to be one of the characteristics displayed by films with reduced whisker counts. (Figures 40-41).

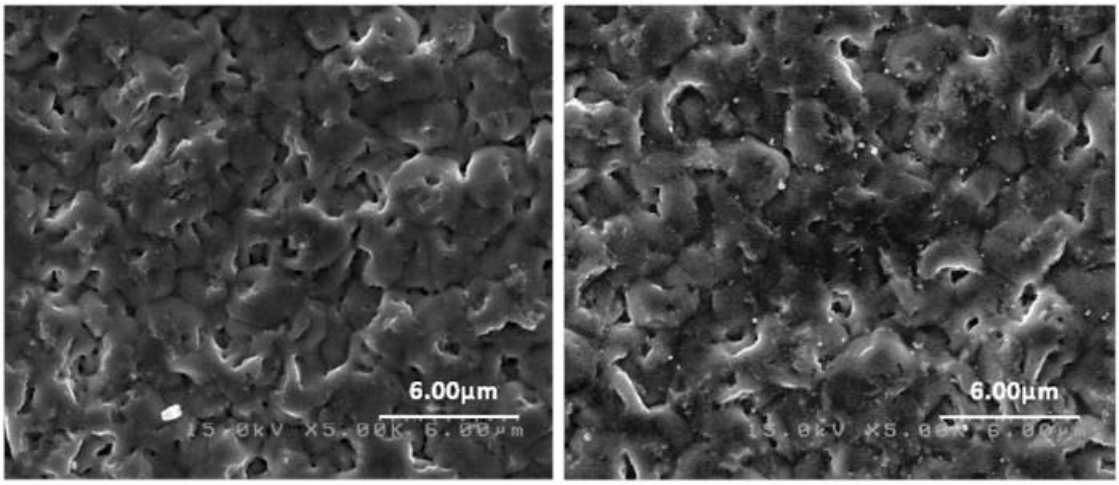

Figure 40. SEM image of particulates in SnCu matrix after aging 8,000 hours (left) and on SnCu surface after 12,000 hours aging (right)

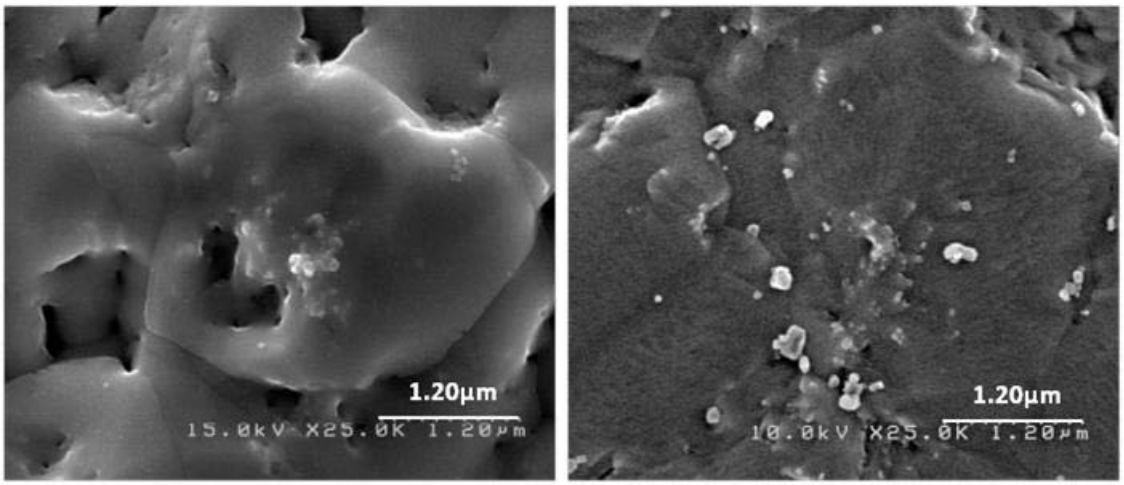

Figure 41. SEM image of particulates in SnCu matrix after aging 8,000 hours (left) and on SnCu surface after 12,000 hours aging (right)

Nearly all of the whiskers that formed on SnCu films formed during the first 8,000 hours of aging. There was a wide variety of whisker characteristics on the SnCu samples, including whiskers with deep striations, with rings, odd shaped whiskers, kinked, and whiskers growing from hillocks (Figures 42-44).

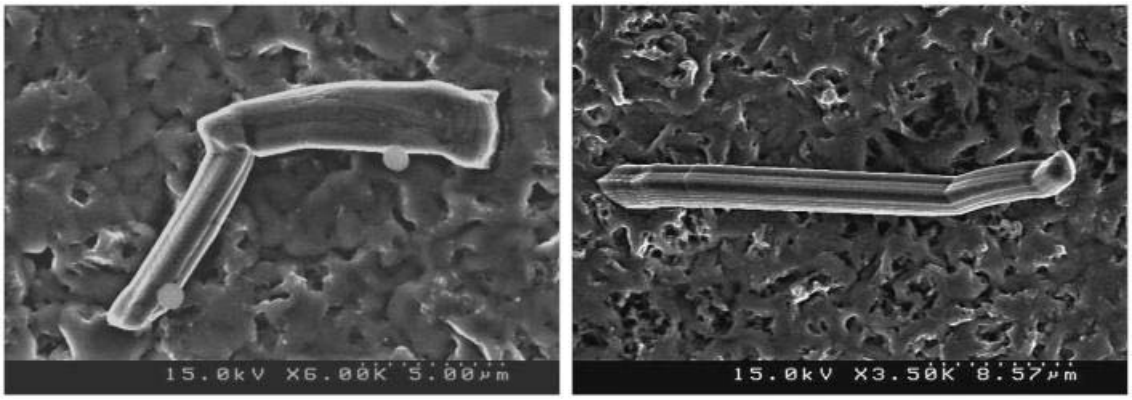

Figure 42. SEM image of whiskers on SnCu film after 8,000 hours of aging

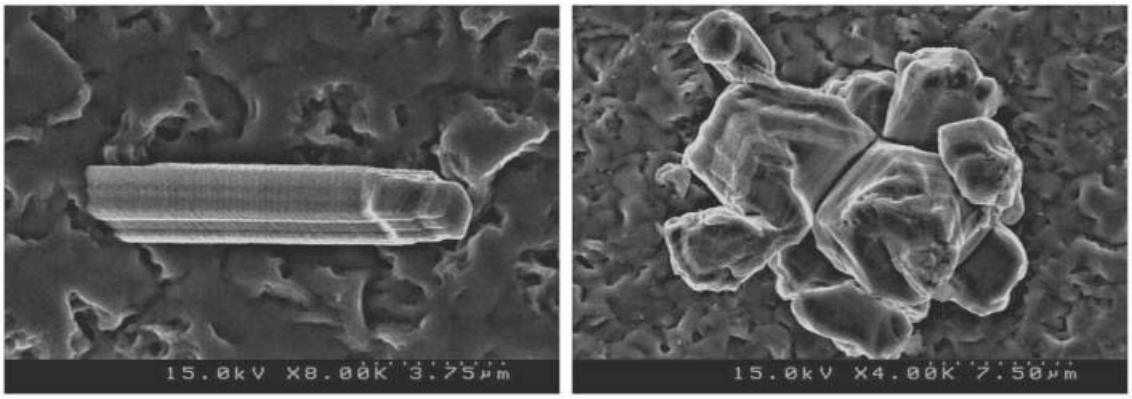

Figure 43. SEM image of whisker (left) and irregular eruption (right) on SnCu film after 8,000 hours of aging

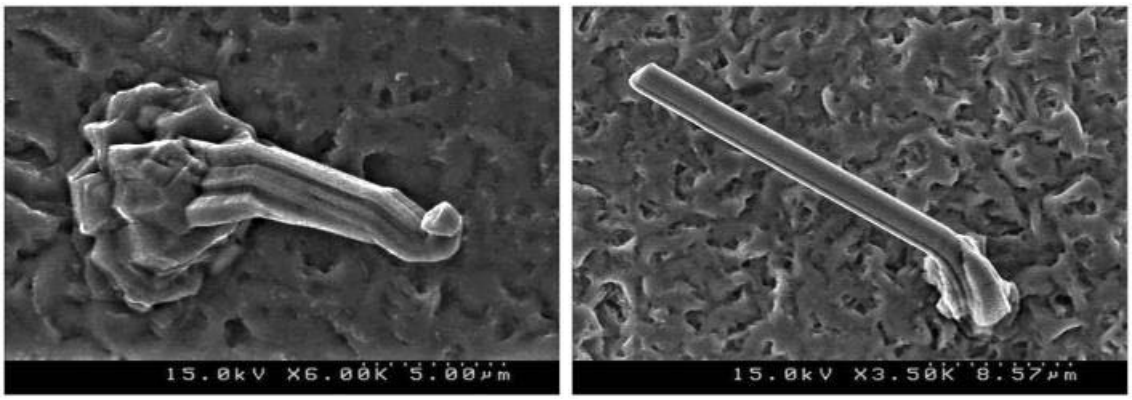

Figure 44. SEM image of whiskers on SnCu film after 8,000 hours of aging

5.4.5 Inspection of Tin with 3.0% Nickel (SnNi) Films

Preliminary inspection of SnNi coupons made after plating found the film to be free of plating nodules, dendrites, and other plating artifacts. At 4,000 hours of aging, nodules plus some short to medium length whiskers were noted.

Inspection data from quantitative inspections can be found in Tables 11 & 12. Typical grain structure for the SnNi films after 12,000 hours of aging are shown in Figures 45-47. During SEM inspection the presence of particles in the film was evident (Figure 47) but they never precipitated out of the matrix as they did on the lower whisker count samples.

Given that the samples had a significantly higher whisker count than the pure Sn samples; coupons were pulled for EBSD and FIB analysis after 8,000 hours. Whisker density varied widely across the sample, with some areas having nodules but few whiskers and other areas with whisker counts so dense it was difficult to make an accurate count (Figures 48-50).

Film	Coupon Number	Inspection Area (cm^2)	Whisker Count at 8,000 hours					Longest Whisker
			10-20μm	21-30μm	31-40μm	41-50μm	>50μm	
SnNi	129	1	41	21	7	2	6	284
	132	1	71	33	12	6	7	217
	131	1	72	33	4	2	10	136
	Average Whiskers/cm^2		61.3	29.0	0.0	3.3	7.7	
	Total Average Number of Whiskers/cm^2 = 109							

Table 11. Average number of whiskers/cm^2 on SnNi films at 8,000 hours

Film	Coupon Number	Inspection Area (cm^2)	Whisker Count at 12,000 hours					Longest Whisker
			10-20μm	21-30μm	31-40μm	41-50μm	>50μm	
SnNi	132	1	287	158	99	64	137	234
	Total Average Number of Whiskers/cm^2 = 745							

Table 12. Average number of whiskers/cm^2 on SnNi films at 12,000 hours

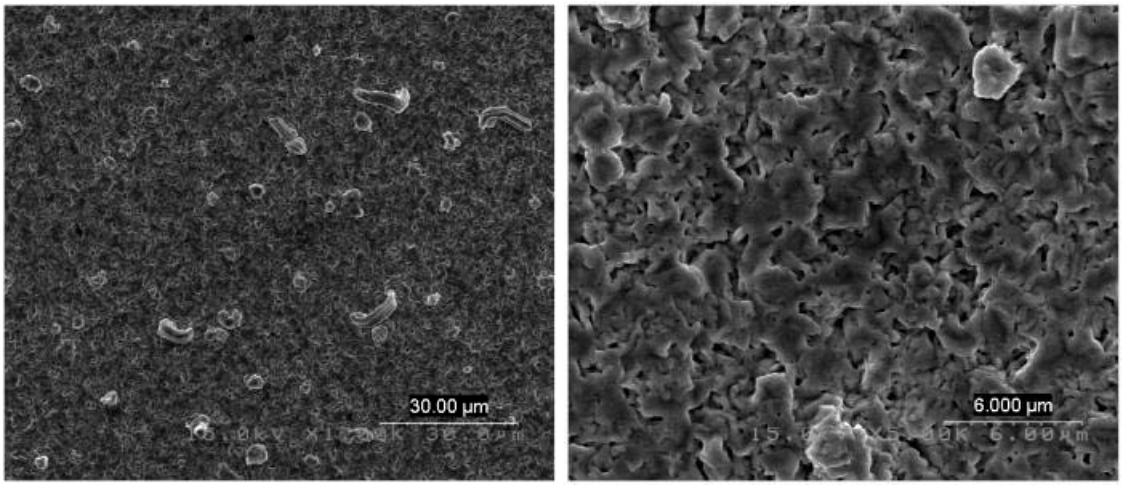

Figure 45. SEM image of SnNi typical grain structure after 12,000 hours of aging

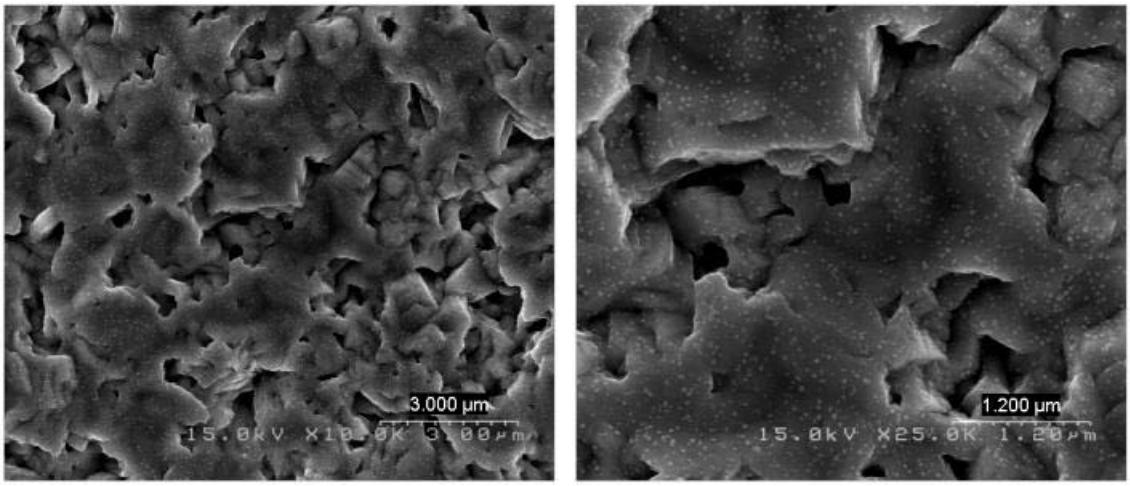

Figure 46. SEM image of SnNi typical grain structure after 12,000 hours of aging

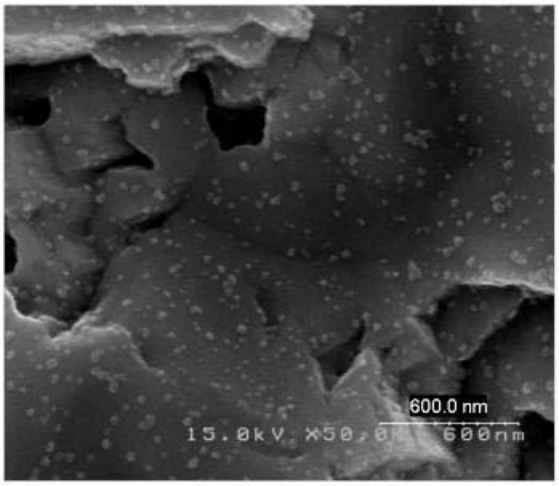

Figure 47. SEM image of SnNi typical grain structure after 12,000 hours of aging

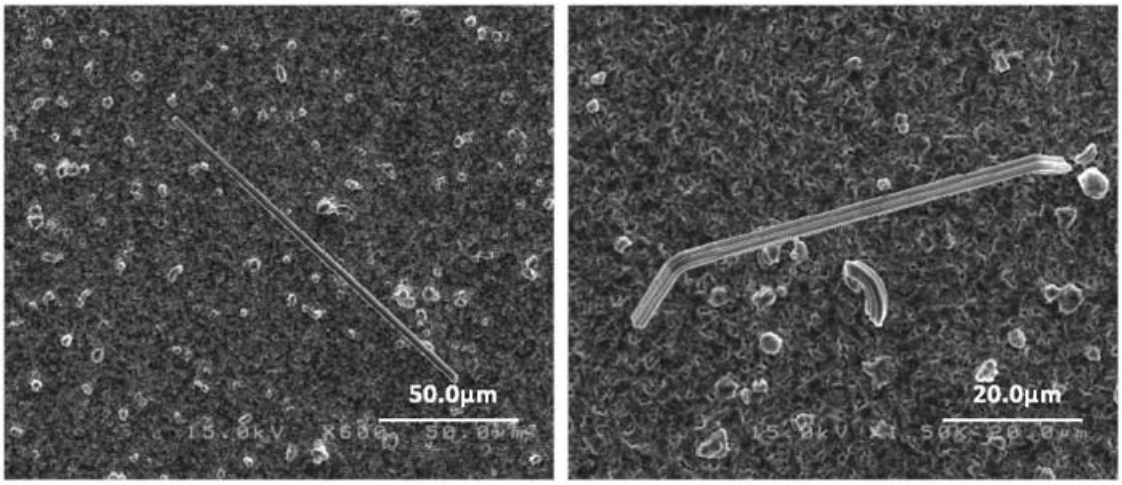

Figure 48. SEM image of whiskers on SnCu film after 8,000 hours of aging

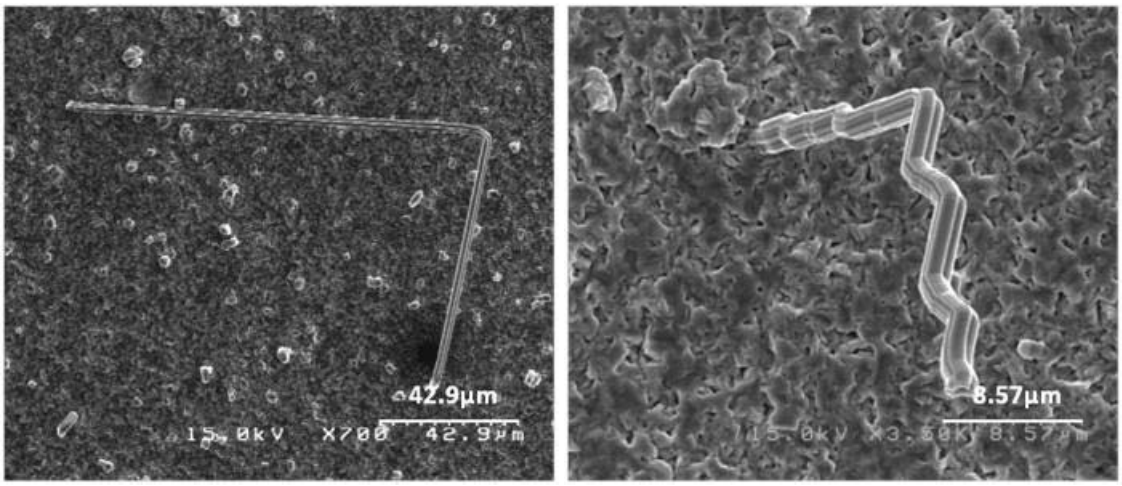

Figure 49. SEM image of whiskers on SnCu film after 8,000 hours of aging

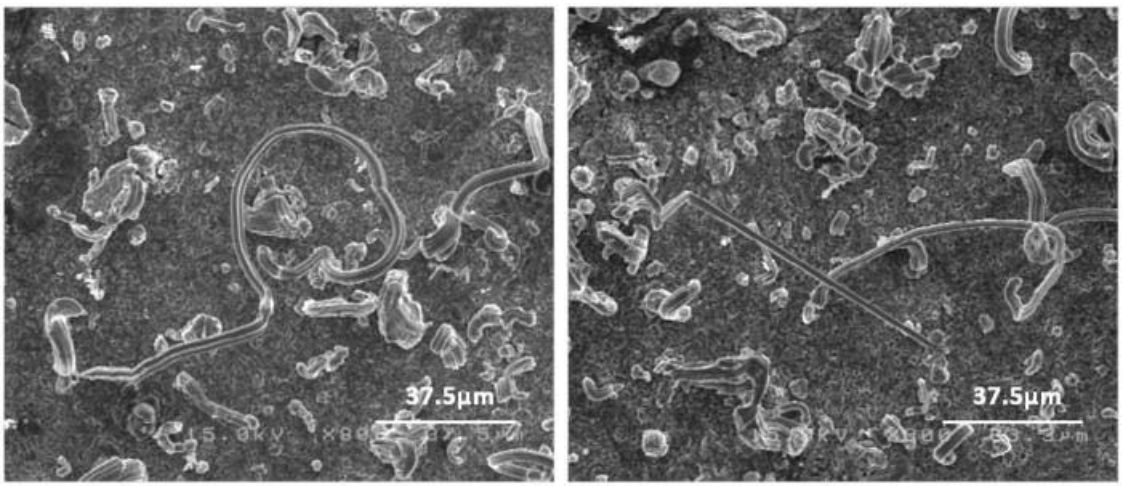

Figure 50. SEM image of whiskers on SnCu film after 12,000 hours of aging

5.4.6 Inspection of Tin with 0.95% Cobalt (SnCo) Films

Inspection of the SnCo films after plating exhibited no defects but after 4,000 hours of aging all coupons had numerous nodules and scattered whisker growth.

Following approximately 8,000 hours of aging, the SnCo coupons had the highest whisker count of all the coupons inspected with an average whisker count of 122 whiskers/cm^2. Inspection data from quantitative inspections can be found in Tables 13 & 14. Typical grain structure for the SnCo films after 12,000 hours of aging are shown in Figures 51-53. The SnCo films, similar to the SnNi films, had particles forming in the matrix that were visible during SEM inspection, but did not precipitate out of the film (Figures 51-52).

Whiskers that formed during the aging of the SnCo film, had no unusual traits (Figures 54-55) and ranged in size from slightly over 10 microns to up to 212 microns in length

Film	Coupon Number	Inspection Area (cm^2)	Whisker Count at 8,000 hours					Longest Whisker
			10-20μm	21-30μm	31-40μm	41-50μm	>50μm	
SnCo	169	1	65	15	4	1	1	56.8
	170	1	87	24	5	0	2	61.8
	171	1	106	37	11	3	5	73.2
	Average Whiskers/cm^2		86.0	25.3	0.0	1.3	2.7	
	Total Average Number of Whiskers/cm^2 = 122							

Table 13. Average number of whiskers/cm^2 on SnCo films at 8,000 hours

Film	Coupon Number	Inspection Area (cm^2)	Whisker Count at 12,000 hours					Longest Whisker
			10-20μm	21-30μm	31-40μm	41-50μm	>50μm	
SnCo	169	1	129	47	23	3	1	212
	Total Average Number of Whiskers/cm^2 = 203							

Table 14. Average number of whiskers/cm^2 on SnCo films at 12,000 hours

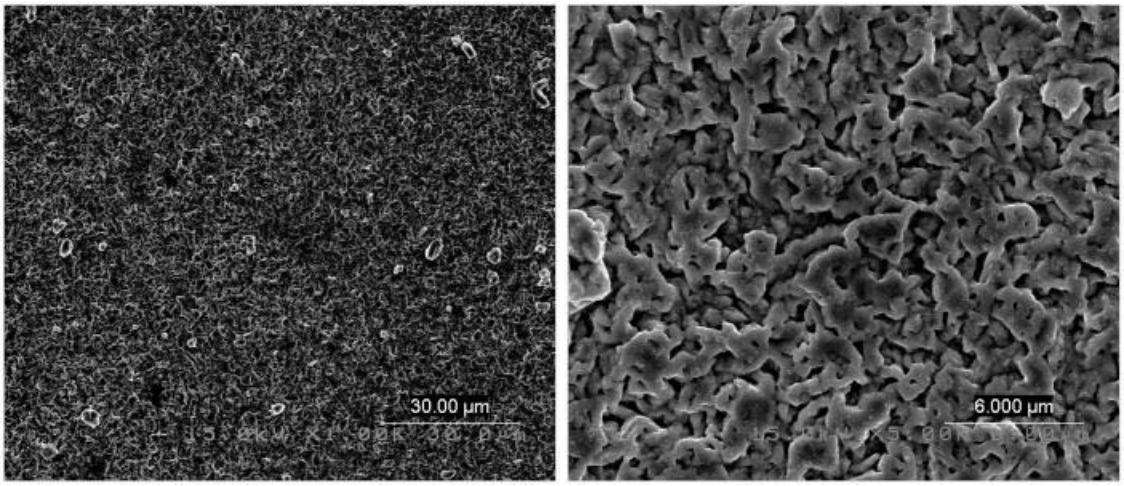

Figure 51. SEM image of SnCo typical grain structure after 12,000 hours of aging

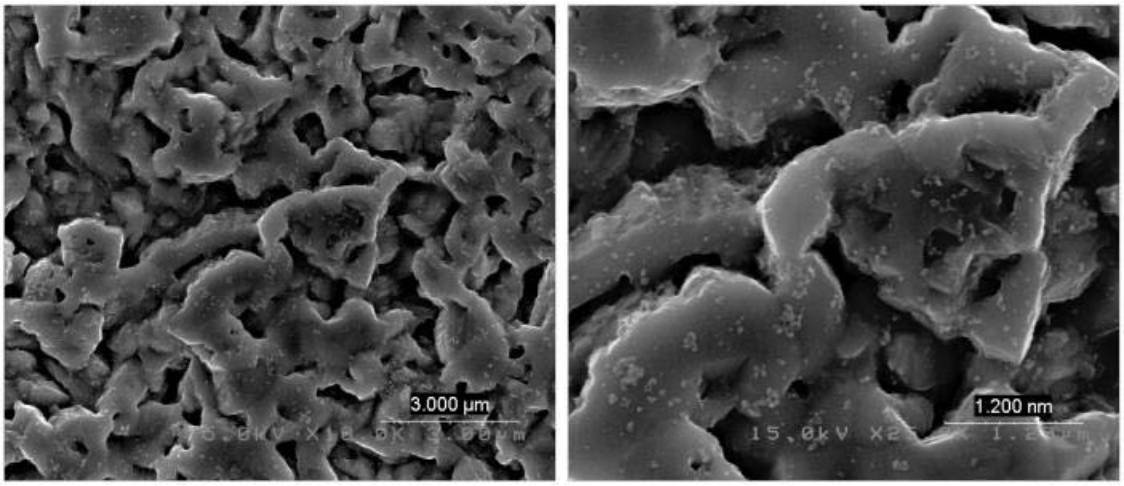

Figure 52. SEM image of SnCo typical grain structure after 12,000 hours of aging

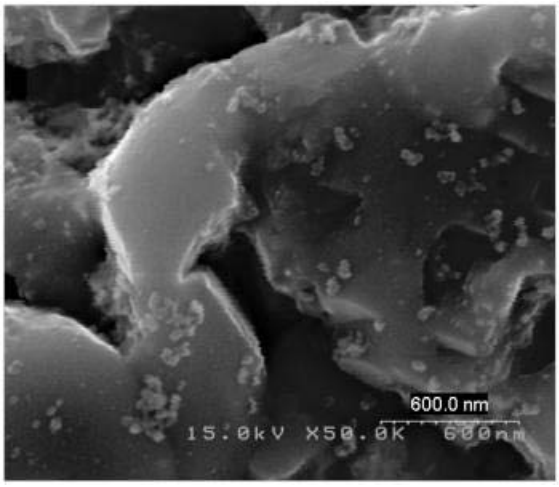

Figure 53. SEM image of SnCo typical grain structure after 12,000 hours of aging

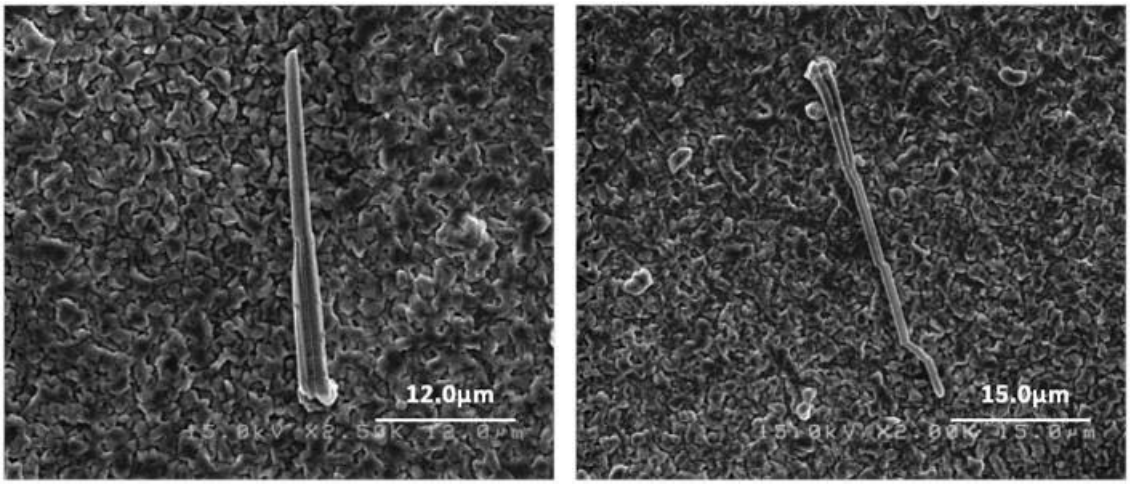

Figure 54. SEM image of whiskers on SnCo film after 8,000 hours of aging

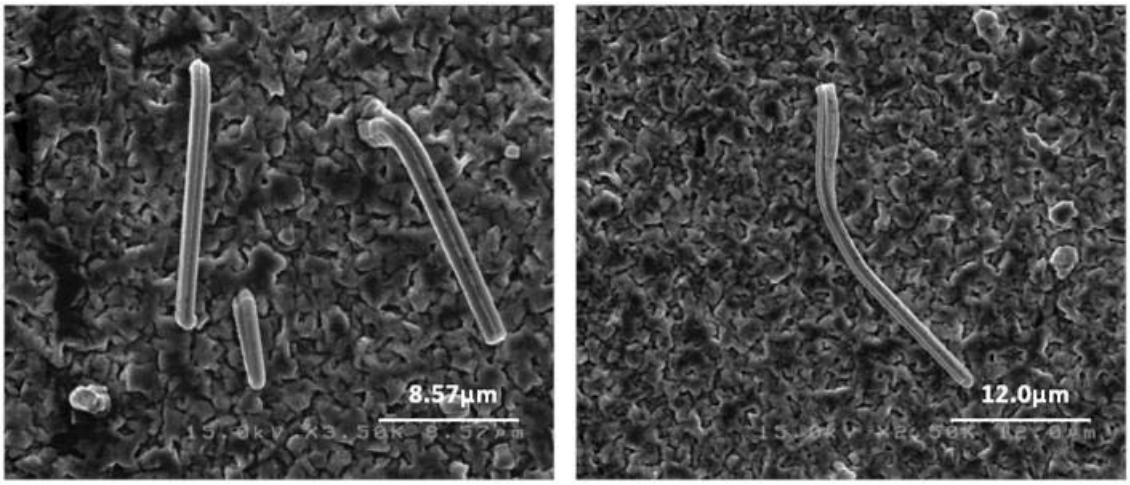

Figure 55. SEM image of whiskers on SnCo film after 8,000 hours of aging

5.4.7 Inspection of Tin with 2.4% Antimony (SnSb) Films

As with most of the other films, the SnSb film had no significant defects immediately after plating. During qualitative inspection at 4,000 hours some nodules and a few short whiskers were noted.

Inspection data from quantitative inspections can be found in Tables 15 & 16. Typical grain structure for the SnCo films after 12,000 hours of aging are shown in Figures 56-57.

Film	Coupon Number	Inspection Area (cm^2)	Whisker Count at 8,000 hours					Longest Whisker
			10-20μm	21-30μm	31-40μm	41-50μm	>50μm	
SnSb	215		11	0	0	0	1	113
	216		4	2	0	0	0	< 20μm
	218		11	1	0	0	0	< 20μm
	Average Whiskers/cm^2		8.7	1.0	0.0	0.0	0.3	
	Total Average Number of Whiskers/cm2 = 10							

Table 15. Average number of whiskers/cm^2 on SnSb films at 8,000 hours

Film	Coupon Number	Inspection Area (cm^2)	Whisker Count at 12,000 hours					Longest Whisker
			10-20μm	21-30μm	31-40μm	41-50μm	>50μm	
SnSb			7	4	0	0	0	25.7
	216		8	2	0	0	0	23.6
	218		21	1	1	0	1	55.2
	Average Whiskers/cm^2		12.0	2.3	0.0	0.0	0.3	
	Total Average Number of Whiskers/cm2 = 15							

Table 16. Average number of whiskers/cm^2 on SnSb films at 12,000 hours

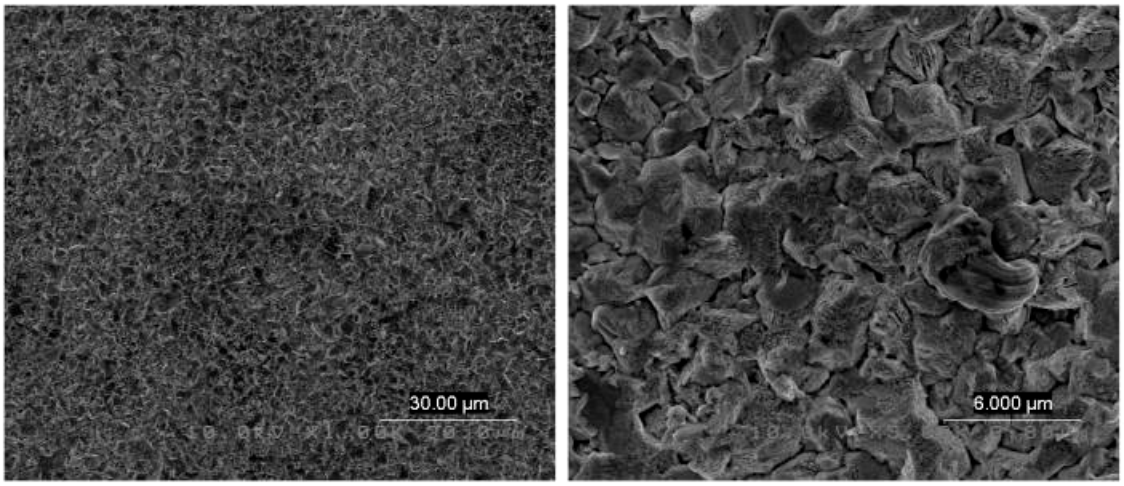

Figure 56. SEM image of SnSb typical grain structure after 12,000 hours of aging

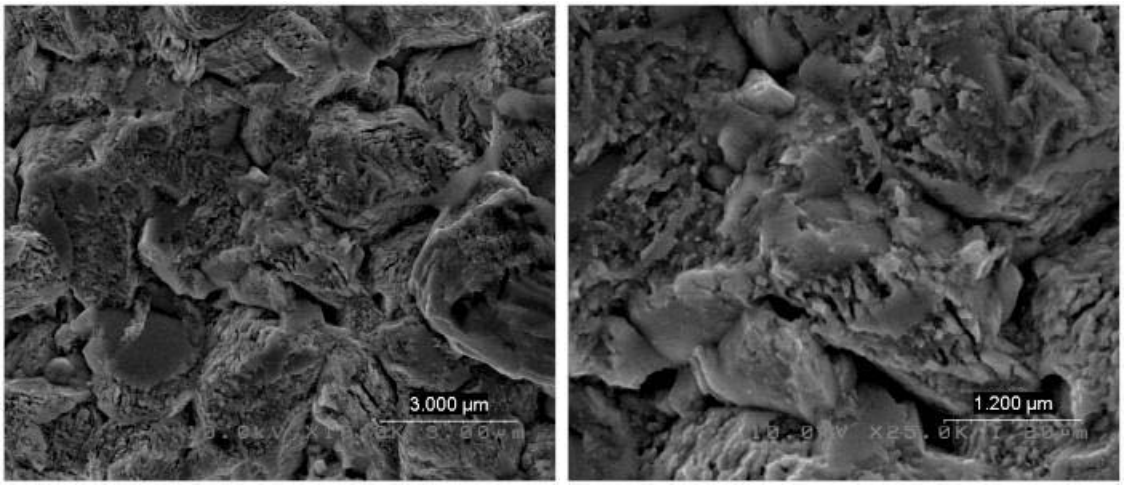

Figure 57. SEM image of SnSb grain structure after 12,000 hours of aging

SEM inspection of the SnSb films showed an unusual microstructure on several areas of the samples. At 8,000 hours of aging the grain structure appeared very porous with parallel open lines in the grains (Figure 58). At 12,000 hours, these voids began to fill, likely due to oxide formation (Figure 59); visually the samples became darker and showed signs of corrosion.

There were also several small areas where the SnSb film appeared to have delaminated (Figure 60, right), visible only under microscopic or SEM inspection. EDX inspection of the area where the metal delaminated showed no significant signs of contamination. Carbon was present on the surface but at relatively low percent. We were unable to determine if the delamination was due to underlying contamination that prevented good adhesion or possibly due to a highly stressed film.

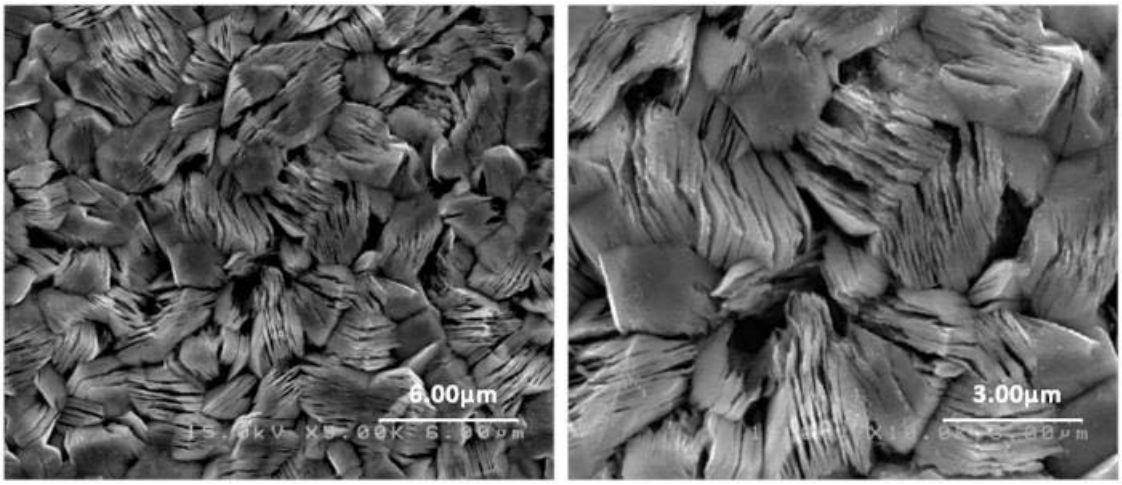

Figure 58. SEM image of SnSb grain structure after aging 8,000 hours

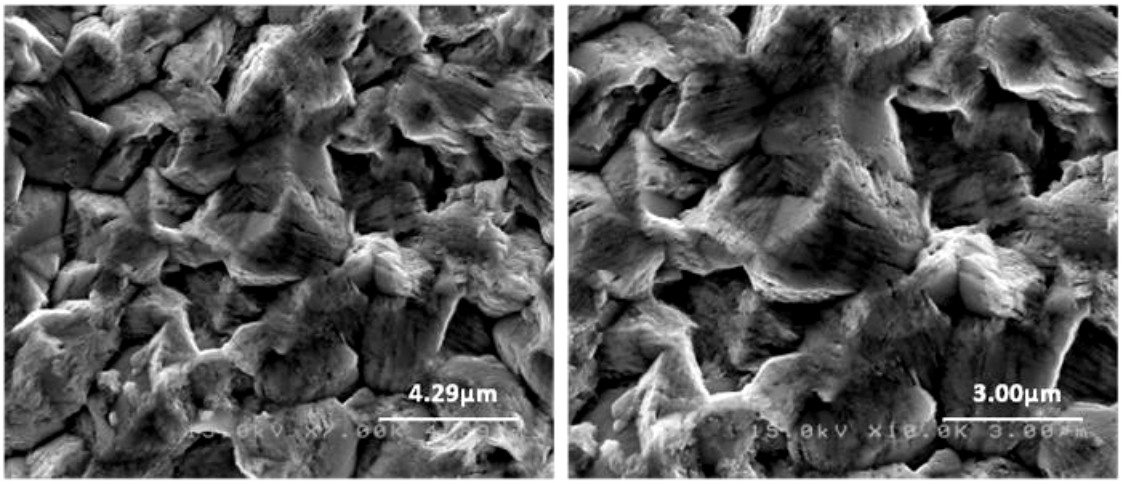

Figure 59. SEM image of SnSb grain structure after aging 12,000 hours

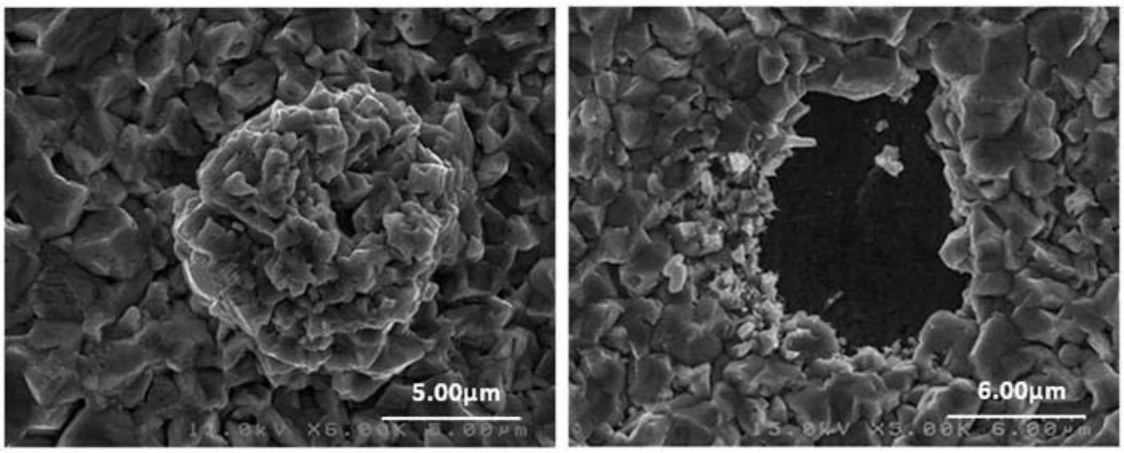

Figure 60. SEM image of SnSb hillock (left) and delamination in SnSb film (right)

Whisker formation was also unusual. Tin whiskers are typically described as "single-crystal" filamentary growths; however, several of the whiskers that formed on the SnSb films appeared to be comprised of multiple grains (Figures 61-62). Cross-sectional images of the whiskers would be required to be certain whether they contain multiple grains. It is feasible that there was a layer of smaller grains on the surface of the plated film that were "pushed up" by a whisker formed from an underlying large grain.

Figure 62 (left) shows a whisker that appears to be two distinct large grains growing in parallel. However, not all whiskers exhibited this multigrain structure, the majority of the SnSb whiskers having a more typical appearance (Figures 63).

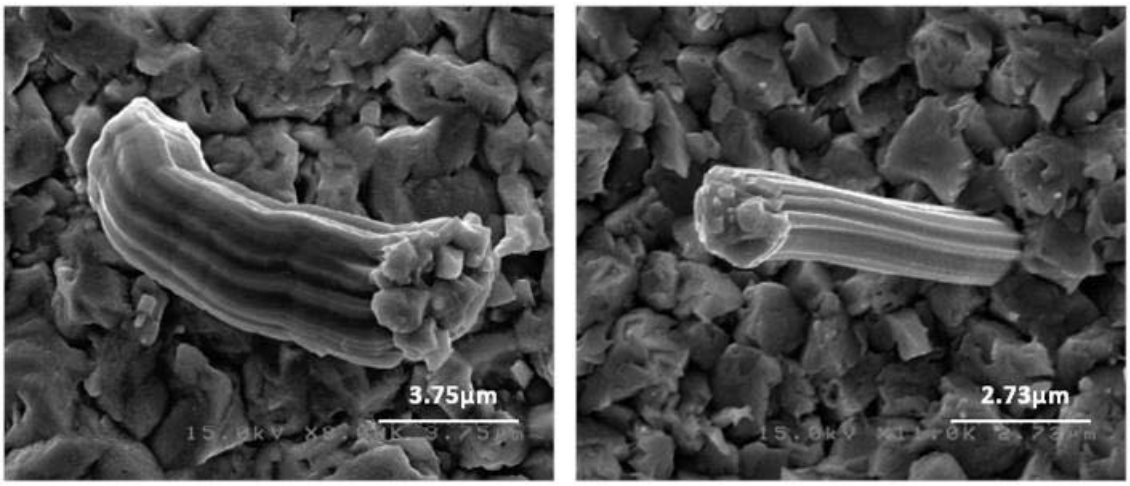

Figure 61. SEM image of whiskers in SnSb film with a multigrain structure after 8,000 hours of aging

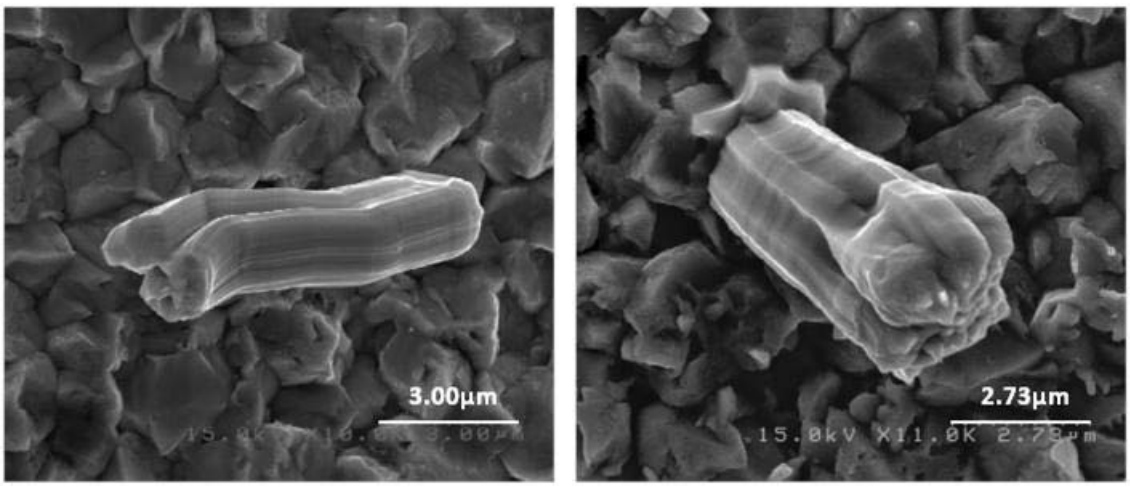

Figure 62. SEM image of whiskers in SnSb film after 12,000 hours of aging

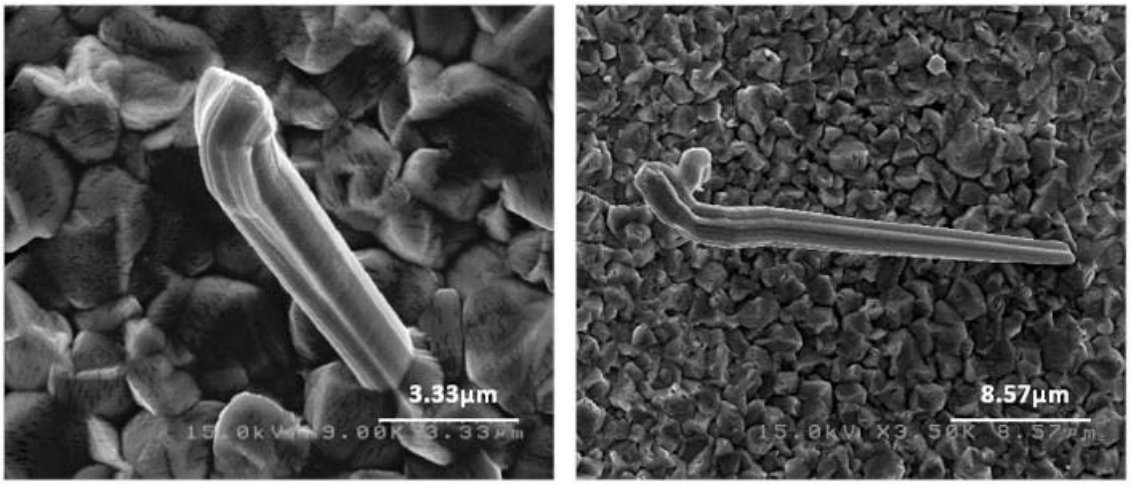

Figure 63. SEM image of whiskers on SnSb film after 12,000 hours of aging

5.4.8 Inspection of Tin with 1.1% Germanium (SnGe) Films

Post plating inspection of the SnGe films found no significant defects, although the film did exhibit a unique "Phillips head" grain structure (Figure 64). The qualitative inspection at 4,000 hours showed no whisker growth and few nodules on the SnGe samples.

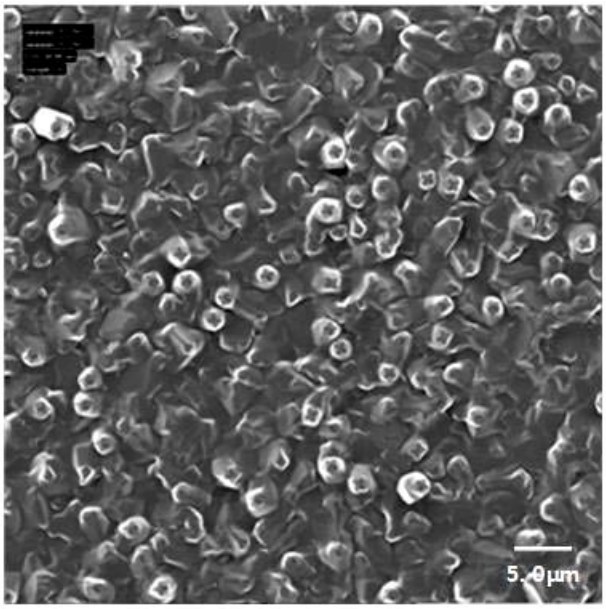

Figure 64. Ion image of SnGe film taken by Evans Analytical Group prior to aging

At the 8,000 and 12,000 hour inspections, there was very little visible change to the morphology after aging (Figures 65-66), when compared to the ion images taken by Evans Analytical after plating (Figure 64). Inspection data from 8,000 and 12,000 hour quantitative inspections can be found in Tables 17 & 18.

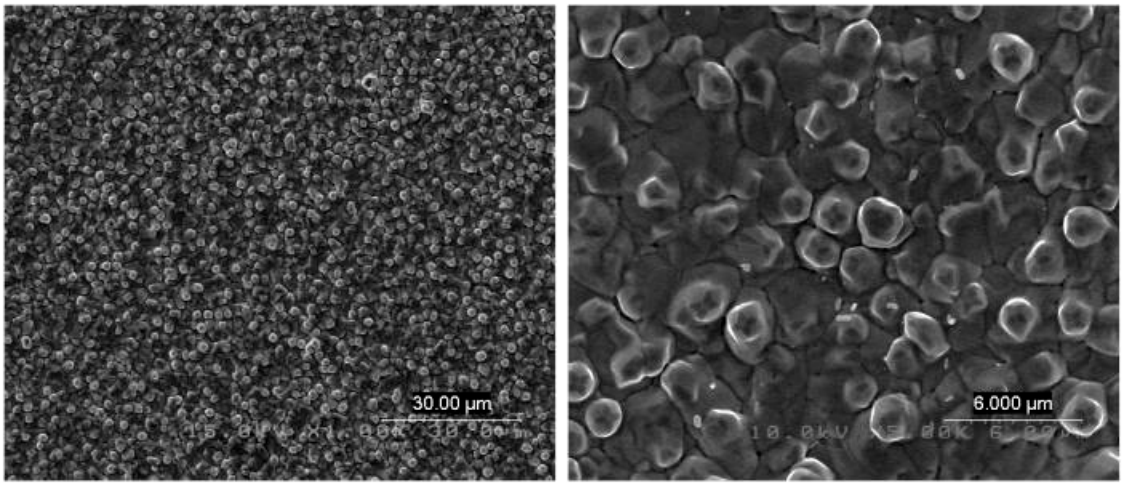

Figure 65. SEM image of SnGe typical grain structure after 12,000 hours of aging

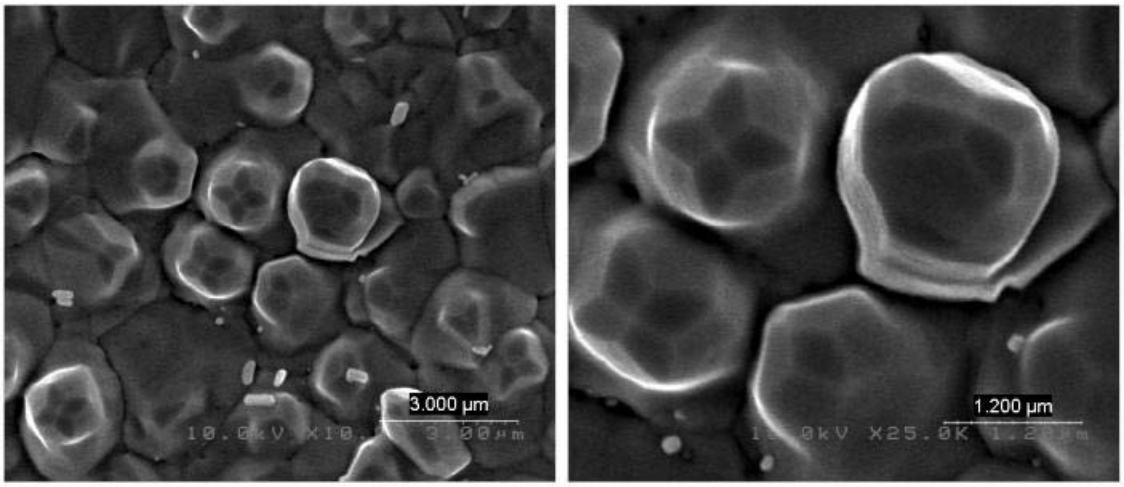

Figure 66. SEM image of SnGe typical grain structure after 12,000 hours of aging

Film	Coupon Number	Inspection Area (cm^2)	Whisker Count at 8,000 hours					Longest Whisker
			10-20μm	21-30μm	31-40μm	41-50μm	>50μm	
SnGe	233		9	0	1	0	1	56.4
	234		19	1	0	0	0	< 20μm
	235		27	0	0	0	0	< 20μm
	Average Whiskers/cm^2		18.3	0.3	0.0	0.0	0.3	
	Total Average Number of Whiskers/cm^2 = 19							

Table 17. Average number of whiskers/cm^2 on SnGe films at 8,000 hours

Film	Coupon Number	Inspection Area (cm^2)	Whisker Count at 12,000 hours					Longest Whisker
			10-20μm	21-30μm	31-40μm	41-50μm	>50μm	
SnGe	233		13	0	0*	0	1	56.4
	234		23	2	0	0	0	25.3
	235		28	0	0	0	0	16.5
	Average Whiskers/cm^2		21.3	0.7	0.0	0.0	0.3	
	Total Average Number of Whiskers/cm2 = 23							

Table 18. Average number of whiskers/cm^2 on SnGe films at 12,000 hours

The SEM inspection performed at a tilt (Figure 67) demonstrates the conical grain structure of this plated film. This highly unusual grain structure may have contributed to stress relief during the aging process.

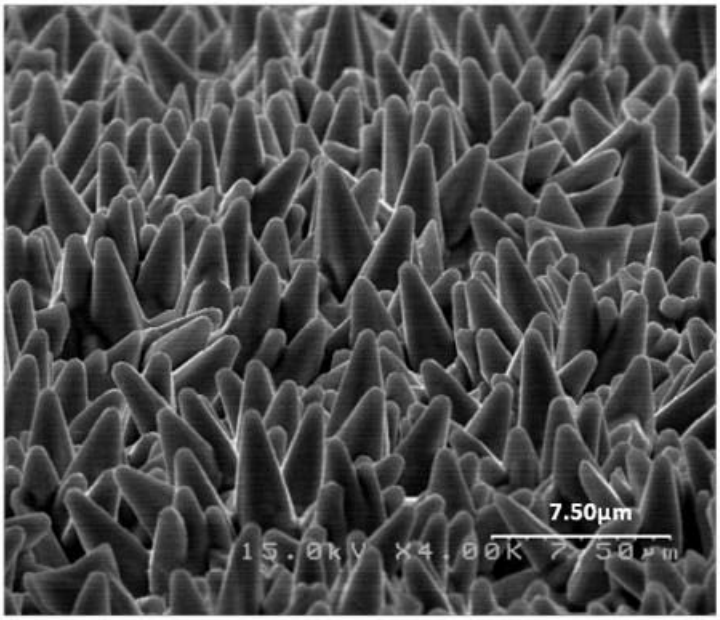

Figure 67. SEM image of SnGe grain structure at 12,000 hours of aging

As seen on many of the low whisker count samples, there was evidence of particles precipitating out of the SnGe during aging (Figures 66, 69). Most of the whiskers that formed were relatively short and had standard features (Figures 68-69).

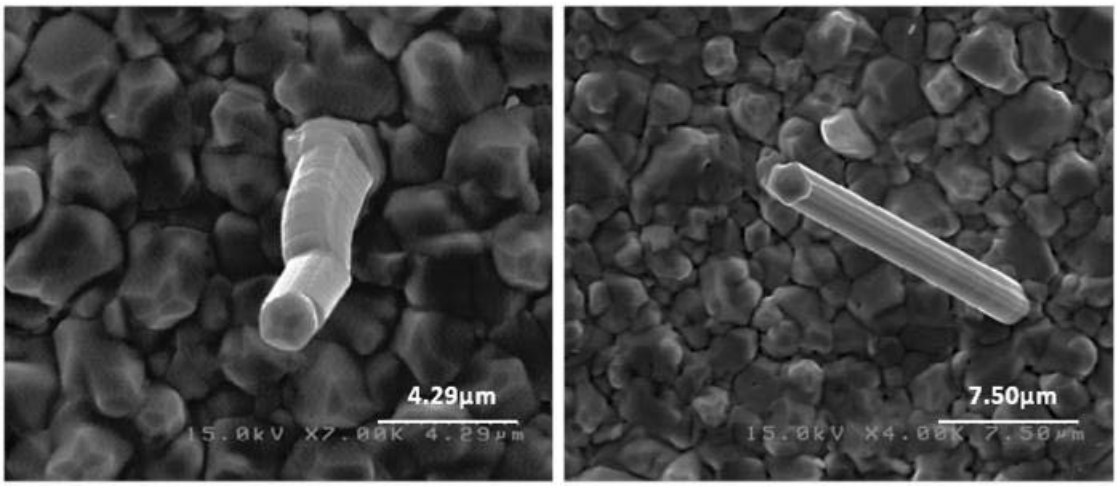

Figure 68. SEM image of whiskers on SnGe film after 8,000 hours of aging

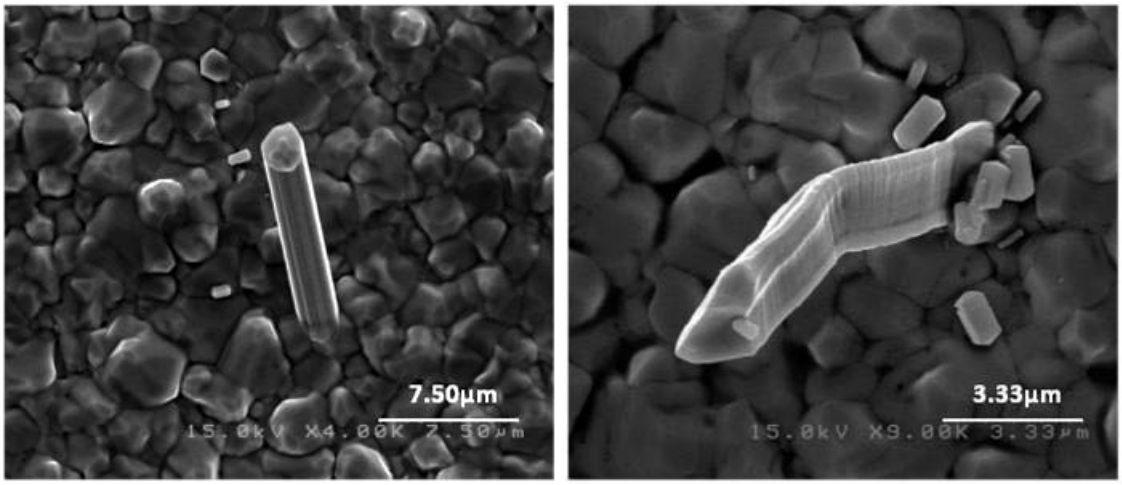

Figure 69. SEM images of whiskers on SnGe film after 12,000 hours of aging

5.4.9 Inspection of Tin with 1.3% Gold (SnAu) Films

Initial inspection of the SnAu film after plating showed it to be free of defects. After 4,000 hours of aging the coupons only had a few scattered nodules and a couple of short whiskers <20 microns in length.

Inspection data from quantitative inspections can be found in Tables 19 & 20. Typical grain structure for the SnAu films after 12,000 hours of aging are shown in Figures 70-71.

It was noted during SEM inspection after both the 8,000 and 12,000 hours aging exposure that there were a number of sub-micron sized particles on the surface of the plated SnAu film (Figures 70-73). This presence of precipitates seems to correlate strongly with suppression of whisker formation in all tin-alloy samples studied.

Film	Coupon Number	Inspection Area (cm^2)	Whisker Count at 8,000 hours					Longest Whisker
			10-20μm	21-30μm	31-40μm	41-50μm	>50μm	
SnAu	268		2	0	0	0	0	< 20μm
	269		4	0	0	0	0	< 20μm
	270		2	0	0	0	0	< 20μm
	Average Whiskers/cm^2		2.7	0.0	0.0	0.0	0.0	
	Total Average Number of Whiskers/cm^2 = 2.7							

Table 19. Average number of whiskers/cm^2 on SnAu films at 8,000 hours

Film	Coupon Number	Inspection Area (cm^2)	Whisker Count at 12,000 hours					Longest Whisker
			10-20μm	21-30μm	31-40μm	41-50μm	>50μm	
SnAu	268		3	0	0	0	0	19.9
	269		14	0	0	0	0	19.8
	270		3	0	0	0	0	15.4
	Average Whiskers/cm^2		6.7	0.0	0.0	0.0	0.0	
	Total Average Number of Whiskers/cm2 = 6.7							

Table 20. Average number of whiskers/cm^2 on SnAu films at 12,000 hours

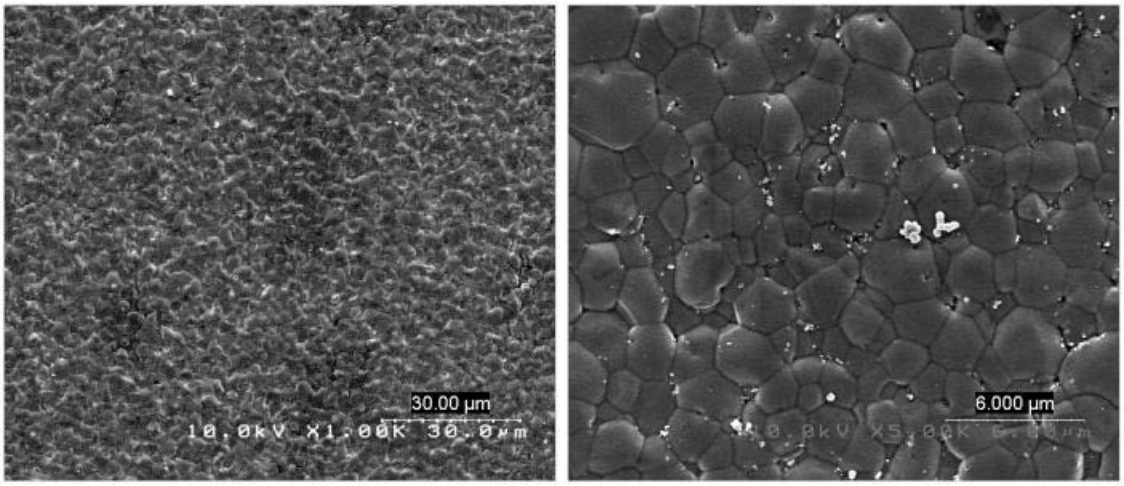

Figure 70. SEM image of SnAu typical grain structure after 12,000 hours of aging

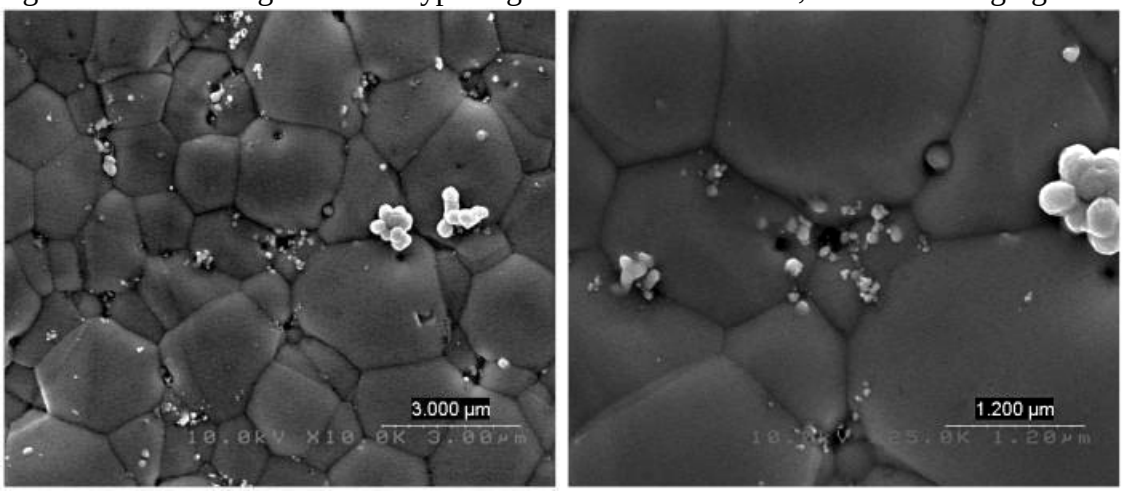

Figure 71. SEM image of SnAu typical grain structure after 12,000 hours of aging

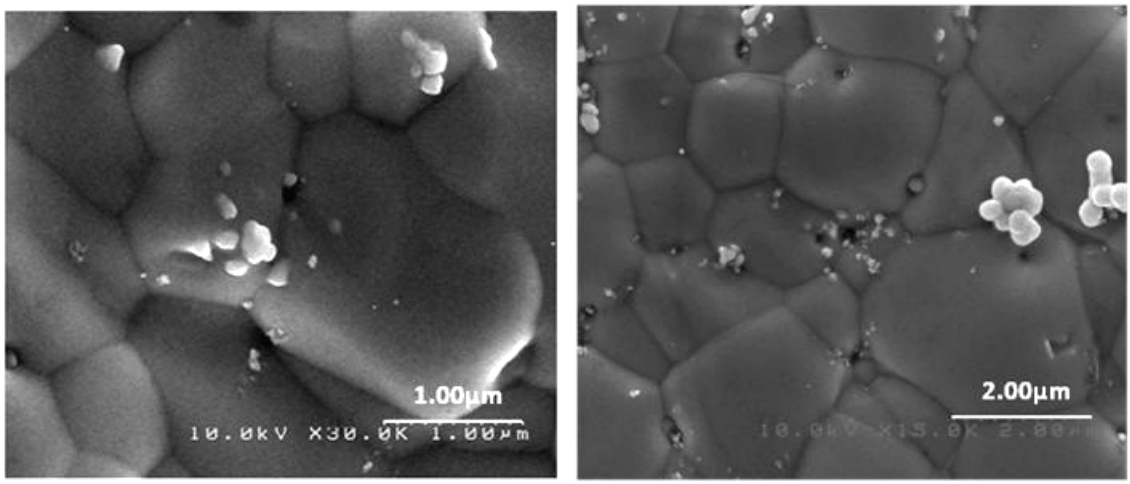

Figure 72: SEM image showing formation of intermetallics on the surface of the SnAu film at 8,000 hours aging and at 12,000 hours aging

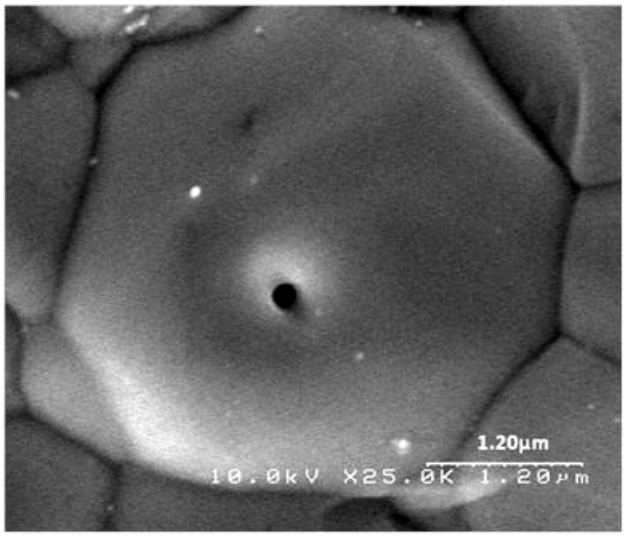

Figure 73: SEM image showing formation of intermetallics on the surface of the SnAu film after 12,000 hours aging

In areas where the precipitates conglomerated, we were able to do Energy Dispersive Spectrometry (EDX). It was determined that the particles were comprised primarily of gold, although it was not possible to obtain an exact composition with this method of analysis. Copper did show up in the EDX scan, although it was not prominent in the particles, and was likely due to intermetallic formation between the Sn and the Cu substrate (Figures 74-75).

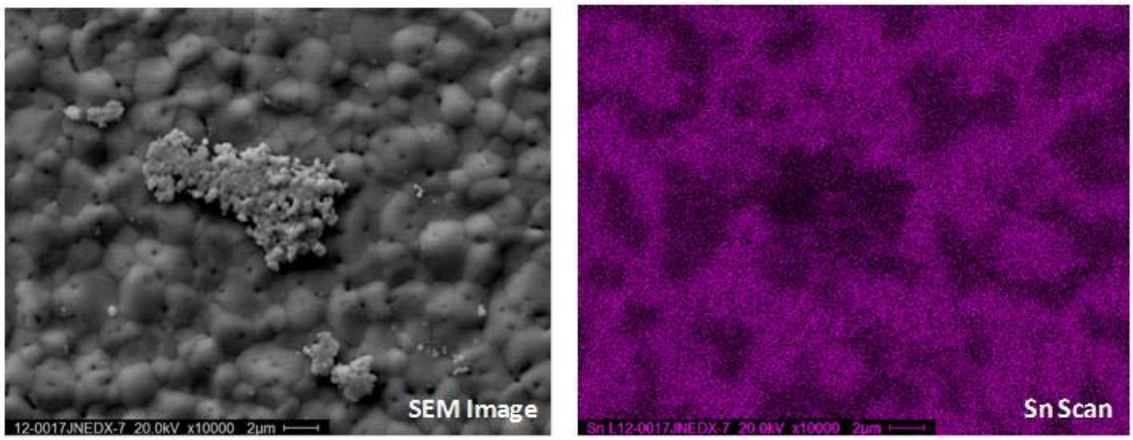

Figure 74. Electron image of particles on SnAu film (left) and EDX Sn scan (right) after 8,000 hours of aging

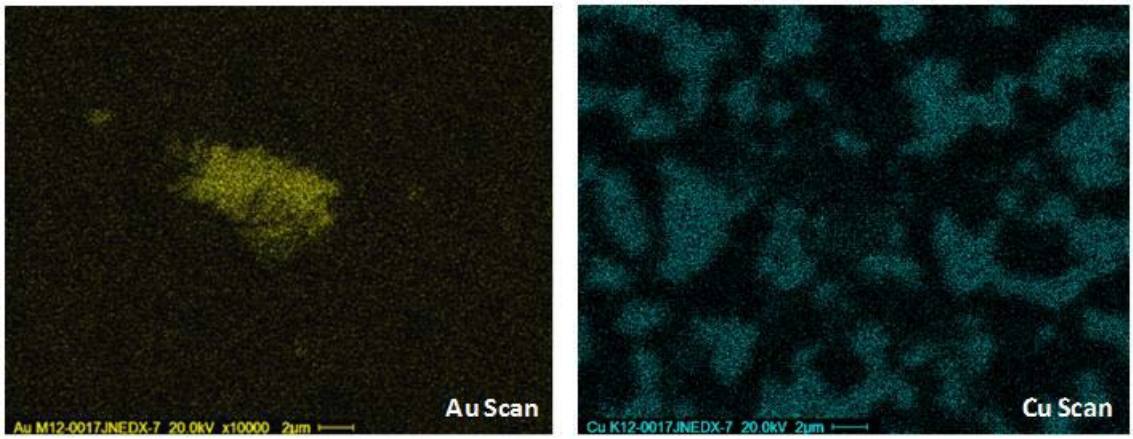

Figure 75. EDX Au scan (left) and EDX Cu Scan (right) after 8,000 hours of aging

The whiskers that did form on the surface of the SnAu film were typical with no unusual formations.

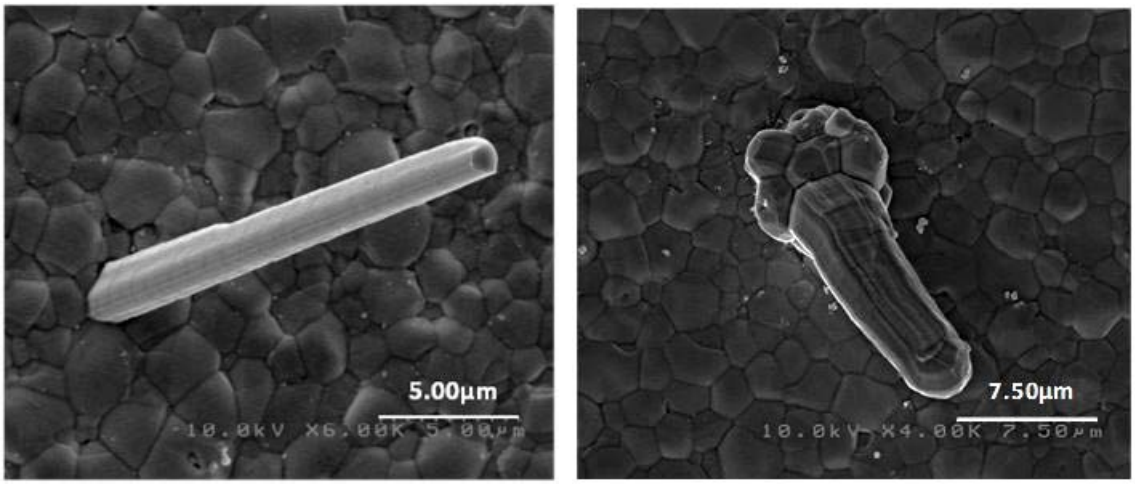

Figure 76. SEM image of whiskers on SnAu film after 12,000 hours of aging

5.4.10 Influence of Inspection on Whisker Growth and Development

During the course of this study, we mapped a few whiskers' precise locations, photographed them, and then inspected the exact same whiskers after an additional 4,000 hours of aging to determine if removing the samples from the environmental chamber and inspecting them influences the whisker development or growth.

A total of ten whiskers were photographed for this purpose and their locations documented using the micromanipulator readings from the stage of the Hitachi S-4000 field emission scanning electron microscope. No tilt was used when documenting these whiskers, since a slight variation in tilt could alter the length of the whisker. All inspections were performed on the same SEM; differences in the size and format of the micrographs are due to an upgrade of the image capture software during the time the samples were in the environmental chamber.

Nine of the whiskers documented were on a pure Sn sample and one was on a Sn/Au sample. Only one whisker was documented from the Sn/Au sample because of the extremely low whisker count on this coupon. The whiskers were documented at 8,000 and 12,000 hours of aging. None of the nine whiskers on the pure tin sample showed any visible change in size or shape during this time. Representative images are shown in Figures 77-80. The one whisker on the Sn/Au sample did show a slight increase in length; note that there was a decrease in magnification on the second image in order to document the entire whisker (Figures 81a and b).

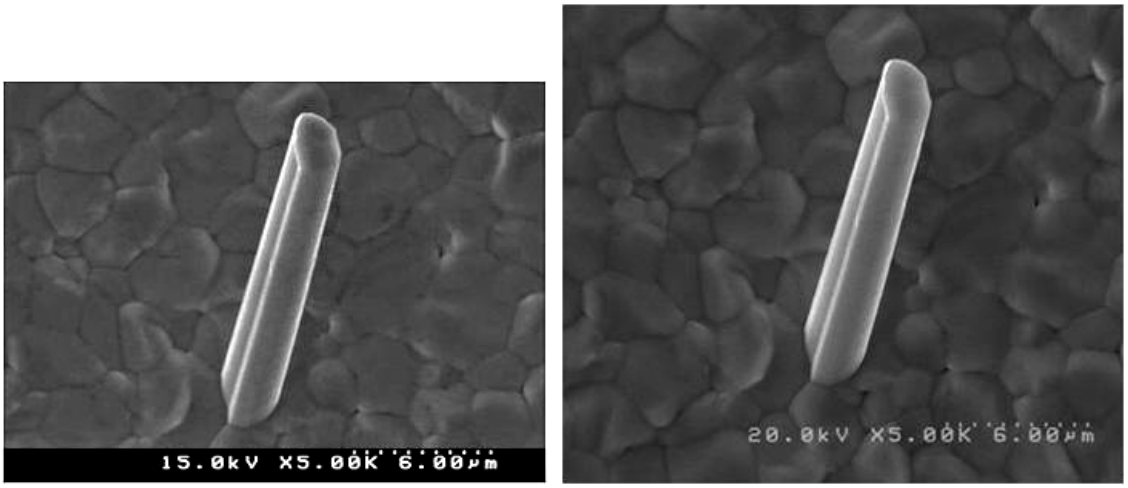

Figure 77. SEM images of a whisker on the Sn sample at 8,000 hours (left) and 12,000 hours (right)

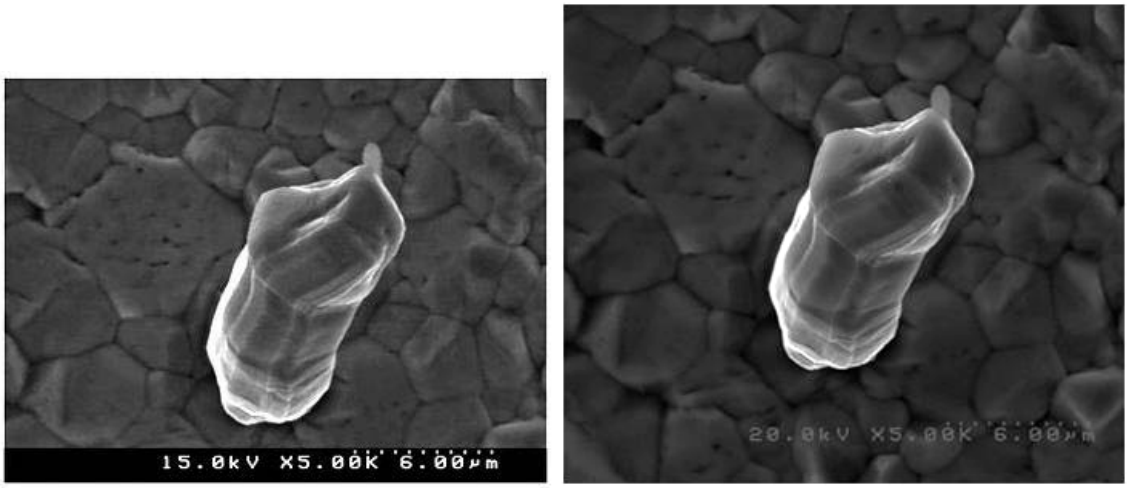

Figure 78. SEM images of a whisker on the Sn sample at 8,000 hours (left) and 12,000 hours (right)

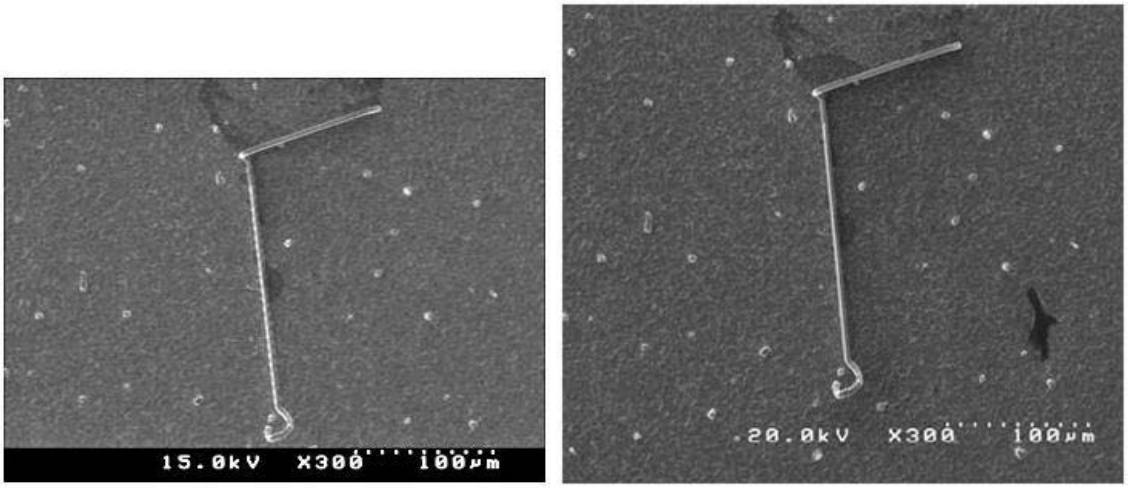

Figure 79. SEM images of a whisker on the Sn sample at 8,000 hours (left) and 12,000 hours (right)

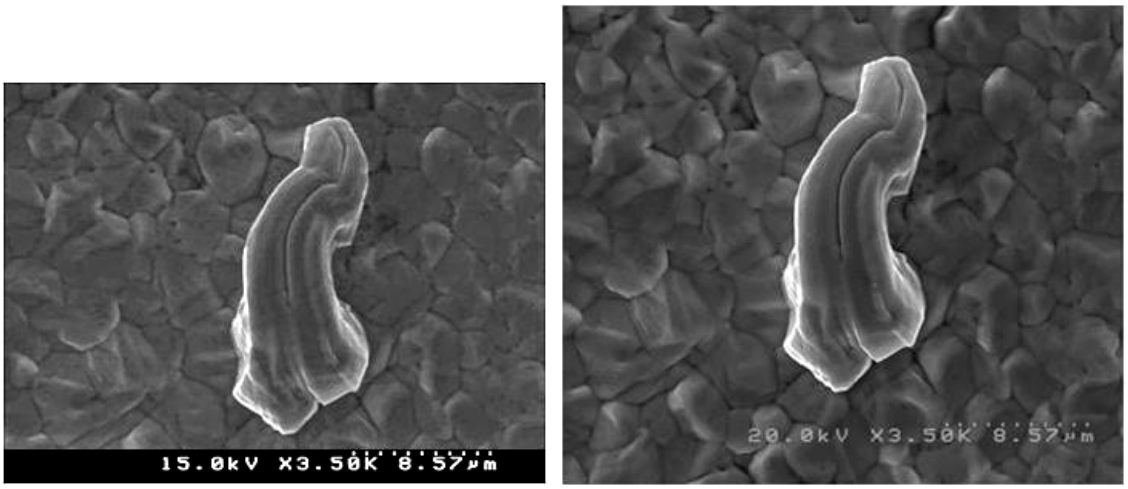

Figure 80. SEM images of a whisker on the Sn sample at 8,000 hours (left) and 12,000 hours (right)

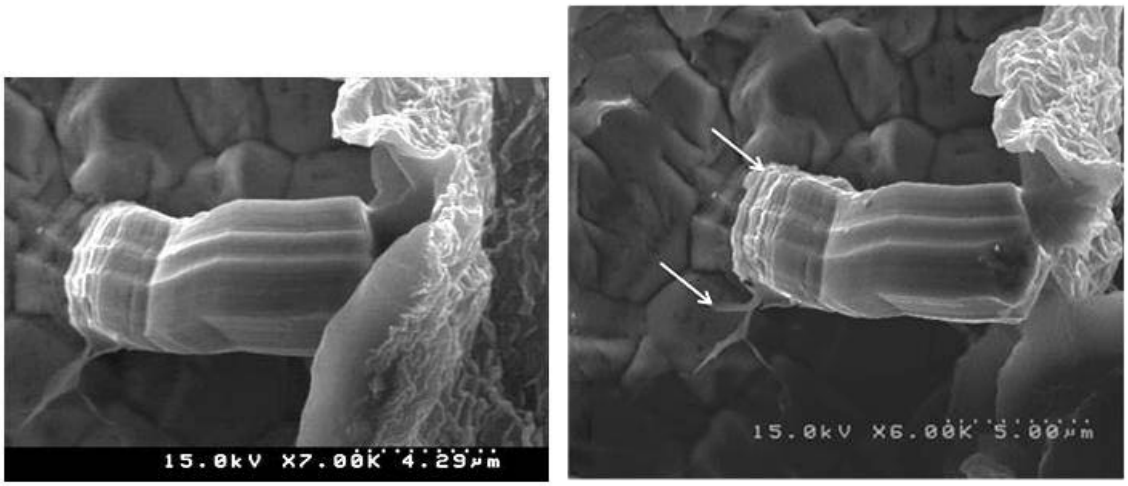

Figure 81. SEM images of a whisker on the Sn/Au sample at 8,000 hours (left) and 12,000 hours (right)

It is noteworthy that none of the whiskers that were photographed and recorded on the pure Sn samples increased in size after inspection, although the average whisker density and length across the sample increased significantly during this time. It will require further investigation to determine if the cause is due to removal from the environmental oven, the SEM inspection, or if the stresses in the area had simply already been relieved by the initial whisker formation.

Undoubtedly, removing the samples from the environmental chamber could cause changes to the Sn surface as the samples cool and the condensation on the samples dries, which will effect whisker formation and growth. For instance, tin oxidation, which is well documented to induce compressive stress, is altered by removal from the chamber. However, SEM inspection may also have an affect depending on the length of time in the chamber, the voltage used during inspection, the time spent on the inspection, and the amount of charging on a particular whisker.

It has long been known that during SEM inspection, a high beam current focused on a small area can cause the temperature of a localized area to rise due to electron beam irradiation. The calculations for temperature rise of a specimen can be frequently found in SEM manuals [20]. However, temperature increase of metal samples is typically not considered a concern during SEM inspection, because of good thermal and electrical conductivity. Still, during whisker inspection it is not uncommon to dwell on a particular whisker for a considerable amount of time, at different angles in order to get accurate measurements and to use higher accelerating voltages in order to get better images. Even moderate increases in temperature over a localized area directly over a whisker may be sufficient to reduce stress. In addition to temperature changes, there is also charging of the metal oxide in the area surrounding the whiskers, particularly at higher accelerating voltages. This charging can lead to breakdown of thin oxide layers [21] which may also have an effect on whisker formation. Additional research in this area is certainly warranted.

5.5 Focused Ion Beam (FIB) Analysis

Evans Analytical Group in Sunnyvale, CA used a FEI Micrion 9500 Focused Ion Beam System equipped with a gallium ion source to create microsections through the plated films so that the morphology of the grains could be visualized. The thickness of each film was also measured using the FIB microsections. A protective coating was used to protect the tin surface morphology around the microsection from the ion beam. This protective coating appears rough and has surface bubbles as seen Figure 82.

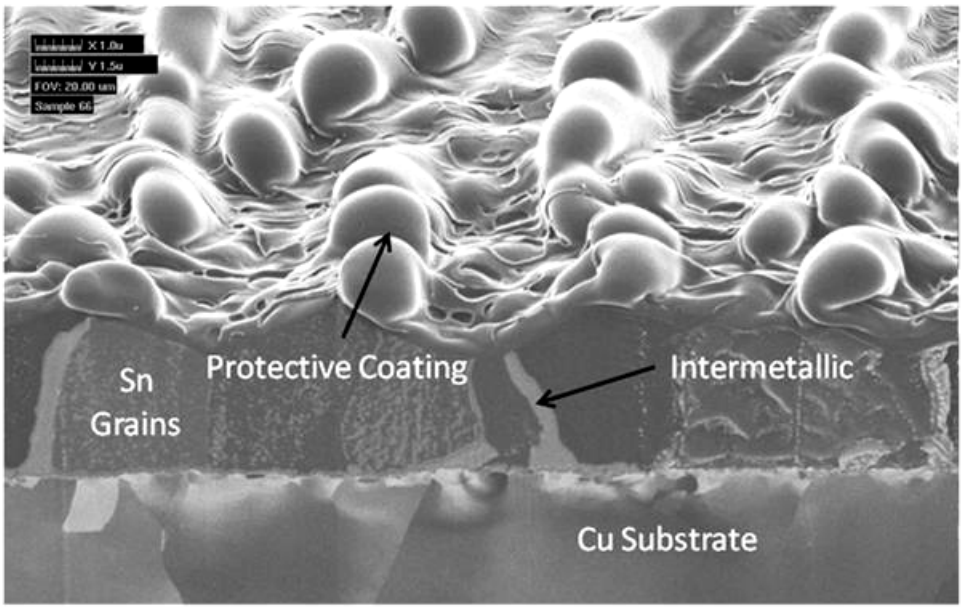

Figure 82. Focused ion beam microsection of tin plated on copper

FIB analysis was performed on one specimen from each of the electroplated films after electroplating. These initial results showed that all of the films had a columnar grain structure (Figure 83) that extended from the copper substrate to the surface of the plated film with the exception of the SnCo and the SnNi films. The SnCo film had a mixture of columnar and equiaxial grains (Figure 84) and the SnNi film had predominately equiaxial grains (Figure 85).

Even prior to aging, all of the plated films exhibited SnCu intermetallic formation between the plated film and the copper substrate. Although typical in appearance to the Cu_6Sn_5 intermetallic formation that is well documented to occur at the interface between Sn plated films and Cu substrates, these intermetallics may be an alloy containing the trace element added as a dopant as well as the Cu and Sn, although the exact phase is not known. The SnNi film had considerably more intermetallic growth when compared to

the other plated films. The SnCu intermetallic appeared to swirl throughout the plated SnNi film, occasionally completely surrounding some grains completely (Figure 82). The SnNi had the longest whiskers of any of the films in this study.

The SnNi film had considerably more intermetallic growth when compared to the other plated films. The SnCu intermetallic appeared to swirl throughout the plated SnNi film, occasionally completely surrounding some grains completely (Figure 82). The SnNi had the longest whiskers of any of the films in this study.

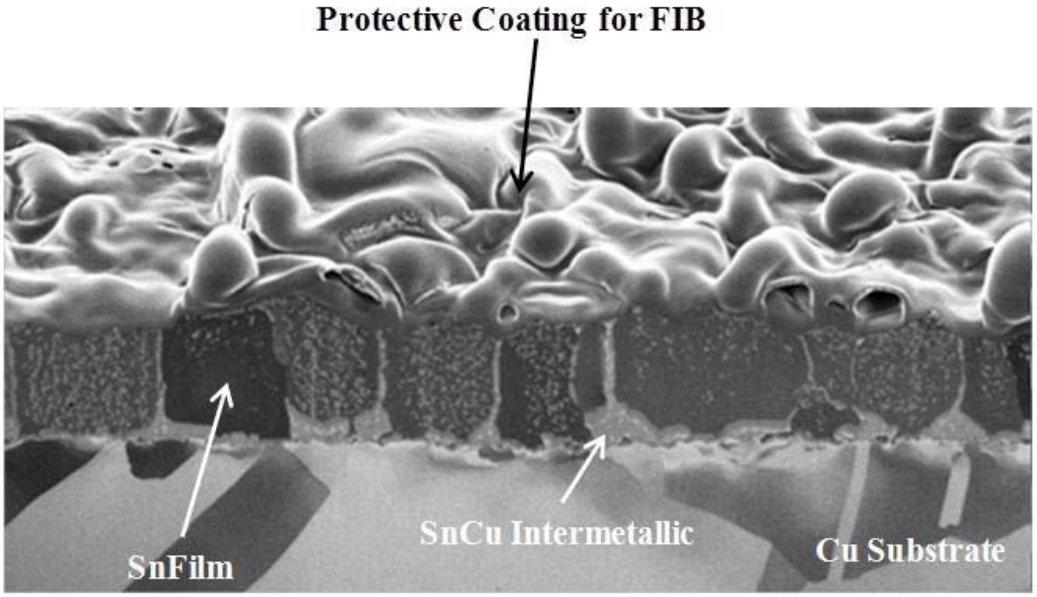

Figure 83. FIB micro-section of Sn plated film taken after electroplating; note the columnar grain structure and the SnCu intermetallic formation

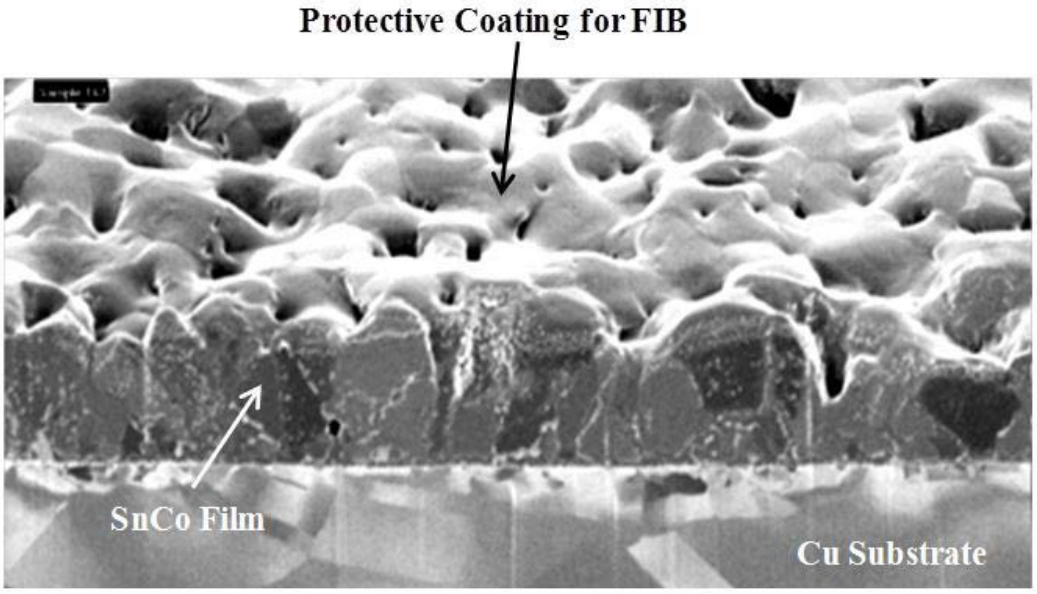

Figure 84. FIB micro-section of SnCo plated film taken after electroplating; note the columnar and equiaxial grains

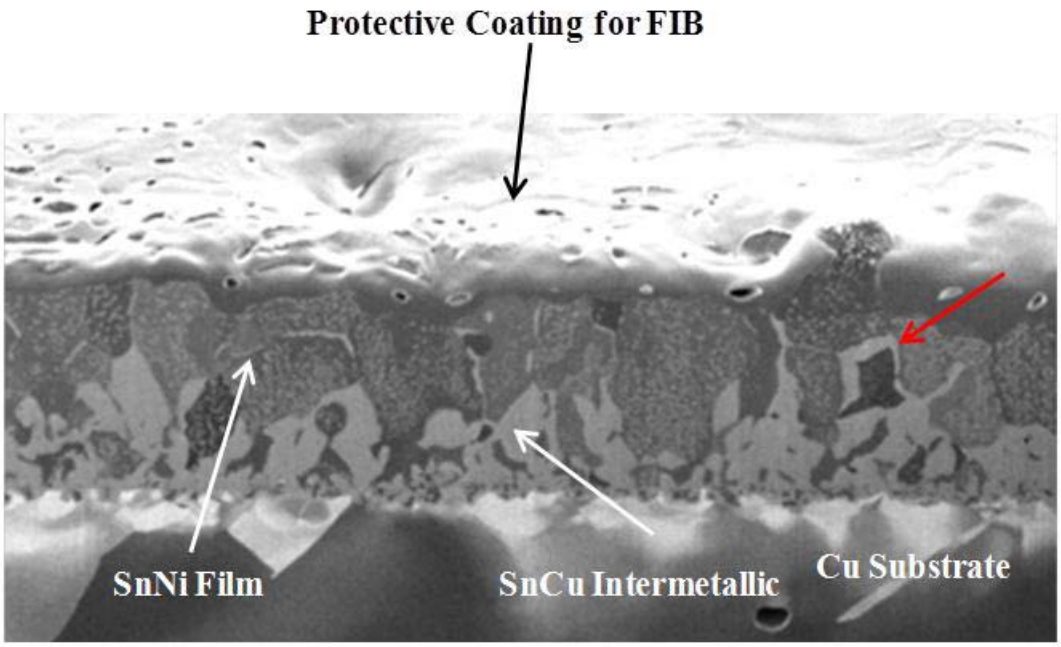

Figure 85. FIB micro-section of SnNi plated film taken after electroplating; note that the SnCu intermetallic completely surrounding some Sn grains

One coupon from each plated film was sent for FIB analysis again after 8,000 hours of aging for films with higher whisker density than pure tin and after 12,000 hours of aging for films with low whisker density. The post aging FIB micro-sections were performed in two areas for each sample, both micro-sections taken at the base of whiskers that formed on the samples with the exception of the Sn/Au sample, because Evans Analytical was unable to locate a whisker on the sample.

As expected, all samples showed significant intermetallic growth after aging. Intermetallics pushed up from the plated film, consistent with the formation of Cu_6Sn_5 intermetallics which are frequently reported [22, 23]. While the formation of intermetallic is evident from the FIB microsections, the composition is not. The dopants in the films may have formed more complex intermetallic.

The SnAu sample showed some of the most significant changes. Prior to aging the grain structure was extremely columnar with little intermetallic formation (Figure 86), after 12,000 hours aging, the SnAu appears to have almost completely transformed in intermetallic compounds (Figure 87-88).

Another noteworthy observation is that one of the whiskers cross sectioned during FIB microsection of the SnAu film appears to be comprised of more than one grain (Figures 80-81). Whiskers that appeared to have multiple grains were seen during SEM inspection on the SnSb films, but were not noted on the SnAu film.

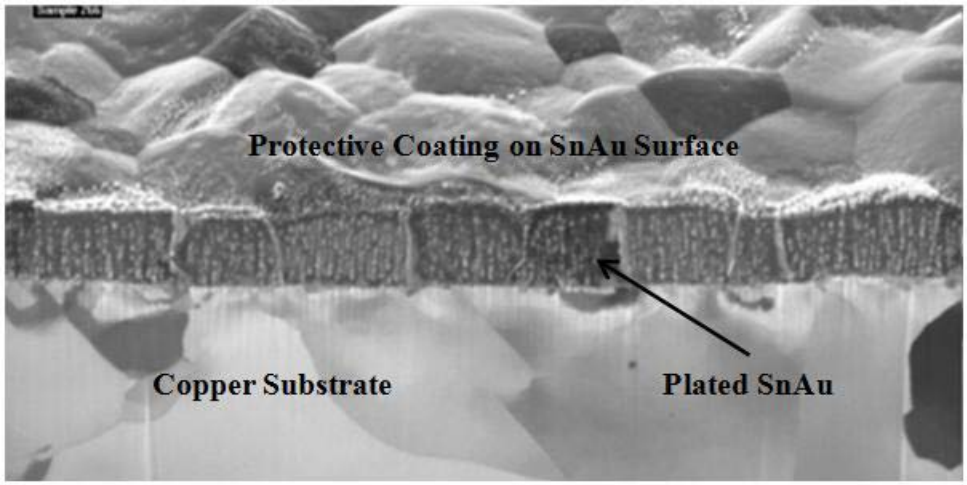

Figure 86. FIB micro-section of SnAu plated film prior to aging

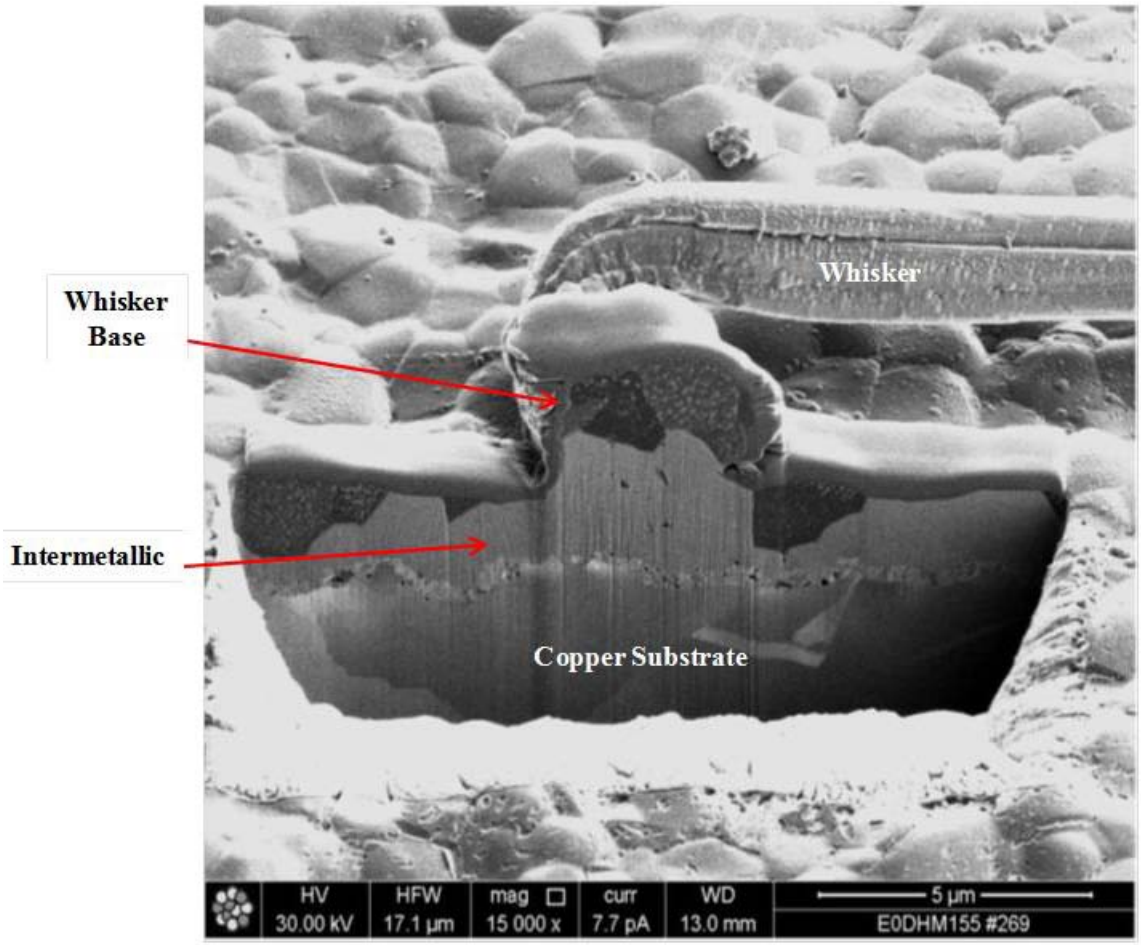

Figure 87. FIB micro-section of the root of a SnAu whisker after 12,000 hours of aging

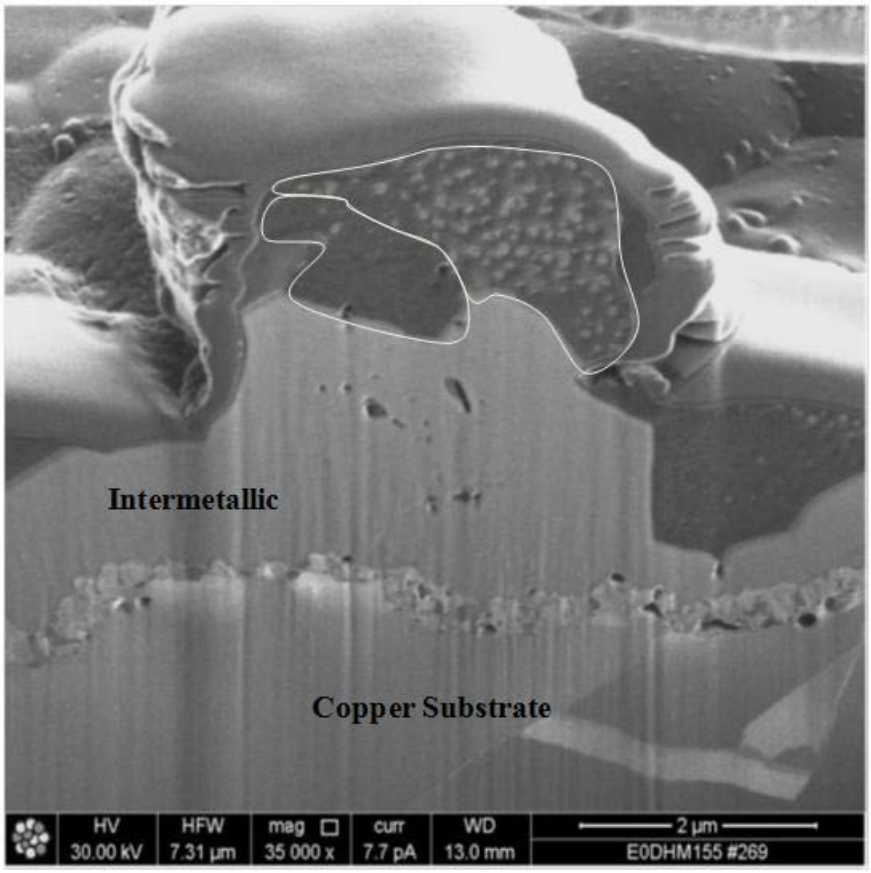

Figure 88. FIB micro-section of a whisker on the SnAu film after 12,000 hours aging

In most cases, the FIB microsections were taken at the base of a whisker that formed during aging. On the Sn/Au microsections, the Evans FIB operator could not locate a whisker due to the extremely low number of whiskers to start and possibly due to a whisker breaking off during transport. Therefore FIB analysis on the Sn/Au sample was performed in a bulk area, rather than at the base of a whisker.

The microsections on most films indicate an area of intermetallic growth that extends from the substrate to at or near the surface of the plated film in the area adjacent to the whisker growth (84-87). On the Sn/Au sample, there were no large intermetallic wedges that extended up to the surface of the plated film (88).

The complete FIB report can be found in Appendices A - I.

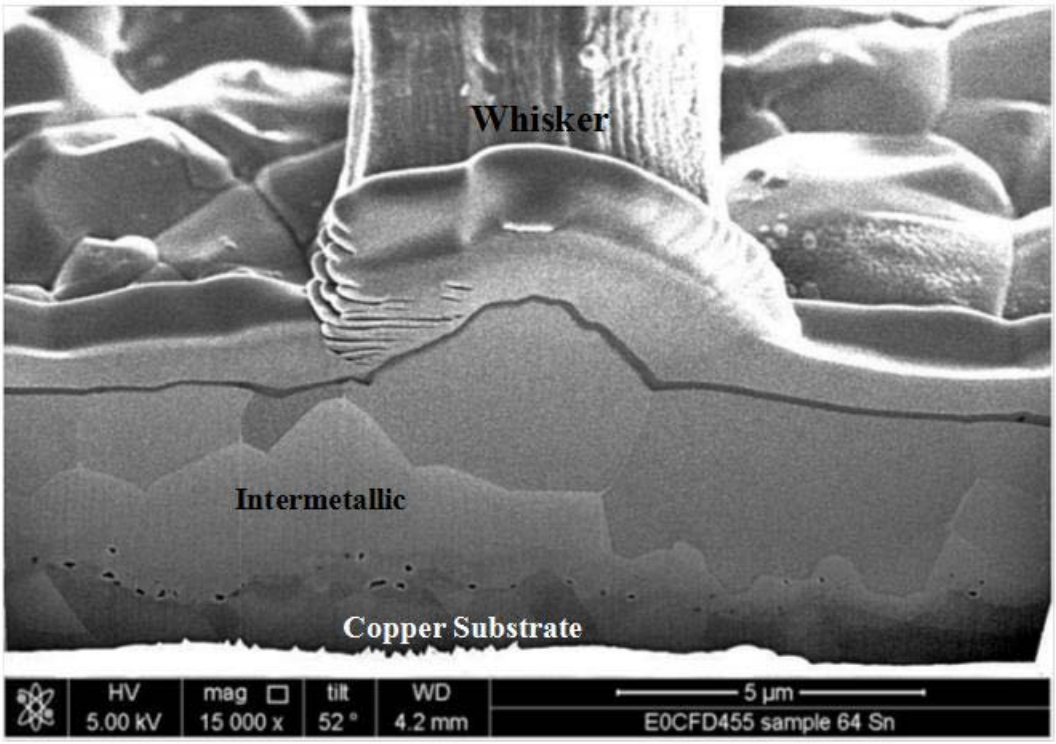

Figure 89. FIB micro-section of the root of a whisker on a pure Sn plated film after 8,000 hours of aging

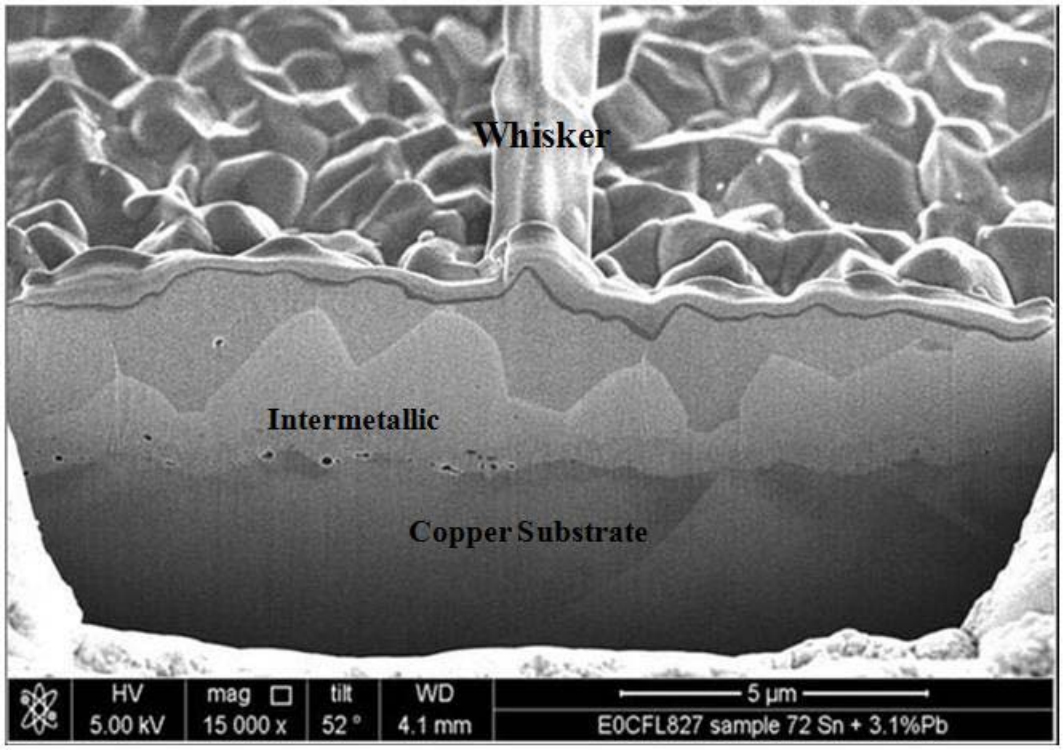

Figure

Figure 90. FIB microsection of the root of a whisker on a SnPb plated film after 8,000 hours of aging

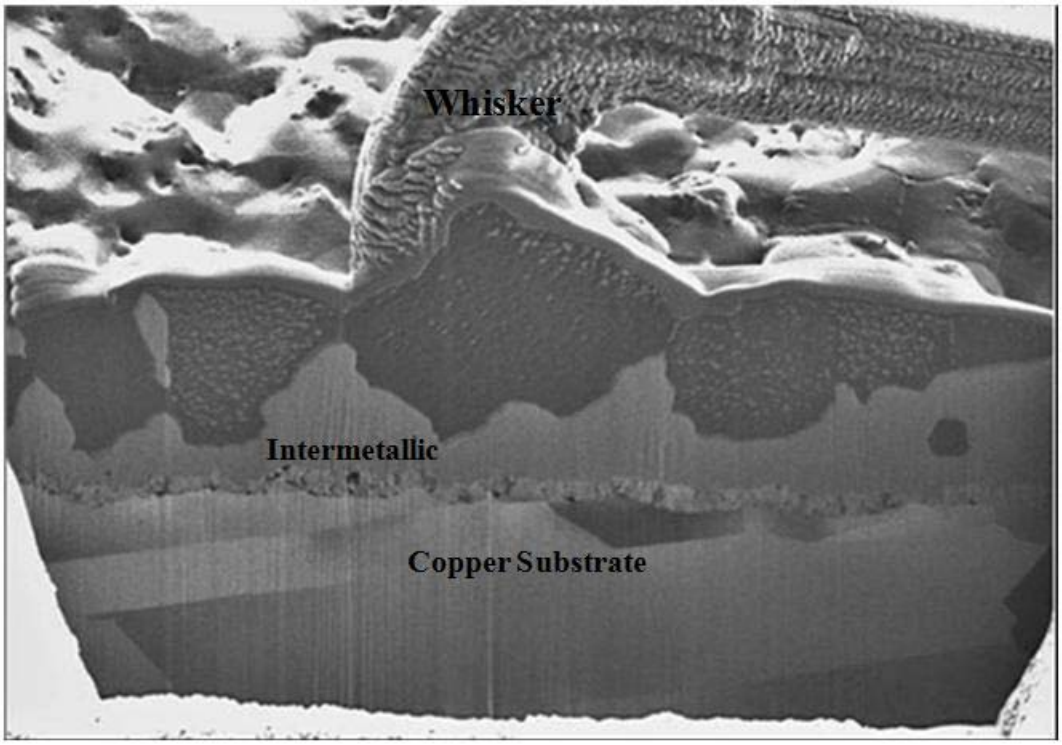

Figure 91. FIB micro-section of the root of a whisker on a SnCu plated film after 8,000 hours of aging

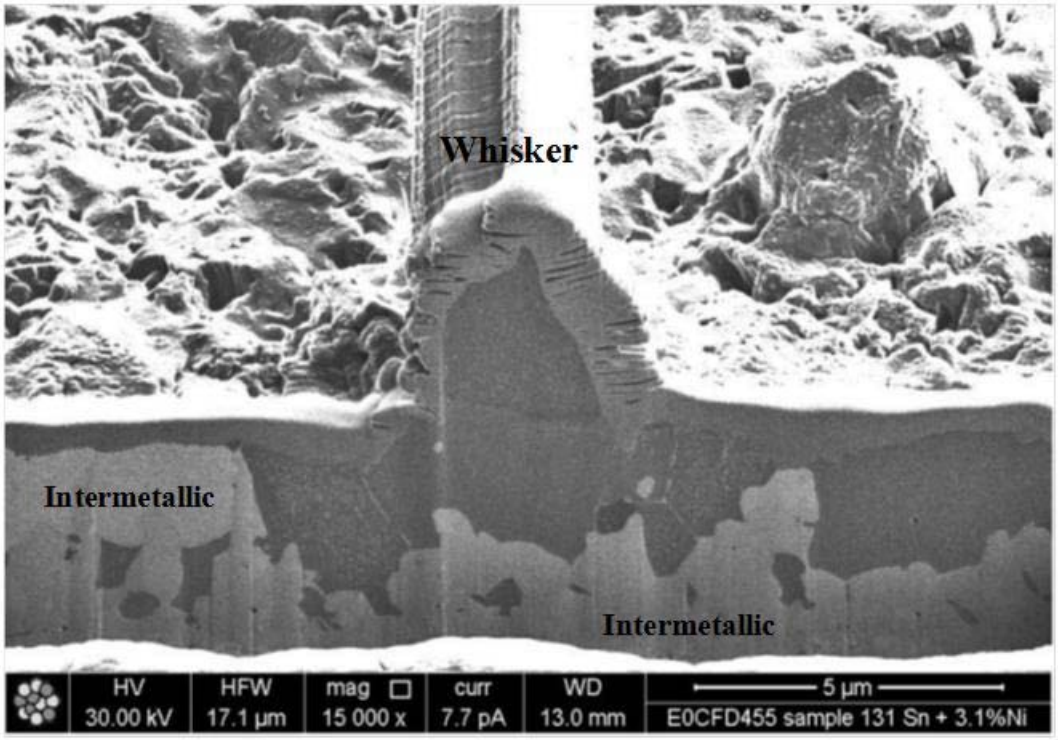

Figure 92. FIB micro-section of the root of a whisker on a SnNi plated film after 8,000 hours of aging

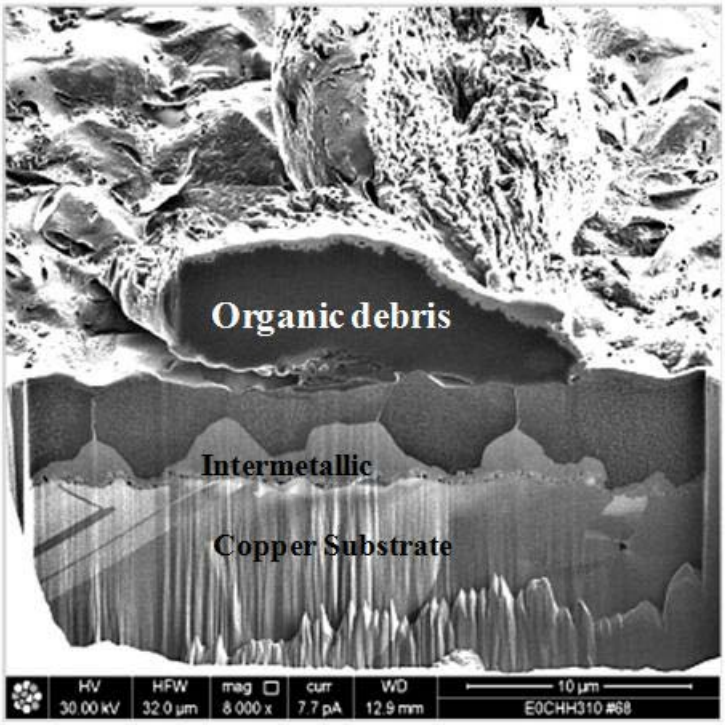

Figure 93. FIB micro-section of bulk Sn plated film capped with 53nm of Au after 12,000 hours of aging

5.6 Electron Backscatter Diffraction (EBSD) Analysis

One objective of the study was to investigate the correlation between whisker growth or suppression with the crystallographic properties of the films. Plated film coupons were sent to EBSD Analytical Inc. for electron backscatter diffraction analysis (EBSD). This included both as plated films and films after aging in the environmental chamber.

Electron backscatter diffraction (EBSD) is a powerful technique that Boeing has used to measure the crystal orientation of single tin grains. The crystallographic data is often presented using inverse pole figures (Figure 94). Each point within the inverse pole figure represents a specific crystallographic orientation. In this study, EBSD was used in an attempt to determine the effects of the dopants on the crystal structure of the films. Tin plated films can have preferred crystal orientations (i.e., fiber textures) which are usually aligned with the specimen normal direction. Figure 94 shows the EBSD orientation measurements for a bright tin plated film. In this case, the plating grains had a predominant 113 crystal orientation (fiber texture) in the specimen normal direction but no predominant fiber textures were observed in the transverse or reference directions. We examined the effects of the elemental dopants on the fiber texture of the films; generated inverse pole figures for the normal, transverse, and reference directions; and looked for correlations between the crystal orientations of the grains and the propensity of the plated films to grow whiskers. The relative orientation of the lattices of adjacent grains (i.e., misorientations) were also examined.

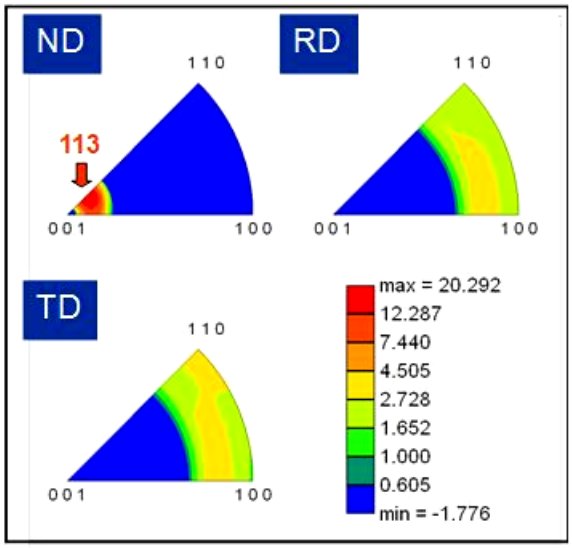

Figure 94. EBSD measurements on a bright tin plated film. Inverse pole figures are shown for the normal (ND), reference (RD), and transverse (TD) directions. The tin plated film has a strong 113 orientation in the normal direction.

It is known from earlier work at Boeing that a matte plated tin film with an average surface roughness (Ra) of approximately 50nm is smooth enough to allow indexing of most of the grains using EBSD. A smooth surface is required to eliminate shadowing of the diffraction pattern by neighboring grains which could lead to erroneous results. Although every effort was made to electroplate films that were as smooth as possible, all of the films produced for this study were rougher than the Ra = 50nm benchmark. The EBSD scans conducted on the first four plated films gave marginal indexing results (Table 21). For that reason, the films had to be polished so that a higher percentage of the grains could be indexed.

Specimen polishing prior to EBSD is standard practice and normal metallographic polishing methods were used to prepare the specimens for EBSD analysis. These methods have been shown to give the required flat surface without distortion of the crystal lattice. The final polishing step used 0.04 micron colloidal silica to remove any surface damage.

Since the films in this study were thin, 2.2 – 4.9 microns thick, it was required that any polishing be done carefully so as not to remove excessive amounts of the electroplated films. No smearing of the grains, significant changes in grain size, or changes in crystallographic orientation of the grains was noted. After polishing, the number of grains that could be indexed by EBSD was increased for every film (See Table 21). For example, for the SnPb film, polishing increased the number of grains that could be indexed from 59% to 92.2%. Had the polishing technique introduced surface damage such as scratches or lifted grains, the percentage of grains indexed would have decreased, not increased.

Plating	Percentage of Grain Indexed with Confidence	
	As Plated	Polished
Sn	70.9%	97.7%
SnPb	59.0%	92.2%
SnCu	50.0%	64.6%
SnNi	63.6%	71.1%
SnCo	n/a	85.9%
SnSb	n/a	94.2%
SnGe	n/a	96.3%
SnAu	n/a	98.6%

Table 21. Percentage of Grains Indexed by EBSD before and after polishing of films

Direct evidence that the crystal orientations of the grains in the films were not changed by the polishing technique is shown in Figures 89 and 90. The inverse pole figures for the SnPb and the SnCu films are shown before and after polishing and the textures observed are essentially the same.

For some films, such as the SnSb, the polishing of the sample was essential since no useful EBSD data would have been obtained on the unpolished film due to surface roughness. Conversely, the polishing of the SnCu and the SnNi films did not significantly increase the number of grains indexed (see Table 21). The reason is that the grains that did not index in the SnCu and SnNi films were actually Cu_6Sn_5 intermetallics that were formed by reaction of the copper substrate with the Sn in the films. These intermetallic wedges extended from the copper substrate to near the plated film surface and their composition was verified by EBSD results.

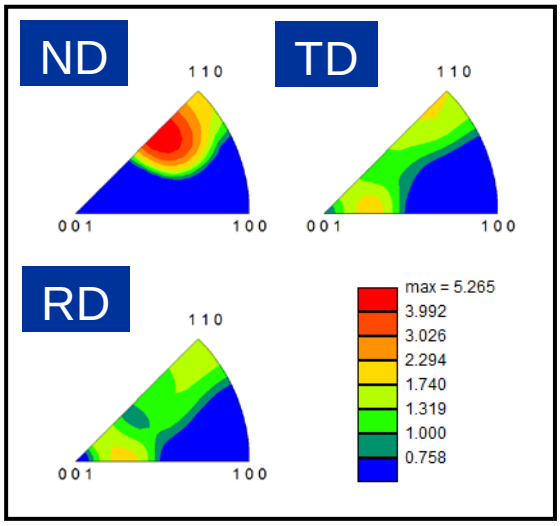

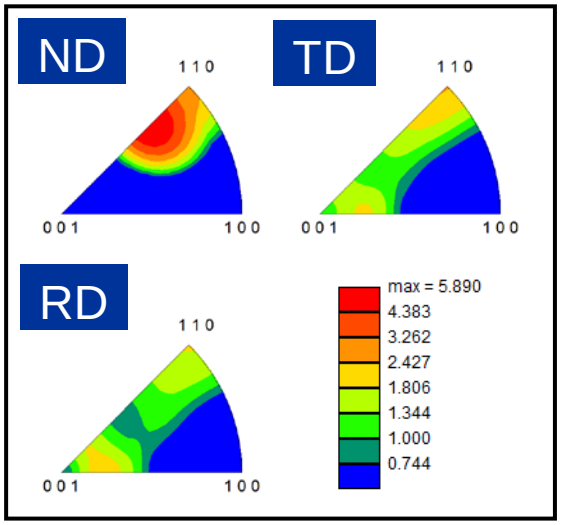

Figure 95. (a) SnPb film as plated (b) SnPb film after polishing

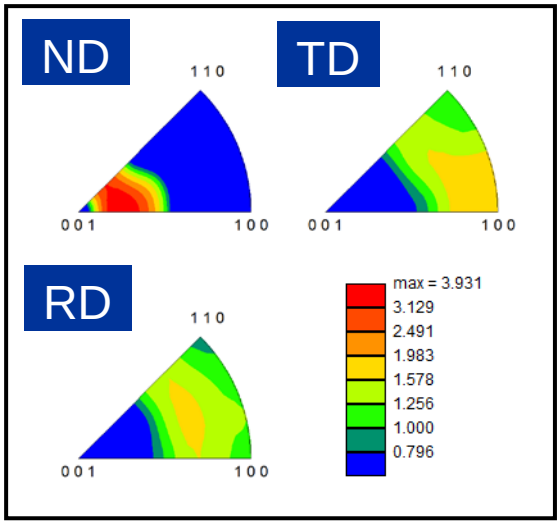

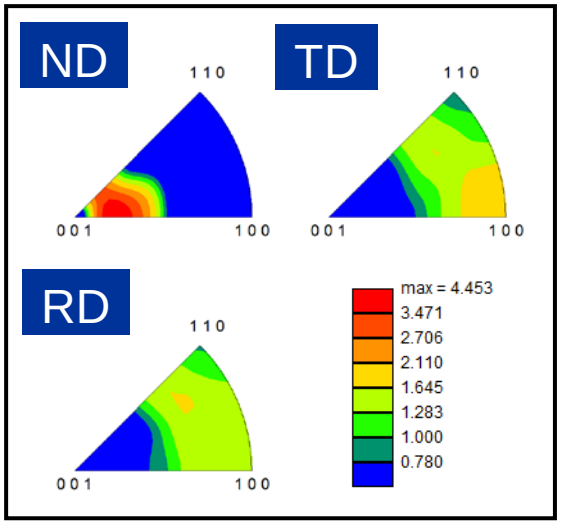

Figure 96. (a) SnCu film as plated (b) SnCu film after polishing

5.6.1 Grain Size

The average grain size within each plated film was determined using EBSD. The results are summarized in Figures 92-93. The data was collected after plating and after the aging of the films. Although it appears that there was a significant change in grain size on some of the films after aging, the changes would include not only changes to the doped tin films, but intermetallics that formed during the aging process.

Figure 97 does indicate a general trend between initial grain size and the propensity to grow whiskers which is supported by some reports that link grain size or finish (matte vs. bright) to whisker growth [6,24,25]. However, this is not true when the data set is limited to only low whisker density samples as seen in Figure 98.

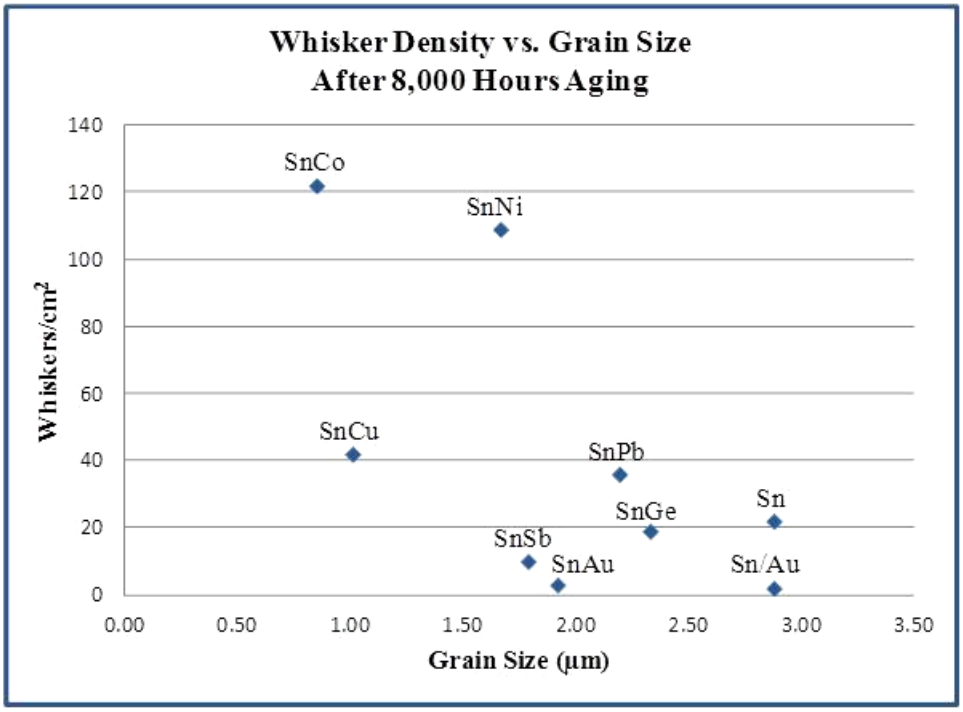

Figure 97. Whisker density after 8,000 hours aging versus post plating grain size

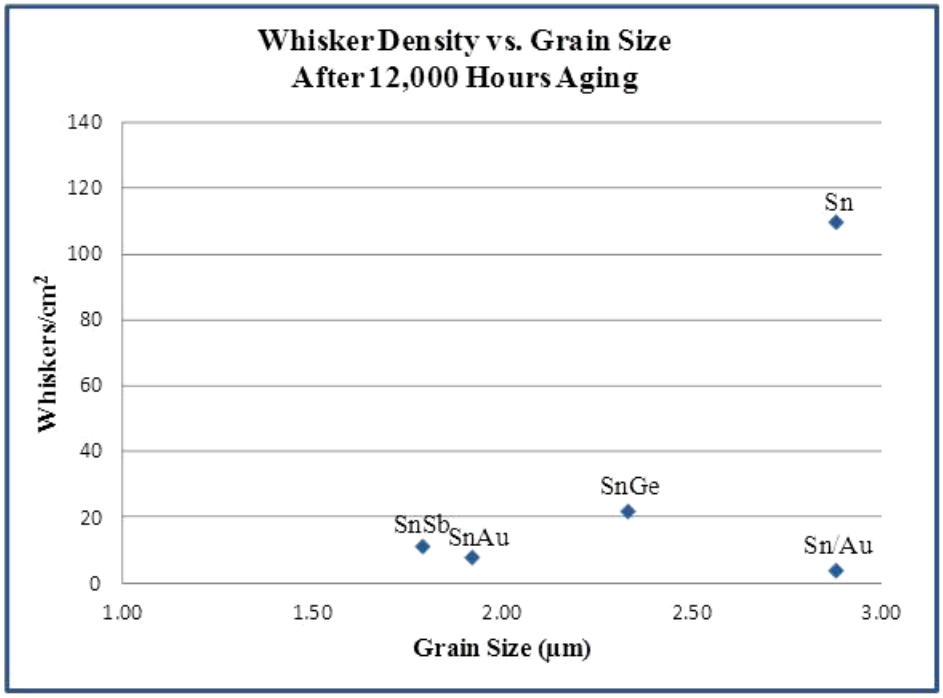

Figure 98. Whisker density after 12,000 hours aging versus post plating grain size

Figure 94 shows a phase ID map for the SnAu sample after aging and nearly half of the grains indexed were actually copper intermetallics, rather than the SnAu. Grain size measurements include both the copper intermetallics as well as the SnAu grains (Table 22) which may distort the data. Furthermore, the SnGe showed the largest decrease in grain size, but given the extremely conical grain shape found during SEM inspection (Figure 67); different polishing depths would greatly change the grain size measurement.

Plated film	Grain Size Post Plating (µm)	Grain Size Post Aging (µm)
SnCo	0.85	0.97
SnCu	1.01	1.31
SnNi	1.67	1.05
SnPb	2.19	1.30
Sn	2.88	1.94
Sn/Au	2.88	1.89
SnAu	1.92	1.56
SnGe	2.33	1.27
SnSb	1.79	1.33

Table 22. Grain size measurements from EBSD post plating and post aging

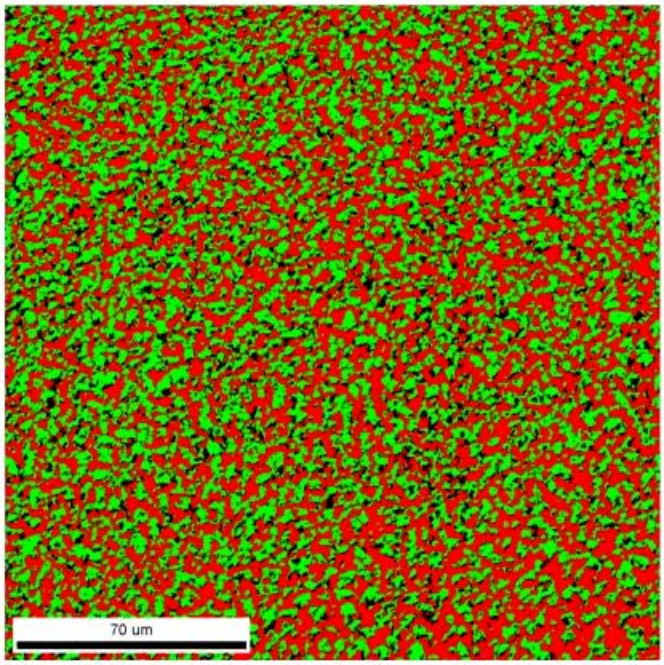

Color Coded Map Type: Phase

Phase	Total Fraction	Partition Fraction
Tin	0.477	0.547
Copper Tin	0.395	0.453

Figure 99. Phase ID map of tin and copper tin on the SnAu film taken after 12,000 hours of aging

5.6.2 Crystallographic Texture

The primary crystallographic orientation and maximum texture intensity were determined by EBSD analysis. The results are summarized in Table 23.

Film	Primary Grain Texture		Pole Figure Maximum Texture Intensity		Percentage of Grains with Primary Crystallographic Texture		Percentage of Grains with Primary Crystallographic Texture	
	Post Plating	Post Aging	Post Plating	Post Aging	15 Degree Tolerance Post Plating	20 Degree Tolerance Post Plating	15 Degree Tolerance Post Aging	20 Degree Tolerance Post Aging
Sn	<111>	<111>	4.499	4.121	47.1%	69.5%	41.4%	61.6%
Sn/Au	<111>	<111>	4.499	4.474	47.1%	69.5%	45.6%	63.3%
SnAu	<111>	<111>	3.013	3.251	32.7%	51.3%	34.5%	54.5%
SnCo	<749>	<215>	2.576	2.092	36.9%	53.9%	38.0%	57.9%
SnCu	<104>	<014>	4.825	6.056	48.3%	69.0%	58.0%	82.3%
SnGe	<001>	<001>	6.424	3.395	18.9%	34.5%	9.1%	16.2%
SnNi	<214>	<216>	3.013	3.508	55.7%	75.3%	46.6%	66.8%
SnPb	<111>	<111>	5.003	4.837	61.5%	84.8%	54.0%	77.6%
SnSb	<110>	<110>	8.666	9.735	45.2%	64.3%	47.6%	65.7%

Table 23. Primary Crystallographic Textures of the Plated Films

The only films with primary crystallographic texture change after aging were the SnNi and SnCo films (Figures 95-96); most films had little or no change (Figures 97-98). Since the SnNi and SnCo films had the highest whisker density, there is a correlation between the whisker formation and change in grain texture/ reorientation of the grains.

It should also be noted that SnNi and SnCo, along with SnAu, had the lowest maximum texture intensity prior to aging. The lower the maximum texture intensity the more random the crystallographic texture. A maximum value of 1.0 would indicate a perfectly random texture, while a maximum value of 5 would indicate that particular orientation is 5 times more likely to be identified than in a random distribution.

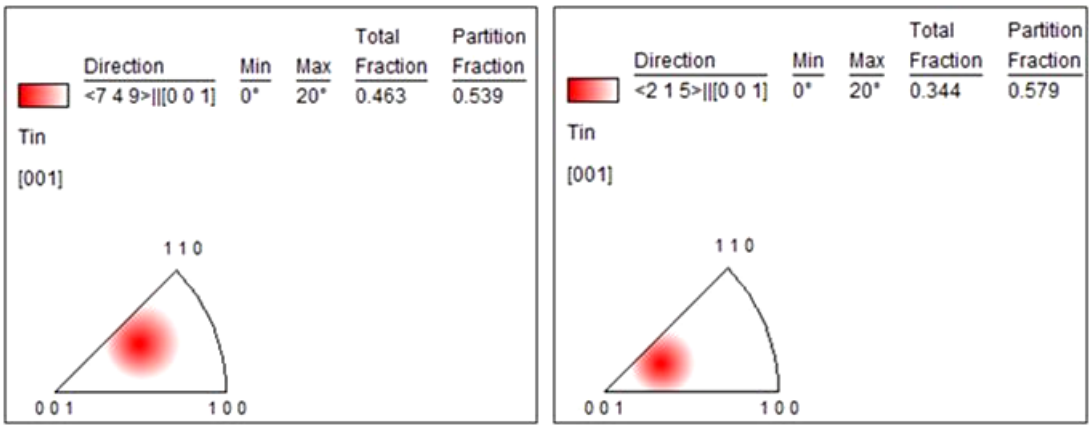

Figure 100. Crystal direction map showing <111> crystal direction in ND direction 20 degree tolerance for SnCo film (left) pre-aging and (right) after 8,000 hours aging

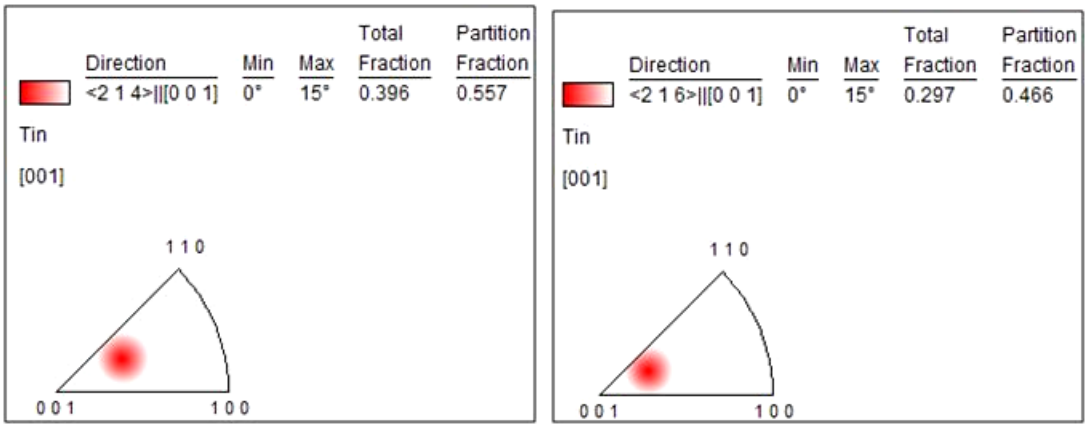

Figure 101. Crystal direction map showing <111> crystal direction in ND direction 20 degree tolerance for SnNi film (left) pre-aging and (right) after 8,000 hours aging

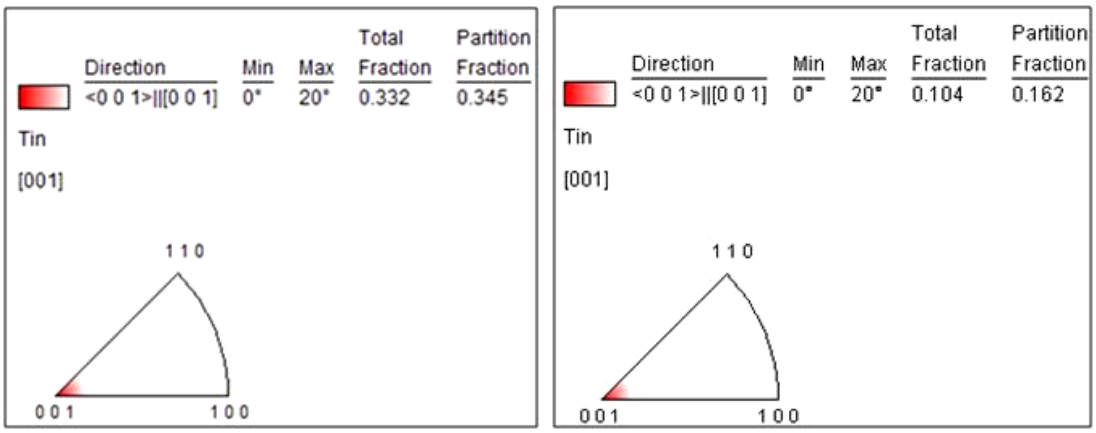

Figure 102. Crystal direction map showing <111> crystal direction in ND direction 20 degree tolerance for SnGe film (left) pre-aging and (right) after 12,000 hours aging

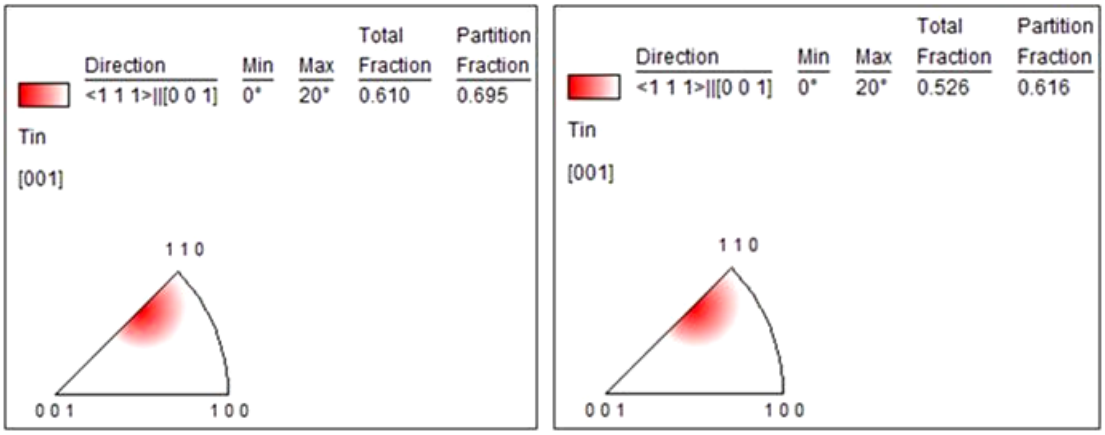

Figure 103. Crystal direction map showing <111> crystal direction in ND direction 20 degree tolerance for Sn film (left) pre-aging and (right) after 8,000 hours aging

It has been postulated in the literature that texture may play a role in whisker formation. For example, Osenbach [26] believes that for plated Sn with columnar grains, the most whisker growth will be seen with either the <100> or the <010> directions oriented perpendicular to the substrate. Conversely, Osenbach says that the least amount of whisker growth will be seen when the <001> direction is perpendicular to the substrate. Osenbach also evokes grain size and temperature as critical parameters. For example, he states that a plated film with the whisker resistant <001> fiber texture will not grow whiskers if the grain size is below 4.5 microns in diameter (at 25 degrees C), whereas the whisker prone plated films, i.e. having <100> or a <010> fiber texture would grow whiskers if the grain diameter were to exceed 0.6 microns (at 25 degrees C).

The plated film in this study that came closest to meeting Osenbach's requirements for a whisker resistant plated film is the SnGe film which had a <001> primary texture and an average grain size of 2.33 microns before aging. This film did have a lower whisker density than the pure tin baseline sample and one of the lowest whisker densities in this study which could indicate that Osenbach's hypothesis has some validity. Unfortunately, from a practical standpoint, this correlation between texture and whisker density is very hard to implement in electroplating, since it is not possible to plate a film with 100% of the grains with the desired texture.

Prior to starting the electroplating step of this project, it was hoped that a single electrolyte chemistry could be used for all plated films, the only change being the addition of individual dopant salts to the electrolyte. This proved impractical; the chemistries used for many of the doped plated films differed significantly from each other (see Section 4). As a result, crystallographic differences between the plated films could be attributed to the different chemistries used, the dopants used, or a combination of the two.

5.6.3 Grain Boundary Types Present in the Plated Films

In this study, EBSD was used to determine the misorientation relationships between the grains in the plated films. The number of low angle grain boundaries, high angle grain boundaries, and coincident site lattice boundaries present in each plated film are summarized in Table 24.

A grain boundary is the interface between two grains, or crystallites, in a polycrystalline material. It is convenient to separate grain boundaries by the extent of the misorientation between the lattices of the two grains. Low angle grain boundaries (LAGB's) are those with a misorientation less than about 15 degrees and are low energy grain boundaries. The energy of a low-angle boundary is dependent on the degree of misorientation between the neighboring grains up to the transition to high-angle status. In contrast, high angle grain boundaries (HSGB's) have a misorientation of greater than about 15 degrees and are generally higher energy grain boundaries. However, there are "special boundaries" at particular orientations whose interfacial energies are notably lower than those of general HAGB's. Coincident site lattice boundaries (CSLB's) are an example of these "special boundaries".

The simplest boundary is that of a tilt boundary where the rotation axis is parallel to the boundary plane. In the case of simple tilt boundaries, the energy of a boundary made up of dislocations can be predicted by the Read-Shockley equation [27]. Similarly, a twist boundary is where the misorientation occurs around an axis that is normal to the boundary plane. As the misorientation angle between the grains increases, dislocations must be introduced to accommodate the deformation. As the misorientation angle approaches 15 degrees, the dislocations will begin to overlap; the ordered nature of the boundary will begin to break down; and the low angle boundary becomes a high angle boundary. In comparison to low angle boundaries, high angle boundaries are

considerably more disordered with large areas of poor fit and a comparatively open structure.

At certain misorientation angles in a grain boundary, some lattice sites of the two grains can coincide. At coincident site lattice (CSL) grain boundaries, the degree of fit (Sigma, Σ) between the lattices of the two grains is described by the reciprocal of the ratio of coincident sites to the total number of sites. For example, boundaries where every third atom in the two adjacent lattices is coincident are designated as Σ3. Low-angle boundaries, where the distortion is entirely accommodated by dislocations, are Σ1. Some low Σ boundaries have special properties. Examples include coherent twin boundaries (Σ3) and high-mobility boundaries in FCC materials (Σ7) [28]. A CSL boundary with a low Σ might be expected to have a lower energy than a non-CSL boundary due to the better fit between the lattices.

Plating	Post Plating			Post Aging		
	Grain Boundary Character Distribution			Grain Boundary Character Distribution		
	2≤ angle	CSL	Angle >15	2≤ angle	CSL	Angle >15
Sn	22.9%	1.9%	75.2%	10.5%	2.1%	87.3%
Sn/Au	22.9%	1.9%	75.2%	27.8%	3.2%	69.0%
SnAu	5.4%	2.9%	91.7%	4.4%	1.2%	94.5%
SnCo	10.4%	2.3%	87.3%	11.2%	1.7%	87.1%
SnCu	18.6%	3.3%	78.1%	12.6%	1.7%	85.7%
SnGe	5.6%	2.0%	92.5%	22.6%	4.8%	72.6%
SnNi	17.8%	1.8%	80.4%	10.2%	1.7%	88.1%
SnPb	13.2%	1.5%	85.3%	17.9%	1.6%	80.5%
SnSb	16.7%	3.8%	79.5%	17.7%	6.7%	75.6%

Table 24. Grain Boundary Character of the Plated Films

There was a hypothesis proposed at the start of this study based on work by Boguslavsky and Bush [29] that low angle (low energy) grain boundaries may act as whisker nucleation sites and that high energy grain boundaries are necessary to supply Sn atoms required for whisker growth. According to their theory, if most grain boundaries in a plated film are high angle (high energy), then there are fewer sites for whisker initiation, but once growth begins, the whiskers will get longer [29]. On the other hand, if most sites are low energy then there will be a high whisker density, but the whiskers will grow slowly.

Most of the films plated in this study had high angle (high energy) grain boundaries, from 75-93%. According to Boguslavsky and Bush this should have indicated few, but long whiskers. In fact, most of the plated films in this study did have relatively low whisker density, but most also had primarily short whiskers. There was also no correlation

between the films that had the longest whiskers and the largest number of high energy grain boundaries. For example, SnCu had the longest whisker at 1.74mm, but its percentage of high energy grain boundaries was one of the lowest at 78.1%. SnAu and SnGe had the largest amount of high energy grain boundaries, 91.7% and 92.5% respectively, but nearly all of the whiskers were less the 20 microns in length, the longest being 56 microns.

One other hypothesis regarding grain boundary contribution to whisker growth, which was put forth at the beginning of this study, was that there may be an association between CSL grain boundaries and whisker formation. The hypothesis, based on literature data [28-29], was that the higher the percentage of CSL boundaries, the more likely the films would be to form whiskers.

The Σ values found for the plated films used in this study are shown in Figures 94-95. Σ33a and Σ35 were the predominant CSL boundaries in all of the films both before and after aging (Note: Σ33a and Σ33b have the same number of coincident sites but are associated with different crystallographic planes).

There was no correlation found between the CSL boundary percentage before aging and the propensity to grow whiskers. The overall percentage of CSL boundaries increased after aging, but given that the percentage of CSL boundaries are extremely low, the likelihood that they play any significant role is probably low. Interestingly, the films with the lowest whisker densities actually had a higher percentage of CSL boundaries after aging, with SnGe, SnAu, SnSb, and Sn/Au having the highest CSL boundary percentage. SnNi, SnCu, and SnCo had the lowest. This apparent relationship may not be real, however, since it is unlikely that a CSL of Σ33 (in which only one out of 33 lattice sites is coincident) would have an interfacial energy significantly lower than a non-CSL high angle grain boundary.

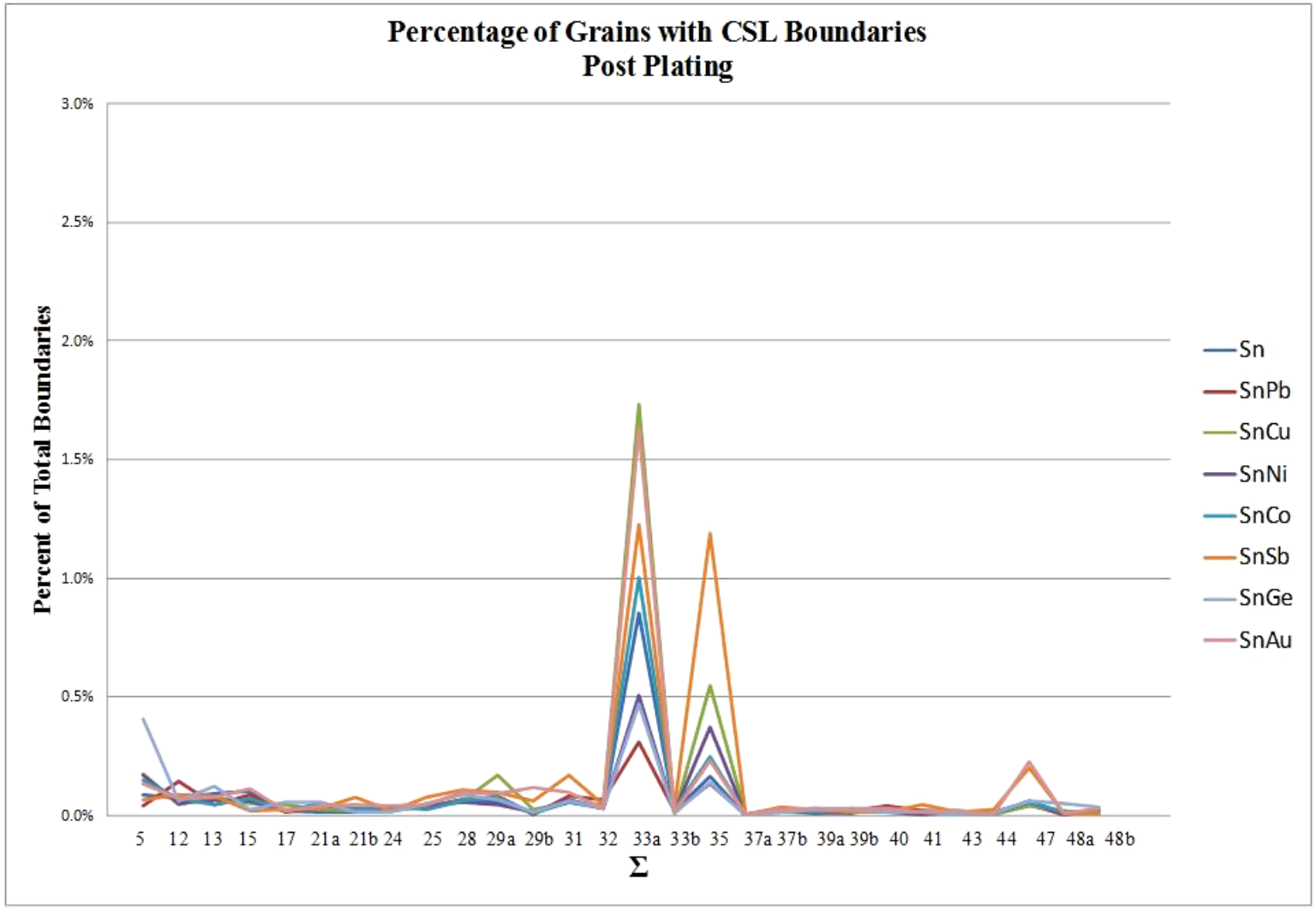

Figure 104. Percentage of grains that have CSL Boundaries after plating

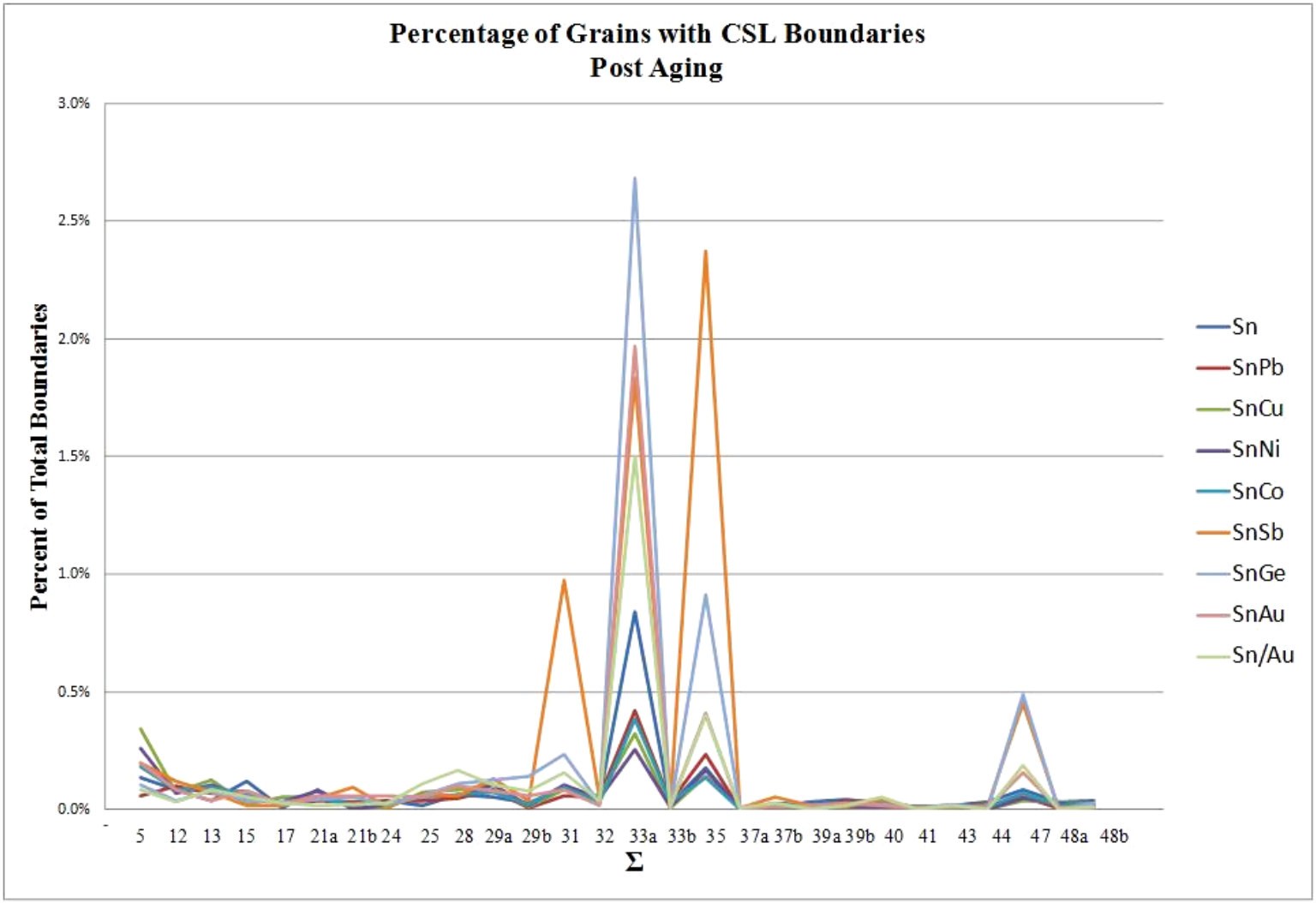

Figure 105. Percentage of grains that have CSL Boundaries after aging

5.6.4 Misorientation Angle Distribution

The distribution of the misorientations for all grains in each plated film was determined using EBSD. The histograms for all of the films can be found in Appendices J-R. The misorientation angle histograms of SnAu and SnGe, taken prior to aging, are shown in Figures 101-102. The blue line in each figure shows what the misorientation angle distribution between all adjacent grains would be if the distribution was completely random (note that the low angle misorientations are not shown). The red line is the actual measured misorientation angle distribution between all grains of the bright tin plated film. The histogram for the SnAu shows that the misorientations are nearly random while the histogram for SnGe deviates significantly from a random distribution with a peak around 44 degrees. The misorientation angle shown can be due to tilt, twist, or a combination of the two.

In the misorientation angle distribution taken prior to aging only the SnGe film deviates significantly from random distribution (Figure 108),. After aging (Figure 109), the SnGe becomes more random, but the SnCu and the SnNi increase with the peak at approximately the same 44 degree point that the SnGe spiked prior to aging. It should be noted that, that there is a spike at approximately 4.5° for all of the films. This measurement is suspect, because the rest of the data forms a nice skewed Gaussian distribution. Regardless of whether the spike is included in the analysis, there does not appear to be a direct correlation between grain misorientation and whisker growth.

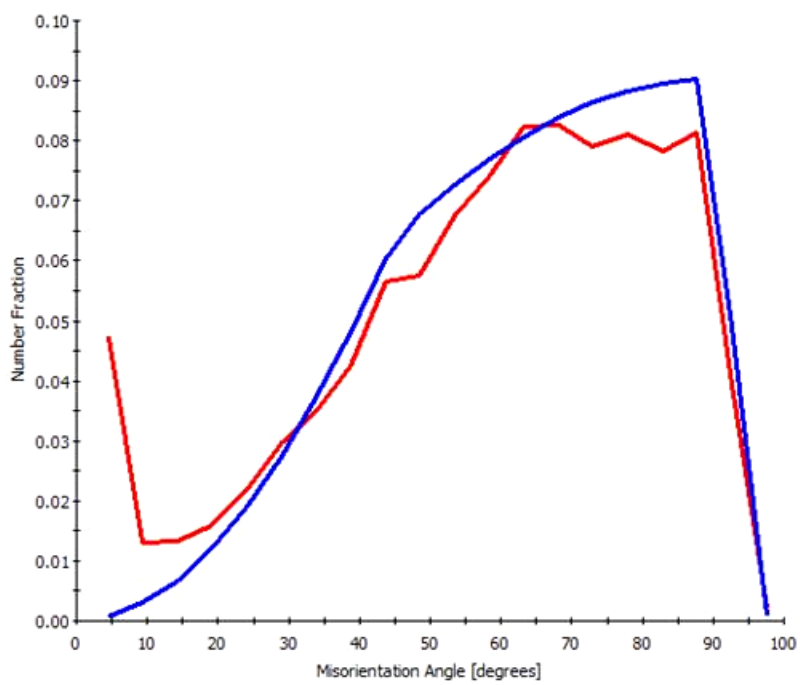

Figure 106. Misorientation Angle Distribution prior to aging for SnAu

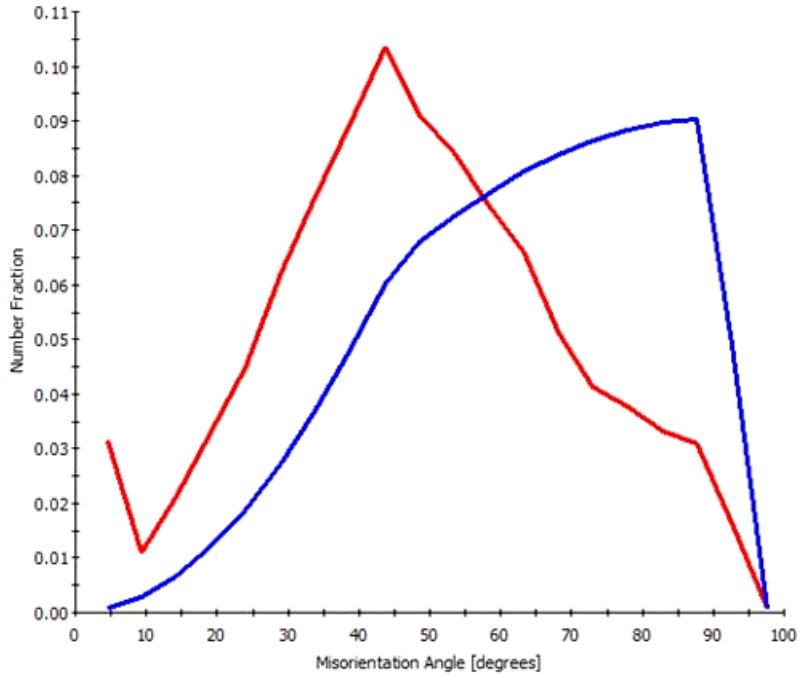

Figure 107. Misorientation Angle Distribution prior to aging for SnGe

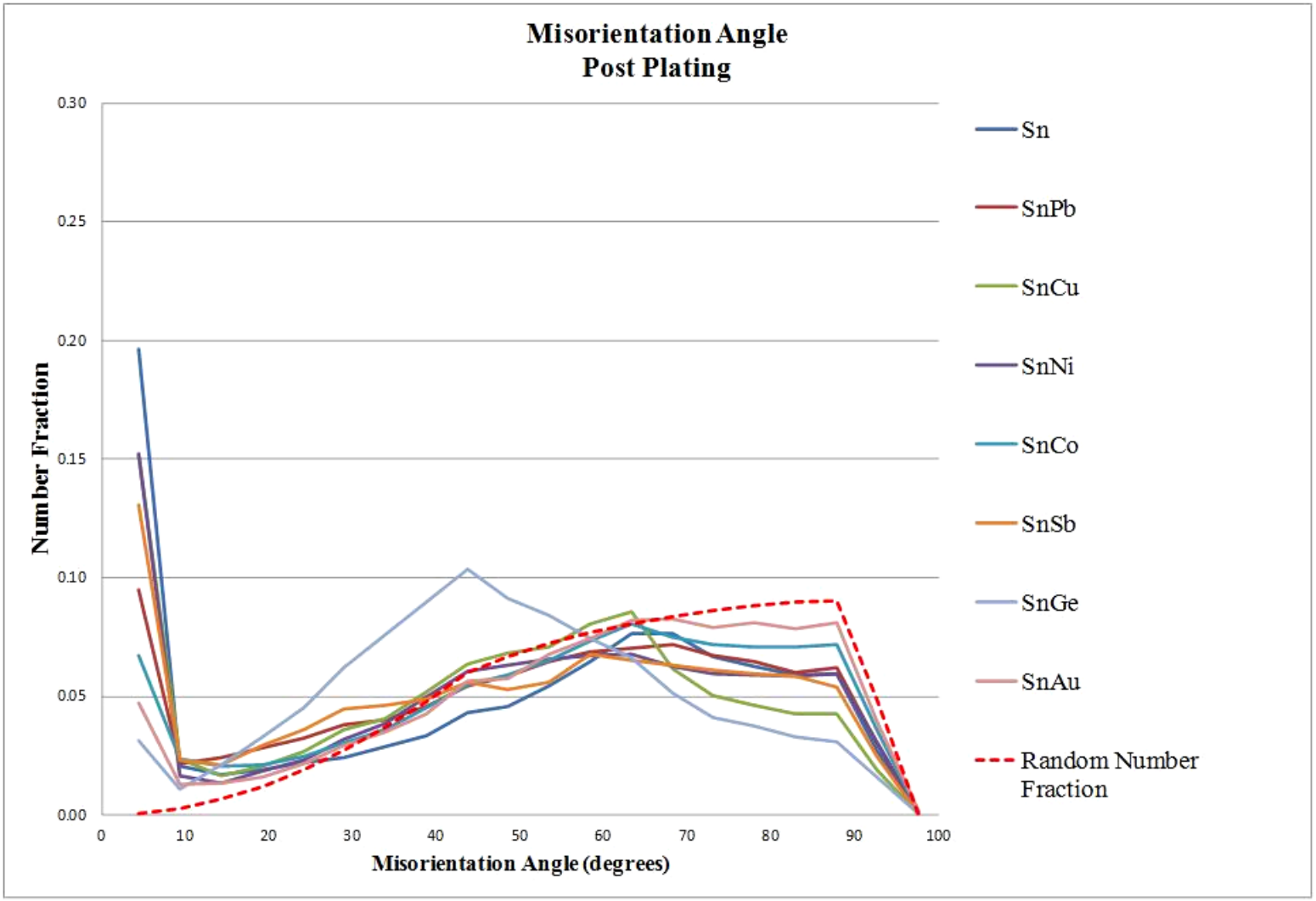

Figure 108. Misorientation angle distribution for all films prior to aging

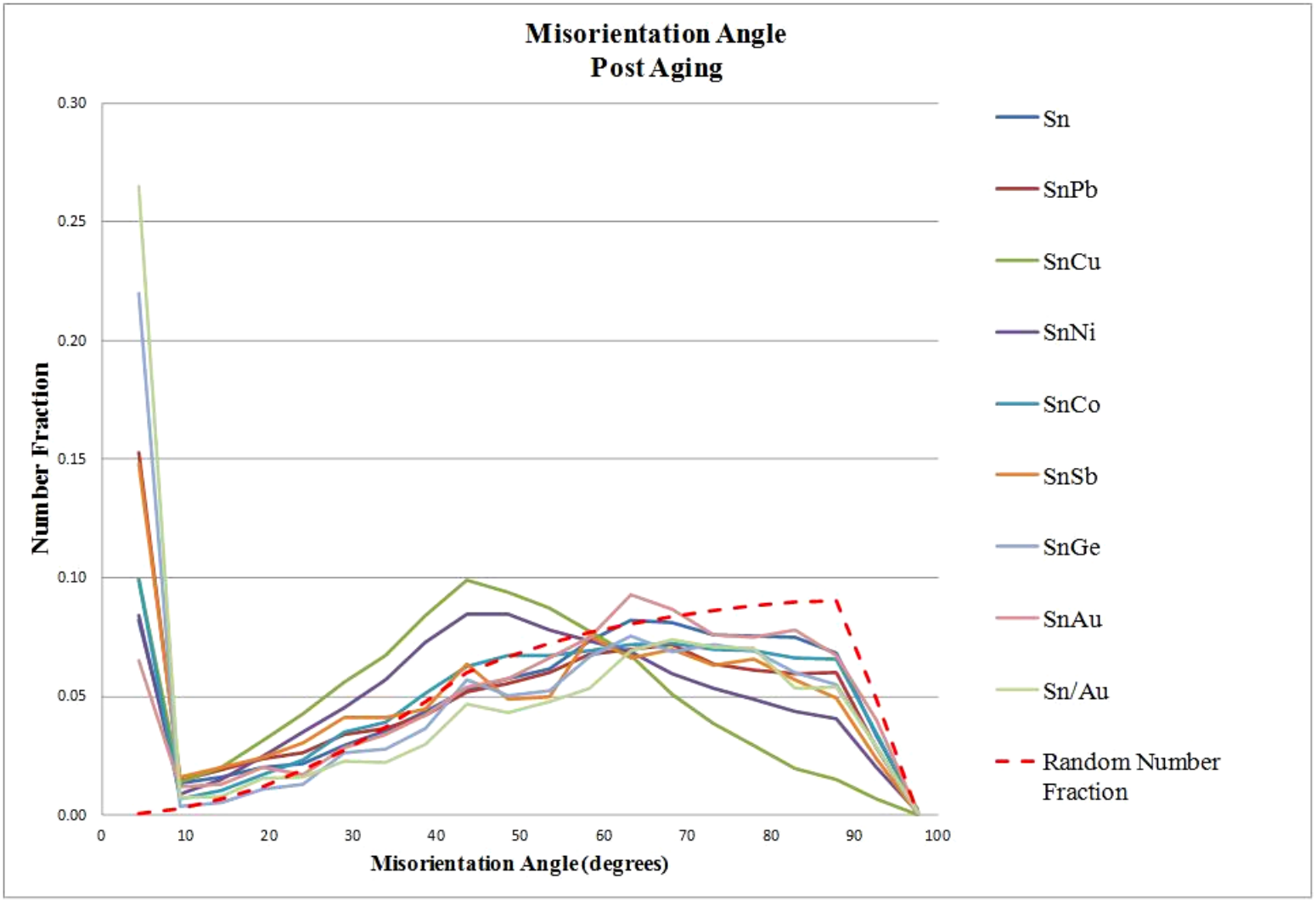

Figure 109. Misorientation angle distribution for all films post aging

5.6.5 Misorientation Distribution Function (MODF) Plots

The misorientation data for each film was also plotted on Misorientation Distribution Function (MODF) Plots which show the axis/angle character of all grain boundaries in a scan. Rotation of a single grain around the misorientation axis using the given misorientation angle will bring the two misoriented grains into coincidence. As examples, the MODF plots for pure Sn and for SnGe are shown in Figures 105-106 (note that the values in the legend are different). The plots for all of the films can be found in Appendices J-R.

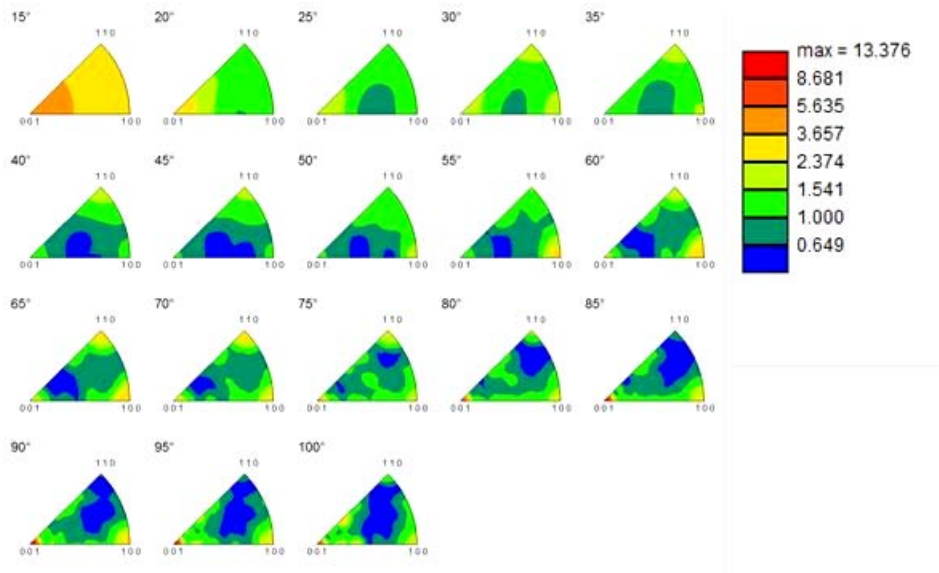

Figure 110. MODF Plot of pure Sn prior to aging

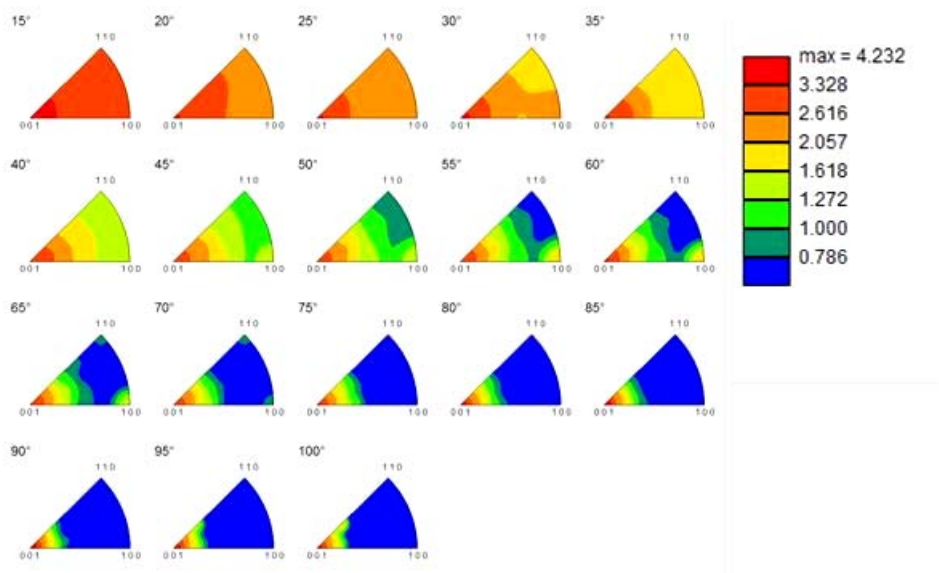

Figure 111. MODF Plot of SnGe prior to aging

As in the pole figure data, there did appear to be a trend between the maximum intensity number and the whisker density for all films except the SnAu and Sn/Au films. This is to be expected since they are both measuring the random distribution.

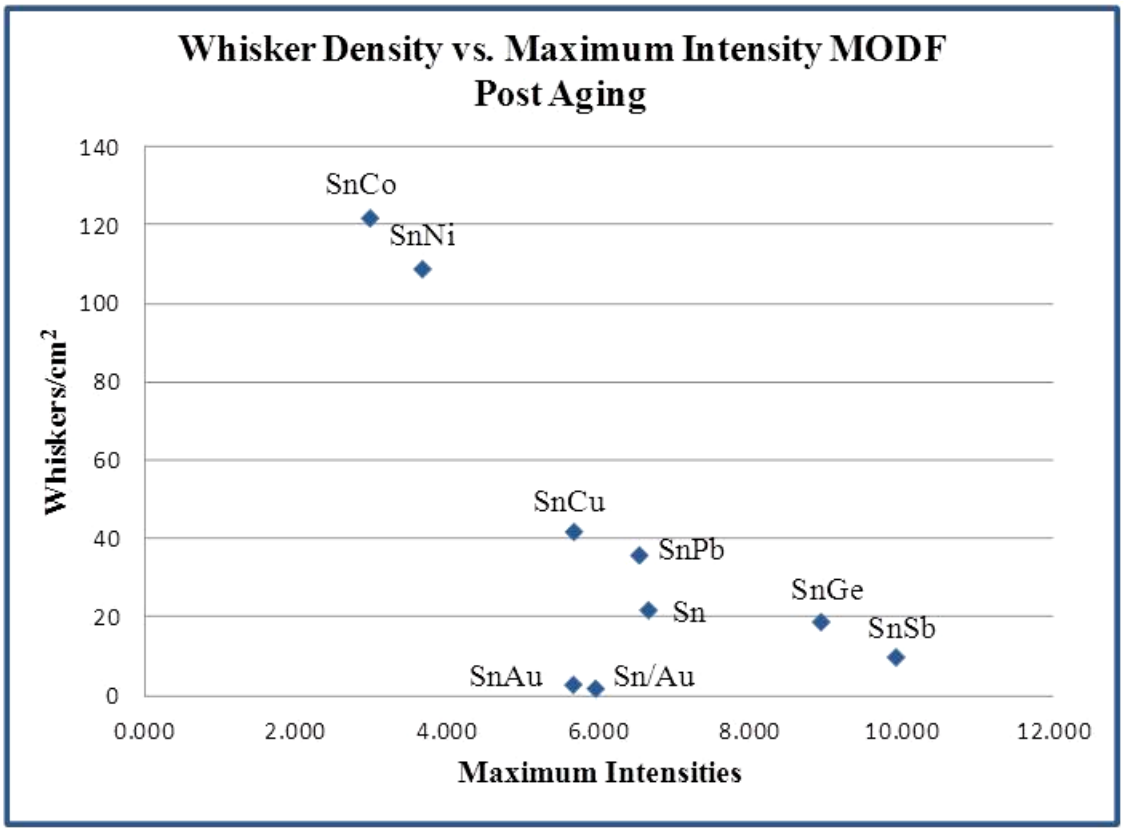

Figure 112. MODF maximum intensity vs. whisker density post aging

5.6.6 Stiffness vs. Crystallographic Orientation

It is known that the c-direction of the tin lattice has a higher single-crystal directional stiffness than the a-direction [32] (about 1.6 times the a-direction). Tin grains with the c-direction oriented normal to the substrate that are surrounded by one or more tin grains also c-direction oriented but in the plane of the substrate might experience high stresses, if intermetallics form between the grains or if exposed to thermal cycling. We theorized at the beginning of the program that these grains might be more prone to form whiskers.

For example, Figure 113 shows an EBSD map of a the SnSb plated film in which the grains with the c-direction oriented normal to the substrate are colored blue and tin grains with the c-direction oriented in the plane of the substrate are colored red. The colored grains in Figure 113 have a tolerance of 15 degrees. The red grains would transmit the stresses caused by intermetallic growth to the blue grains (due to their higher stiffness in the plane of the substrate)

which in turn might make the blue grains more susceptible to whisker formation than other grains.

The percentages of grains with their c-direction oriented normal and parallel to the specimen substrates are shown in Table 25 (15 degree tolerance). If the grains in the substrate plane (red grains) did transmit stresses to the grains normal to the substrate (blue grains), then it would be expected that SnSb, which had approximately 65% of the grains c-direction aligned in the substrate plane to have a lot of stress transmitted to the normal grains (~0.6%) resulting in few, but very long whiskers. This was not the case, the SnSb longest whisker was approximately 55 microns and most were <20 microns.

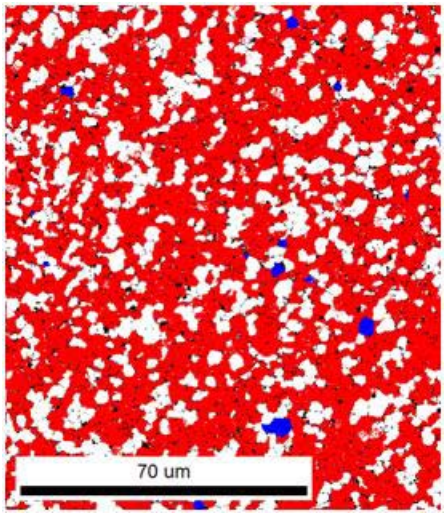

Figure 113. EBSD crystal direction map of SnSb prior to aging; blue grains indicate C-direction normal to the substrate, red indicates grains in plane (15 degree tolerance)

Film	Post Plating		Post Aging	
	C-Direction Aligned with Sample Normal	C-Direction Aligned with Sample Plane	C-Direction Aligned with Sample Normal	C-Direction Aligned with Sample Plane
Sn	0.1%	13.6%	0.1%	13.1%
Sn/Au	0.1%	13.6%	0.3%	11.8%
SnAu	0.7%	22.6%	0.1%	25.1%
SnCo	3.3%	17.6%	4.8%	3.7%
SnCu	4.1%	1.5%	10.2%	0.5%
SnGe	18.9%	3.6%	9.1%	13.4%
SnNi	5.0%	1.0%	10.5%	1.3%
SnPb	0.1%	32.9%	0.2%	31.1%
SnSb	0.6%	65.4%	0.3%	65.3%

Table 25. EBSD crystal direction data for c-Direction aligned grains normal to the plane of the substrate and in the plane of the substrate

6.0 Conclusions and Implications for Future Research

6.1 Conclusions and Observations

We have demonstrated that a small addition of Au, Sb, and Ge to electroplated Sn significantly suppresses the formation of tin whiskers. A thin film layer of sputtered Au over plated pure Sn has an even greater impact in reducing the formation of whiskers.

It was observed during the scanning electron microscope inspection, that on the gold-doped and germanium-doped films, intermetallics or elemental gold and germanium precipitated out as fine particles leaving small nano-pores in the films. Although there were no obvious precipitates noted on the surface of the antimony-doped film, the film was very porous. Whether this change in porosity was the cause of the reduction in whisker formation will require additional research.

It was also observed during SEM inspection, that although there were particles of intermetallics or elemental nickel and cobalt in the SnNi and SnCo samples, there was no

evidence that they precipitated out of the film. These were the samples with the highest whisker densities.

The SnCu film had a higher whisker density than pure tin at 8,000 hours and SEM images taken at that time show particles still in matrix. By 12,000 hours, the particles began to precipitate out of the matrix and the whisker growth dropped off significantly, which reinforces the notion that void or stress relief formation may mitigate whisker formation.

EBSD data shows a general trend that the lower the pole figure maximum intensity (the more random the texture), the more likely a film was to form whiskers.

There was general trend that indicated that the smaller the grain size, the more likely the film was to form whiskers.

6.2 Implications for future research

The Sn/Au had the lowest whisker density of all the films in this study. This thin Au film was applied using sputtering, which may be impractical with circuit board processes and manufacturing. However, the thin film Au layer could also be deposited using either electroplating or as an electroless gold film on the surface of the tin. Plated Au is commonly used is the electronics industry and is readily available. Studies should be performed to determine if the strike of plated Au has the same effect as the sputtered film. Different thicknesses of plated gold should be investigated as well.

It was not clear from Arnold's original paper whether these films were incorporated into tin plated films or whether some of them were simply applied to the surface of the pure tin as a thin layer. Since the Au thin film layer deposited on top of the pure tin electroplating had the best results, we would suggest depositing thin film layers of Cu, Ge, Ni, Sb, and Co on the surface of the plated Sn. All of these metals can easily be evaporated or sputtered on the surface as a pure tin film to determine if they mitigate whisker formation more readily than when incorporated into the plating. Strikes of plated Cu or Ni films could also be easily implemented since they are both commonly plated materials.

Removal of the samples from the environmental chamber and/or SEM inspection likely has an effect on whisker growth and formation. Additional systemic research into the effect of sample inspection on whisker growth and formation needs to be studied.

Scanning transmission electron microscopy (STEM) analysis of the intermetallics formed during the aging process of the doped films is recommended. STEM has the best elemental mapping resolution of any analytical tool with resolution <0.25nm. It will help identify the composition of intermetallic formation, not only between the pure tin film and the dopants, but possibly more complex compositions formed from the tin, copper substrate, and dopant materials.

This study was preliminary and only one dopant level per element was investigated. Additional studies with multiple dopant levels of the same elements may yield even better results for some of the elements and should be investigated.

6.0 Literature Cited

1. S.M. Arnold, “Repressing the Growth of Tin Whiskers”, Plating, Vol. 53, 1966, pp. 96-99.
2. Keun-Soo Kim, Sun-Sik Kim, Alongheng Baated, Kyoko Hamasaki, Katsuaki Suganuma, Masanobu Tsujimoto, Isamu Yanada, “Whisker Growth on Sn Plating with or without Surface Treatment during Heat and Humid Environments”, TMS 2009 Annual Meeting & Exhibition, San Francisco, CA, February 15-19, 2009
3. EM/P-576, Thomas A. Woodrow, et. al., “Tin Whisker Mitigation Study: Phase I. Evaluation of Environments for Growing Tin Whiskers”, Project ID: CBTP-051-010-5132, The Boeing Company, August 1, 2003.
4. T. Gutowski, C. Murphy, & et.al., (2005). Environmentally beign manufacturing: Observations from japan, europe and the united states. *Journal of Cleaner Production*, *13*(1), 1-17. doi: 10.1016/j.jclepro.2003.10.004
5. Capt. M.E. McDowell, "Tin Whiskers: A Case Study", Aerospace App. Conf., 1993, pp. 207-215, http://nepp.nasa.gov/whisker/reference/tech_papers/mcdowell1992-tin-whiskers-a-case-study.pdf
6. Osterman, M. (2002). Mitigation strategies for tin whiskers. *CALCE EPSC*, Retrieved from http://www.calce.umd.edu/lead-free/tin-whiskers/TINWHISKERMITIGATION.pdf
7. H. Taylor (2000). *Inductively coupled plasma-mass spectrometry: Practices and techniques* . (2 ed.). San Diego, CA: Academic Press.
8. C. Johnson, R. Gemmen, C. Cross, “Alloy Films Deposited by Electroplating as Precursors for Protective Oxide Coatings on Solid Oxide Fuel Cells Metallic Interconnect Materials”, MS&T’06 conference, Cincinnati.
9. R. G. Canham, D. A. Aikens, Nicholas Winograd, and Glenn Mazepa, “Mechanism of Polarographic Reduction of Germanium(IV)in Acidic Catechol Medium”, The Journal of Physical Chemistry, Vol. 74, Number 6, March 6, 1970, pp. 1082-1087.
10. U.S. Patent 5750017, May 12, 1998.
11. U.S. Patent 6808614 B2, October 26, 2004.
12. U.S. Patent 3772168, November 13, 1973.
13. G. I. Medvedev, S. S. Kruglikov, and N. Yu. Fursova, Russian Journal of Applied Chemistry, Vol. 74, No. 11, 2001, pp. 1817-1820.
14. Yahui Zhang and Douglas G. Ivey, “Phase Formation in Gold-Tin Alloys Electroplated from a Non-cyanide Bath”, 2003 International Conference on Compound Semiconductor Manufacturing.
15. Test method for measuring whisker growth on tin and tin alloy surface finishes. (2008). *JEDEC Standard*. Arlington, VA: JEDEC Solid State Technology Association. Retrieved from http://www.jedec.org/Catalog/catalog.cfm
16. Boettinger, et. al., “Whisker and Hillock Formation on Sn, Sn–Cu and Sn–Pb Electrodeposits”, Acta Materialia, Vol. 53, 2005, pp. 5033–5050.
17. Cavalotti, et. al., “Phase Structure of Electrodeposited Alloys”, Electrochimica Acta, Vol. 50, 2005, pp. 4557–4565.
18. J. B. LeBret and M. G. Norton (2003). Electron microscopy study of tin whisker growth. Journal of Materials Research, 18, pp 585-593. doi:10.1557/JMR.2003.0076.
19. R. F Champaign & R. R. Ogden, (2010). Microscopy study of tin whiskers. *Journal of Failure Analysis and Prevention*, *10*, 444-449. doi: 10.1007/s11668-010-9392-1

20. "SEM Q & A." *Jeol Ltd*. n.d. 29. Print. <http://www.medicine.mcgill.ca/femr/SEM Sample Prep JEOL.pdf>.
21. Wang, S.B. "SEM metrology damage in polysilicon line and its impact on LWR evaluation." *Proc. SPIE 7272, Metrology, Inspection, and Process Control for Microlithography XXIII*. 72720N . (2009): n. page. Print. <http://proceedings.spiedigitallibrary.org/proceeding.aspx?articleid=1336378>.
22. Murakami, K., & Okano, M. (2010). Mechanism of generation and suppression of tin whiskers on tin. *Materials Transactions,, 51*(1), 143-151. Retrieved from http://www.jim.or.jp/journal/e/pdf3/51/01/143.pdf
23. Lee, B., & Lee, D. (1998). Spontaneous growth mechanism of tin whiskers. *Acta Materialia* , *46*(10), 3701-3714. Retrieved from http://www.sciencedirect.com/science/article/pii/S1359645498000457
24. Kaeshita, T., & et.al., (1982). Grain size effect of electro-plated tin coatings on whisker growth. *Journal of Material Science*, *17*(9), 2560-2566. doi: 10.1007/BF00543888
25. Brusse, J. A., Ewell, G. J., & Siplon, J. P. (2002, March). *Tin whiskers: Attributes and mitigation*. Carts 2002: 22nd capacitor and resistor technology symposium,. Retrieved from http://nepp.nasa.gov/DocUploads/5A676ED4-A9EF-4F3E-975B05515589AF7F/CARTS2002_JBRUSSE_article.pdf
26. John W. Osenbach, "Creep and its effect on Sn whisker growth''J. Applied Physics, Vol. 106, Issue 9, November 17, 2009, pp. 094903 through 094903-10.
27. W T Read and W Shockley, Dislocation models of crystal grain boundaries, *Physical Review*, Vol. 78, No. 3, pp. 275-289, 1950.
28. Grain boundary. In (2013). *Wikipedia*. Retrieved from http://en.wikipedia.org/wiki/Grain_boundary
29. Irina Boguslavsky and P. Bush, "Recrystallization Principles Applied to Whisker Growth in Tin", Proceedings of the APEX Conference, pp.S12-4-1 - S12-4-10 , March 31, 2003.
30. K.N. Tu, J.O. Suh, and Albert T. Wu, "Tin Whisker Growth on Lead-Free Finishes" in *Lead-Free Solder Interconnect Reliability*, ed. Dongkai Shangguan, ASM International, Materials Park, OH, August 2005.
31. George T.T. Sheng, C.F. Hu, W.J. Choi, K.N. Tu, Y.Y. Bong, and Luu Nguyen, "Tin whiskers studied by focused ion beam imaging and transmission electron microscopy", J. Applied Physics, Vol. 92, No. 1, July 1, 2002 2, pp. 64-69.
32. J.G. Lee, A. Telang, K.N. Subramanian, and T.R. Bieler, "Modeling Thermomechanical Fatigue Behavior of Sn-Ag Solder Joints", J. Electronic Materials, Vol. 31, 2002, pp. 1152-1159.

Appendix A: FIB Images for Pure Sn

FIB Images for Pure Sn
Post Plating

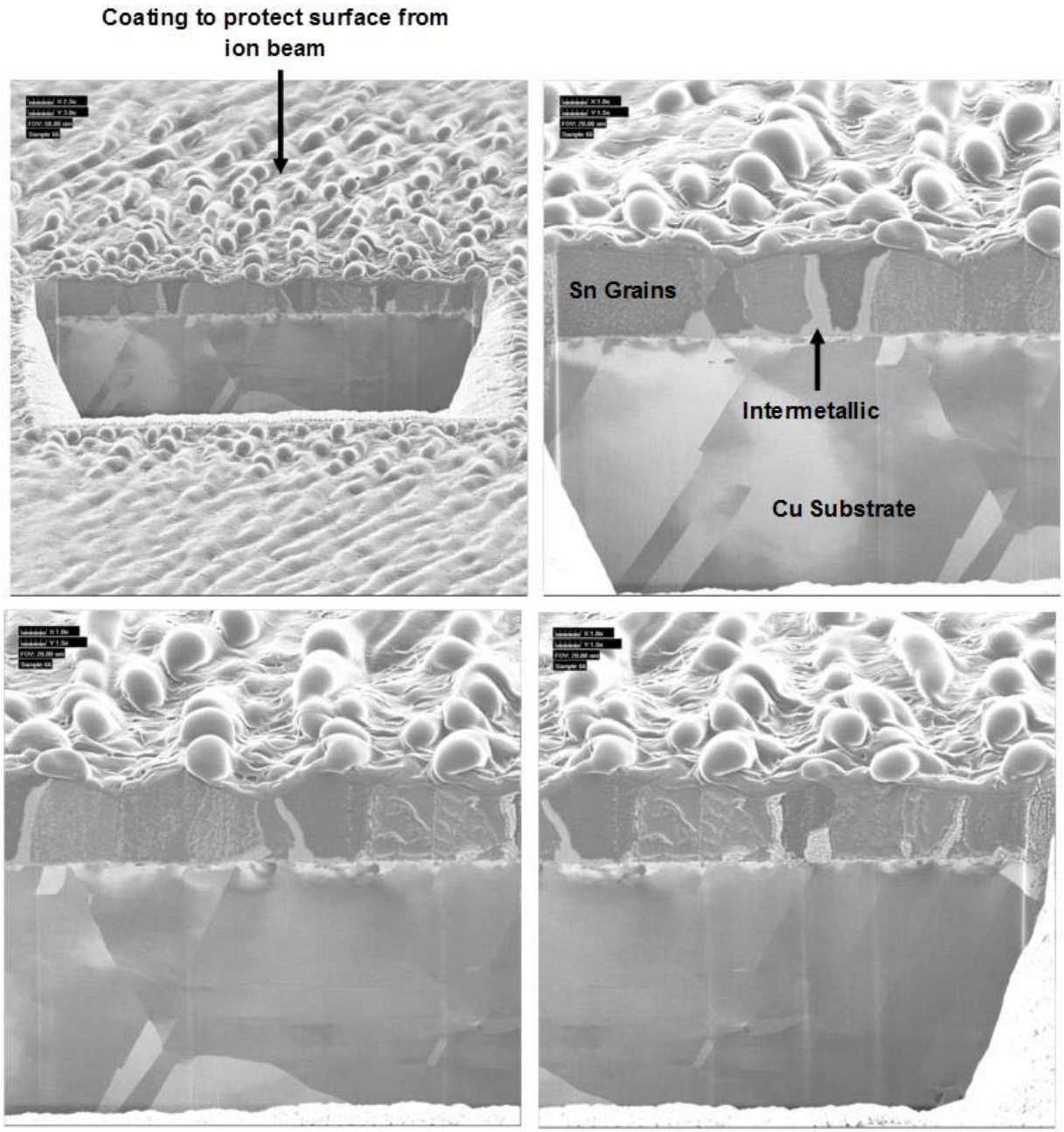

FIB Ion Images for Pure Sn – 1st Whisker
Post Aging 8,000 Hours at 50°C/ 50% Relative Humdity

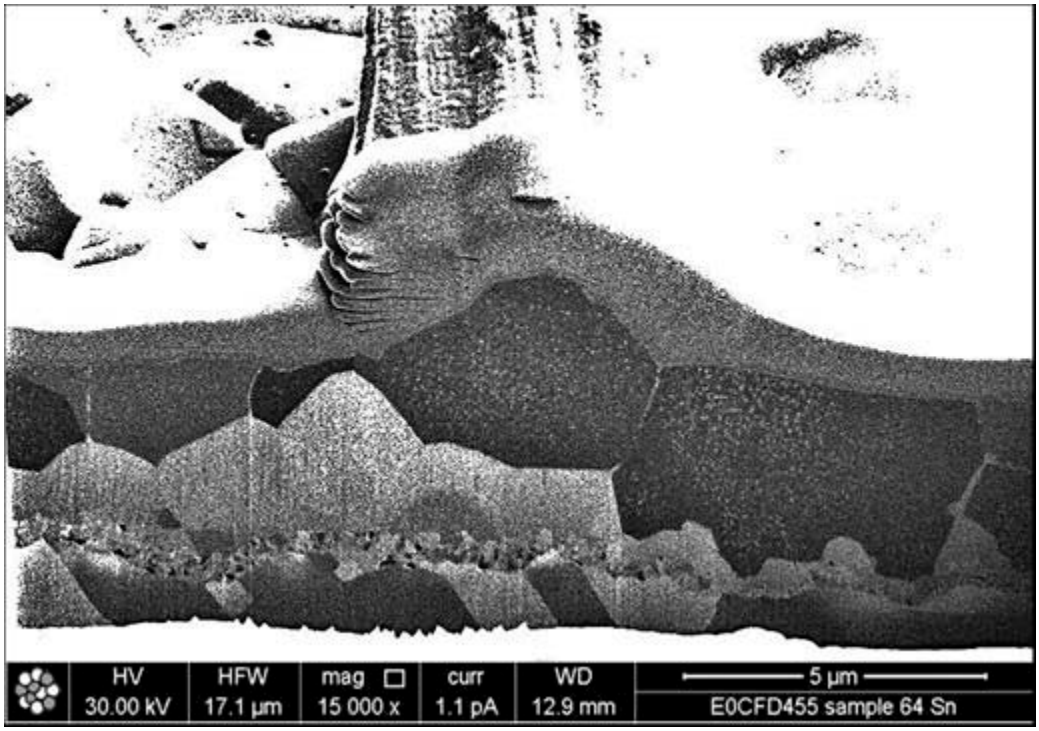

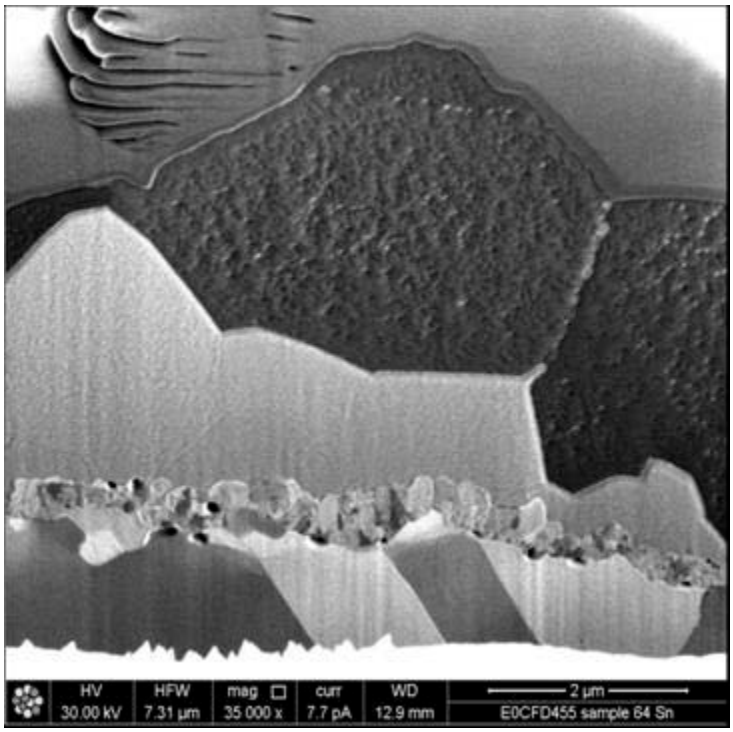

FIB Electron Images for Pure Sn – 1st Whisker
Post Aging 8,000 Hours at 50°C/ 50% Relative Humidity

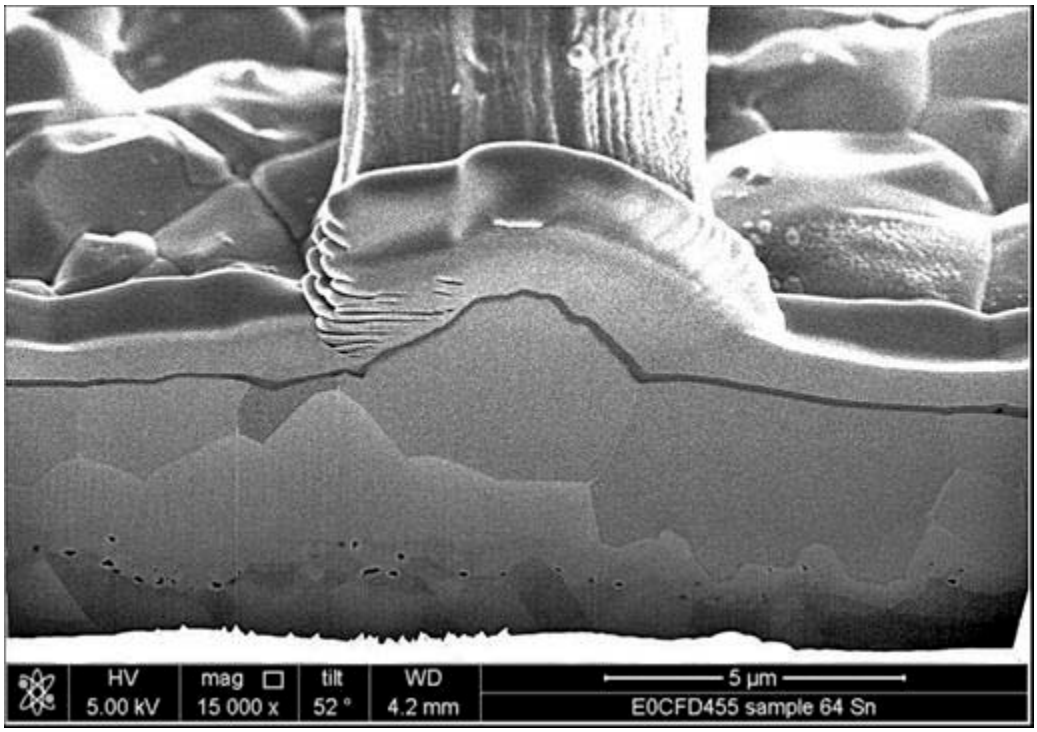

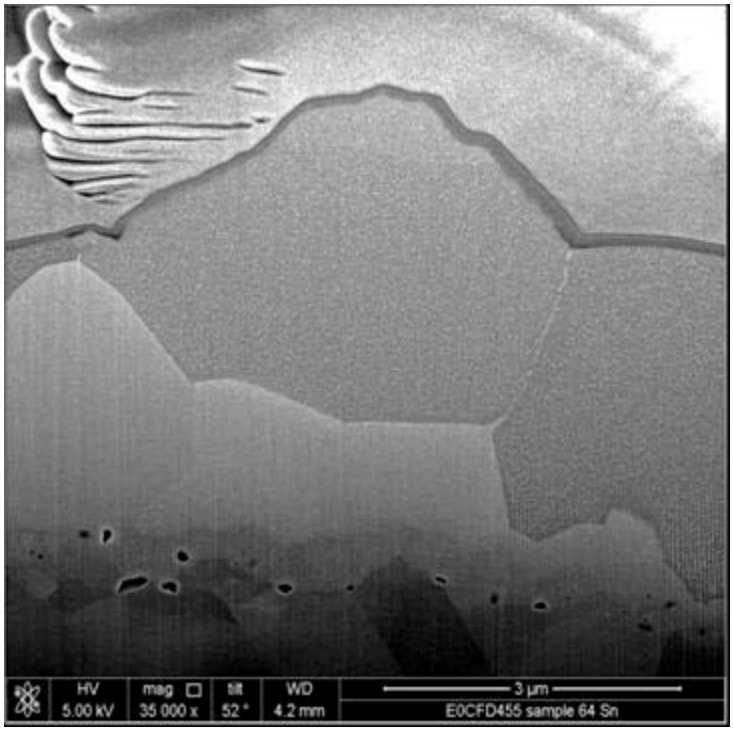

FIB Electron Images for Pure Sn – 1st Whisker
Post Aging 8,000 Hours at 50°C/ 50% Relative Humidity

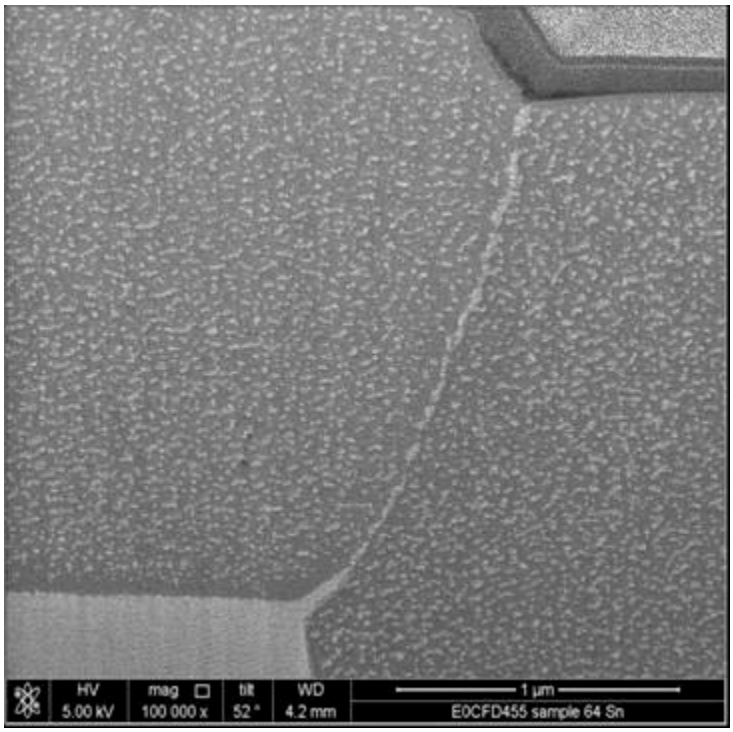

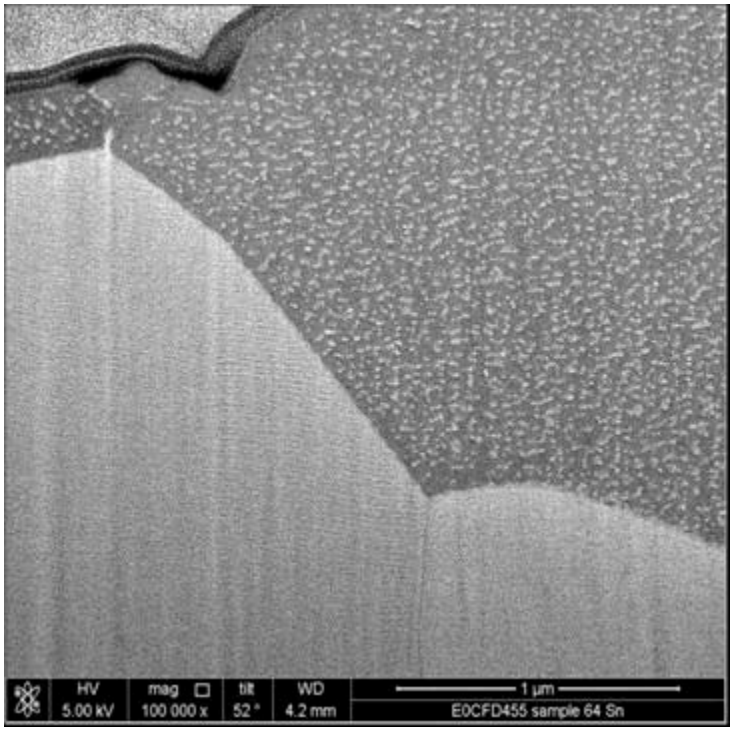

FIB Ion Images for Pure Sn – 2nd Whisker
Post Aging 8,000 Hours at 50°C/ 50% Relative Humidity

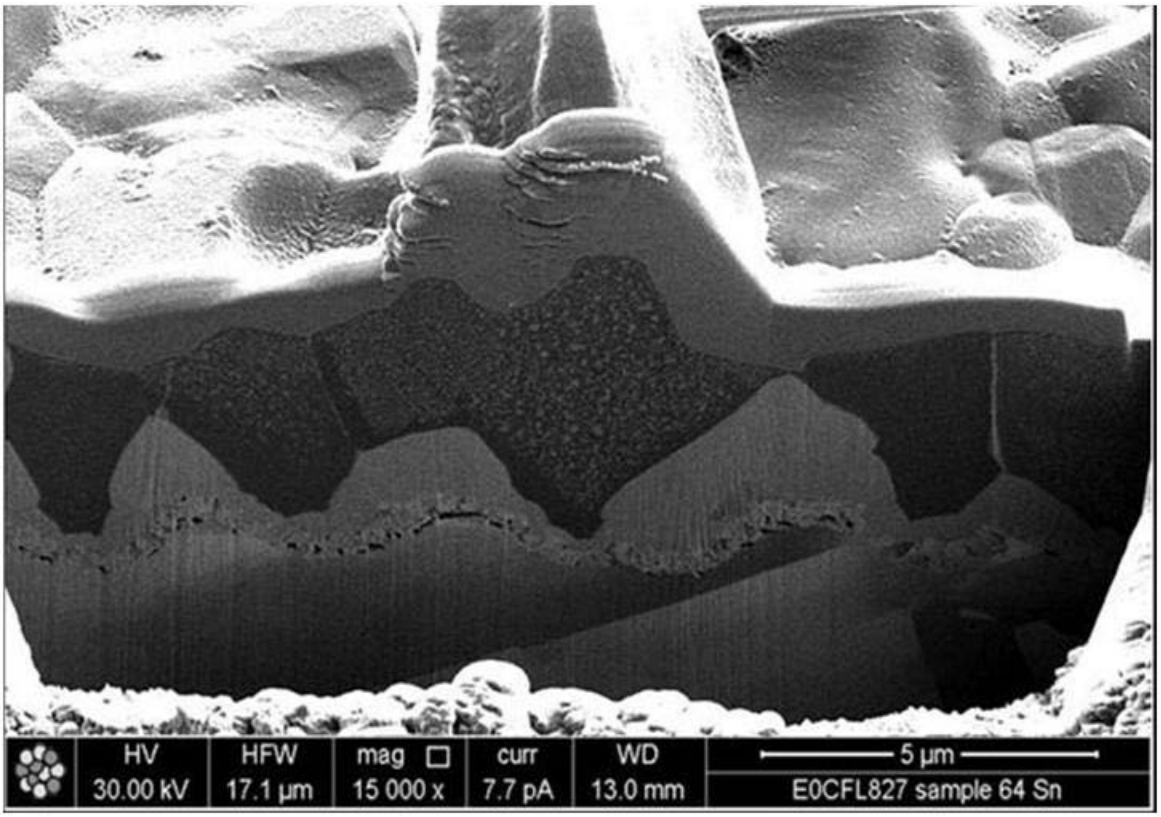

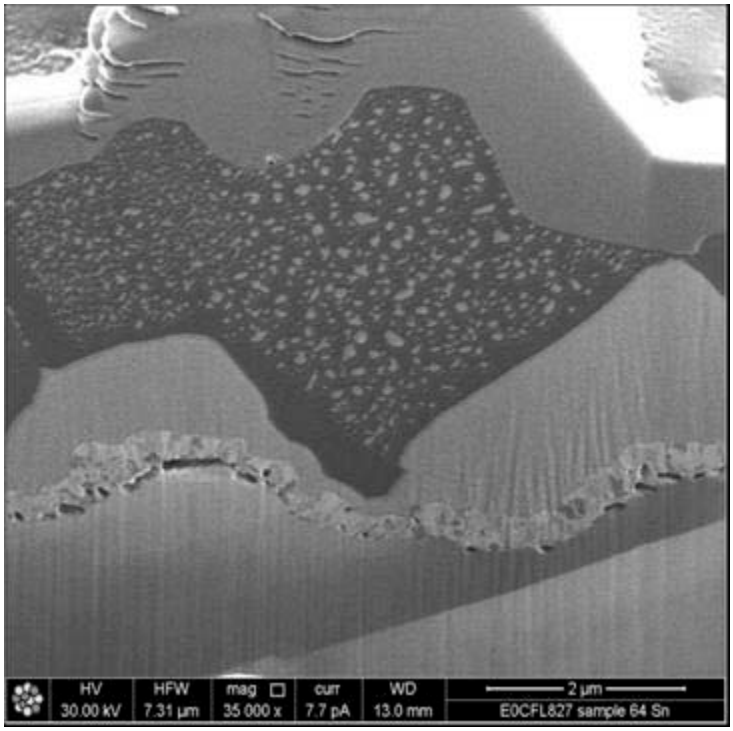

FIB Electron Images for Pure Sn – 2nd Whisker
Post Aging 8,000 Hours at 50°C/ 50% Relative Humidity

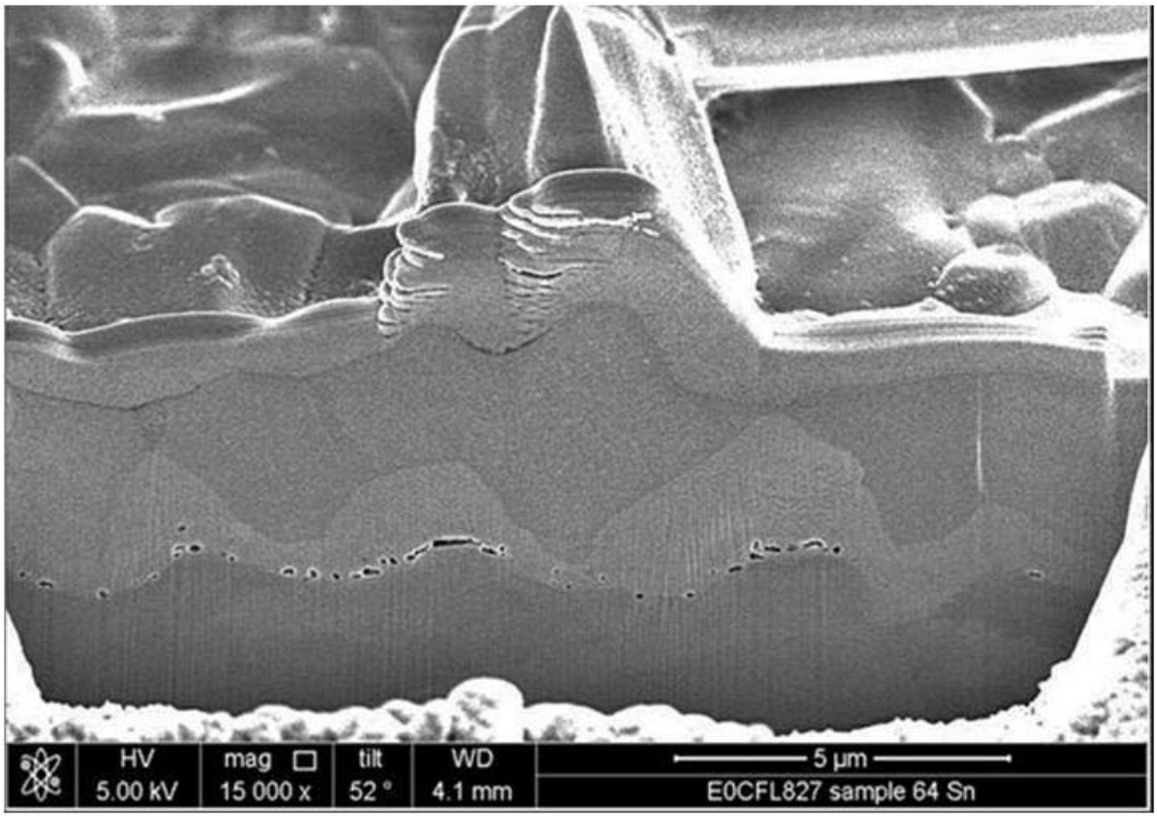

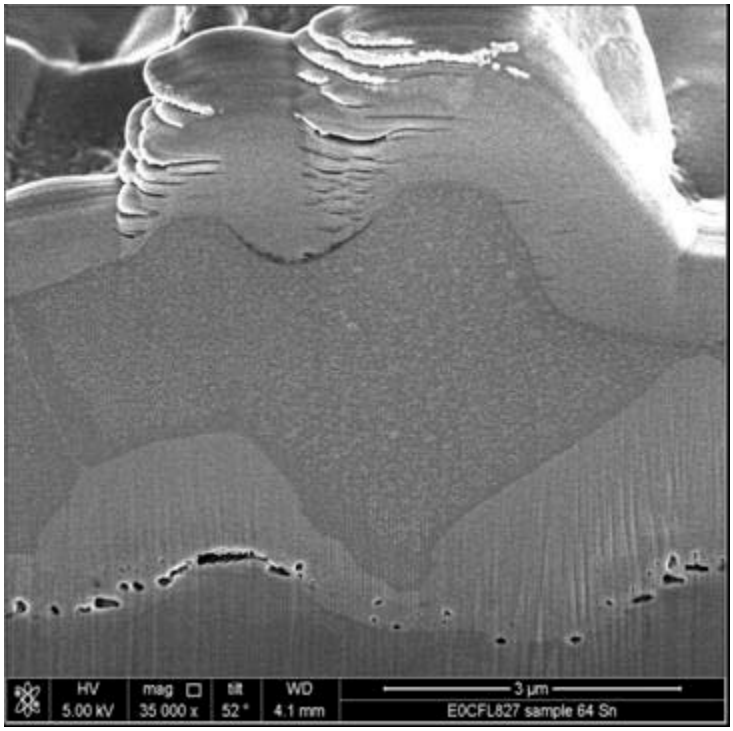

Appendix B: FIB Images for Sn with 3.1% Pb

FIB Images for Sn with 3.1% Pb
Post Plating

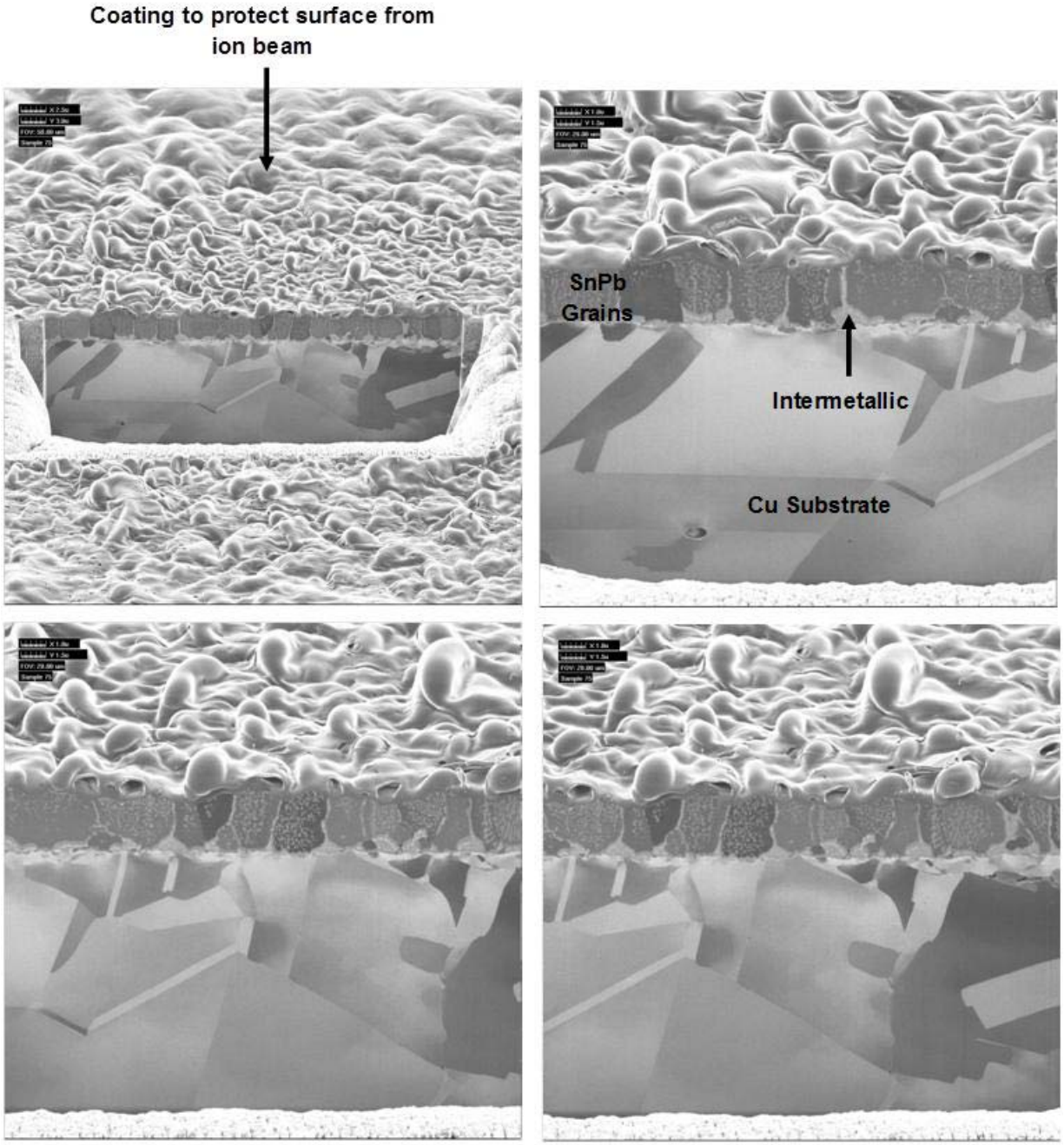

FIB Ion Images for Sn with 3.1% Pb – 1st Whisker
Post Aging 8,000 Hours at 50°C/ 50% Relative Humidity

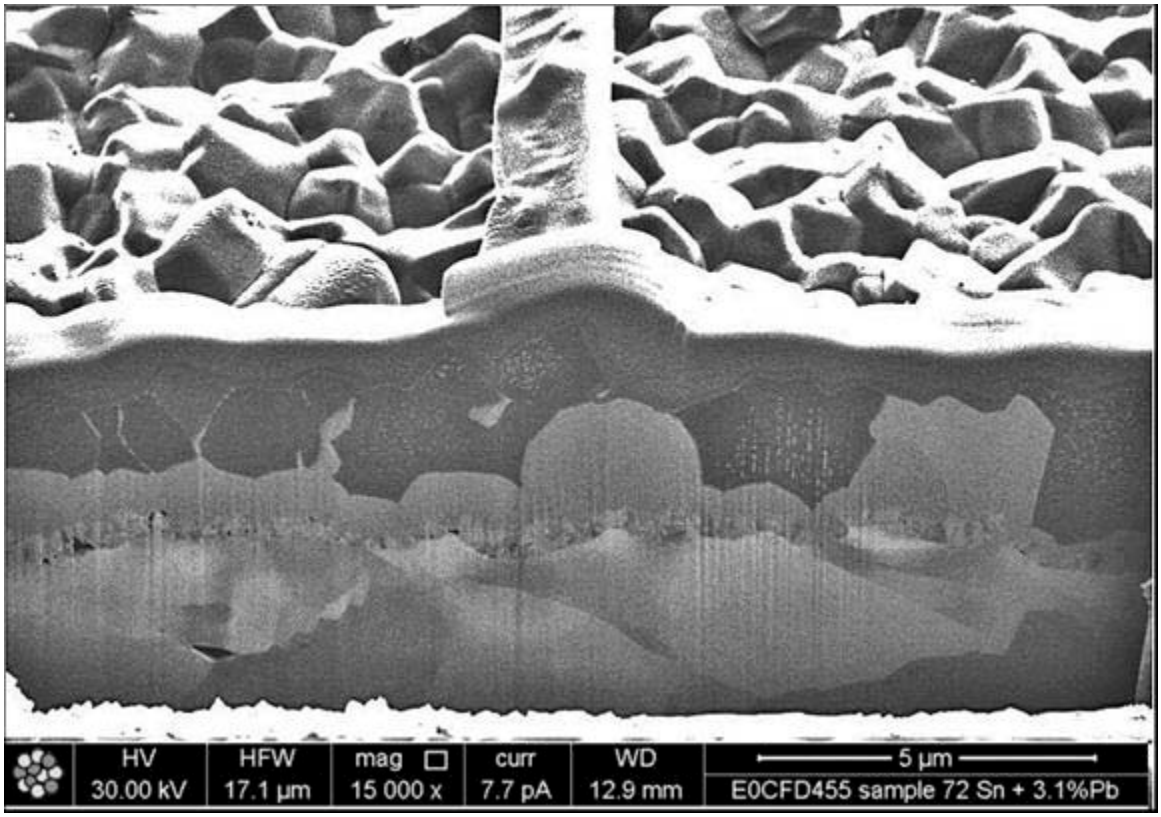

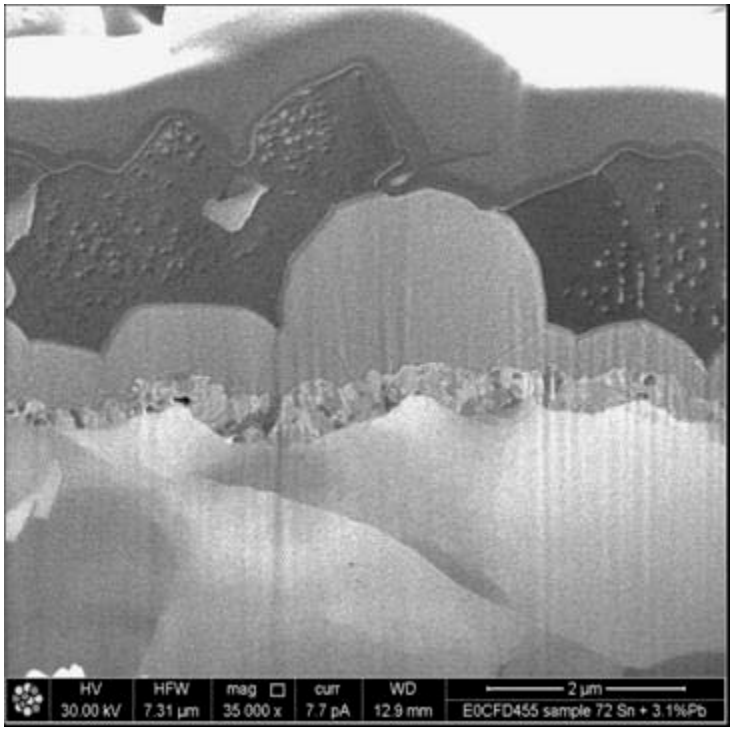

FIB Electron Images for Sn with 3.1% Pb – 1st Whisker Post Aging 8,000 Hours at 50°C/ 50% Relative Humdity

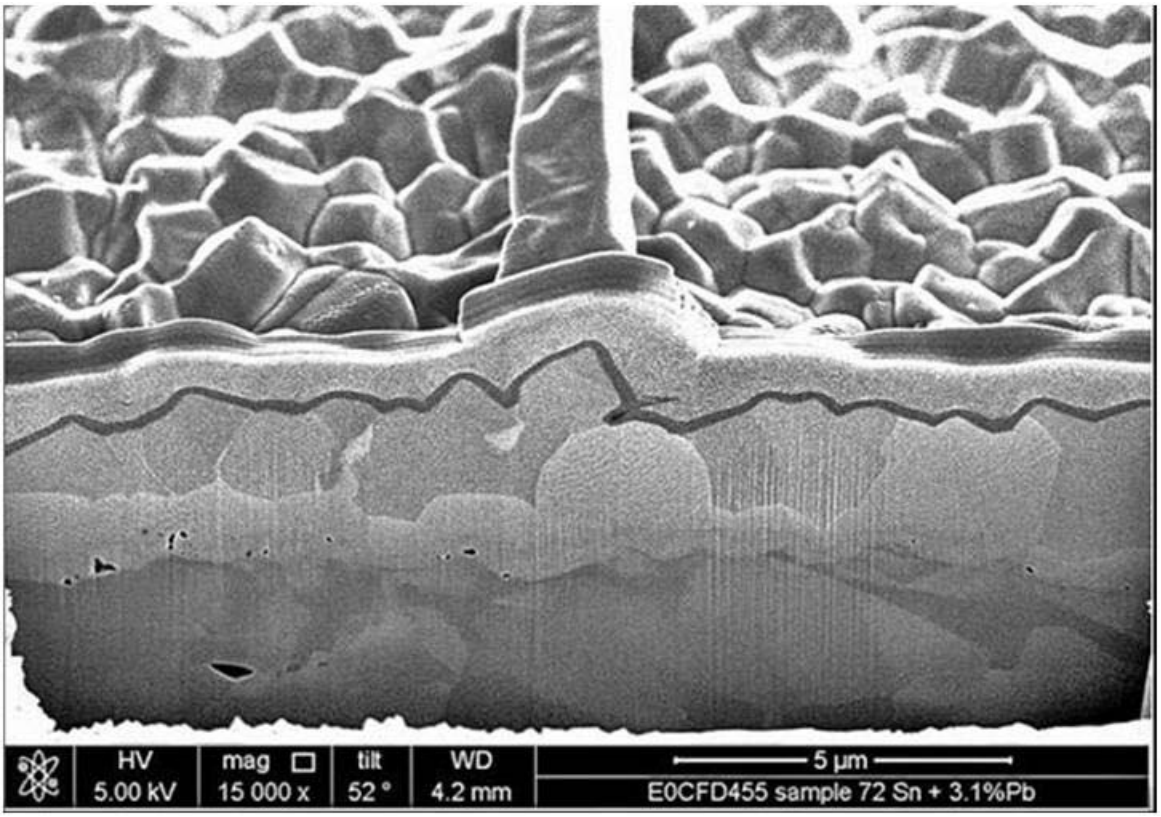

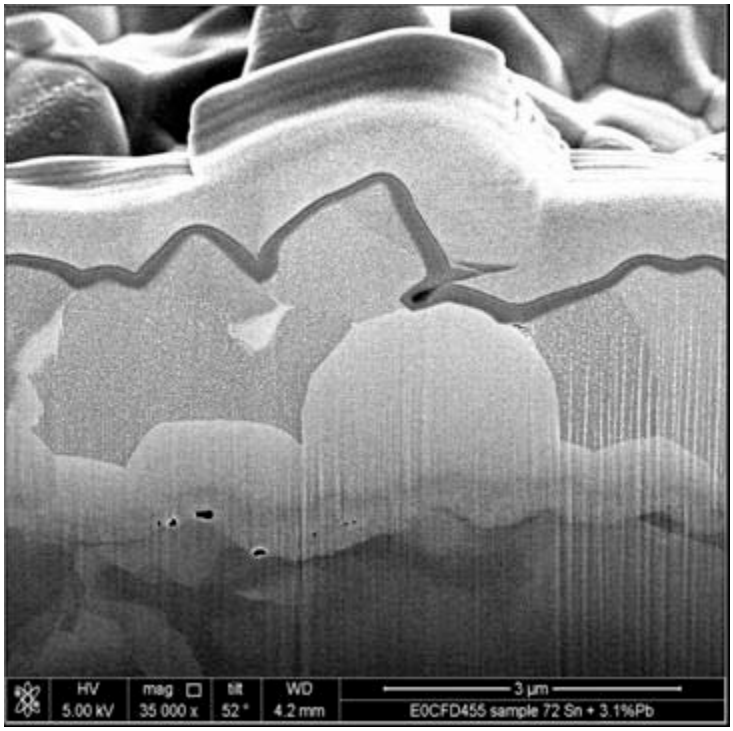

FIB Electron Images for Sn with 3.1% Pb – 1st Whisker Post Aging 8,000 Hours at 50°C/ 50% Relative Humidity

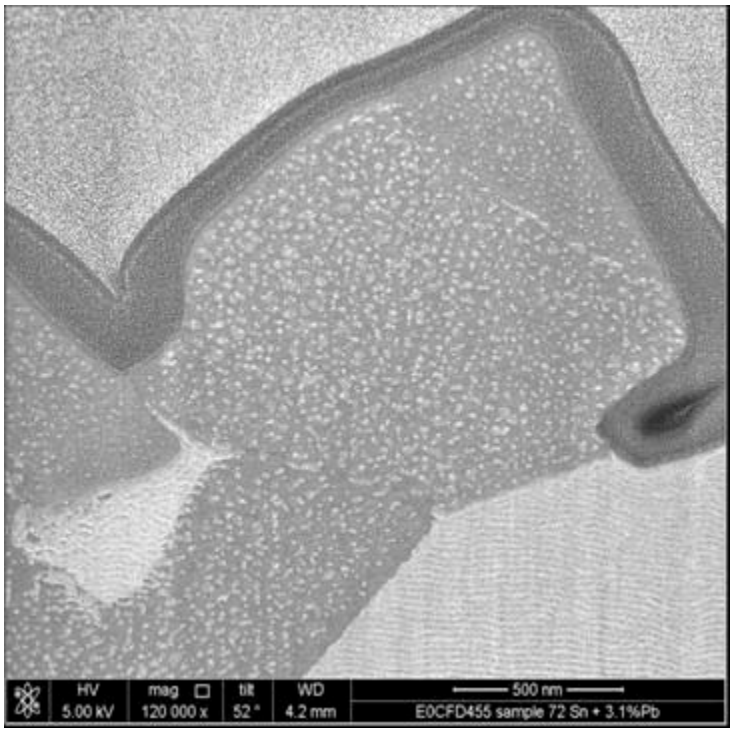

FIB Ion Images for Sn with 3.1% Pb –2nd Whisker
Post Aging 8,000 Hours at 50°C/ 50% Relative Humidity

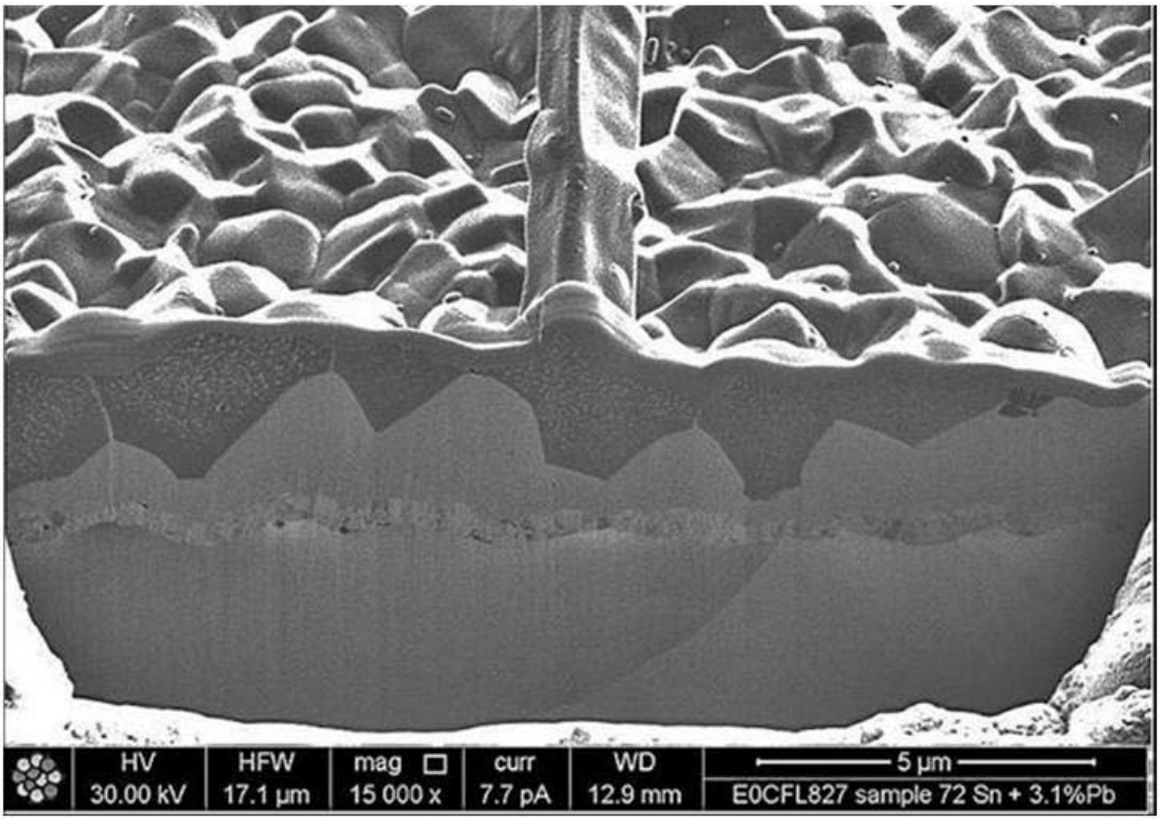

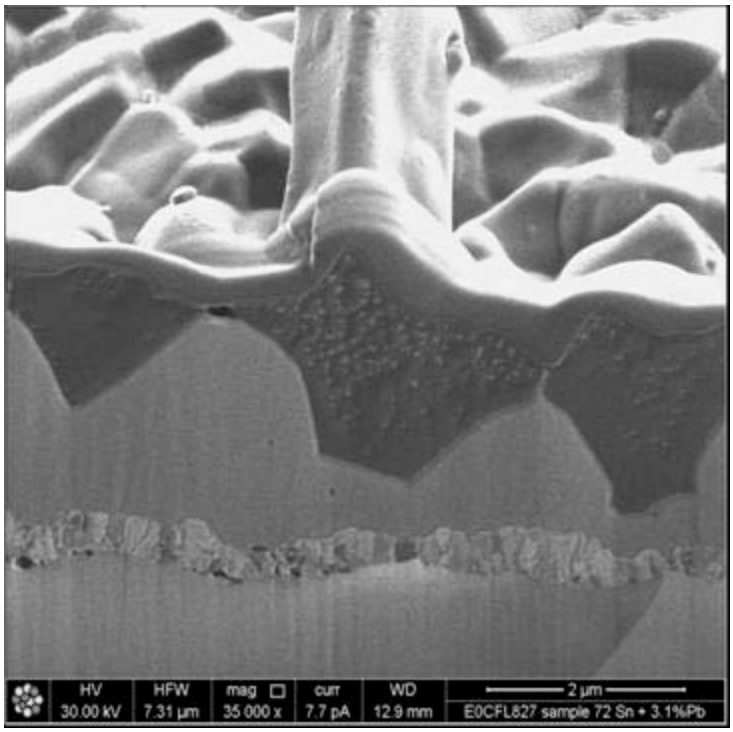

FIB Ion Images for Sn with 3.1% Pb –2nd Whisker
Post Aging 8,000 Hours at 50°C/ 50% Relative Humidity

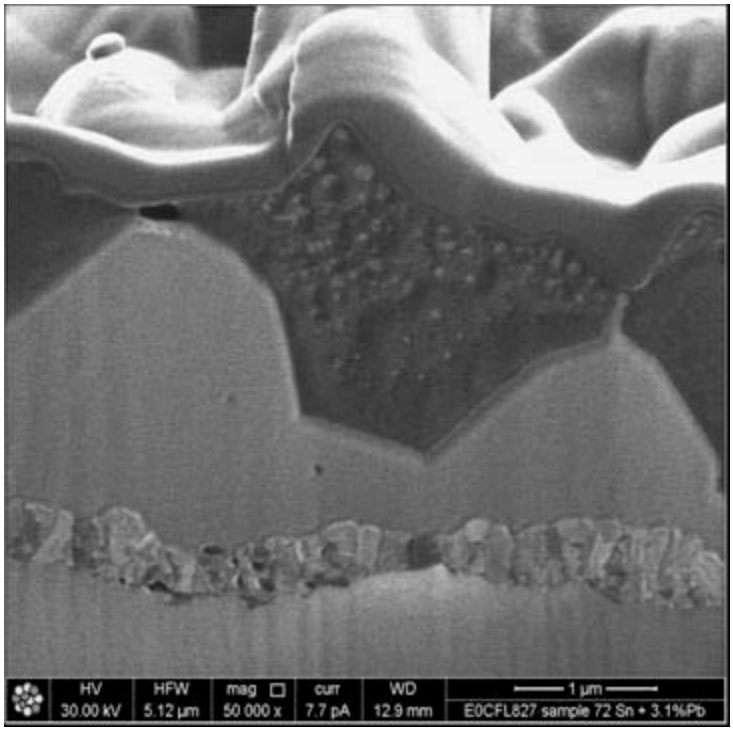

FIB Electron Images for Sn with 3.1% Pb –2nd Whisker Post Aging 8,000 Hours at 50°C/ 50% Relative Humidity

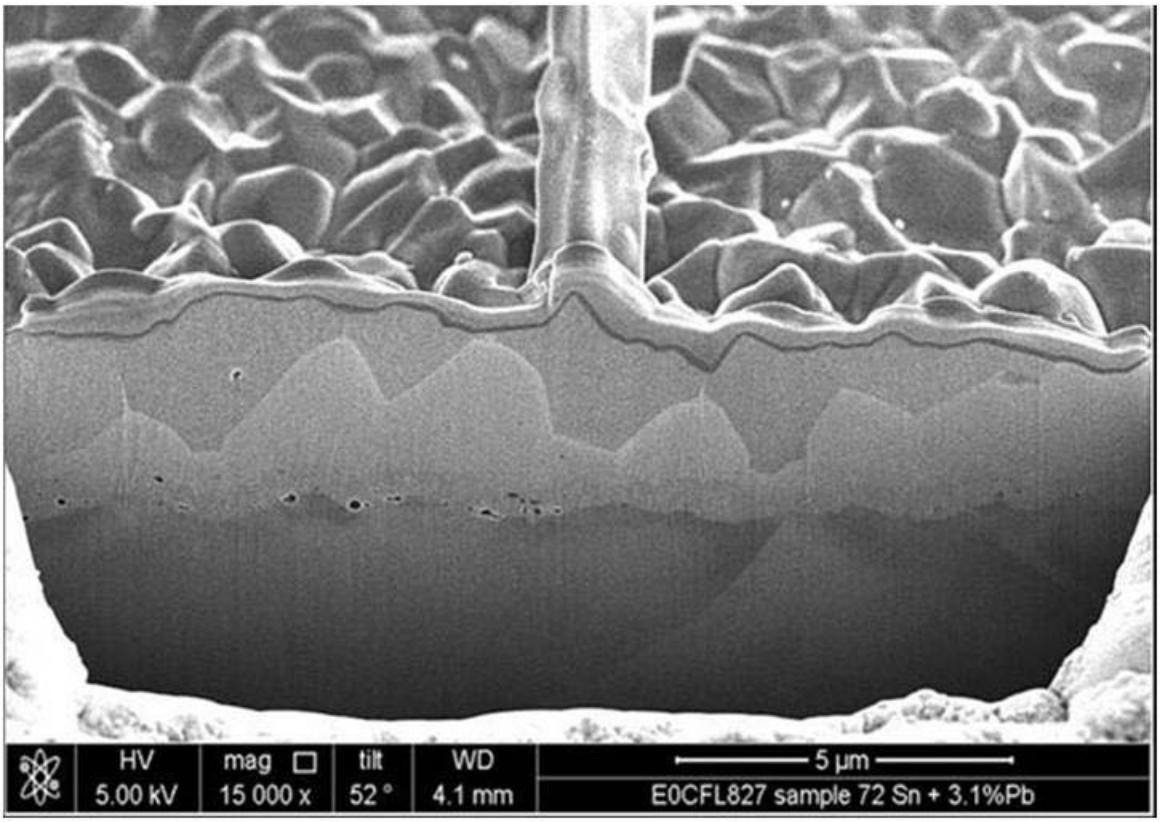

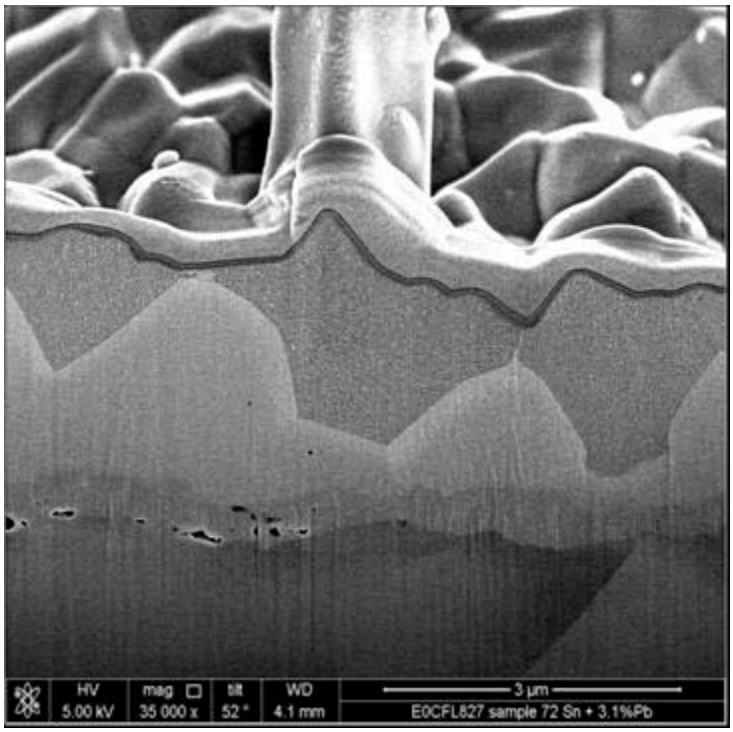

FIB Electron Images for Sn with 3.1% Pb –2nd Whisker Post Aging 8,000 Hours at 50°C/ 50% Relative Humidity

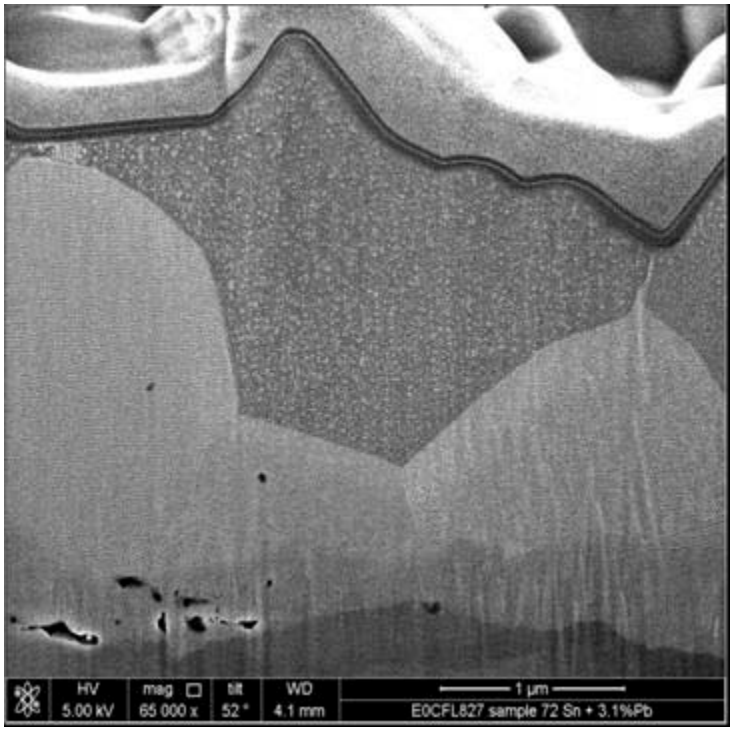

Appendix C: FIB Images for Sn with 2.1% Cu

FIB Images for Sn with 2.1% Cu
Post Plating

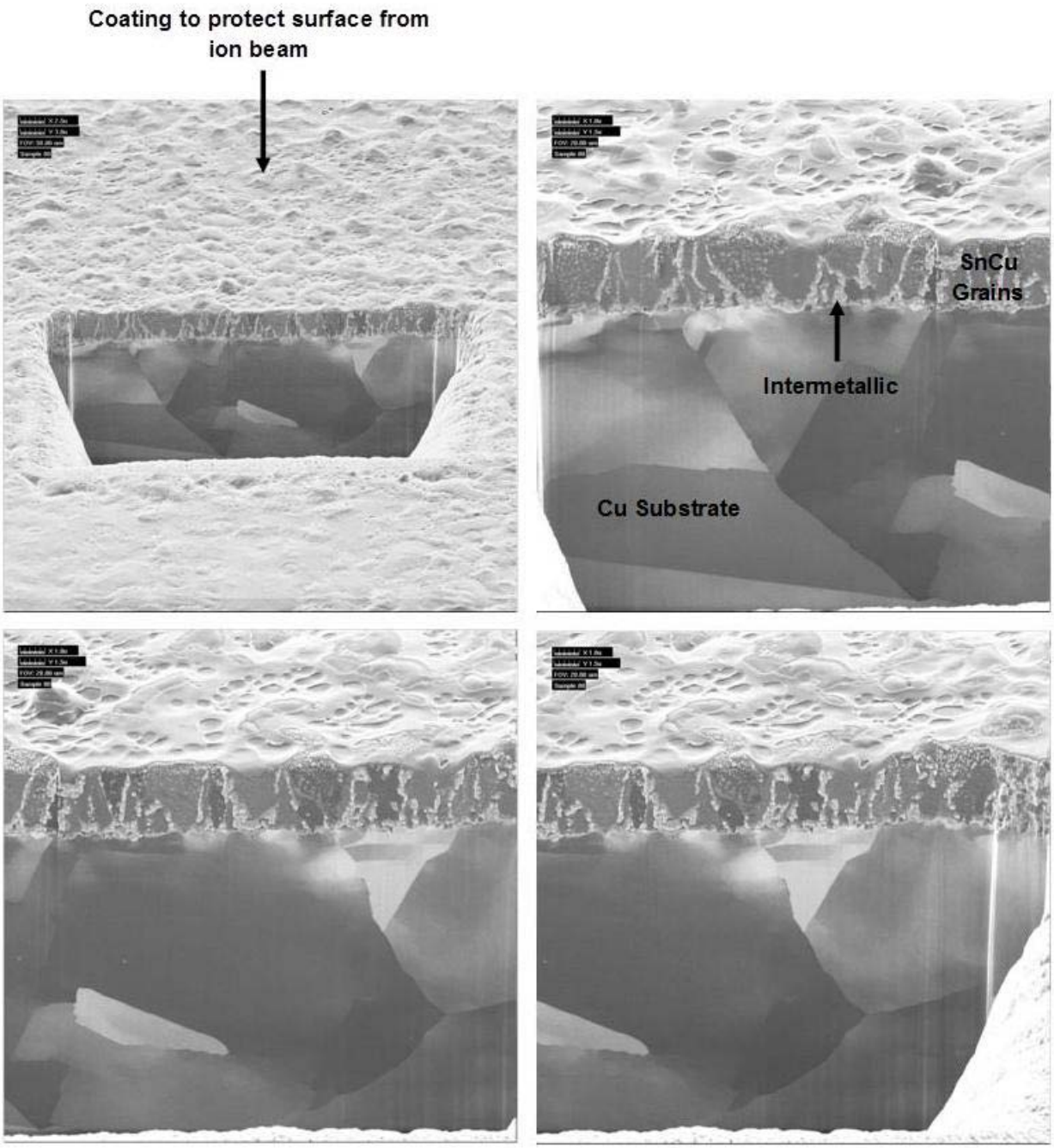

FIB Ion Images for Sn with 2.1% Cu – 1st Whisker
Post Aging 8,000 Hours at 50°C/ 50% Relative Humdity

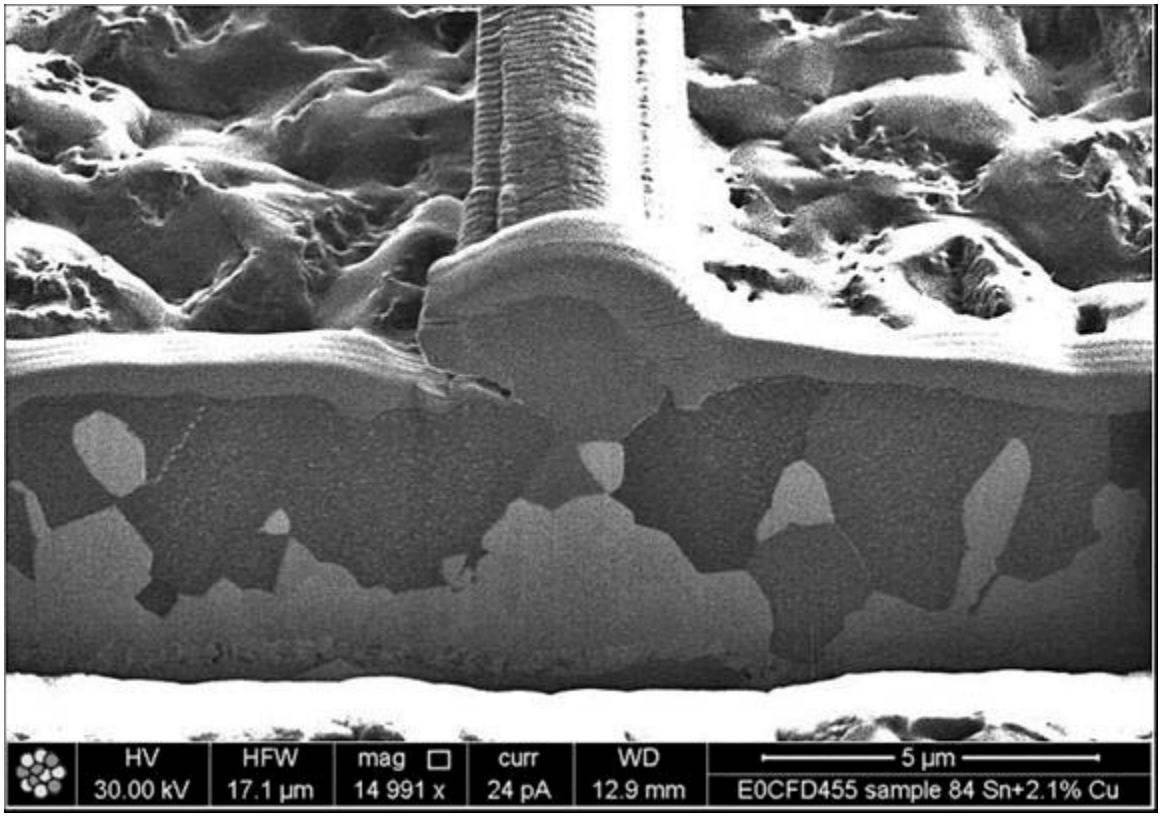

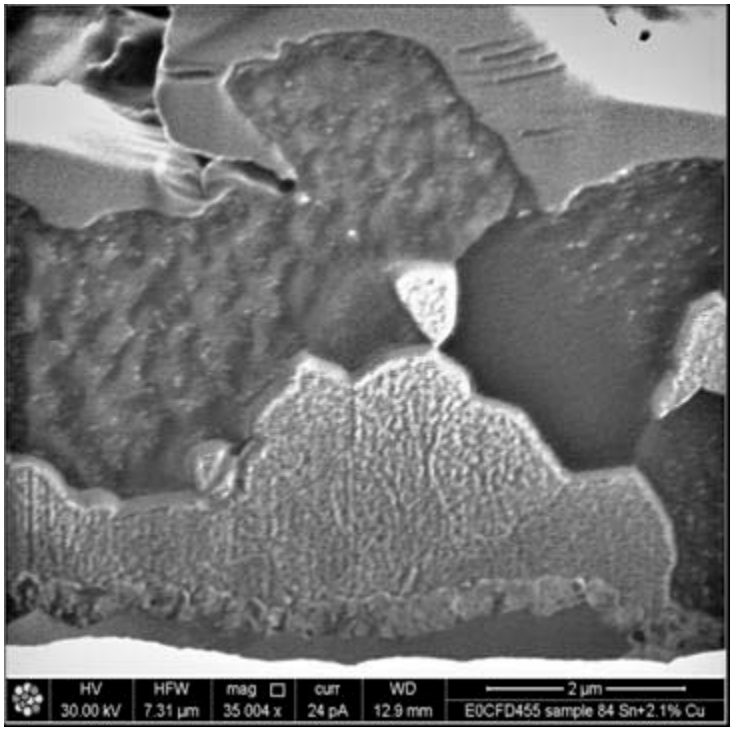

FIB Electron Images for Sn with 2.1% Cu – 1st Whisker Post Aging 8,000 Hours at 50°C/ 50% Relative Humdity

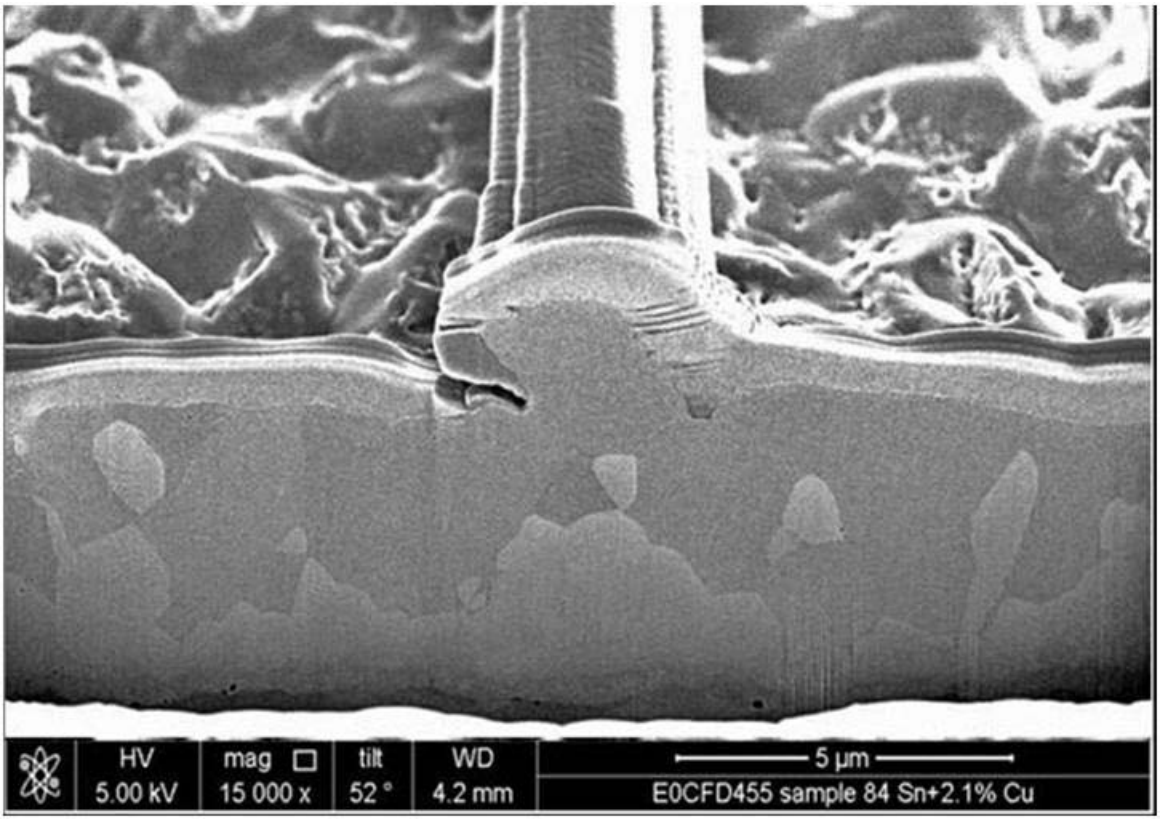

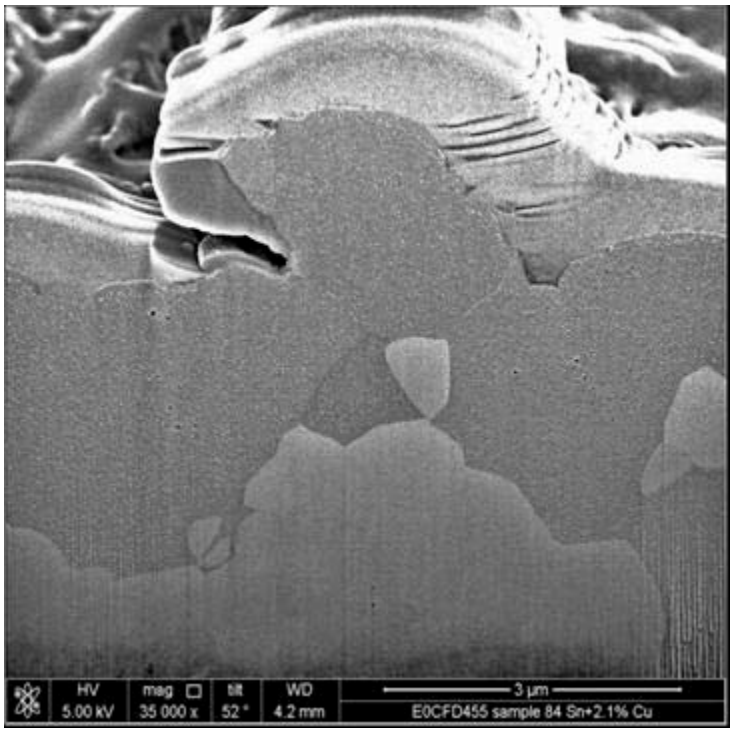

FIB Electron Images for Sn with 2.1% Cu – 1st Whisker Post Aging 8,000 Hours at 50°C/ 50% Relative Humdity

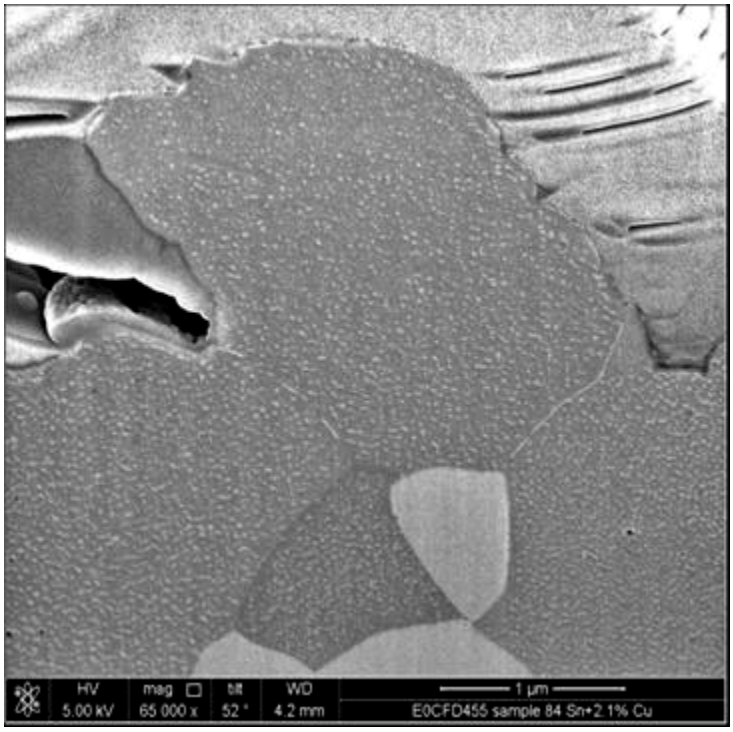

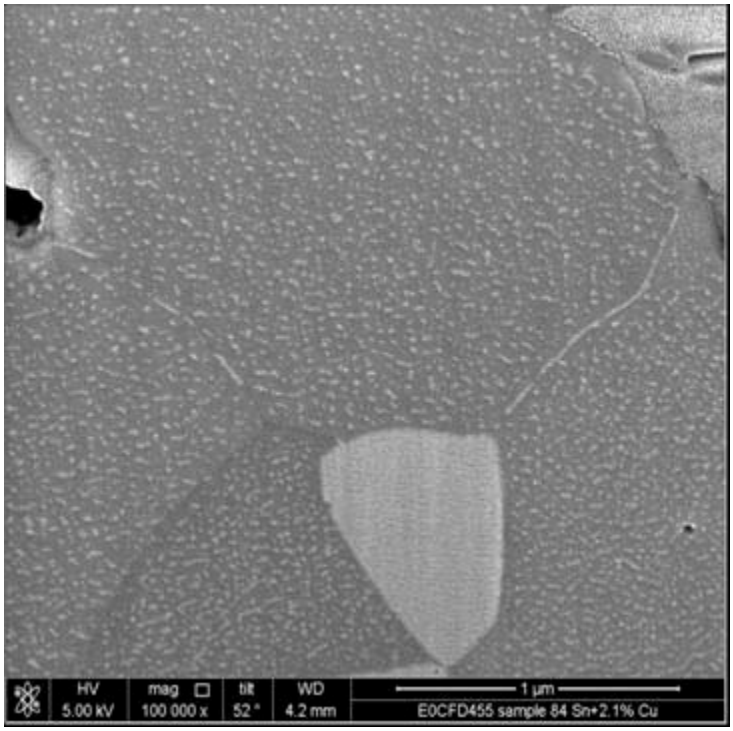

FIB Ion Images for Sn with 2.1% Cu – 2nd Whisker
Post Aging 8,000 Hours at 50°C/ 50% Relative Humdity

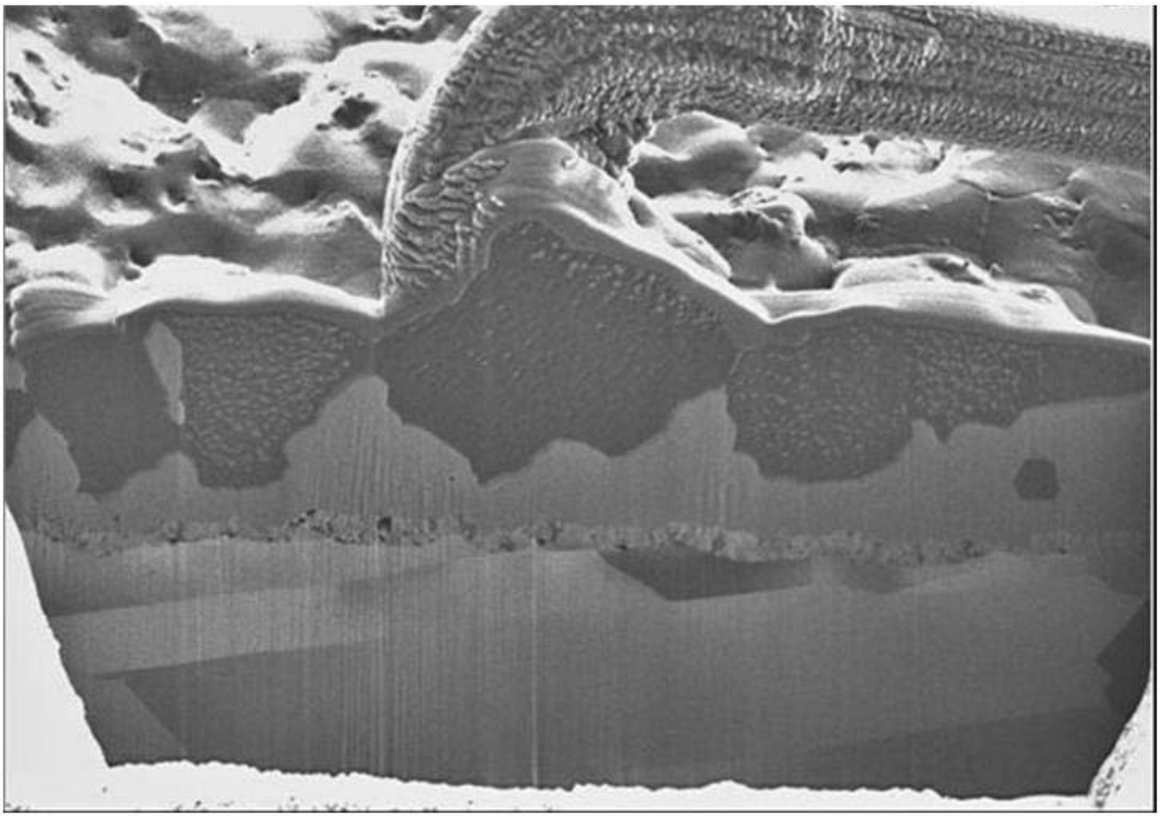

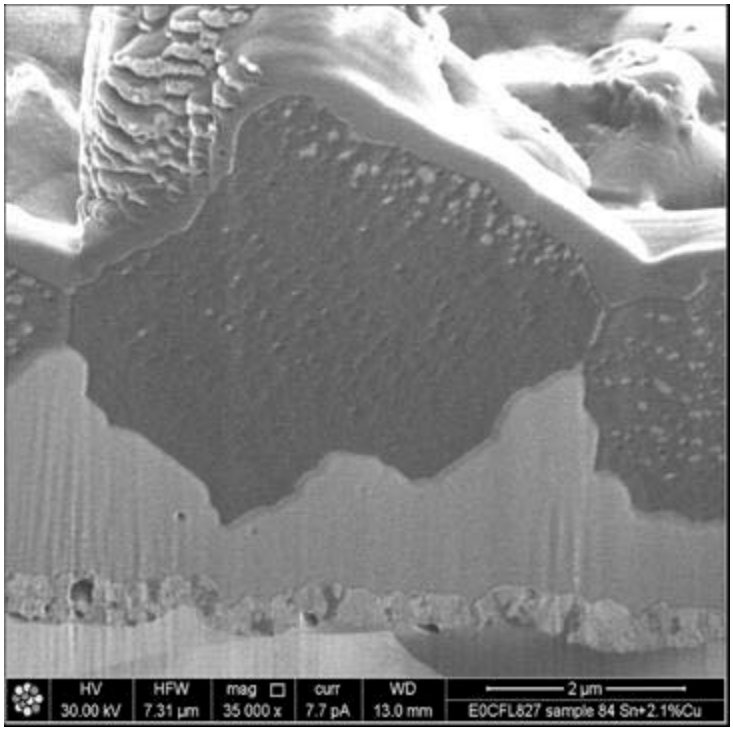

FIB Electron Images for Sn with 2.1% Cu – 2nd Whisker Post Aging 8,000 Hours at 50°C/ 50% Relative Humdity

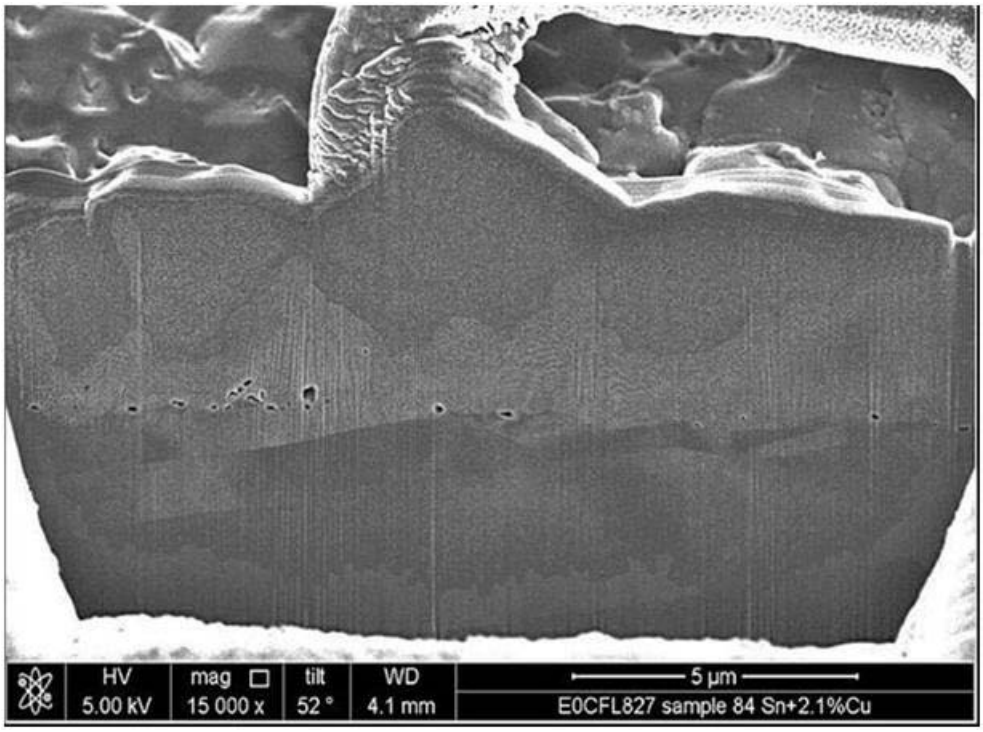

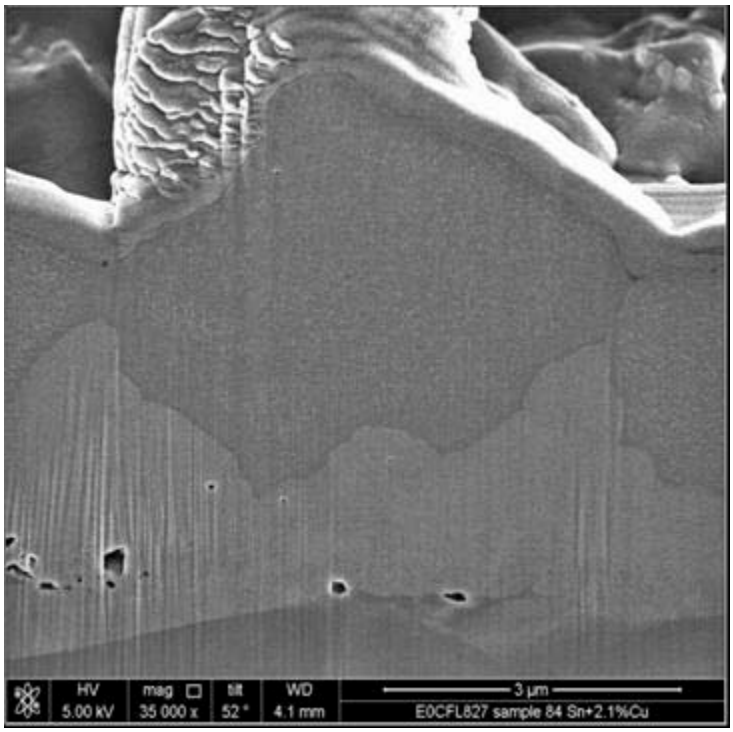

Appendix D: FIB Images for Sn with 3.0% Ni

FIB Images for Sn with 3.0% Ni
Post Plating

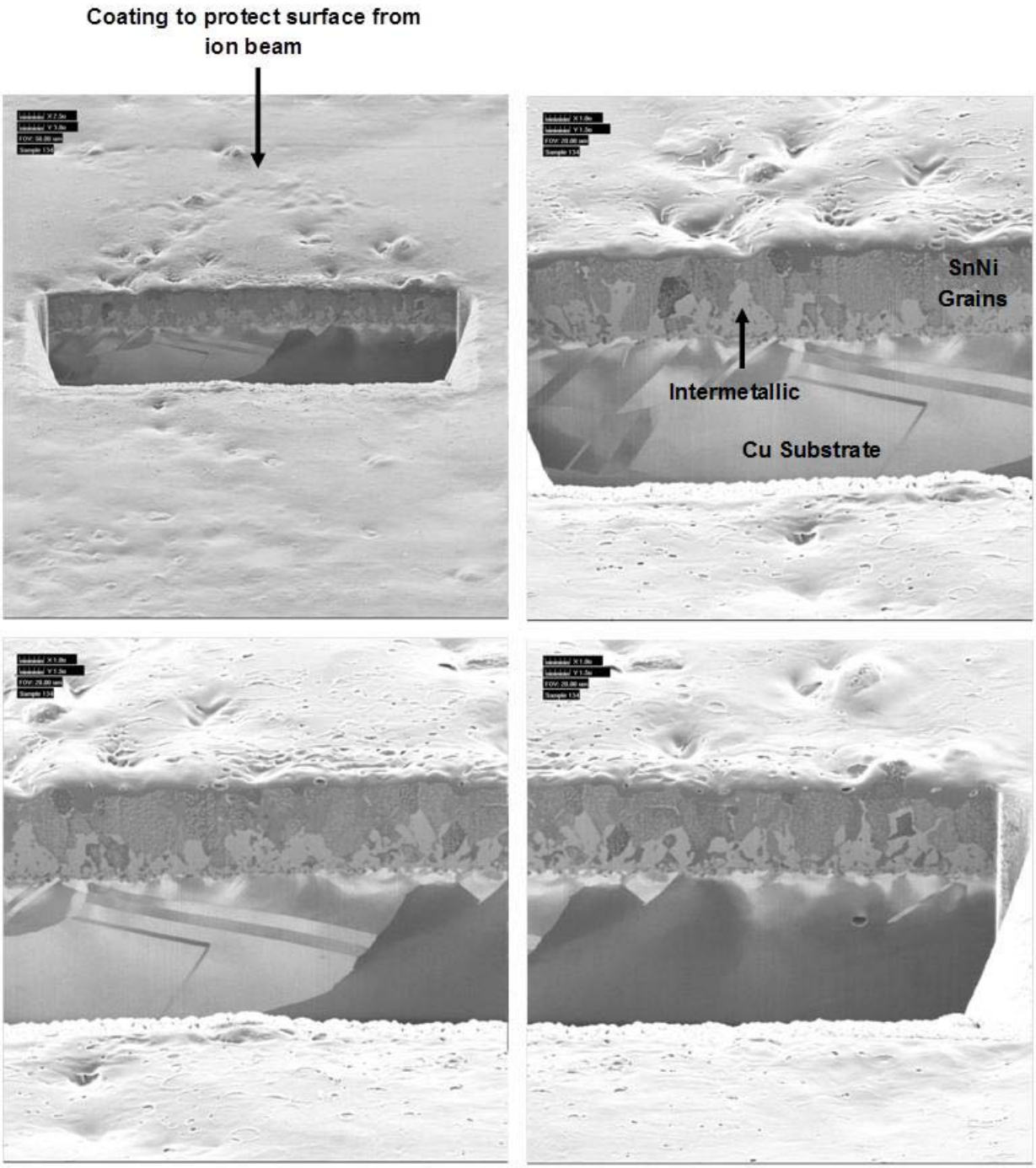

FIB Ion Images for Sn with 3.0% Ni – 1st Whisker
Post Aging 8,000 Hours at 50°C/ 50% Relative Humdity

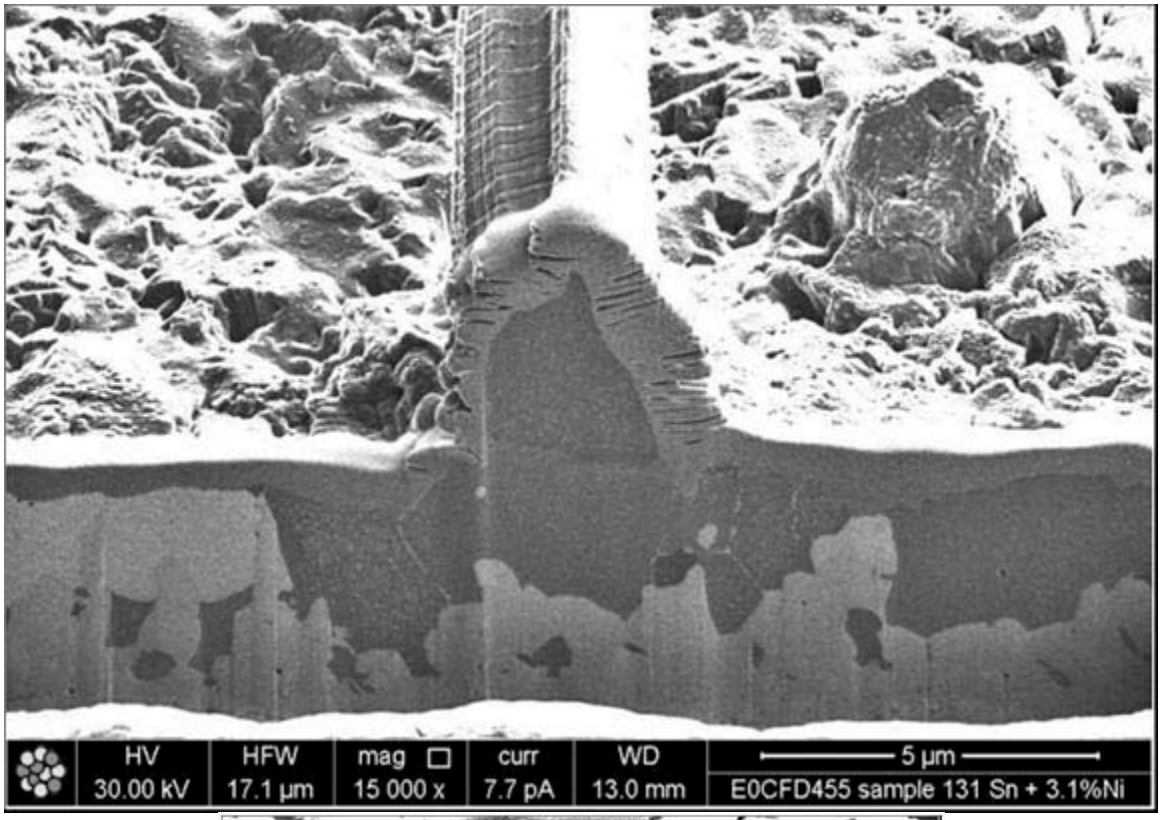

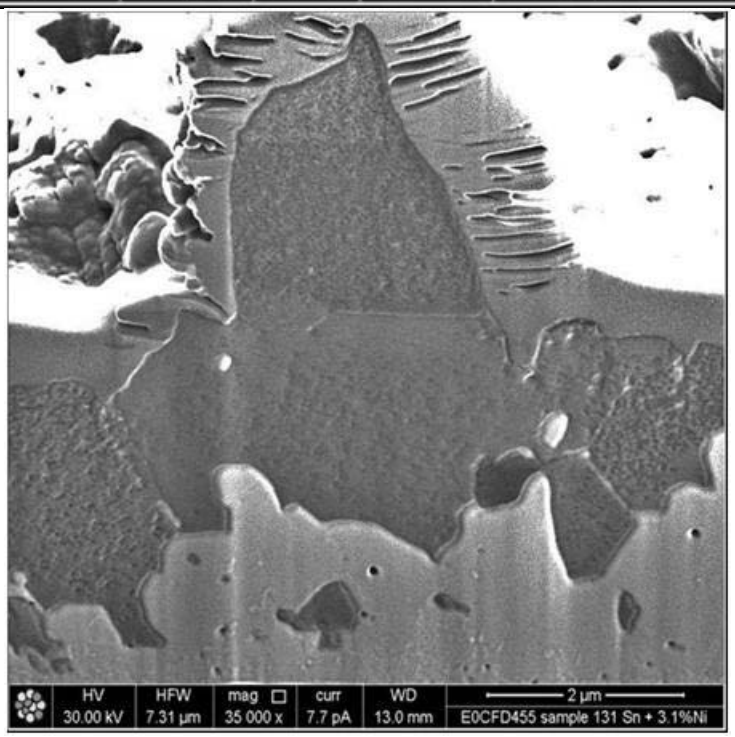

FIB Electron Images for Sn with 3.0% Ni – 1st Whisker Post Aging 8,000 Hours at 50°C/ 50% Relative Humdity

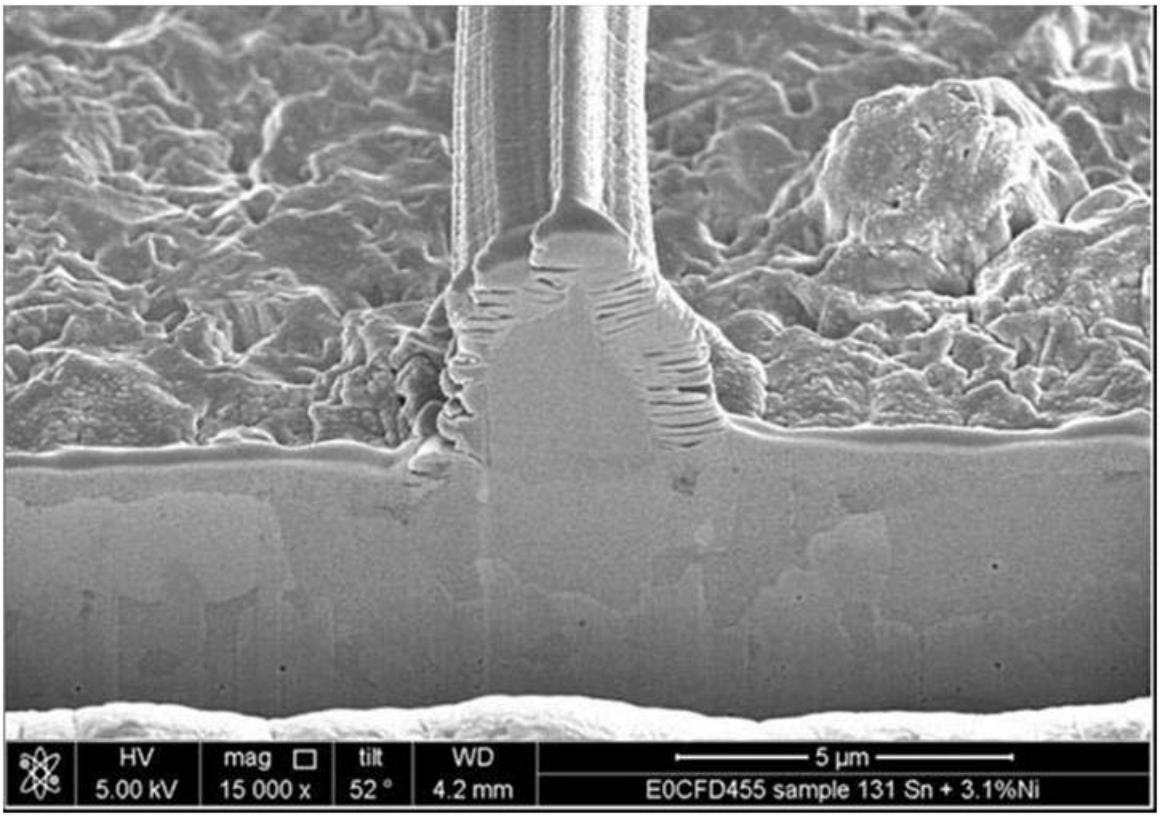

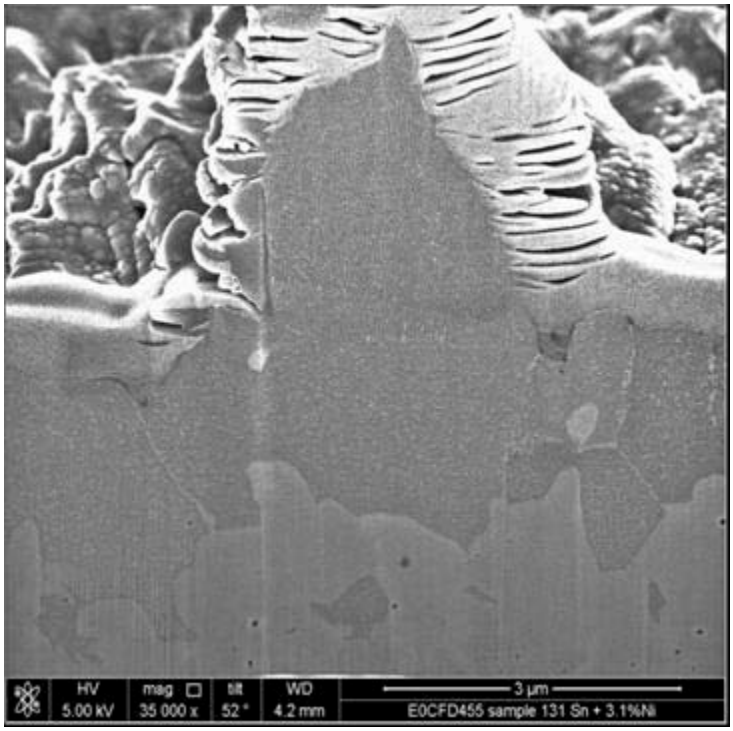

FIB Ion Images for Sn with 3.0% Ni – 2nd Whisker
Post Aging 8,000 Hours at 50°C/ 50% Relative Humidity

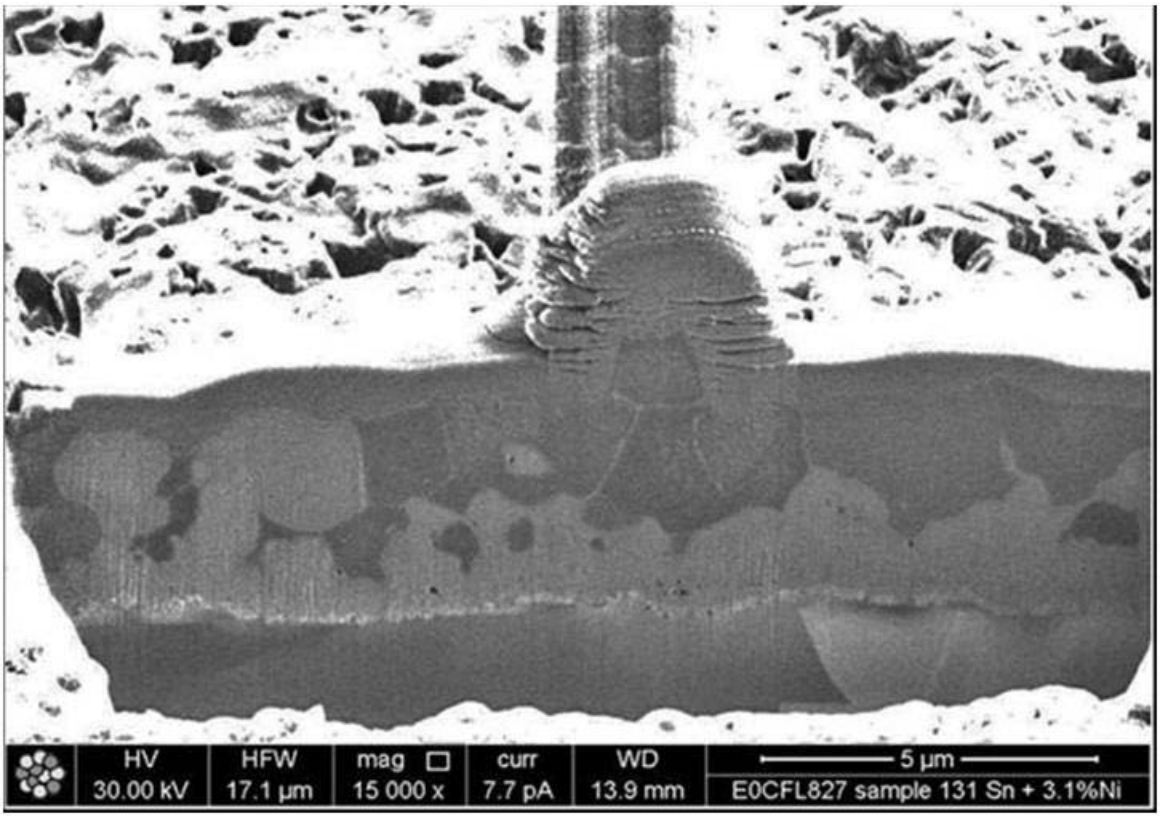

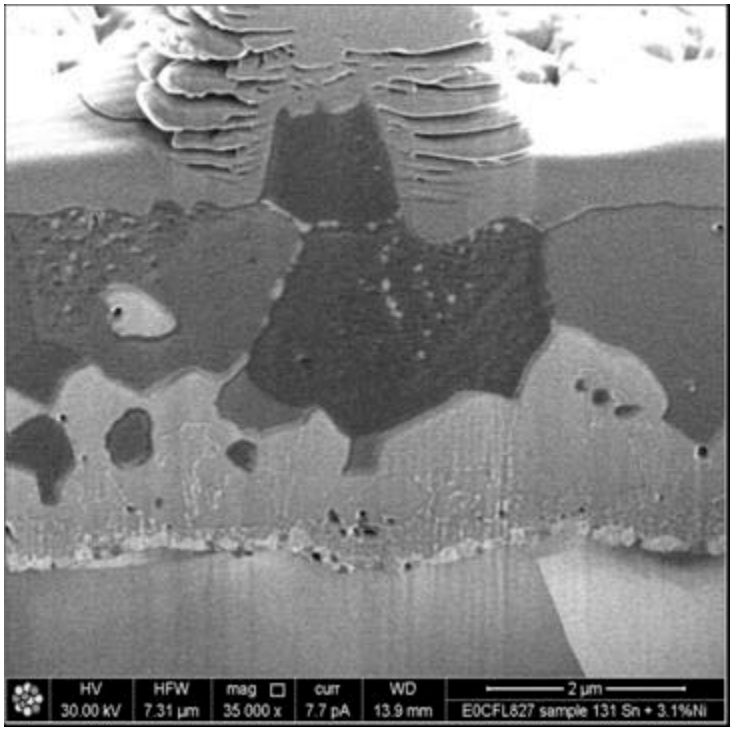

FIB Ion Images for Sn with 3.0% Ni – 2nd Whisker
Post Aging 8,000 Hours at 50°C/ 50% Relative Humdity

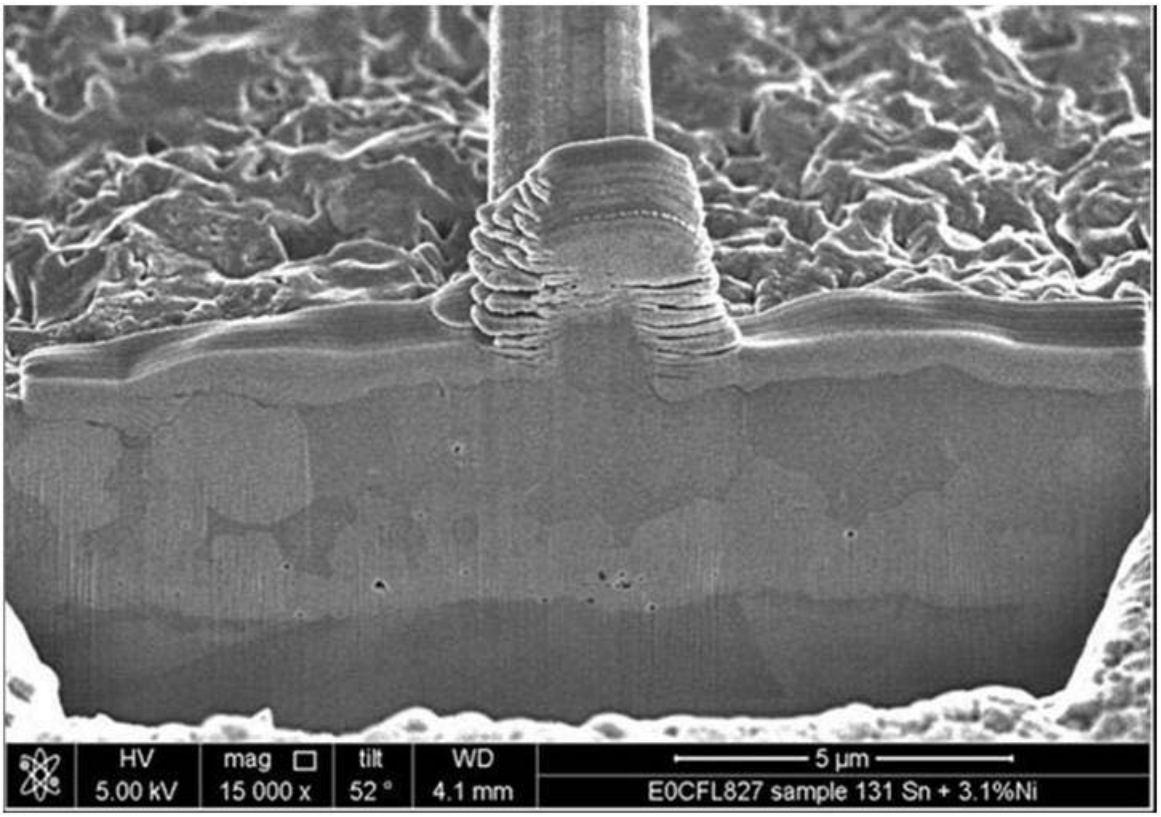

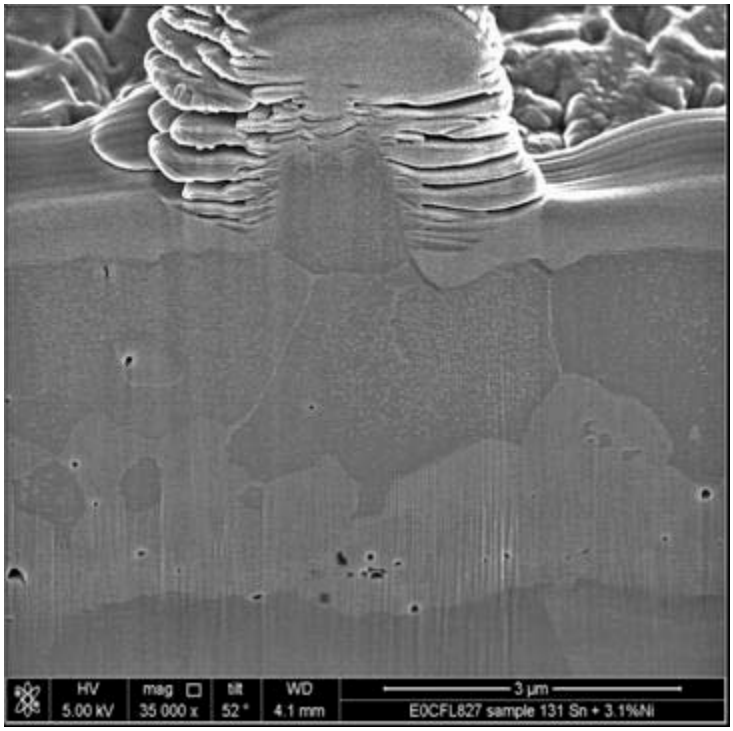

FIB Electron Images for Sn with 3.0% Ni – 2nd Whisker Post Aging 8,000 Hours at 50°C/ 50% Relative Humdity

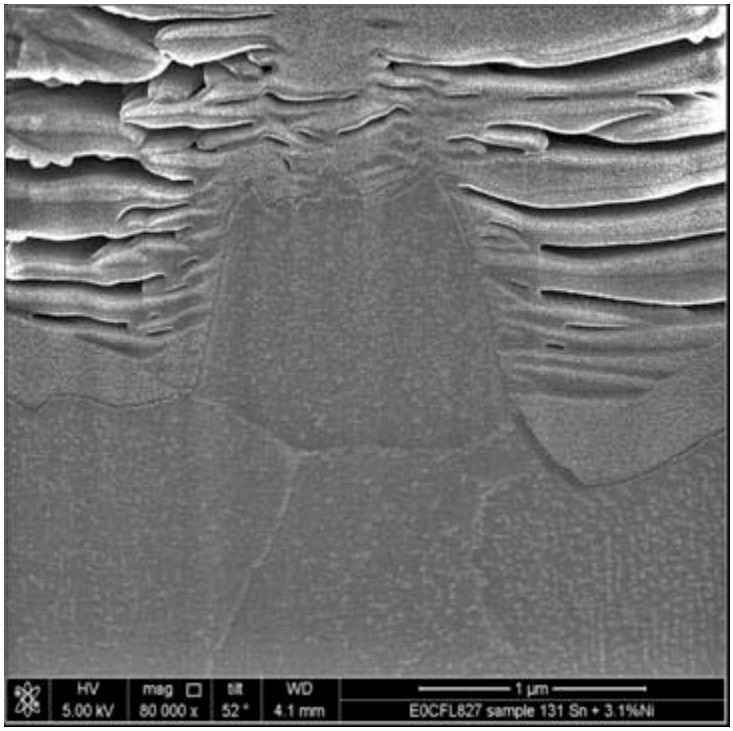

Appendix E: FIB Images for Sn with 0.95% Co

FIB Images for Sn with 0.95% Co
Post Plating

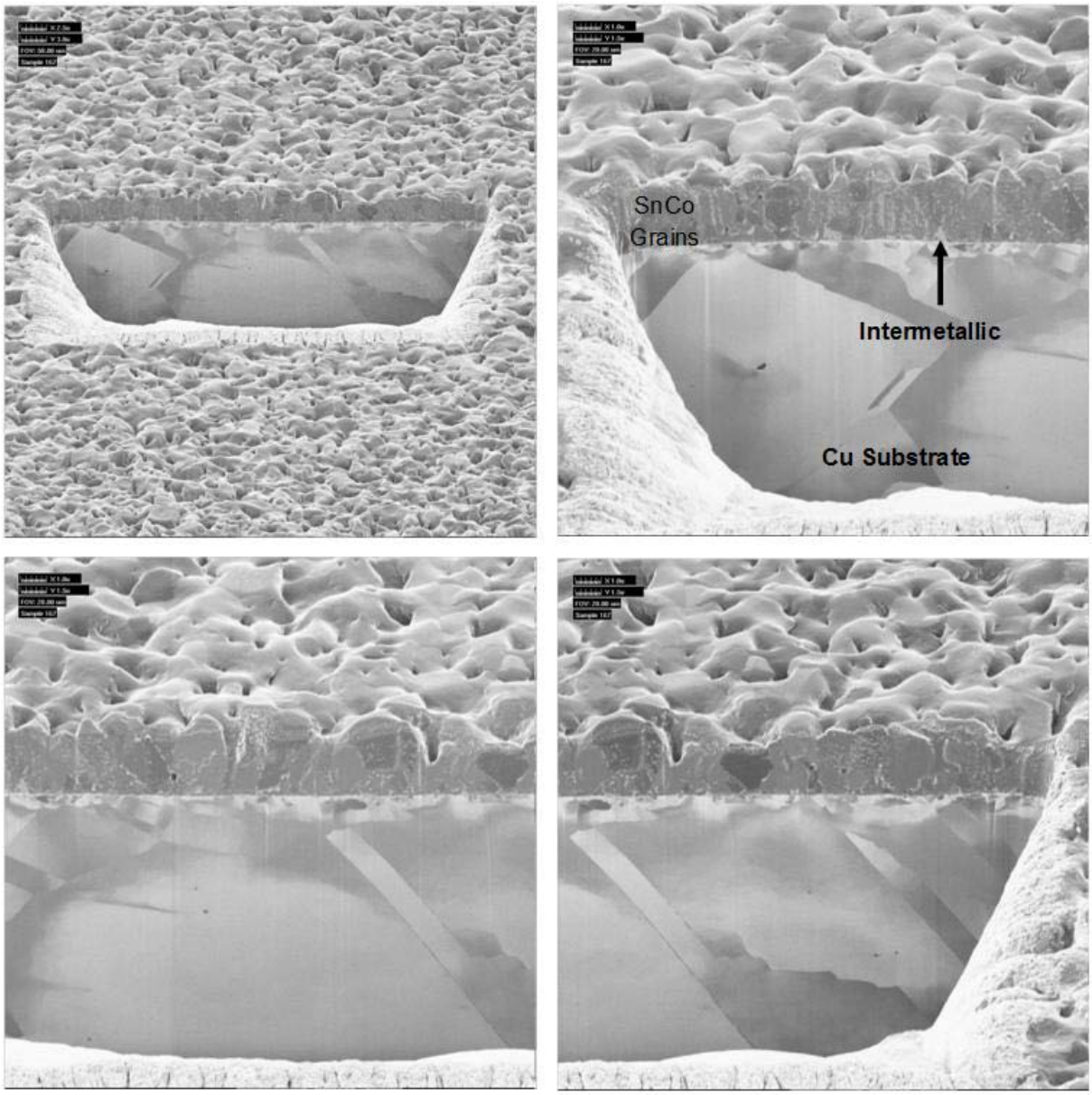

FIB Ion Images for Sn with 0.95% Co – 1st Whisker
Post Aging 8,000 Hours at 50°C/ 50% Relative Humdity

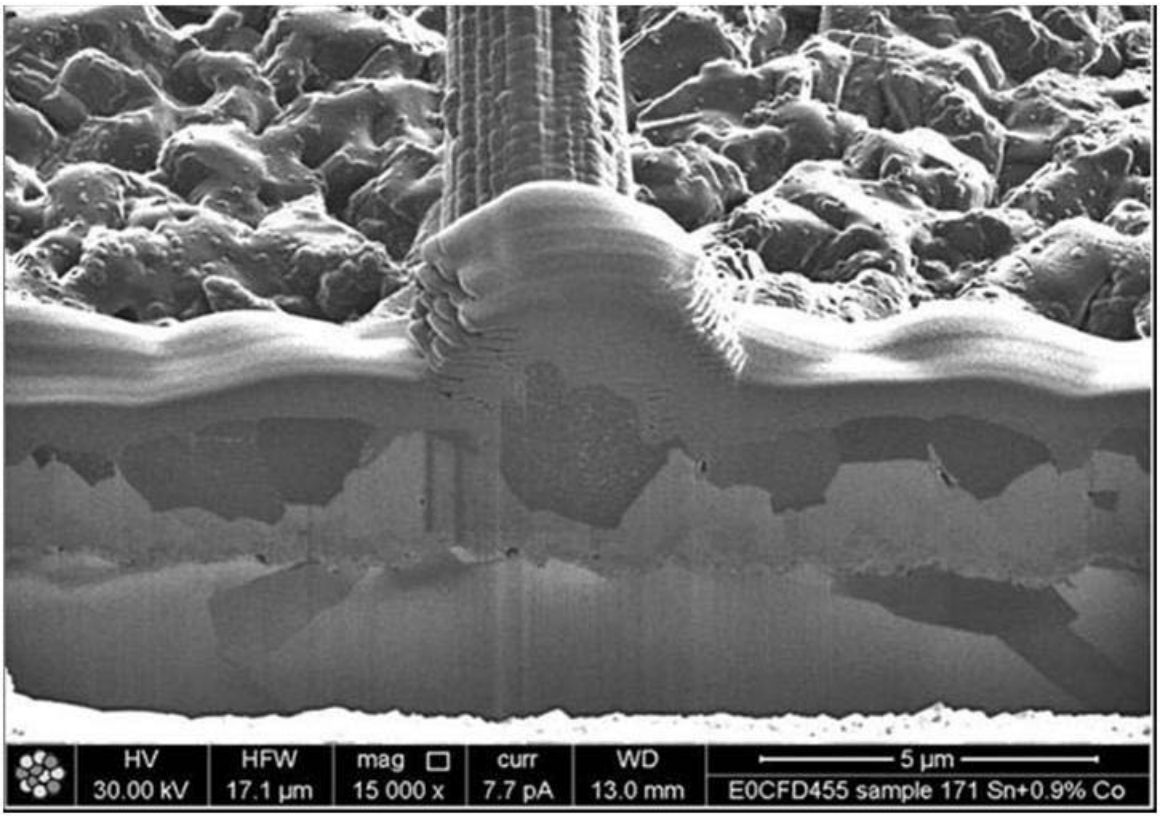

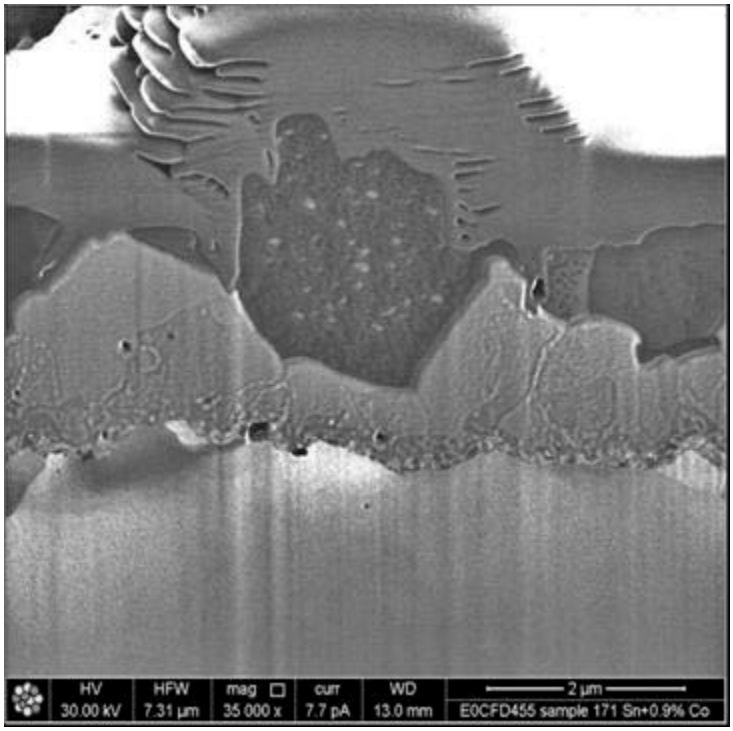

FIB Ion Images for Sn with 0.95% Co – 1st Whisker Post Aging 8,000 Hours at 50°C/ 50% Relative Humdity

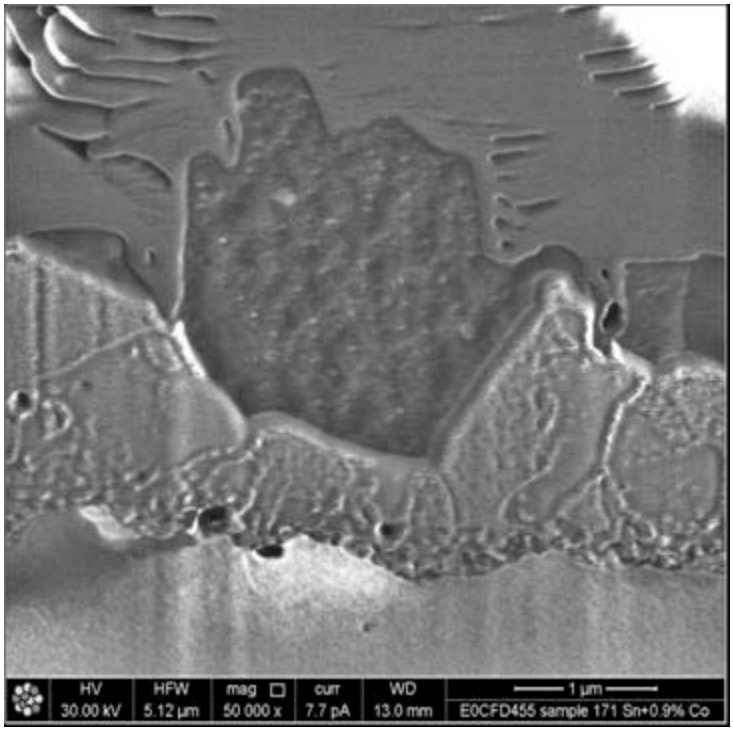

FIB Electron Images for Sn with 0.95% Co – 1st Whisker Post Aging 8,000 Hours at 50°C/ 50% Relative Humidity

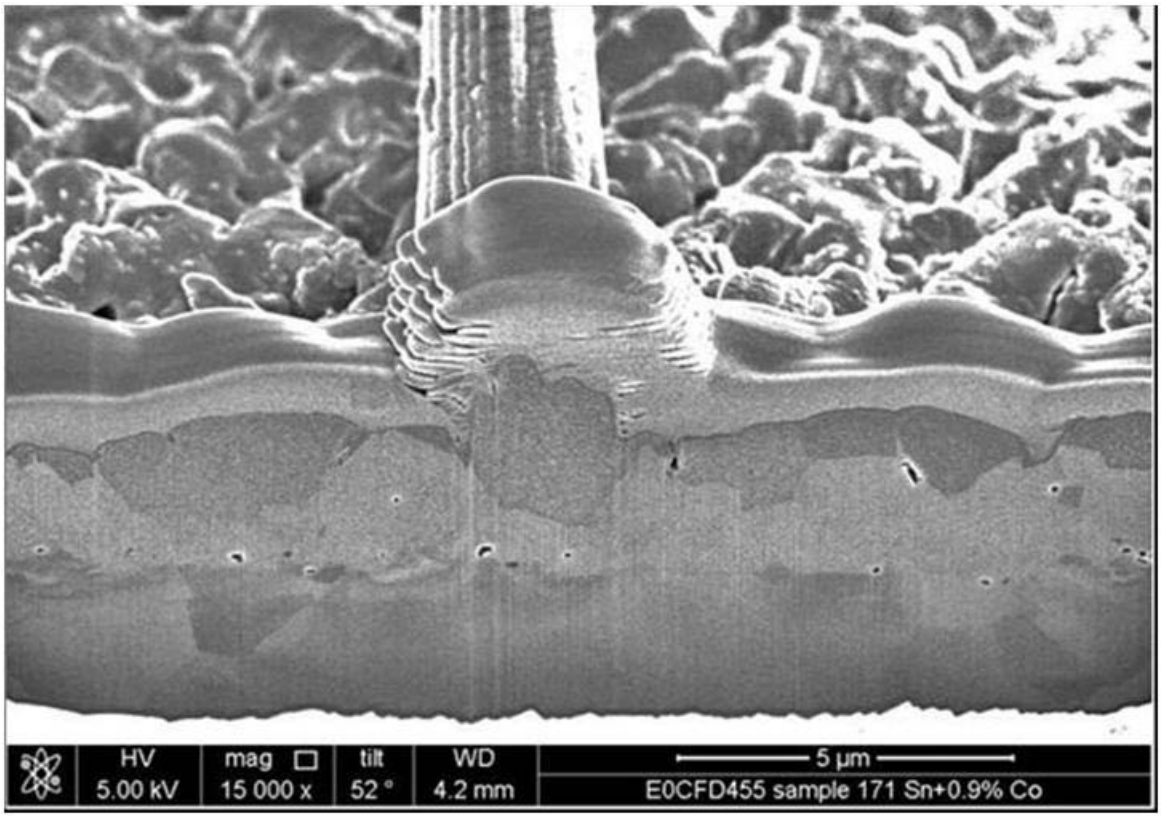

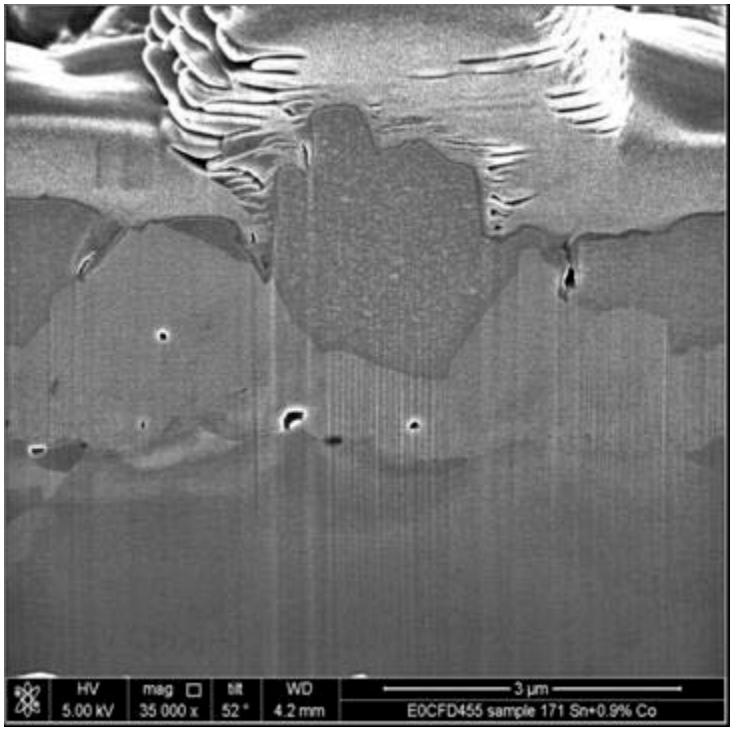

FIB Electron Images for Sn with 0.95% Co – 1st Whisker Post Aging 8,000 Hours at 50°C/ 50% Relative Humidity

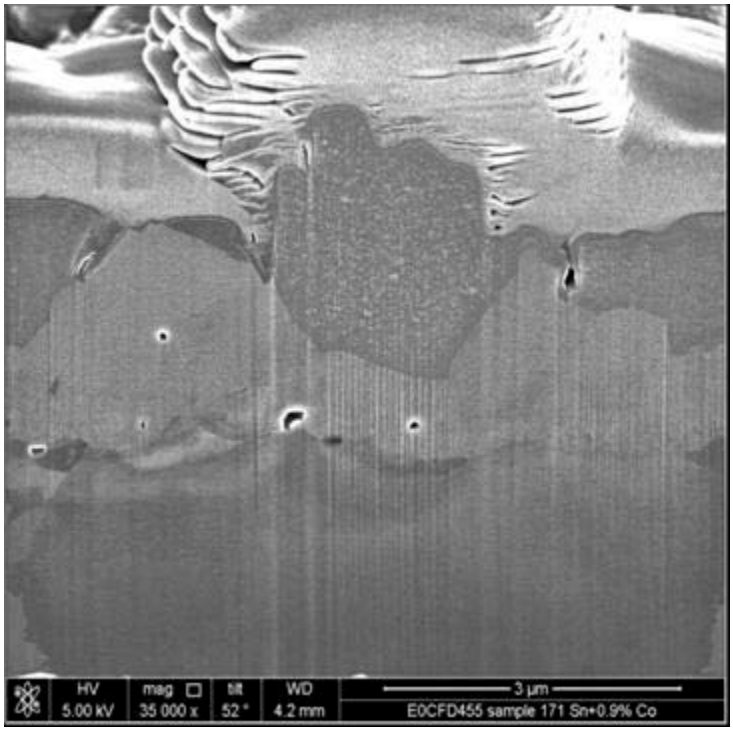

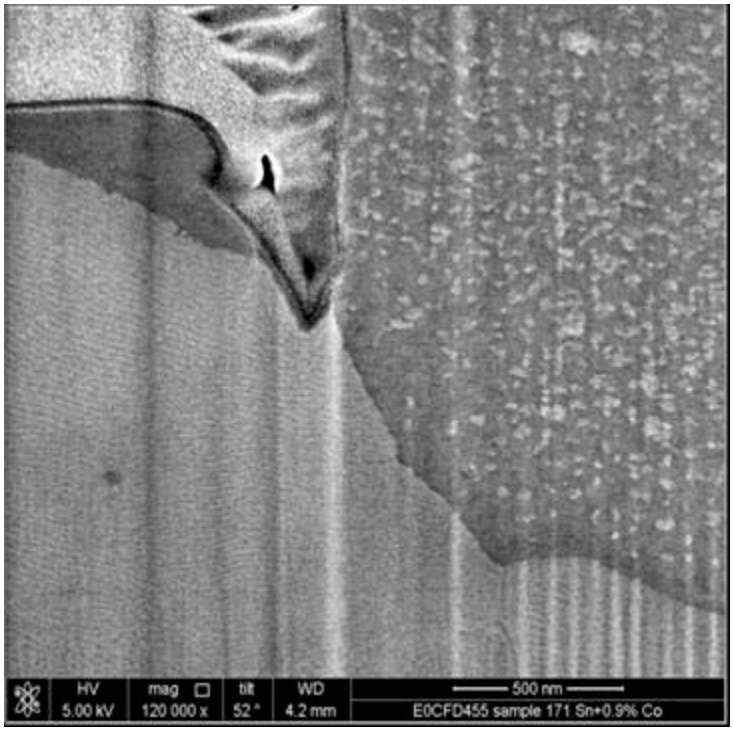

Appendix F: FIB Images for Sn with 2.4% Sb

FIB Images for Sn with 2.4% Sb
Post Plating

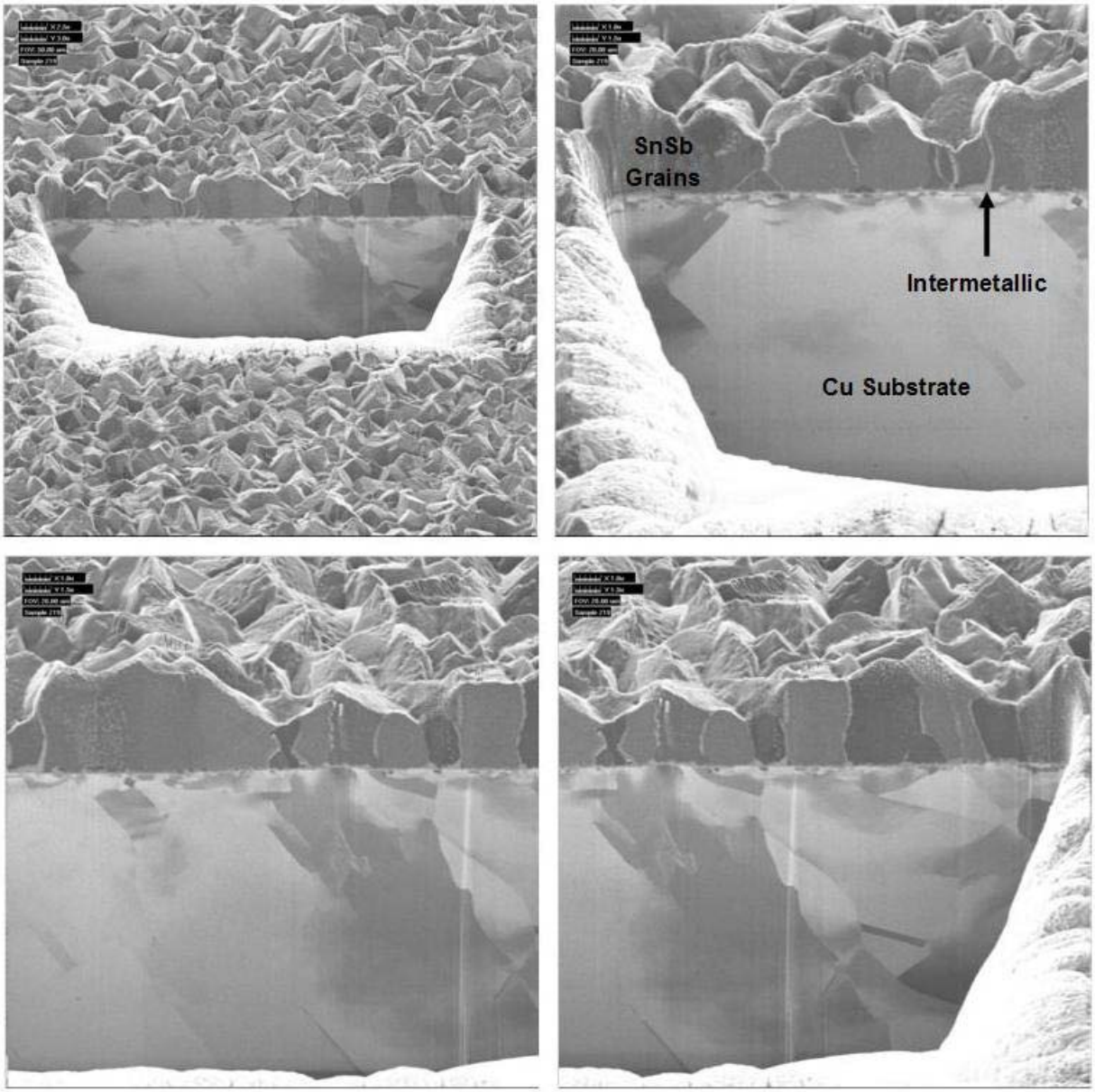

FIB Ion Images for Sn with 2.4% Sb – 1st Whisker
Post Aging 12,000 Hours at 50°C/ 50% Relative Humidity

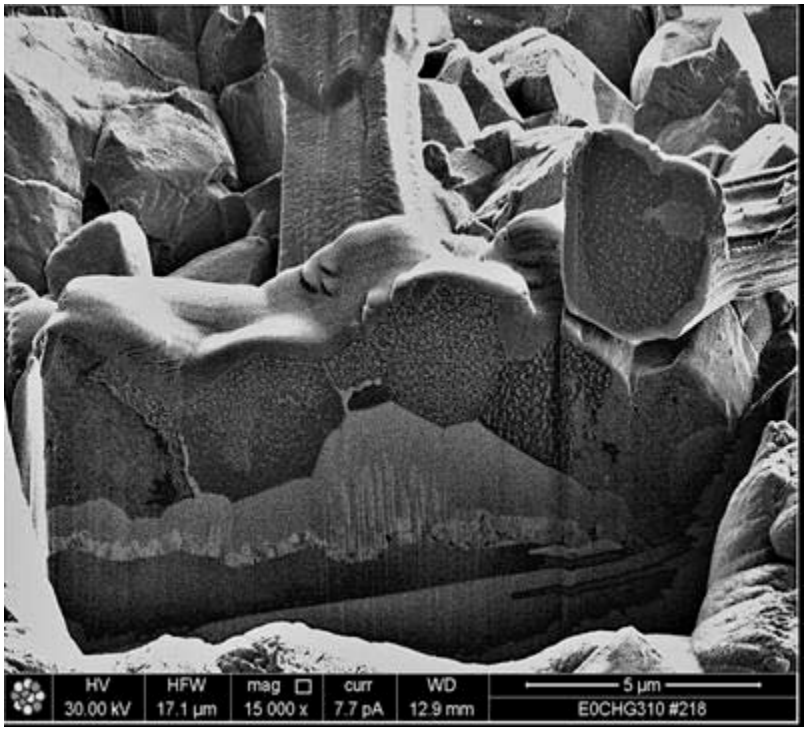

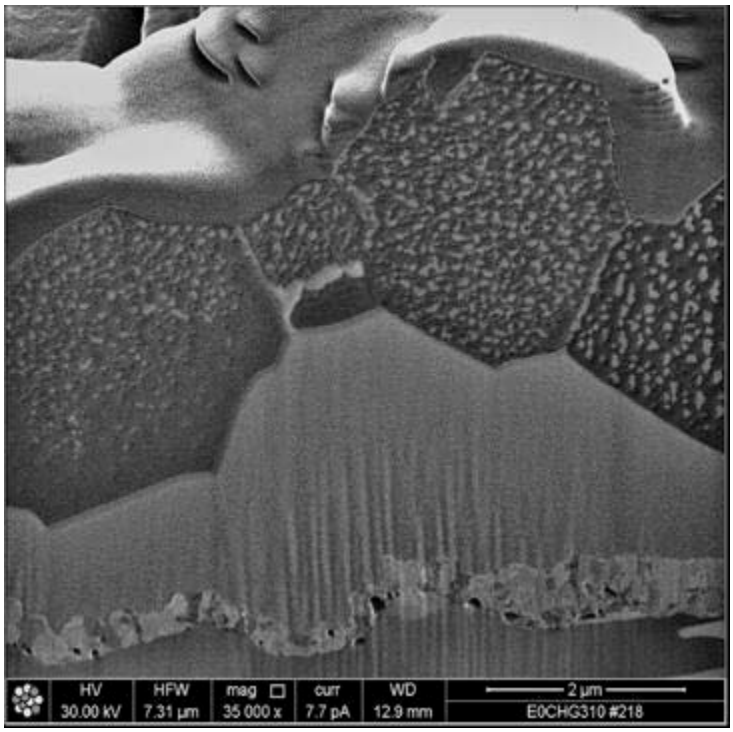

FIB Electron Images for Sn with 2.4% Sb – 1st Whisker Post Aging 12,000 Hours at 50°C/ 50% Relative Humidity

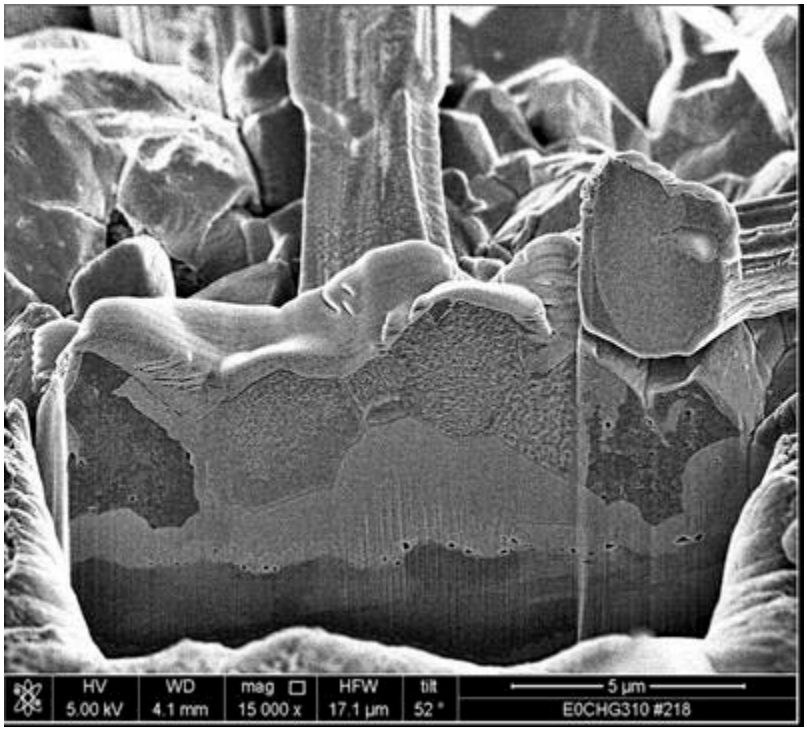

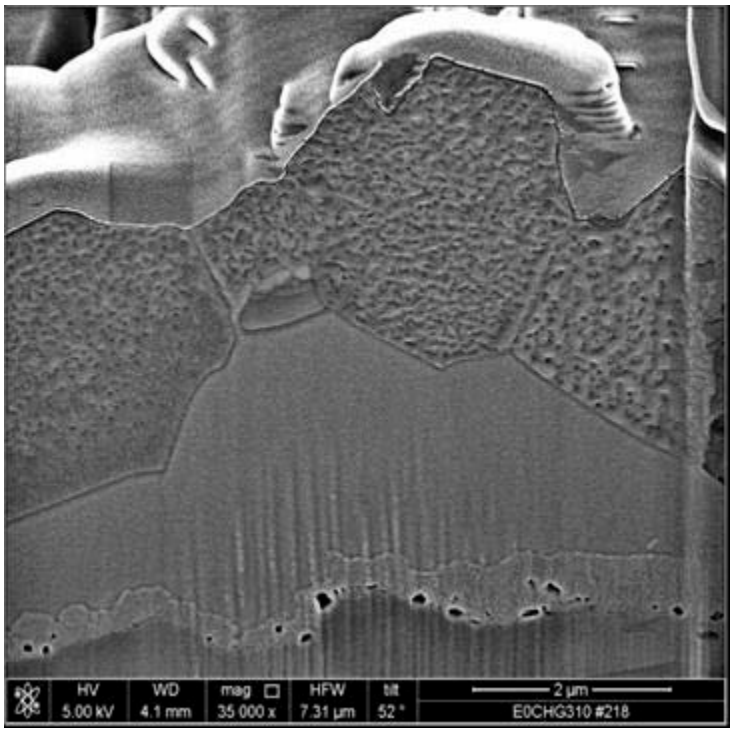

FIB Ion Images for Sn with 2.4% Sb – 2nd Whisker
Post Aging 12,000 Hours at 50°C/ 50% Relative Humidity

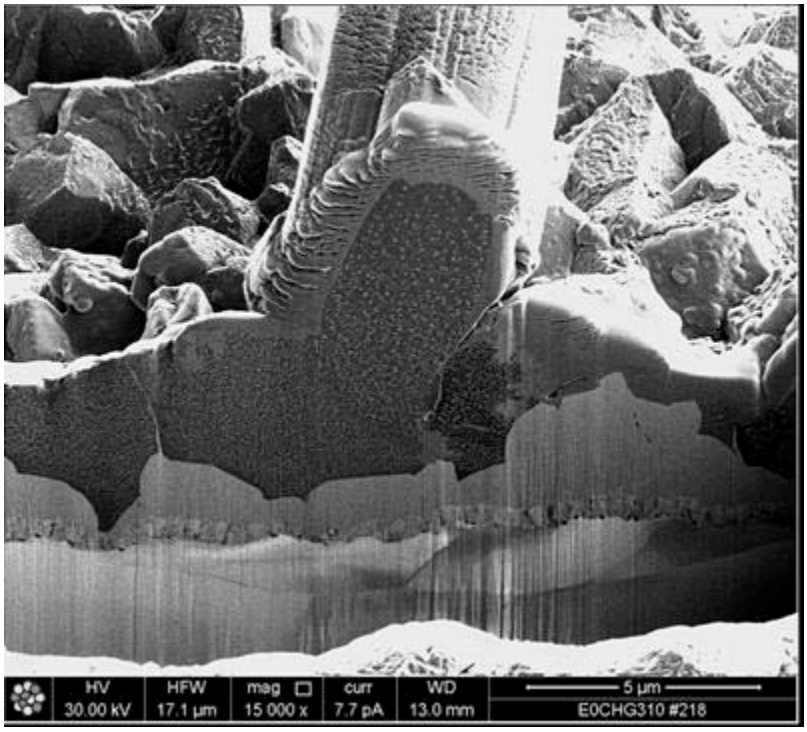

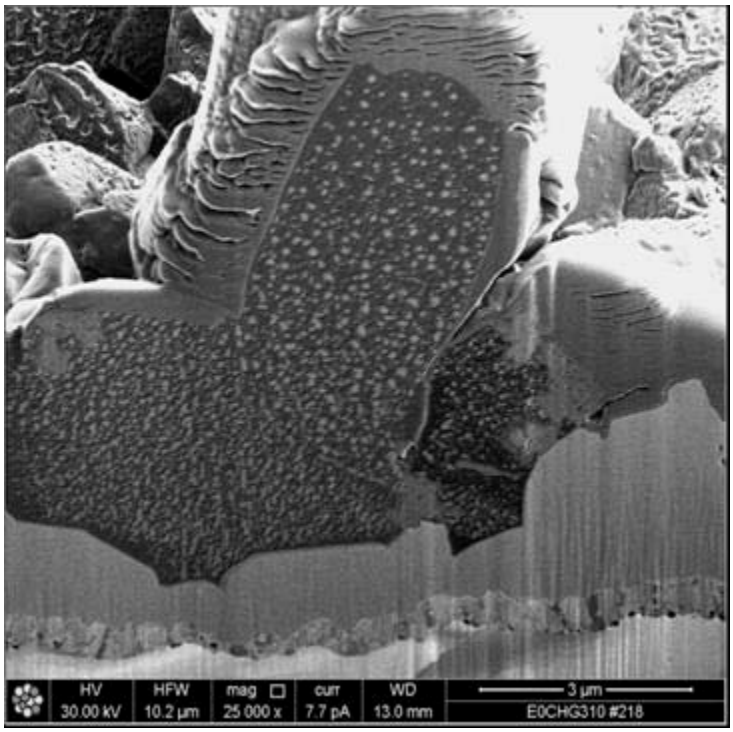

FIB Ion Images for Sn with 2.4% Sb – 2nd Whisker
Post Aging 12,000 Hours at 50°C/ 50% Relative Humidity

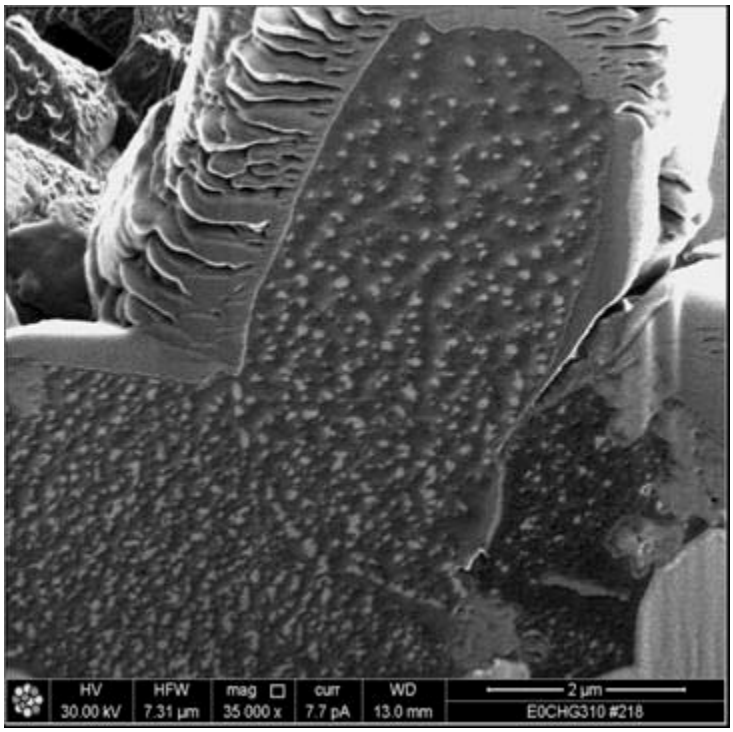

FIB Electron Images for Sn with 2.4% Sb – 2nd Whisker Post Aging 12,000 Hours at 50°C/ 50% Relative Humidity

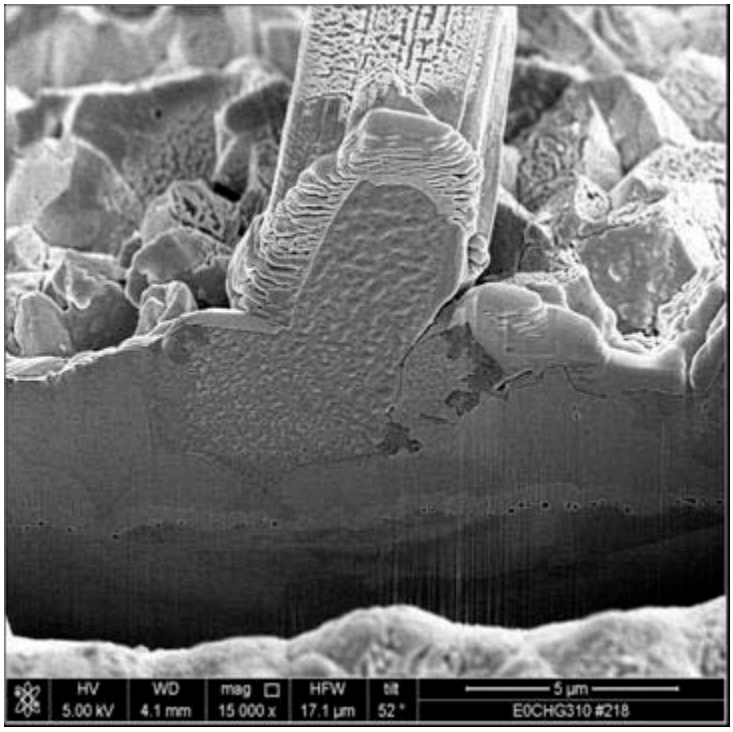

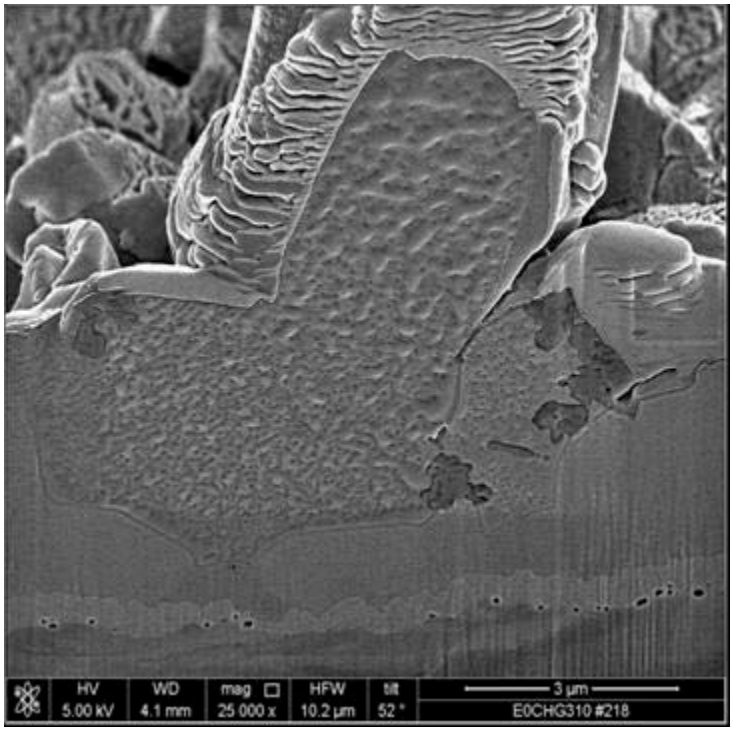

FIB Electron Images for Sn with 2.4% Sb – 2nd Whisker Post Aging 12,000 Hours at 50°C/ 50% Relative Humidity

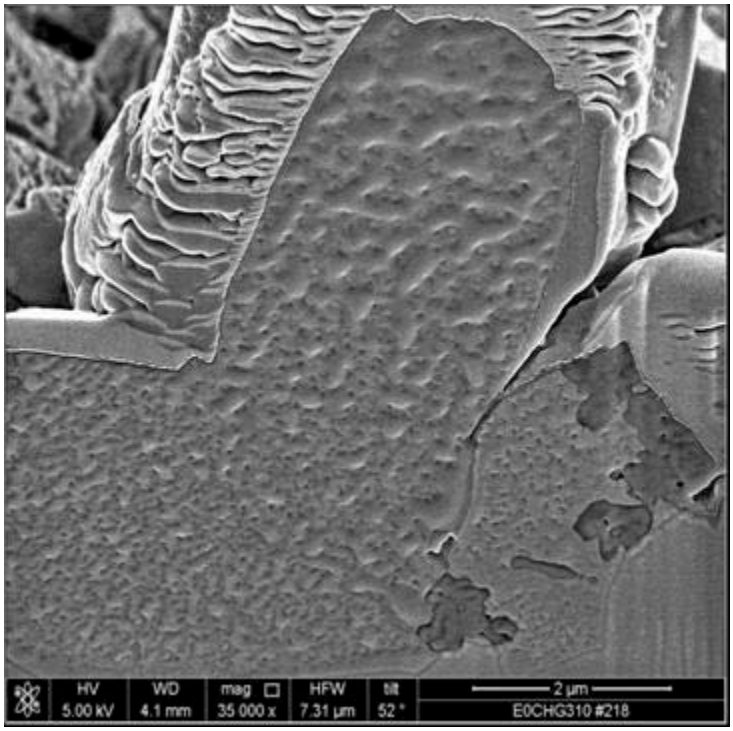

Appendix G: FIB Images for Sn with 1.1% Ge

FIB Images for Sn with 1.1% Ge
Post Plating

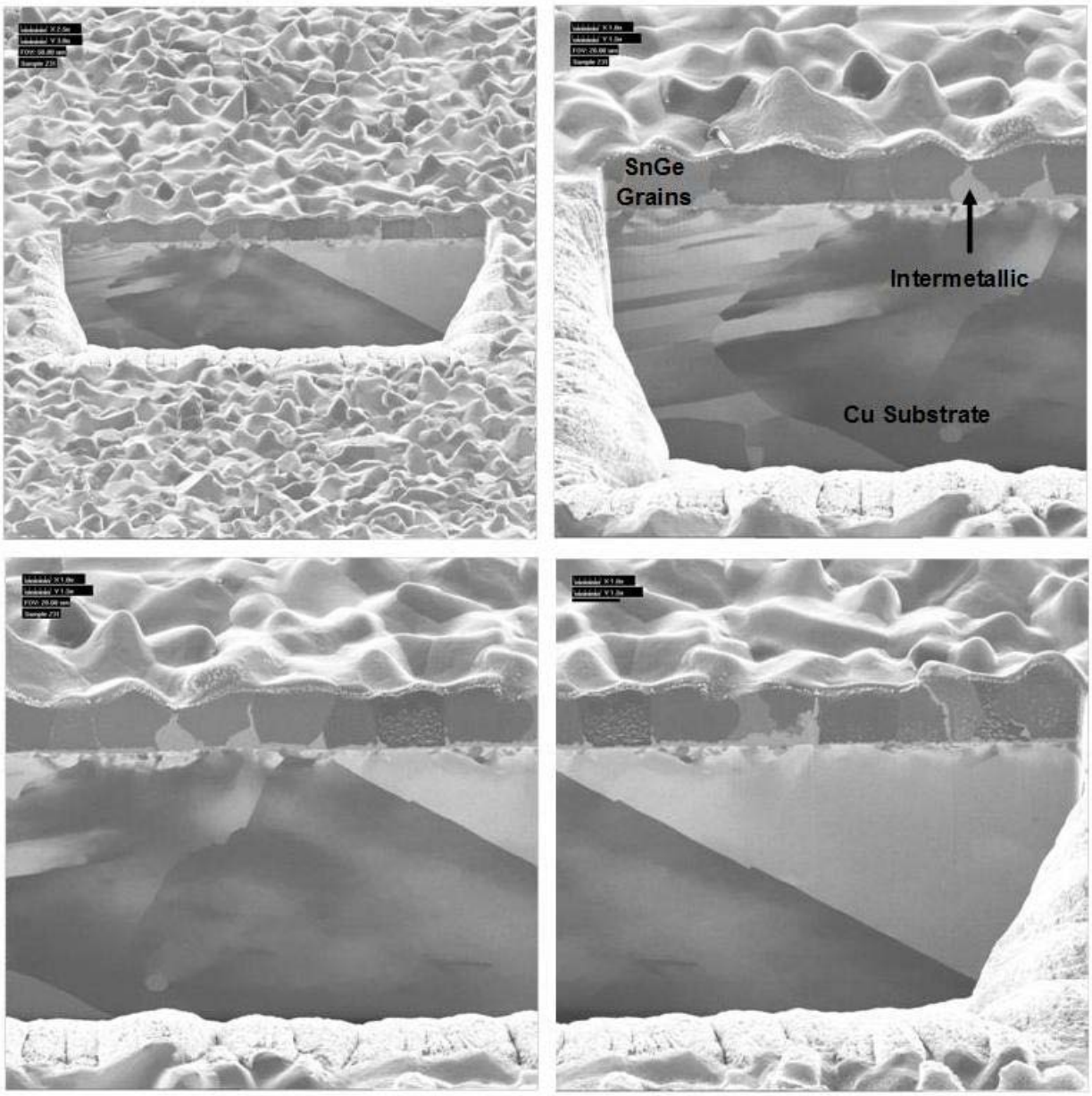

FIB Ion Images for Sn with 1.1% Ge – 1st Whisker
Post Aging 12,000 Hours at 50°C/ 50% Relative Humidity

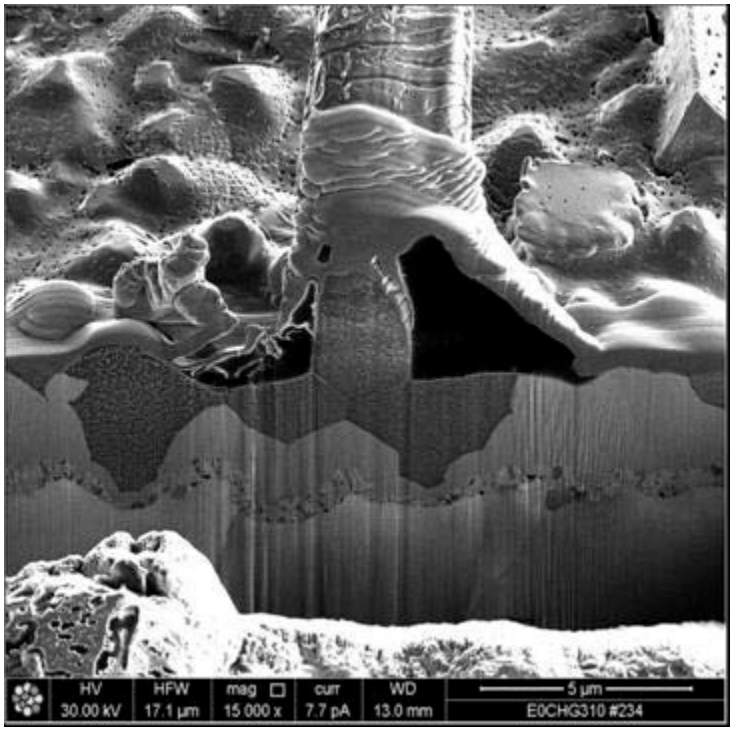

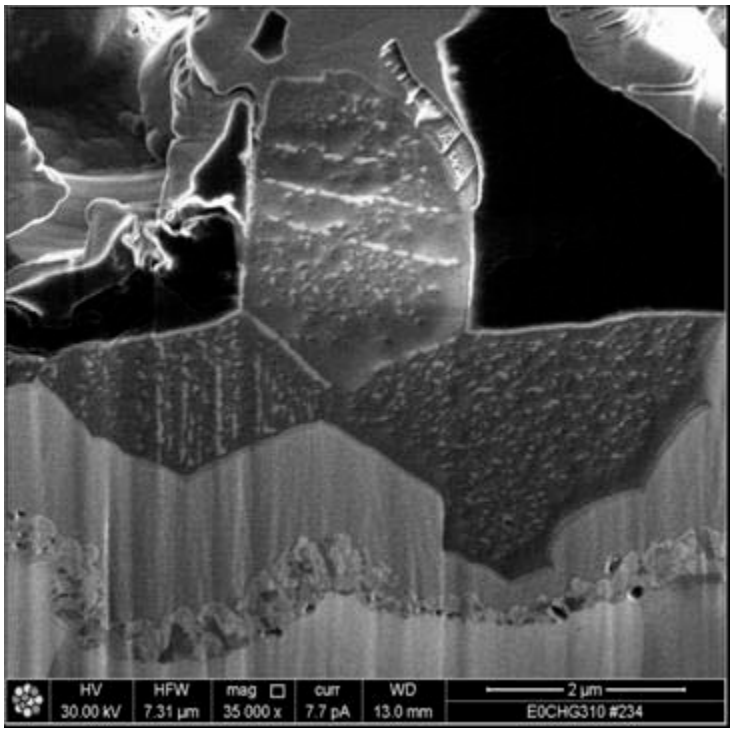

FIB Electron Images for Sn with 1.1% Ge – 1st Whisker Post Aging 12,000 Hours at 50°C/ 50% Relative Humidity

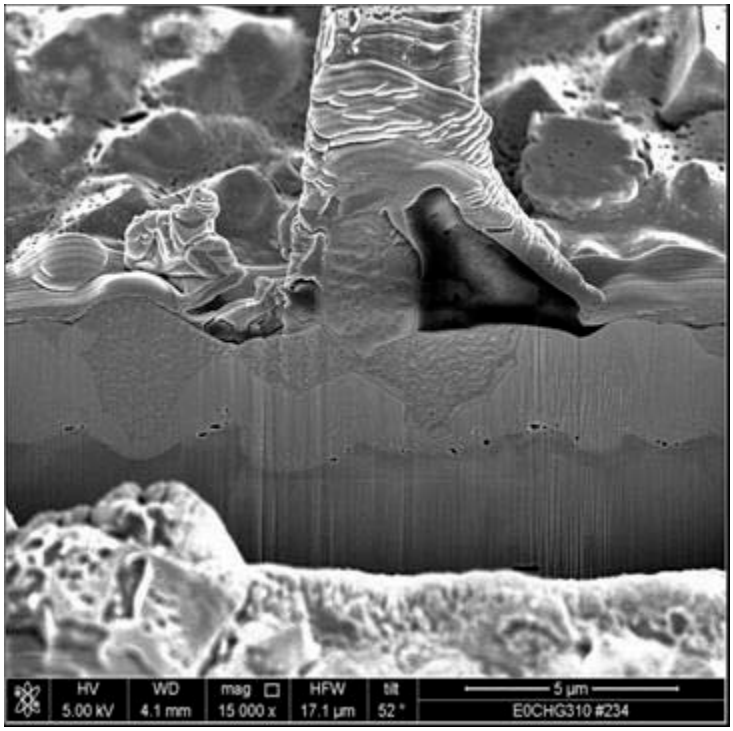

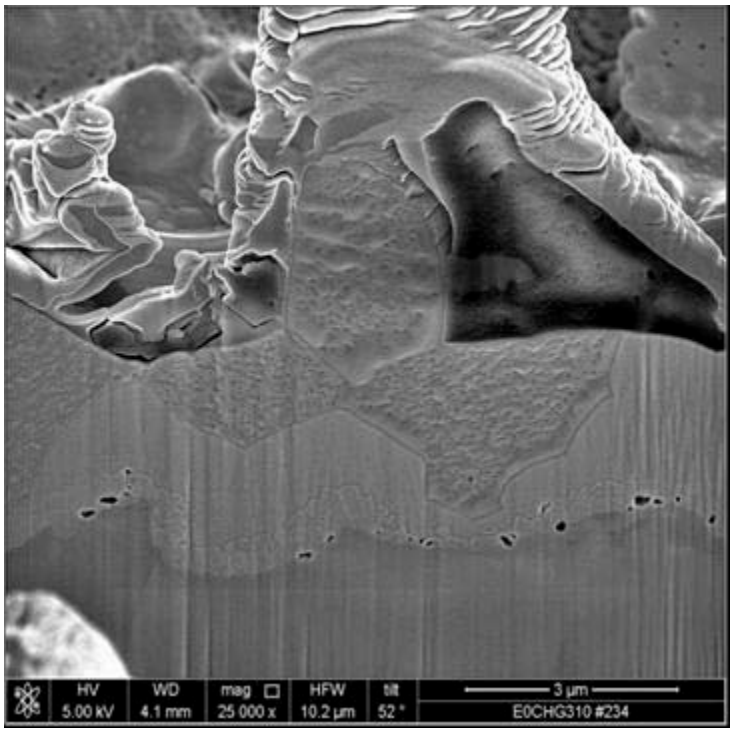

FIB Electron Images for Sn with 1.1% Ge – 1st Whisker Post Aging 12,000 Hours at 50°C/ 50% Relative Humidity

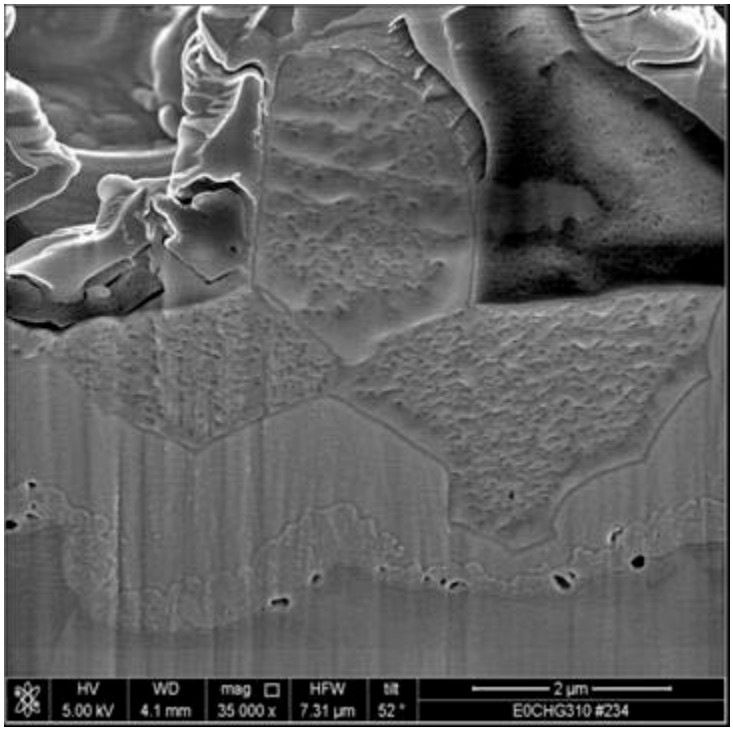

FIB Ion Images for Sn with 1.1% Ge – 2nd Whisker
Post Aging 12,000 Hours at 50°C/ 50% Relative Humidity

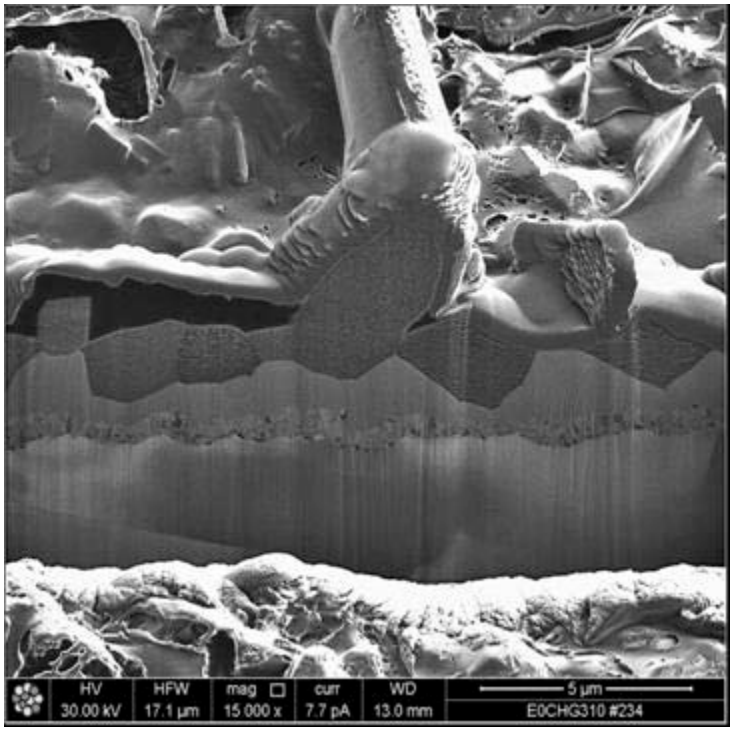

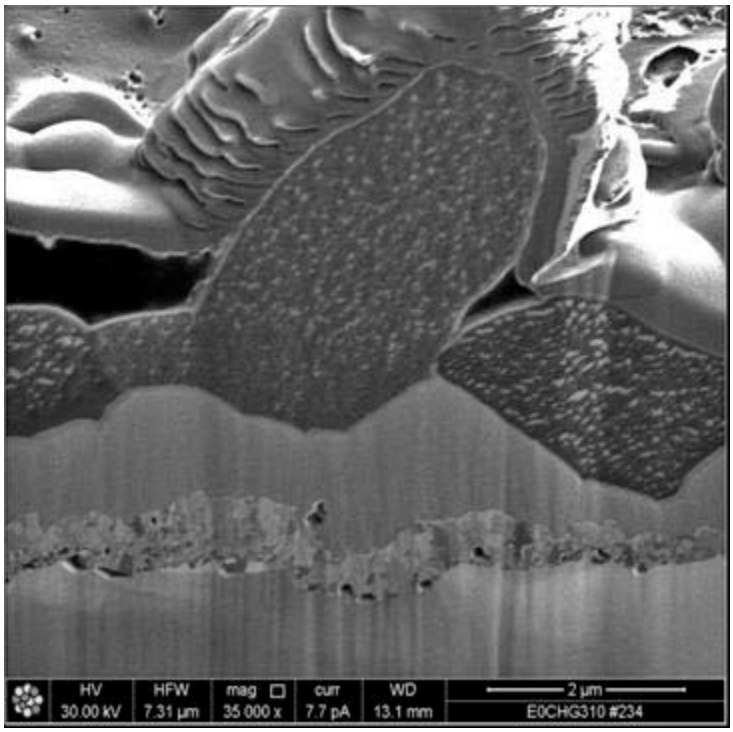

FIB Electron Images for Sn with 1.1% Ge – 2nd Whisker Post Aging 12,000 Hours at 50°C/ 50% Relative Humidity

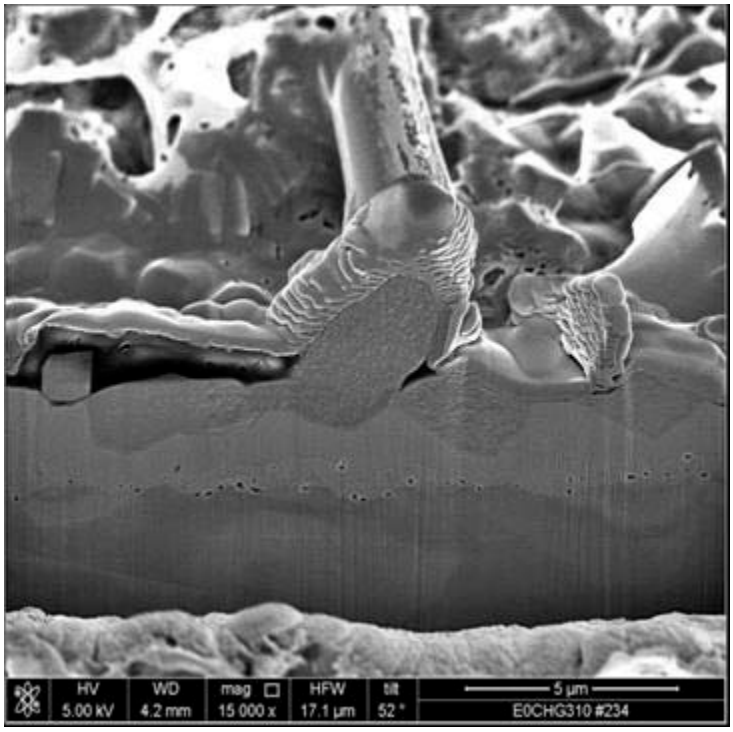

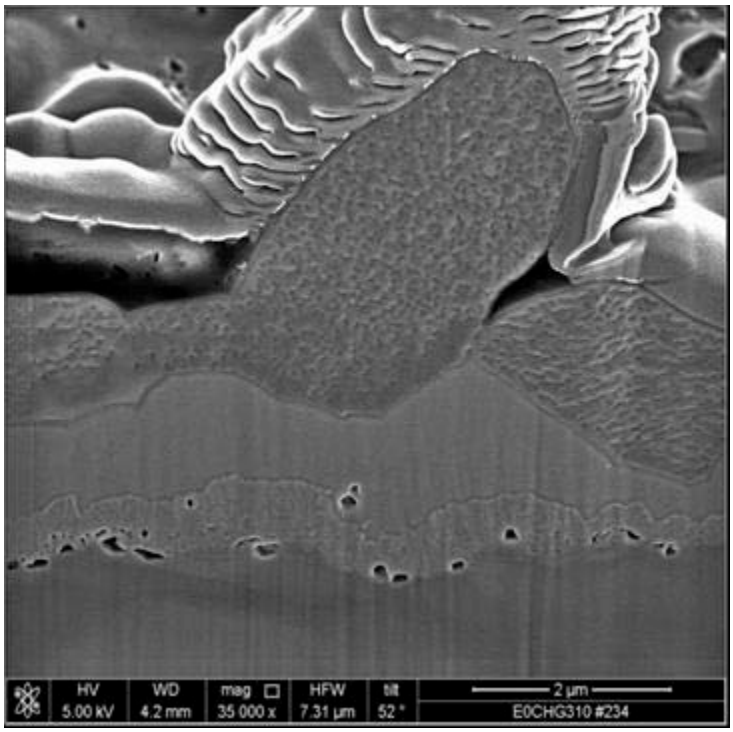

FIB Electron Images for Sn with 1.1% Ge – 2nd Whisker Post Aging 12,000 Hours at 50°C/ 50% Relative Humidity

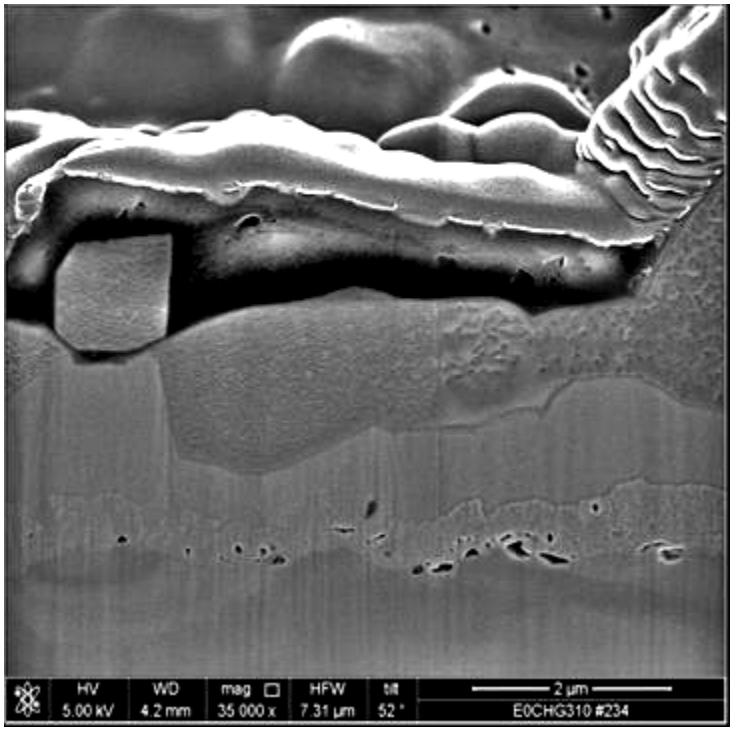

Appendix H: FIB Images for Sn with 1.3% Au

FIB Images for Sn with 1.3% Au
Post Plating

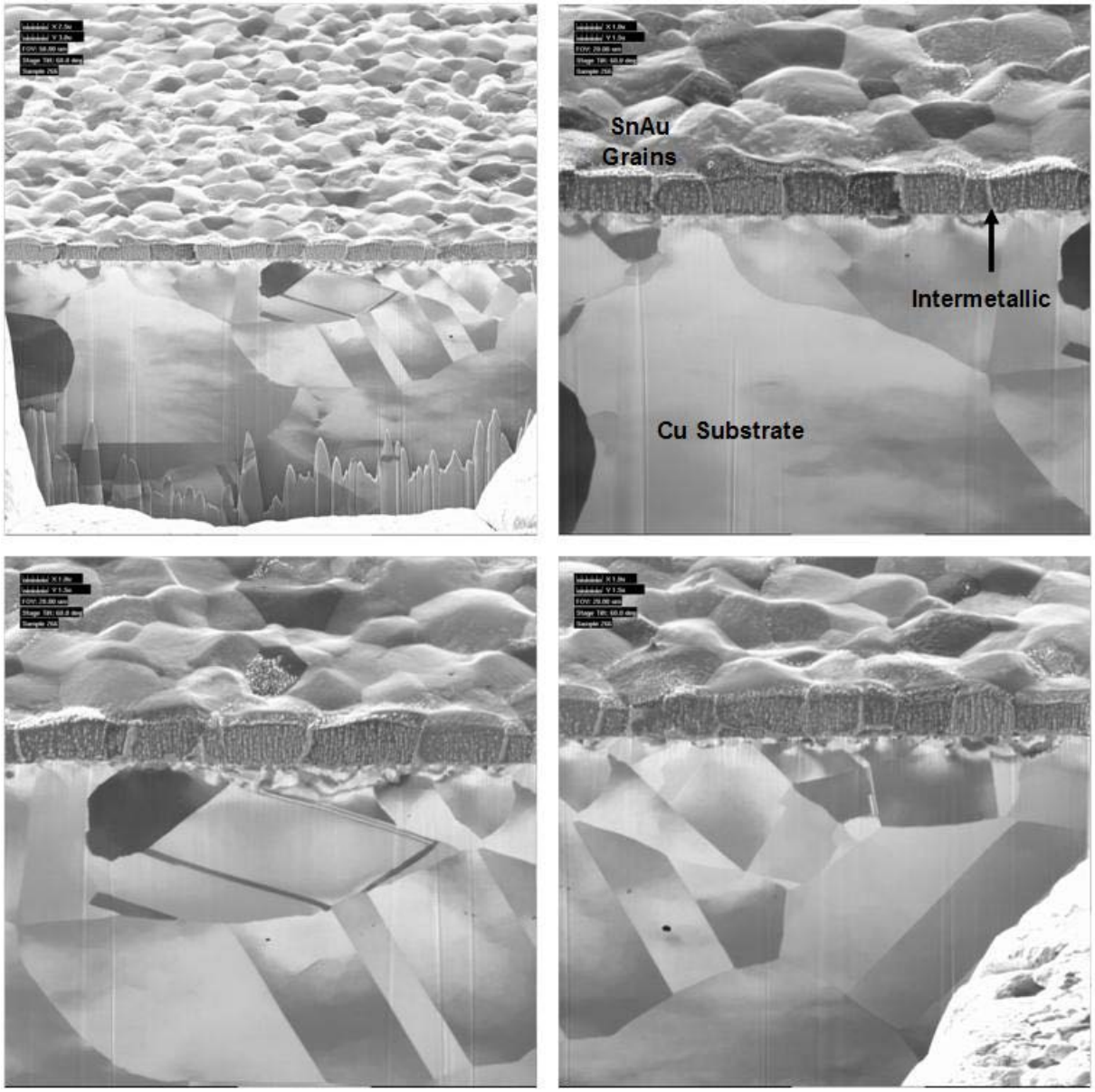

FIB Ion Images for Sn with 1.3% Au – 1st Whisker
Post Aging 12,000 Hours at 50°C/ 50% Relative Humdity

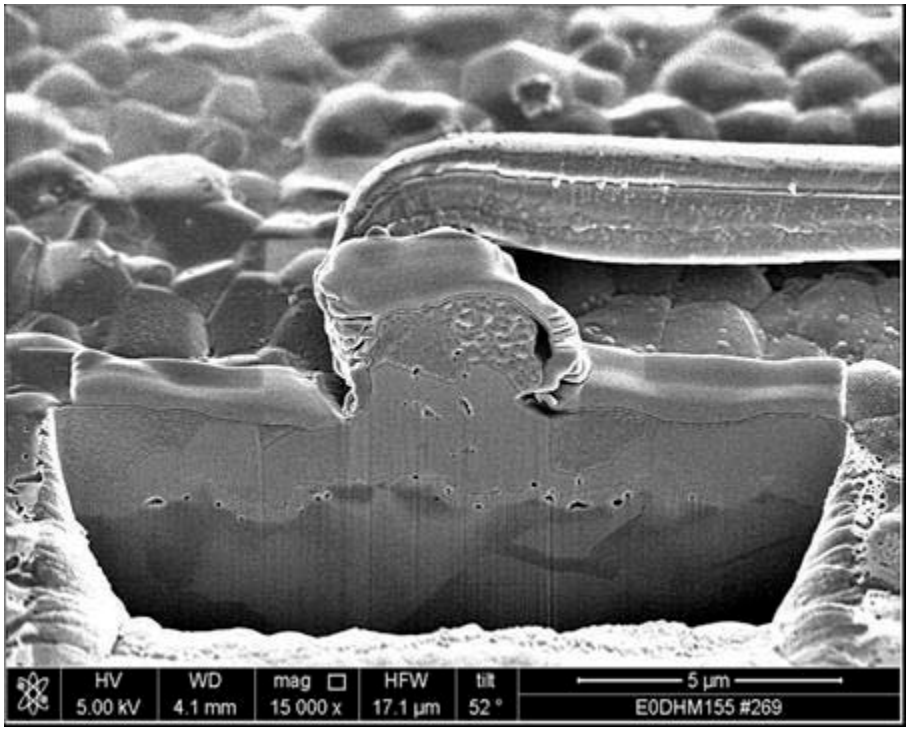

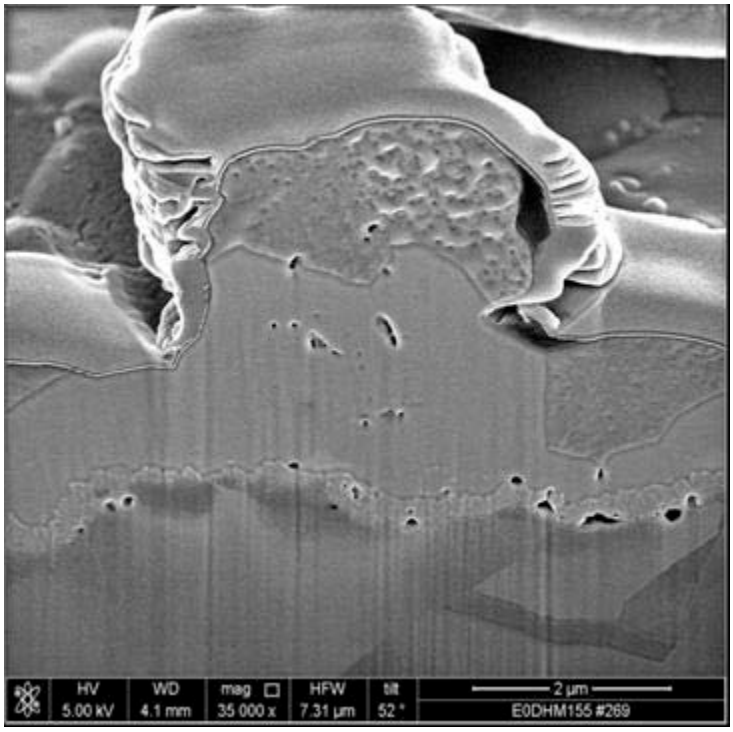

FIB Ion Images for Sn with 1.3% Au – 1st Whisker
Post Aging 12,000 Hours at 50°C/ 50% Relative Humdity

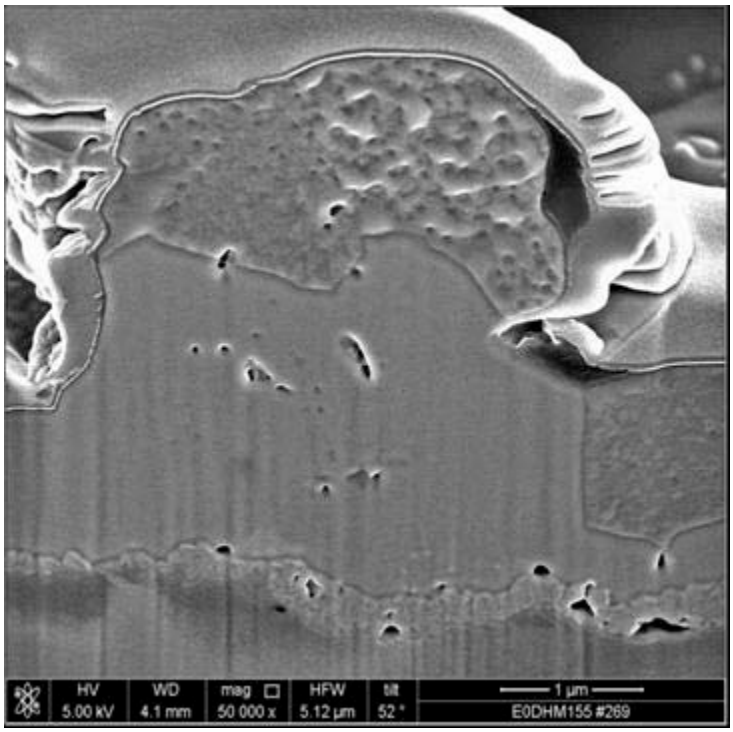

FIB Electron Images for Sn with 1.3% Au – 1st Whisker Post Aging 12,000 Hours at 50°C/ 50% Relative Humdity

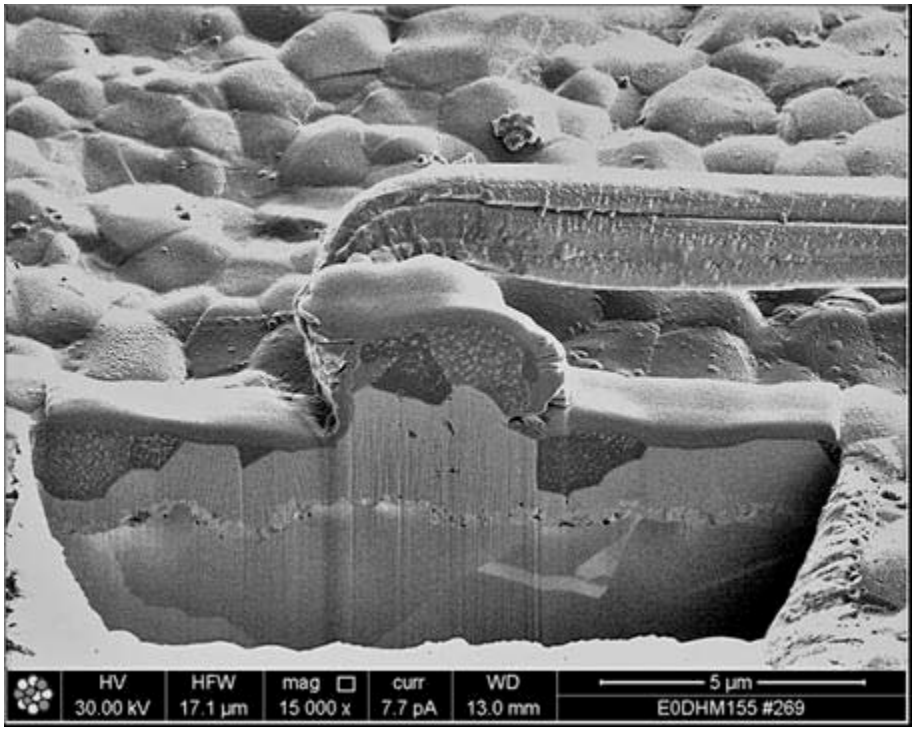

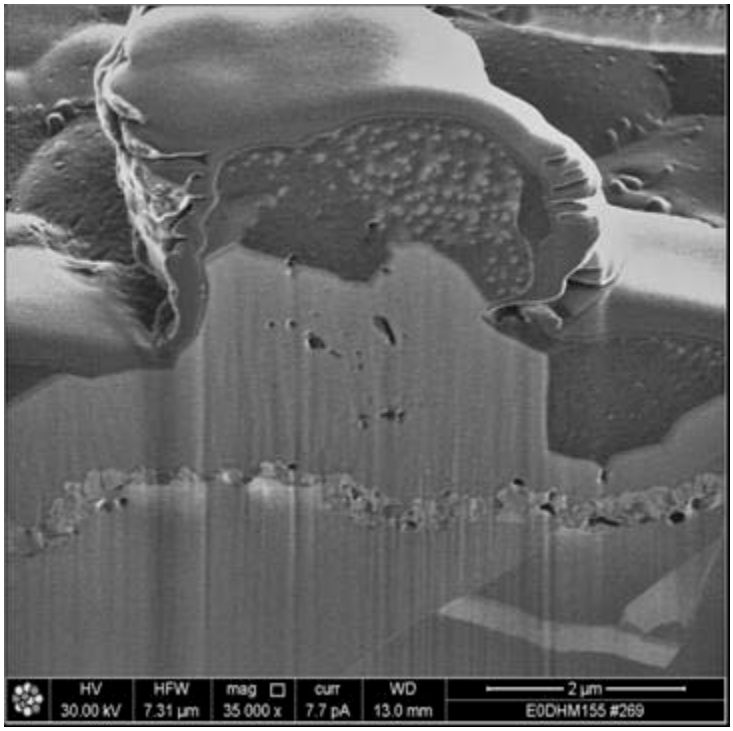

FIB Ion Images for Sn with 1.3% Au – 2nd Whisker
Post Aging 12,000 Hours at 50°C/ 50% Relative Humdity

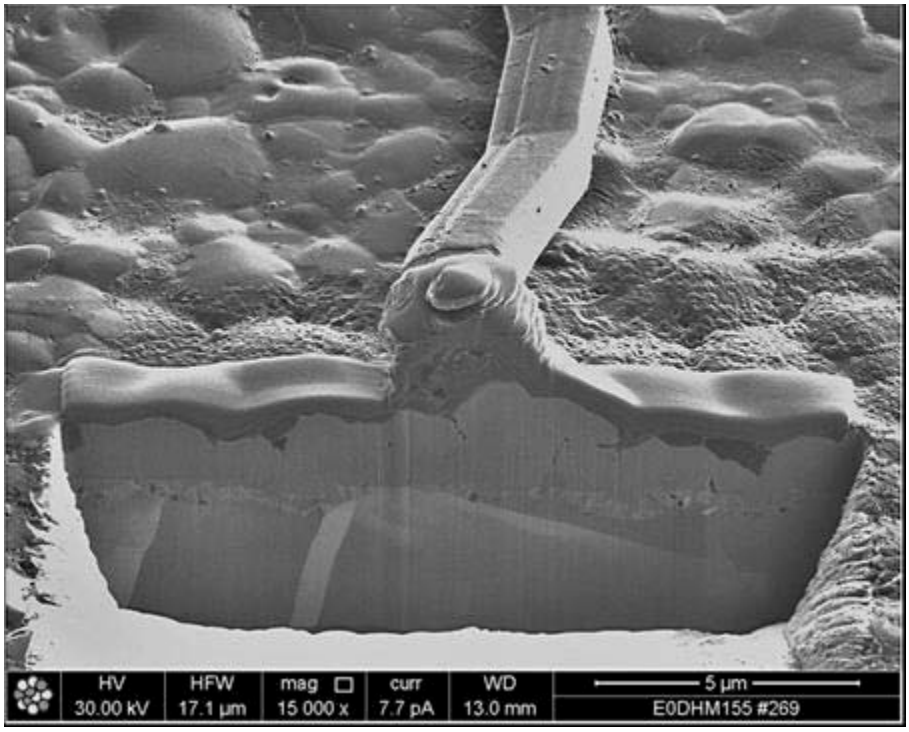

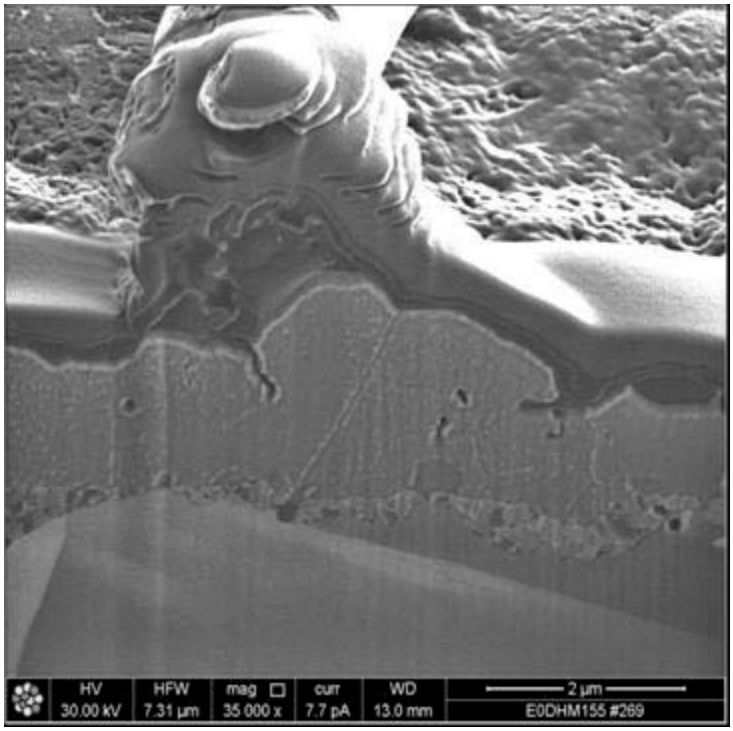

FIB Electron Images for Sn with 1.3% Au – 2nd Whisker Post Aging 12,000 Hours at 50°C/ 50% Relative Humdity

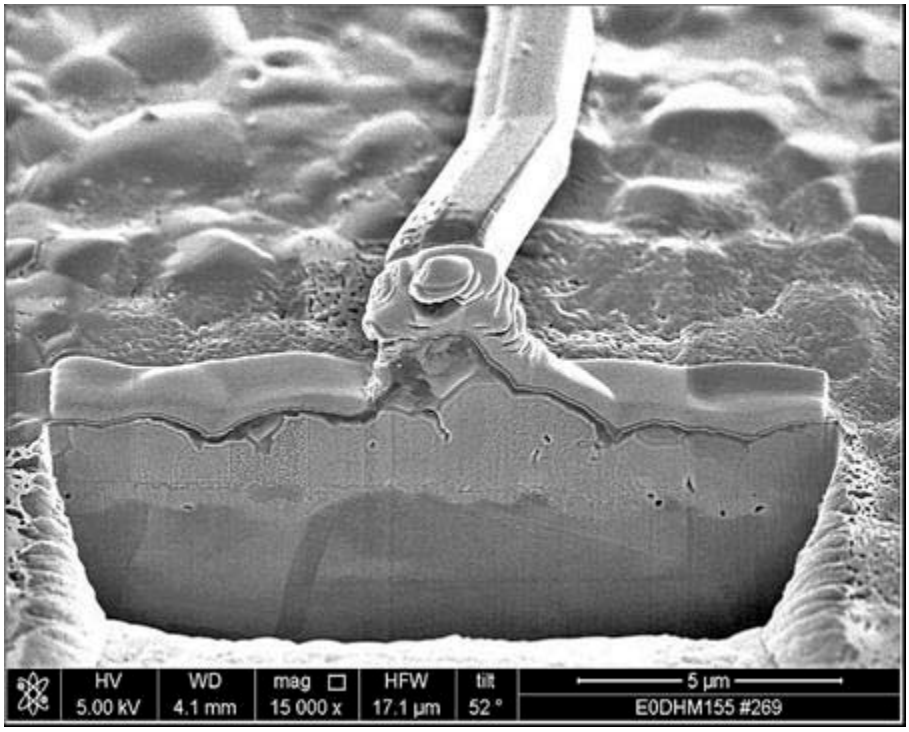

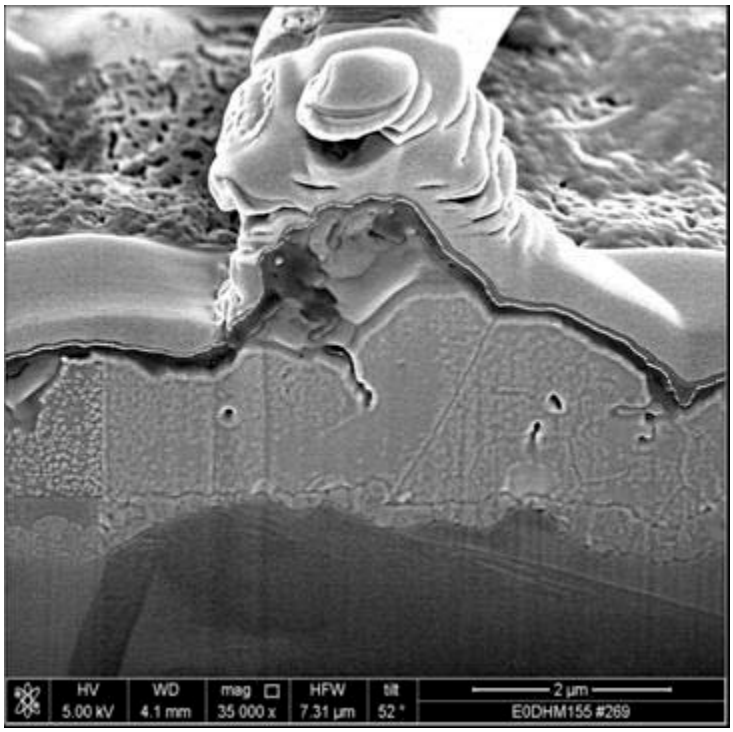

FIB Electron Images for Sn with 1.3% Au – 2nd Whisker
Post Aging 12,000 Hours at 50°C/ 50% Relative Humdity

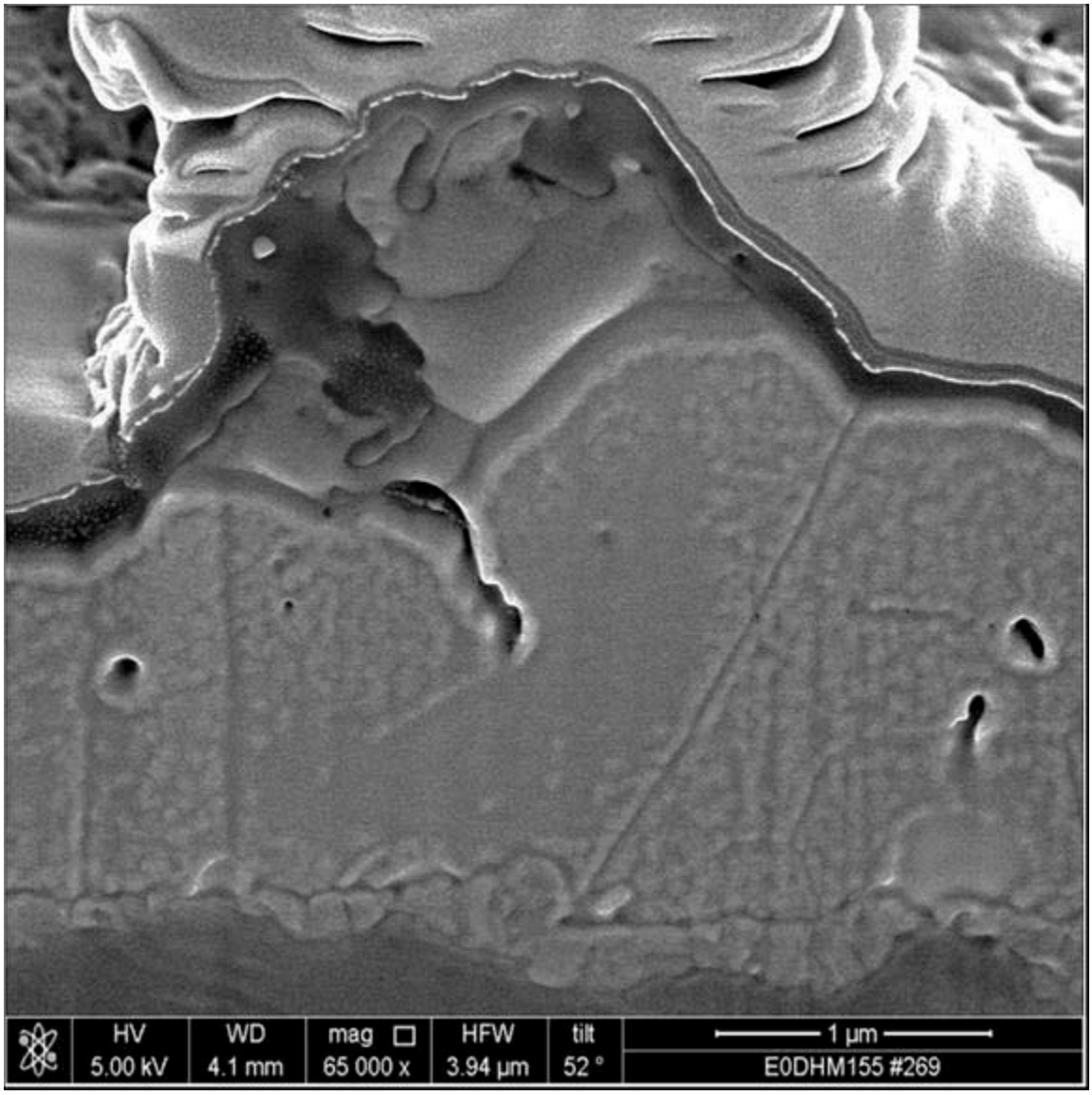

Appendix I: FIB Images for Pure Tin with 53nm Au Cap Layer

FIB Electron Images for Tin with 53nm Au Cap– 1st Whisker Post Aging 12,000 Hours at 50°C/ 50% Relative Humidity

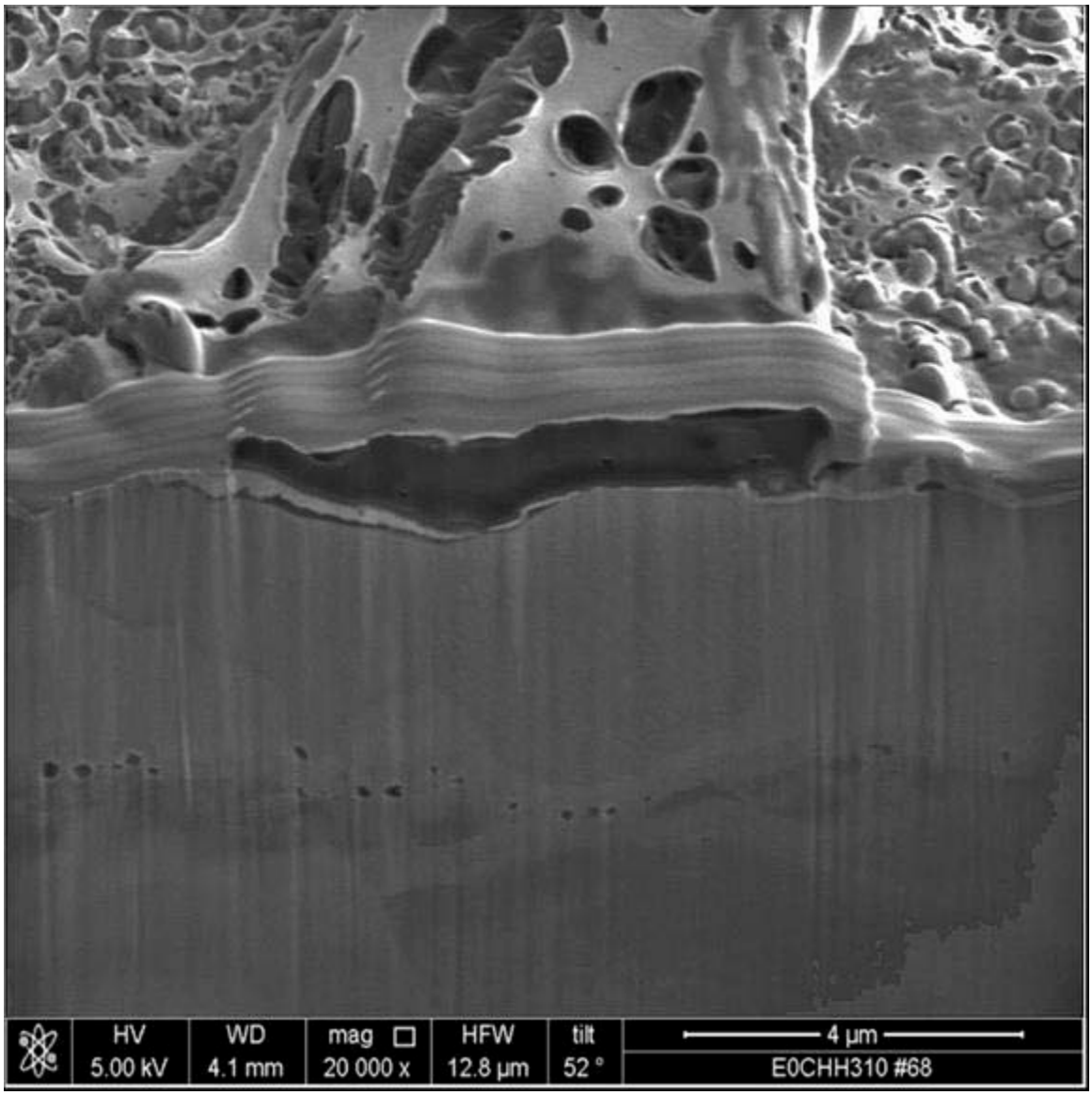

FIB Ion Images for Tin with 53nm Au Cap – 1st Whisker Post Aging 12,000 Hours at 50°C/ 50% Relative Humidity

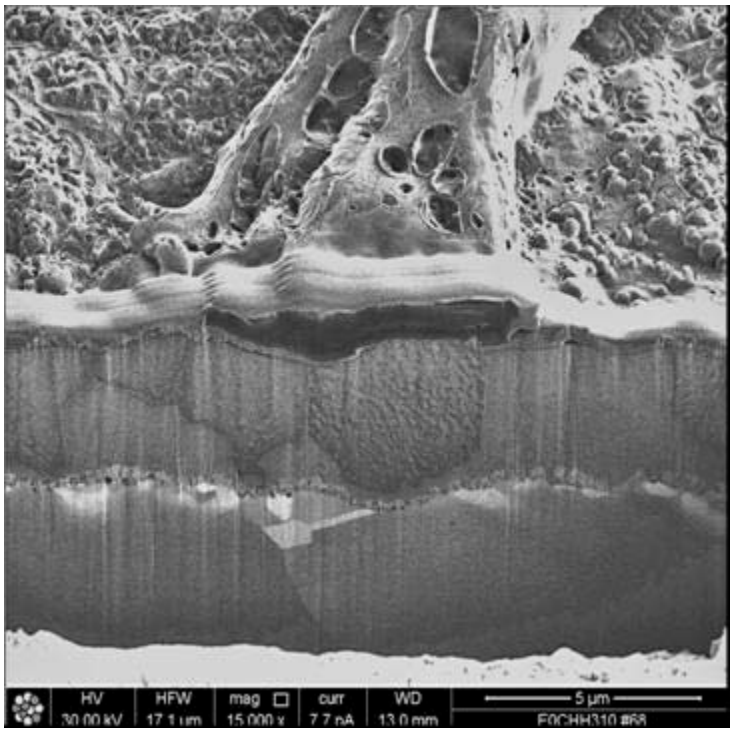

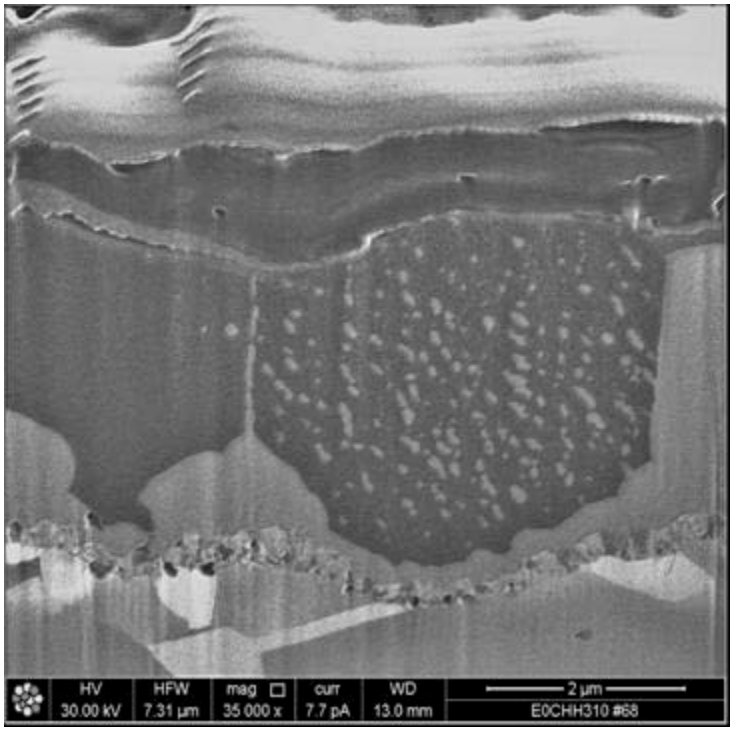

FIB Electron Images for Tin with 53nm Au Cap– 2nd Whisker Post Aging 12,000 Hours at 50°C/ 50% Relative Humidity

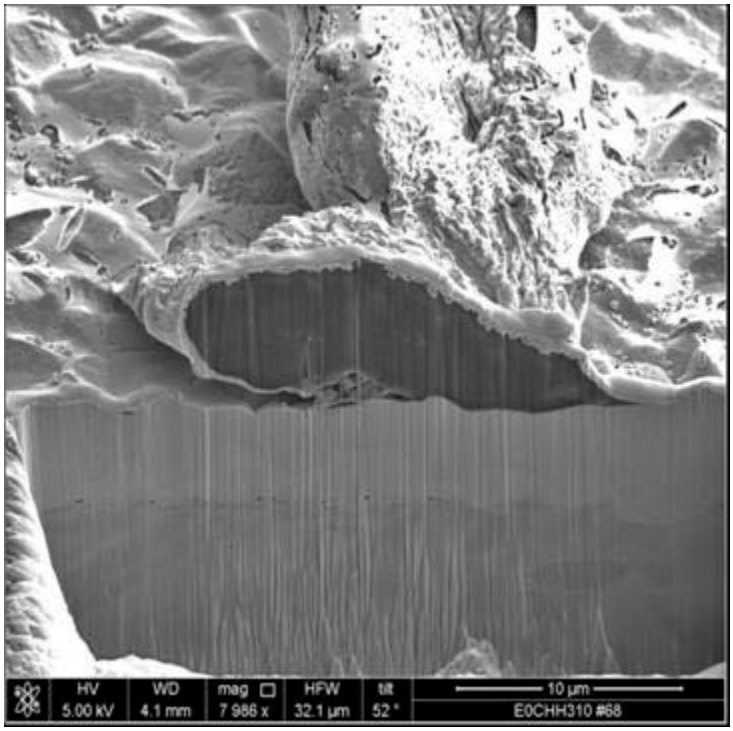

FIB Ion Images for Tin with 53nm Au Cap – 2nd Whisker Post Aging 12,000 Hours at 50°C/ 50% Relative Humidity

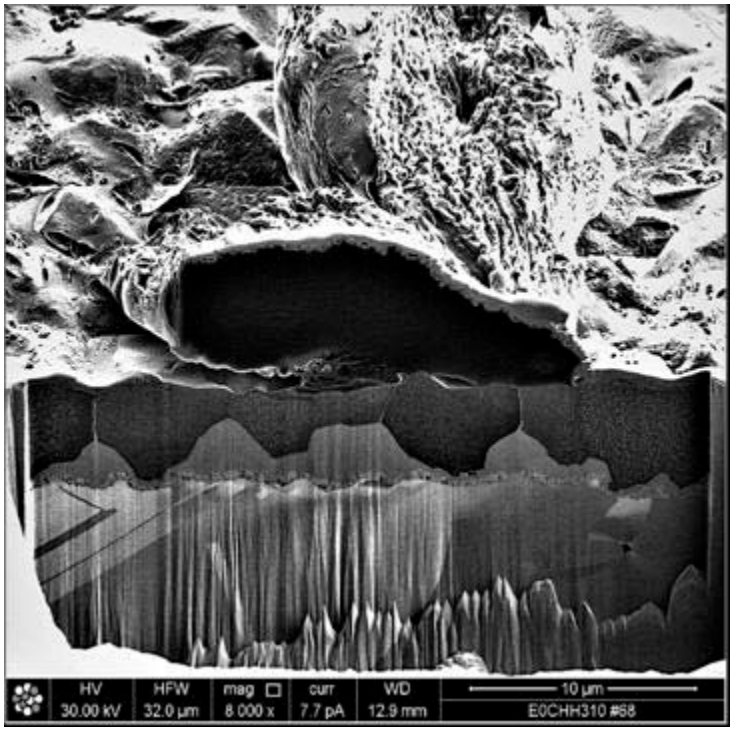

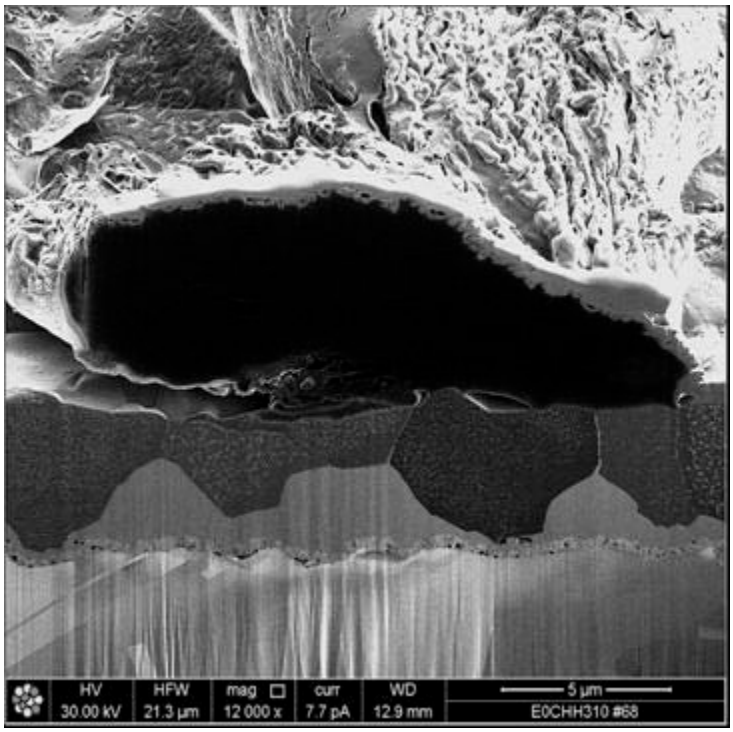

FIB Ion Images for Tin with 53nm Au Cap – 2nd Whisker Post Aging 12,000 Hours at 50°C/ 50% Relative Humidity

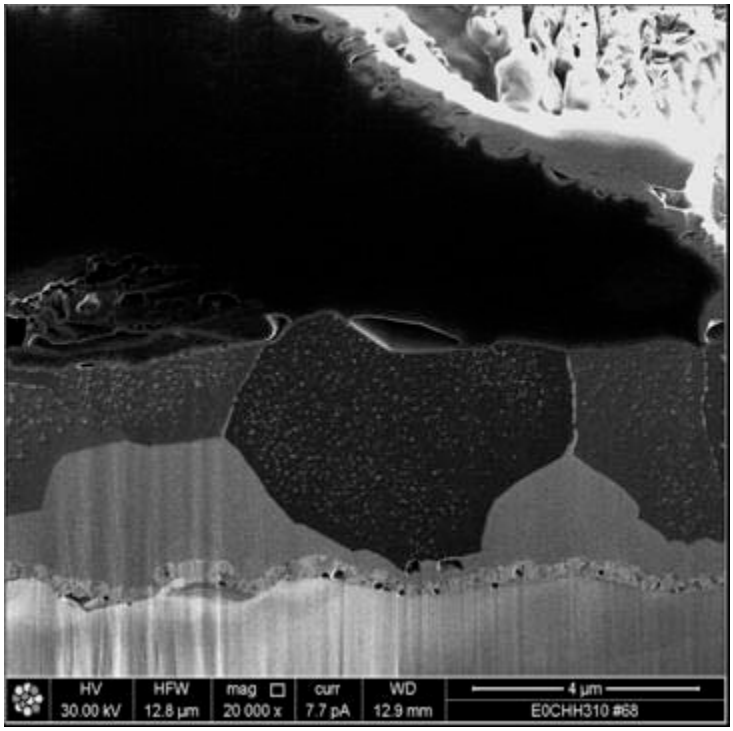

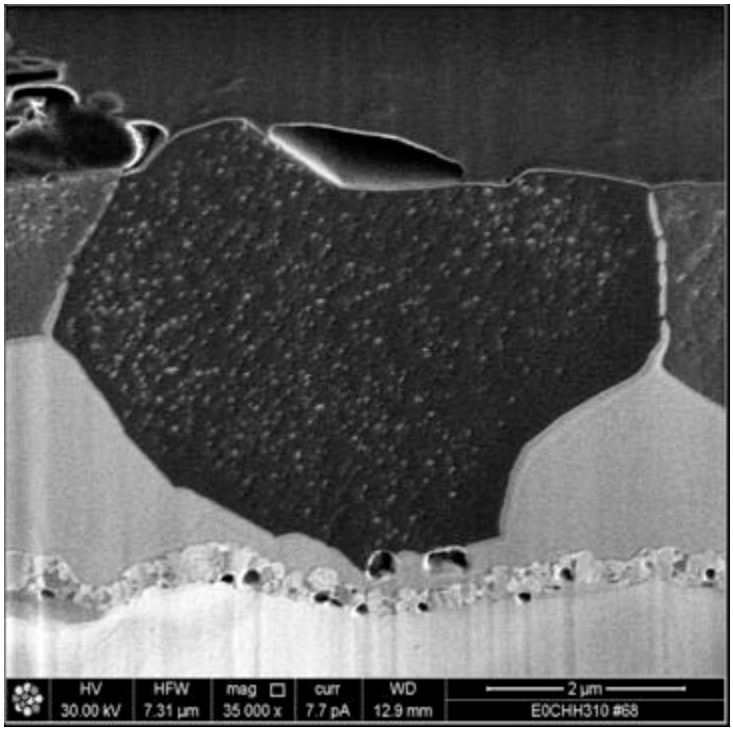

Appendix J: EBSD Data for Pure Sn

Pure Tin
Image Quality Map

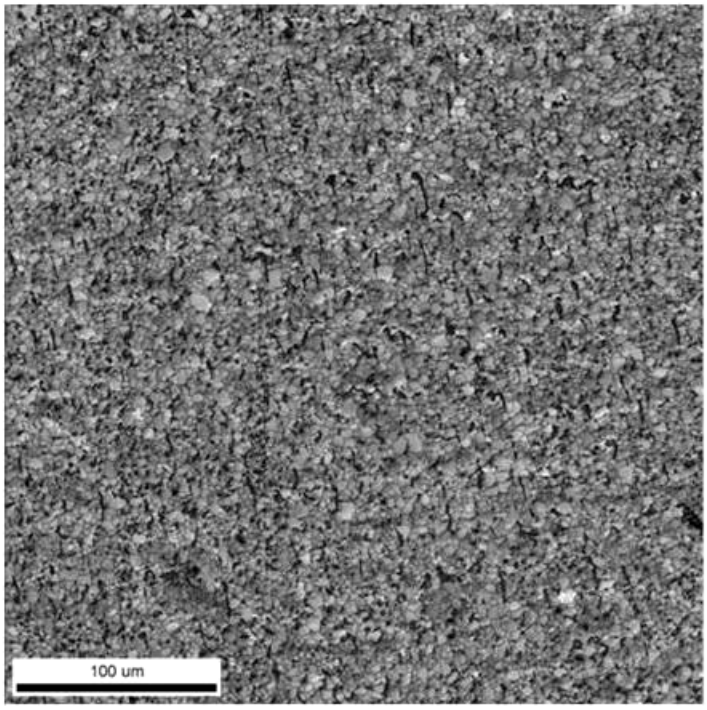

X = 350 microns
Y = 350 microns
Step size = 0.4 microns

a) Pure Tin, Sample 65, post plating

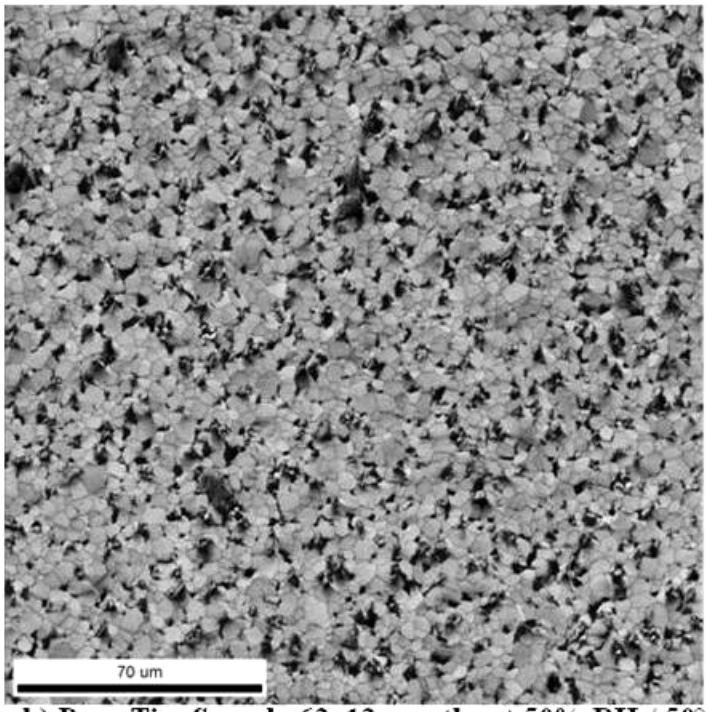

X = 200 microns
Y = 200 microns
Step size = 0.2 microns

b) Pure Tin, Sample 62, 12 months at 50% RH / 50°C

Pure Tin
Color Coded Orientation Map

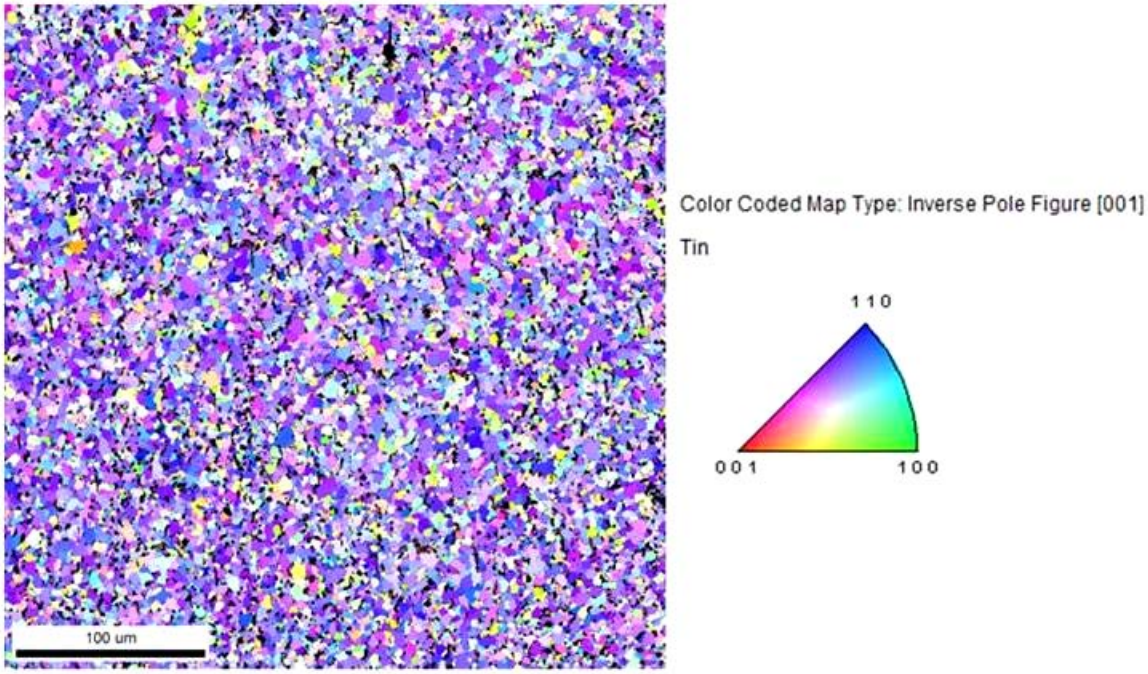

a) Pure Tin, Sample 65, post plating

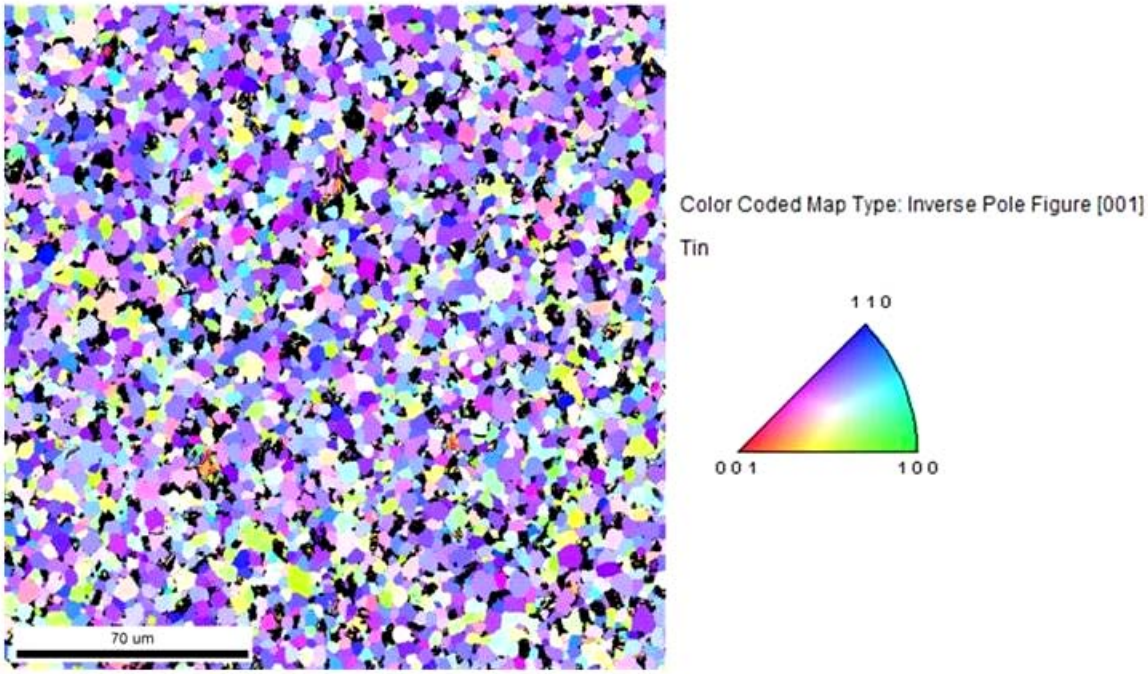

b) Pure Tin, Sample 62, 12 months at 50% RH / 50°C

Pure Tin

Crystal Direction Map Showing <111> crystal direction in ND direction 15º Tolerance

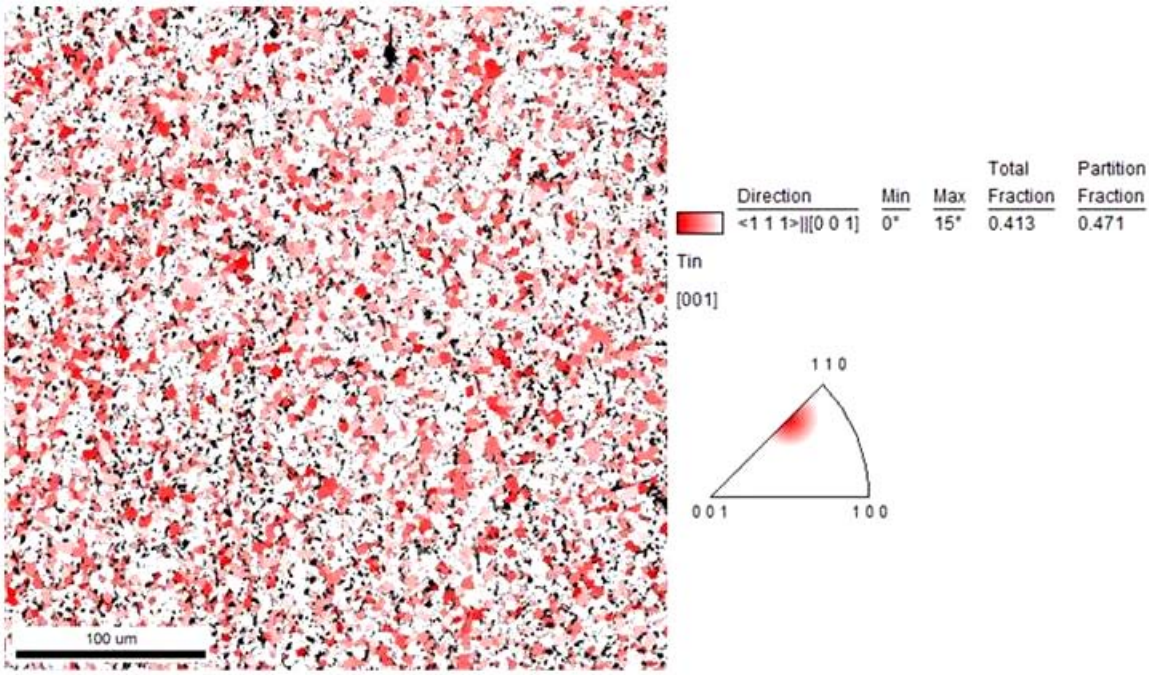

a) Pure Tin, Sample 65, post plating

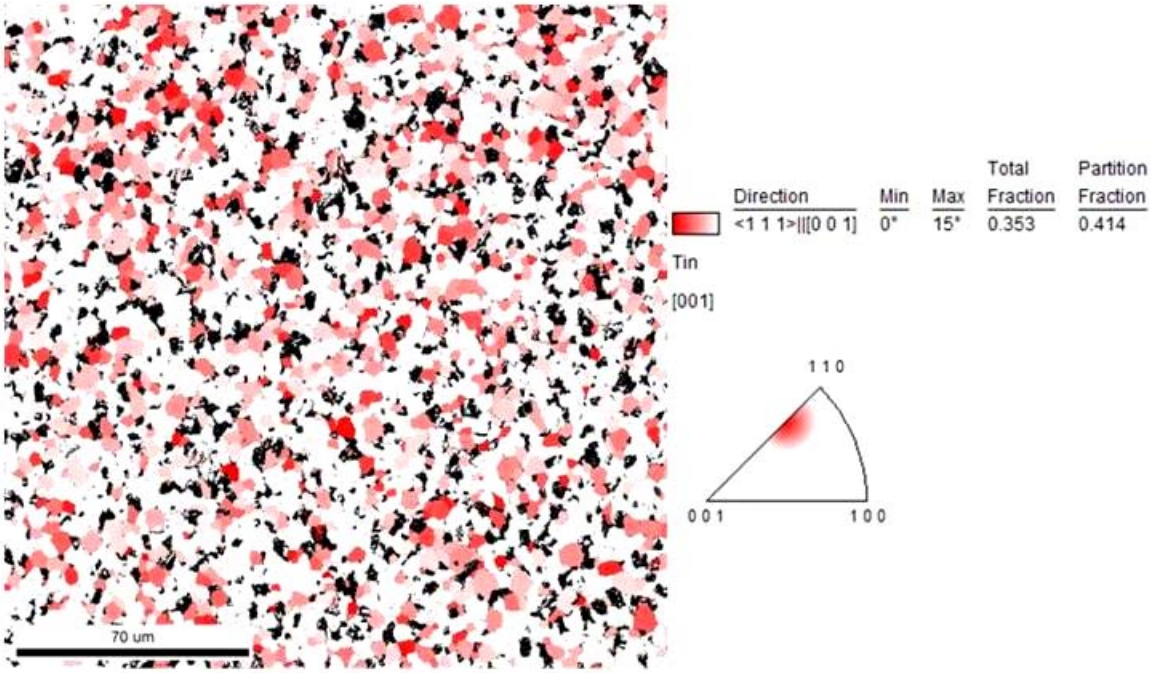

b) Pure Tin, Sample 62, 12 months at 50% RH / 50°C

Pure Tin
Crystal Direction Map Showing <111> crystal direction in ND direction 20º Tolerance

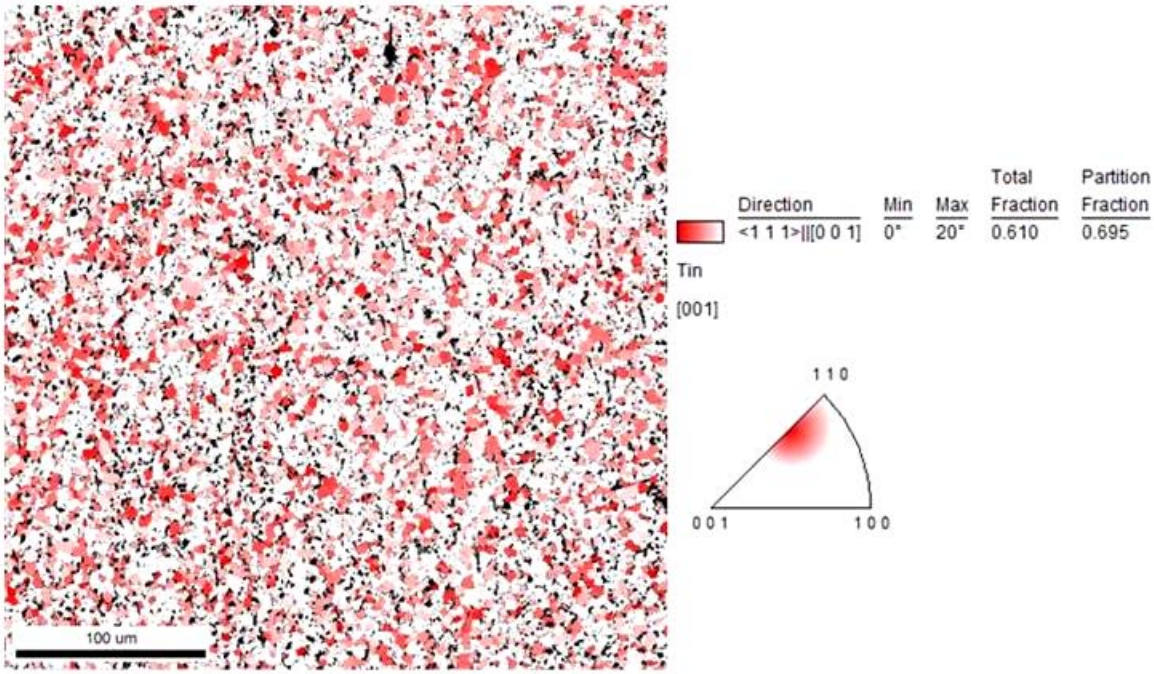

a) Pure Tin, Sample 65, post plating

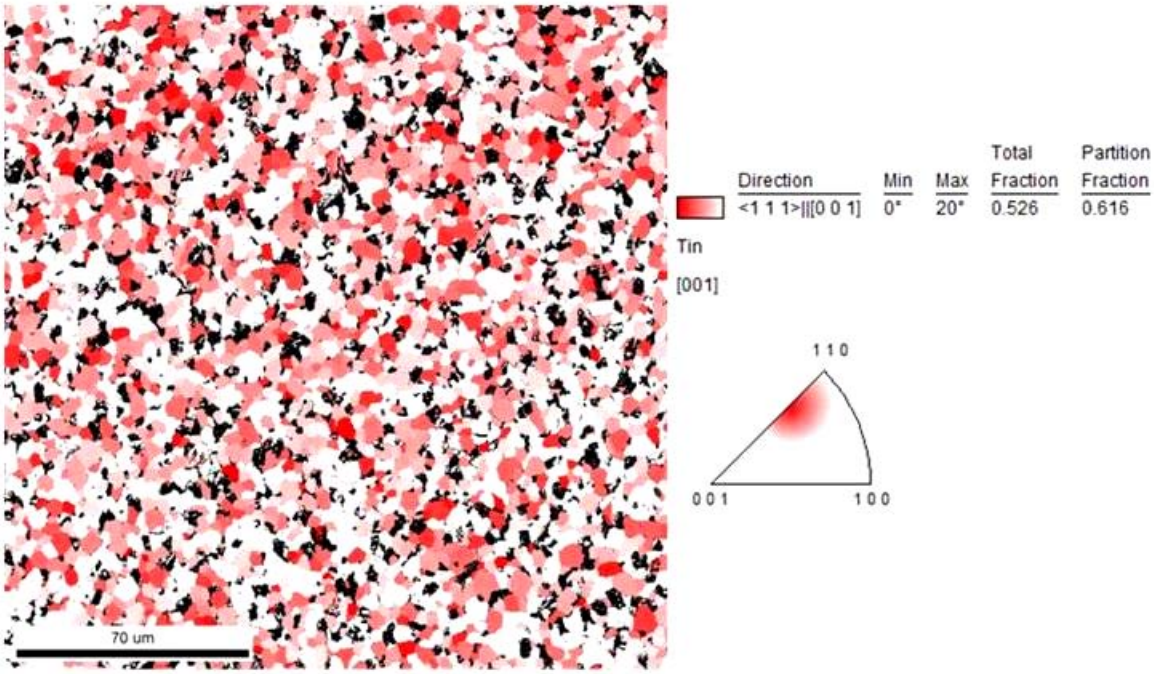

b) Pure Tin, Sample 62, 12 months at 50% RH / 50°C

Pure Tin

Confidence Index (CI) Chart

Data points with a CI above 0.1 are generally considered to be indexed correctly.

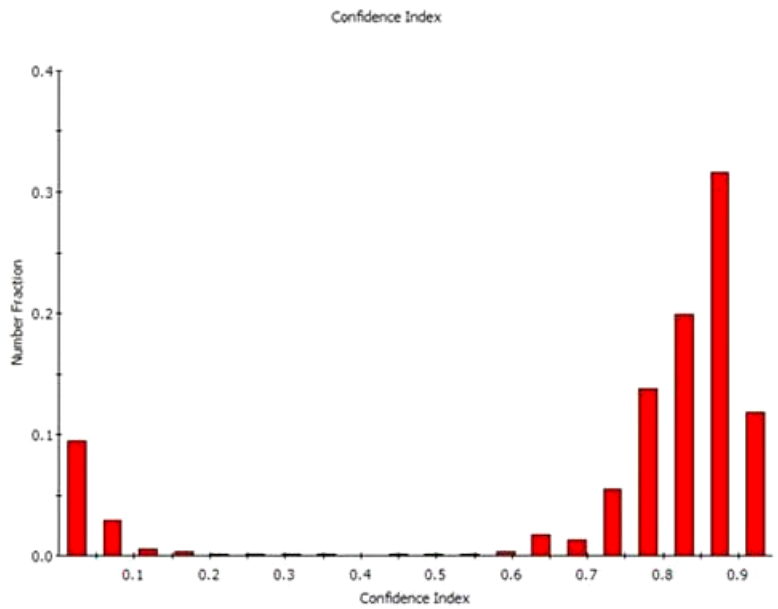

(a) Pure Tin, Sample 65, post plating. Indicates that about 12.3% of data points were not indexed with a high degree of confidence

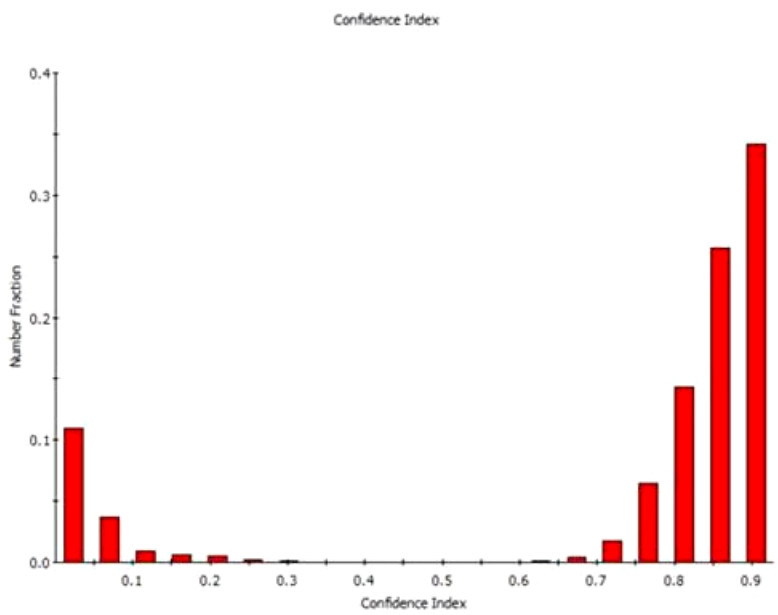

(b) Pure Tin, Sample 62, 12 months at 50% RH / 50°C. Indicates that about 14.6.% of data points were not indexed with a high degree of confidence

Pure Tin
Pole Figure and Inverse Pole Figure Plots

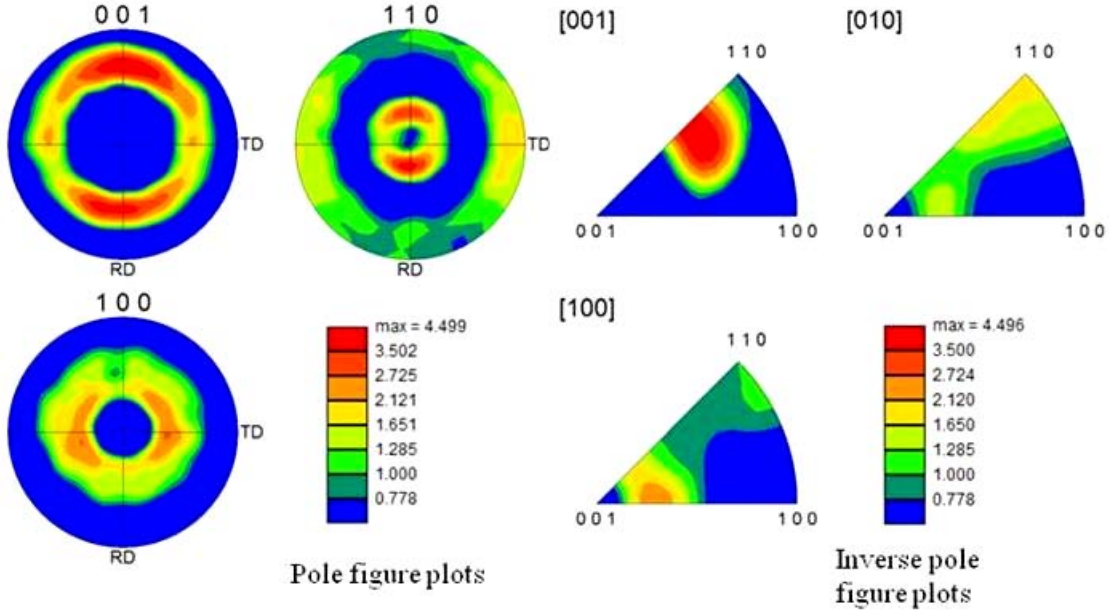

a) Pure Tin, Sample 65, post plating

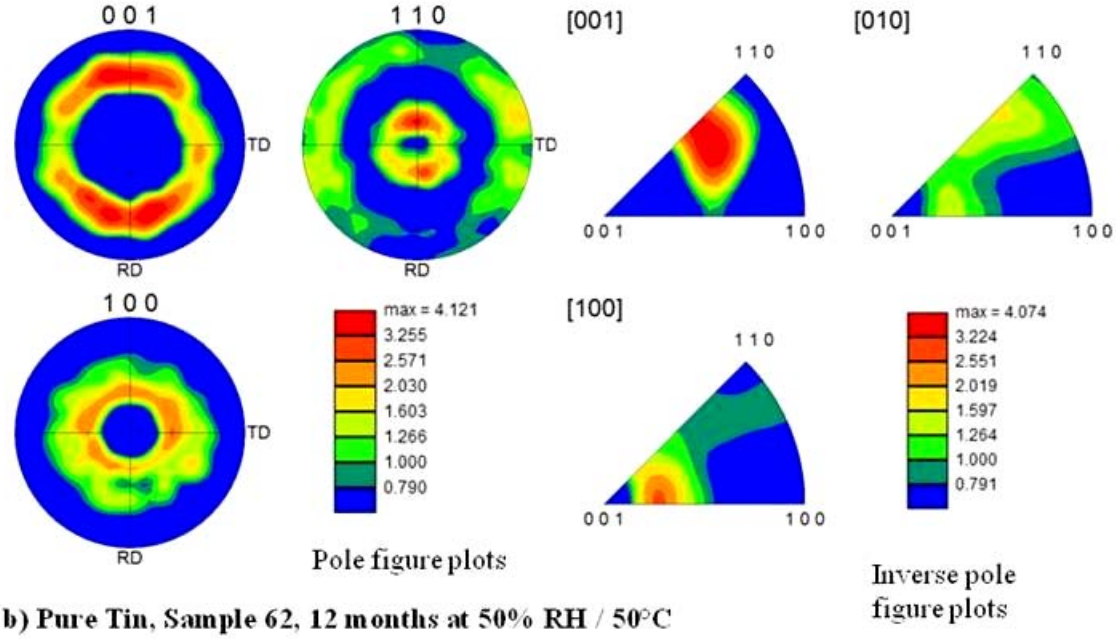

b) Pure Tin, Sample 62, 12 months at 50% RH / 50°C

Pure Tin
Grain Size Histogram and Data

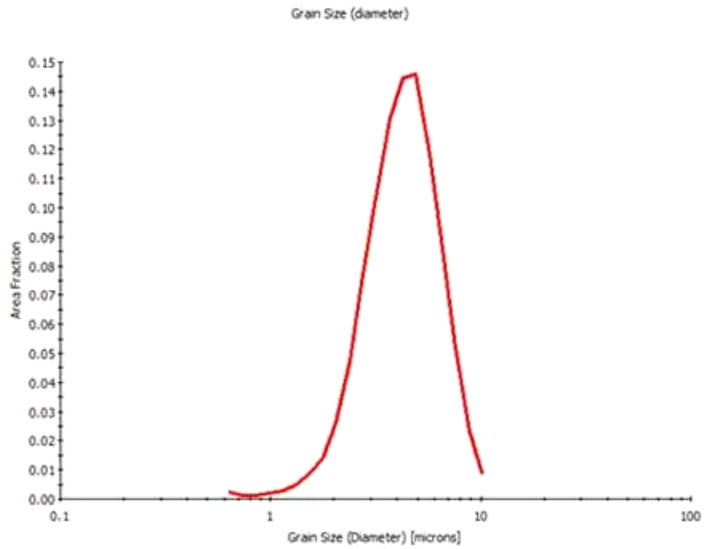

Chart: Grain Size (diameter)

Edge grains included in analysis

Diameter [microns]	Area Fraction
0.638932	0.00253414
0.73922	0.00140641
0.855249	0.00118242
0.98949	0.0021643
1.1448	0.00275552
1.32449	0.00487555
1.53239	0.00874968
1.77291	0.0142047
2.05119	0.0260784
2.37315	0.0470756
2.74564	0.0771349
3.1766	0.10313
3.6752	0.130137
4.25207	0.14427
4.91948	0.145863
5.69164	0.118551
6.58501	0.0857153
7.61861	0.052123
8.81443	0.0233919
10.198	0.00865722

Average	
Number	2.87793
Standard Deviation	1.59386
Area	4.49422

a) Pure Tin, Sample 65, post plating

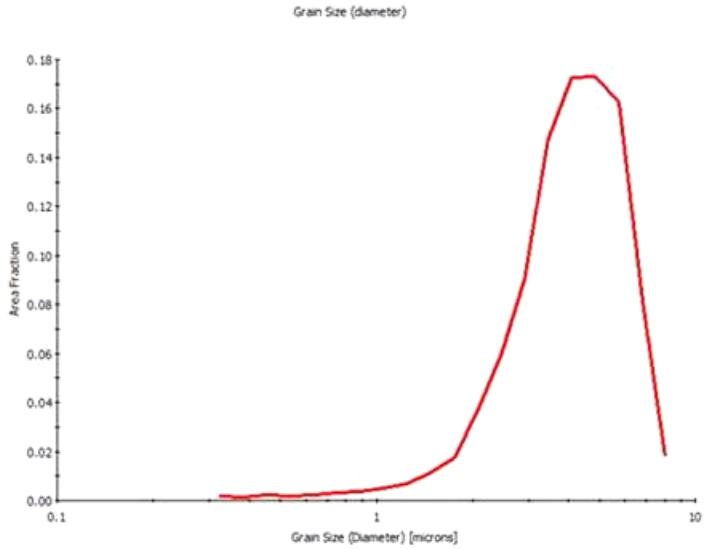

Chart: Grain Size (diameter)

Edge grains included in analysis

Diameter [microns]	Area Fraction
0.323238	0.00185176
0.382855	0.00149471
0.453469	0.00217301
0.537107	0.00190906
0.63617	0.00229885
0.753505	0.00340377
0.892482	0.00360838
1.05709	0.00503557
1.25206	0.00684028
1.48299	0.0115423
1.75651	0.0173339
2.08048	0.0374548
2.4642	0.060166
2.9187	0.0901144
3.45703	0.147262
4.09464	0.172492
4.84985	0.172927
5.74436	0.162567
6.80384	0.0817058
8.05874	0.0178189

Average	
Number	1.94112
Standard Deviation	1.67702
Area	4.24034

b) Pure Tin, Sample 62, 12 months at 50% RH / 50°C

Pure Tin
Misorientation Angle Histogram, 2º minimum misorientation

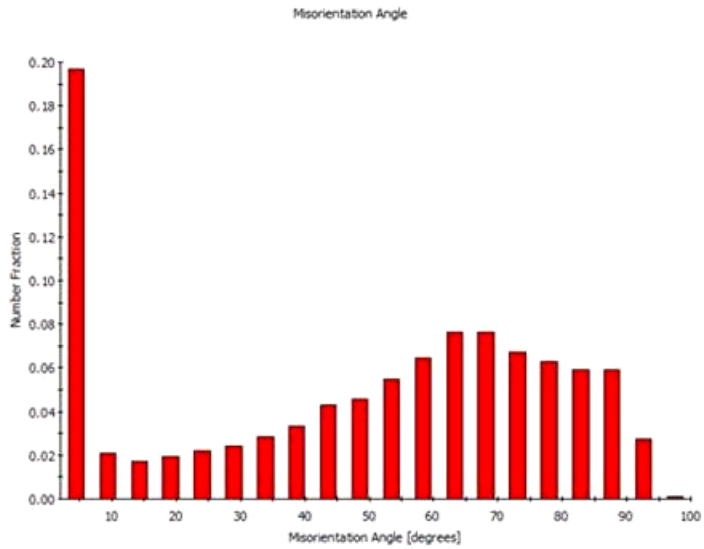

Chart: Misorientation Angle

Angle [degrees]	Number Fraction
4.45	0.196949
9.35	0.0208752
14.25	0.0169873
19.15	0.0192069
24.05	0.0221032
28.95	0.024151
33.85	0.0286046
38.75	0.0333804
43.65	0.043247
48.55	0.0455847
53.45	0.0545885
58.35	0.0644981
63.25	0.0766094
68.15	0.0764125
73.05	0.0669648
77.95	0.0627439
82.85	0.0591101
87.75	0.0593214
92.65	0.0275234
97.55	0.00113845

Average Number 48.297

a) Pure Tin, Sample 65, post plating

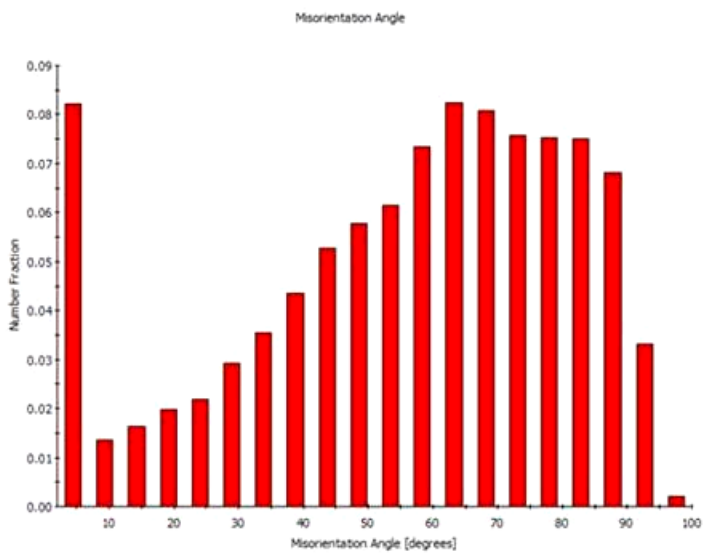

Chart: Misorientation Angle

Angle [degrees]	Number Fraction
4.45	0.0822471
9.35	0.0135542
14.25	0.0162583
19.15	0.0199067
24.05	0.0218622
28.95	0.0292259
33.85	0.0353493
38.75	0.0435232
43.65	0.0527642
48.55	0.0577311
53.45	0.0614912
58.35	0.0734587
63.25	0.0823253
68.15	0.0808727
73.05	0.075822
77.95	0.0752354
82.85	0.0749895
87.75	0.0681007
92.65	0.0332486
97.55	0.00203369

Average Number 55.5331

b) Pure Tin, Sample 62, 12 months at 50% RH / 50°C

Pure Tin
Misorientation Angle Histogram, 2º minimum misorientation

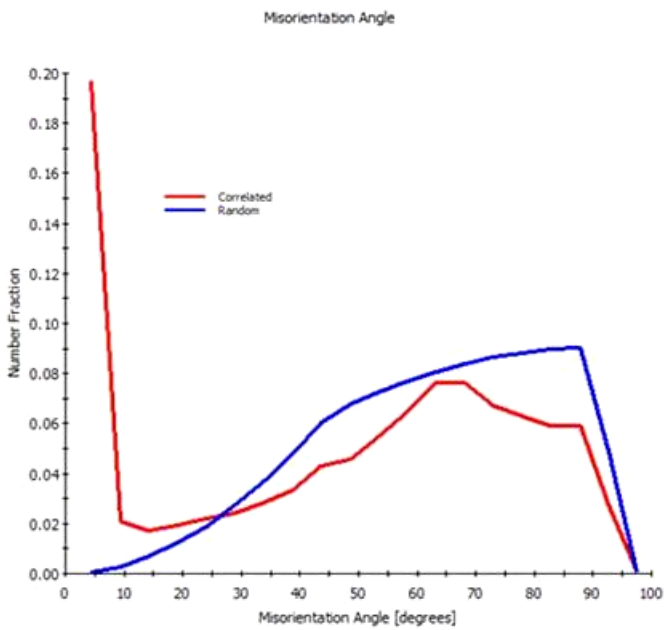

Chart: Misorientation Angle

Angle [degrees]	Correlated Number Fraction	Random Number Fraction
4.45	0.196949	0.000708709
9.35	0.0208752	0.00294711
14.25	0.0169873	0.00675729
19.15	0.0192069	0.0121114
24.05	0.0221032	0.0189703
28.95	0.024151	0.0272839
33.85	0.0286046	0.0369914
38.75	0.0333804	0.0480218
43.65	0.043247	0.0602946
48.55	0.0455847	0.0677123
53.45	0.0545885	0.0725691
58.35	0.0644981	0.076896
63.25	0.0766094	0.0806611
68.15	0.0764125	0.083837
73.05	0.0669648	0.0864005
77.95	0.0627439	0.0883329
82.85	0.0591101	0.0896199
87.75	0.0593214	0.0902523
92.65	0.0275234	0.0489891
97.55	0.00113845	0.000673135
Average Number	48.297	63.0123

a) Pure Tin, Sample 65, post plating

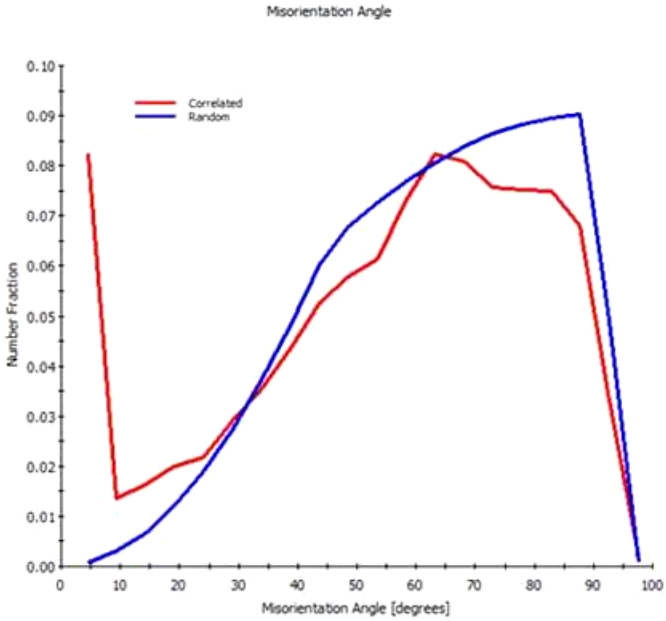

Chart: Misorientation Angle

Angle [degrees]	Correlated Number Fraction	Random Number Fraction
4.45	0.0822471	0.000709712
9.35	0.0135542	0.00294811
14.25	0.0162583	0.00675829
19.15	0.0199067	0.0121124
24.05	0.0218622	0.0189713
28.95	0.0292259	0.0272849
33.85	0.0353493	0.0369924
38.75	0.0435232	0.0480228
43.65	0.0527642	0.0602956
48.55	0.0577311	0.0677133
53.45	0.0614912	0.0725702
58.35	0.0734587	0.076897
63.25	0.0823253	0.0806621
68.15	0.0808727	0.083838
73.05	0.075822	0.0864015
77.95	0.0752354	0.0883339
82.85	0.0749895	0.0896209
87.75	0.0681007	0.0902533
92.65	0.0332486	0.0489901
97.55	0.00203369	0.000674138
Average Number	55.5331	63.0123

b) Pure Tin, Sample 62, 12 months at 50% RH / 50°C

Pure Tin
Grain Boundary Characterization Chart

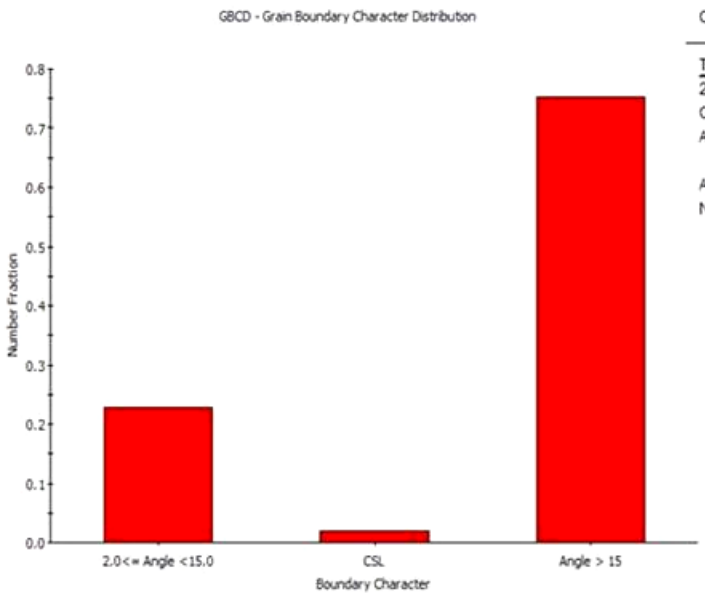

Chart: GBCD - Grain Boundary Character Distribution

Type	Number Fraction
2.0<= Angle <15.0	0.228862
CSL	0.0194755
Angle > 15	0.751663
Average Number	0.333333

a) Pure Tin, Sample 65, post plating

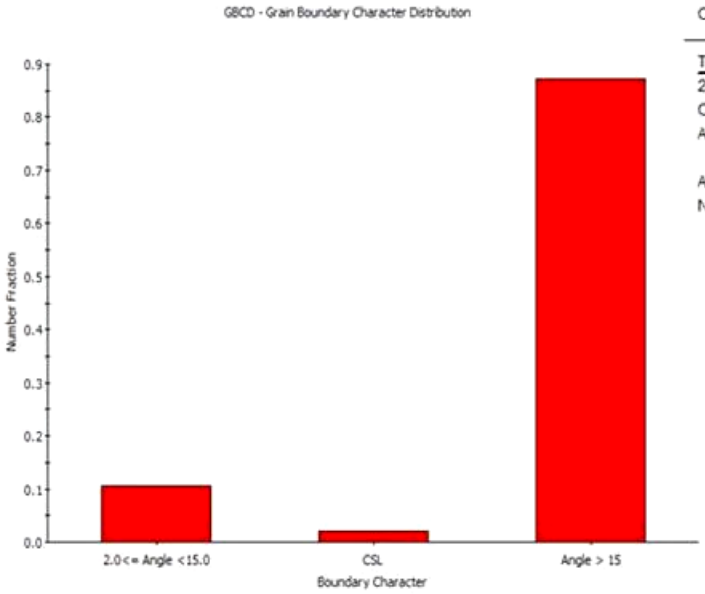

Chart: GBCD - Grain Boundary Character Distribution

Type	Number Fraction
2.0<= Angle <15.0	0.105143
CSL	0.0213761
Angle > 15	0.873481
Average Number	0.333333

b) Pure Tin, Sample 62, 12 months at 50% RH / 50°C

Pure Tin

Coincident Site Lattice Boundary Chart

The total fraction of CSL boundaries is approximately 2% of boundaries measured

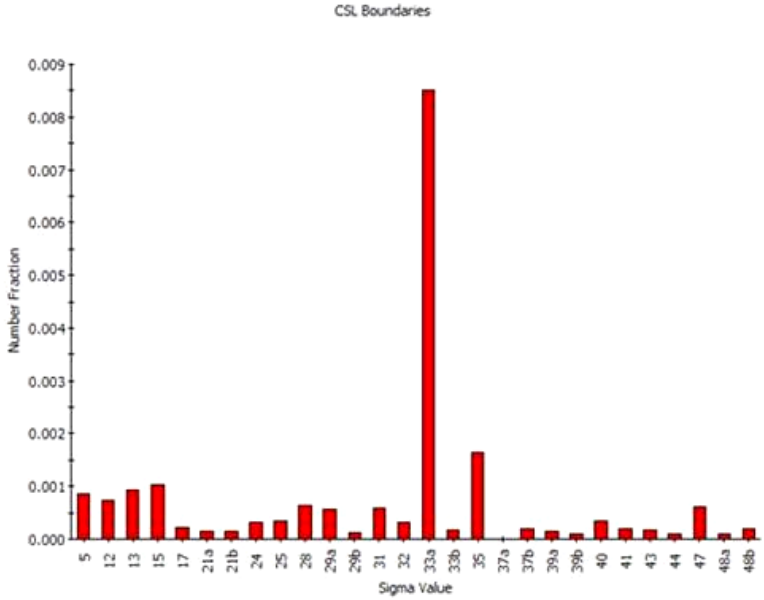

Chart: CSL Boundaries

Overall fraction of CSL boundaries: 0.019

Sigma	Number Fraction
5	0.000866371
12	0.000730329
13	0.000930812
15	0.00103463
17	0.000211223
21a	0.000146782
21b	0.000146782
24	0.000311464
25	0.000336524
28	0.000640828
29a	0.000572807
29b	0.000132462
31	0.000583548
32	0.000325784
33a	0.00851335
33b	0.000179002
35	0.00165398
37a	1.07401e-005
37b	0.000196903
39a	0.000157522
39b	8.95012e-005
40	0.000350845
41	0.000186162
43	0.000179002
44	8.59211e-005
47	0.000612188
48a	8.95012e-005
48b	0.000200483

a) Pure Tin, Sample 65, post plating

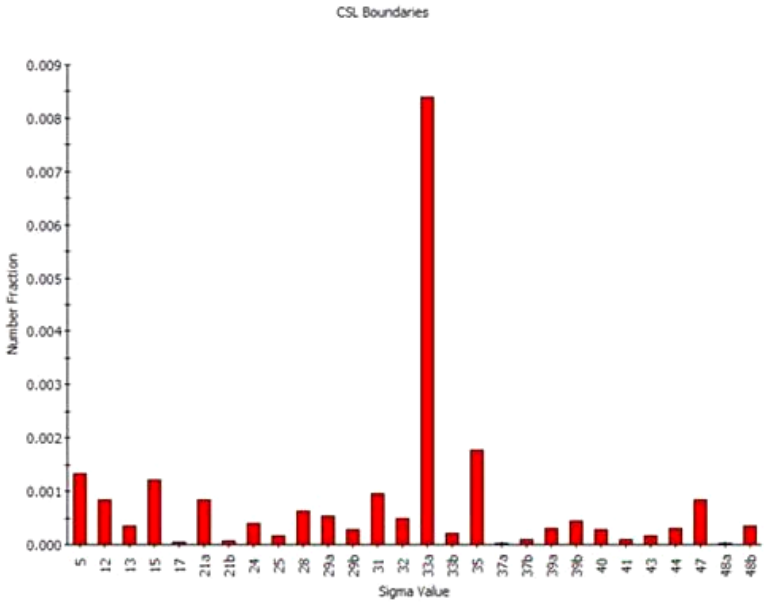

Chart: CSL Boundaries

Overall fraction of CSL boundaries: 0.021

Sigma	Number Fraction
5	0.00133531
12	0.000832472
13	0.000346398
15	0.0012068
17	4.46965e-005
21a	0.000849233
21b	6.70447e-005
24	0.000385507
25	0.000156438
28	0.000625751
29a	0.000525184
29b	0.000273766
31	0.0009498
32	0.000491661
33a	0.00838618
33b	0.000201134
35	0.00176551
37a	2.79353e-005
37b	9.498e-005
39a	0.000296114
39b	0.000435791
40	0.000279353
41	9.498e-005
43	0.000167612
44	0.000296114
47	0.000849233
48a	3.35224e-005
48b	0.000357572

b) Pure Tin, Sample 62, 12 months at 50% RH / 50°C

Pure Tin
Misorientation Distribution Function (MODF) Plot

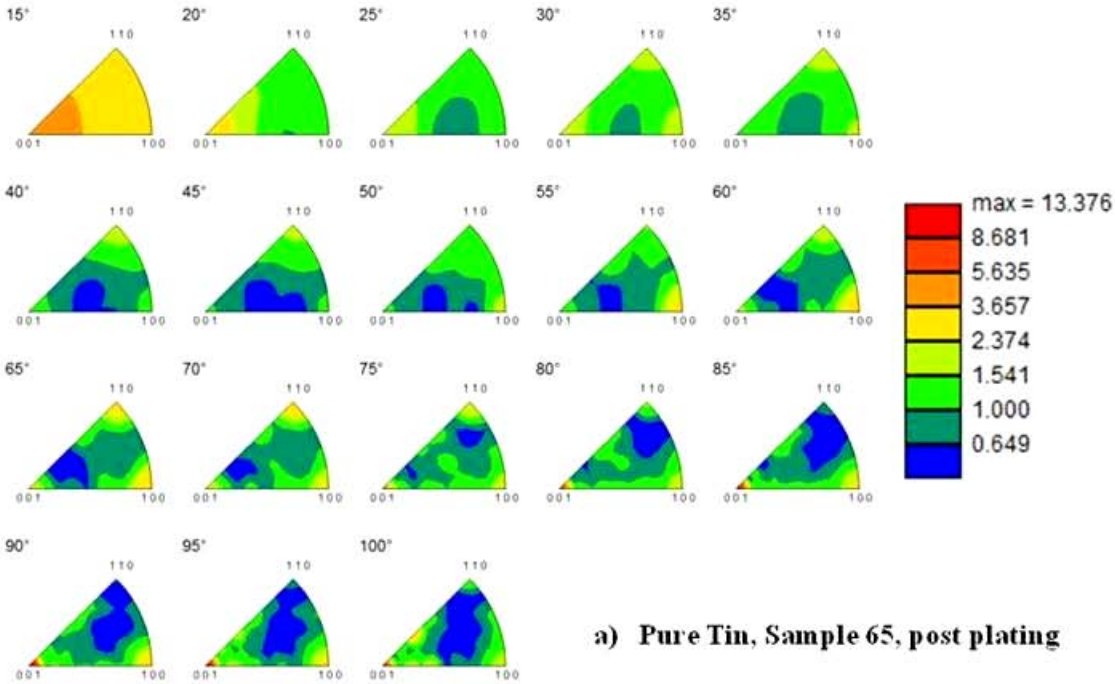

a) Pure Tin, Sample 65, post plating

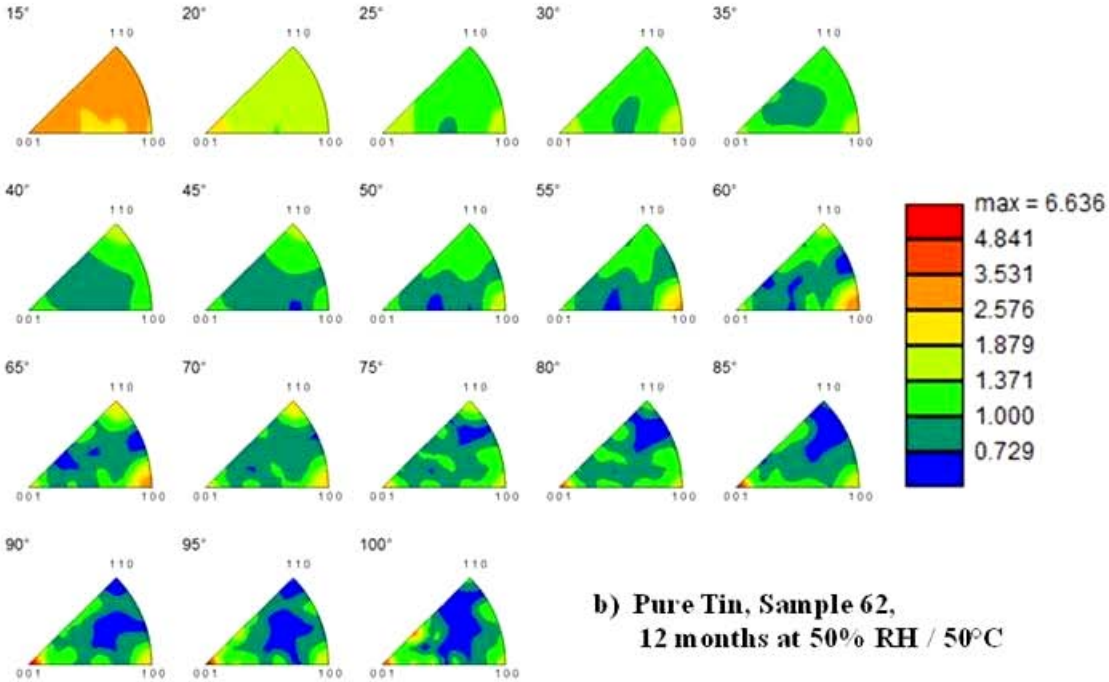

b) Pure Tin, Sample 62,
12 months at 50% RH / 50°C

Pure Tin

Crystal Direction Map

Blue Indicates C-Direction in sample normal

Red indicates C-direction in sample plane 15º tolerance

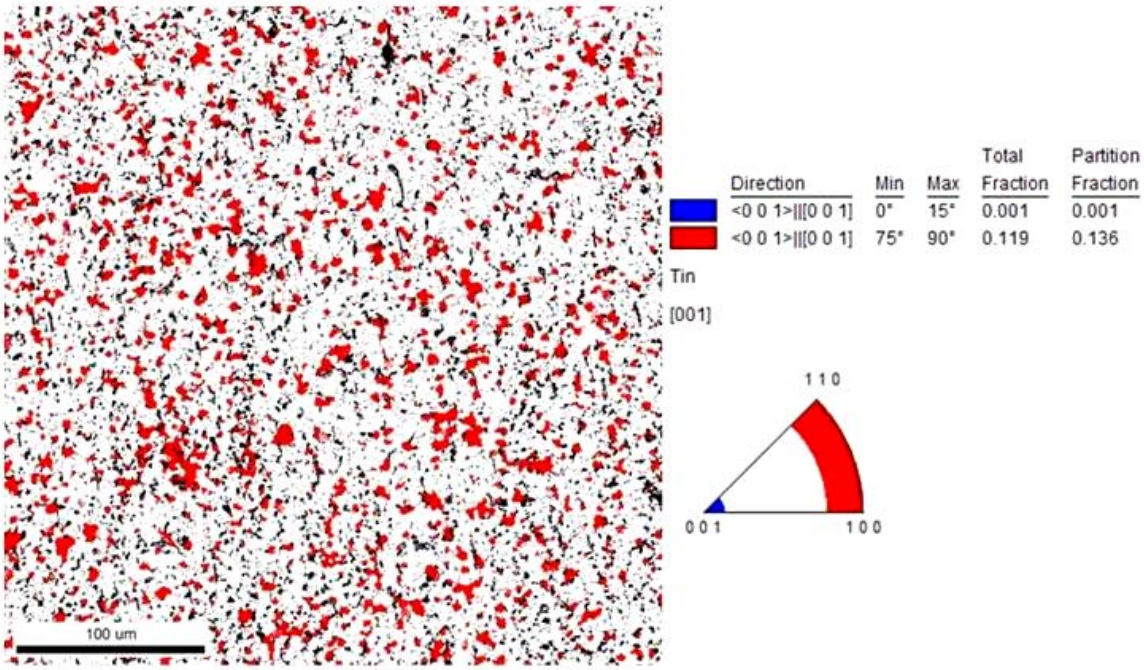

a) Pure Tin, Sample 65, post plating

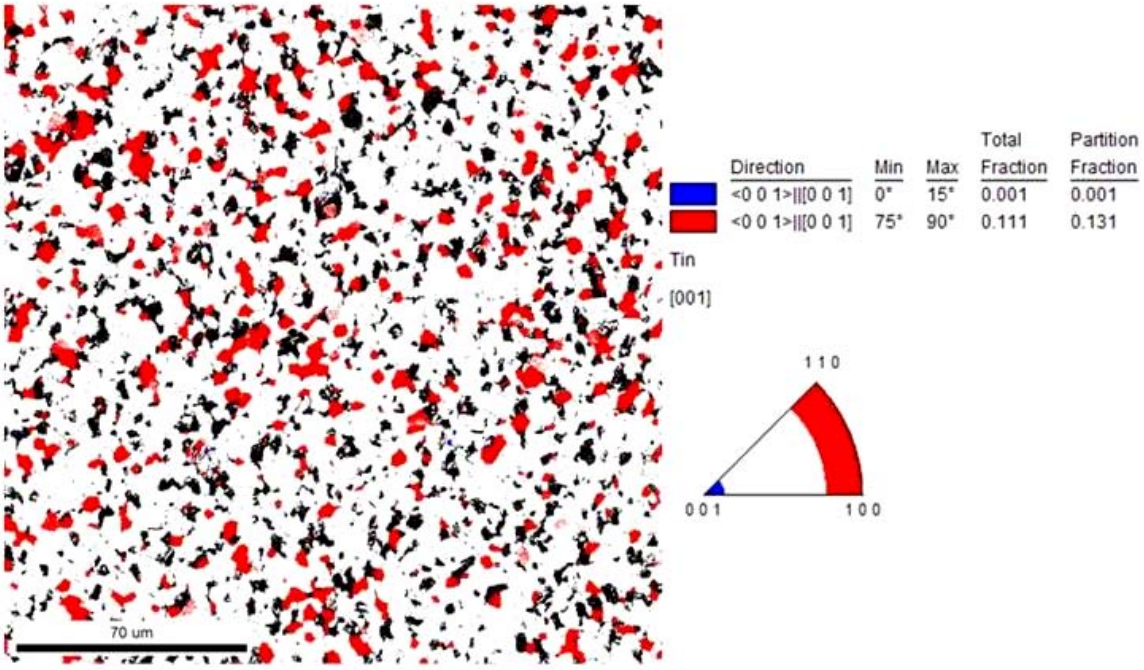

b) Pure Tin, Sample 62, 12 months at 50% RH / 50°C

Appendix K: EBSD Data for Sn with 3.1% Pb

Electroplated Sn with 3.1% Pb
Image Quality Map

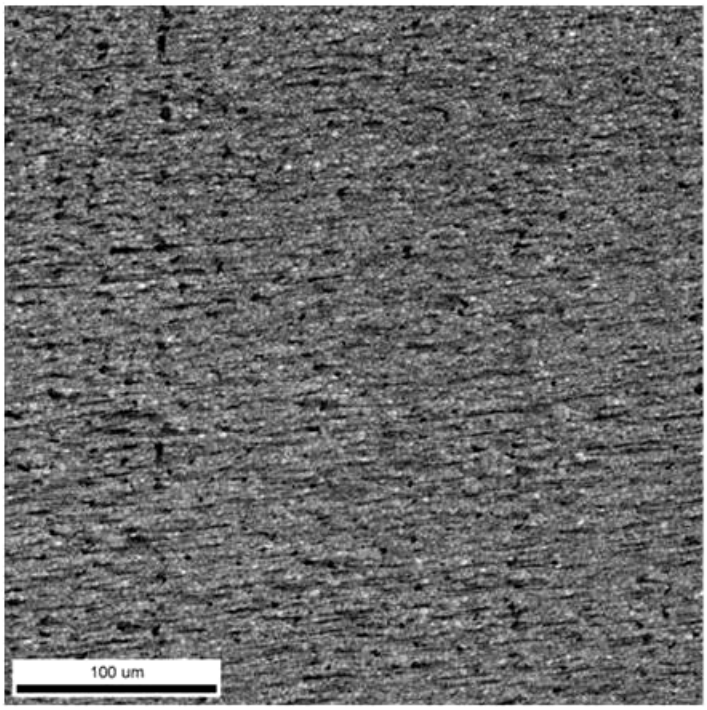

X = 350 microns
Y = 350 microns
Step size = 0.4 microns

a) Sn with 3.1% Pb, Sample 74, post plating

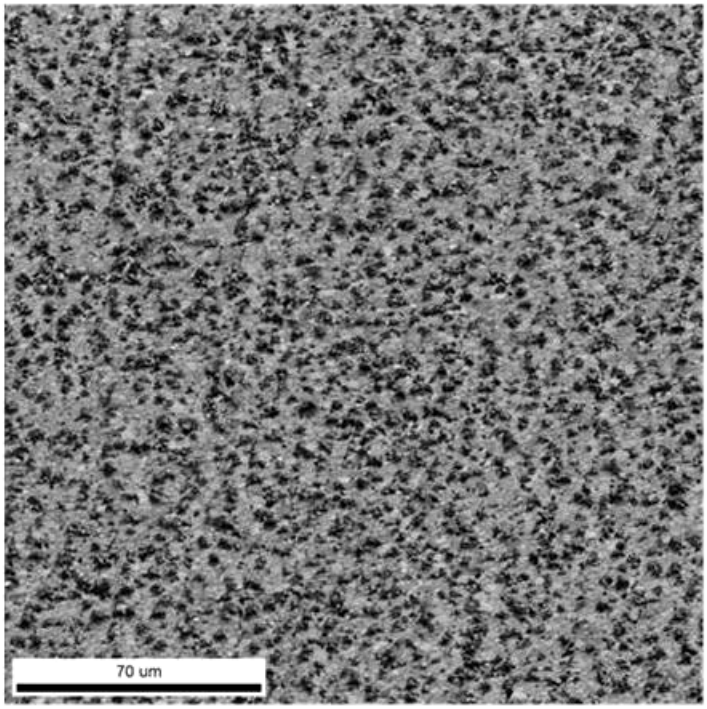

X = 200 microns
Y = 200 microns
Step size = 0.2 microns

b) Sn with 3.1% Pb, Sample 73, 12 months at 50% RH / 50°C

Electroplated Sn with 3.1% Pb
Color Coded Orientation Map

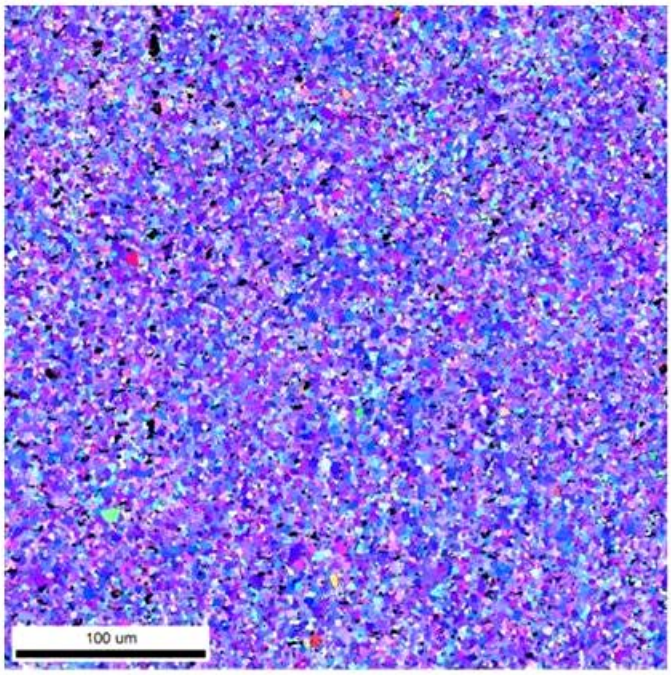

Color Coded Map Type: Inverse Pole Figure [001]

Tin

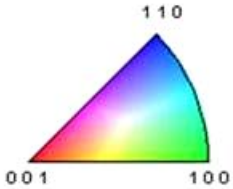

a) Sn with 3.1% Pb, Sample 74, post plating

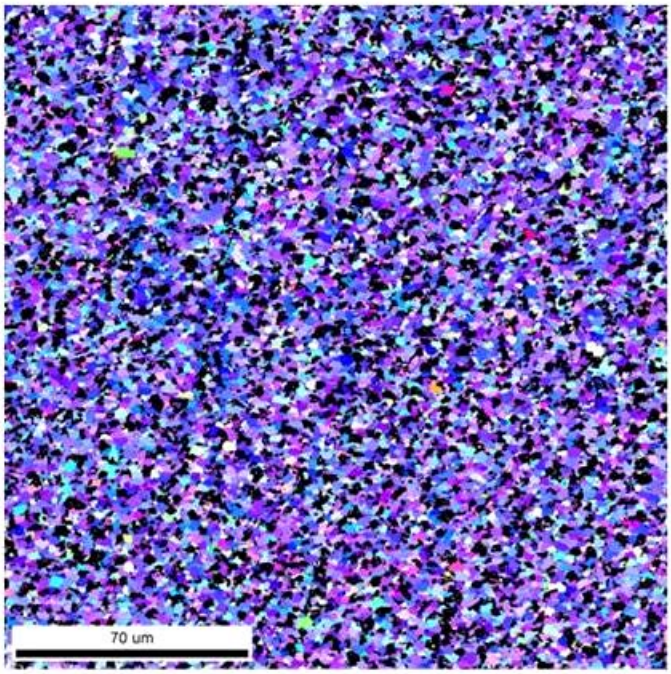

Color Coded Map Type: Inverse Pole Figure [001]

Tin

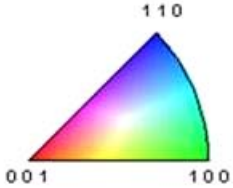

b) Sn with 3.1% Pb, Sample 73, 12 months at 50% RH / 50°C

Electroplated Sn with 3.1% Pb
Crystal Direction Map Showing <111> crystal direction in ND direction 15º Tolerance

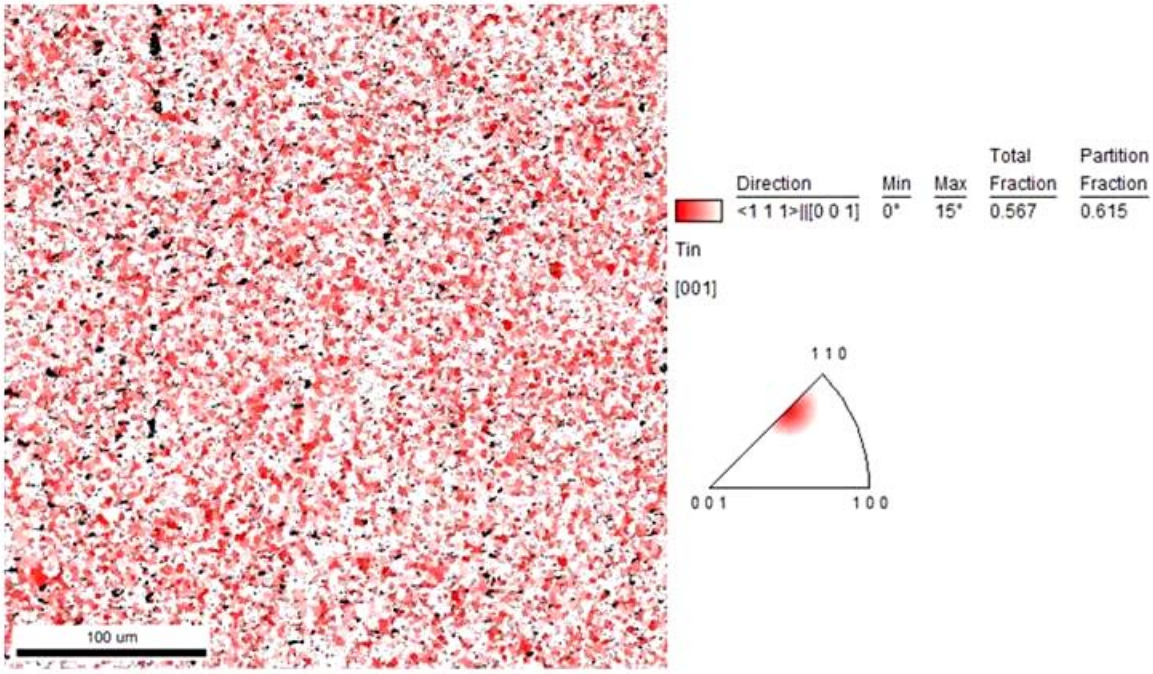

a) Sn with 3.1% Pb, Sample 74, post plating

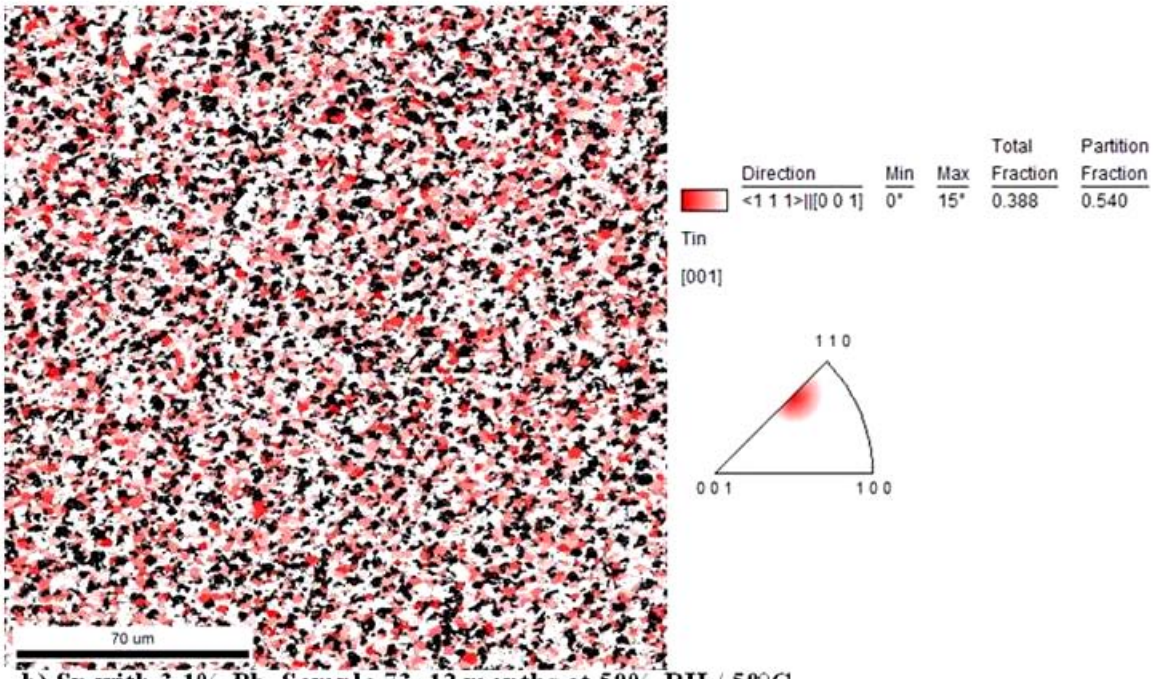

b) Sn with 3.1% Pb, Sample 73, 12 months at 50% RH / 50°C

Electroplated Sn with 3.1% Pb
Crystal Direction Map Showing <111> crystal direction in ND direction 20º Tolerance

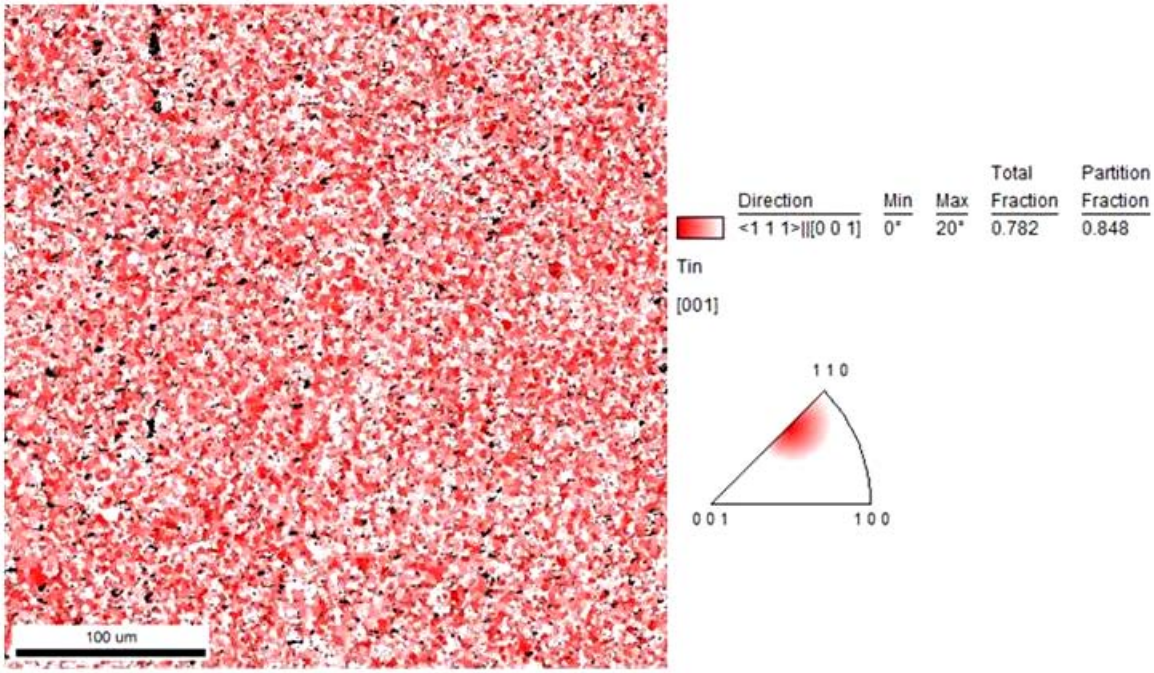

a) Sn with 3.1% Pb, Sample 74, post plating

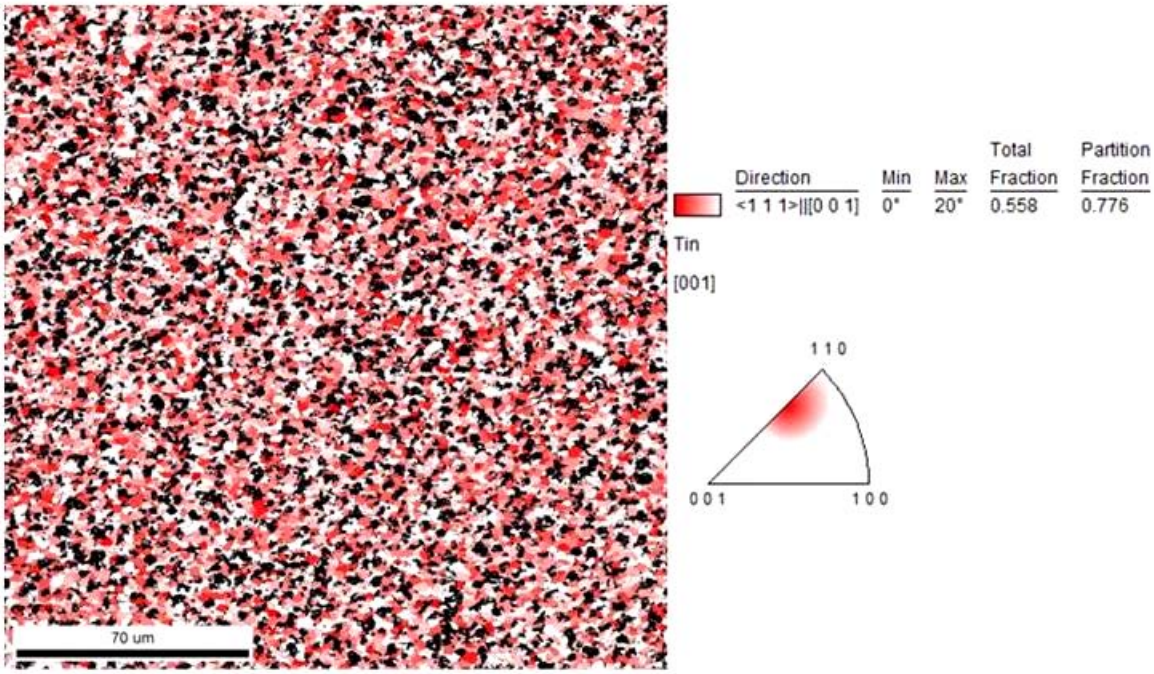

b) Sn with 3.1% Pb, Sample 73, 12 months at 50% RH / 50°C

Electroplated Sn with 3.1% Pb

Confidence Index (CI) Chart

Data points with a CI above 0.1 are generally considered to be indexed correctly.

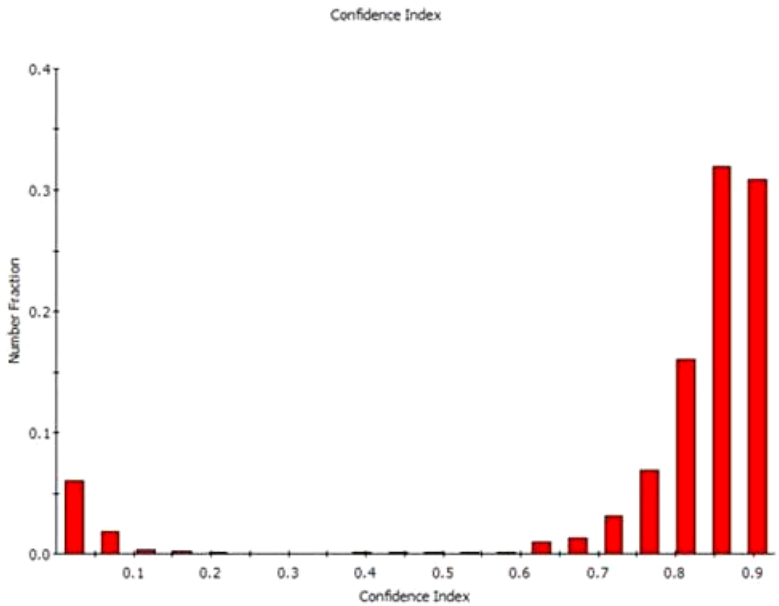

Chart: Confidence Index

CI	Number Fraction
0.023225	0.0603651
0.069675	0.0179239
0.116125	0.00299165
0.162575	0.0016924
0.209025	0.000737744
0.255475	0.000334414
0.301925	0.000406719
0.348375	0.000349101
0.394825	0.000576186
0.441275	0.000976127
0.487725	0.000685774
0.534175	0.00143933
0.580625	0.0011535
0.627075	0.00978612
0.673525	0.0125631
0.719975	0.0306859
0.766425	0.0686825
0.812875	0.160733
0.859325	0.319038
0.905775	0.30888
Average	
Number	0.780914
Standard Deviation	0.239504

(a) Sn with 3.1% Pb, Sample 74, post plating. Indicates that about 12.3% of data points were not indexed with a high degree of confidence

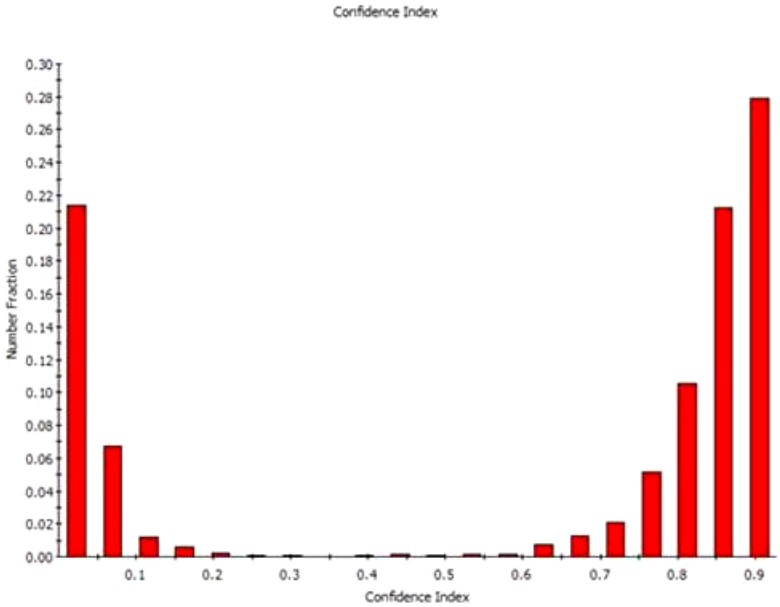

Chart: Confidence Index

CI	Number Fraction
0.023225	0.214035
0.069675	0.0670631
0.116125	0.0119757
0.162575	0.00563896
0.209025	0.00235844
0.255475	0.000766233
0.301925	0.000666666
0.348375	0.000358441
0.394825	0.000917748
0.441275	0.0013013
0.487725	0.000999999
0.534175	0.00185281
0.580625	0.00165541
0.627075	0.0074277
0.673525	0.0124727
0.719975	0.0212615
0.766425	0.0517826
0.812875	0.105733
0.859325	0.212735
0.905775	0.278997
Average	
Number	0.606044
Standard Deviation	0.381675

Electroplated Sn with 3.1% Pb
Pole Figure and Inverse Pole Figure Plots

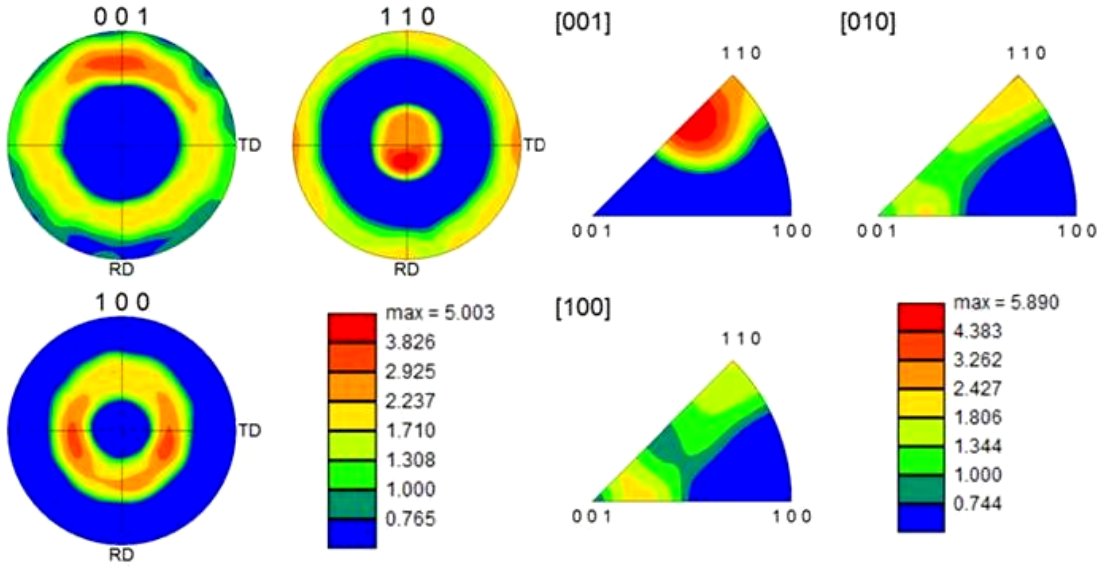

Pole figure plots

Inverse pole figure plots

a) Sn with 3.1% Pb, Sample 74, post plating

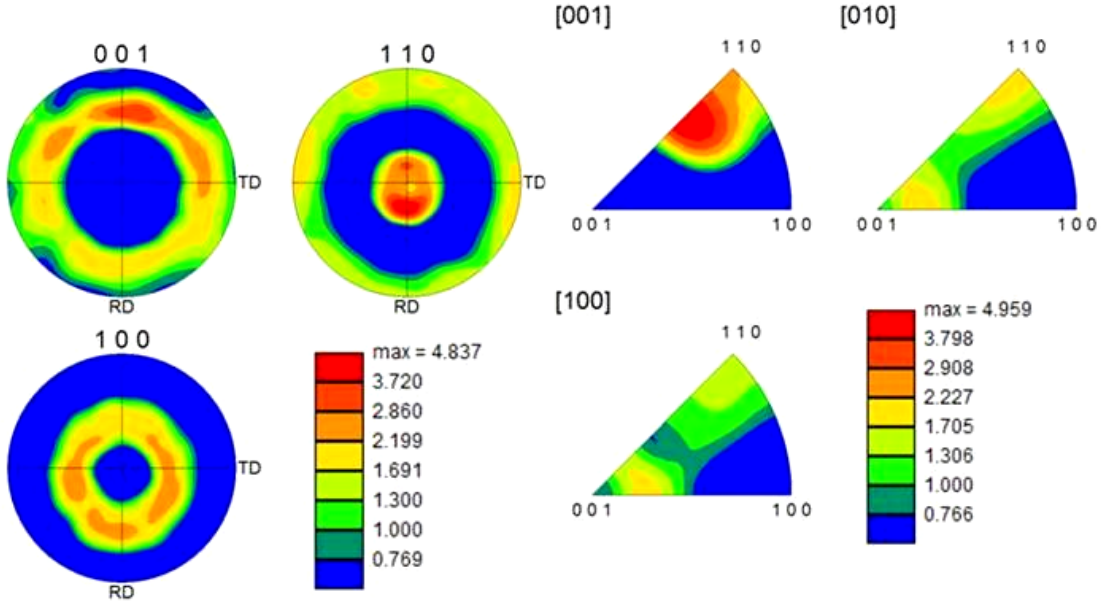

Pole figure plots

Inverse pole figure plots

b) Sn with 3.1% Pb, Sample 73, 12 months at 50% RH / 50°C

Electroplated Sn with 3.1% Pb
Grain Size Histogram and Data

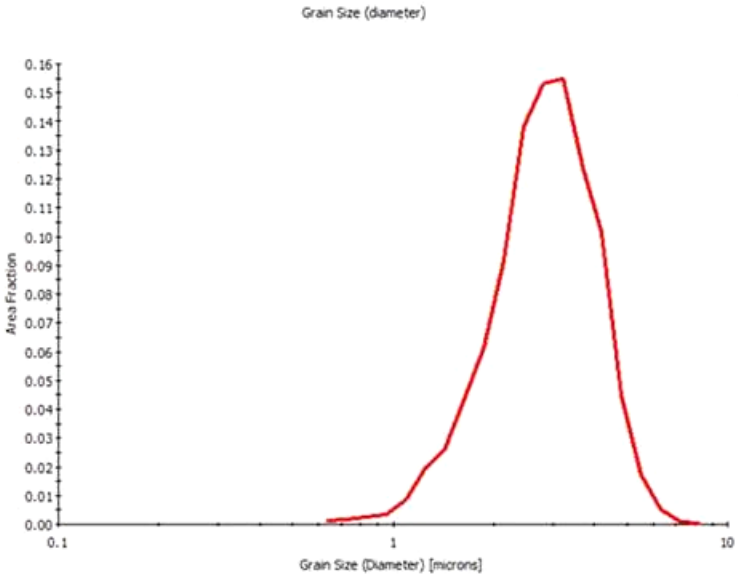

Chart: Grain Size (diameter)

Edge grains included in analysis

Diameter [microns]	Area Fraction
0.635531	0.00141544
0.727479	0.00193451
0.832729	0.0026188
0.953206	0.00343379
1.09111	0.00859618
1.24897	0.0199197
1.42967	0.0256492
1.63651	0.0433002
1.87328	0.061495
2.1443	0.091642
2.45454	0.138108
2.80965	0.153067
3.21615	0.154933
3.68145	0.123726
4.21408	0.101353
4.82376	0.0446195
5.52165	0.0172972
6.32051	0.00533747
7.23495	0.00100486
8.28169	0.000548666

Average	
Number	2.19355
Standard Deviation	0.941862
Area	2.96881

a) Sn with 3.1% Pb, Sample 74, post plating

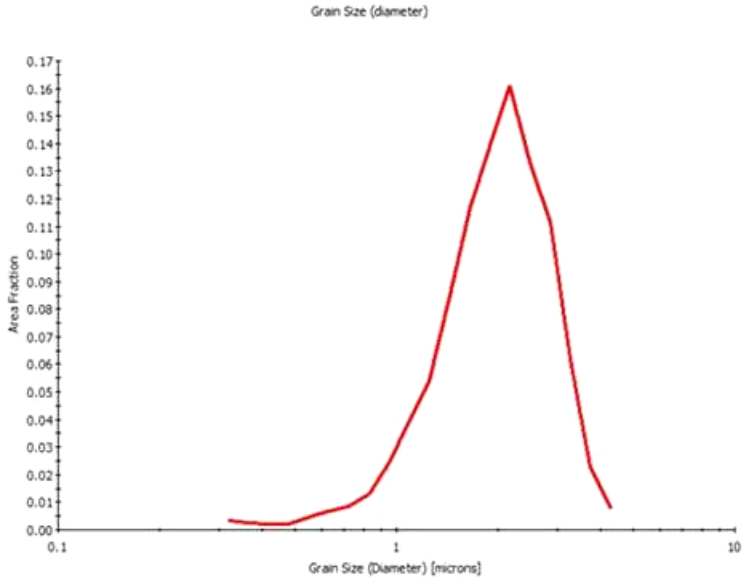

Chart: Grain Size (diameter)

Edge grains included in analysis

Diameter [microns]	Area Fraction
0.318075	0.00356511
0.364802	0.00237183
0.418394	0.00195934
0.479858	0.00200722
0.550352	0.00467614
0.631202	0.0067742
0.72393	0.00860463
0.83028	0.0132943
0.952253	0.0247508
1.09214	0.0395747
1.25259	0.0537455
1.4366	0.0854227
1.64765	0.116606
1.88969	0.13905
2.1673	0.16125
2.48569	0.132177
2.85086	0.111475
3.26966	0.061988
3.75	0.0229645
4.3009	0.00774282

Average	
Number	1.30258
Standard Deviation	0.747314
Area	2.05565

b) Sn with 3.1% Pb, Sample 73, 12 months at 50% RH / 50°C

Electroplated Sn with 3.1% Pb

Misorientation Angle Histogram, 2º minimum misorientation

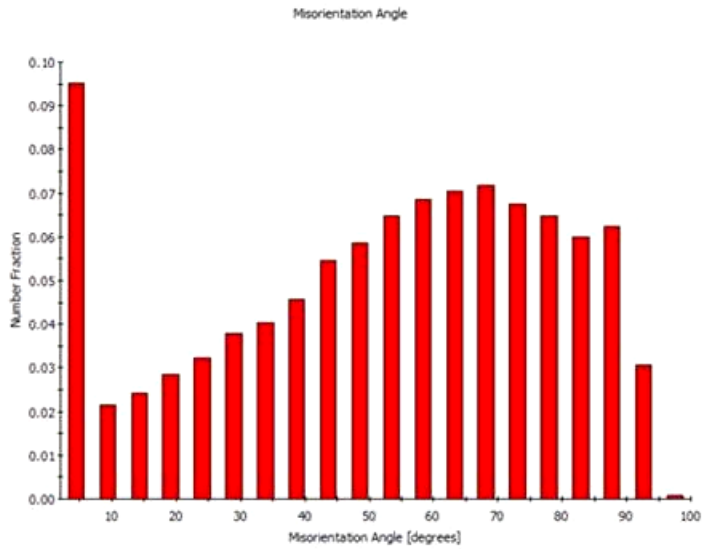

Chart: Misorientation Angle

Angle [degrees]	Number Fraction
4.45	0.0950271
9.35	0.0214325
14.25	0.024113
19.15	0.0284265
24.05	0.0322437
28.95	0.037998
33.85	0.040276
38.75	0.0456804
43.65	0.0545727
48.55	0.0585134
53.45	0.0646772
58.35	0.0686133
63.25	0.0705368
68.15	0.0717741
73.05	0.067456
77.95	0.0648967
82.85	0.0600504
87.75	0.0623375
92.65	0.0305169
97.55	0.000857666
Average Number	51.7772

a) Sn with 3.1% Pb, Sample 74, post plating

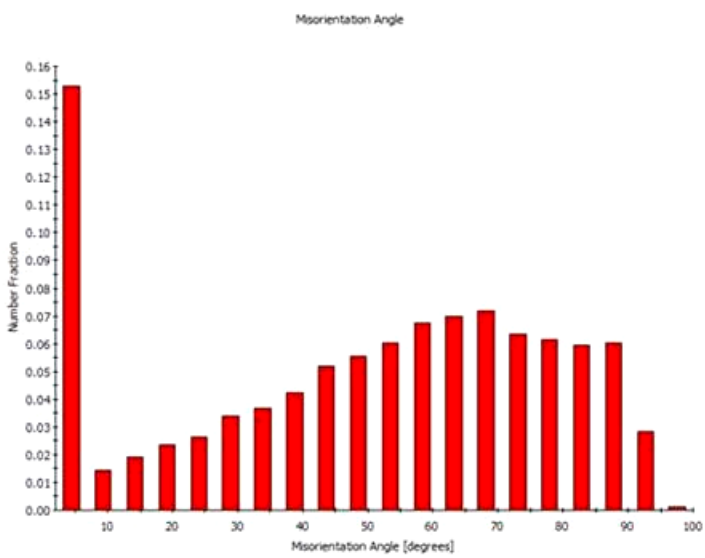

Chart: Misorientation Angle

Angle [degrees]	Number Fraction
4.45	0.152718
9.35	0.0143517
14.25	0.0191465
19.15	0.0235448
24.05	0.0264079
28.95	0.0338111
33.85	0.0366487
38.75	0.0423494
43.65	0.0516735
48.55	0.055446
53.45	0.060299
58.35	0.0675568
63.25	0.0697395
68.15	0.0718895
73.05	0.0635441
77.95	0.0613177
82.85	0.059586
87.75	0.0602045
92.65	0.0284633
97.55	0.00130239
Average Number	49.6015

b) Sn with 3.1% Pb, Sample 73, 12 months at 50% RH / 50°C

Electroplated Sn with 3.1% Pb
Misorientation Angle Histogram, 2º minimum misorientation

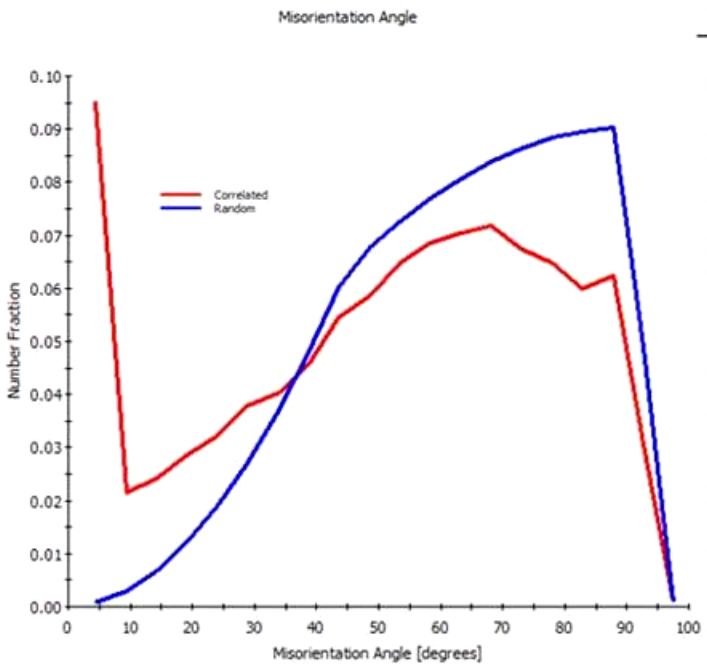

Chart: Misorientation Angle

Angle [degrees]	Correlated Number Fraction	Random Number Fraction
4.45	0.0950271	0.000708071
9.35	0.0214325	0.00294649
14.25	0.024113	0.00675672
19.15	0.0284265	0.0121109
24.05	0.0322437	0.0189699
28.95	0.037998	0.0272836
33.85	0.040276	0.0369912
38.75	0.0456804	0.0480217
43.65	0.0545727	0.0602946
48.55	0.0585134	0.0677124
53.45	0.0646772	0.0725693
58.35	0.0686133	0.0768962
63.25	0.0705368	0.0806613
68.15	0.0717741	0.0838373
73.05	0.067456	0.0864008
77.95	0.0648967	0.0883332
82.85	0.0600504	0.0896203
87.75	0.0623375	0.0902527
92.65	0.0305169	0.048989
97.55	0.000857666	0.000672497
Average Number	51.7772	63.0123

a) Sn with 3.1% Pb, Sample 74, post plating

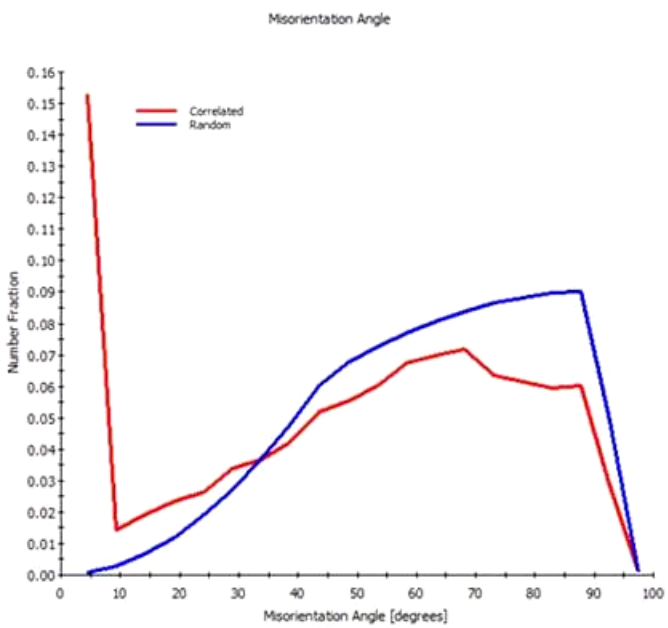

Chart: Misorientation Angle

Angle [degrees]	Correlated Number Fraction	Random Number Fraction
4.45	0.152718	0.000708742
9.35	0.0143517	0.00294715
14.25	0.0191465	0.00675736
19.15	0.0235448	0.0121115
24.05	0.0264079	0.0189705
28.95	0.0338111	0.0272841
33.85	0.0366487	0.0369916
38.75	0.0423494	0.0480221
43.65	0.0516735	0.0602949
48.55	0.055446	0.0677127
53.45	0.060299	0.0725696
58.35	0.0675568	0.0768964
63.25	0.0697395	0.0806616
68.15	0.0718895	0.0838375
73.05	0.0635441	0.086401
77.95	0.0613177	0.0883334
82.85	0.059586	0.0896204
87.75	0.0602045	0.0902528
92.65	0.0284633	0.0489894
97.55	0.00130239	0.000673168
Average Number	49.6015	63.0123

b) Sn with 3.1% Pb, Sample 73, 12 months at 50% RH / 50°C

Electroplated Sn with 3.1% Pb
Grain Boundary Characterization Chart

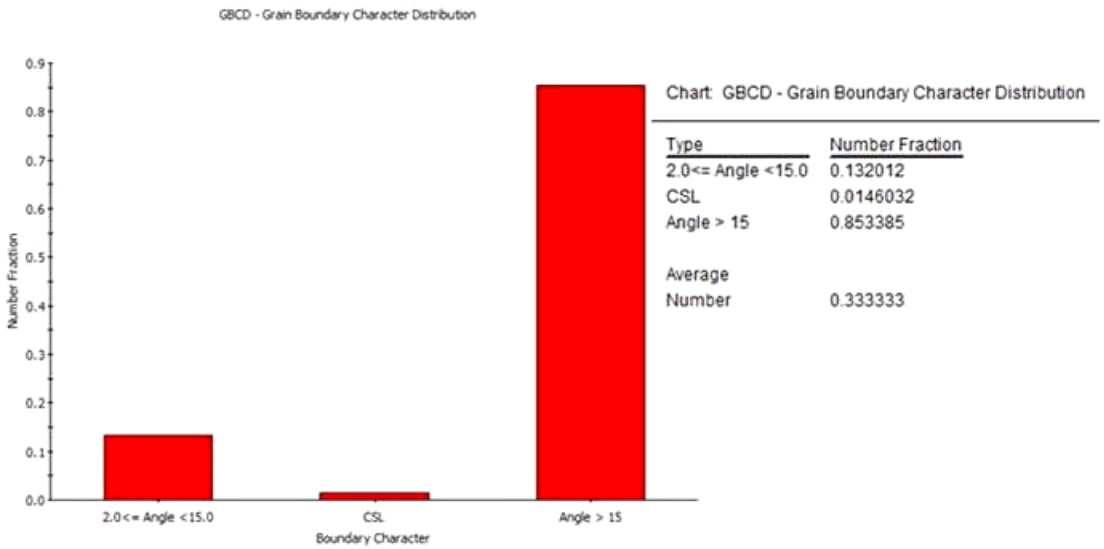

a) Sn with 3.1% Pb, Sample 74, post plating

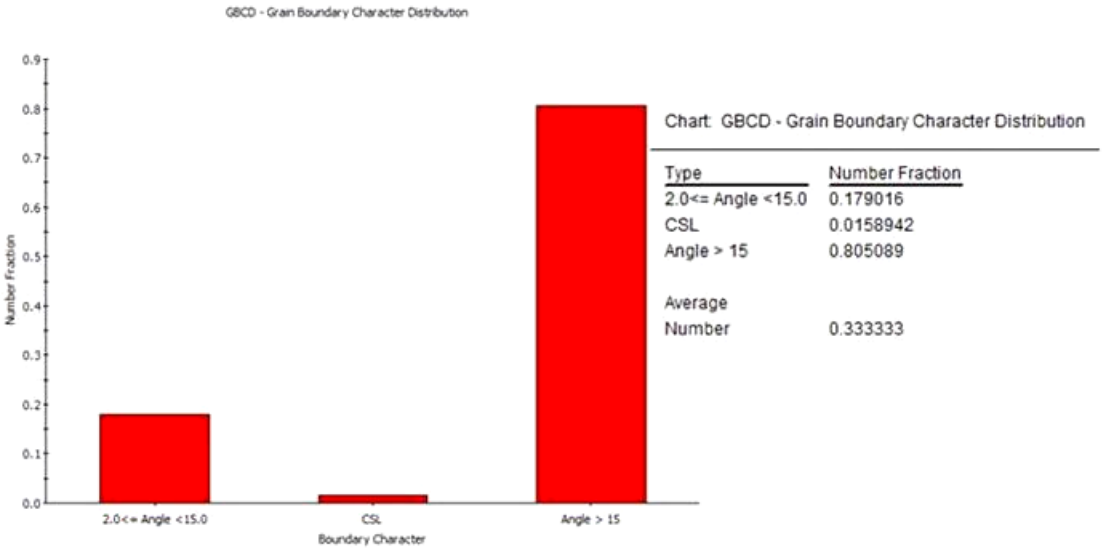

b) Sn with 3.1% Pb, Sample 73, 12 months at 50% RH / 50°C

Electroplated Sn with 3.1% Pb

Coincident Site Lattice Boundary Chart

The total fraction of CSL boundaries is approximately 2% of boundaries measured

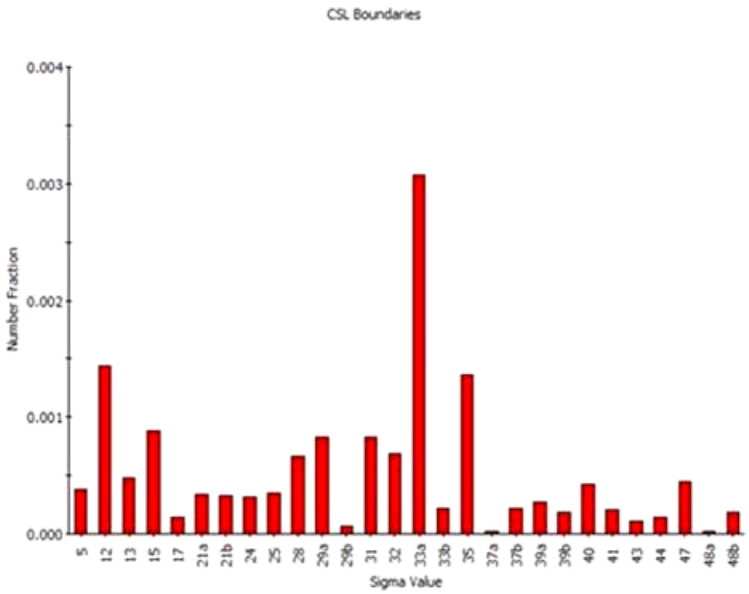

Chart: CSL Boundaries

Overall fraction of CSL boundaries: 0.015

Sigma	Number Fraction
5	0.000386522
12	0.00143402
13	0.000475719
15	0.000882824
17	0.000146375
21a	0.000340779
21b	0.000322483
24	0.000313334
25	0.000347641
28	0.000670123
29a	0.00082336
29b	6.1752e-005
31	0.000830221
32	0.000681559
33a	0.00307388
33b	0.000214988
35	0.00136083
37a	2.0584e-005
37b	0.000219563
39a	0.00027674
39b	0.000182969
40	0.000420828
41	0.000210414
43	0.000112068
44	0.000144088
47	0.000443699
48a	1.82969e-005
48b	0.000187543

a) Sn with 3.1% Pb, Sample 74, post plating

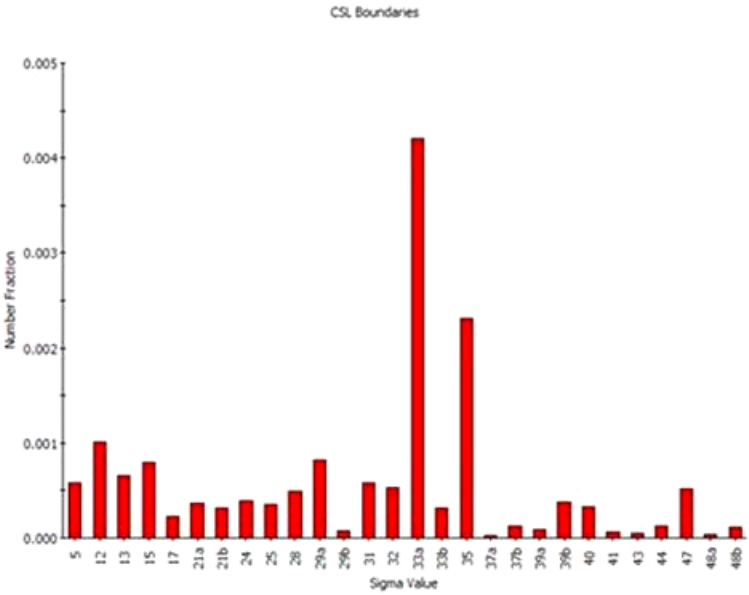

Chart: CSL Boundaries

Overall fraction of CSL boundaries: 0.016

Sigma	Number Fraction
5	0.000578434
12	0.00101135
13	0.000658469
15	0.000793073
17	0.000229191
21a	0.000367433
21b	0.00032014
24	0.000389261
25	0.000352881
28	0.000491123
29a	0.000818539
29b	7.6397e-005
31	0.000582072
32	0.000534779
33a	0.00420547
33b	0.00032014
35	0.00231374
37a	2.54657e-005
37b	0.00012369
39a	8.73108e-005
39b	0.000378347
40	0.000327416
41	6.91211e-005
43	4.72934e-005
44	0.000120052
47	0.000516589
48a	4.00175e-005
48b	0.000116414

b) Sn with 3.1% Pb, Sample 73, 12 months at 50% RH / 50°C

Electroplated Sn with 3.1% Pb
Misorientation Distribution Function (MODF) Plot

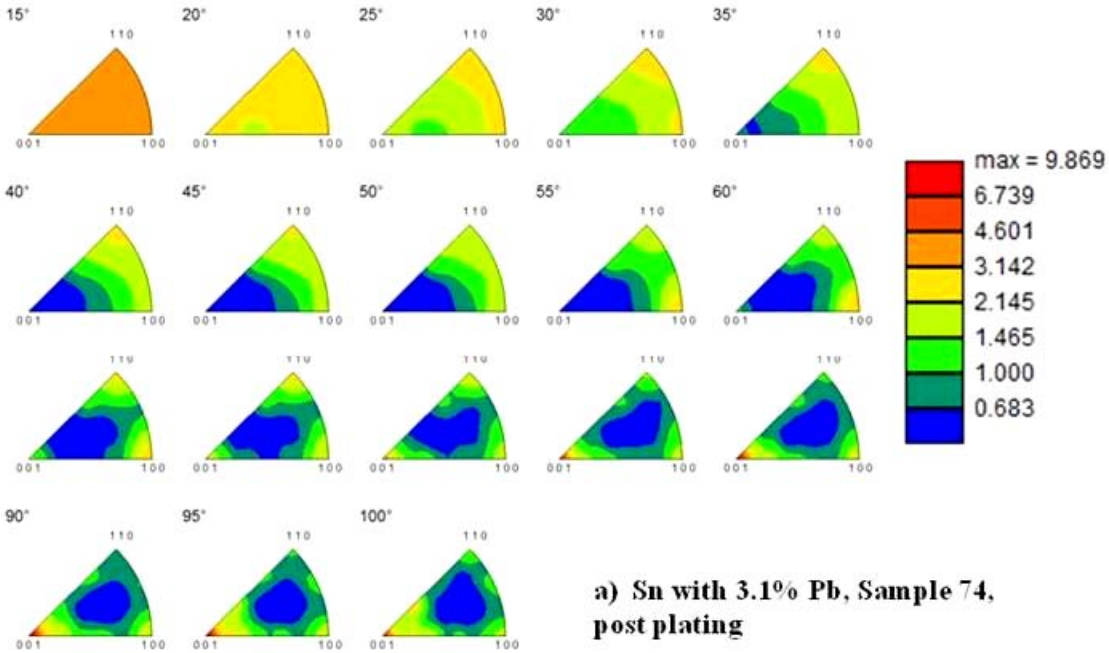

a) Sn with 3.1% Pb, Sample 74, post plating

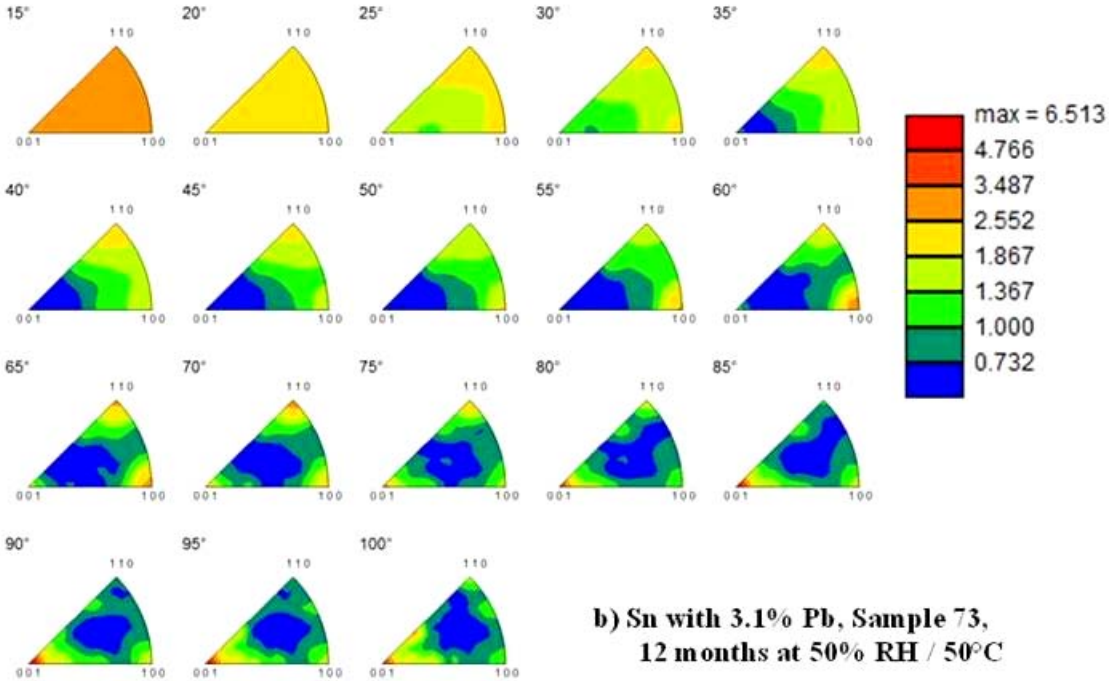

b) Sn with 3.1% Pb, Sample 73, 12 months at 50% RH / 50°C

Electroplated Sn with 3.1% Pb

Crystal Direction Map

Blue Indicates C-Direction in sample normal

Red indicates C-direction in sample plane 15º tolerance

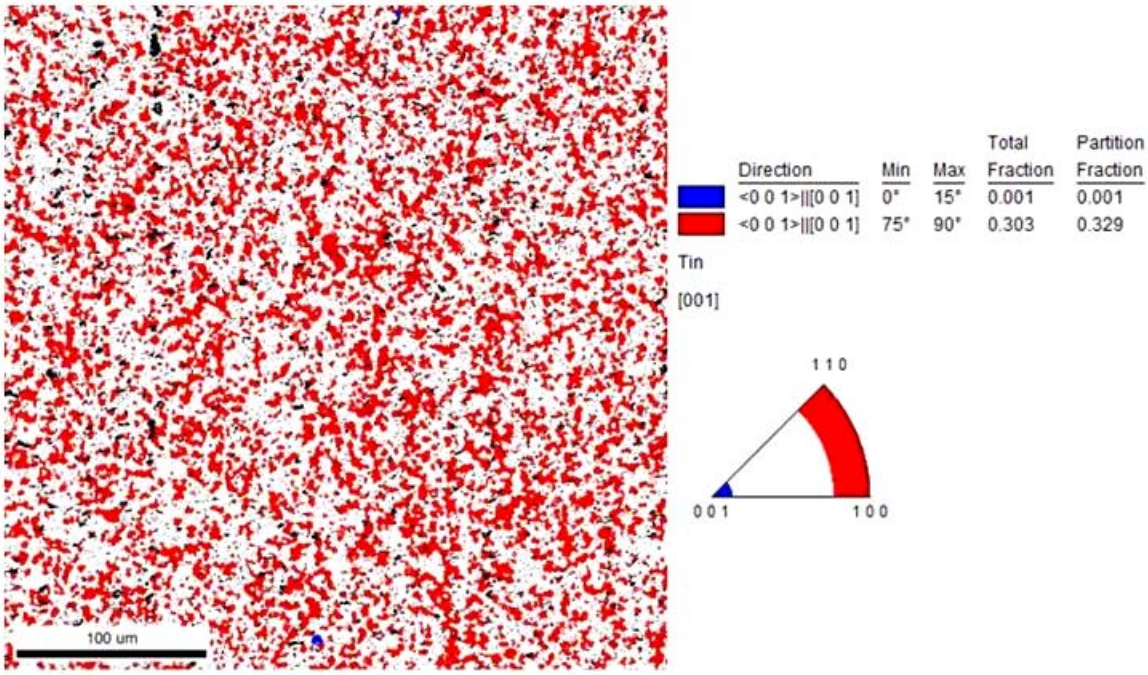

a) Sn with 3.1% Pb, Sample 74, post plating

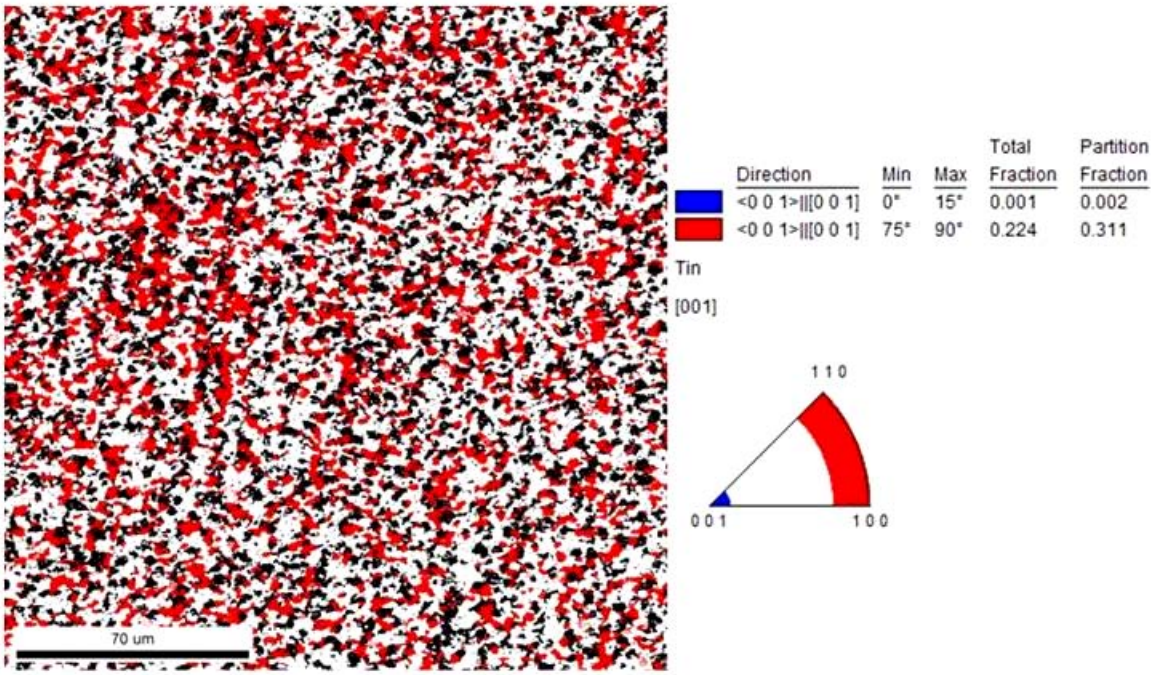

b) Sn with 3.1% Pb, Sample 73, 12 months at 50% RH / 50°C

Appendix L: EBSD Data for Sn with 2.1% Cu

Electroplated Sn with 2.1% Cu
Image Quality Map

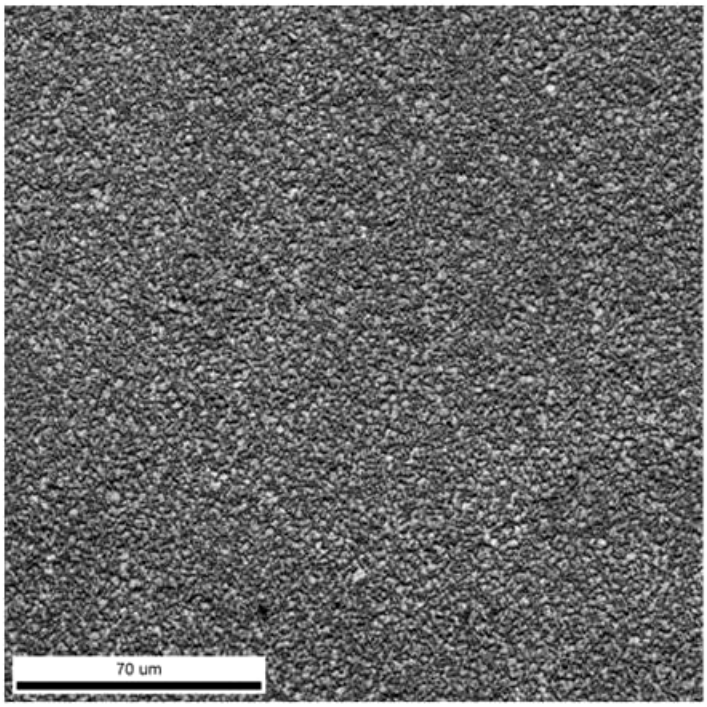

X = 200 microns
Y = 200 microns
Step size = 0.25 microns

a) Sn with 2.1% Cu, Sample 79, post plating

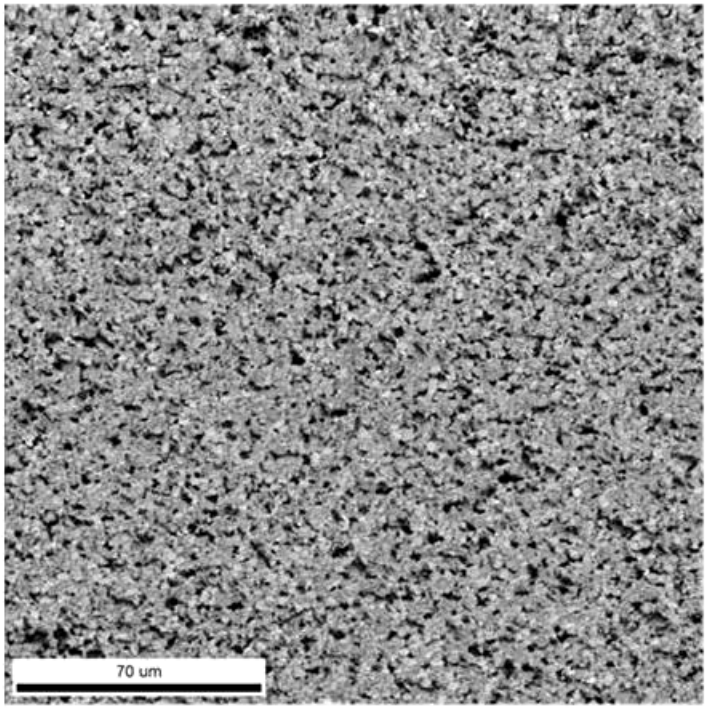

X = 200 microns
Y = 200 microns
Step size = 0.2 microns

b) Sn with 2.1% Cu, Sample 82, 12 months at 50% RH / 50°C

Electroplated Sn with 2.1% Cu
Color Coded Orientation Map

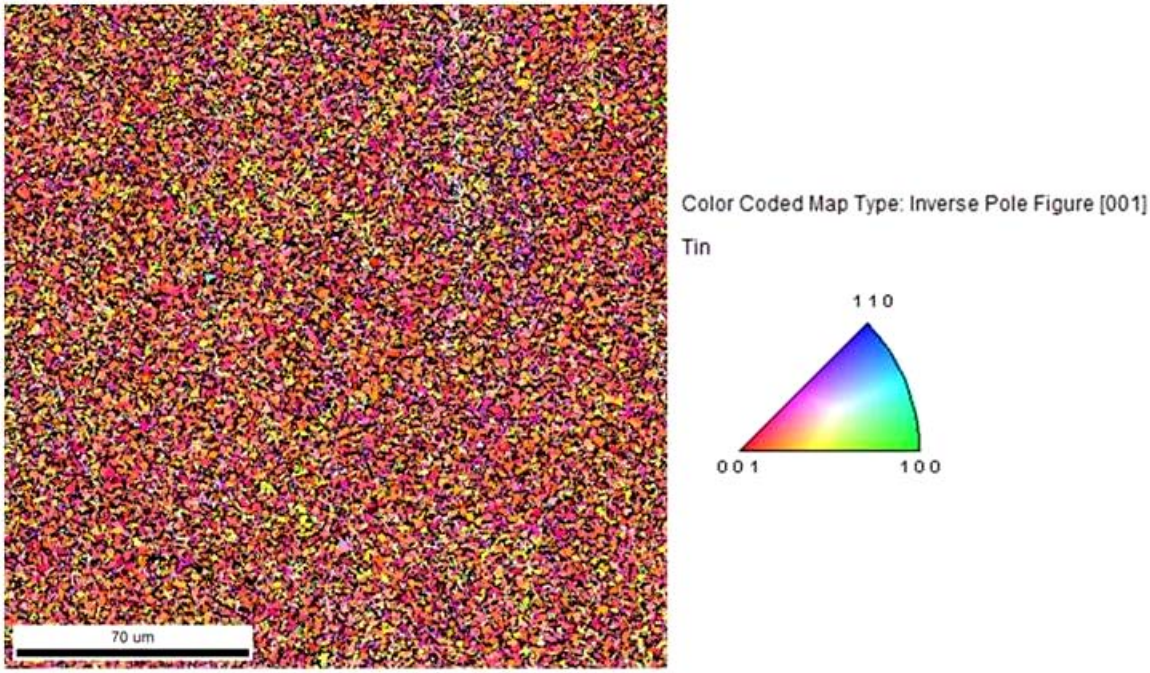

a) Sn with 2.1% Cu, Sample 79, post plating

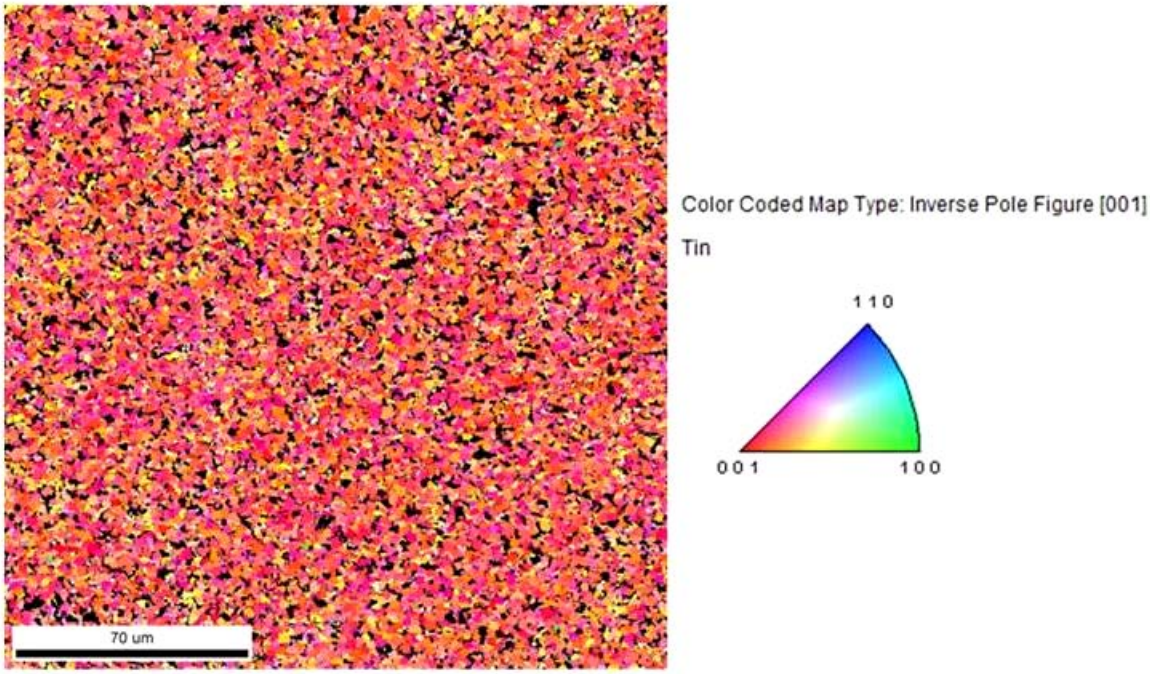

b) Sn with 2.1% Cu, Sample 82, 12 months at 50% RH / 50°C

Electroplated Sn with 2.1% Cu
Crystal Direction Map Showing <111> crystal direction in ND direction 15º Tolerance

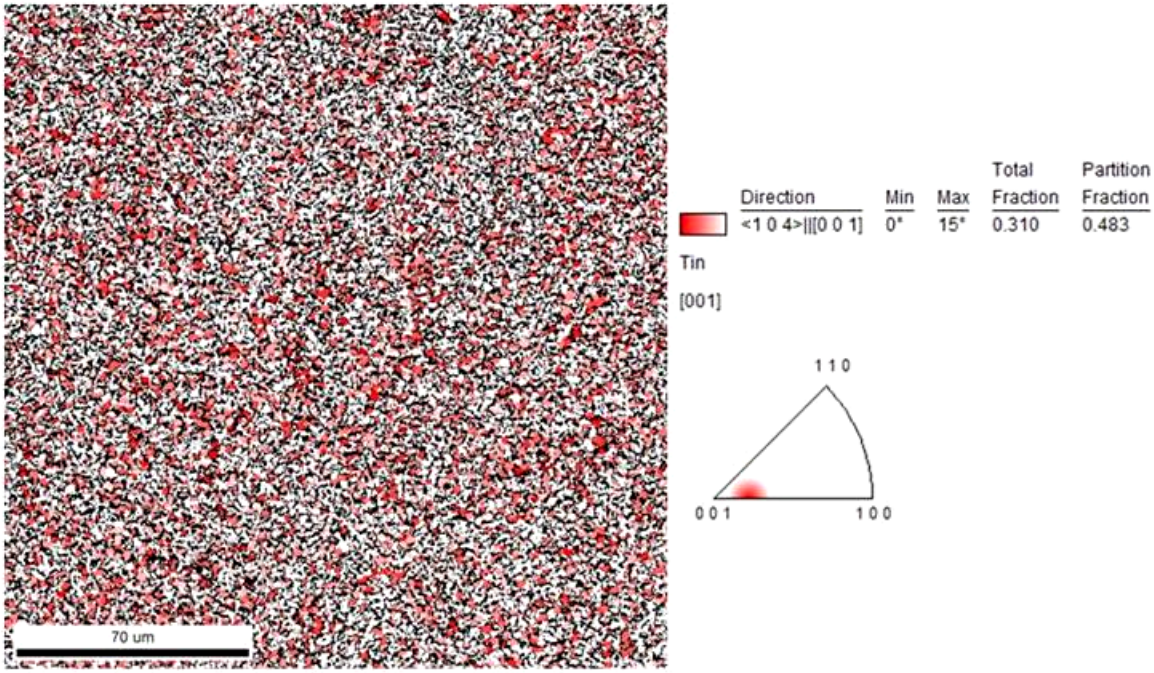

a) Sn with 2.1% Cu, Sample 79, post plating

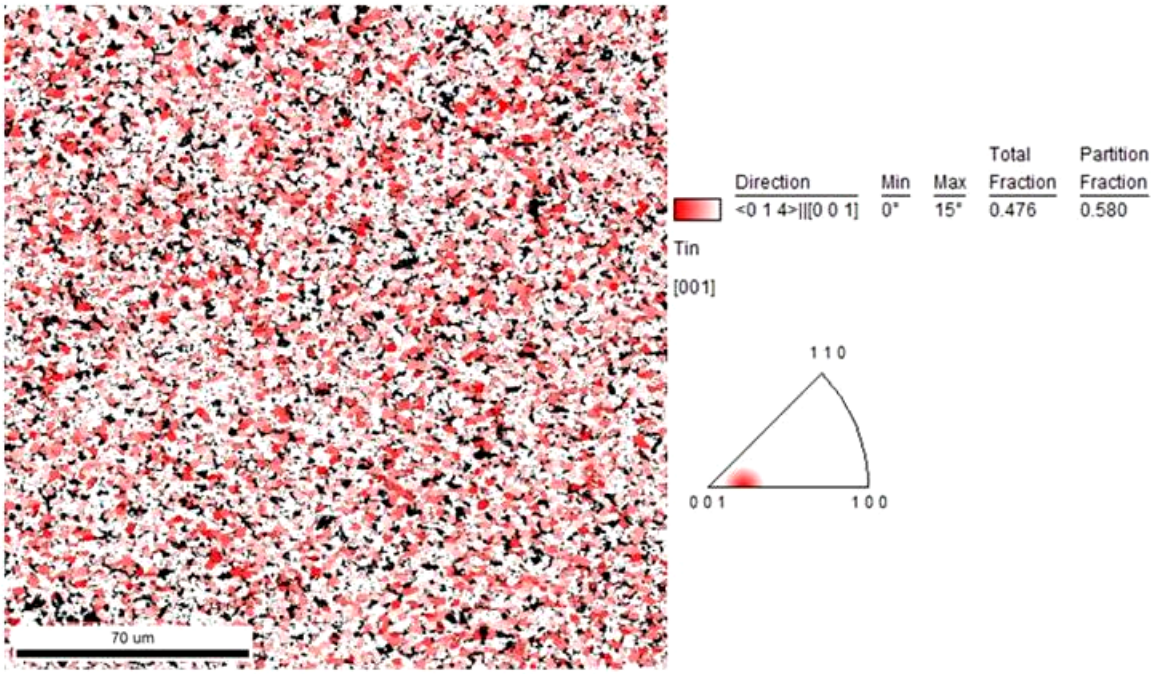

b) Sn with 2.1% Cu, Sample 82, 12 months at 50% RH / 50°C

Electroplated Sn with 2.1% Cu
Crystal Direction Map Showing <111> crystal direction in ND direction 20º Tolerance

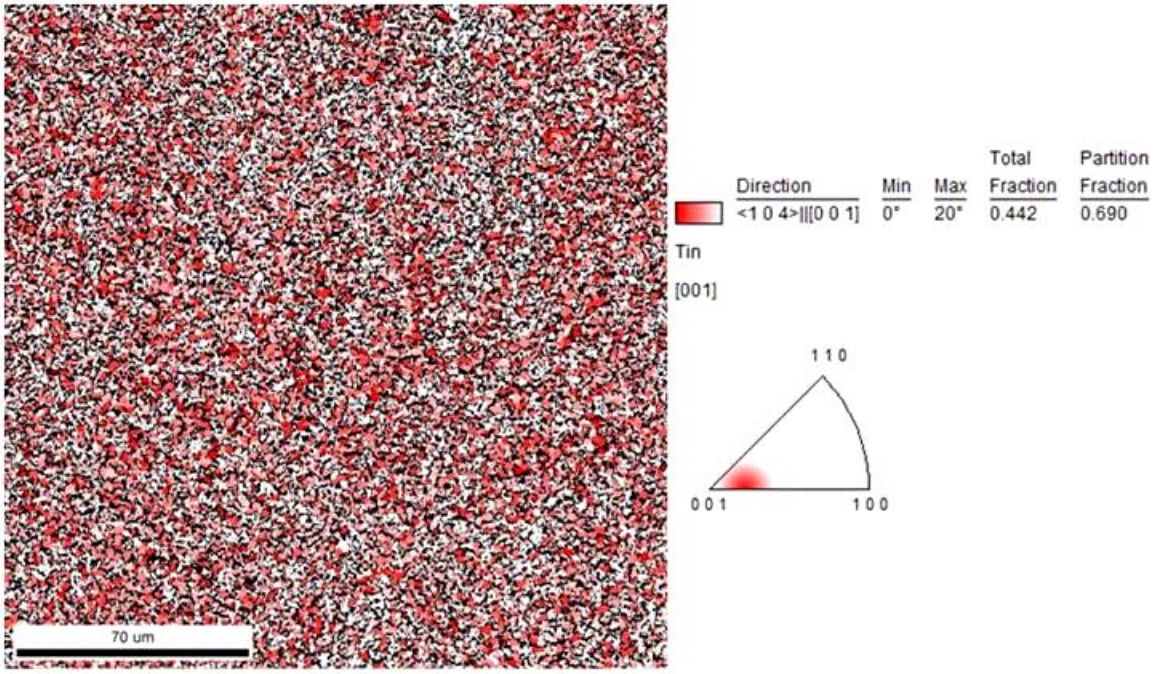

a) Sn with 2.1% Cu, Sample 79, post plating

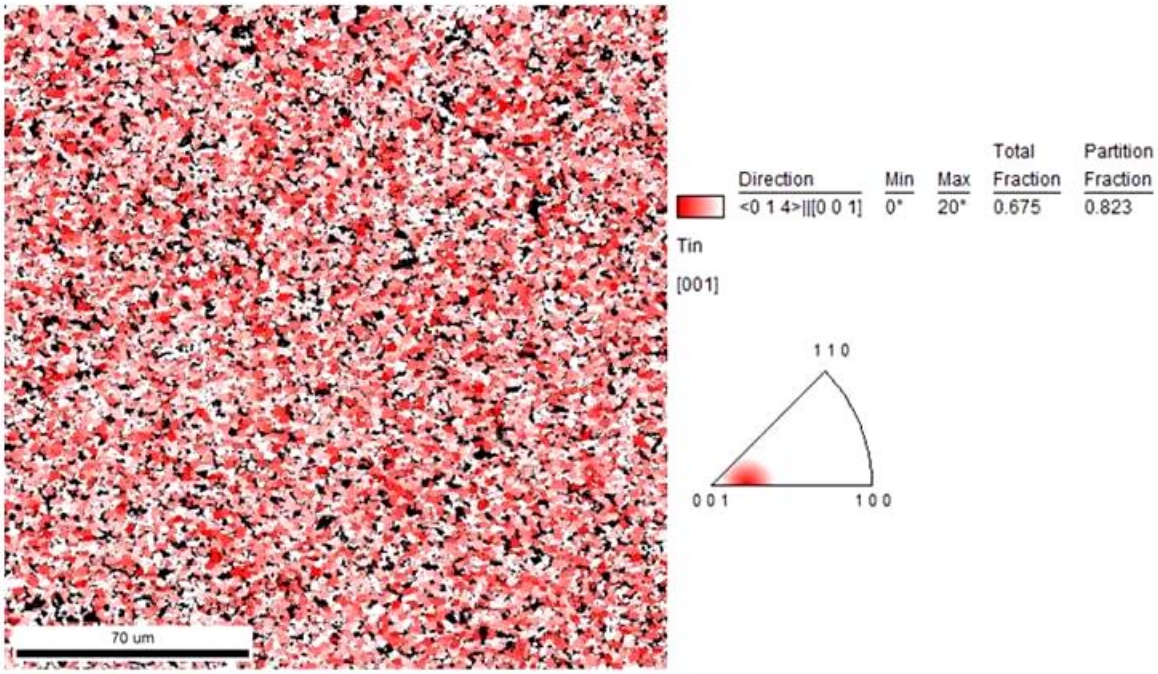

b) Sn with 2.1% Cu, Sample 82, 12 months at 50% RH / 50°C

Electroplated Sn with 2.1% Cu

Confidence Index (CI) Chart

Data points with a CI above 0.1 are generally considered to be indexed correctly.

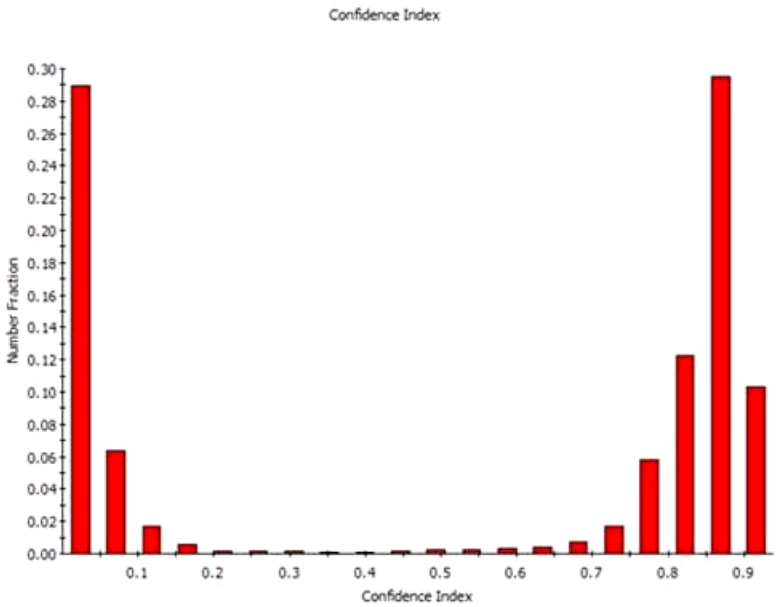

Chart: Confidence Index

CI	Number Fraction
0.0235	0.289699
0.0705	0.0639644
0.1175	0.0167752
0.1645	0.00602708
0.2115	0.00171024
0.2585	0.00138982
0.3055	0.00144931
0.3525	0.000919339
0.3995	0.00117351
0.4465	0.00180488
0.4935	0.00209961
0.5405	0.00238082
0.5875	0.00307708
0.6345	0.00419786
0.6815	0.00733984
0.7285	0.0169118
0.7755	0.058301
0.8225	0.122399
0.8695	0.295189
0.9165	0.103192
Average	
Number	0.535597
Standard Deviation	0.399951

(a) Sn with 2.1% Cu, Sample 79. Indicates that about 35.4% of data points were not indexed with a high degree of confidence

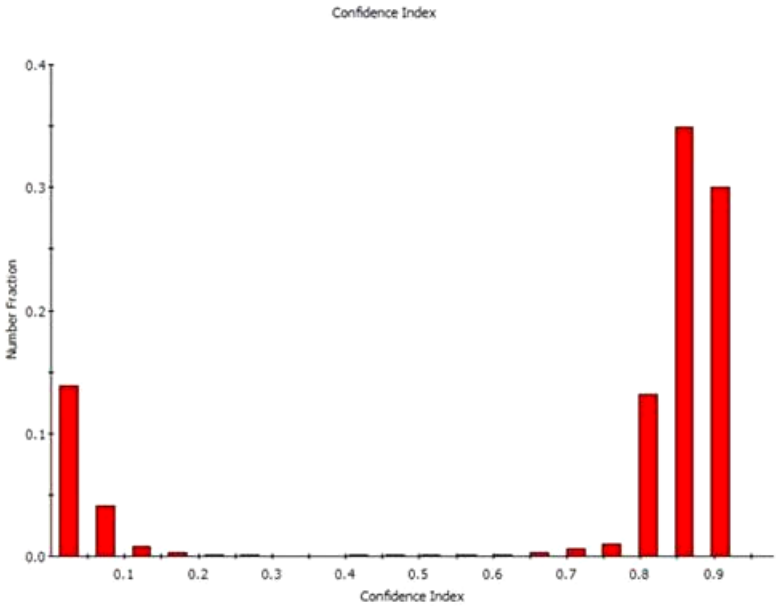

Chart: Confidence Index

CI	Number Fraction
0.02455	0.138181
0.07365	0.0410727
0.12275	0.00814285
0.17185	0.00288917
0.22095	0.00102424
0.27005	0.000954112
0.31915	0.00044329
0.36825	0.000381818
0.41735	0.000737662
0.46645	0.00106493
0.51555	0.00115584
0.56465	0.00108312
0.61375	0.00100173
0.66285	0.00270995
0.71195	0.00637575
0.76105	0.0103411
0.81015	0.132013
0.85925	0.349316
0.90835	0.300692
0.95745	0.000419913
Average	
Number	0.70502
Standard Deviation	0.331916

(b) Sn with 2.1% Cu, Sample 82, 12 months at 50% RH / 50°C. Indicates that about 17.9.% of data points were not indexed with a high degree of confidence

Electroplated Sn with 2.1% Cu
Pole Figure and Inverse Pole Figure Plots

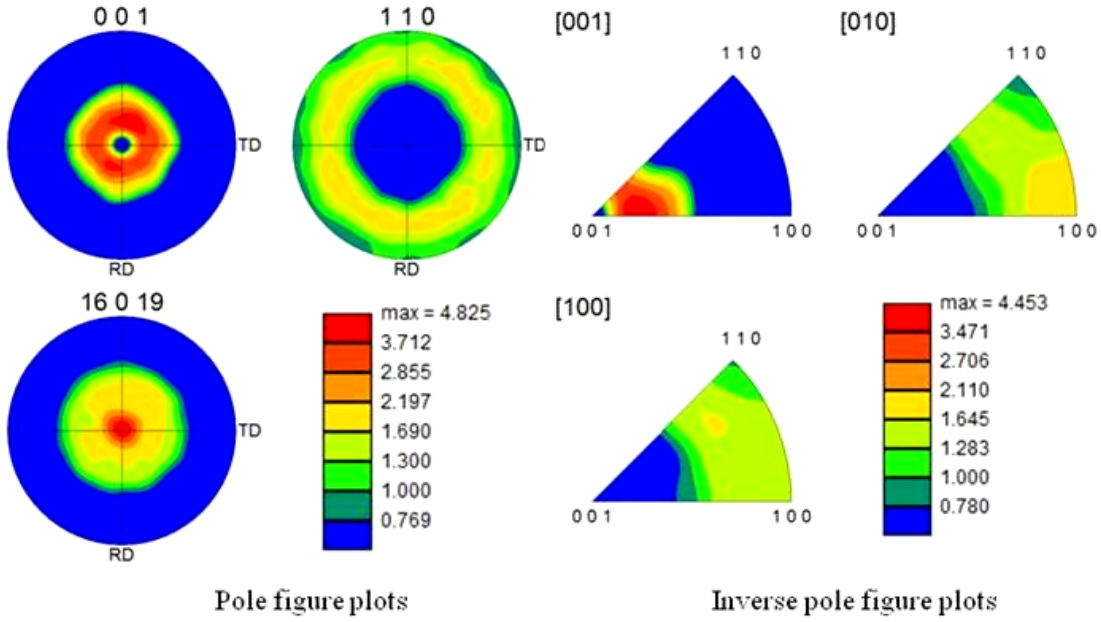

Pole figure plots

Inverse pole figure plots

a) Sn with 2.1% Cu, Sample 79, post plating

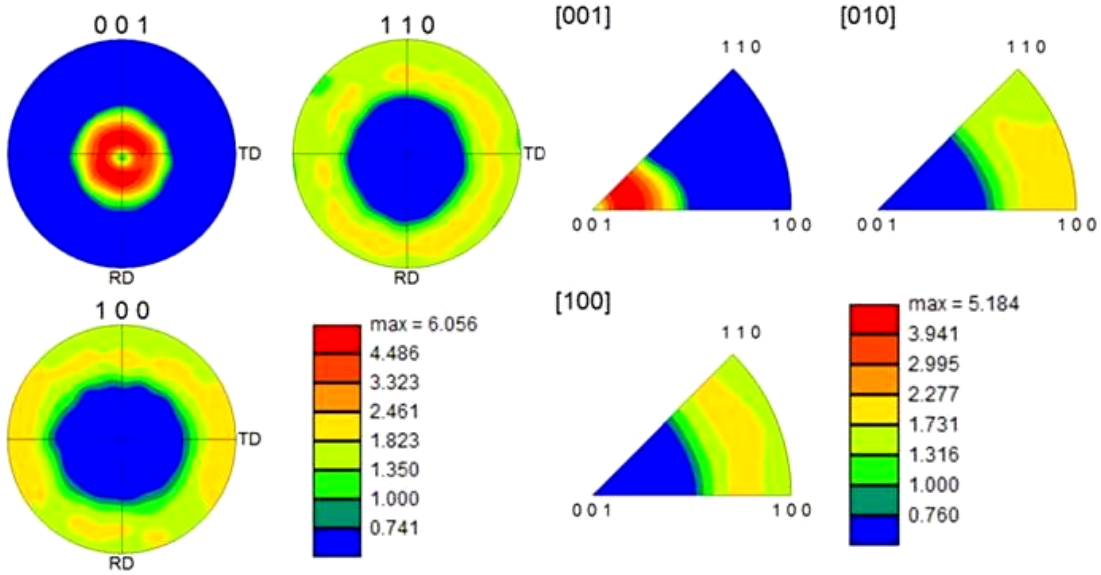

Pole figure plots

Inverse pole figure plots

b) Sn with 2.1% Cu, Sample 82, 12 months at 50% RH / 50°C

Electroplated Sn with 2.1% Cu
Grain Size Histogram and Data

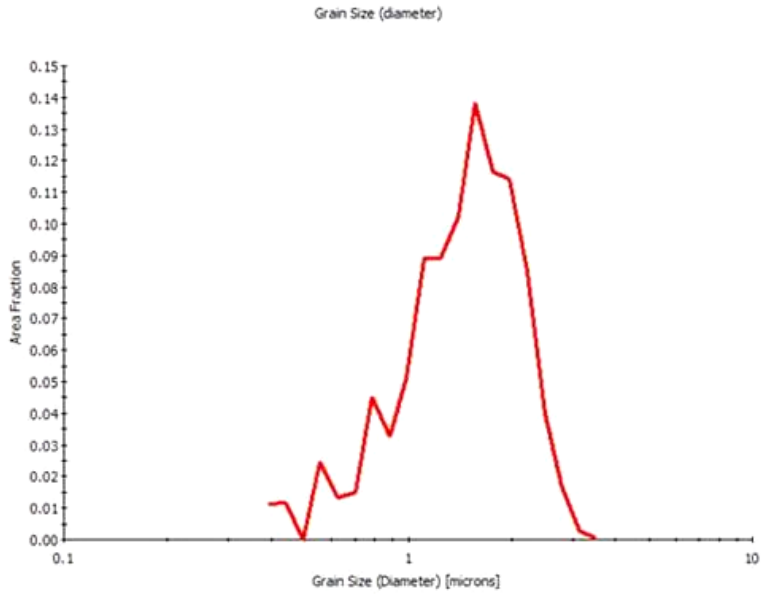

Chart: Grain Size (diameter)

Edge grains included in analysis

Diameter [microns]	Area Fraction
0.393281	0.0111794
0.441323	0.0116624
0.495234	0
0.555731	0.0246878
0.623619	0.0132401
0.699799	0.015011
0.785285	0.0449837
0.881214	0.0327546
0.988862	0.0513483
1.10966	0.0892074
1.24521	0.0891795
1.39733	0.102473
1.56802	0.138343
1.75957	0.116593
1.97452	0.114052
2.21572	0.0850538
2.48639	0.0398211
2.79012	0.0170653
3.13096	0.0029129
3.51343	0.000431462

Average	
Number	1.00994
Standard Deviation	0.512674
Area	1.50391

a) Sn with 2.1% Cu, Sample 79, post plating

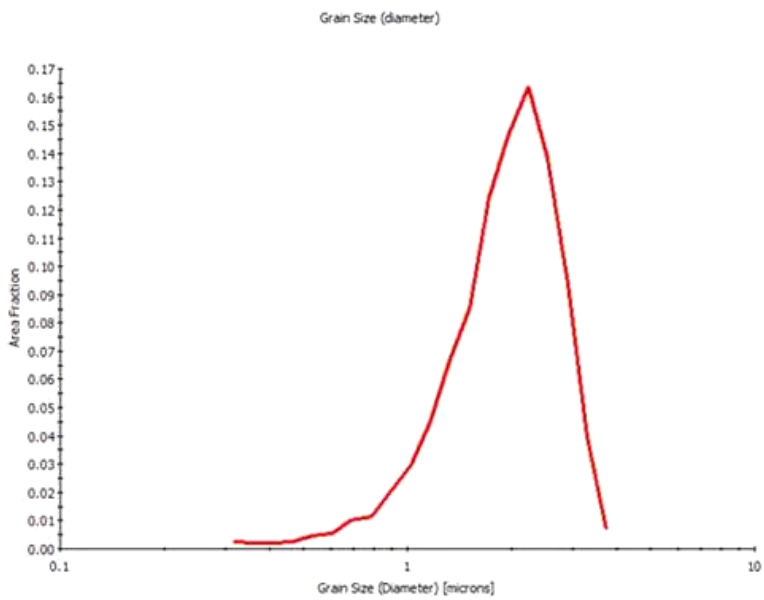

Chart: Grain Size (diameter)

Edge grains included in analysis

Diameter [microns]	Area Fraction
0.316947	0.00249177
0.360934	0.00224196
0.411027	0.00211384
0.468072	0.00243946
0.533033	0.00449245
0.60701	0.00563905
0.691255	0.0100279
0.787191	0.0113753
0.896442	0.0201958
1.02085	0.0294668
1.16253	0.0449405
1.32388	0.0663491
1.50761	0.0854239
1.71685	0.12432
1.95512	0.146139
2.22646	0.163741
2.53547	0.138348
2.88735	0.0938536
3.28807	0.039657
3.74441	0.00674402

Average	
Number	1.30695
Standard Deviation	0.711033
Area	1.97982

b) Sn with 2.1% Cu, Sample 82, 12 months at 50% RH / 50°C

Electroplated Sn with 2.1% Cu
Misorientation Angle Histogram, 2º minimum misorientation

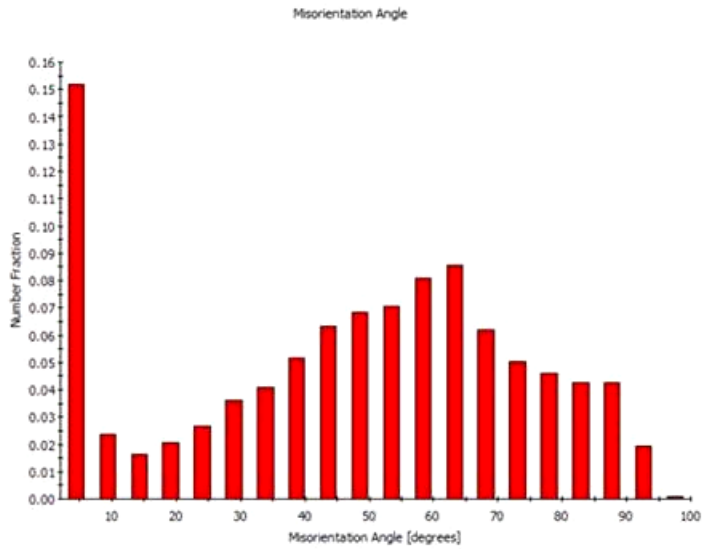

Chart: Misorientation Angle

Angle [degrees]	Number Fraction
4.45	0.151775
9.35	0.0235733
14.25	0.0162881
19.15	0.0206536
24.05	0.0268162
28.95	0.0359269
33.85	0.0407062
38.75	0.0517898
43.65	0.0634404
48.55	0.0682537
53.45	0.0706519
58.35	0.0806867
63.25	0.0857154
68.15	0.0617849
73.05	0.0505199
77.95	0.0461715
82.85	0.0427585
87.75	0.0425261
92.65	0.0191682
97.55	0.000793714
Average Number	47.0467

a) Sn with 2.1% Cu, Sample 79, post plating

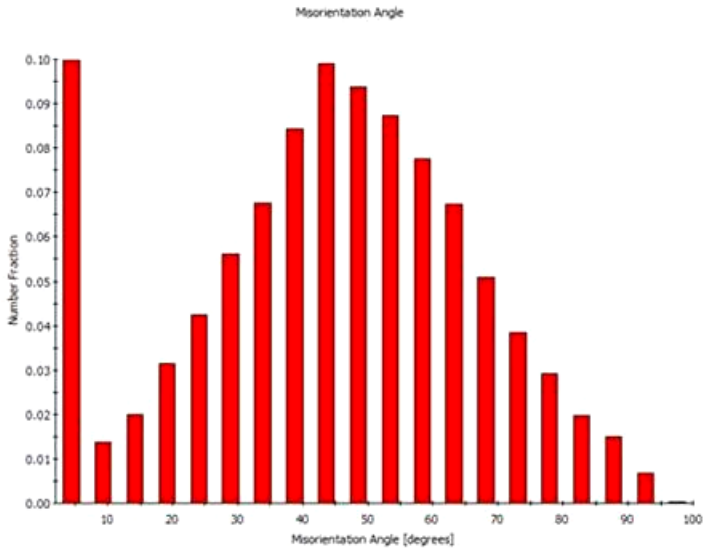

Chart: Misorientation Angle

Angle [degrees]	Number Fraction
4.45	0.0997238
9.35	0.013812
14.25	0.0199567
19.15	0.0312995
24.05	0.0424931
28.95	0.0560036
33.85	0.0674867
38.75	0.0842427
43.65	0.0990102
48.55	0.0936657
53.45	0.0872703
58.35	0.0775726
63.25	0.0673225
68.15	0.050898
73.05	0.0383817
77.95	0.0292872
82.85	0.0196223
87.75	0.0150243
92.65	0.00663731
97.55	0.000289617
Average Number	43.9335

b) Sn with 2.1% Cu, Sample 82, 12 months at 50% RH / 50°C

Electroplated Sn with 2.1% Cu
Misorientation Angle Histogram, 2º minimum misorientation

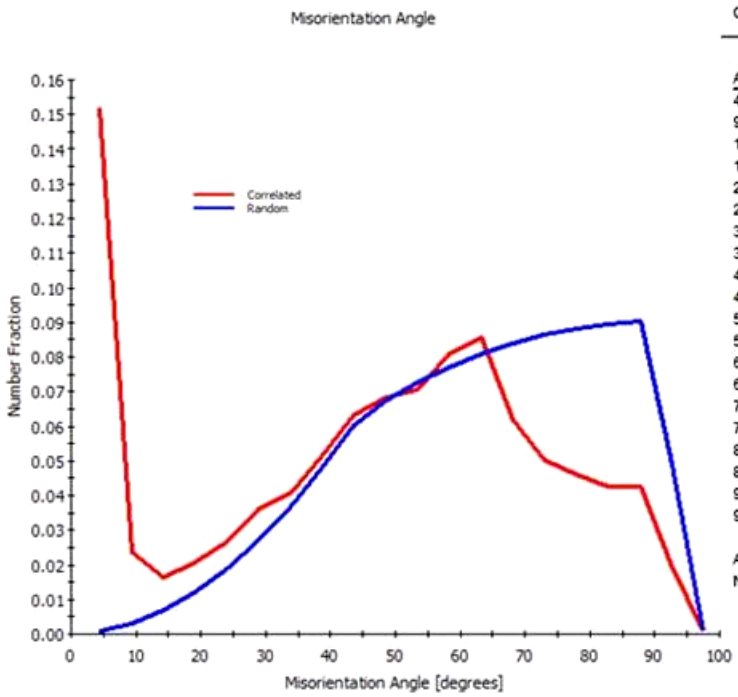

Chart: Misorientation Angle

Angle [degrees]	Correlated Number Fraction	Random Number Fraction
4.45	0.151775	0.000709754
9.35	0.0235733	0.00294816
14.25	0.0162881	0.00675835
19.15	0.0206536	0.0121125
24.05	0.0268162	0.0189714
28.95	0.0359269	0.027285
33.85	0.0407062	0.0369925
38.75	0.0517898	0.048023
43.65	0.0634404	0.0602958
48.55	0.0682537	0.0677135
53.45	0.0706519	0.0725704
58.35	0.0806867	0.0768972
63.25	0.0857154	0.0806623
68.15	0.0617849	0.0838383
73.05	0.0505199	0.0864018
77.95	0.0461715	0.0883341
82.85	0.0427585	0.0896212
87.75	0.0425261	0.0902536
92.65	0.0191682	0.0489902
97.55	0.000793714	0.00067418
Average Number	47.0467	63.0123

a) Sn with 2.1% Cu, Sample 79, post plating

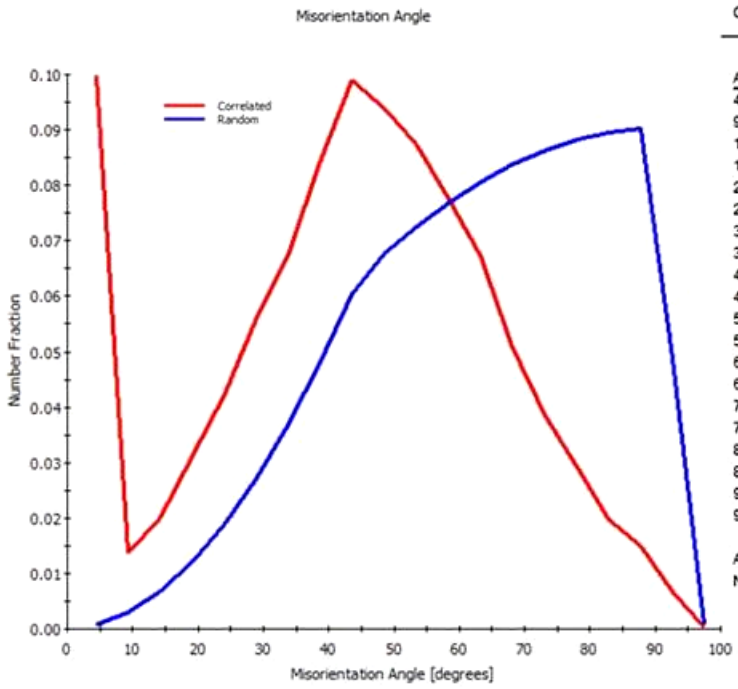

Chart: Misorientation Angle

Angle [degrees]	Correlated Number Fraction	Random Number Fraction
4.45	0.0997238	0.000708414
9.35	0.013812	0.00294682
14.25	0.0199567	0.00675701
19.15	0.0312995	0.0121111
24.05	0.0424931	0.0189701
28.95	0.0560036	0.0272837
33.85	0.0674867	0.0369912
38.75	0.0842427	0.0480217
43.65	0.0990102	0.0602944
48.55	0.0936657	0.0677122
53.45	0.0872703	0.072569
58.35	0.0775726	0.0768959
63.25	0.0673225	0.080661
68.15	0.050898	0.0838369
73.05	0.0383817	0.0864004
77.95	0.0292872	0.0883328
82.85	0.0196223	0.0896199
87.75	0.0150243	0.0902523
92.65	0.00663731	0.0489889
97.55	0.000289617	0.00067284
Average Number	43.9335	63.0123

b) Sn with 2.1% Cu, Sample 82, 12 months at 50% RH / 50°C

Electroplated Sn with 2.1% Cu
Grain Boundary Characterization Chart

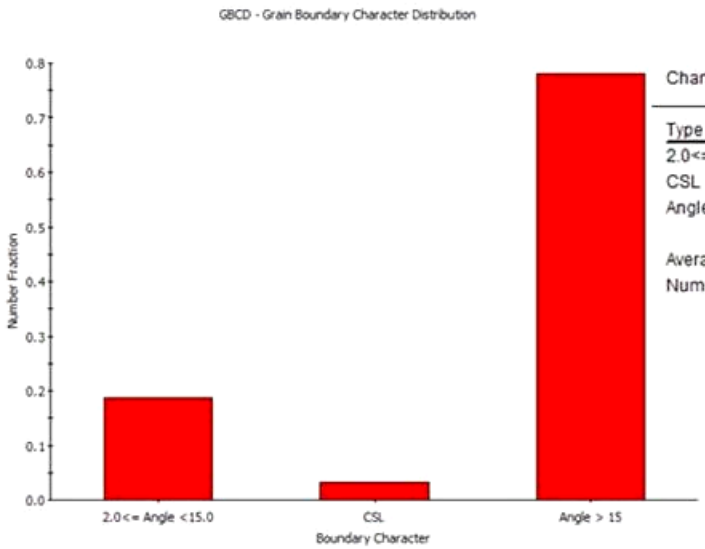

Chart: GBCD - Grain Boundary Character Distribution

Type	Number Fraction
2.0<= Angle <15.0	0.186126
CSL	0.0332113
Angle > 15	0.780663
Average Number	0.333333

a) Sn with 2.1% Cu, Sample 79, post plating

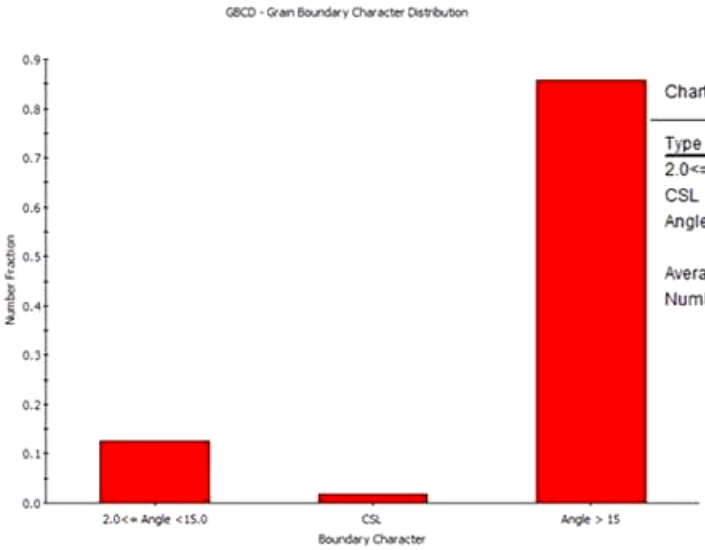

Chart: GBCD - Grain Boundary Character Distribution

Type	Number Fraction
2.0<= Angle <15.0	0.125571
CSL	0.0174696
Angle > 15	0.856959
Average Number	0.333333

b) Sn with 2.1% Cu, Sample 82, 12 months at 50% RH / 50°C

Electroplated Sn with 2.1% Cu

Coincident Site Lattice Boundary Chart

The total fraction of CSL boundaries is approximately 2% of boundaries measured

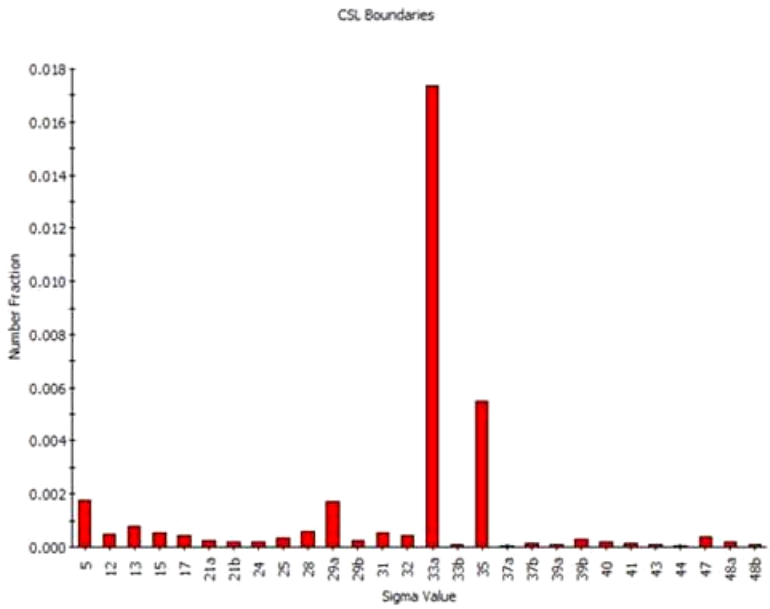

Chart: CSL Boundaries

Overall fraction of CSL boundaries: 0.033

Sigma	Number Fraction
5	0.00176885
12	0.000476228
13	0.000771036
15	0.000532922
17	0.000453551
21a	0.000255122
21b	0.000204098
24	0.00018709
25	0.000351502
28	0.000612293
29a	0.00171782
29b	0.000226775
31	0.0005556
32	0.00046489
33a	0.0173483
33b	9.07101e-005
35	0.00547096
37a	5.10245e-005
37b	0.000141735
39a	8.50408e-005
39b	0.000300477
40	0.000175751
41	0.000136065
43	7.3702e-005
44	6.23632e-005
47	0.000413865
48a	0.000175751
48b	0.000107718

a) Sn with 2.1% Cu, Sample 79, post plating

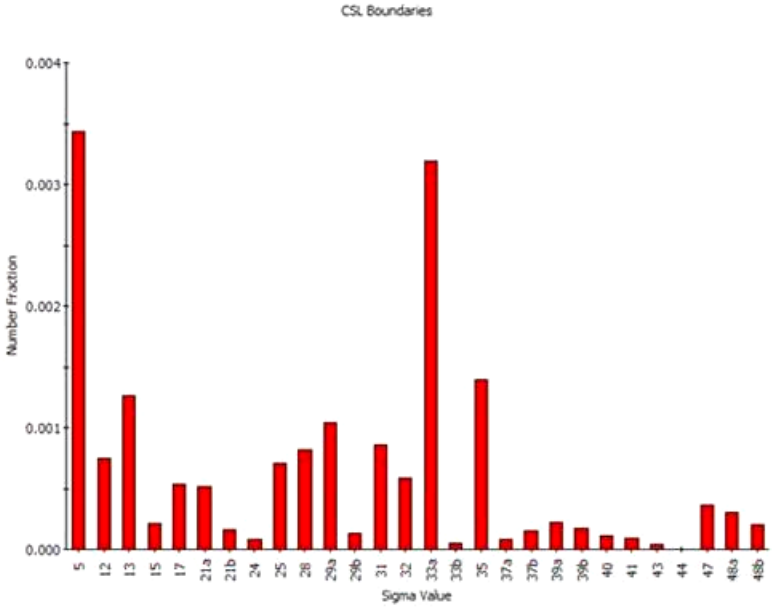

Chart: CSL Boundaries

Overall fraction of CSL boundaries: 0.017

Sigma	Number Fraction
5	0.0034336
12	0.000746436
13	0.00126297
15	0.000214974
17	0.000537434
21a	0.000516534
21b	0.000164216
24	8.06151e-005
25	0.000710607
28	0.000818094
29a	0.00103605
29b	0.000134358
31	0.000859894
32	0.000588191
33a	0.00319475
33b	4.77719e-005
35	0.00139733
37a	8.36008e-005
37b	0.000152273
39a	0.000217959
39b	0.000167202
40	0.000107487
41	9.55438e-005
43	3.58289e-005
44	2.98574e-006
47	0.000361275
48a	0.00030156
48b	0.000200045

b) Sn with 2.1% Cu, Sample 82, 12 months at 50% RH / 50°C

Electroplated Sn with 2.1% Cu
Misorientation Distribution Function (MODF) Plot

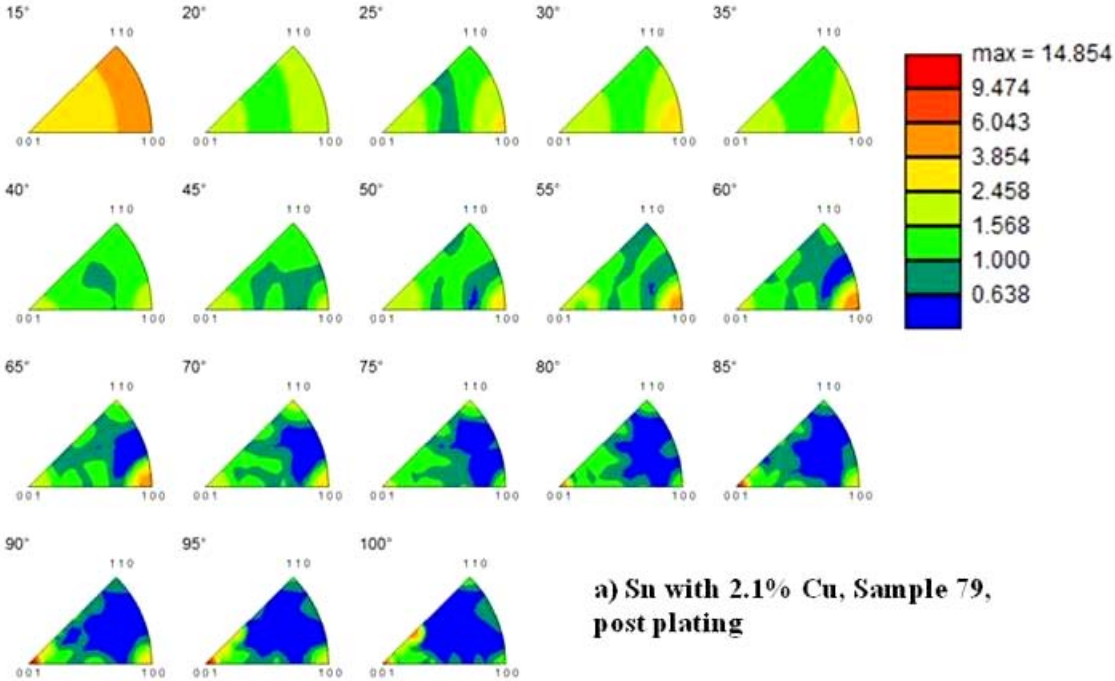

a) Sn with 2.1% Cu, Sample 79, post plating

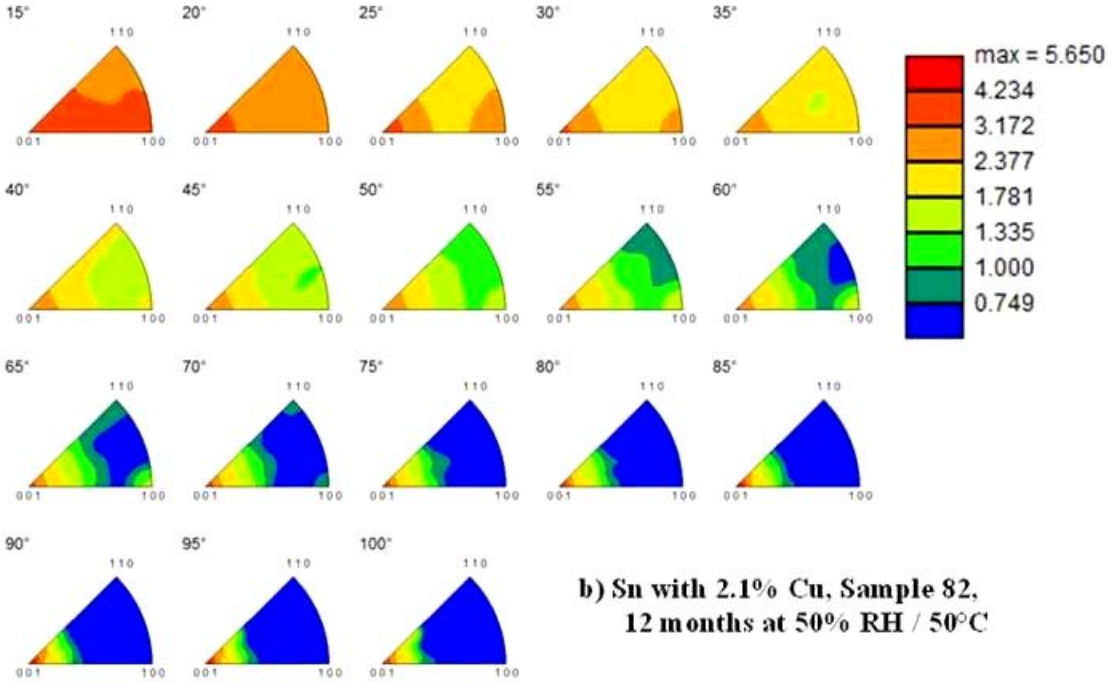

b) Sn with 2.1% Cu, Sample 82, 12 months at 50% RH / 50°C

Electroplated Sn with 2.1% Cu

Crystal Direction Map

Blue Indicates C-Direction in sample normal

Red indicates C-direction in sample plane 15º tolerance

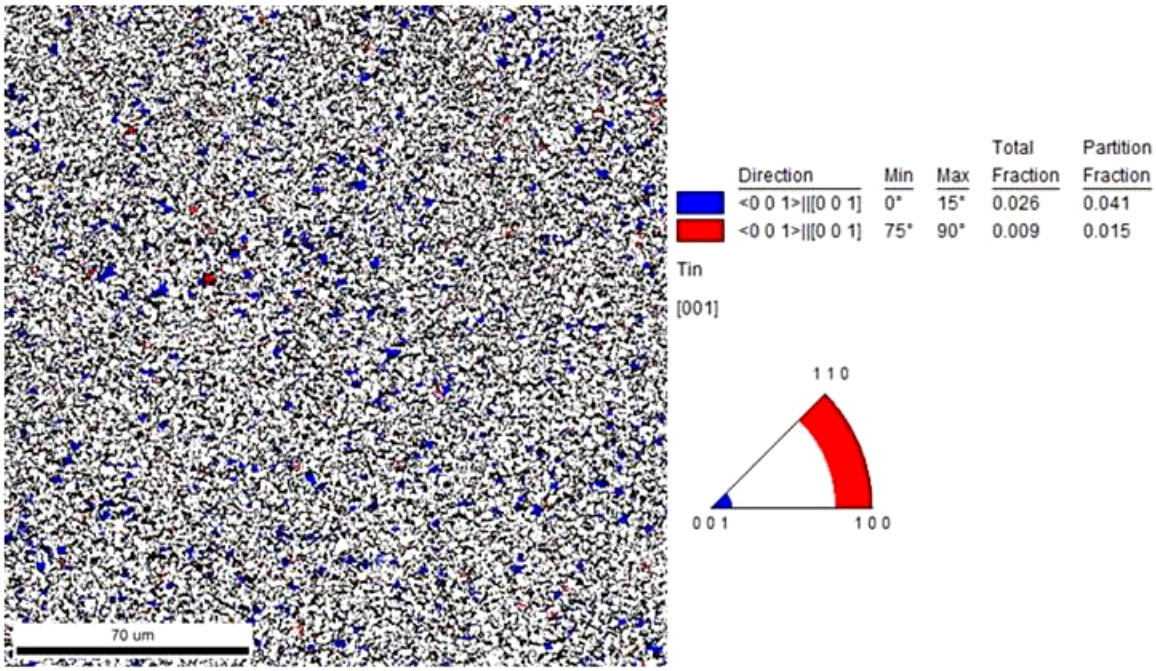

a) Sn with 2.1% Cu, Sample 79, post plating

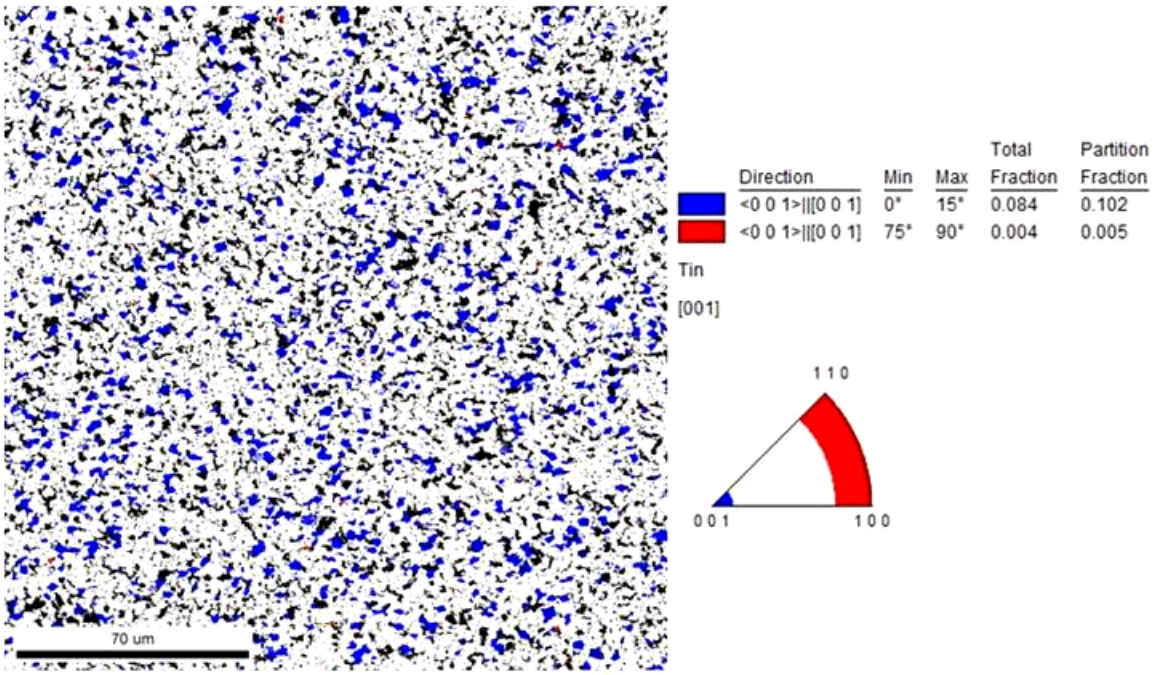

b) Sn with 2.1% Cu, Sample 82, 12 months at 50% RH / 50°C

Appendix M: EBSD Data for Sn with 3.0% Ni

Electroplated Sn with 3.0% Ni
Image Quality Map

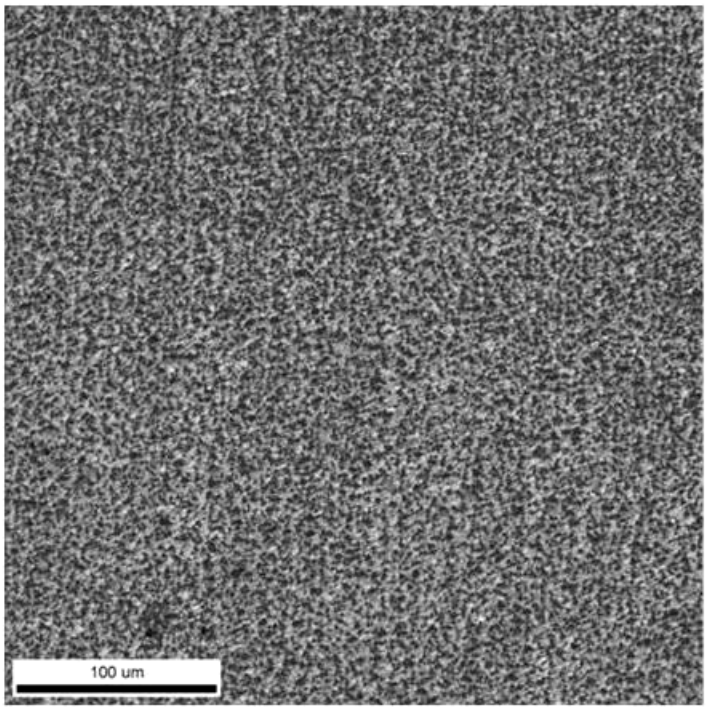

X = 350 microns
Y = 350 microns
Step size = 0.4 microns

a) Sn with 3.0% Ni, Sample 130, post plating

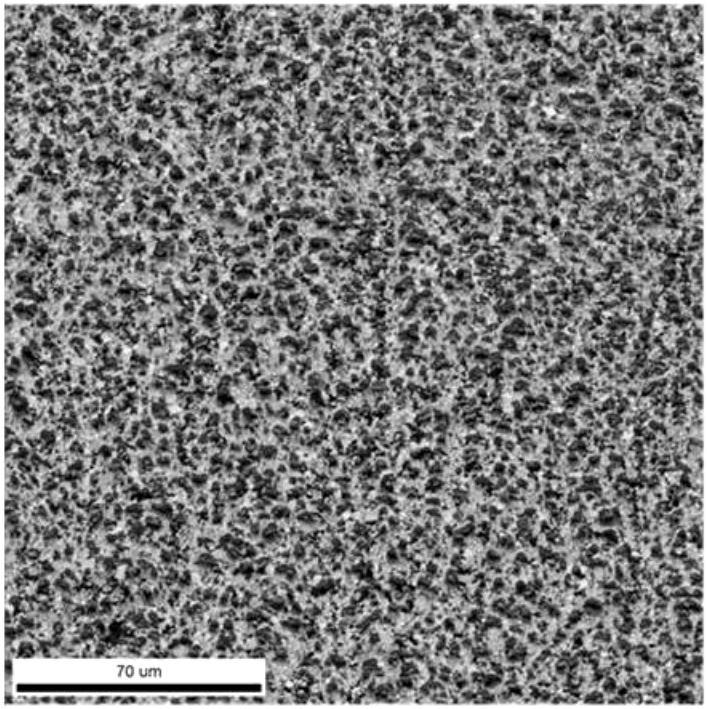

X = 200 microns
Y = 200 microns
Step size = 0.2 microns

b) Sn with 3.0% Ni, Sample 129, 12 months at 50% RH / 50°C

Electroplated Sn with 3.0% Ni
Color Coded Orientation Map

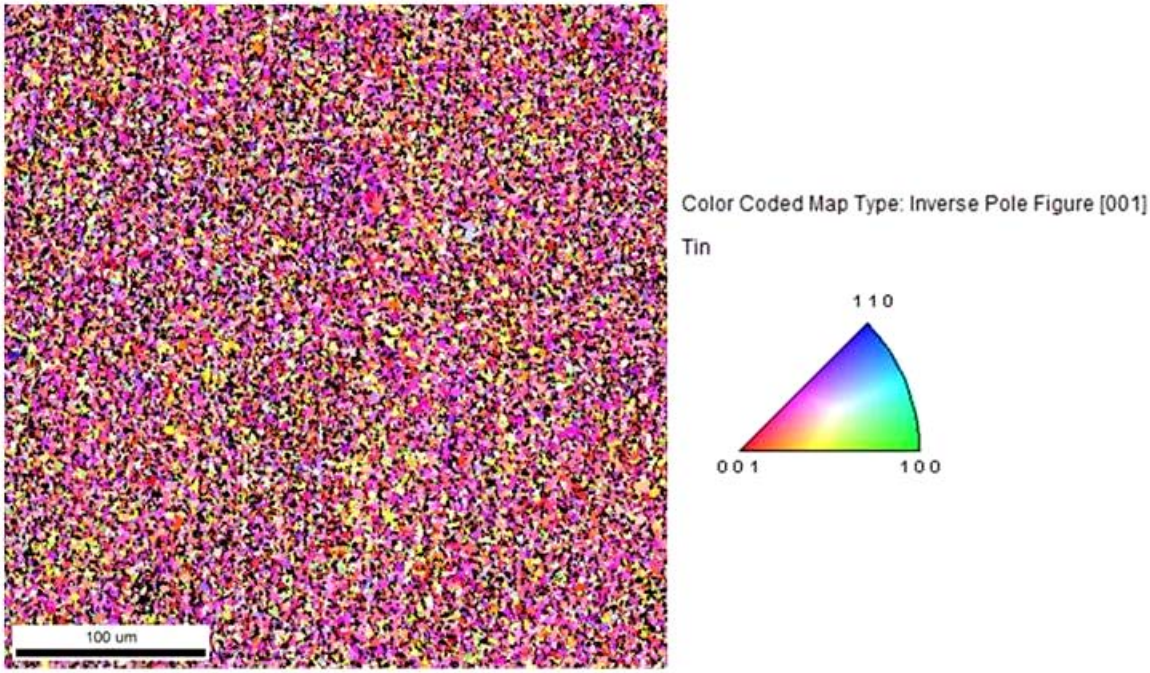

a) Sn with 3.0% Ni, Sample 130, post plating

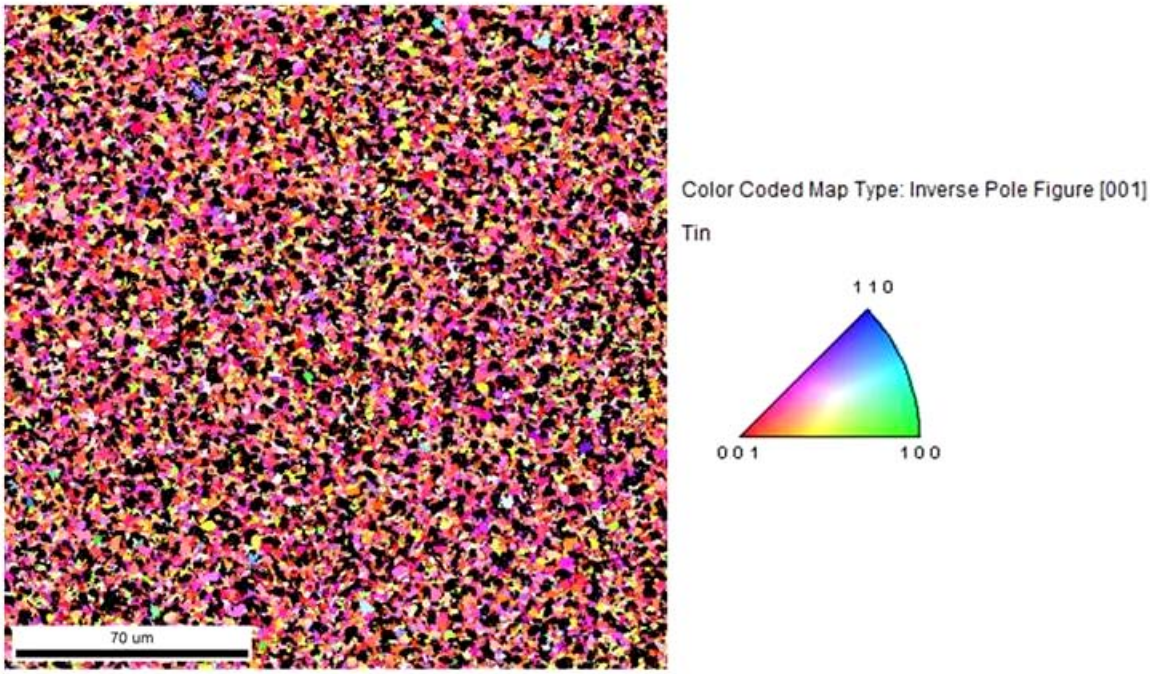

b) Sn with 3.0% Ni, Sample 129, 12 months at 50% RH / 50°C

Electroplated Sn with 3.0% Ni
Crystal Direction Map Showing <111> crystal direction in ND direction 15º Tolerance

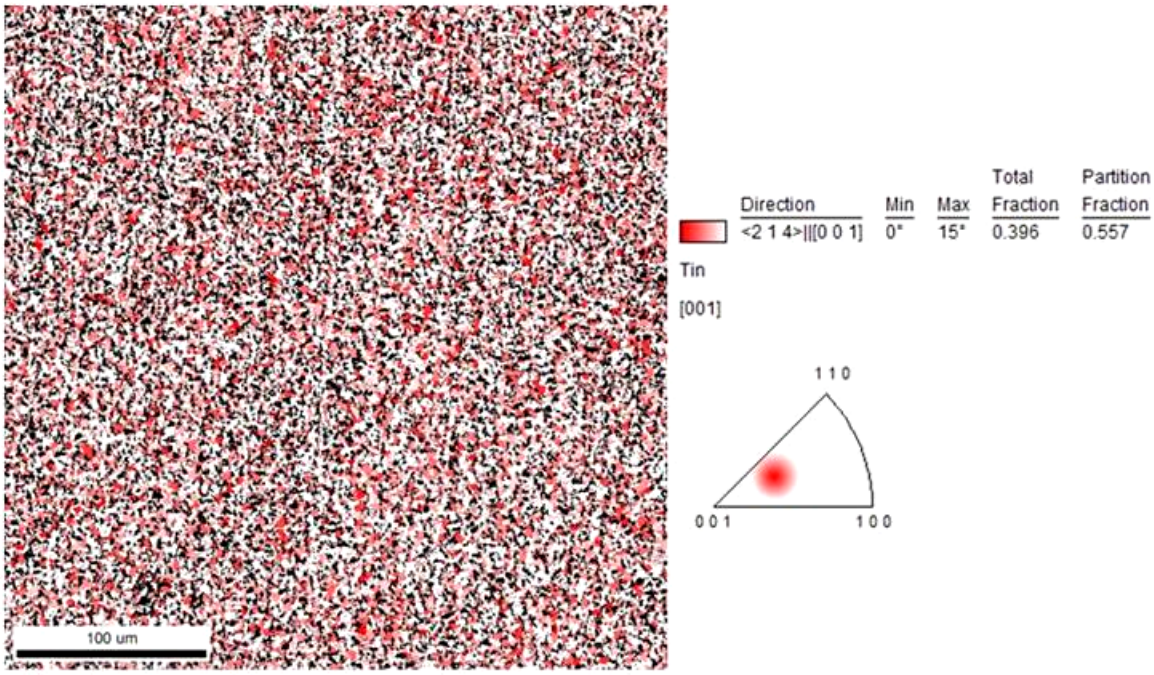

a) Sn with 3.0% Ni, Sample 130, post plating

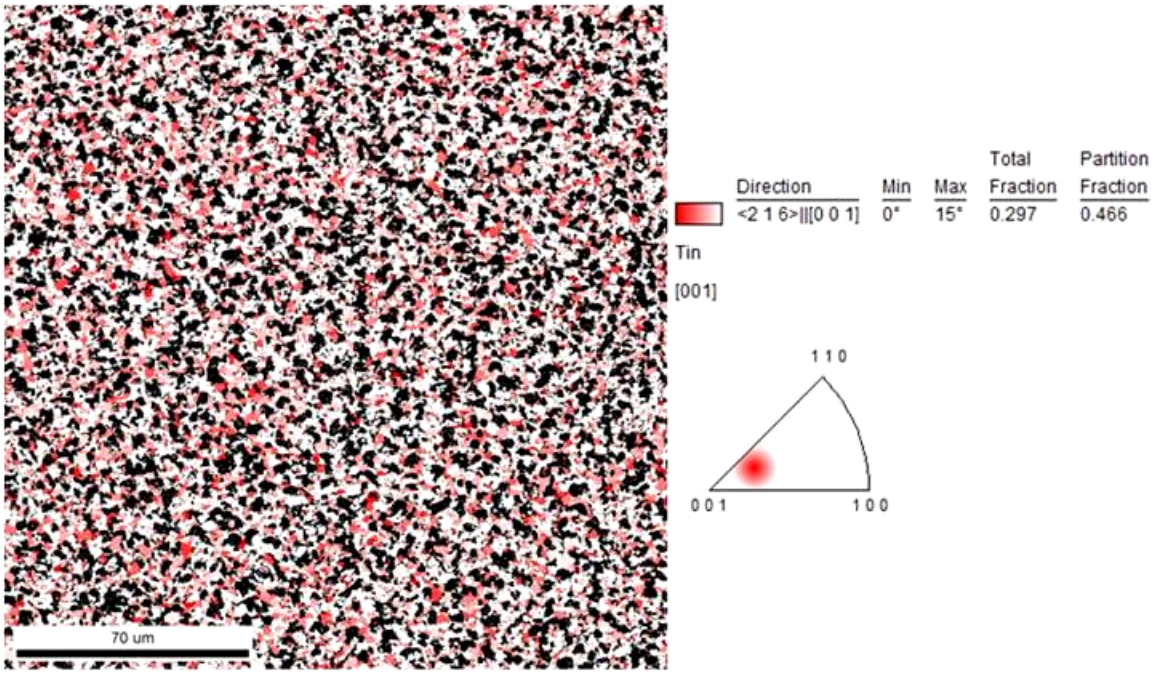

b) Sn with 3.0% Ni, Sample 129, 12 months at 50% RH / 50°C

Electroplated Sn with 3.0% Ni
Crystal Direction Map Showing <111> crystal direction in ND direction 20º Tolerance

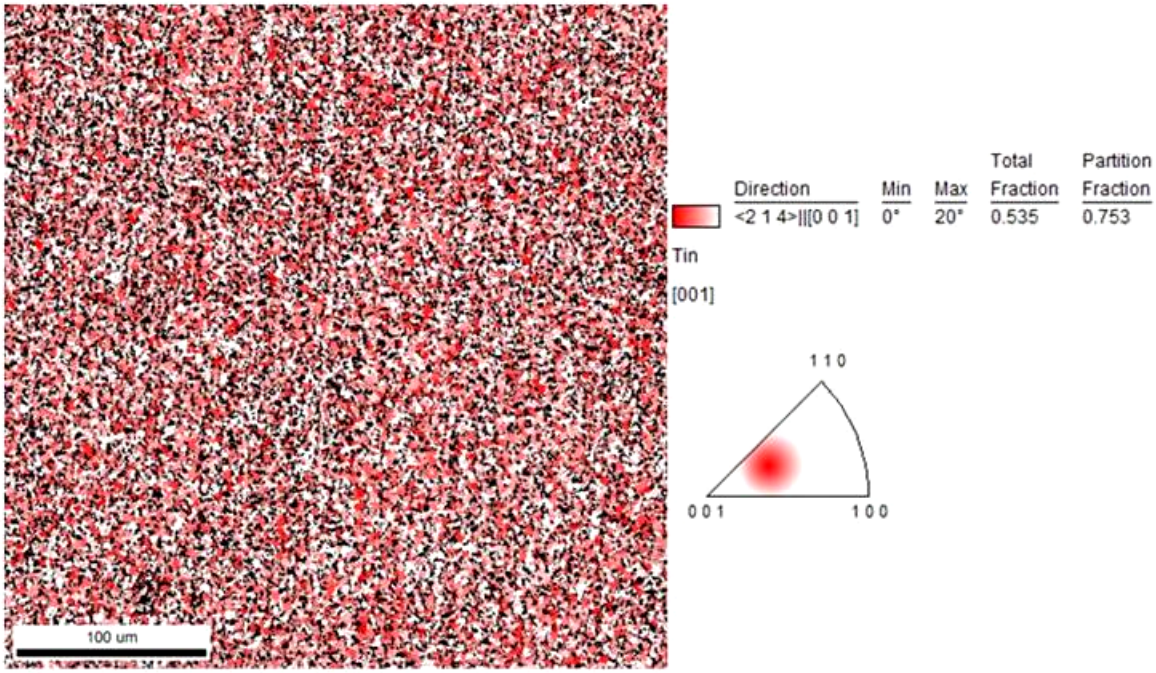

a) Sn with 3.0% Ni, Sample 130, post plating

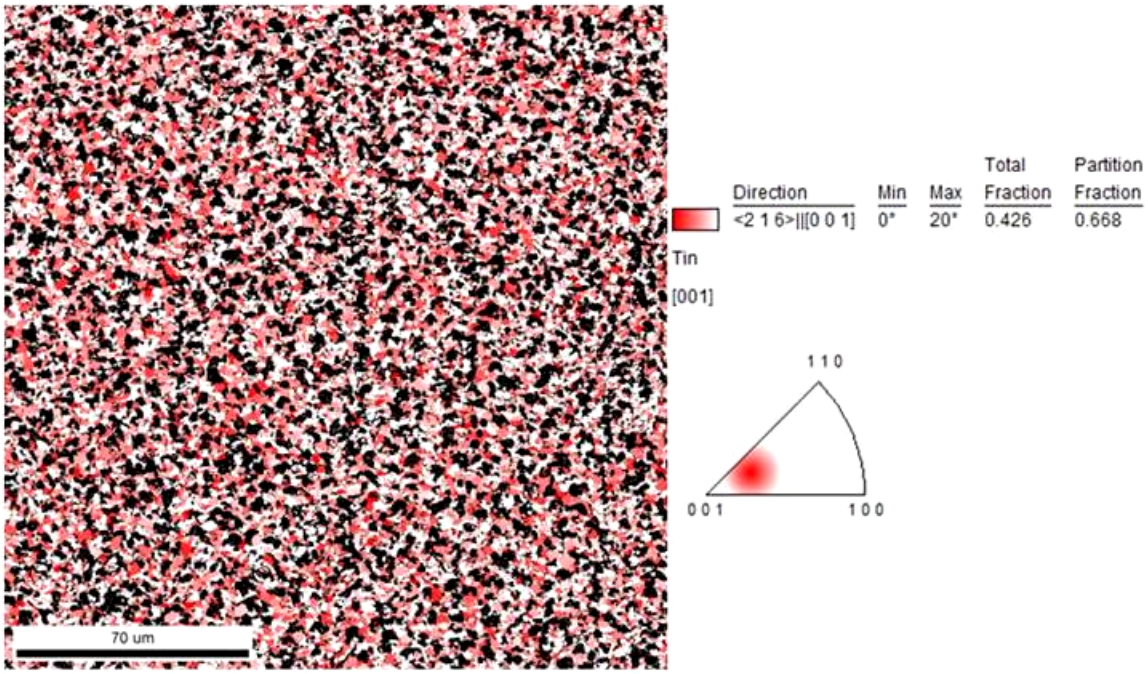

b) Sn with 3.0% Ni, Sample 129, 12 months at 50% RH / 50°C

Electroplated Sn with 3.0% Ni

Confidence Index (CI) Chart

Data points with a CI above 0.1 are generally considered to be indexed correctly.

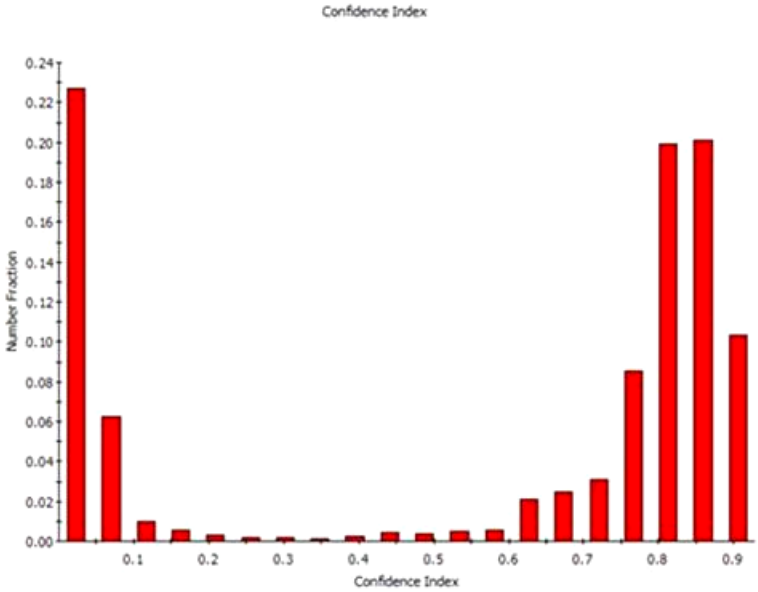

Chart: Confidence Index

CI	Number Fraction
0.023225	0.22728
0.069675	0.0624405
0.116125	0.0101251
0.162575	0.00540259
0.209025	0.00314869
0.255475	0.00159637
0.301925	0.00164382
0.348375	0.00146306
0.394825	0.00240642
0.441275	0.00438353
0.487725	0.00344017
0.534175	0.00523764
0.580625	0.00537774
0.627075	0.0207958
0.673525	0.024994
0.719975	0.0310914
0.766425	0.0856224
0.812875	0.199224
0.859325	0.200835
0.905775	0.103492
Average	
Number	0.569377
Standard Deviation	0.36827

(a) Sn with 3.0% Ni, Sample 130, post plating. Indicates that about 28.9% of data points were not indexed with a high degree of confidence

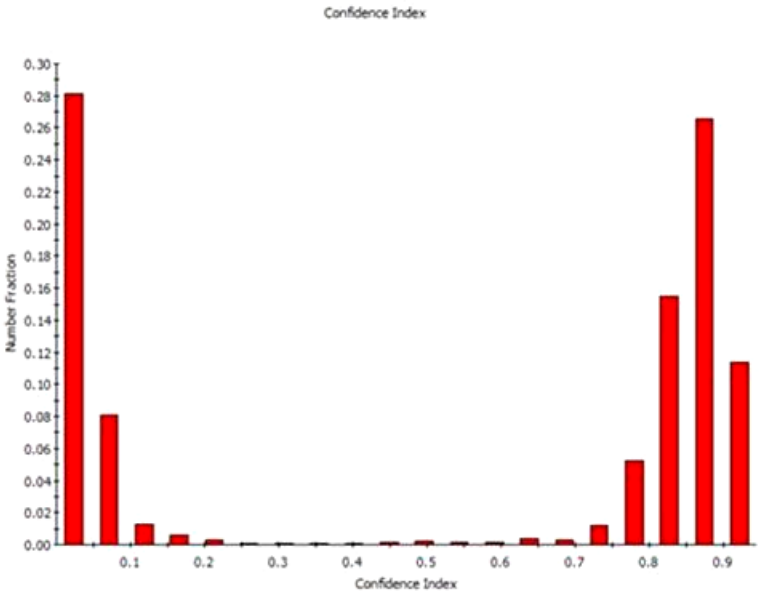

Chart: Confidence Index

CI	Number Fraction
0.02365	0.281234
0.07095	0.0811637
0.11825	0.0127252
0.16555	0.00616748
0.21285	0.00279254
0.26015	0.000918155
0.30745	0.000739889
0.35475	0.000893925
0.40205	0.000733832
0.44935	0.00152478
0.49665	0.00218419
0.54395	0.00140103
0.59125	0.0018216
0.63855	0.00372887
0.68585	0.00330311
0.73315	0.0119793
0.78045	0.0521116
0.82775	0.155016
0.87505	0.26581
0.92235	0.113751
Average	
Number	0.537702
Standard Deviation	0.404384

(b) Sn with 3.0% Ni, Sample 129, 12 months at 50% RH / 50°C. Indicates that about 36.2% of data points were not indexed with a high degree of confidence

Electroplated Sn with 3.0% Ni
Pole Figure and Inverse Pole Figure Plots

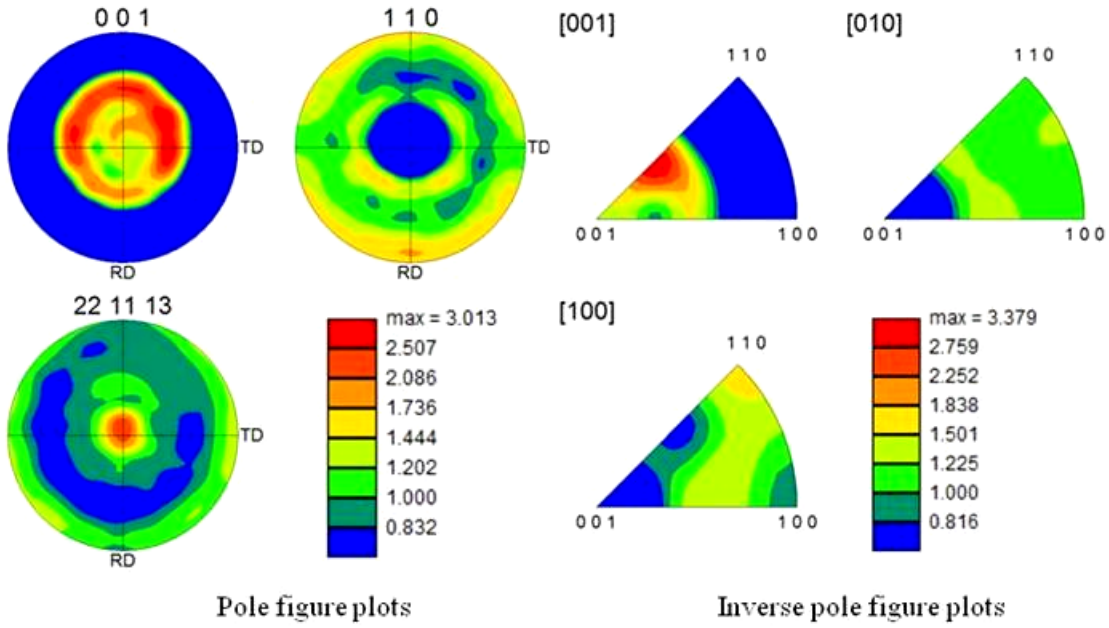

a) Sn with 3.0% Ni, Sample 130, post plating

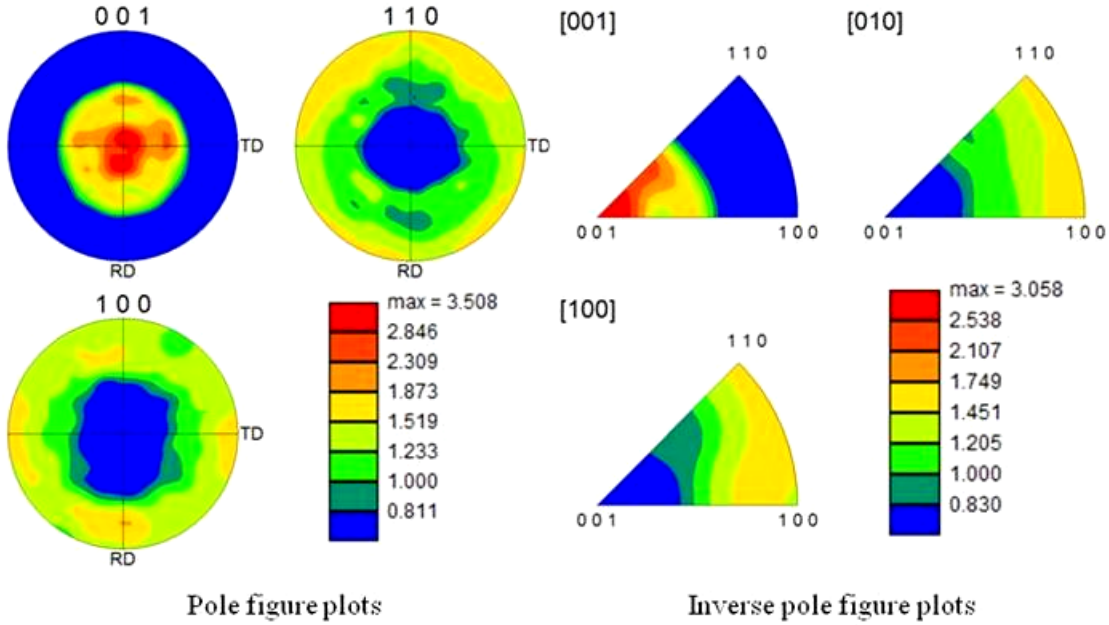

b) Sn with 3.0% Ni, Sample 129, 12 months at 50% RH / 50°C

Electroplated Sn with 3.0% Ni
Grain Size Histogram and Data

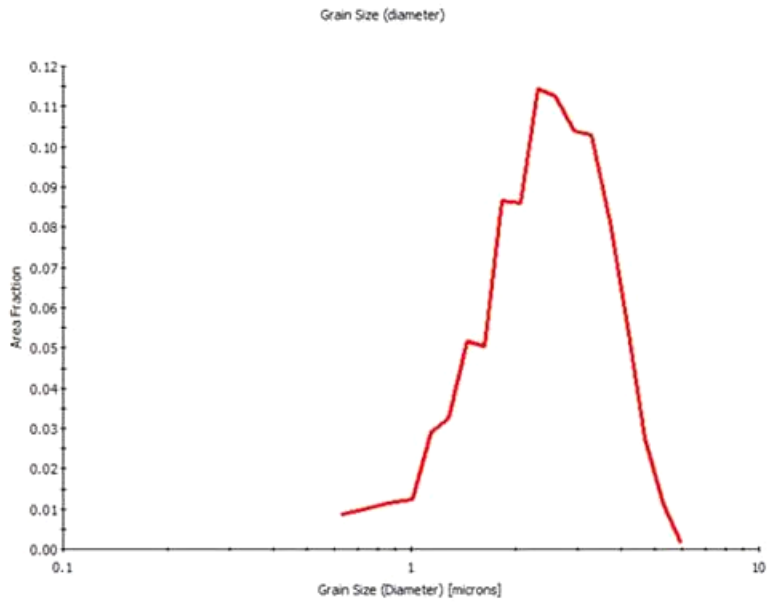

Edge grains included in analysis

Diameter [microns]	Area Fraction
0.630206	0.00869521
0.709345	0.00951059
0.798422	0.0106978
0.898685	0.0118964
1.01154	0.0122209
1.13856	0.0290259
1.28154	0.0323282
1.44247	0.0515255
1.62361	0.0505324
1.8275	0.0866292
2.05699	0.0860128
2.3153	0.114488
2.60604	0.112648
2.9333	0.103966
3.30165	0.102921
3.71626	0.0812526
4.18294	0.0555192
4.70821	0.0274245
5.29945	0.0110712
5.96494	0.00163565

a) Sn with 3.0% Ni, Sample 130, post plating

Average	
Number	1.66567
Standard Deviation	0.86062
Area	2.54667

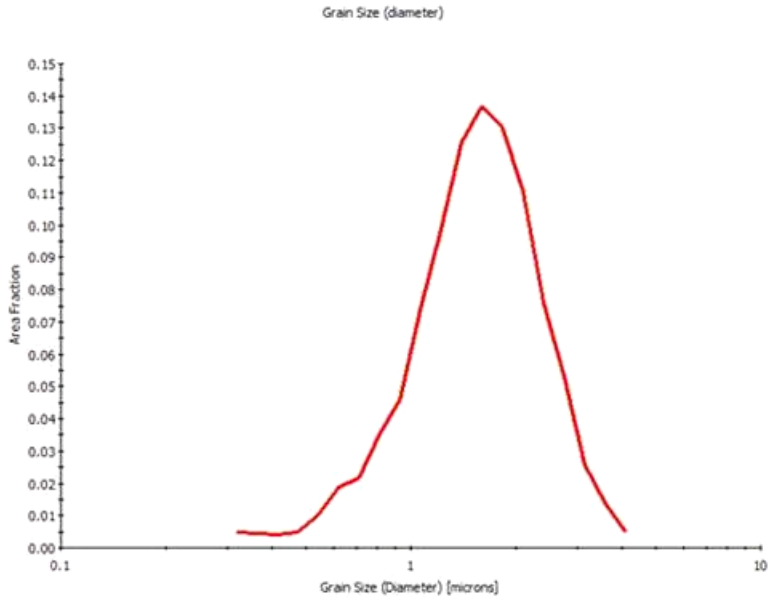

Edge grains included in analysis

Diameter [microns]	Area Fraction
0.317694	0.00503139
0.363492	0.00435457
0.415893	0.00430144
0.475847	0.00490834
0.544445	0.0102642
0.622931	0.0185706
0.712732	0.0216414
0.815479	0.0352519
0.933037	0.0461328
1.06754	0.0741131
1.22144	0.0989009
1.39752	0.125635
1.59898	0.136999
1.82949	0.130279
2.09323	0.110317
2.39498	0.0758569
2.74024	0.0530408
3.13527	0.0257555
3.58725	0.0139195
4.10438	0.00472655

b) Sn with 3.0% Ni, Sample 129, 12 months at 50% RH / 50°C

Average	
Number	1.04502
Standard Deviation	0.5747
Area	1.65108

Electroplated Sn with 3.0% Ni
Misorientation Angle Histogram, 2º minimum misorientation

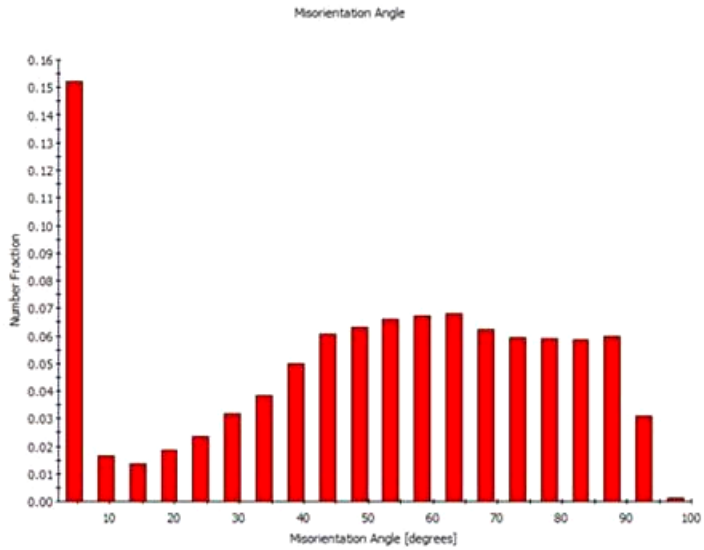

Chart: Misorientation Angle

Angle [degrees]	Number Fraction
4.45	0.152029
9.35	0.0165947
14.25	0.0134892
19.15	0.0184457
24.05	0.0233667
28.95	0.031764
33.85	0.0384909
38.75	0.0500002
43.65	0.0604549
48.55	0.063067
53.45	0.0658725
58.35	0.0672205
63.25	0.0679525
68.15	0.0624575
73.05	0.0593262
77.95	0.0590199
82.85	0.0586103
87.75	0.0597196
92.65	0.0307998
97.55	0.00131893
Average Number	49.5892

a) Sn with 3.0% Ni, Sample 130, post plating

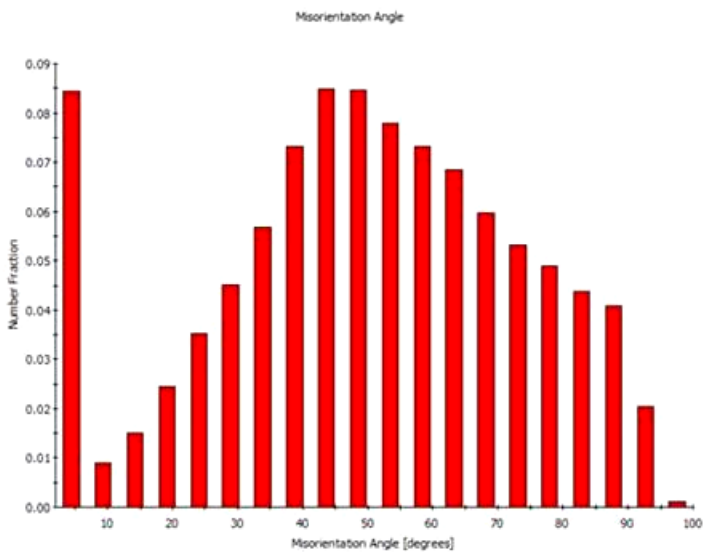

Chart: Misorientation Angle

Angle [degrees]	Number Fraction
4.45	0.0843406
9.35	0.00898551
14.25	0.0150201
19.15	0.0244962
24.05	0.0351711
28.95	0.0451784
33.85	0.0568714
38.75	0.0731014
43.65	0.084787
48.55	0.0845804
53.45	0.0779261
58.35	0.07326
63.25	0.0685607
68.15	0.0597264
73.05	0.0532639
77.95	0.0489002
82.85	0.0436587
87.75	0.0407779
92.65	0.0203281
97.55	0.00106602
Average Number	49.4451

b) Sn with 3.0% Ni, Sample 129, 12 months at 50% RH / 50°C

Electroplated Sn with 3.0% Ni

Misorientation Angle Histogram, 2º minimum misorientation

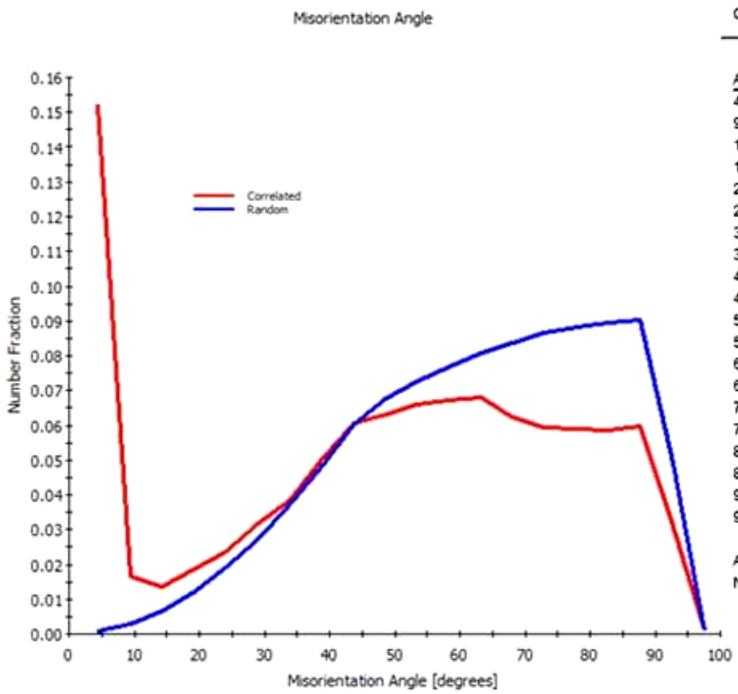

Chart: Misorientation Angle

Angle [degrees]	Correlated Number Fraction	Random Number Fraction
4.45	0.152029	0.000708536
9.35	0.0165947	0.00294695
14.25	0.0134892	0.00675716
19.15	0.0184457	0.0121113
24.05	0.0233667	0.0189703
28.95	0.031764	0.0272839
33.85	0.0384909	0.0369915
38.75	0.0500002	0.0480219
43.65	0.0604549	0.0602948
48.55	0.063067	0.0677125
53.45	0.0658725	0.0725694
58.35	0.0672205	0.0768963
63.25	0.0679525	0.0806614
68.15	0.0624575	0.0838374
73.05	0.0593262	0.0864009
77.95	0.0590199	0.0883332
82.85	0.0586103	0.0896203
87.75	0.0597196	0.0902527
92.65	0.0307998	0.0489892
97.55	0.00131893	0.000672962
Average Number	49.5892	63.0123

a) Sn with 3.0% Ni, Sample 130, post plating

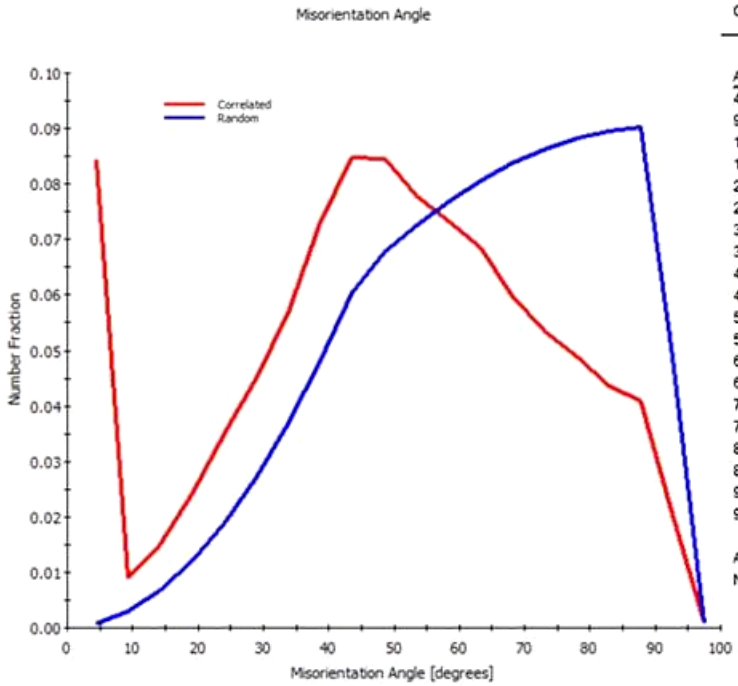

Chart: Misorientation Angle

Angle [degrees]	Correlated Number Fraction	Random Number Fraction
4.45	0.0843406	0.000708768
9.35	0.00898551	0.00294718
14.25	0.0150201	0.00675739
19.15	0.0244962	0.0121115
24.05	0.0351711	0.0189705
28.95	0.0451784	0.0272841
33.85	0.0568714	0.0369917
38.75	0.0731014	0.0480222
43.65	0.084787	0.060295
48.55	0.0845804	0.0677127
53.45	0.0779261	0.0725696
58.35	0.07326	0.0768965
63.25	0.0685607	0.0806616
68.15	0.0597264	0.0838376
73.05	0.0532639	0.0864011
77.95	0.0489002	0.0883335
82.85	0.0436587	0.0896205
87.75	0.0407779	0.0902529
92.65	0.0203281	0.0489894
97.55	0.00106602	0.000673193
Average Number	49.4451	63.0123

b) Sn with 3.0% Ni, Sample 129, 12 months at 50% RH / 50°C

Electroplated Sn with 3.0% Ni
Grain Boundary Characterization Chart

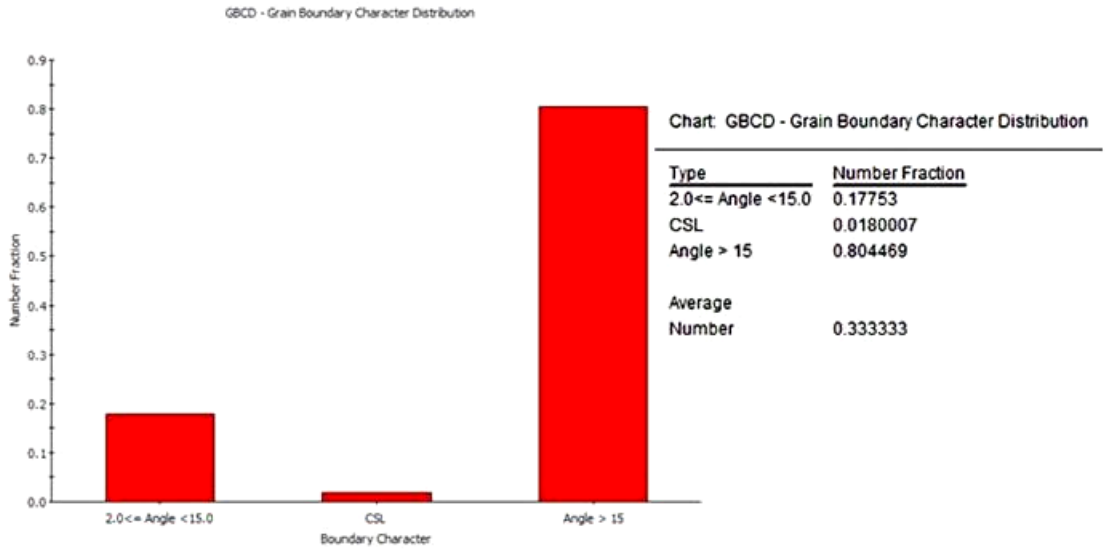

a) Sn with 3.0% Ni, Sample 130, post plating

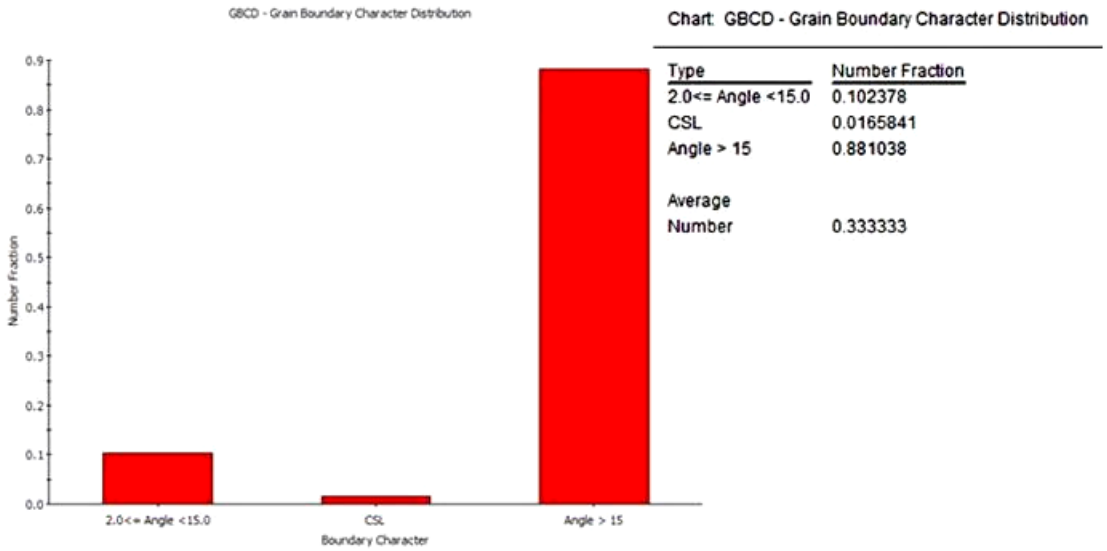

b) Sn with 3.0% Ni, Sample 129, 12 months at 50% RH / 50°C

Electroplated Sn with 3.0% Ni
Coincident Site Lattice Boundary Chart
The total fraction of CSL boundaries is approximately 2% of boundaries measured

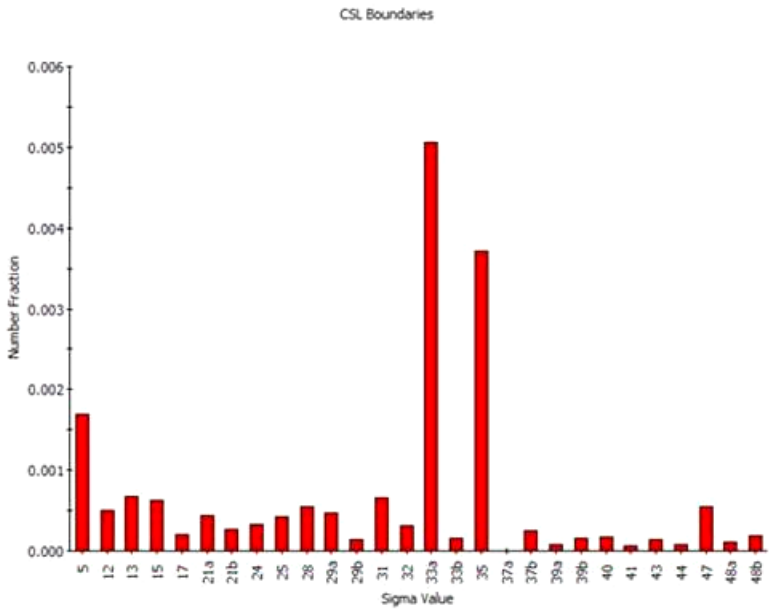

Overall fraction of CSL boundaries: 0.018

Sigma	Number Fraction
5	0.00168656
12	0.00049984
13	0.000667529
15	0.000622382
17	0.000206386
21a	0.000445019
21b	0.000274106
24	0.000322478
25	0.000419221
28	0.000554662
29a	0.000467593
29b	0.000138665
31	0.000657854
32	0.000306354
33a	0.00506612
33b	0.000161239
35	0.00370527
37a	3.22478e-006
37b	0.000254757
39a	8.38442e-005
39b	0.000161239
40	0.000170913
41	5.8046e-005
43	0.00014189
44	8.06194e-005
47	0.000544987
48a	0.000109642
48b	0.000190262

a) Sn with 3.0% Ni, Sample 130, post plating

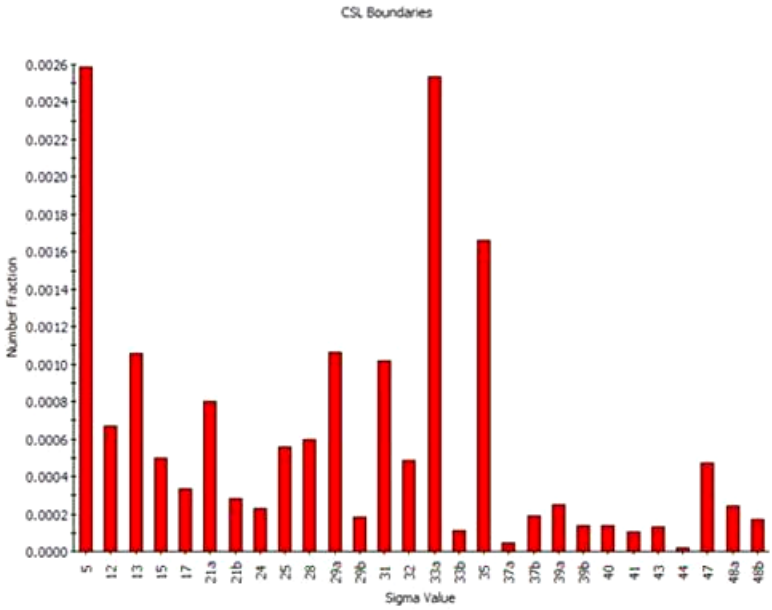

Overall fraction of CSL boundaries: 0.017

Sigma	Number Fraction
5	0.00258573
12	0.000671332
13	0.00105864
15	0.000497966
17	0.000331977
21a	0.000804122
21b	0.000280336
24	0.000232384
25	0.000560672
28	0.000597559
29a	0.00106233
29b	0.000184432
31	0.00101806
32	0.0004869
33a	0.00253409
33b	0.000114348
35	0.00165989
37a	4.79523e-005
37b	0.00018812
39a	0.000247139
39b	0.000136479
40	0.000136479
41	0.00010697
43	0.000129102
44	2.21318e-005
47	0.000472145
48a	0.00024345
48b	0.000173366

b) Sn with 3.0% Ni, Sample 129, 12 months at 50% RH / 50°C

Electroplated Sn with 3.0% Ni
Misorientation Distribution Function (MODF) Plot

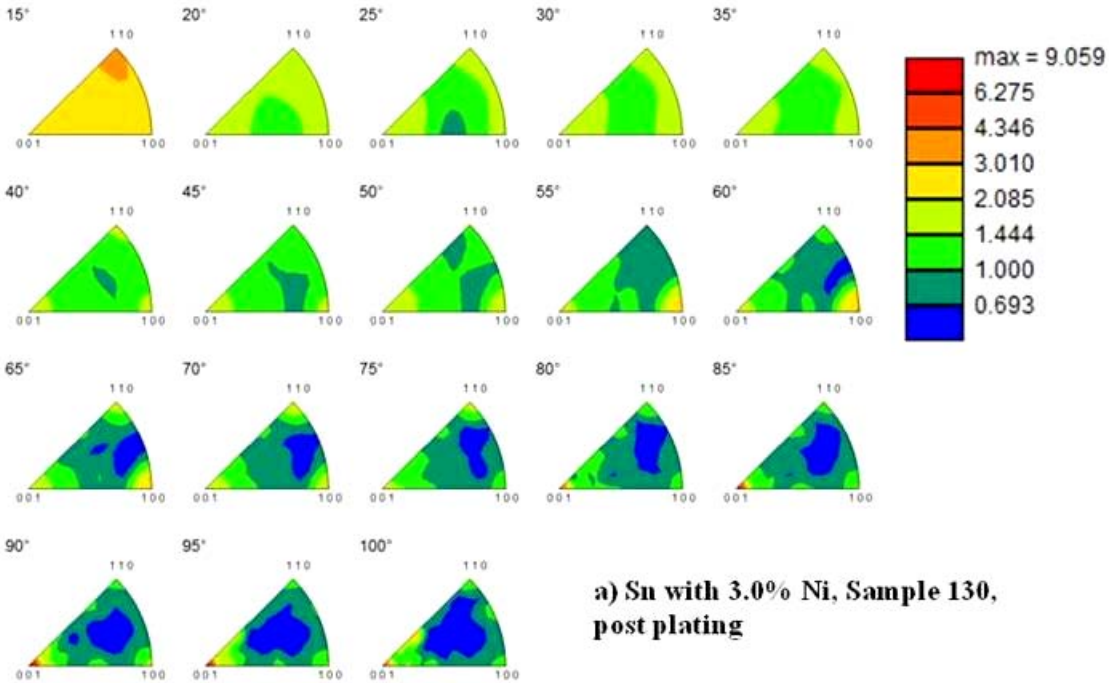

a) Sn with 3.0% Ni, Sample 130, post plating

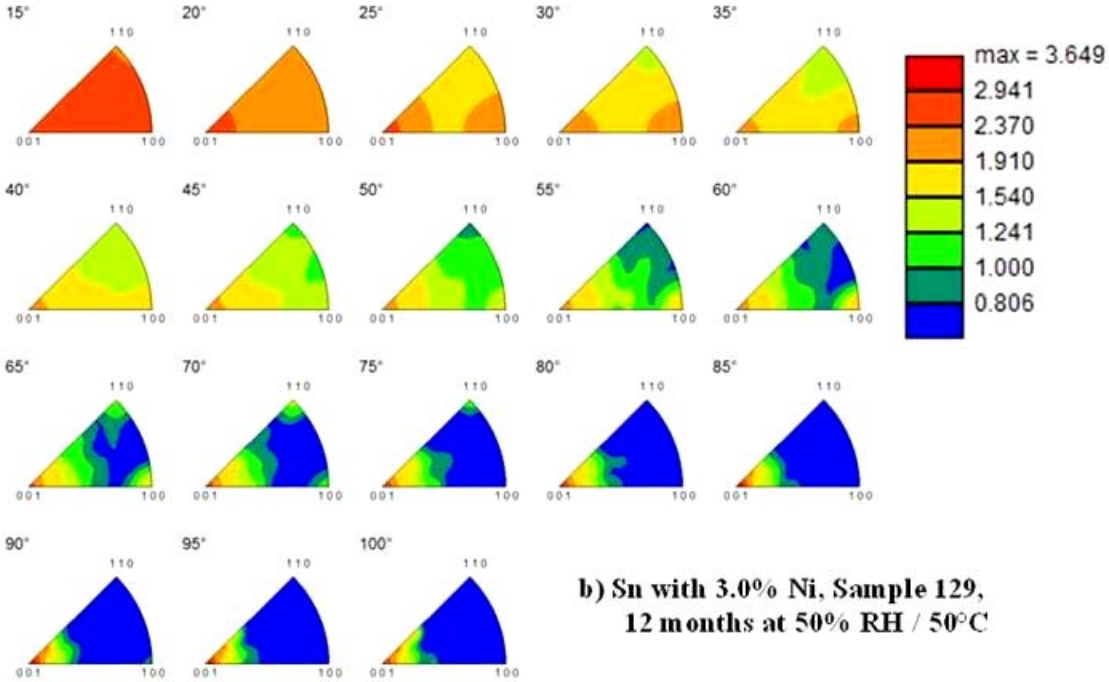

b) Sn with 3.0% Ni, Sample 129, 12 months at 50% RH / 50°C

Electroplated Sn with 3.0% Ni

Crystal Direction Map

Blue Indicates C-Direction in sample normal

Red indicates C-direction in sample plane 15º tolerance

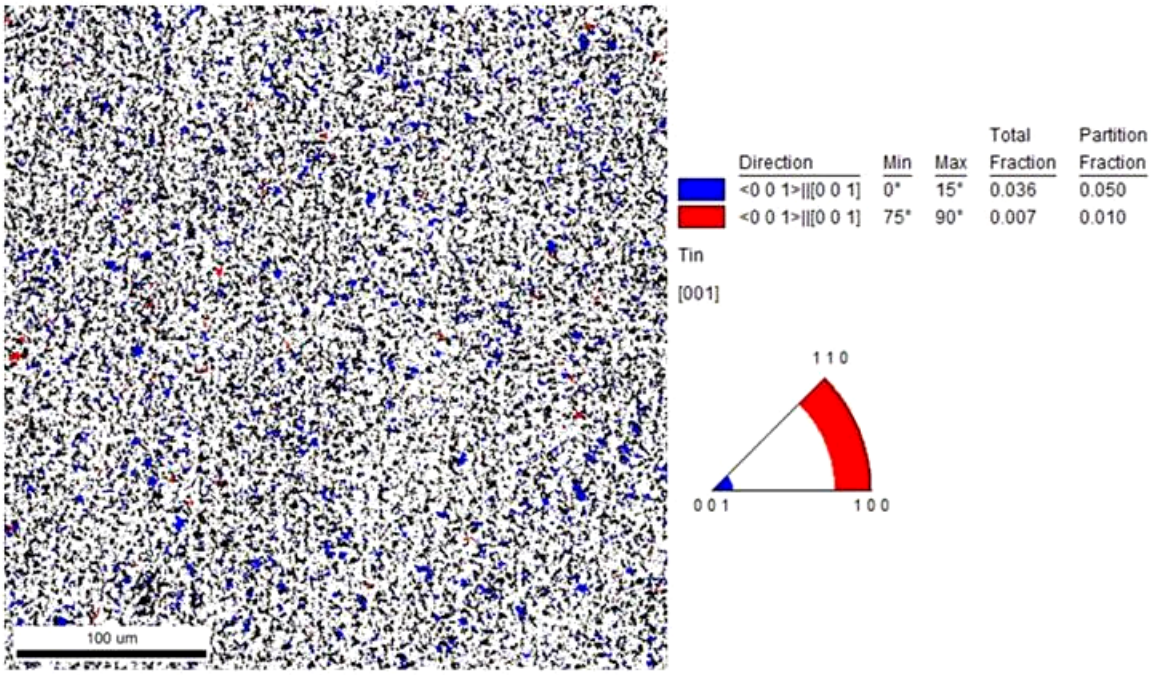

a) Sn with 3.0% Ni, Sample 130, post plating

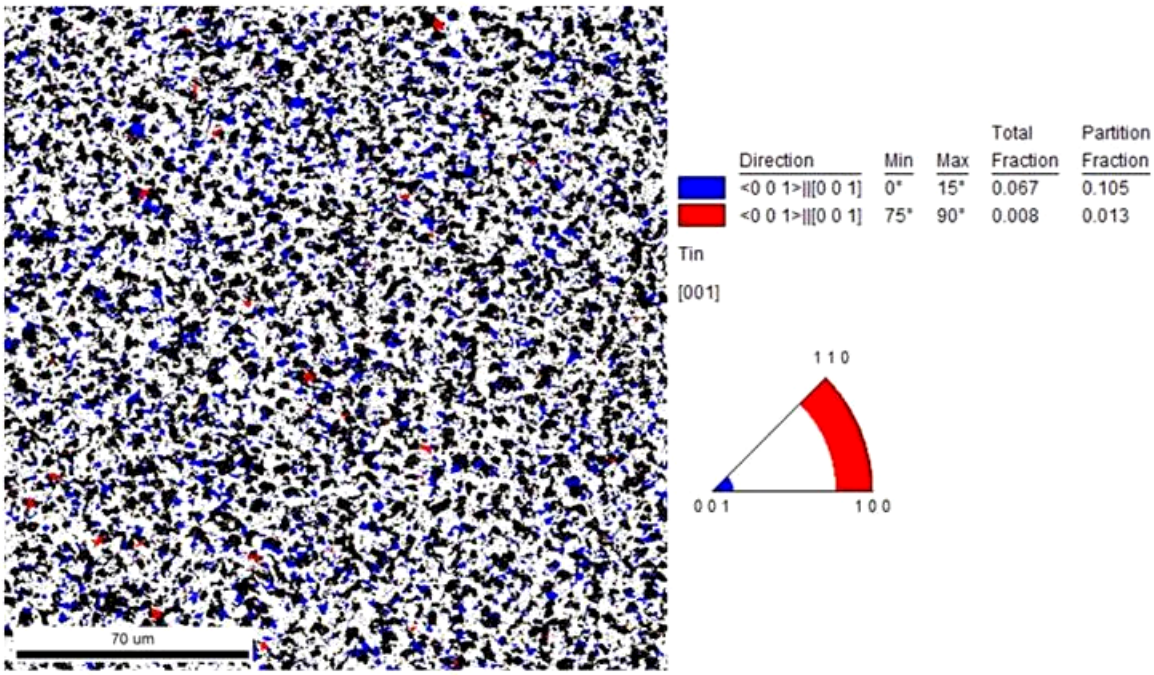

b) Sn with 3.0% Ni, Sample 129, 12 months at 50% RH / 50°C

Appendix N: EBSD Data for Sn with 0.95% Co

Electroplated Sn with 0.95% Co
Image Quality Map

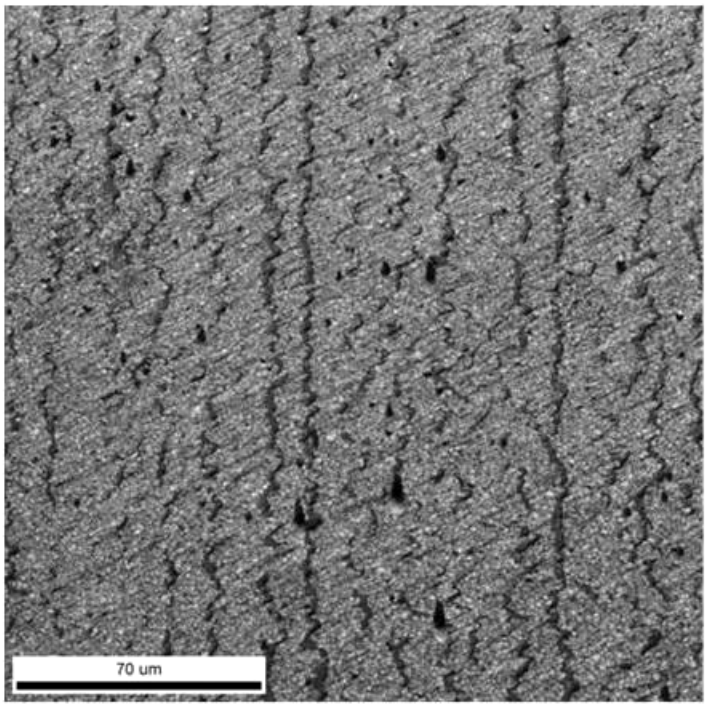

X = 200 microns
Y = 200 microns
Step size = 0.25 microns

a) Sn with 0.95% Co, Sample 168, post plating

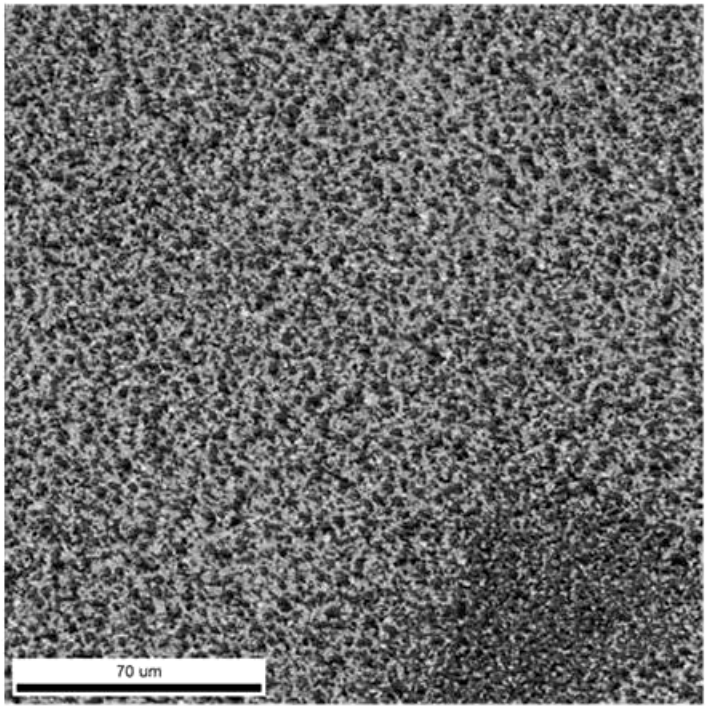

X = 200 microns
Y = 200 microns
Step size = 0.2 microns

b) Sn with 0.95% Co, Sample 171, 12 months at 50% RH / 50°C

Electroplated Sn with 0.95% Co
Color Coded Orientation Map

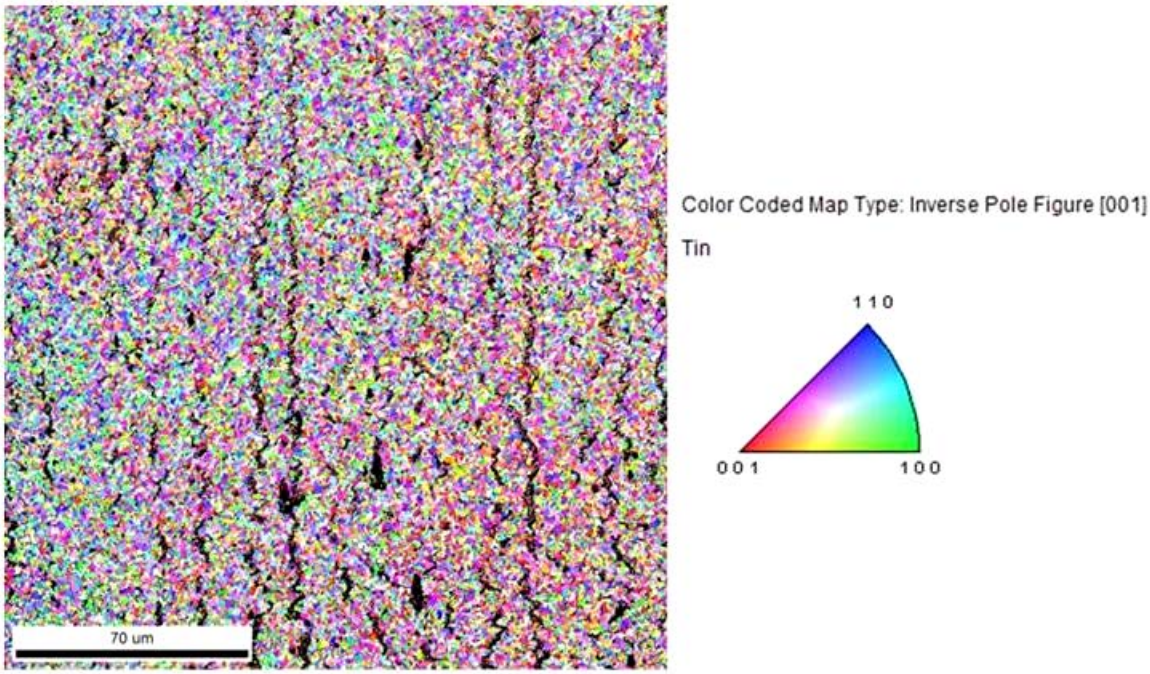

a) Sn with 0.95% Co, Sample 168, post plating

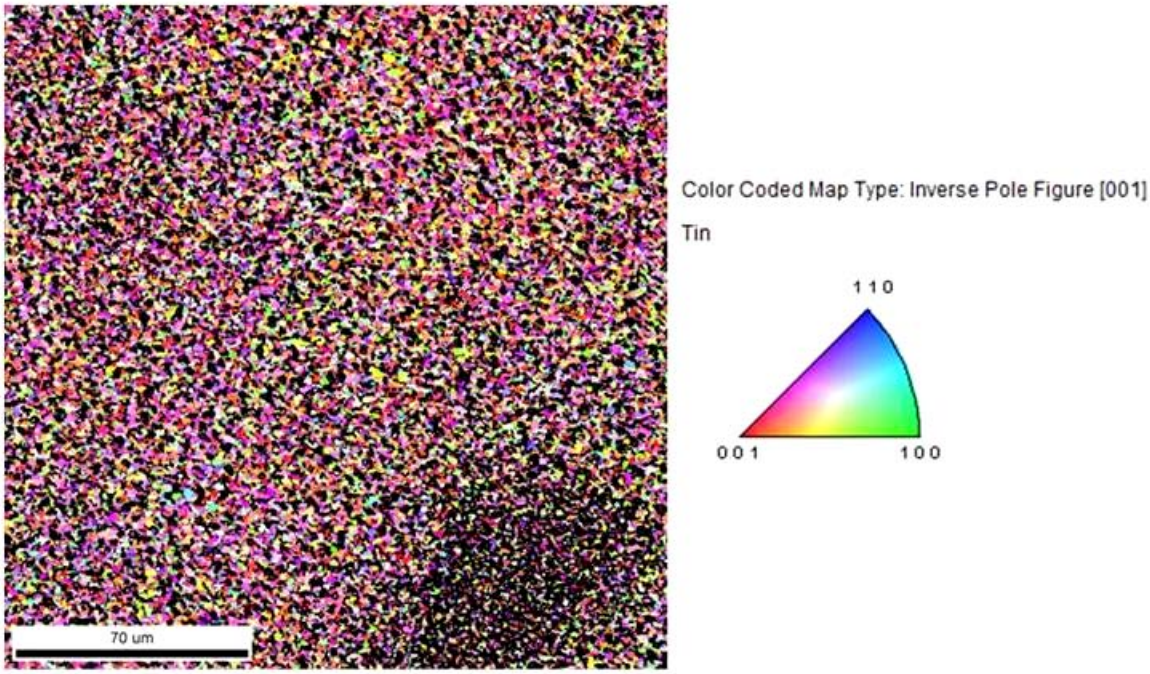

b) Sn with 0.95% Co, Sample 171, 12 months at 50% RH / 50°C

Electroplated Sn with 0.95% Co
Crystal Direction Map Showing <111> crystal direction in ND direction 15º Tolerance

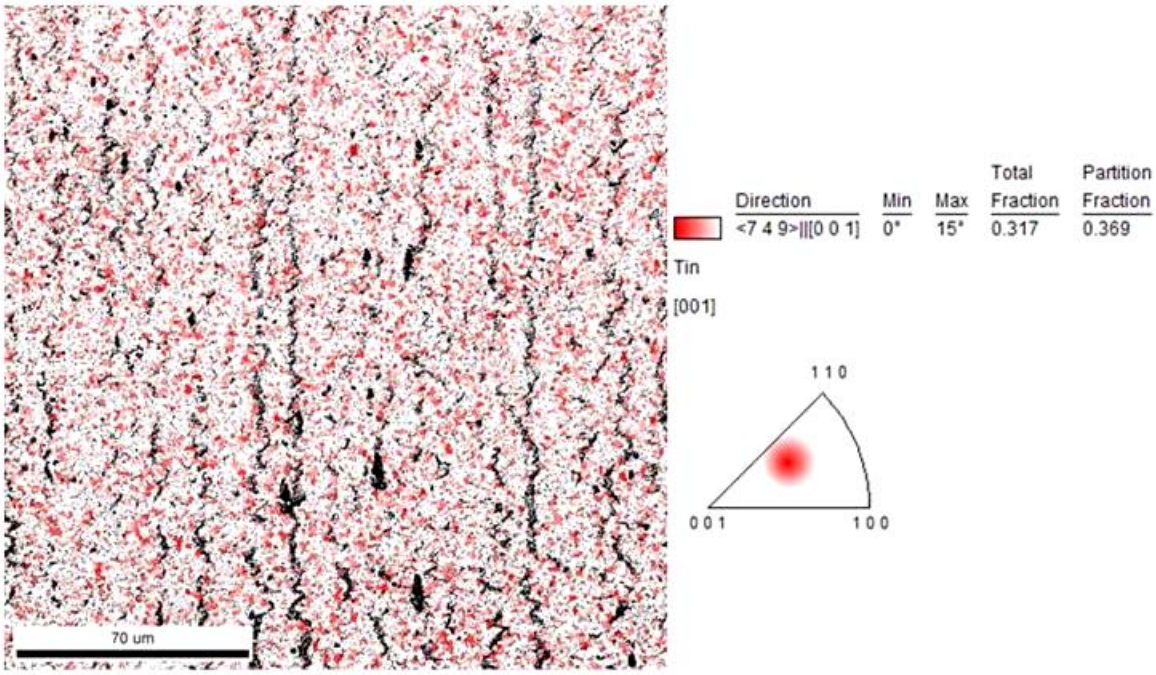

a) Sn with 0.95% Co, Sample 168, post plating

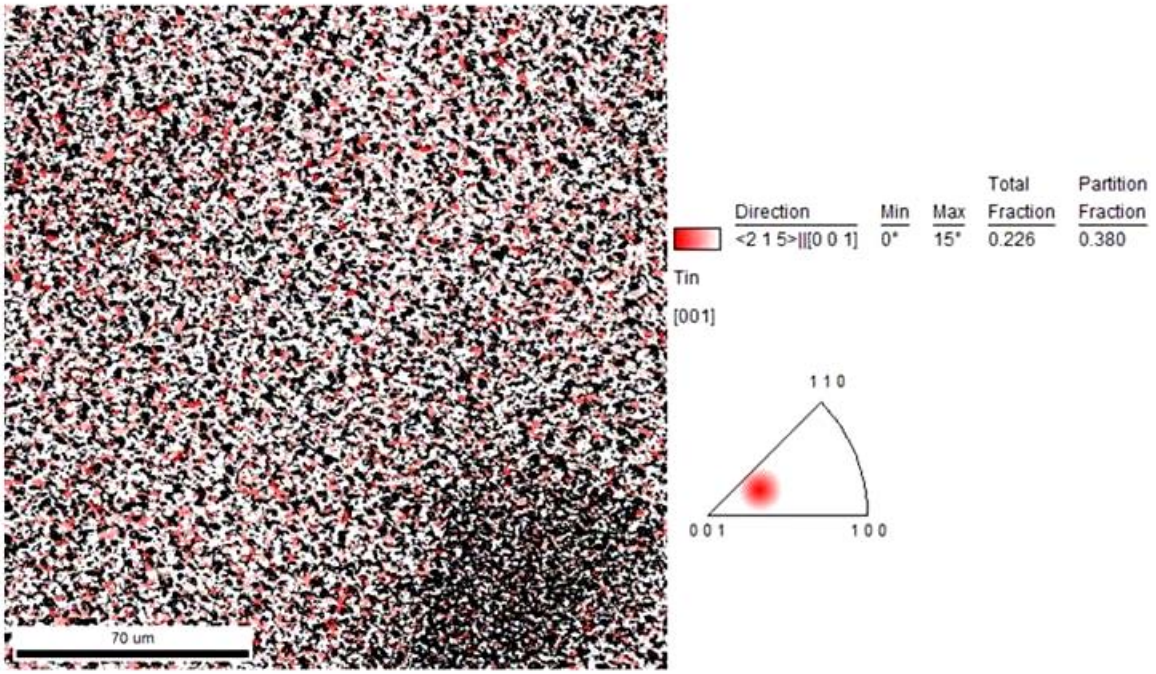

b) Sn with 0.95% Co, Sample 171, 12 months at 50% RH / 50°C

Electroplated Sn with 0.95% Co
Crystal Direction Map Showing <111> crystal direction in ND direction 20º Tolerance

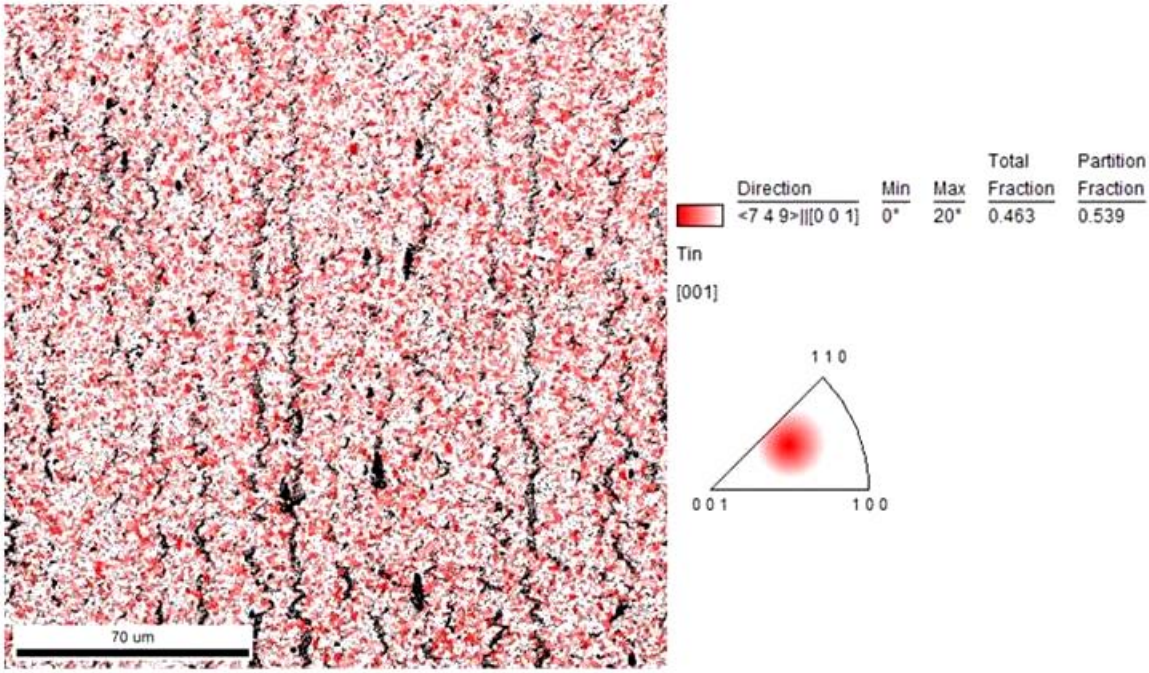

a) Sn with 0.95% Co, Sample 168, post plating

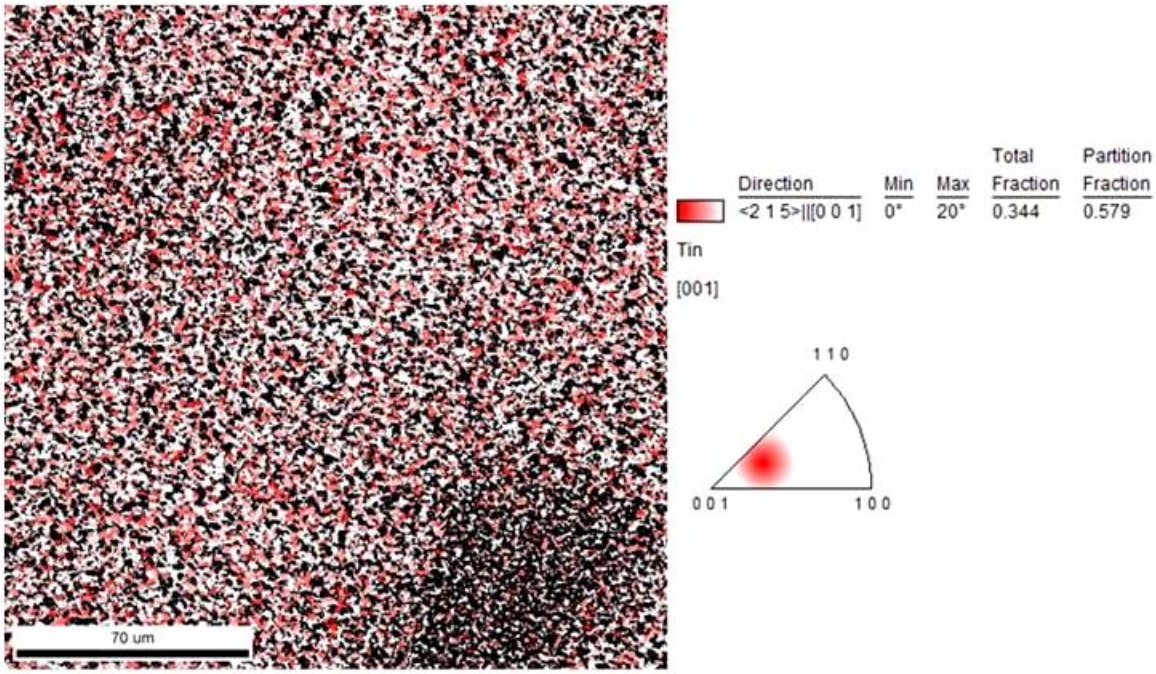

b) Sn with 0.95% Co, Sample 171, 12 months at 50% RH / 50°C

Electroplated Sn with 0.95% Co

Confidence Index (CI) Chart

Data points with a CI above 0.1 are generally considered to be indexed correctly.

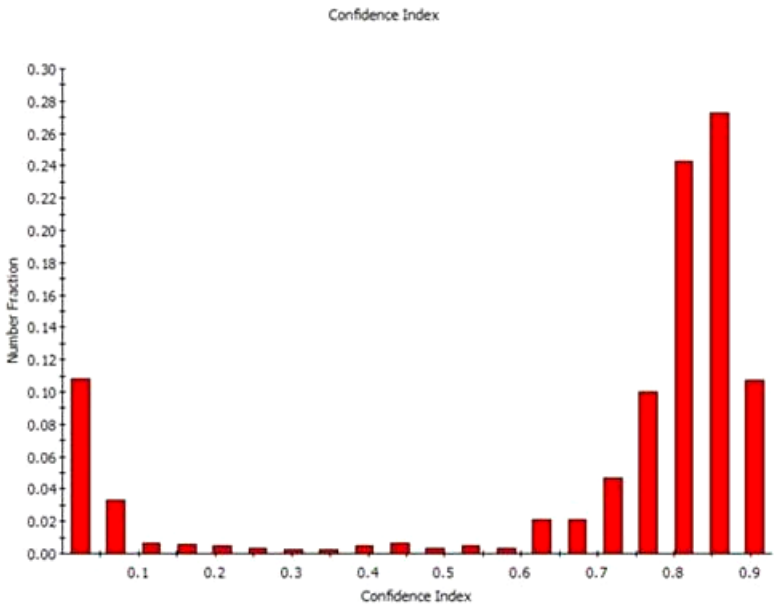

CI	Number Fraction
0.023225	0.108057
0.069675	0.0330935
0.116125	0.00683015
0.162575	0.005804
0.209025	0.00452639
0.255475	0.0028851
0.301925	0.00278641
0.348375	0.00217532
0.394825	0.00457777
0.441275	0.00670036
0.487725	0.00323797
0.534175	0.00462779
0.580625	0.00341913
0.627075	0.0206419
0.673525	0.0208893
0.719975	0.0471526
0.766425	0.0997794
0.812875	0.24247
0.859325	0.272715
0.905775	0.10763
Average	
Number	0.686965
Standard Deviation	0.296591

(a) Sn with 0.95% Co, Sample 168, post plating. Indicates that about 14.1% of data points were not indexed with a high degree of confidence

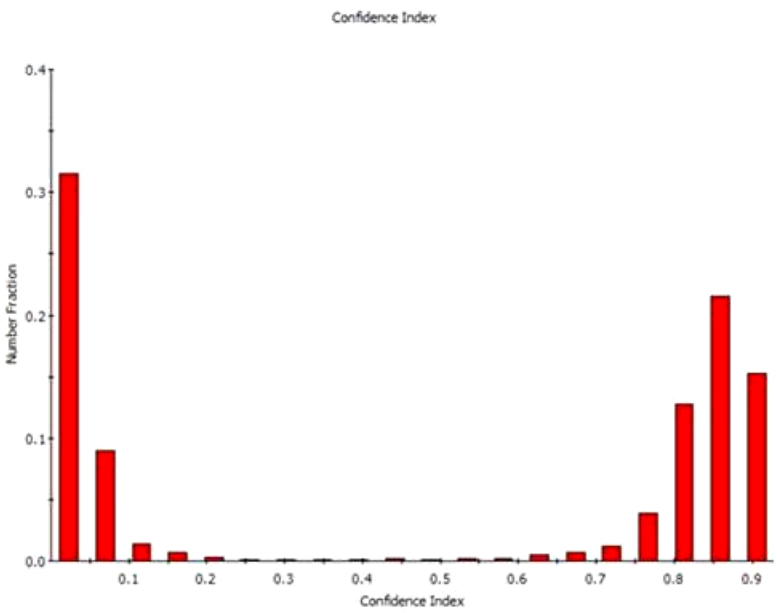

CI	Number Fraction
0.023225	0.315448
0.069675	0.0899168
0.116125	0.0139195
0.162575	0.00663896
0.209025	0.00284675
0.255475	0.00116104
0.301925	0.000977488
0.348375	0.000651082
0.394825	0.00145022
0.441275	0.00232987
0.487725	0.00149177
0.534175	0.00220519
0.580625	0.00154545
0.627075	0.00483636
0.673525	0.00727012
0.719975	0.0119991
0.766425	0.0387047
0.812875	0.128116
0.859325	0.215873
0.905775	0.152618
Average	
Number	0.494531
Standard Deviation	0.405934

(b) Sn with 0.95% Co, Sample 171, 12 months at 50% RH / 50°C. Indicates that about 40.4% of data points were not indexed with a high degree of confidence

Electroplated Sn with 0.95% Co
Pole Figure and Inverse Pole Figure Plots

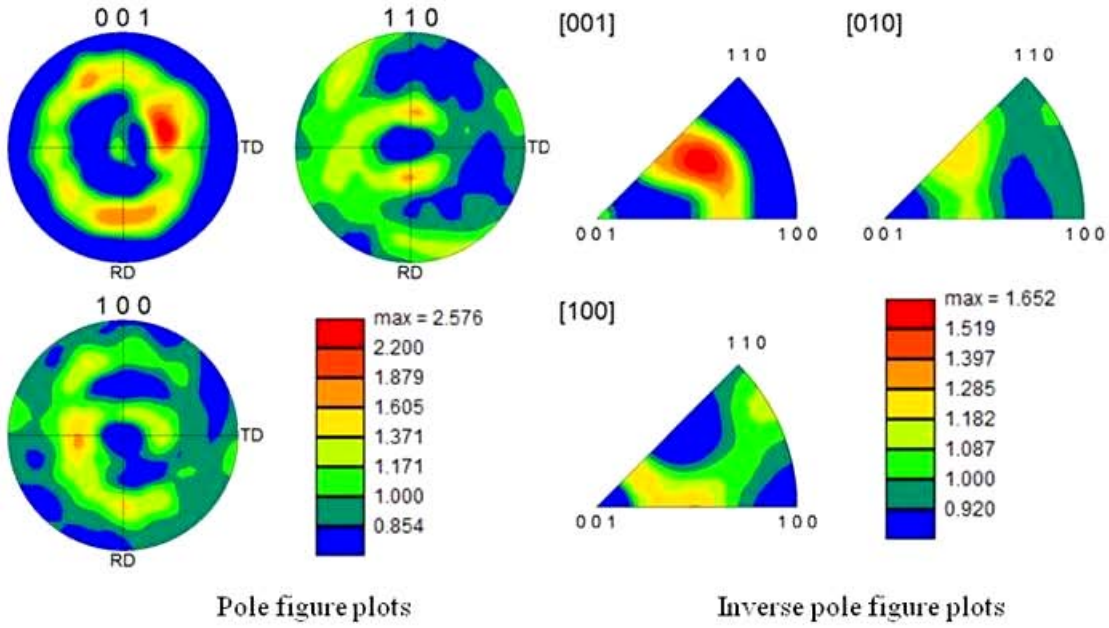

a) Sn with 0.95% Co, Sample 168, post plating

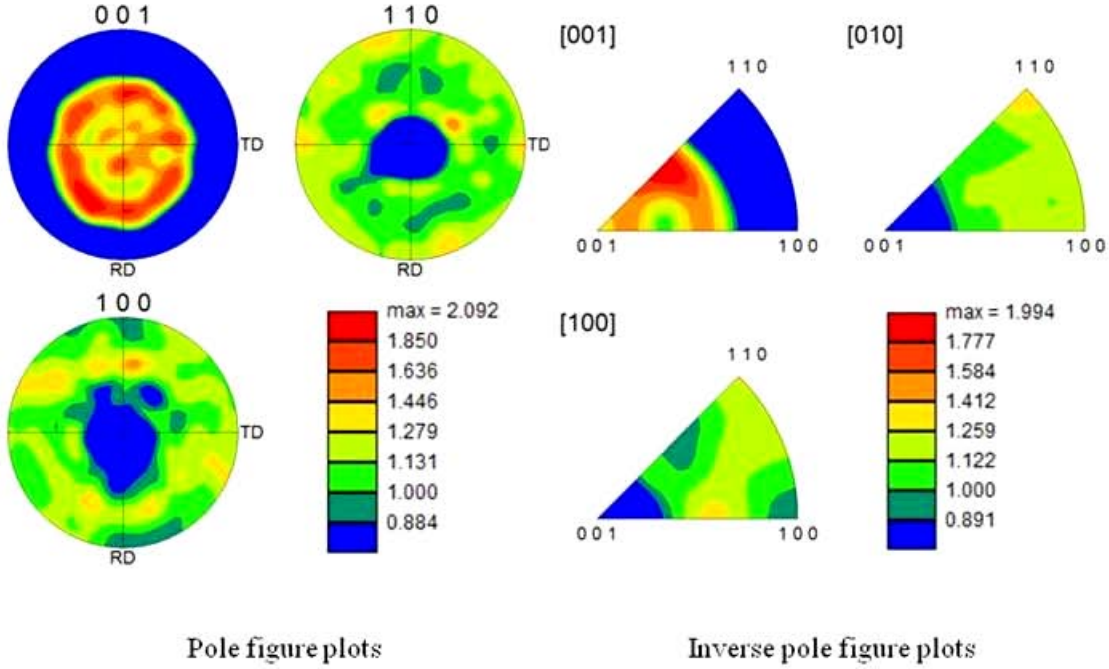

b) Sn with 0.95% Co, Sample 171, 12 months at 50% RH / 50°C

Electroplated Sn with 0.95% Co
Grain Size Histogram and Data

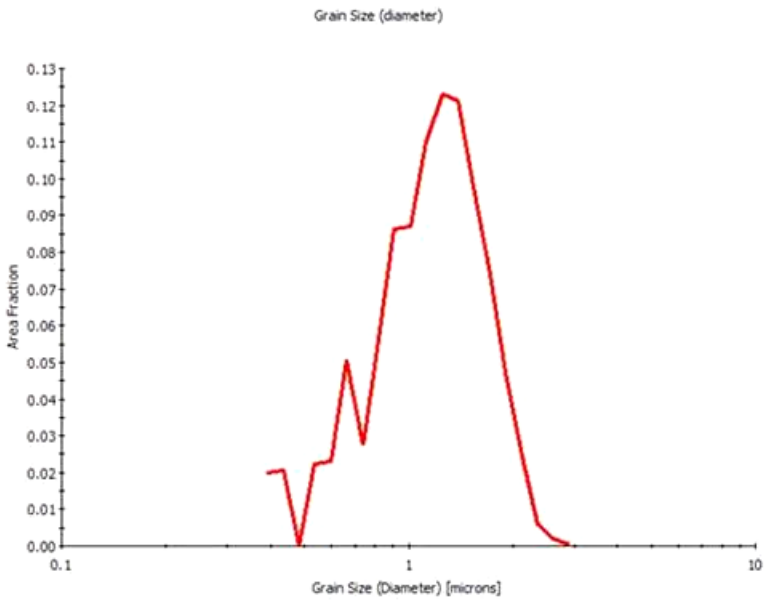

Edge grains included in analysis

Diameter [microns]	Area Fraction
0.391365	0.0198915
0.434905	0.0205702
0.483289	0
0.537056	0.0224807
0.596805	0.0230788
0.663201	0.0505381
0.736984	0.0273947
0.818975	0.0560889
0.910088	0.0864453
1.01134	0.0870241
1.12385	0.110019
1.24888	0.123134
1.38782	0.121432
1.54222	0.097784
1.7138	0.0739136
1.90446	0.0472411
2.11634	0.0243912
2.35179	0.00607966
2.61343	0.00208137
2.90418	0.000411115

a) Sn with 0.95% Co, Sample 168, post plating

Average	
Number	0.850216
Standard Deviation	0.388534
Area	1.19698

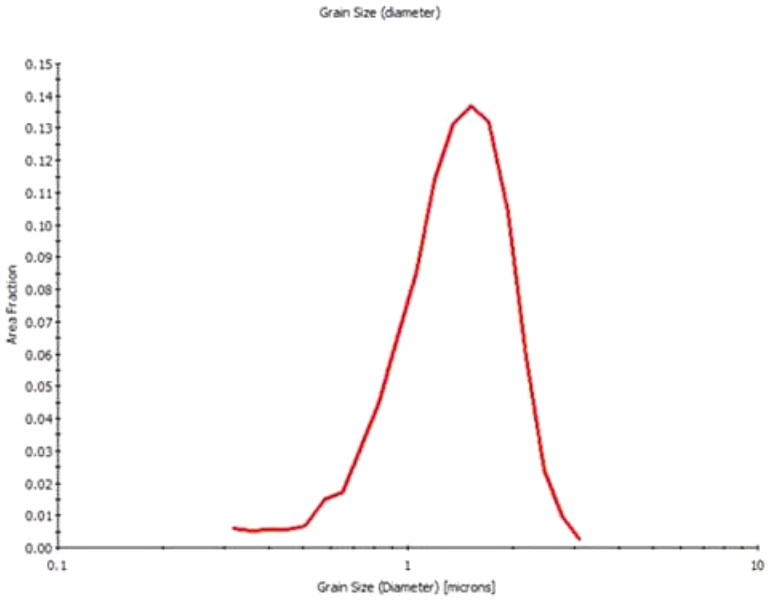

Edge grains included in analysis

Diameter [microns]	Area Fraction
0.315468	0.00597854
0.355905	0.00509792
0.401526	0.00546799
0.452994	0.00558883
0.51106	0.00681535
0.576569	0.0148874
0.650475	0.0172272
0.733854	0.0311192
0.827921	0.0450384
0.934046	0.0646038
1.05377	0.0851073
1.18885	0.113775
1.34124	0.130954
1.51316	0.137021
1.70712	0.132182
1.92594	0.104073
2.17281	0.0592355
2.45133	0.0238794
2.76555	0.00973665
3.12004	0.00221136

b) Sn with 0.95% Co, Sample 171, 12 months at 50% RH / 50°

Average	
Number	0.970436
Standard Deviation	0.480971
Area	1.40817

Electroplated Sn with 0.95% Co
Misorientation Angle Histogram, 2º minimum misorientation

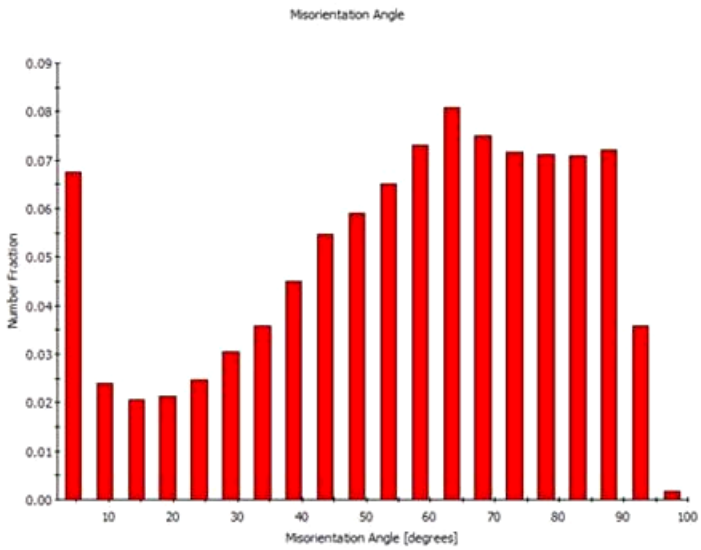

Angle [degrees]	Number Fraction
4.45	0.0673899
9.35	0.0238359
14.25	0.0204991
19.15	0.0213367
24.05	0.0247555
28.95	0.0304255
33.85	0.0357948
38.75	0.0450652
43.65	0.0547202
48.55	0.0590996
53.45	0.0650293
58.35	0.073138
63.25	0.0807409
68.15	0.0749518
73.05	0.0716287
77.95	0.0710176
82.85	0.0709649
87.75	0.0720387
92.65	0.0358573
97.55	0.00171037

a) Sn with 0.95% Co, Sample 168, post plating

Average Number	55.2554

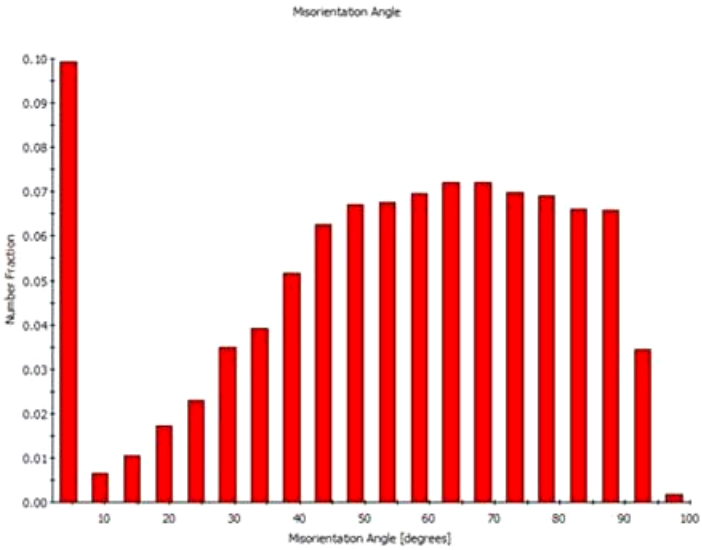

Angle [degrees]	Number Fraction
4.45	0.0991479
9.35	0.00656475
14.25	0.0103732
19.15	0.0172887
24.05	0.0230365
28.95	0.0348497
33.85	0.0391533
38.75	0.0515566
43.65	0.062524
48.55	0.0671618
53.45	0.0674713
58.35	0.0695344
63.25	0.0720555
68.15	0.0721792
73.05	0.069947
77.95	0.0691754
82.85	0.0660725
87.75	0.0658249
92.65	0.0343917
97.55	0.00169173

b) Sn with 0.95% Co, Sample 171, 12 months at 50% RH / 50°C

Average Number	53.9281

Electroplated Sn with 0.95% Co
Misorientation Angle Histogram, 2º minimum misorientation

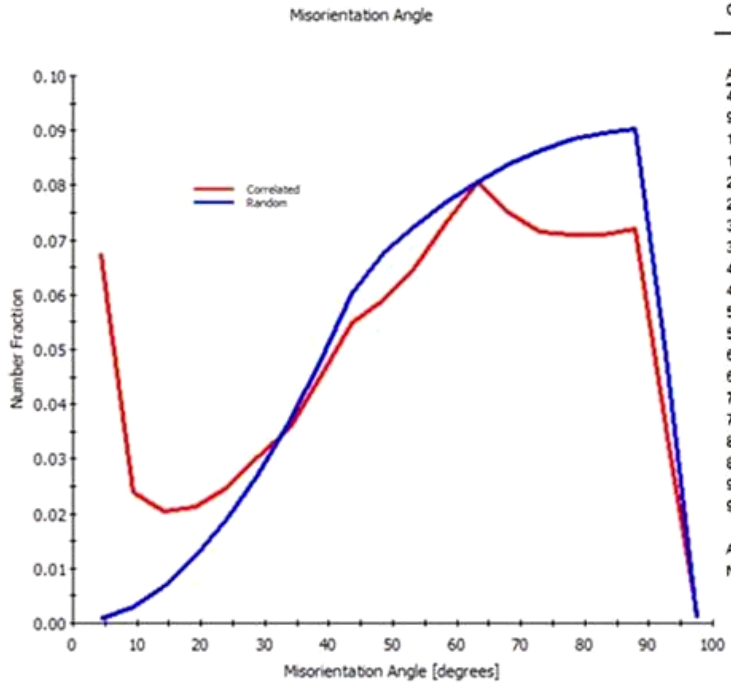

Chart: Misorientation Angle

Angle [degrees]	Correlated Number Fraction	Random Number Fraction
4.45	0.0673899	0.000707903
9.35	0.0238359	0.00294632
14.25	0.0204991	0.00675655
19.15	0.0213367	0.0121107
24.05	0.0247555	0.0189697
28.95	0.0304255	0.0272834
33.85	0.0357948	0.036991
38.75	0.0450652	0.0480215
43.65	0.0547202	0.0602944
48.55	0.0590996	0.0677121
53.45	0.0650293	0.0725691
58.35	0.073138	0.0768959
63.25	0.0807409	0.0806611
68.15	0.0749518	0.0838371
73.05	0.0716287	0.0864006
77.95	0.0710176	0.0883329
82.85	0.0709649	0.08962
87.75	0.0720387	0.0902524
92.65	0.0358573	0.0489887
97.55	0.00171037	0.000672329
Average Number	55.2554	63.0123

a) Sn with 0.95% Co, Sample 168, post plating

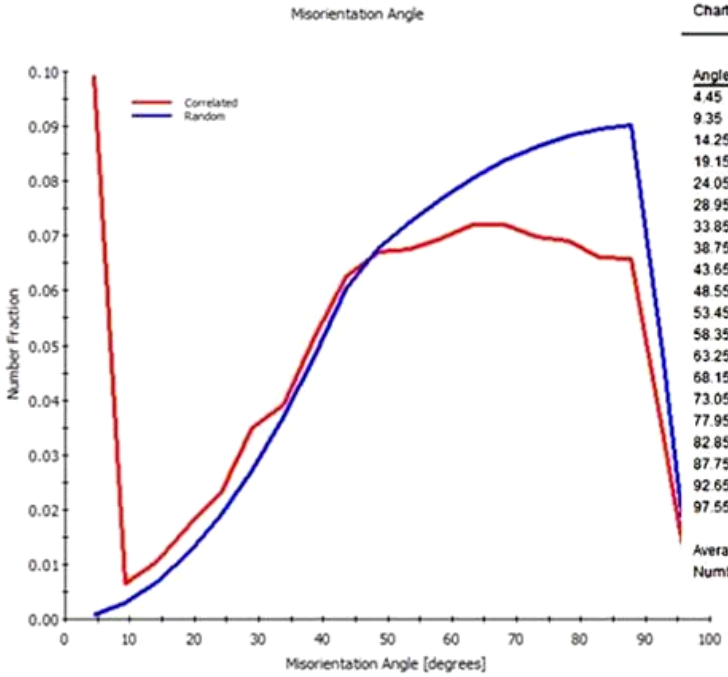

Chart: Misorientation Angle

Angle [degrees]	Correlated Number Fraction	Random Number Fraction
4.45	0.0991479	0.000708984
9.35	0.00656475	0.00294739
14.25	0.0103732	0.00675759
19.15	0.0172887	0.0121117
24.05	0.0230365	0.0189707
28.95	0.0348497	0.0272843
33.85	0.0391533	0.0369918
38.75	0.0515566	0.0480223
43.65	0.062524	0.0602951
48.55	0.0671618	0.0677128
53.45	0.0674713	0.0725696
58.35	0.0695344	0.0768965
63.25	0.0720555	0.0806616
68.15	0.0721792	0.0838376
73.05	0.069947	0.0864011
77.95	0.0691754	0.0883334
82.85	0.0660725	0.0896205
87.75	0.0658249	0.0902529
92.65	0.0343917	0.0489895
97.55	0.00169173	0.00067341
Average Number	53.9281	63.0123

b) Sn with 0.95% Co, Sample 171, 12 months at 50% RH / 50°C

Electroplated Sn with 0.95% Co
Grain Boundary Characterization Chart

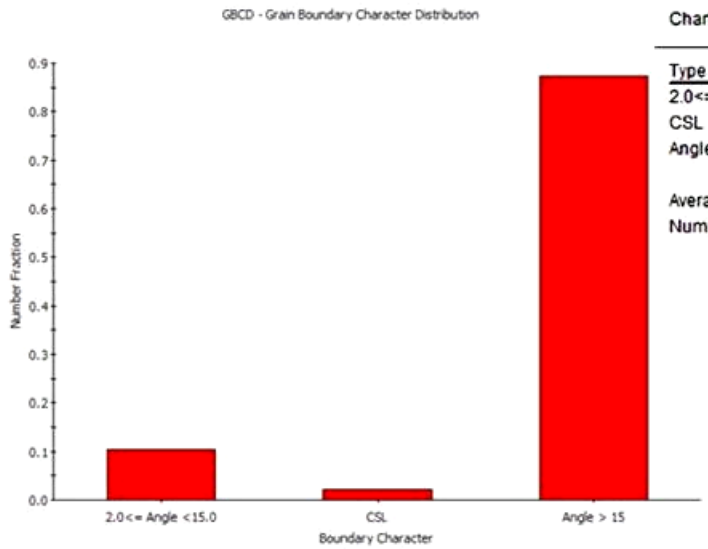

Chart: GBCD - Grain Boundary Character Distribution

Type	Number Fraction
2.0<= Angle <15.0	0.104272
CSL	0.0225023
Angle > 15	0.873225
Average Number	0.333333

a) Sn with 0.95% Co, Sample 168, post plating

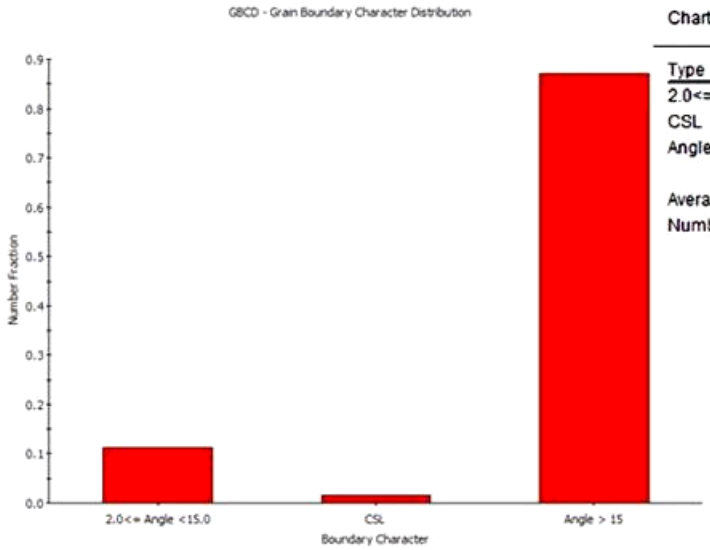

Chart: GBCD - Grain Boundary Character Distribution

Type	Number Fraction
2.0<= Angle <15.0	0.111984
CSL	0.0166037
Angle > 15	0.871412
Average Number	0.333333

b) Sn with 0.95% Co, Sample 171, 12 months at 50% RH / 50°C

Electroplated Sn with 0.95% Co

Coincident Site Lattice Boundary Chart

The total fraction of CSL boundaries is approximately 2% of boundaries measured

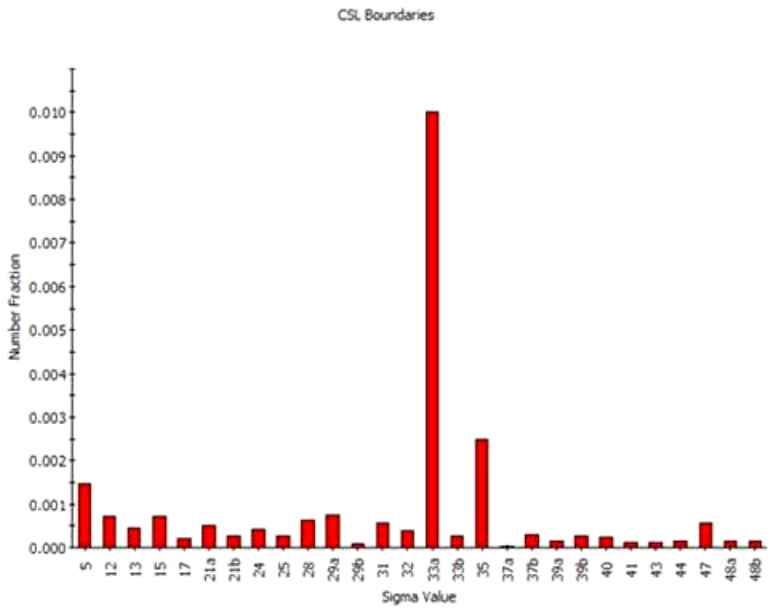

Overall fraction of CSL boundaries: 0.023

Sigma	Number Fraction
5	0.00148193
12	0.000712655
13	0.000439308
15	0.000722418
17	0.000203058
21a	0.00051936
21b	0.00026749
24	0.000417831
25	0.00025968
28	0.000620889
29a	0.000743895
29b	9.7624e-005
31	0.000574029
32	0.000392449
33a	0.0100162
33b	0.0002753
35	0.00248941
37a	1.75723e-005
37b	0.000308492
39a	0.000150341
39b	0.0002753
40	0.000234298
41	0.000134721
43	0.000128864
44	0.000140579
47	0.000554504
48a	0.000160103
48b	0.000164008

a) Sn with 0.95% Co, Sample 168, post plating

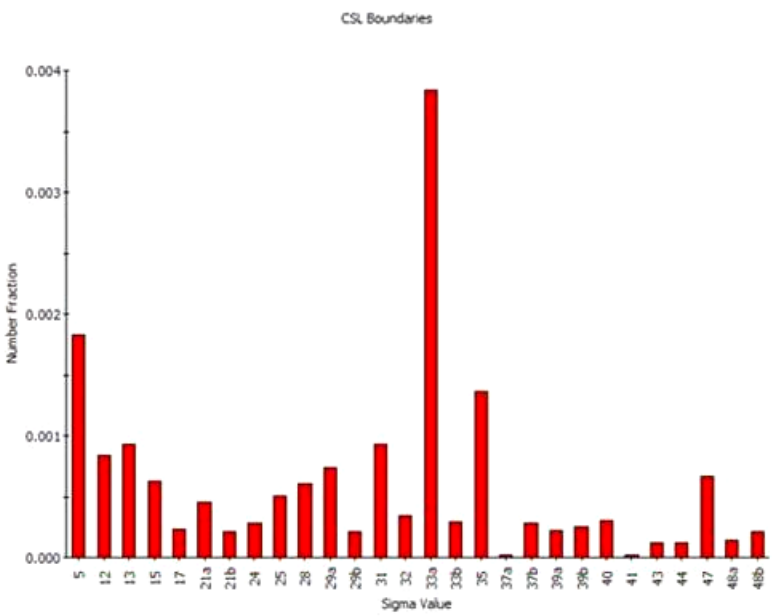

Overall fraction of CSL boundaries: 0.017

Sigma	Number Fraction
5	0.00183202
12	0.00084174
13	0.000924264
15	0.000627179
17	0.000231066
21a	0.00045388
21b	0.000210435
24	0.00028058
25	0.00050752
28	0.000606548
29a	0.000738586
29b	0.000214561
31	0.00092839
32	0.000342473
33a	0.00384147
33b	0.000297085
35	0.00136577
37a	1.65047e-005
37b	0.000284706
39a	0.000222814
39b	0.000251697
40	0.000305337
41	2.47571e-005
43	0.000119659
44	0.000119659
47	0.000664315
48a	0.00014029
48b	0.000210435

b) Sn with 0.95% Co, Sample 171, 12 months at 50% RH / 50°C

Electroplated Sn with 0.95% Co
Misorientation Distribution Function (MODF) Plot

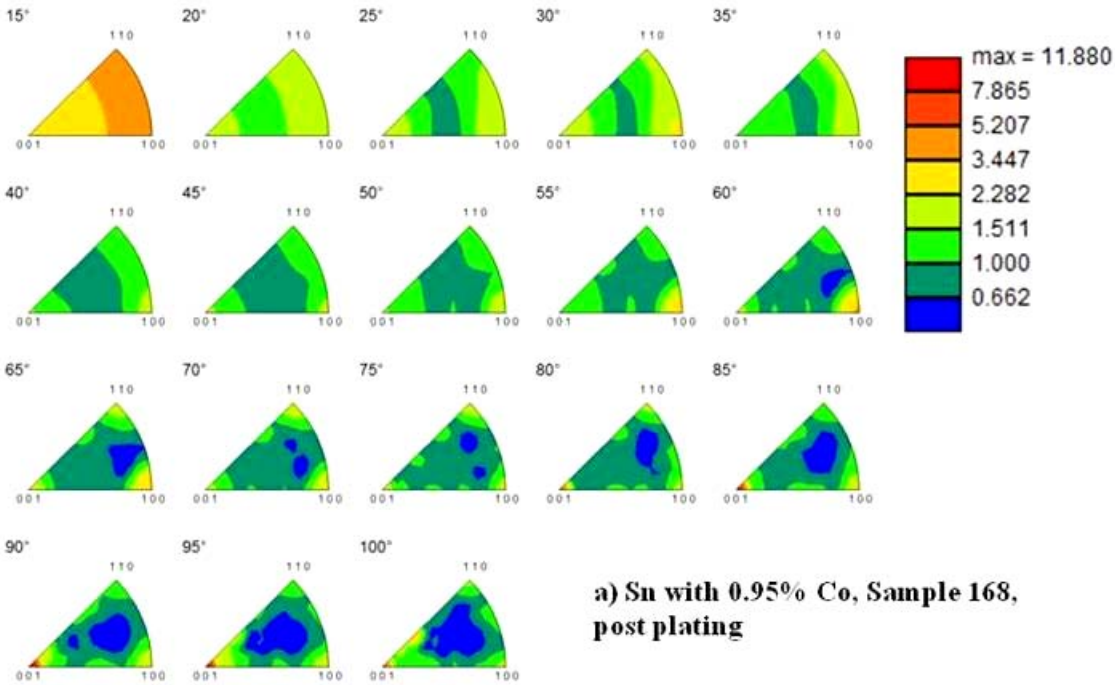

a) Sn with 0.95% Co, Sample 168, post plating

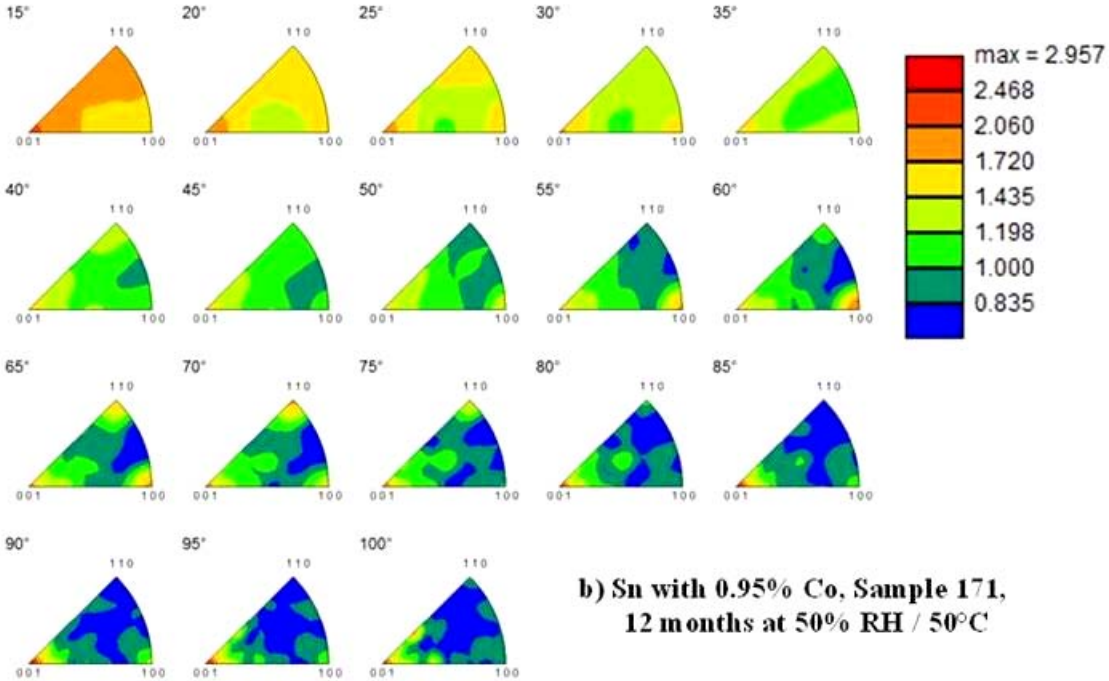

b) Sn with 0.95% Co, Sample 171, 12 months at 50% RH / 50°C

Electroplated Sn with 0.95% Co

Crystal Direction Map

Blue Indicates C-Direction in sample normal

Red indicates C-direction in sample plane 15º tolerance

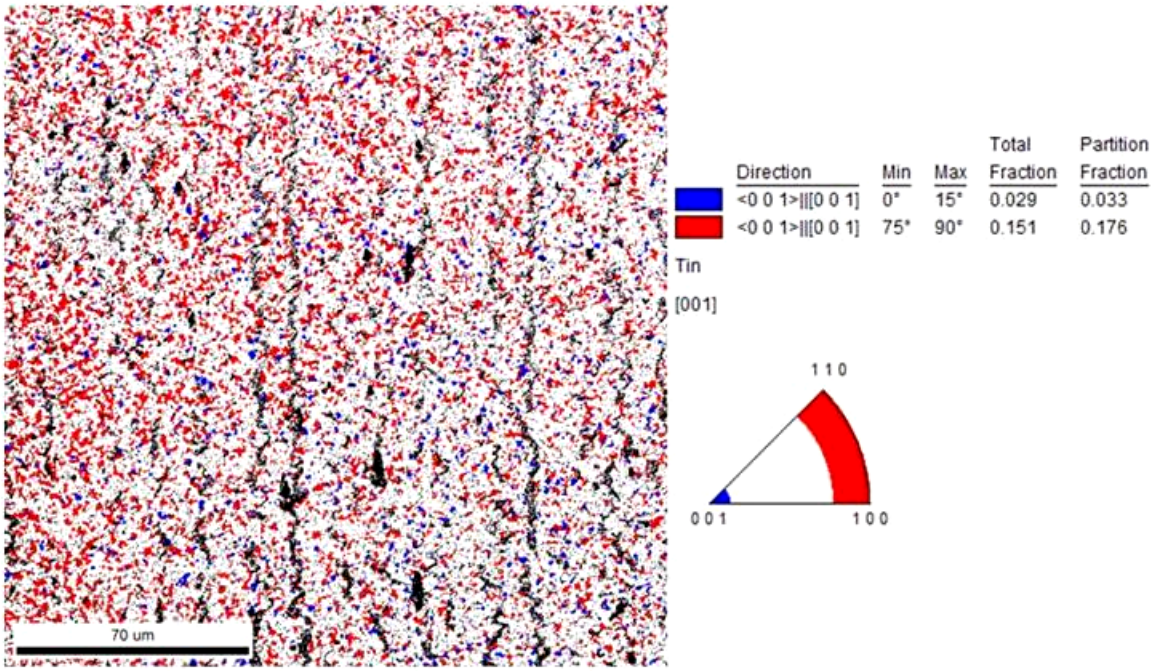

a) Sn with 0.95% Co, Sample 168, post plating

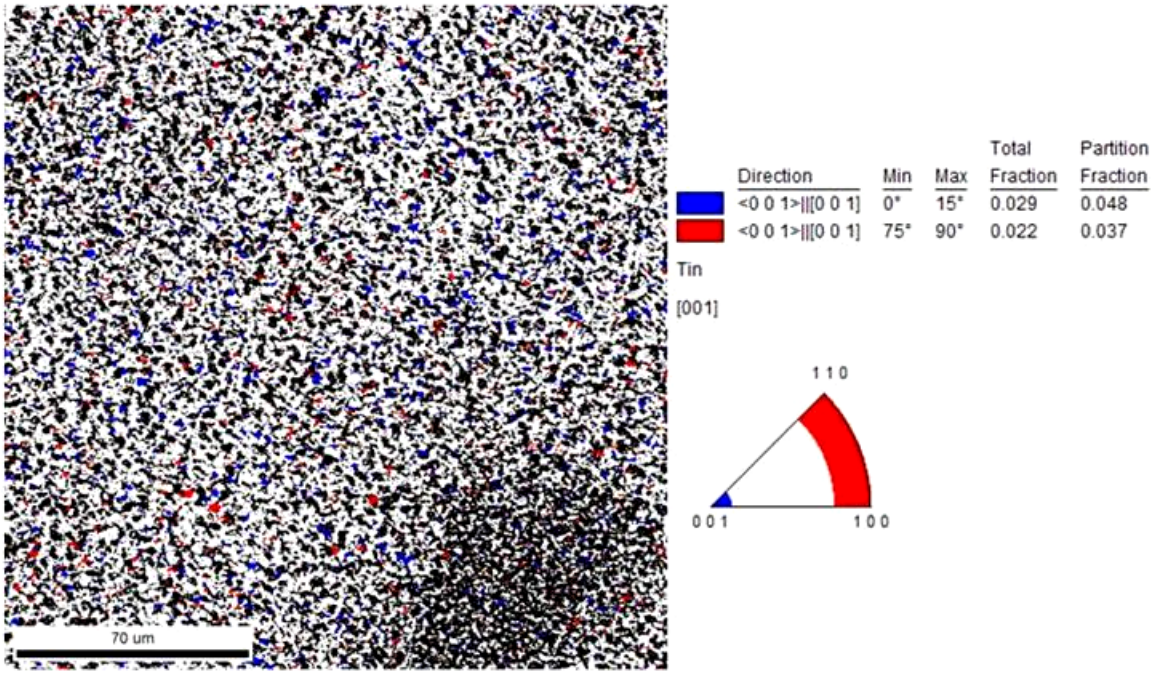

b) Sn with 0.95% Co, Sample 171, 12 months at 50% RH / 50°C

Appendix O: EBSD Data for Sn with 2.4% Sb

Electroplated Sn with 2.4% Sb
Image Quality Map

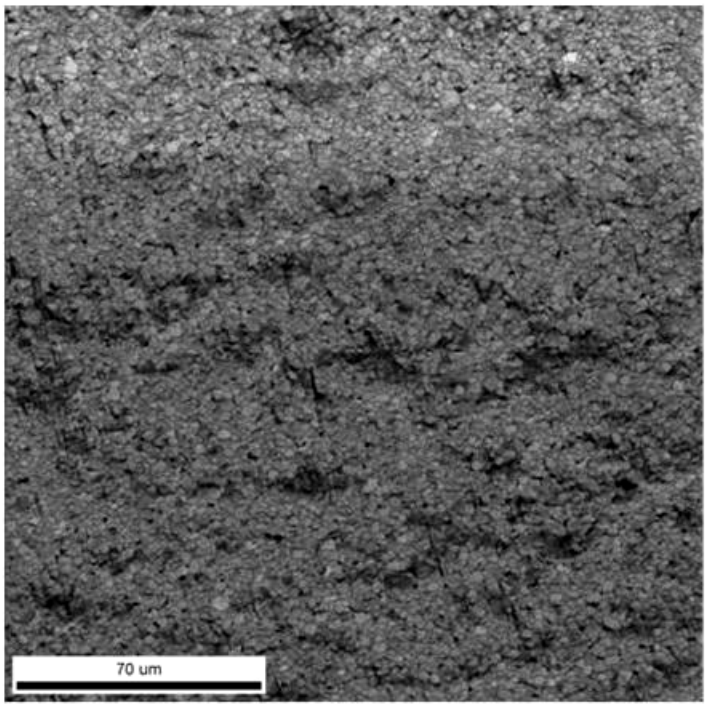

X = 200 microns
Y = 200 microns
Step size = 0.25 microns

a) Sn with 2.4% Sb, Sample 217, post plating

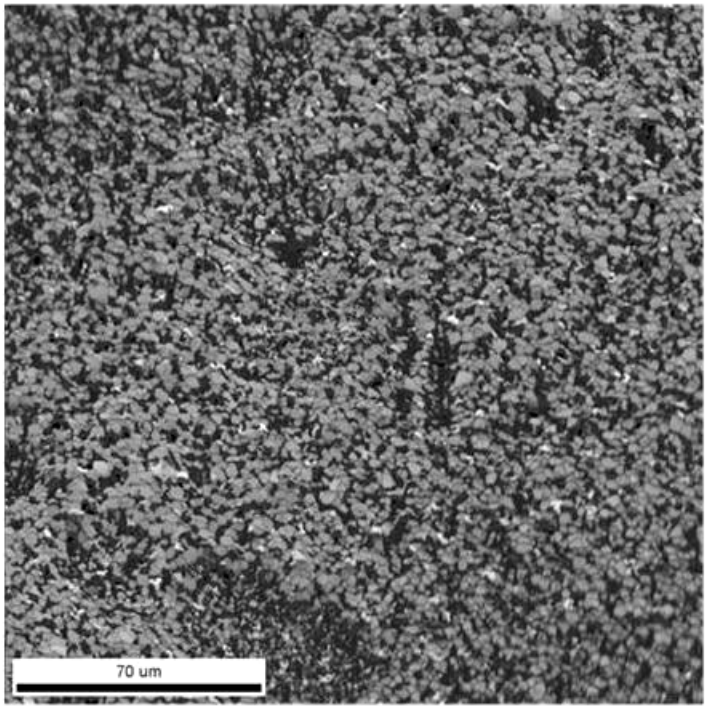

X = 200 microns
Y = 200 microns
Step size = 0.2 microns

b) Sn with 2.4% Sb, Sample 216, 18 months at 50% RH / 50°C

Electroplated Sn with 2.4% Sb
Color Coded Orientation Map

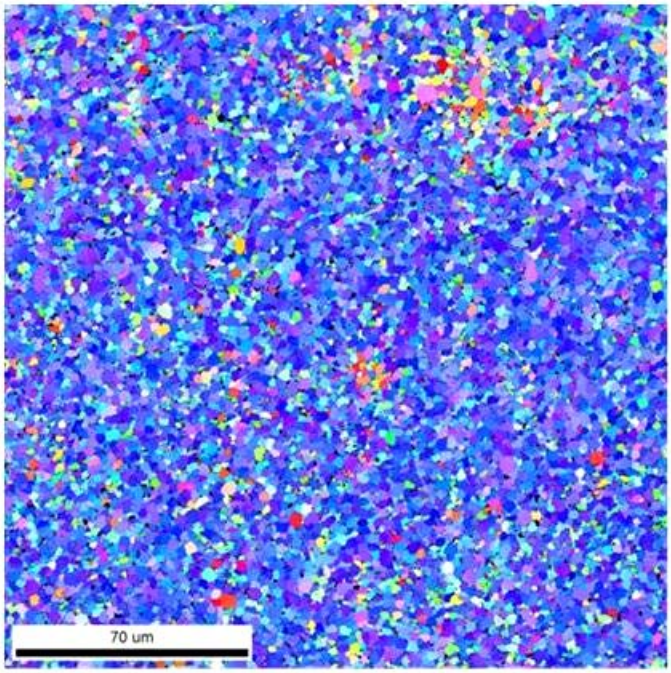

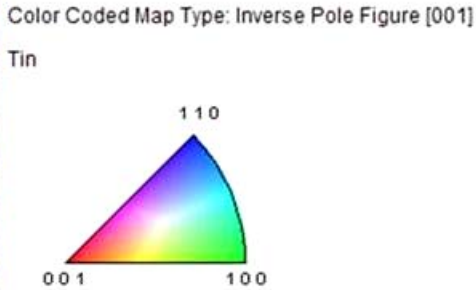

a) Sn with 2.4% Sb, Sample 217, post plating

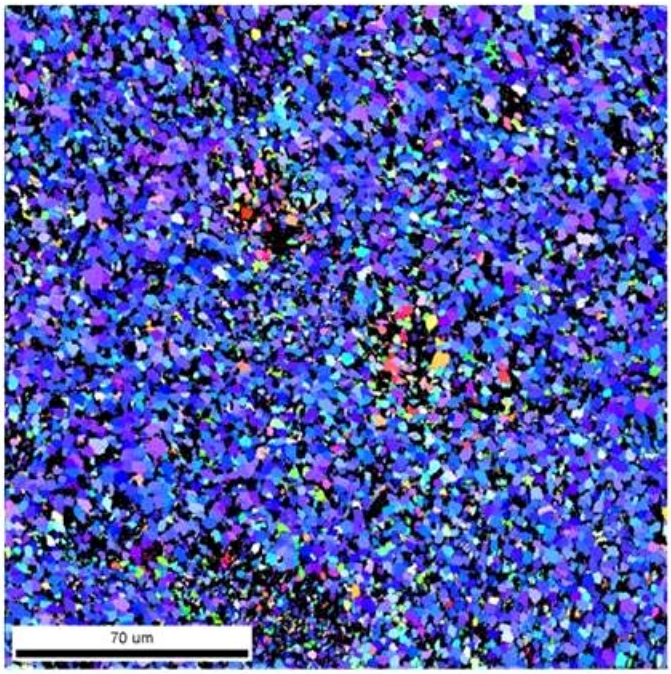

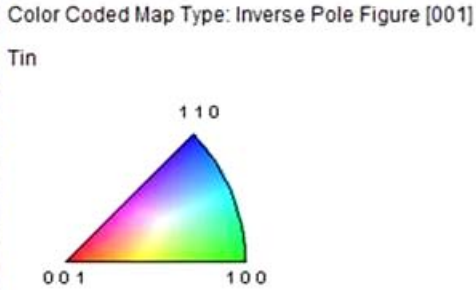

b) Sn with 2.4% Sb, Sample 216, 18 months at 50% RH / 50°C

Electroplated Sn with 2.4% Sb
Crystal Direction Map Showing <111> crystal direction in ND direction 15º Tolerance

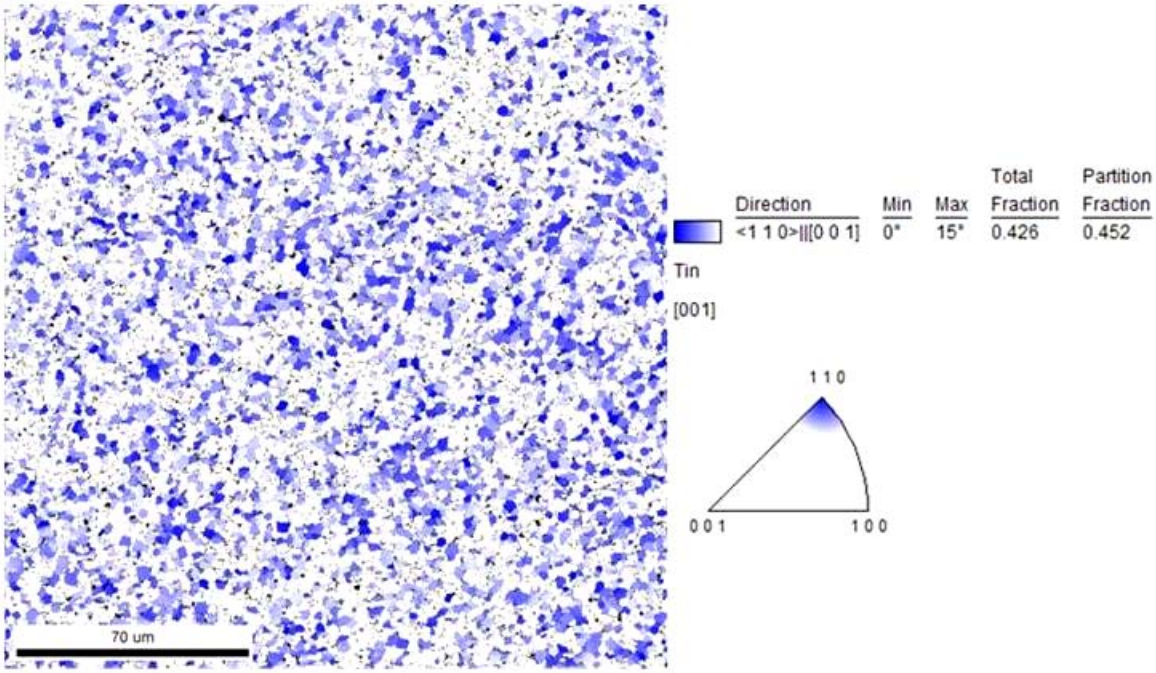

a) Sn with 2.4% Sb, Sample 217, post plating

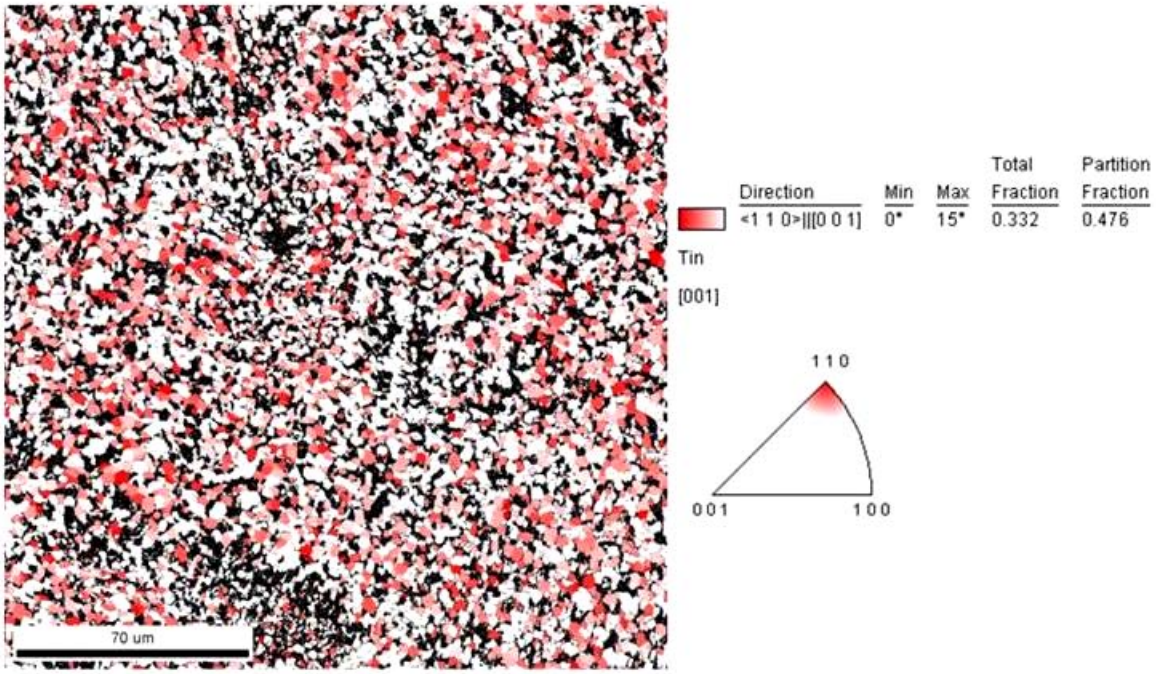

b) Sn with 2.4% Sb, Sample 216, 18 months at 50% RH / 50°C

Electroplated Sn with 2.4% Sb
Crystal Direction Map Showing <111> crystal direction in ND direction 20º Tolerance

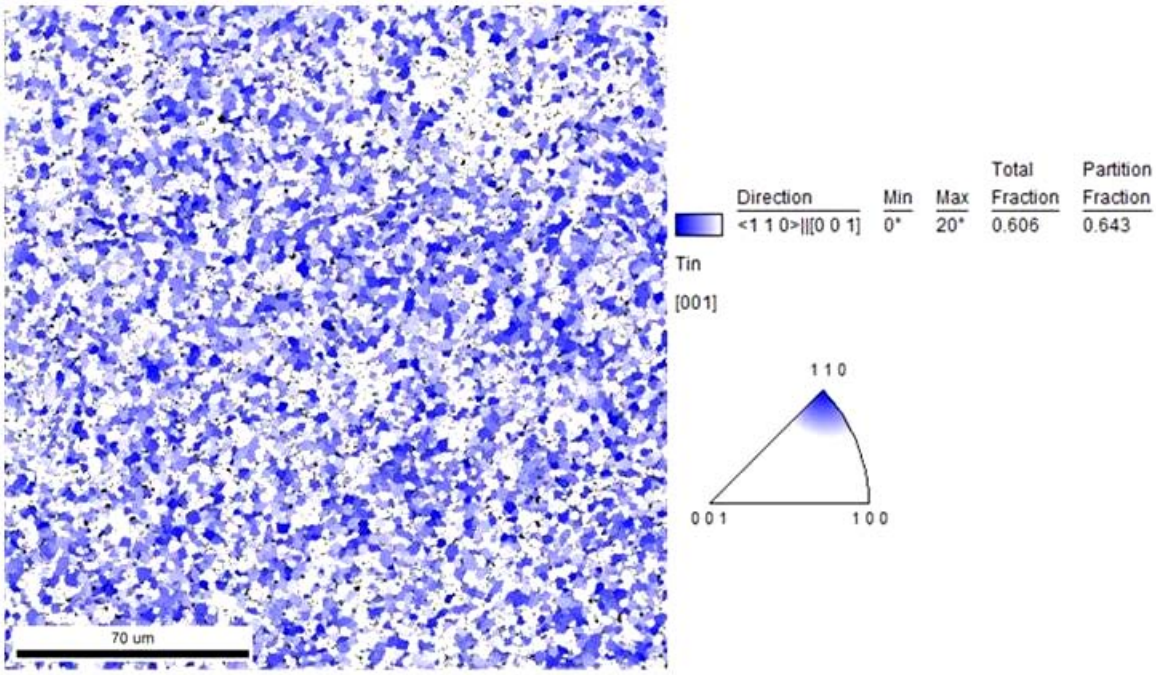

a) Sn with 2.4% Sb, Sample 217, post plating

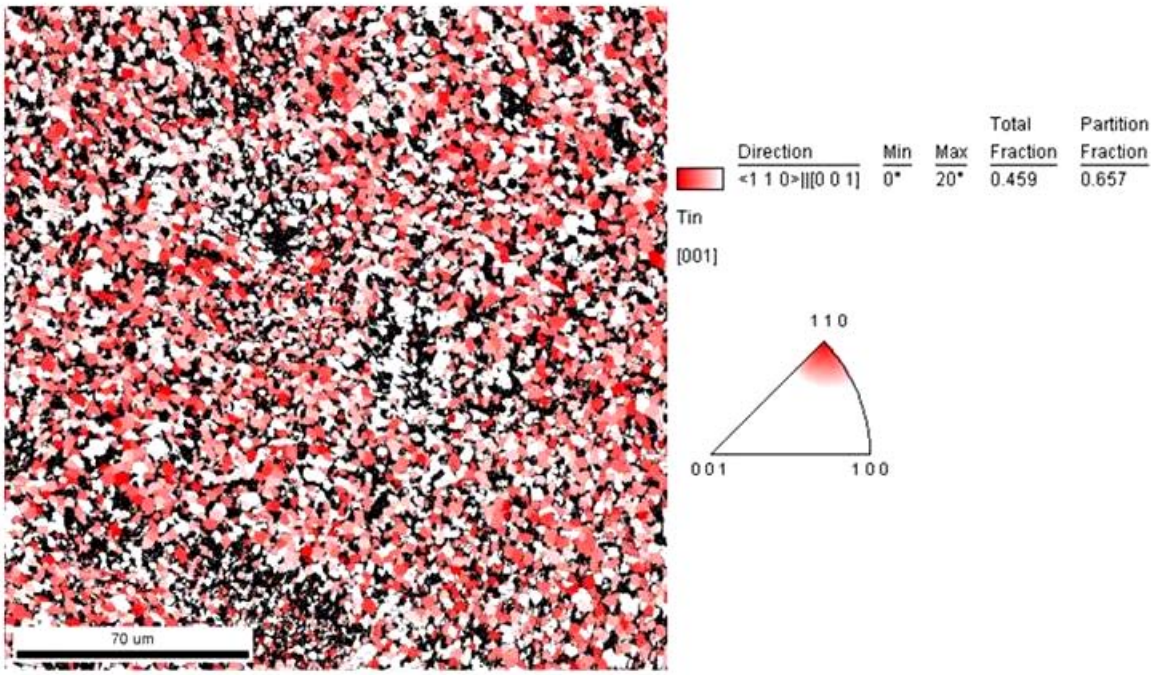

b) Sn with 2.4% Sb, Sample 216, 18 months at 50% RH / 50°C

Electroplated Sn with 2.4% Sb

Confidence Index (CI) Chart

Data points with a CI above 0.1 are generally considered to be indexed correctly.

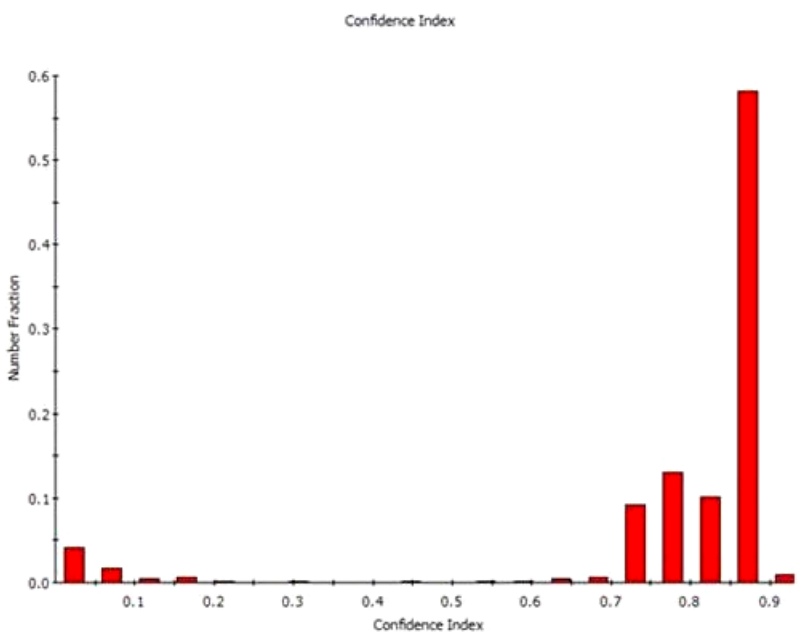

CI	Number Fraction
0.023575	0.0412499
0.070725	0.0167117
0.117875	0.00403157
0.165025	0.0056323
0.212175	0.00149528
0.259325	0.000562419
0.306475	0.000935562
0.353625	0.000623258
0.400775	0.000335288
0.447925	0.000819293
0.495075	0.00036368
0.542225	0.000811181
0.589375	0.00128572
0.636525	0.00434658
0.683675	0.00677336
0.730825	0.0914161
0.777975	0.130529
0.825125	0.101212
0.872275	0.581499
0.919425	0.00936644
Average	
Number	0.782604
Standard Deviation	0.213664

a) Sn with 2.4% Sb, Sample 217, post plating. Indicates that about 5.8% of data points were not indexed with a high degree of confidence

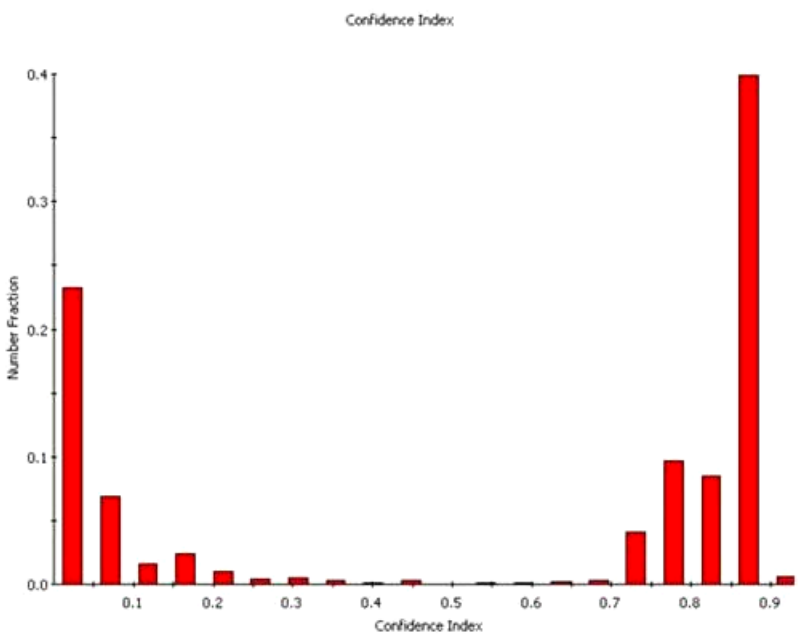

CI	Number Fraction
0.023575	0.232183
0.070725	0.068744
0.117875	0.0155968
0.165025	0.0237503
0.212175	0.00974066
0.259325	0.00355024
0.306475	0.00514785
0.353625	0.00311036
0.400775	0.00107633
0.447925	0.00320648
0.495075	0.000389661
0.542225	0.000917002
0.589375	0.00108586
0.636525	0.00247738
0.683675	0.00278391
0.730825	0.0405611
0.777975	0.0965095
0.825125	0.0845521
0.872275	0.398628
0.919425	0.00598952
Average	
Number	0.554129
Standard Deviation	0.385468

(b) Sn with 2.4% Sb, Sample 216, 18 months at 50% RH / 50°C. Indicates that about 30% of data points were not indexed with a high degree of confidence

Electroplated Sn with 2.4% Sb
Pole Figure and Inverse Pole Figure Plots

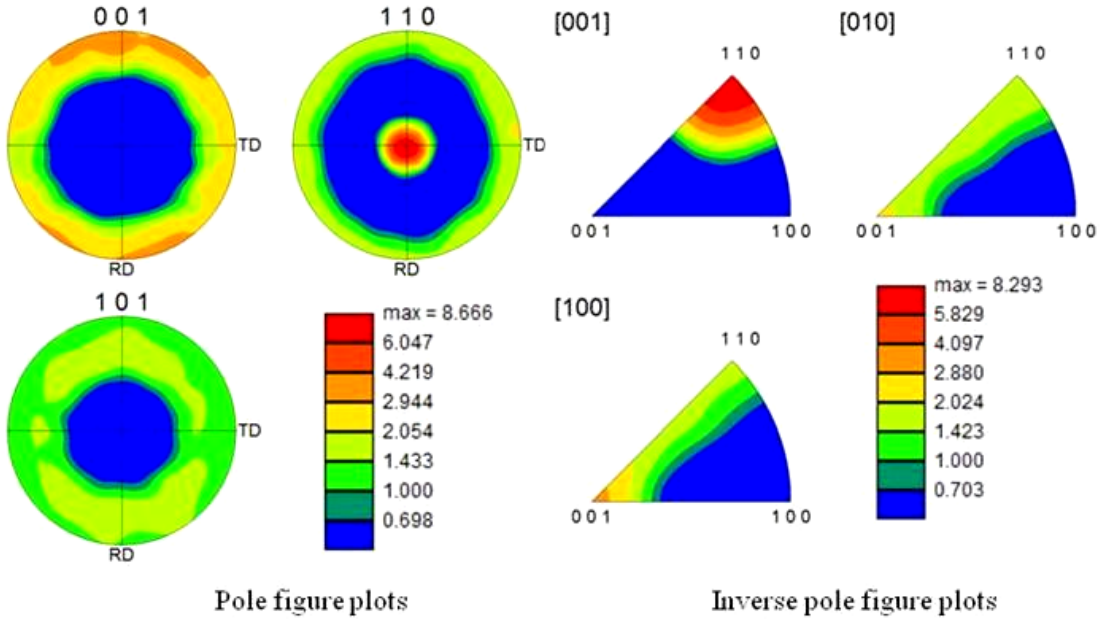

a) Sn with 2.4% Sb, Sample 217, post plating

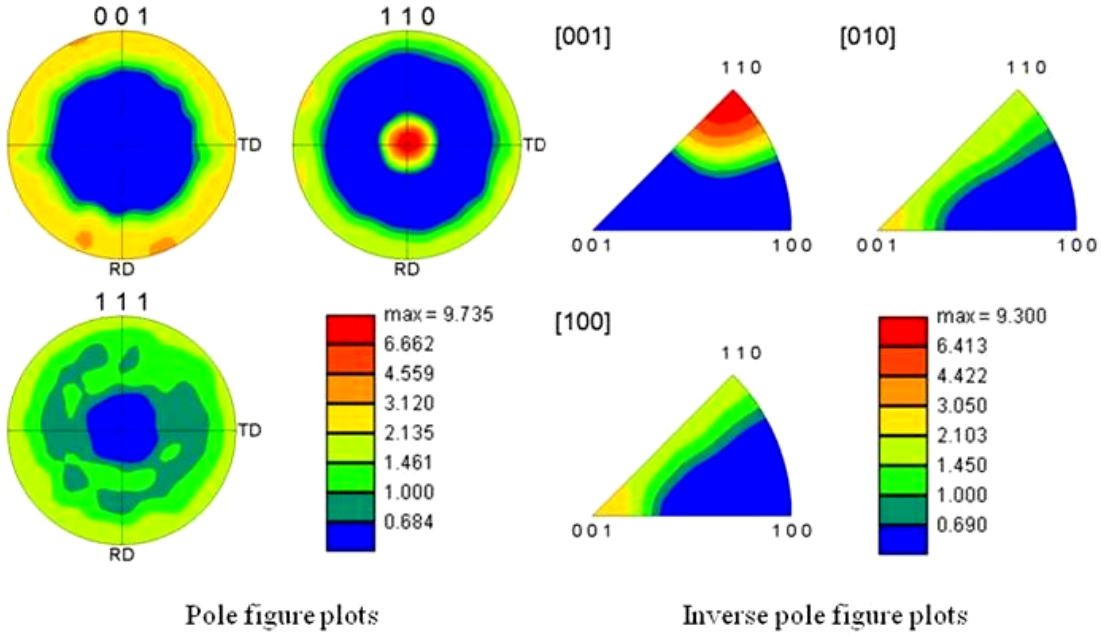

b) Sn with 2.4% Sb, Sample 216, 18 months at 50% RH / 50°C

Electroplated Sn with 2.4% Sb
Grain Size Histogram and Data

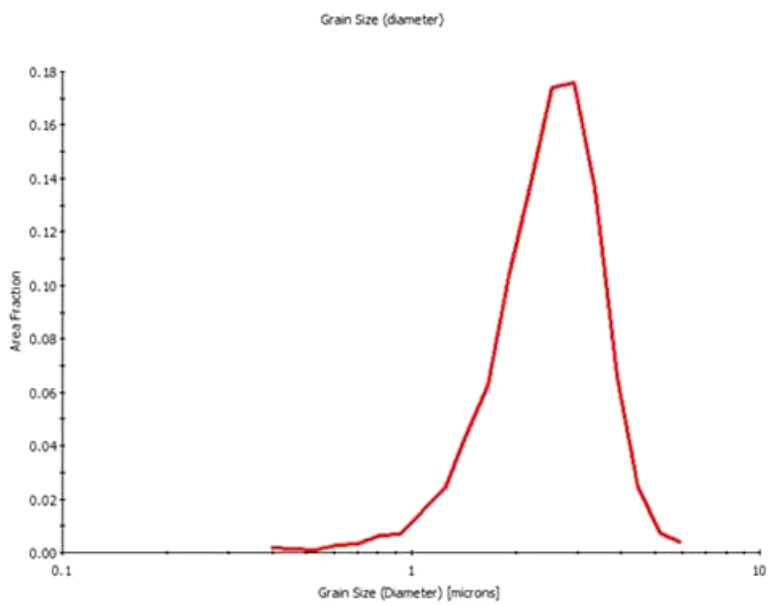

a) Sn with 2.4% Sb, Sample 217, post plating

Edge grains included in analysis

Diameter [microns]	Area Fraction
0.39866	0.00200276
0.459683	0.00116514
0.530046	0.000997032
0.61118	0.00276068
0.704733	0.00339252
0.812606	0.00642129
0.936991	0.00688793
1.08042	0.0158148
1.24579	0.0237143
1.43649	0.0439361
1.65637	0.0624015
1.90991	0.103542
2.20226	0.138635
2.53935	0.174213
2.92805	0.176056
3.37625	0.136435
3.89305	0.0658302
4.48895	0.0244983
5.17607	0.00753571
5.96837	0.00376061

Average	
Number	1.78818
Standard Deviation	0.896904
Area	2.57631

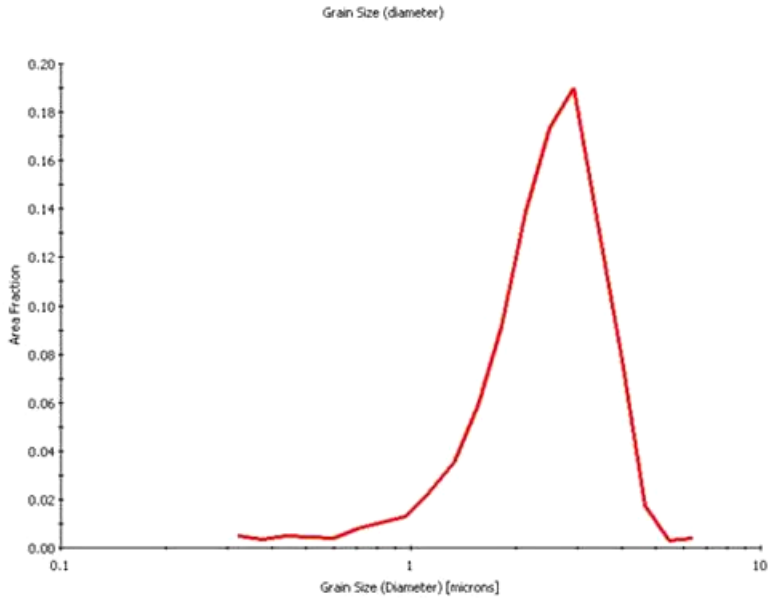

b) Sn with 2.4% Sb, Sample 216, 18 months at 50% RH / 50°C

Edge grains included in analysis

Diameter [microns]	Area Fraction
0.321355	0.00519867
0.376205	0.0032595
0.440418	0.00497517
0.51559	0.00426849
0.603593	0.00418322
0.706617	0.00787552
0.827225	0.0102384
0.968419	0.0129967
1.13371	0.0234392
1.32722	0.0354308
1.55376	0.0591452
1.81896	0.0911886
2.12942	0.138502
2.49288	0.173387
2.91838	0.190054
3.4165	0.13391
3.99964	0.0776997
4.68232	0.0173001
5.48152	0.00318457
6.41713	0.00376335

Average	
Number	1.32859
Standard Deviation	0.978682
Area	2.53456

Electroplated Sn with 2.4% Sb
Misorientation Angle Histogram, 2º minimum misorientation

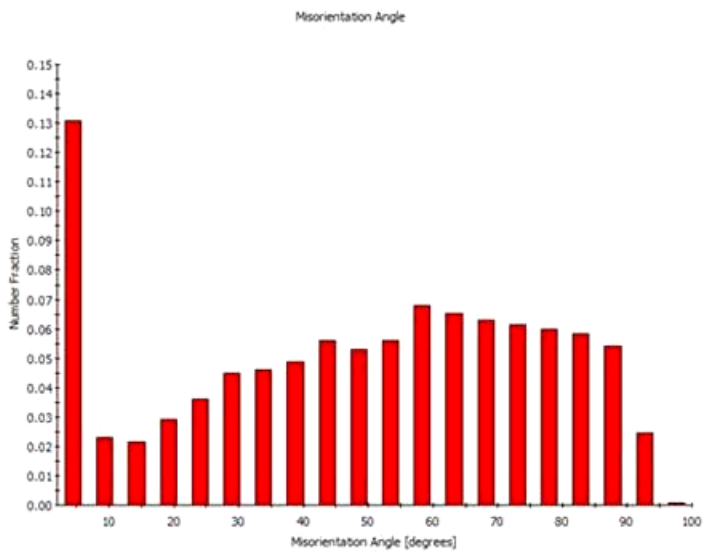

Angle [degrees]	Number Fraction
4.45	0.130681
9.35	0.0230069
14.25	0.0213625
19.15	0.0293127
24.05	0.0360153
28.95	0.0447091
33.85	0.0461604
38.75	0.0487378
43.65	0.0560123
48.55	0.0530811
53.45	0.0558515
58.35	0.0679269
63.25	0.0653102
68.15	0.0629723
73.05	0.0612493
77.95	0.0597086
82.85	0.058461
87.75	0.0541106
92.65	0.0245977
97.55	0.000732818
Average Number	48.5714

a) Sn with 2.4% Sb, Sample 217, post plating

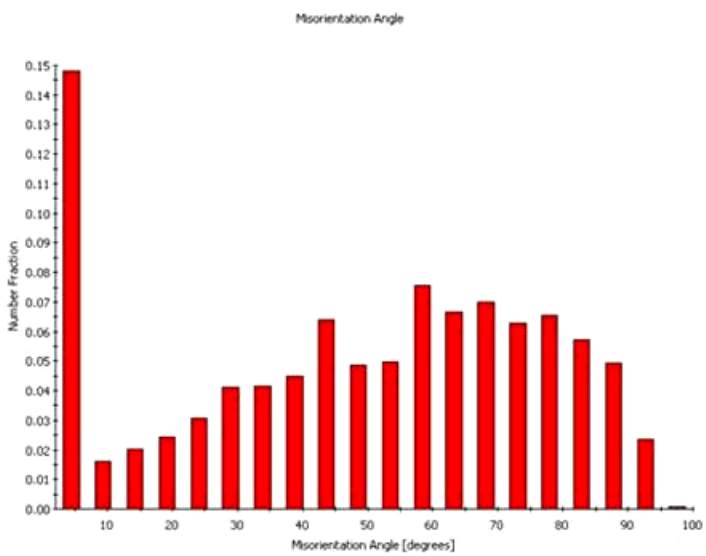

Angle [degrees]	Number Fraction
4.45	0.148017
9.35	0.0159675
14.25	0.0203585
19.15	0.0243789
24.05	0.030552
28.95	0.041178
33.85	0.0413681
38.75	0.0448419
43.65	0.0638413
48.55	0.0487483
53.45	0.049827
58.35	0.0754082
63.25	0.066455
68.15	0.0697768
73.05	0.0630192
77.95	0.0655996
82.85	0.0572215
87.75	0.0493185
92.65	0.0234855
97.55	0.000636797
Average Number	48.5697

b) Sn with 2.4% Sb, Sample 216, 18 months at 50% RH / 50°C

Electroplated Sn with 2.4% Sb
Misorientation Angle Histogram, 2º minimum misorientation

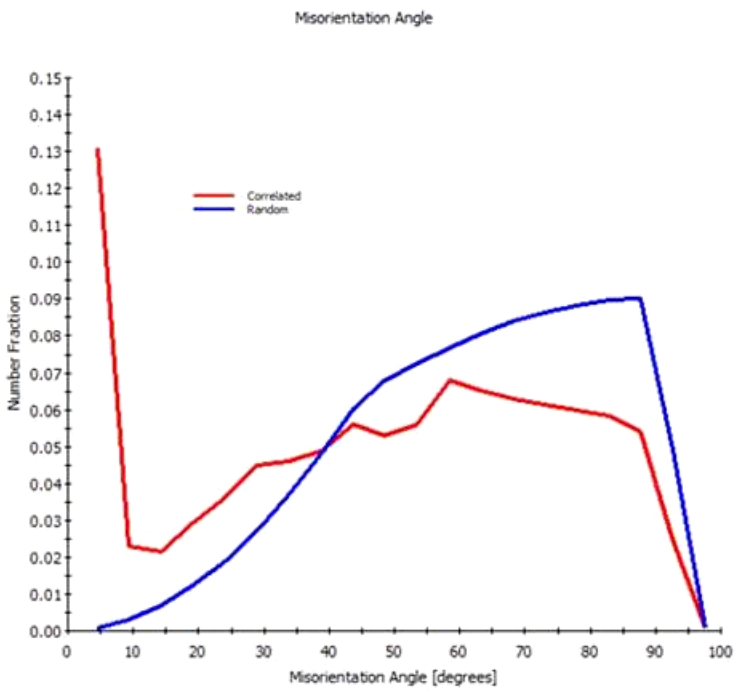

Chart: Misorientation Angle

Angle [degrees]	Correlated Number Fraction	Random Number Fraction
4.45	0.130681	0.000708705
9.35	0.0230069	0.0029471
14.25	0.0213625	0.00675727
19.15	0.0293127	0.0121114
24.05	0.0360153	0.0189703
28.95	0.0447091	0.0272839
33.85	0.0461604	0.0369913
38.75	0.0487378	0.0480217
43.65	0.0560123	0.0602944
48.55	0.0530811	0.0677121
53.45	0.0558515	0.072569
58.35	0.0679269	0.0768958
63.25	0.0653102	0.0806609
68.15	0.0629723	0.0838368
73.05	0.0612493	0.0864003
77.95	0.0597086	0.0883327
82.85	0.058461	0.0896197
87.75	0.0541106	0.0902521
92.65	0.0245977	0.0489889
97.55	0.000732818	0.000673146
Average Number	48.5714	63.0123

a) Sn with 2.4% Sb, Sample 217, post plating

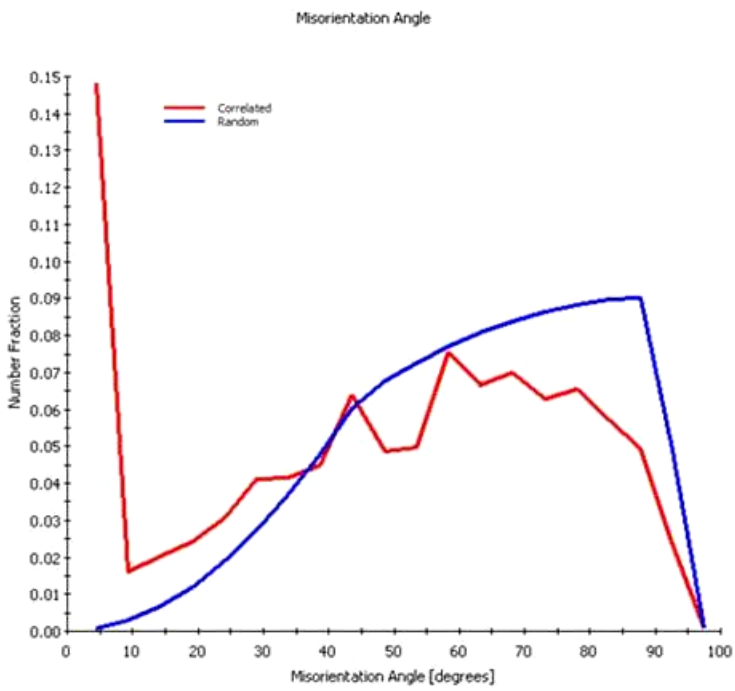

Chart: Misorientation Angle

Angle [degrees]	Correlated Number Fraction	Random Number Fraction
4.45	0.148017	0.000709297
9.35	0.0159675	0.0029477
14.25	0.0203585	0.0067579
19.15	0.0243789	0.012112
24.05	0.030552	0.018971
28.95	0.041178	0.0272846
33.85	0.0413681	0.0369921
38.75	0.0448419	0.0480226
43.65	0.0638413	0.0602954
48.55	0.0487483	0.0677131
53.45	0.049827	0.07257
58.35	0.0754082	0.0768968
63.25	0.066455	0.0806619
68.15	0.0697768	0.0838379
73.05	0.0630192	0.0864014
77.95	0.0655996	0.0883337
82.85	0.0572215	0.0896208
87.75	0.0493185	0.0902532
92.65	0.0234855	0.0489898
97.55	0.000636797	0.000673723
Average Number	48.5697	63.0123

b) Sn with 2.4% Sb, Sample 216, 18 months at 50% RH / 50°C

Electroplated Sn with 2.4% Sb
Grain Boundary Characterization Chart

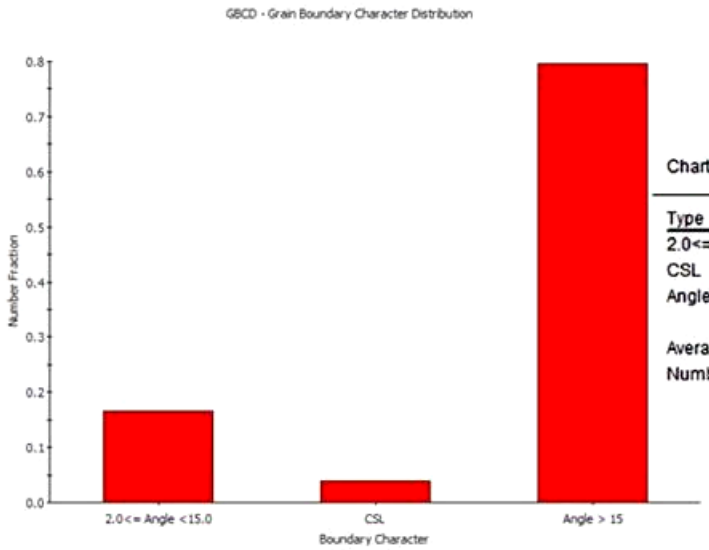

Chart: GBCD - Grain Boundary Character Distribution

Type	Number Fraction
2.0<= Angle <15.0	0.166679
CSL	0.0381673
Angle > 15	0.795154
Average Number	0.333333

a) Sn with 2.4% Sb, Sample 217, post plating

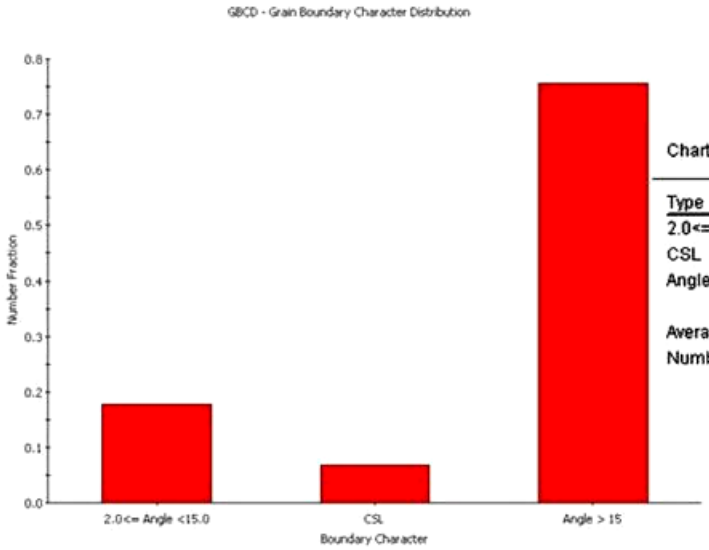

Chart: GBCD - Grain Boundary Character Distribution

Type	Number Fraction
2.0<= Angle <15.0	0.176996
CSL	0.0672582
Angle > 15	0.755745
Average Number	0.333333

b) Sn with 2.4% Sb, Sample 216, 18 months at 50% RH / 50°C

Electroplated Sn with 2.4% Sb

Coincident Site Lattice Boundary Chart

The total fraction of CSL boundaries is approximately 2% of boundaries measured

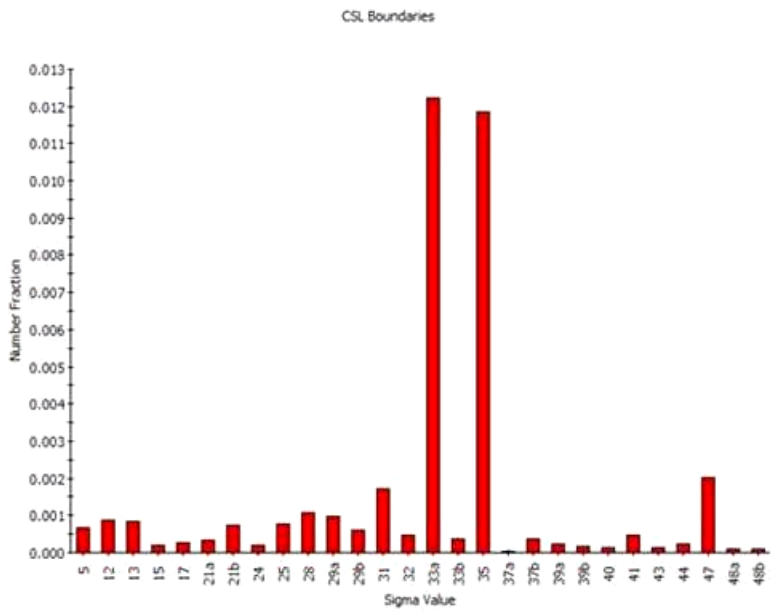

Overall fraction of CSL boundaries: 0.038

Sigma	Number Fraction
5	0.000668473
12	0.000875807
13	0.000836485
15	0.00018946
17	0.000253805
21a	0.000321725
21b	0.000754266
24	0.000193035
25	0.000761416
28	0.00109029
29a	0.000986623
29b	0.000596979
31	0.00170157
32	0.000461139
33a	0.0122398
33b	0.000364622
35	0.0118717
37a	2.85978e-005
37b	0.000378921
39a	0.000239506
39b	0.000164437
40	0.000146564
41	0.000464714
43	0.000139414
44	0.000235932
47	0.00201257
48a	9.65175e-005
48b	9.29428e-005

a) Sn with 2.4% Sb, Sample 217, post plating

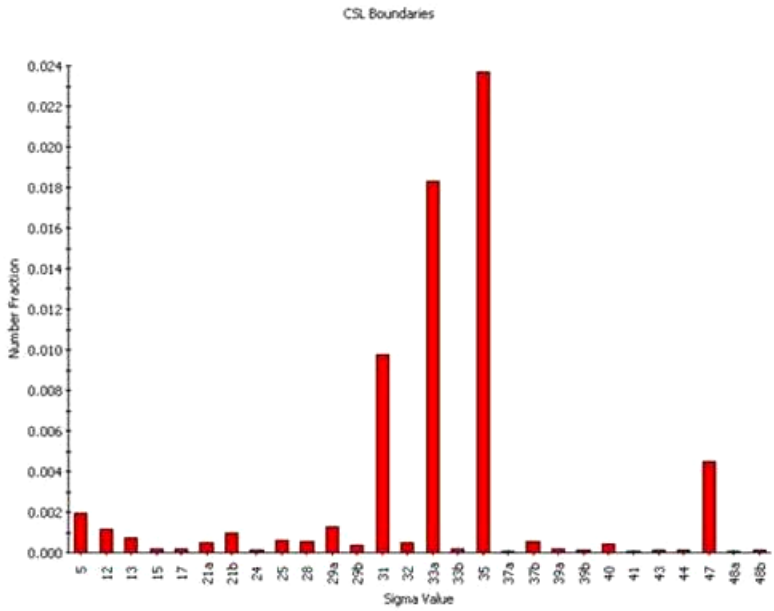

Overall fraction of CSL boundaries: 0.067

Sigma	Number Fraction
5	0.00195316
12	0.0011738
13	0.000731842
15	0.00017108
17	0.000156823
21a	0.000460965
21b	0.000945692
24	0.00012831
25	0.000622541
28	0.000570266
29a	0.0012926
29b	0.000375425
31	0.00973255
32	0.000498983
33a	0.0183103
33b	0.000156823
35	0.0237136
37a	7.60355e-005
37b	0.000517992
39a	0.000161575
39b	0.000133062
40	0.000422948
41	5.22744e-005
43	9.97966e-005
44	0.000147319
47	0.00449085
48a	4.75222e-005
48b	0.000114053

b) Sn with 2.4% Sb, Sample 216, 18 months at 50% RH / 50°C

Electroplated Sn with 2.4% Sb
Misorientation Distribution Function (MODF) Plot

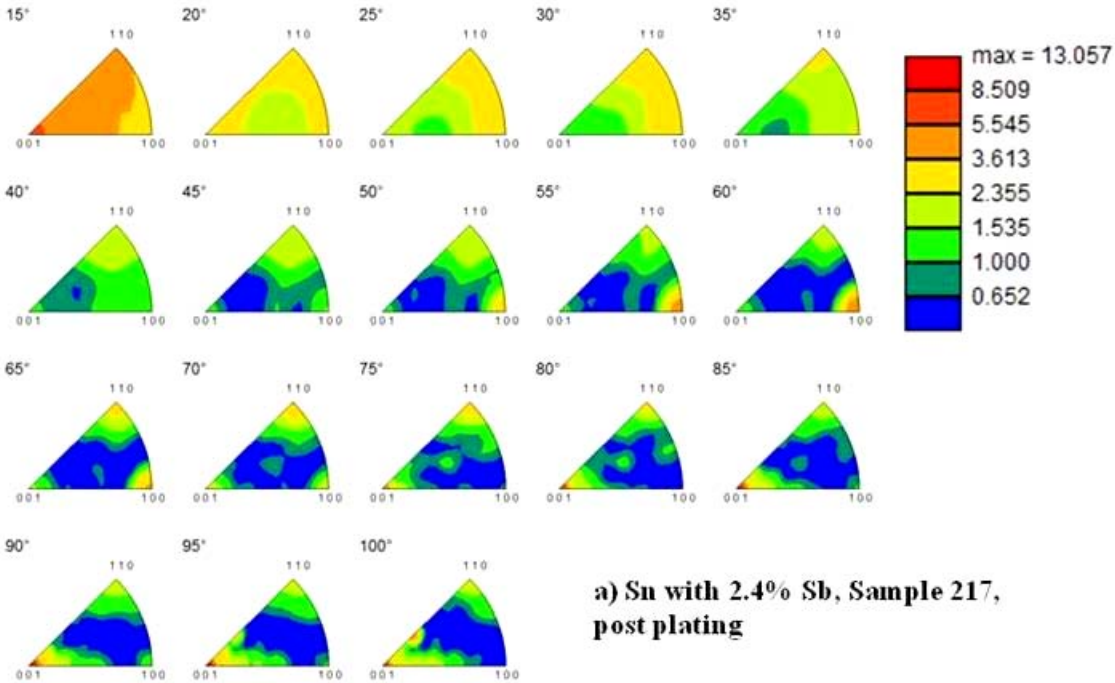

a) Sn with 2.4% Sb, Sample 217, post plating

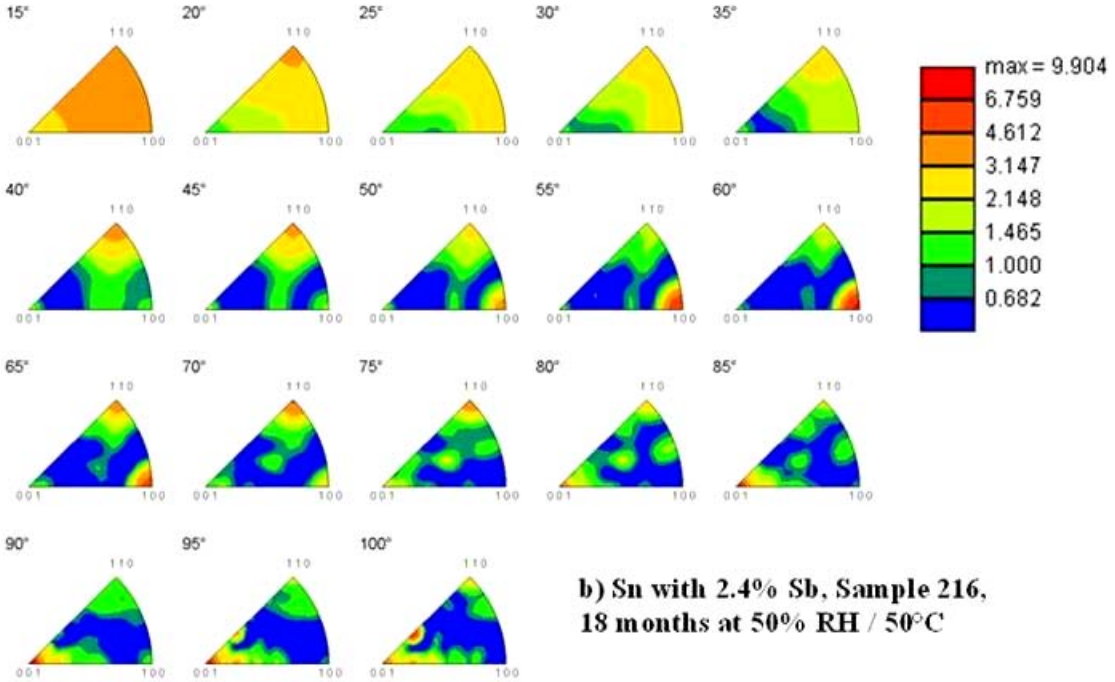

b) Sn with 2.4% Sb, Sample 216, 18 months at 50% RH / 50°C

Electroplated Sn with 2.4% Sb

Crystal Direction Map

Blue Indicates C-Direction in sample normal

Red indicates C-direction in sample plane 15º tolerance

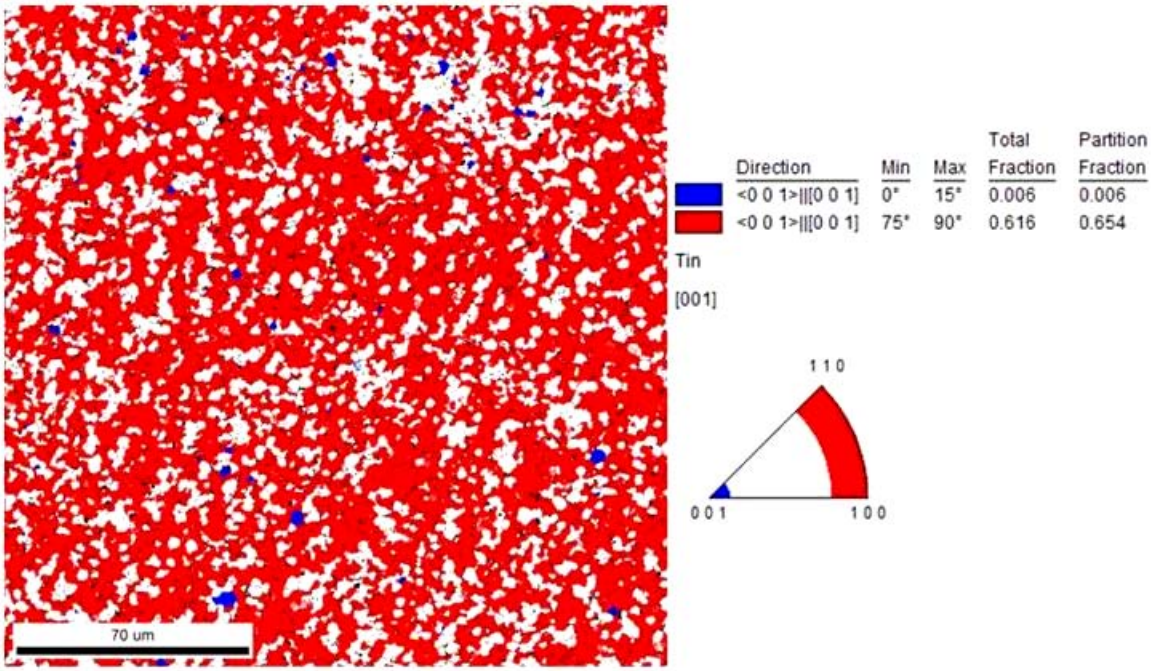

a) Sn with 2.4% Sb, Sample 217, post plating

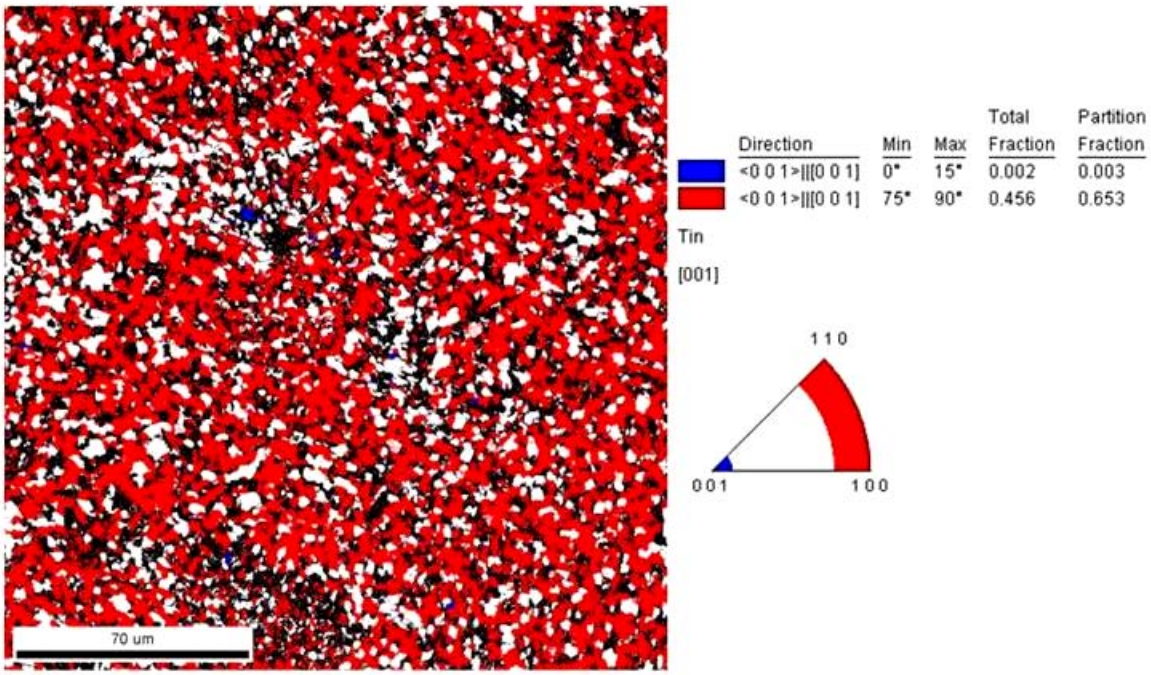

b) Sn with 2.4% Sb, Sample 216, 18 months at 50% RH / 50°C

Appendix P: EBSD Data for Sn with 1.1% Ge

Electroplated Sn with 1.1% Ge
Image Quality Map

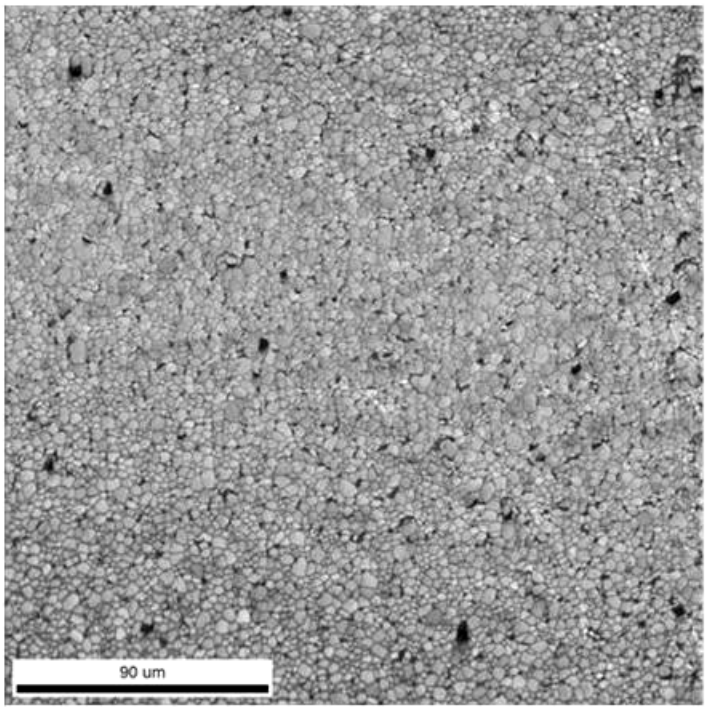

X = 250 microns
Y = 250 microns
Step size = 0.3 microns

a) Sn with 1.1% Ge, Sample 232, post plating

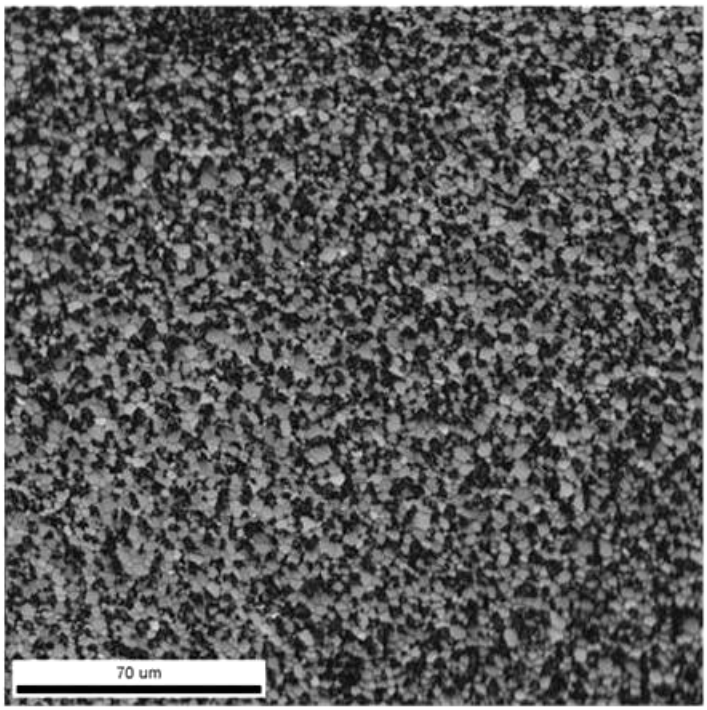

X = 200 microns
Y = 200 microns
Step size = 0.2 microns

b) Sn with 1.1% Ge, Sample 235, 18 months at 50% RH / 50°C

Electroplated Sn with 1.1% Ge
Color Coded Orientation Map

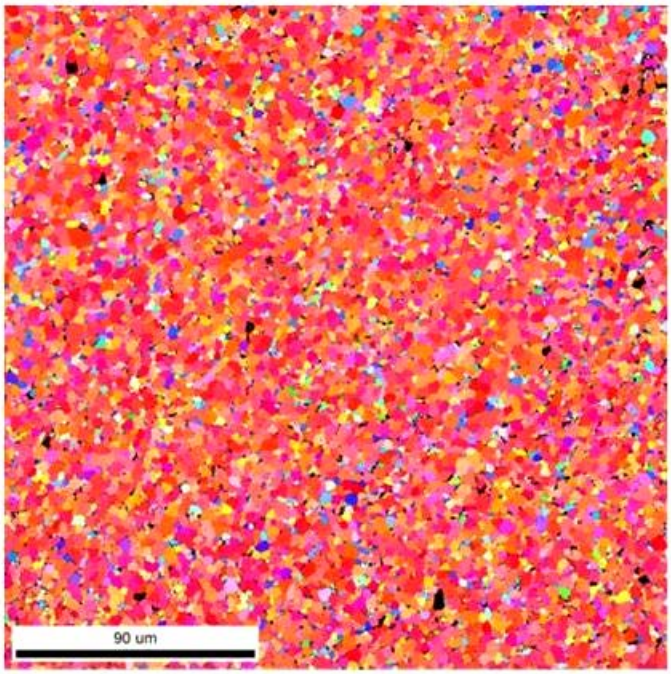

Color Coded Map Type: Inverse Pole Figure [001]

Tin

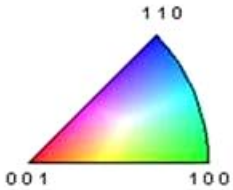

a) Sn with 1.1% Ge, Sample 232, post plating

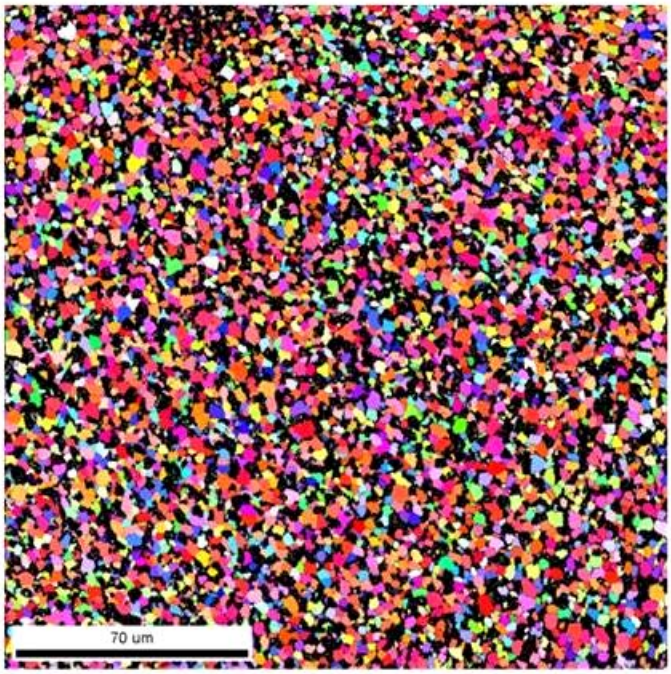

Color Coded Map Type: Inverse Pole Figure [001]

Tin

b) Sn with 1.1% Ge, Sample 235, 18 months at 50% RH / 50°C

Electroplated Sn with 1.1% Ge
Crystal Direction Map Showing <111> crystal direction in ND direction 15º Tolerance

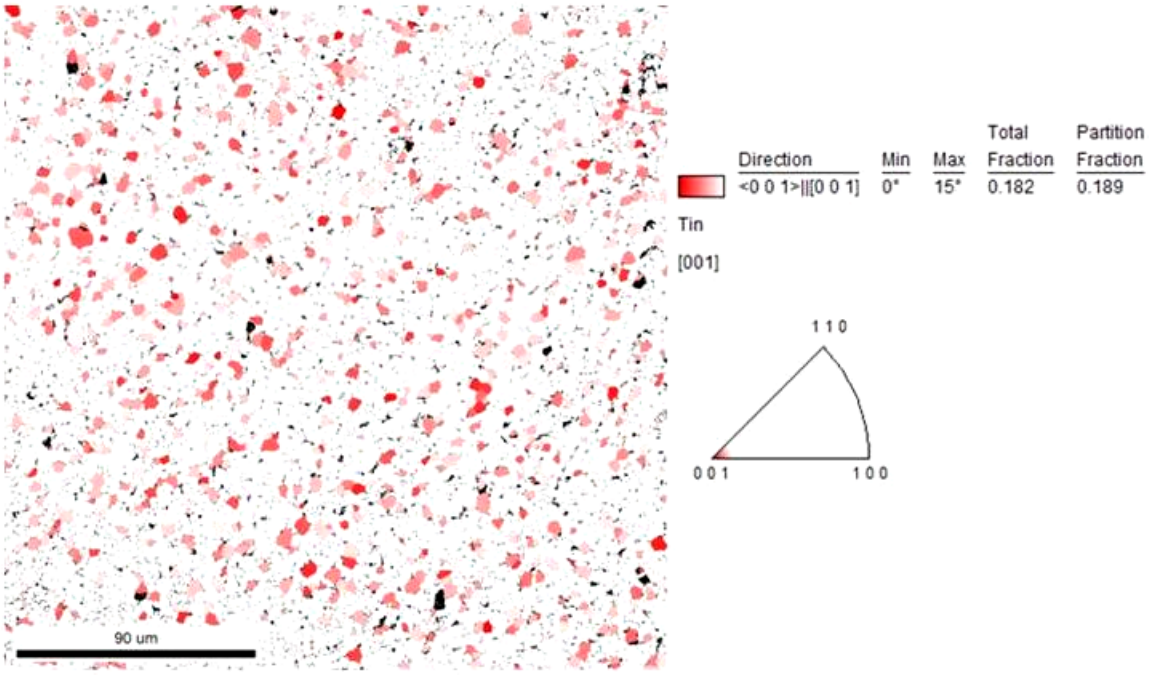

a) Sn with 1.1% Ge, Sample 232, post plating

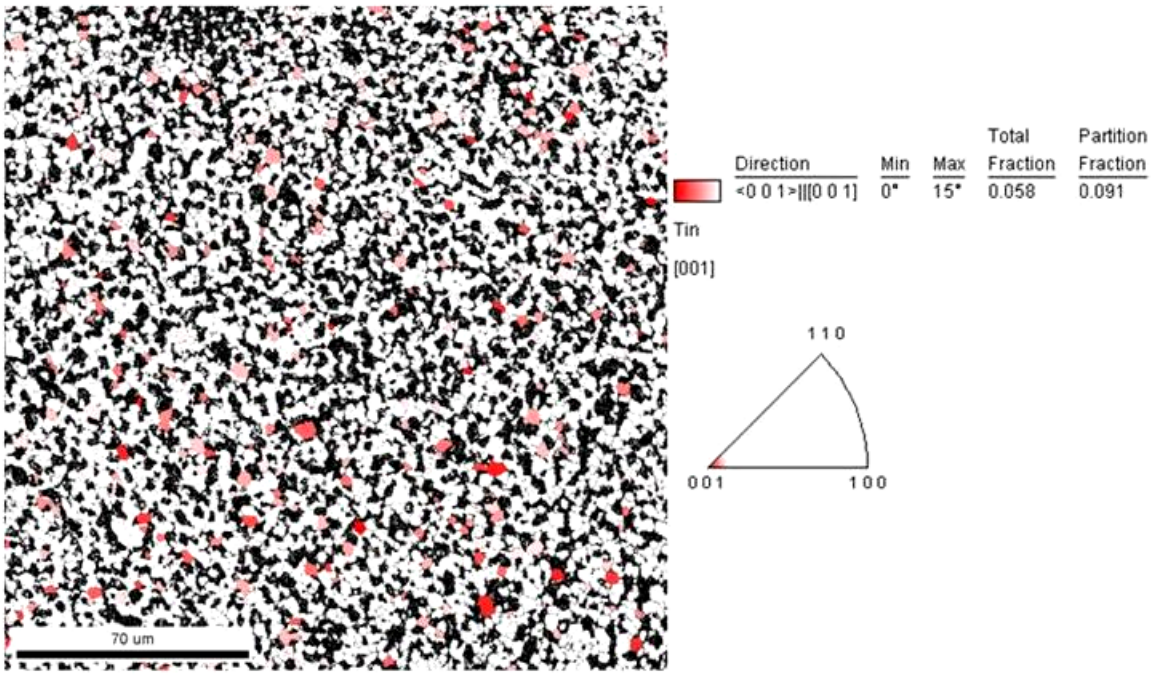

b) Sn with 1.1% Ge, Sample 235, 18 months at 50% RH / 50°C

Electroplated Sn with 1.1% Ge
Crystal Direction Map Showing <111> crystal direction in ND direction 20º Tolerance

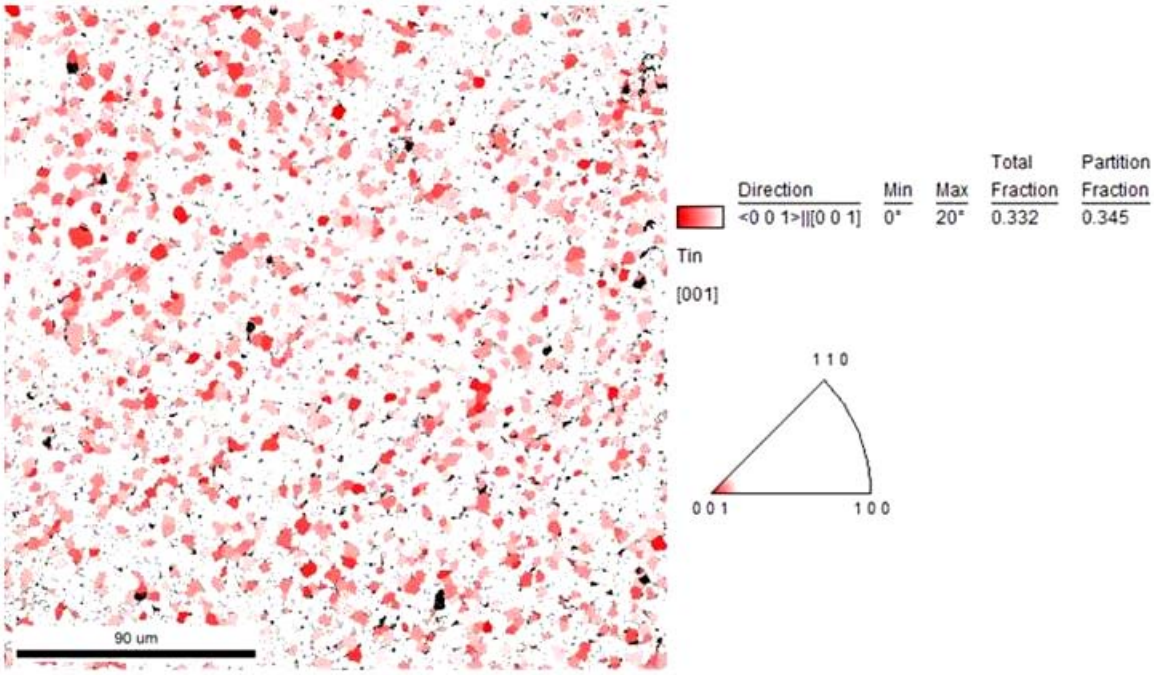

a) Sn with 1.1% Ge, Sample 232, post plating

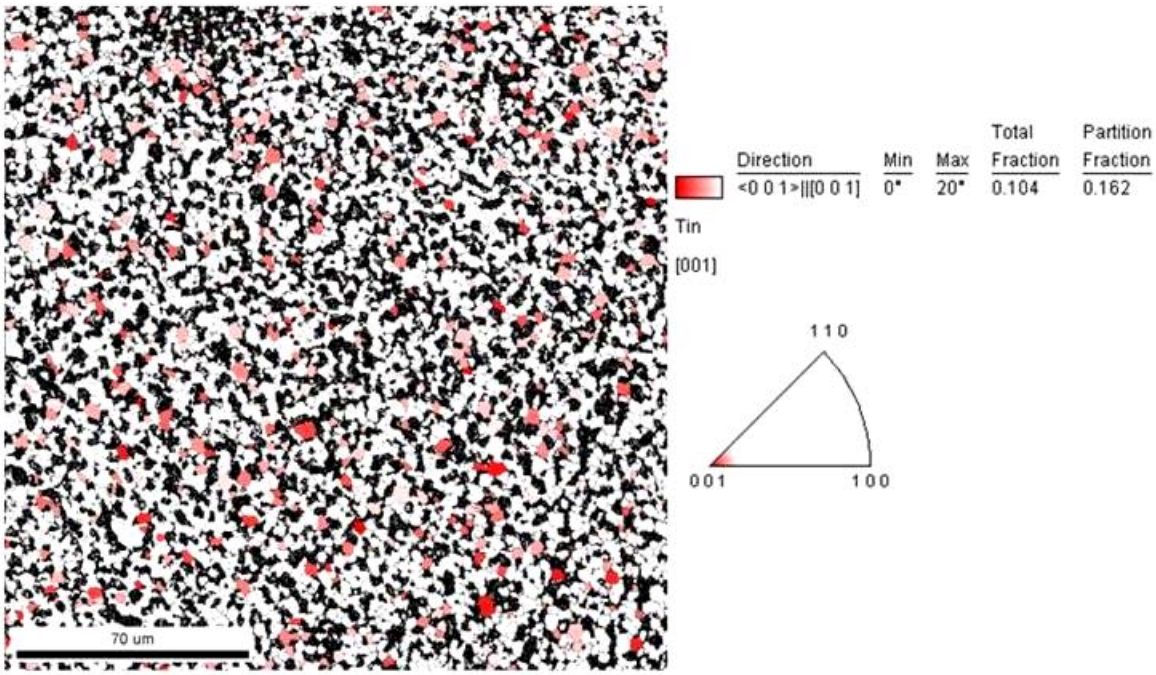

b) Sn with 1.1% Ge, Sample 235, 18 months at 50% RH / 50°C

Electroplated Sn with 1.1% Ge

Confidence Index (CI) Chart

Data points with a CI above 0.1 are generally considered to be indexed correctly.

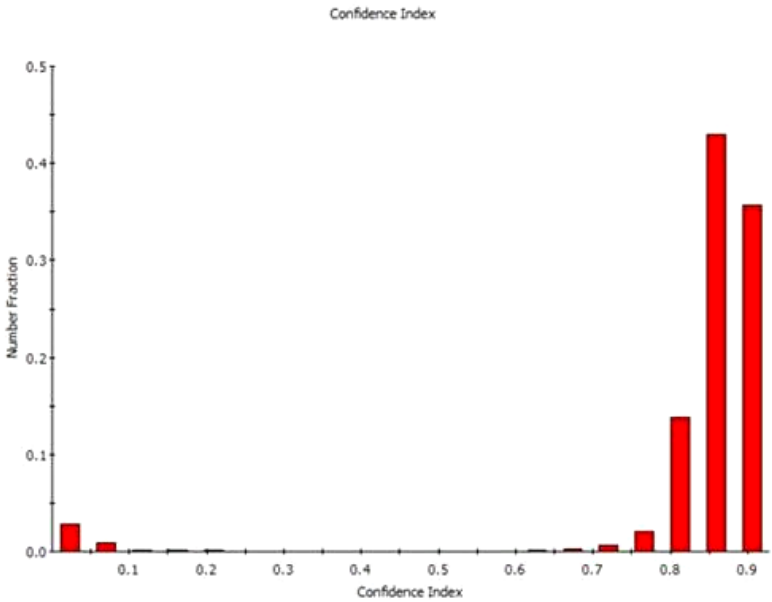

CI	Number Fraction
0.023225	0.0285887
0.069675	0.00935887
0.116125	0.00170309
0.162575	0.00123963
0.209025	0.000659058
0.255475	0.00041487
0.301925	0.000353823
0.348375	0.000246679
0.394825	0.000419853
0.441275	0.00055316
0.487725	0.000347594
0.534175	0.000475917
0.580625	0.000379986
0.627075	0.00184262
0.673525	0.00237709
0.719975	0.00631275
0.766425	0.0207647
0.812875	0.137495
0.859325	0.4295
0.905775	0.356966
Average	
Number	0.831238
Standard Deviation	0.18034

a) Sn with 1.1% Ge, Sample 232, post plating. Indicates that about 3.7% of data points were not indexed with a high degree of confidence

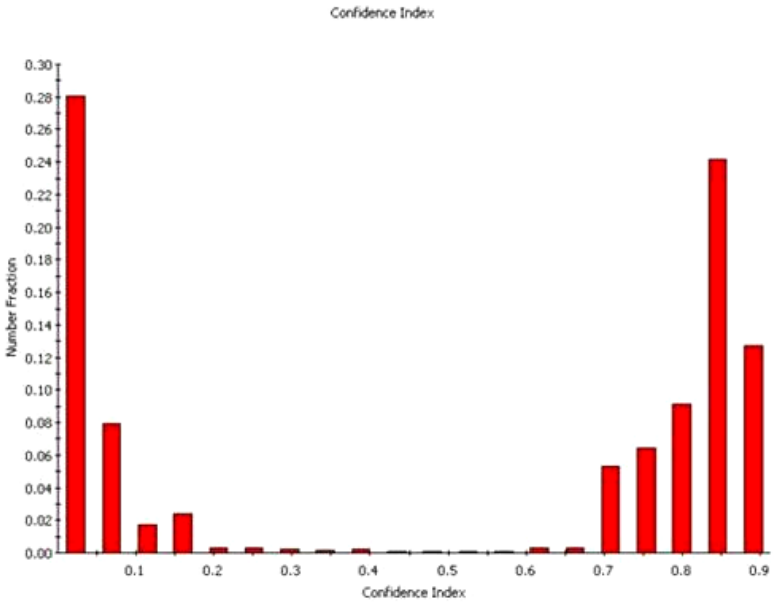

CI	Number Fraction
0.02285	0.280586
0.06855	0.079002
0.11425	0.0170261
0.15995	0.023795
0.20565	0.00284446
0.25135	0.00326244
0.29705	0.0024862
0.34275	0.001202
0.38845	0.0021513
0.43415	0.000797004
0.47985	0.000996904
0.52555	0.000752005
0.57125	0.000801331
0.61695	0.00321225
0.66265	0.00320619
0.70835	0.0534313
0.75405	0.0640398
0.79975	0.0911734
0.84545	0.24183
0.89115	0.127405
Average	
Number	0.501046
Standard Deviation	0.387271

(b) Sn with 1.1% Ge, Sample 235, 18 months at 50% RH / 50°C. Indicates that about 36% of data points were not indexed with a high degree of confidence

Electroplated Sn with 1.1% Ge
Pole Figure and Inverse Pole Figure Plots

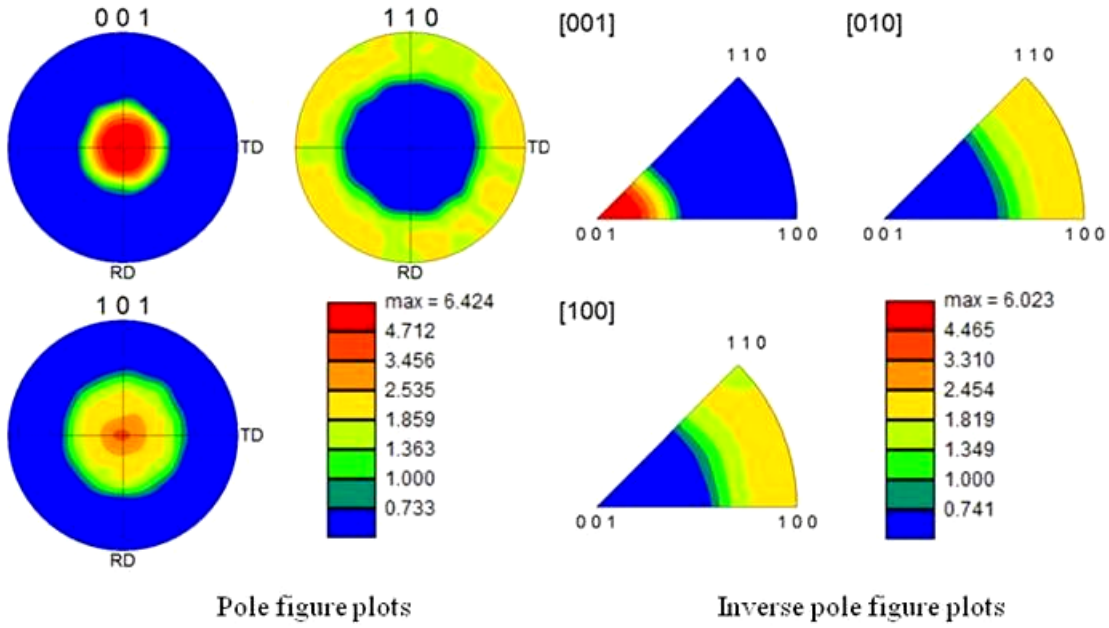

a) Sn with 1.1% Ge, Sample 232, post plating

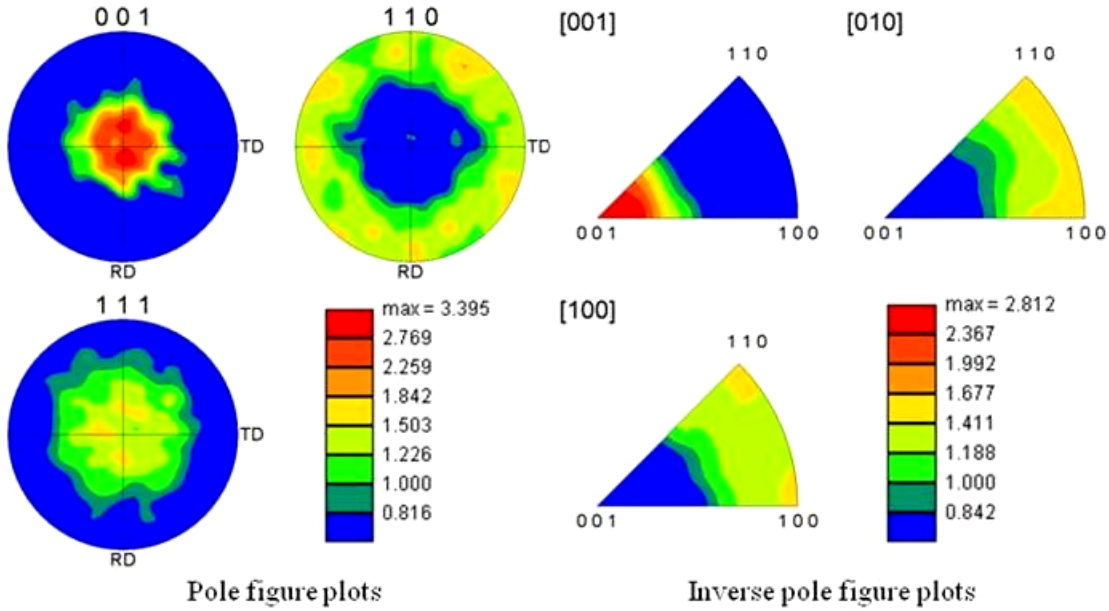

b) Sn with 1.1% Ge, Sample 235, 18 months at 50% RH / 50°C

Electroplated Sn with 1.1% Ge
Grain Size Histogram and Data

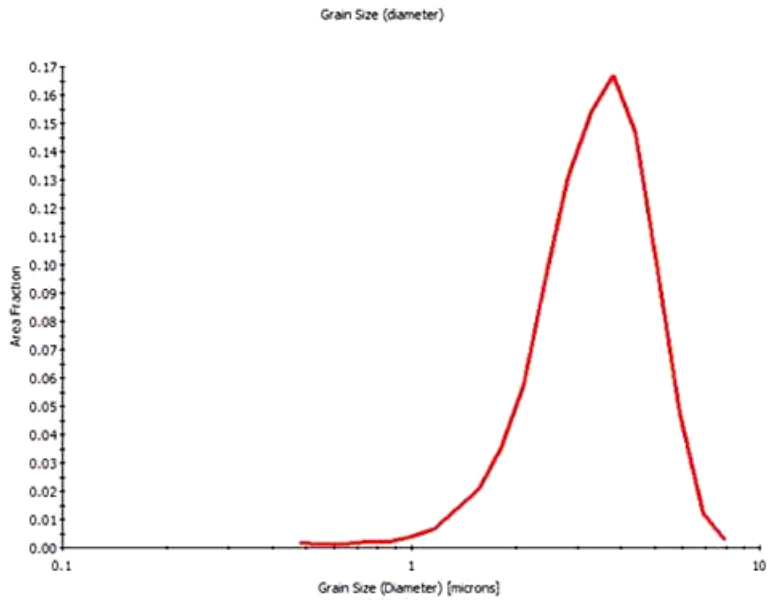

Edge grains included in analysis

Diameter [microns]	Area Fraction
0.47968	0.00184446
0.556086	0.00129945
0.644663	0.00109783
0.747348	0.00202136
0.86639	0.00225289
1.00439	0.00375526
1.16438	0.00650504
1.34985	0.0134939
1.56486	0.0207118
1.81412	0.0355429
2.10308	0.0575203
2.43807	0.0954722
2.82642	0.130654
3.27662	0.153806
3.79854	0.167077
4.40359	0.146645
5.10502	0.0978461
5.91818	0.0475709
6.86086	0.0123766
7.95369	0.00250784

a) Sn with 1.1% Ge, Sample 232, post plating

Average	
Number	2.32923
Standard Deviation	1.26392
Area	3.52558

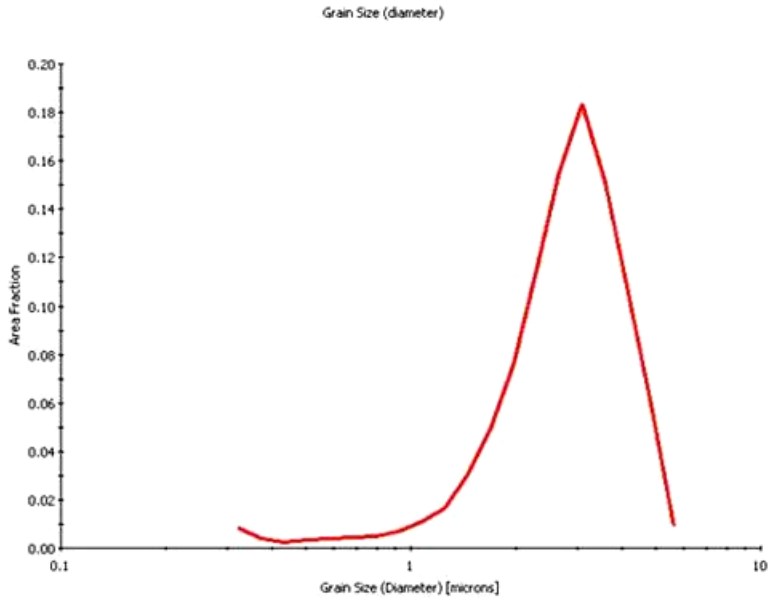

Edge grains included in analysis

Diameter [microns]	Area Fraction
0.320328	0.00850809
0.372609	0.00382177
0.433423	0.0022444
0.504162	0.00373159
0.586447	0.00422828
0.682161	0.00428267
0.793498	0.00500981
0.923005	0.00684913
1.07365	0.0110373
1.24888	0.0163978
1.45271	0.0303938
1.68981	0.049308
1.96561	0.0756897
2.28642	0.114635
2.65958	0.155572
3.09366	0.183456
3.59858	0.150954
4.1859	0.105504
4.86909	0.0592704
5.66378	0.00910641

b) Sn with 1.1% Ge, Sample 235, 18 months at 50% RH / 50°C

Average	
Number	1.27381
Standard Deviation	1.12801
Area	2.89714

Electroplated Sn with 1.1% Ge
Misorientation Angle Histogram, 2º minimum misorientation

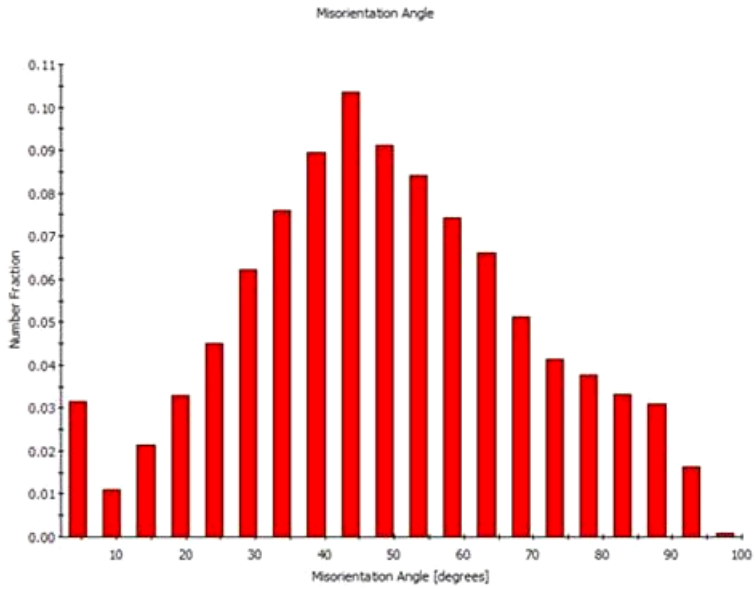

Angle [degrees]	Number Fraction
4.45	0.031487
9.35	0.0110271
14.25	0.0212994
19.15	0.0327941
24.05	0.0450509
28.95	0.0623003
33.85	0.0760924
38.75	0.0895384
43.65	0.10354
48.55	0.0912726
53.45	0.0840709
58.35	0.074211
63.25	0.0660705
68.15	0.0512069
73.05	0.0412181
77.95	0.0376467
82.85	0.0331512
87.75	0.0309163
92.65	0.0162479
97.55	0.000857867
Average Number	48.4928

a) Sn with 1.1% Ge, Sample 232, post plating

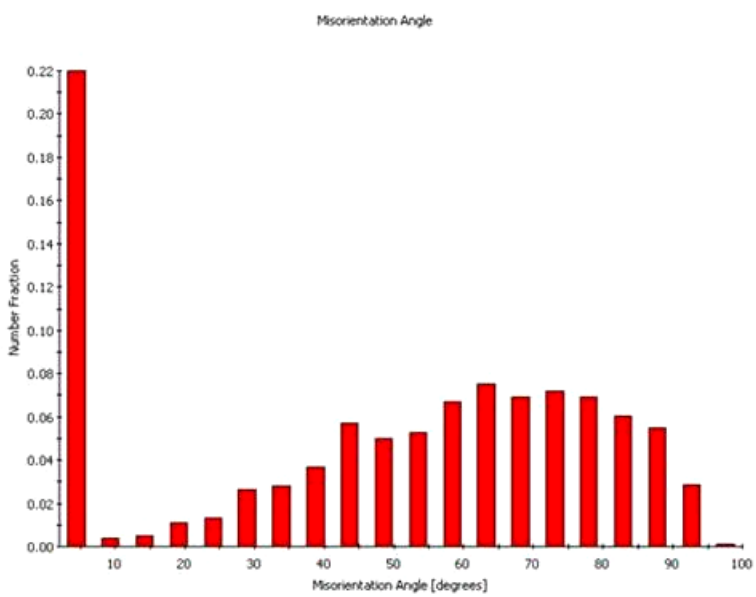

Angle [degrees]	Number Fraction
4.45	0.219843
9.35	0.0036718
14.25	0.00516891
19.15	0.0110089
24.05	0.0129061
28.95	0.0260962
33.85	0.027845
38.75	0.0367438
43.65	0.0570064
48.55	0.0501597
53.45	0.0525667
58.35	0.066828
63.25	0.0753848
68.15	0.0690027
73.05	0.0720098
77.95	0.0692995
82.85	0.0601103
87.75	0.0549027
92.65	0.0285936
97.55	0.000851805
Average Number	48.6274

b) Sn with 1.1% Ge, Sample 235, 18 months at 50% RH / 50°C

Electroplated Sn with 1.1% Ge
Misorientation Angle Histogram, 2º minimum misorientation

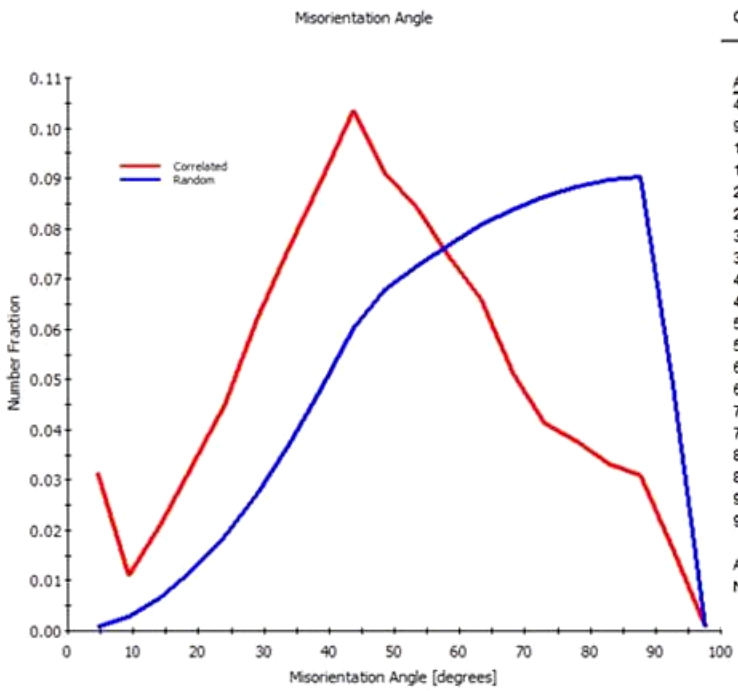

Chart: Misorientation Angle

Angle [degrees]	Correlated Number Fraction	Random Number Fraction
4.45	0.031487	0.000708763
9.35	0.0110271	0.00294717
14.25	0.0212994	0.00675737
19.15	0.0327941	0.0121115
24.05	0.0450509	0.0189705
28.95	0.0623003	0.0272841
33.85	0.0760924	0.0369916
38.75	0.0895384	0.0480221
43.65	0.10354	0.0602949
48.55	0.0912726	0.0677126
53.45	0.0840709	0.0725695
58.35	0.074211	0.0768964
63.25	0.0660705	0.0806615
68.15	0.0512069	0.0838374
73.05	0.0412181	0.0864009
77.95	0.0376467	0.0883333
82.85	0.0331512	0.0896204
87.75	0.0309163	0.0902528
92.65	0.0162479	0.0489893
97.55	0.000857867	0.000673189
Average Number	48.4928	63.0123

a) Sn with 1.1% Ge, Sample 232, post plating

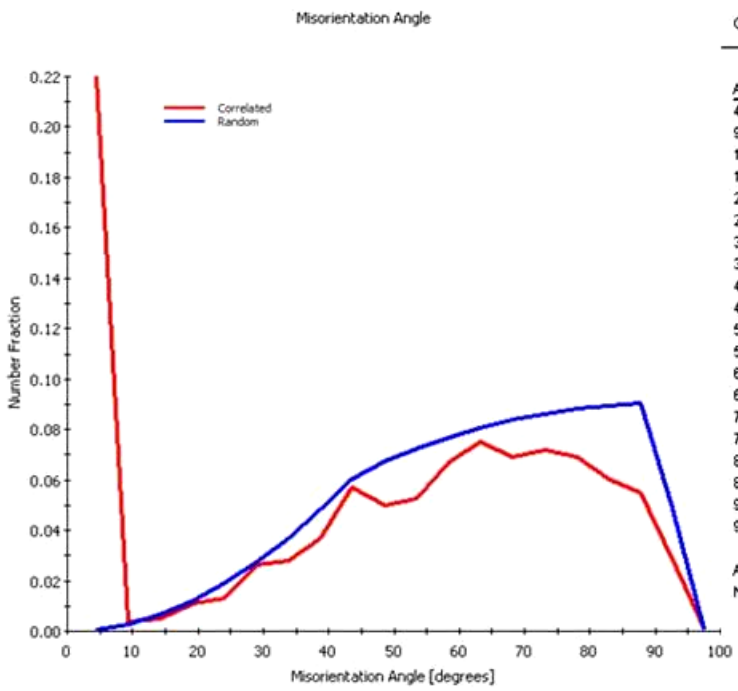

Chart: Misorientation Angle

Angle [degrees]	Correlated Number Fraction	Random Number Fraction
4.45	0.219843	0.000710144
9.35	0.0036718	0.00294854
14.25	0.00516891	0.00675872
19.15	0.0110089	0.0121128
24.05	0.0129061	0.0189718
28.95	0.0260962	0.0272853
33.85	0.027845	0.0369928
38.75	0.0367438	0.0480232
43.65	0.0570064	0.060296
48.55	0.0501597	0.0677136
53.45	0.0525667	0.0725705
58.35	0.066828	0.0768973
63.25	0.0753848	0.0806625
68.15	0.0690027	0.0838384
73.05	0.0720098	0.0864019
77.95	0.0692995	0.0883342
82.85	0.0601103	0.0896213
87.75	0.0549027	0.0902537
92.65	0.0285936	0.0489905
97.55	0.000851805	0.000674569
Average Number	48.6274	63.0123

b) Sn with 1.1% Ge, Sample 235, 18 months at 50% RH / 50°C

Electroplated Sn with 1.1% Ge
Grain Boundary Characterization Chart

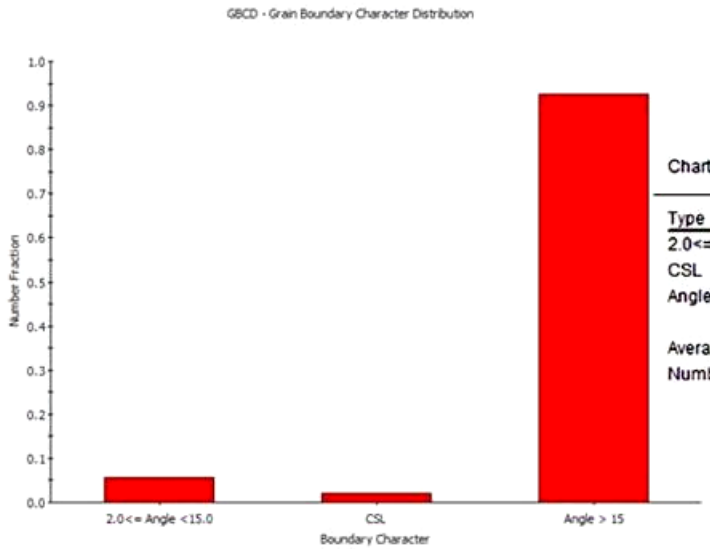

Chart: GBCD - Grain Boundary Character Distribution

Type	Number Fraction
2.0<= Angle <15.0	0.0556987
CSL	0.0196131
Angle > 15	0.924688
Average Number	0.333333

a) Sn with 1.1% Ge, Sample 232, post plating

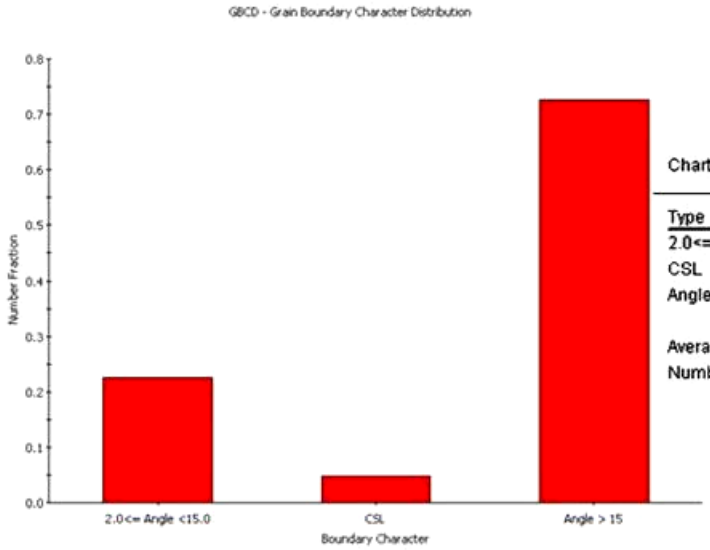

Chart: GBCD - Grain Boundary Character Distribution

Type	Number Fraction
2.0<= Angle <15.0	0.226264
CSL	0.0477011
Angle > 15	0.726035
Average Number	0.333333

b) Sn with 1.1% Ge, Sample 235, 18 months at 50% RH / 50°C

Electroplated Sn with 1.1% Ge

Coincident Site Lattice Boundary Chart

The total fraction of CSL boundaries is approximately 2% of boundaries measured

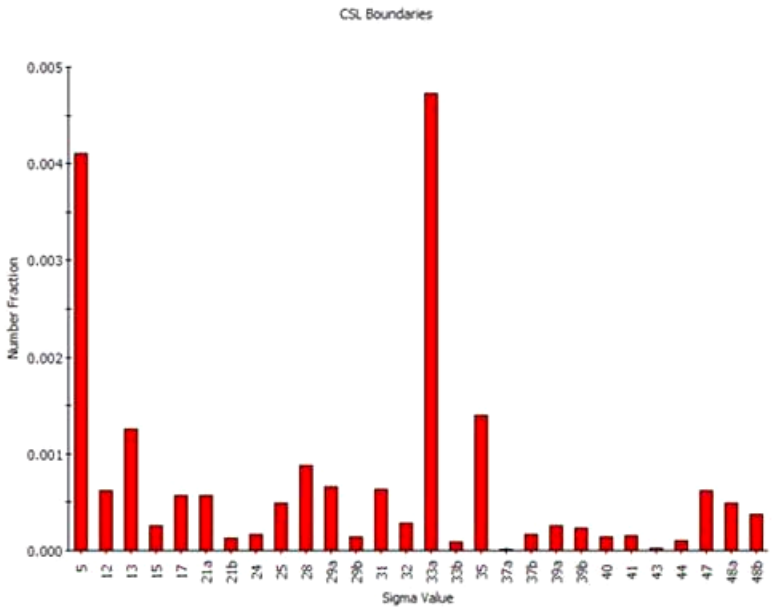

Overall fraction of CSL boundaries: 0.020

Sigma	Number Fraction
5	0.00410524
12	0.000622229
13	0.00125919
15	0.000265092
17	0.000567002
21a	0.000574366
21b	0.000128864
24	0.000165682
25	0.000493365
28	0.000883639
29a	0.00066273
29b	0.000143591
31	0.000636957
32	0.000283501
33a	0.00472379
33b	9.57276e-005
35	0.00140278
37a	1.47273e-005
37b	0.000165682
39a	0.000257728
39b	0.000231955
40	0.00013991
41	0.000158319
43	2.94546e-005
44	0.000103091
47	0.000622229
48a	0.000497047
48b	0.000379229

a) Sn with 1.1% Ge, Sample 232, post plating

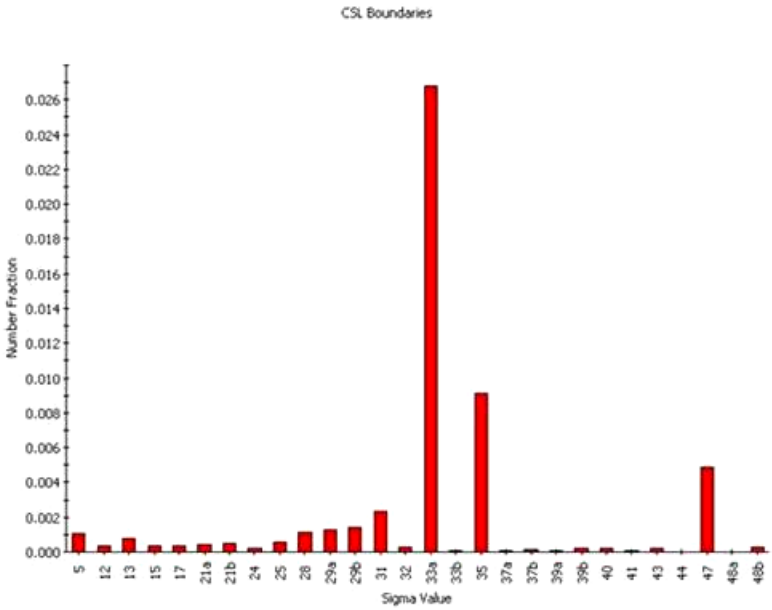

Overall fraction of CSL boundaries: 0.053

Sigma	Number Fraction
5	0.00106476
12	0.000354919
13	0.000787275
15	0.000367825
17	0.000342013
21a	0.000406543
21b	0.000522699
24	0.000193592
25	0.000593682
28	0.00109702
29a	0.0012519
29b	0.00141968
31	0.00236182
32	0.000271029
33a	0.0267931
33b	7.09838e-005
35	0.00912464
37a	3.87184e-005
37b	0.000141968
39a	3.87184e-005
39b	0.000206498
40	0.000206498
41	4.51715e-005
43	0.000193592
44	1.93592e-005
47	0.00485916
48a	2.58123e-005
48b	0.000258123

b) Sn with 1.1% Ge, Sample xxx, 18 months at 50% RH / 50°C

Electroplated Sn with 1.1% Ge
Misorientation Distribution Function (MODF) Plot

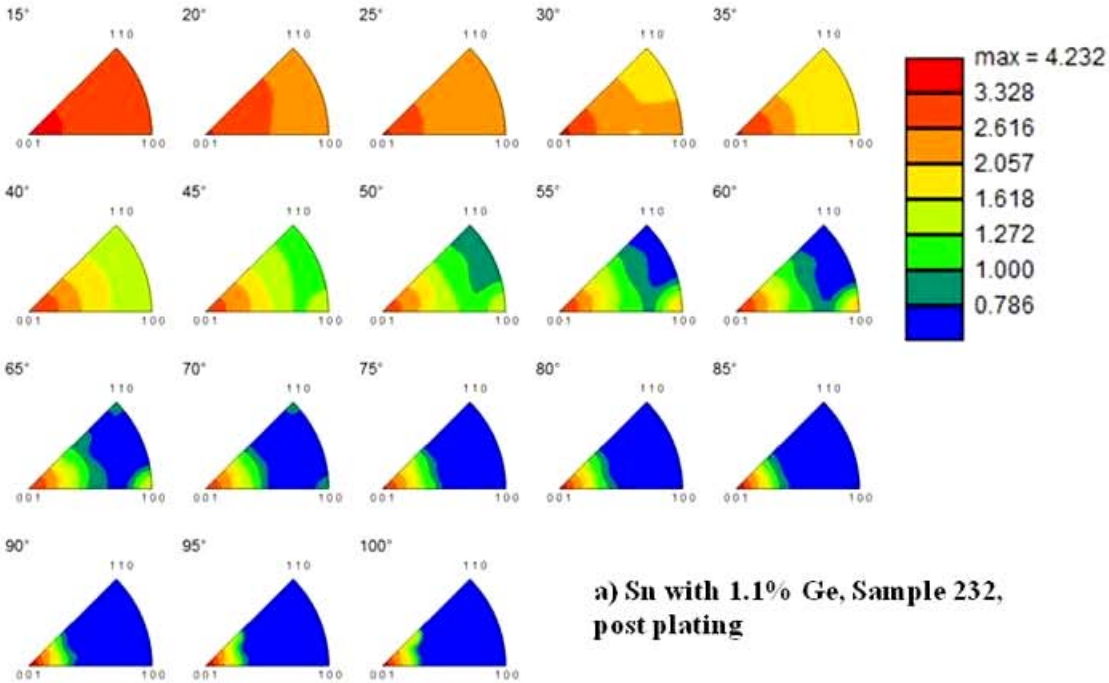

a) Sn with 1.1% Ge, Sample 232, post plating

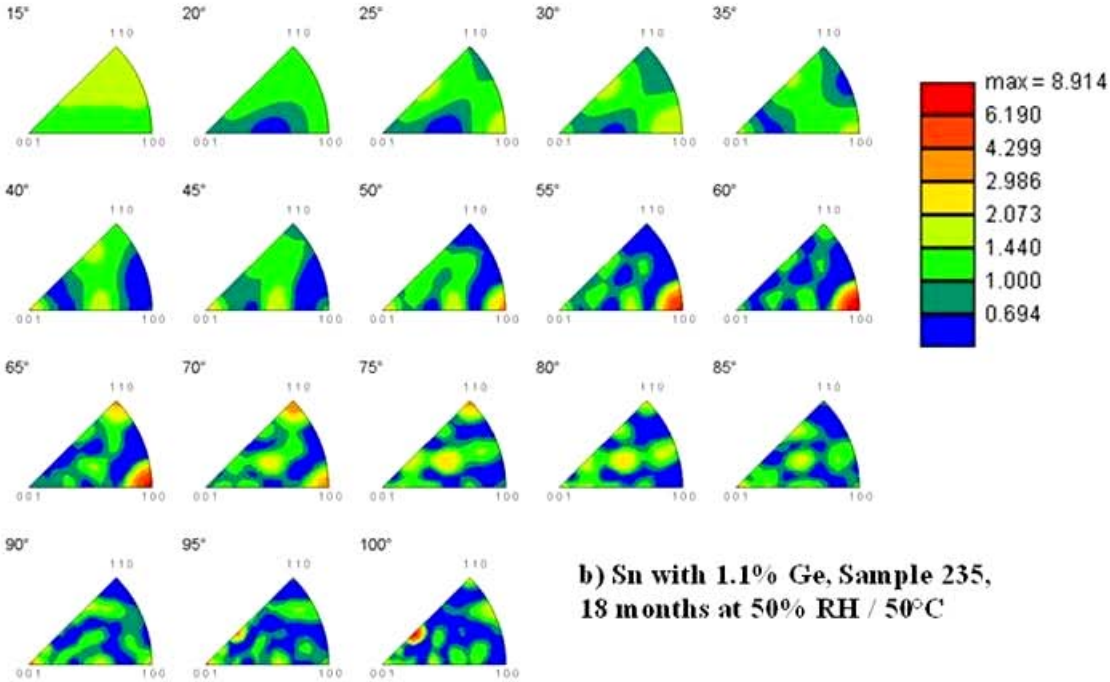

b) Sn with 1.1% Ge, Sample 235, 18 months at 50% RH / 50°C

Electroplated Sn with 1.1% Ge

Crystal Direction Map

Blue Indicates C-Direction in sample normal

Red indicates C-direction in sample plane 15º tolerance

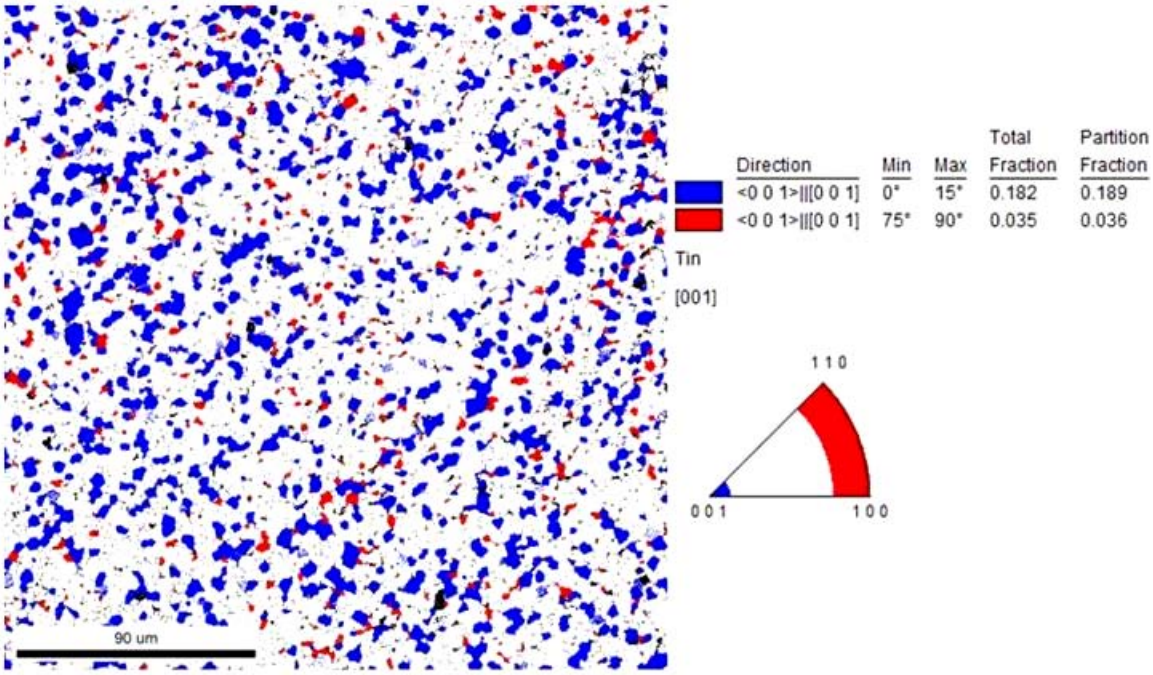

a) Sn with 1.1% Ge, Sample 232, post plating

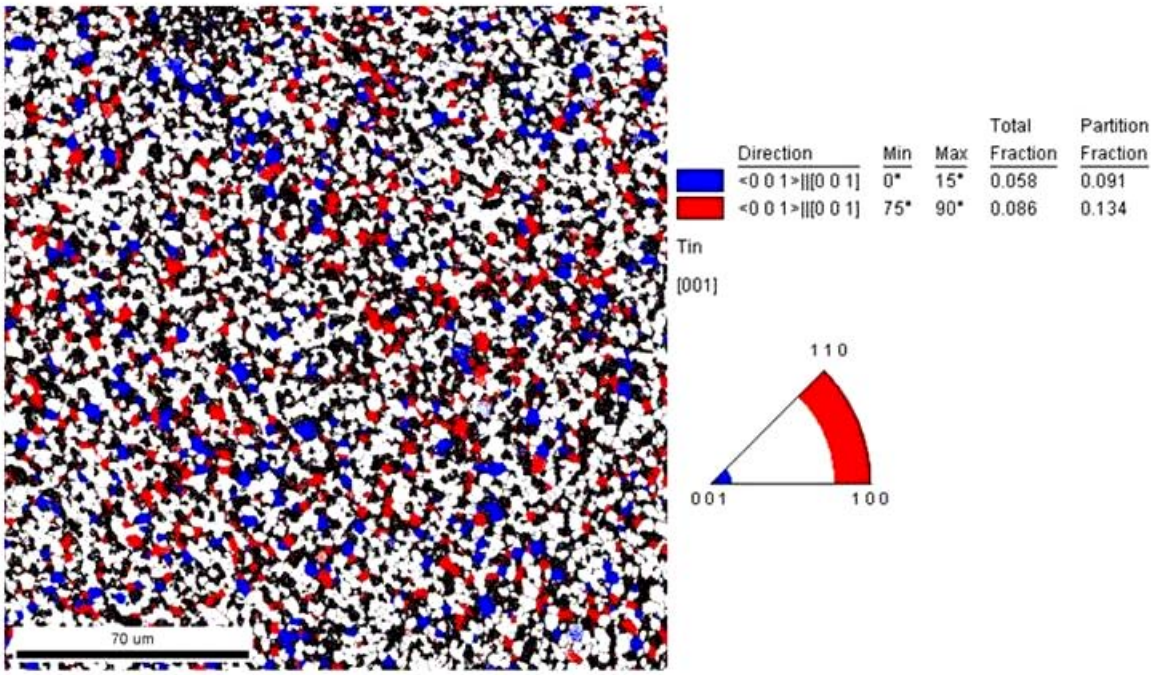

b) Sn with 1.1% Ge, Sample 235, 18 months at 50% RH / 50°C

Appendix Q: EBSD Data for Sn with 1.3% Au

Electroplated Sn with 1.3% Au
Image Quality Map

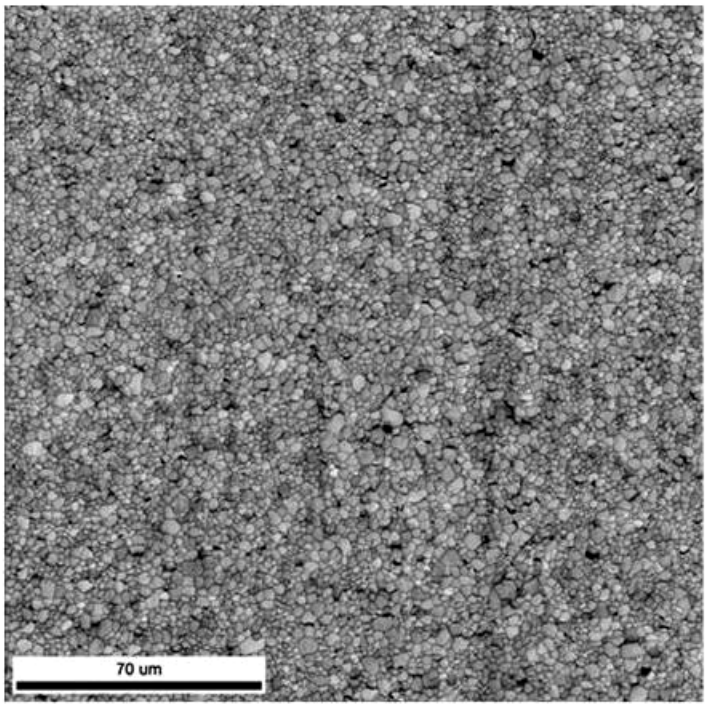

X = 200 microns
Y = 200 microns
Step size = 0.2 microns

a) Sn with 1.3% Au, Sample 267, post plating

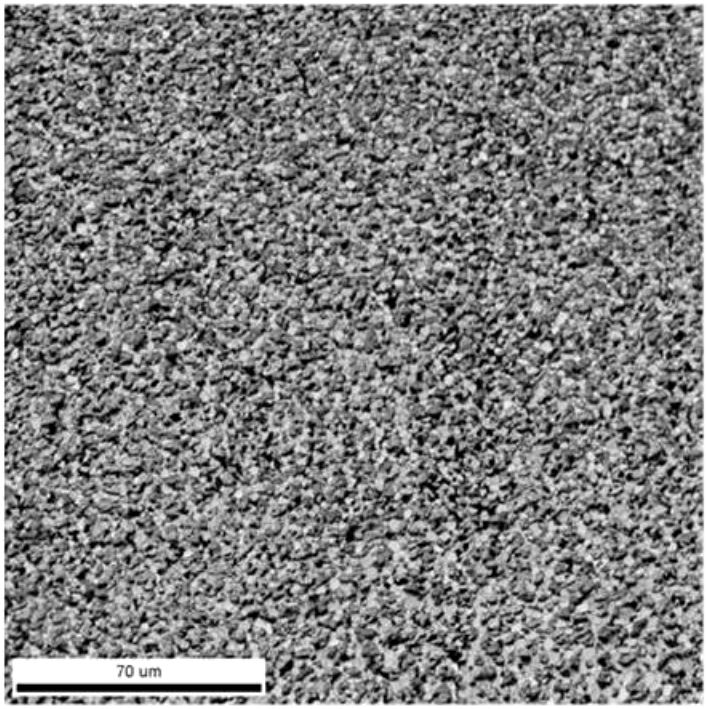

X = 200 microns
Y = 200 microns
Step size = 0.2 microns

b) Sn with 1.3% Au, Sample 268, 18 months at 50% RH / 50°C

Electroplated Sn with 1.3% Au
Color Coded Orientation Map

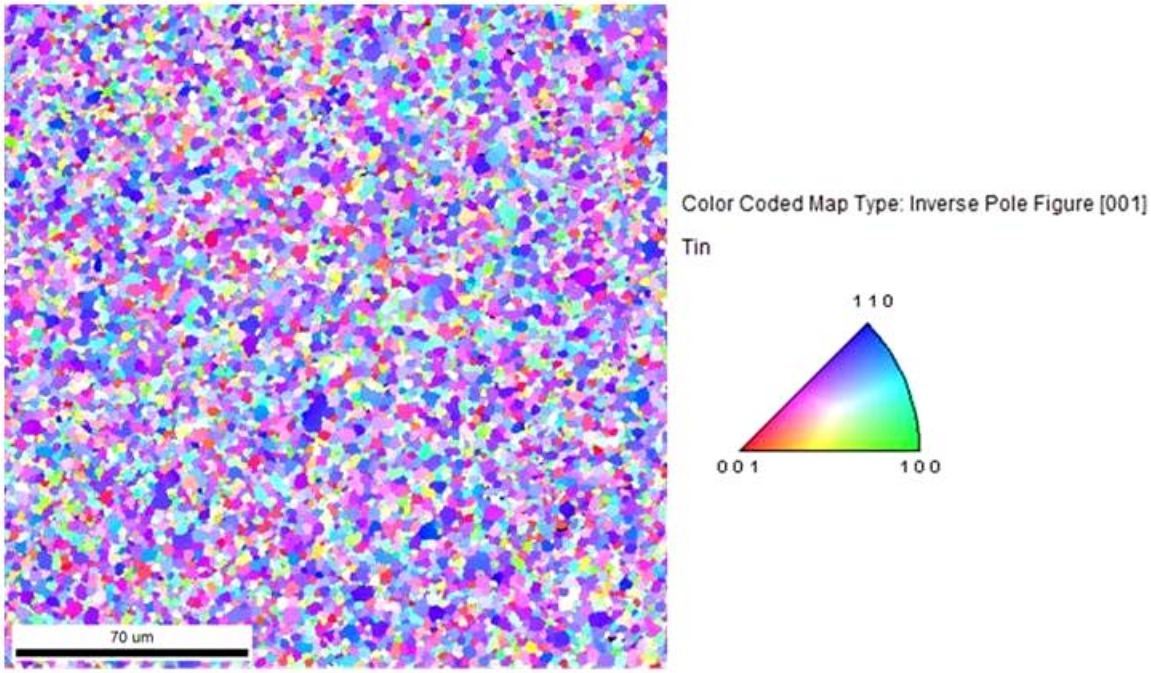

a) Sn with 1.3% Au, Sample 267, post plating

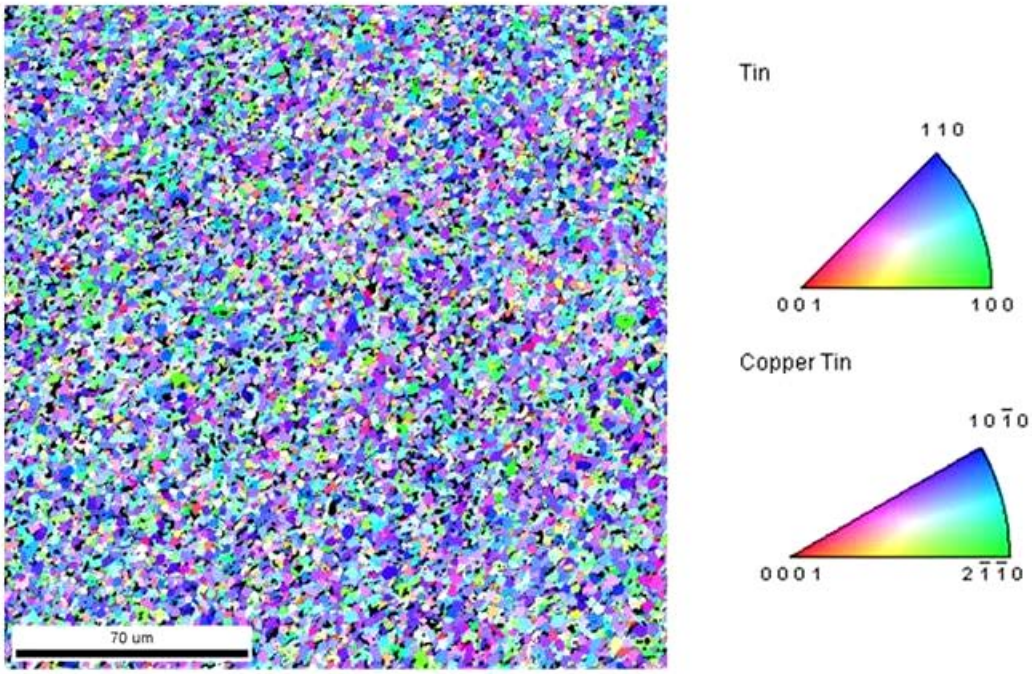

b) Sn with 1.3% Au, Sample 268, 18 months at 50% RH / 50°C

Electroplated Sn with 1.3% Au
Color Coded Orientation Map

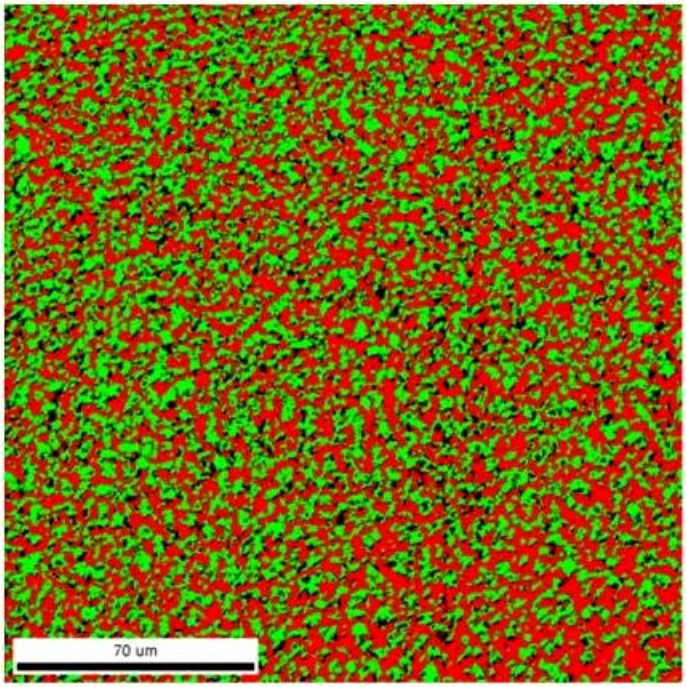

Figure 3. Phase ID map showing 2 phases

Color Coded Map Type: Phase

Phase	Total Fraction	Partition Fraction
Tin	0.477	0.547
Copper Tin	0.395	0.453

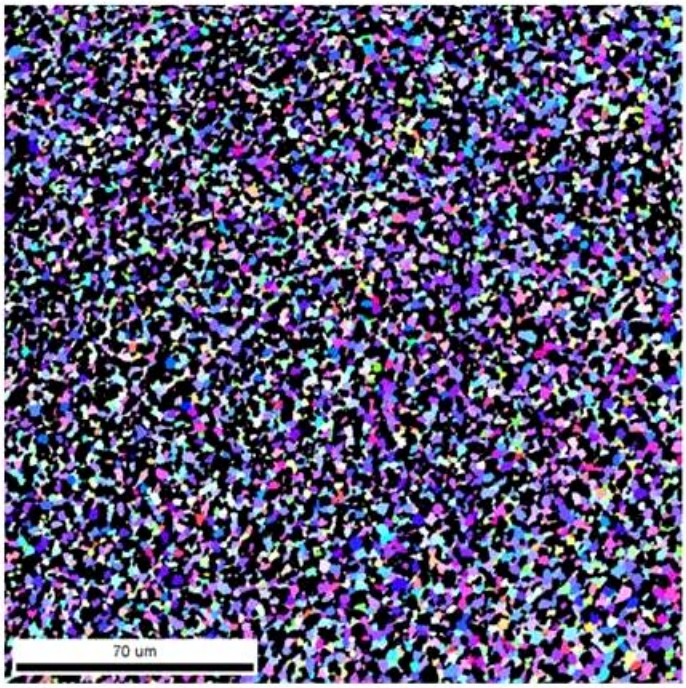

Figure 4. Color coded orientation map

Tin plating sample 268

Tin phase

Color Coded Map Type: Inverse Pole Figure [001]

Tin

Both scans show Sn with 1.3% Au, Sample 268, 18 months at 50% RH / 50°C

Electroplated Sn with 1.3% Au
Crystal Direction Map Showing <111> crystal direction in ND direction 15º Tolerance

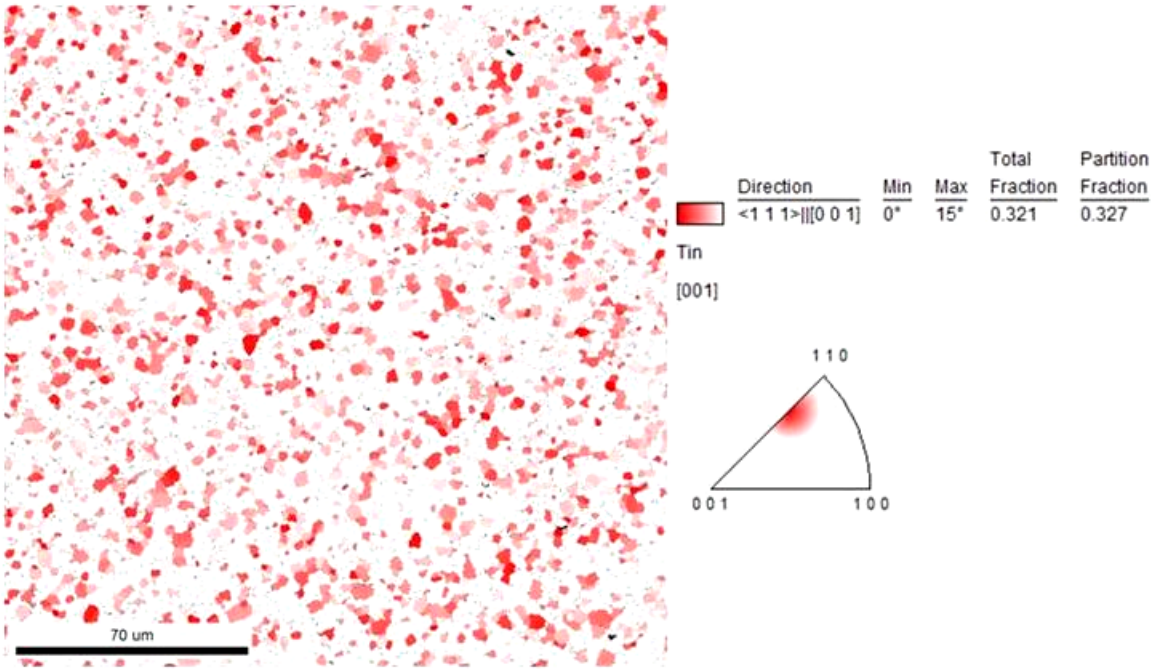

a) Sn with 1.3% Au, Sample 267, post plating

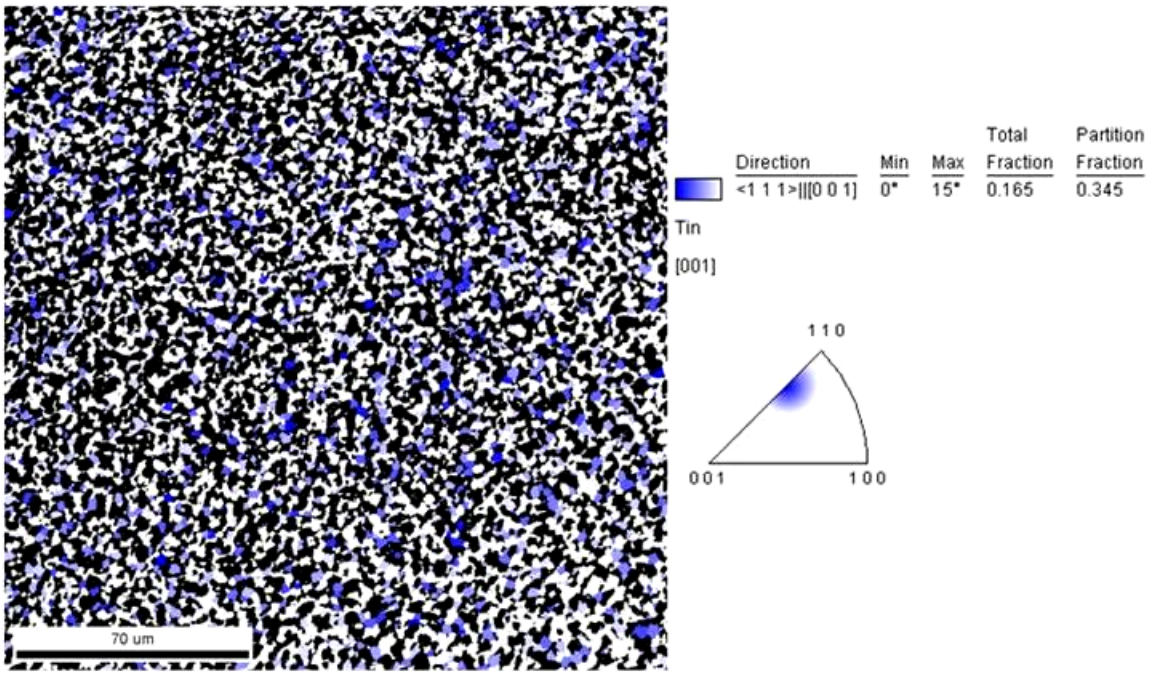

b) Sn with 1.3% Au, Sample 268, 18 months at 50% RH / 50°C

Electroplated Sn with 1.3% Au
Crystal Direction Map Showing <111> crystal direction in ND direction 20º Tolerance

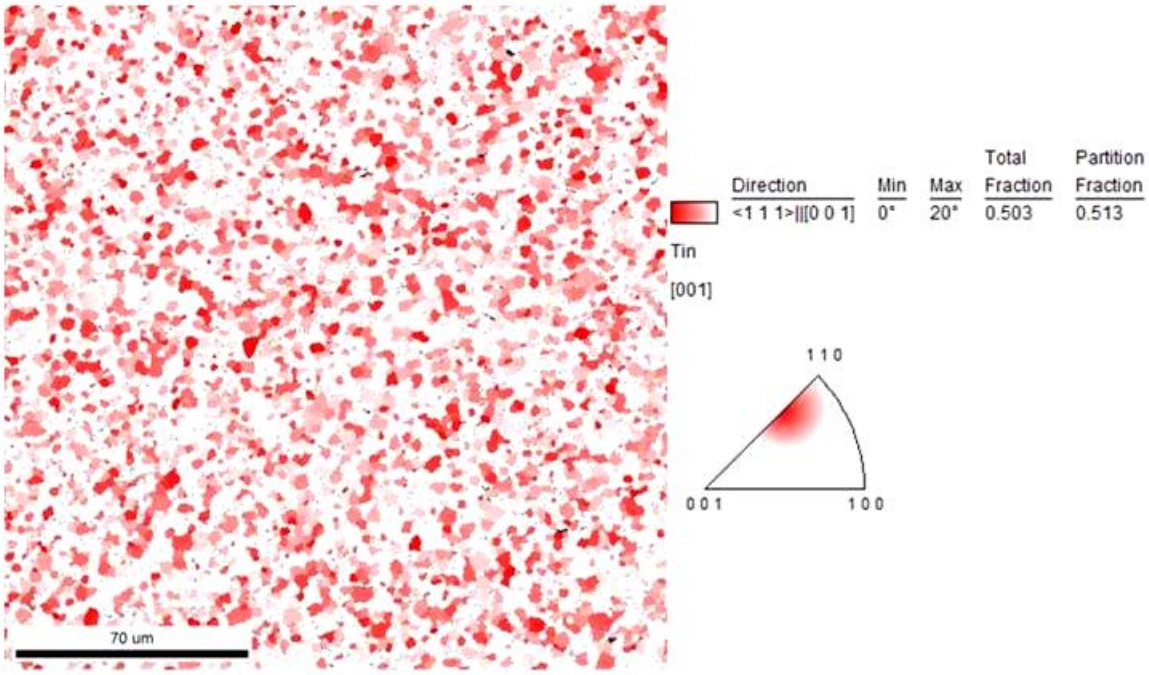

a) Sn with 1.3% Au, Sample 267, post plating

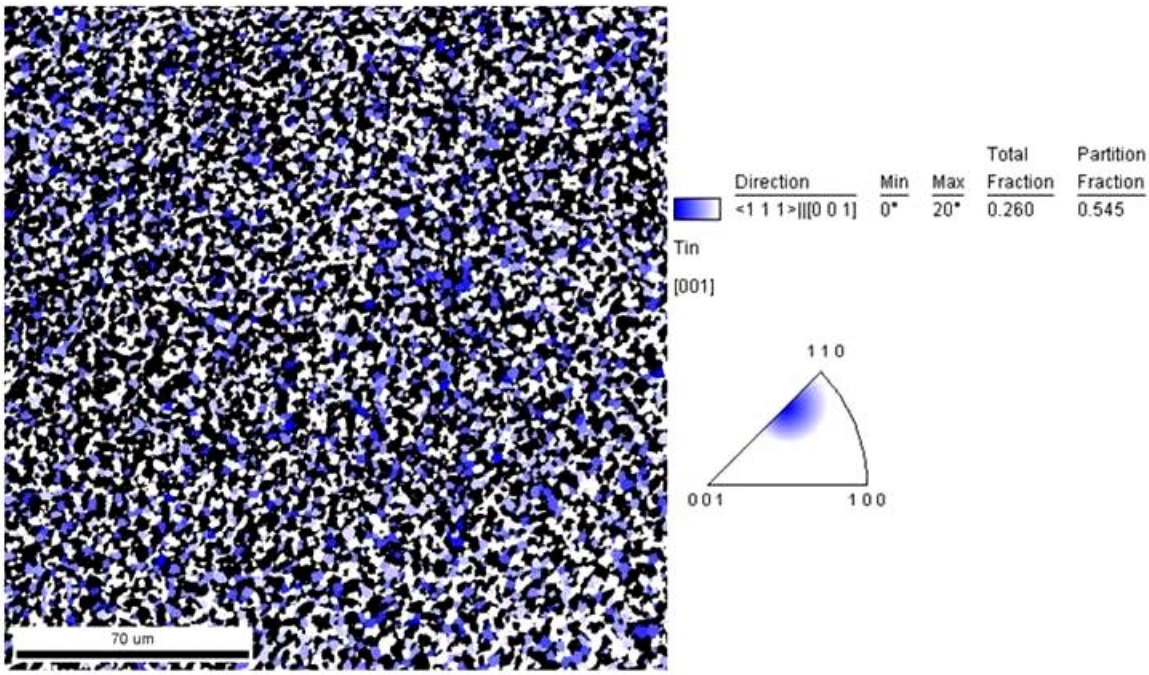

b) Sn with 1.3% Au, Sample 268, 18 months at 50% RH / 50°C

Electroplated Sn with 1.3% Au

Confidence Index (CI) Chart

Data points with a CI above 0.1 are generally considered to be indexed correctly.

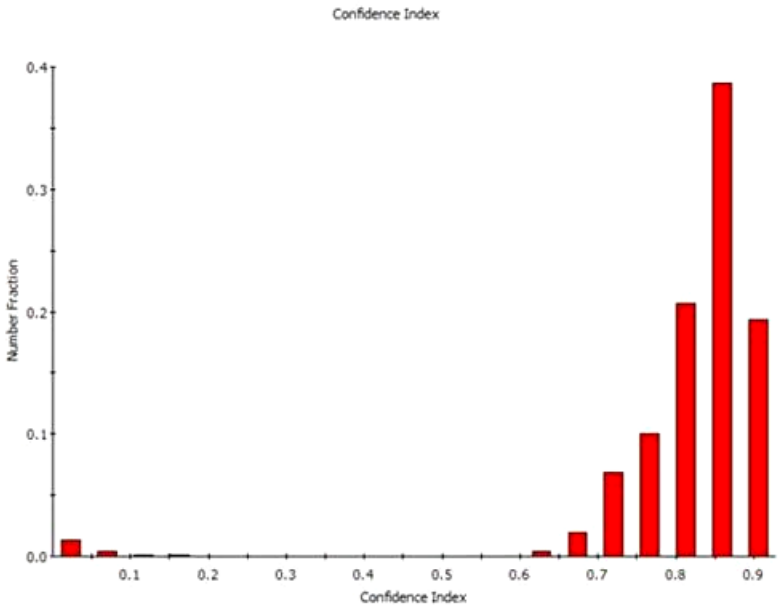

CI	Number Fraction
0.023225	0.0136477
0.069675	0.00419098
0.116125	0.00102892
0.162575	0.000882675
0.209025	0.000266533
0.255475	0.000138459
0.301925	7.5287e-005
0.348375	6.14411e-005
0.394825	8.99983e-005
0.441275	0.000109902
0.487725	5.97104e-005
0.534175	0.000102979
0.580625	7.87485e-005
0.627075	0.00372368
0.673525	0.0197849
0.719975	0.0682256
0.766425	0.100442
0.812875	0.207076
0.859325	0.387039
0.905775	0.192974
Average	
Number	0.818662
Standard Deviation	0.134501

a) Sn with 1.3% Au, Sample 267, post plating. Indicates that about 1.4% of data points were not indexed with a high degree of confidence

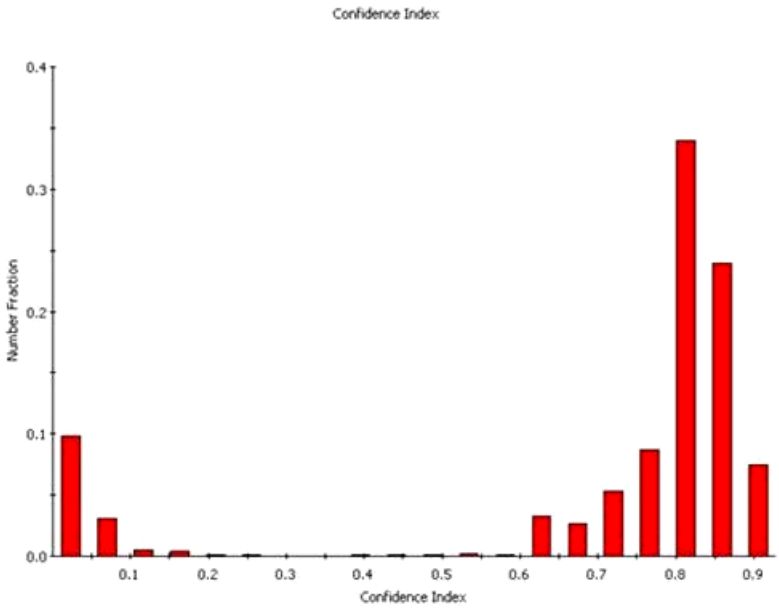

CI	Number Fraction
0.023225	0.0983361
0.069675	0.0302645
0.116125	0.00515327
0.162575	0.00369426
0.209025	0.00131796
0.255475	0.000713928
0.301925	0.000465568
0.348375	0.000460376
0.394825	0.000747678
0.441275	0.00125565
0.487725	0.000572874
0.534175	0.00180602
0.580625	0.00116046
0.627075	0.0322367
0.673525	0.0263418
0.719975	0.0533266
0.766425	0.0874281
0.812875	0.339816
0.859325	0.239794
0.905775	0.0751079
Average	
Number	0.702463
Standard Deviation	0.283941

(b) Sn with 1.3% Au, Sample 268, 18 months at 50% RH / 50°C. Indicates that about 88.0% of data points were not indexed with a high degree of confidence

Electroplated Sn with 1.3% Au
Pole Figure and Inverse Pole Figure Plots

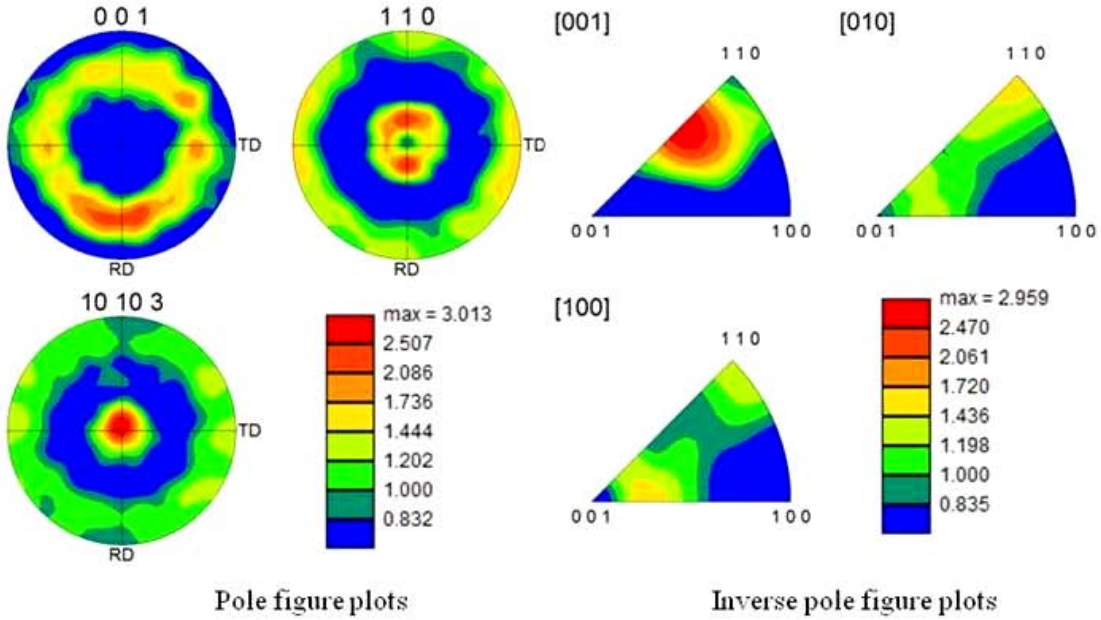

Pole figure plots

Inverse pole figure plots

a) Sn with 1.3% Au, Sample 267, post plating

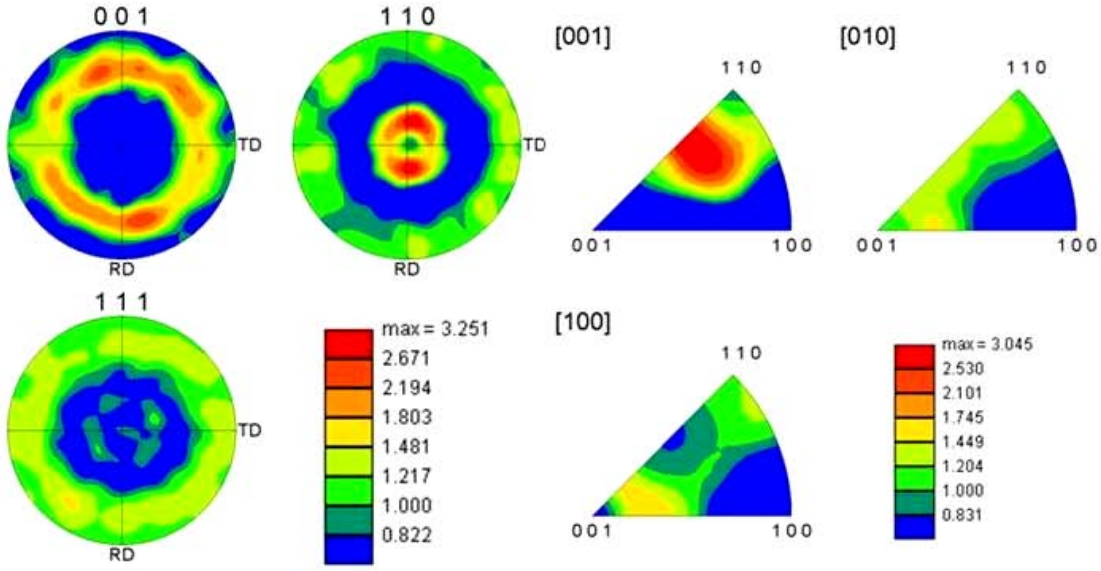

Pole figure plots

Inverse pole figure plots

b) Sn with 1.3% Au, Sample 268, 18 months at 50% RH / 50°C

Electroplated Sn with 1.3% Au
Grain Size Histogram and Data

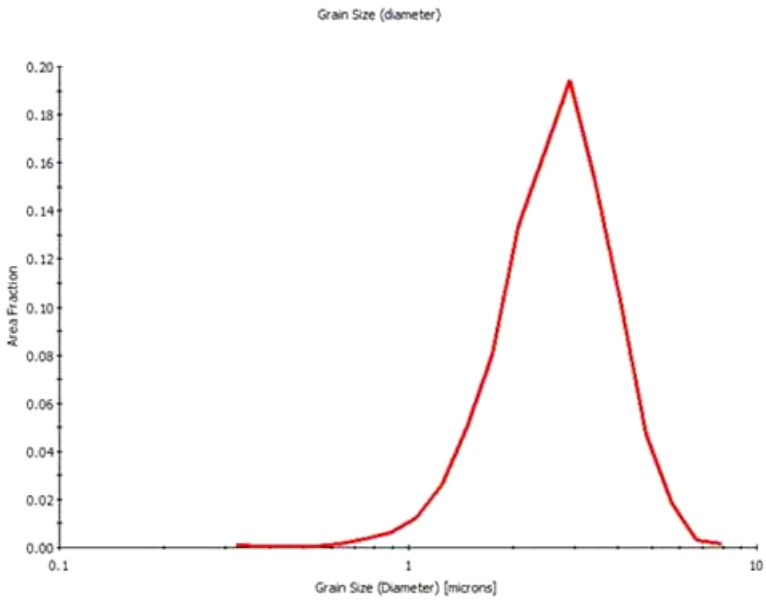

a) Sn with 1.3% Au, Sample 267, post plating

Edge grains included in analysis

Diameter [microns]	Area Fraction
0.323153	0.00102919
0.382556	0.000328353
0.452878	0.000523423
0.536127	0.000550786
0.634679	0.00131606
0.751348	0.00359158
0.889462	0.00603393
1.05296	0.0121138
1.24652	0.026127
1.47566	0.0495813
1.74692	0.0804925
2.06804	0.133365
2.4482	0.163935
2.89823	0.194155
3.43099	0.153706
4.06168	0.102865
4.8083	0.0471452
5.69218	0.0183984
6.73852	0.00323499
7.97721	0.0015076

Average	
Number	1.91866
Standard Deviation	0.973311
Area	2.8133

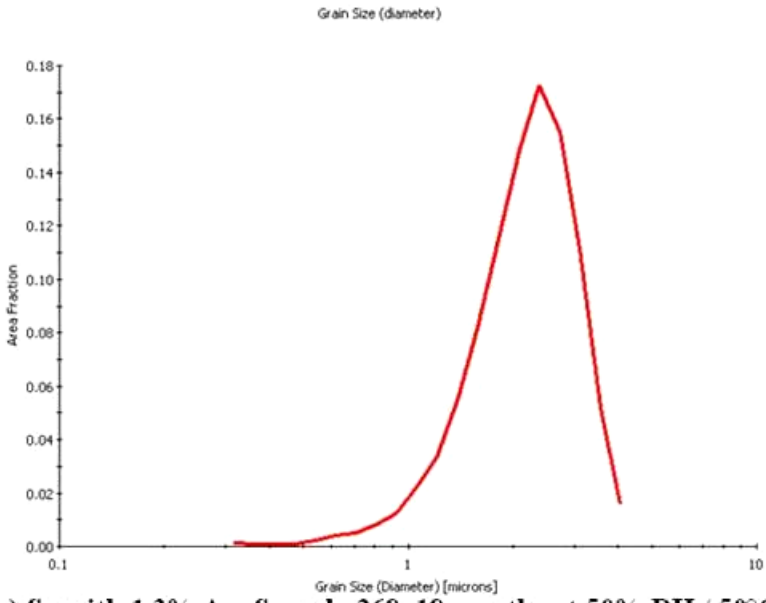

b) Sn with 1.3% Au, Sample 268, 18 months at 50% RH / 50°C

Edge grains included in analysis

Diameter [microns]	Area Fraction
0.317611	0.00150717
0.363208	0.000948413
0.415352	0.000963117
0.474981	0.000955765
0.543171	0.00228648
0.621151	0.00418882
0.710326	0.00526957
0.812303	0.00807254
0.92892	0.0124433
1.06228	0.0224274
1.21478	0.0334168
1.38918	0.0554399
1.58862	0.0818208
1.81669	0.115206
2.0775	0.148381
2.37575	0.172503
2.71682	0.155016
3.10686	0.111426
3.55289	0.0520248
4.06296	0.0157039

Average	
Number	1.55647
Standard Deviation	0.788404
Area	2.24367

Electroplated Sn with 1.3% Au
Misorientation Angle Histogram, 2º minimum misorientation

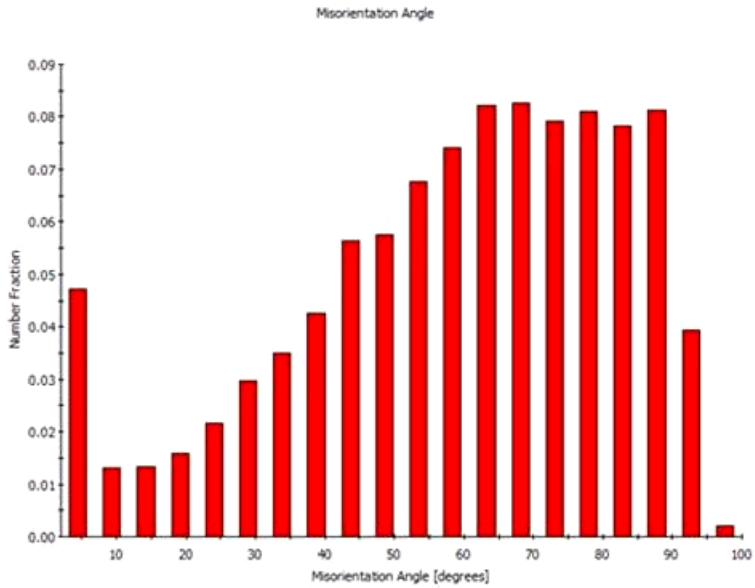

a) Sn with 1.3% Au, Sample 267, post plating

Chart: Misorientation Angle

Angle [degrees]	Number Fraction
4.45	0.0472356
9.35	0.0131578
14.25	0.0132495
19.15	0.0158197
24.05	0.0217482
28.95	0.0295935
33.85	0.0348973
38.75	0.0425765
43.65	0.0564965
48.55	0.0574793
53.45	0.0675712
58.35	0.0741758
63.25	0.0822791
68.15	0.0825914
73.05	0.07911
77.95	0.0810384
82.85	0.0782877
87.75	0.081302
92.65	0.0393587
97.55	0.00203155
Average Number	58.5957

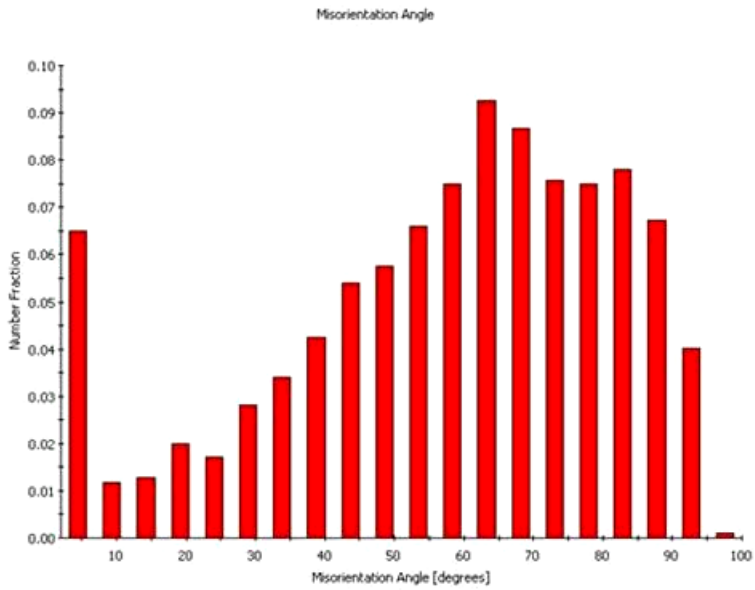

b) Sn with 1.3% Au, Sample 268, 18 months at 50% RH / 50°C

Chart: Misorientation Angle

Angle [degrees]	Number Fraction
4.45	0.0650477
9.35	0.0116822
14.25	0.0127431
19.15	0.0200165
24.05	0.0170223
28.95	0.028174
33.85	0.0339031
38.75	0.0423317
43.65	0.0540493
48.55	0.0576565
53.45	0.066038
58.35	0.0749027
63.25	0.0926677
68.15	0.0866085
73.05	0.0756926
77.95	0.074891
82.85	0.0780384
87.75	0.067205
92.65	0.0402334
97.55	0.00109631
Average Number	57.2659

Electroplated Sn with 1.3% Au
Misorientation Angle Histogram, 2º minimum misorientation

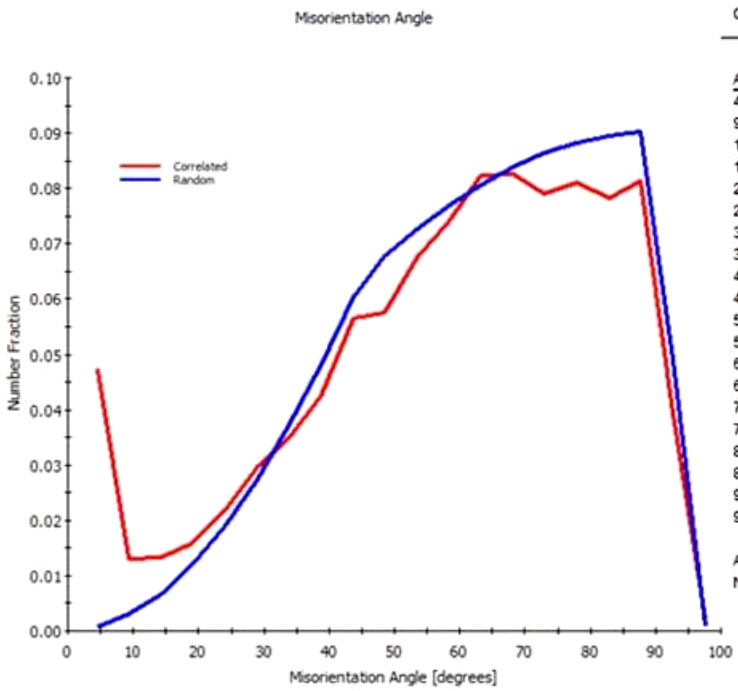

Chart: Misorientation Angle

Angle [degrees]	Correlated Number Fraction	Random Number Fraction
4.45	0.0472356	0.000708352
9.35	0.0131578	0.00294675
14.25	0.0132495	0.00675694
19.15	0.0158197	0.0121111
24.05	0.0217482	0.01897
28.95	0.0295935	0.0272836
33.85	0.0348973	0.0369911
38.75	0.0425765	0.0480215
43.65	0.0564965	0.0602942
48.55	0.0574793	0.0677119
53.45	0.0675712	0.0725688
58.35	0.0741758	0.0768956
63.25	0.0822791	0.0806607
68.15	0.0825914	0.0838367
73.05	0.07911	0.0864002
77.95	0.0810384	0.0883325
82.85	0.0782877	0.0896196
87.75	0.081302	0.090252
92.65	0.0393587	0.0489887
97.55	0.00203155	0.000672778
Average Number	58.5957	63.0123

a) Sn with 1.3% Au, Sample 267, post plating

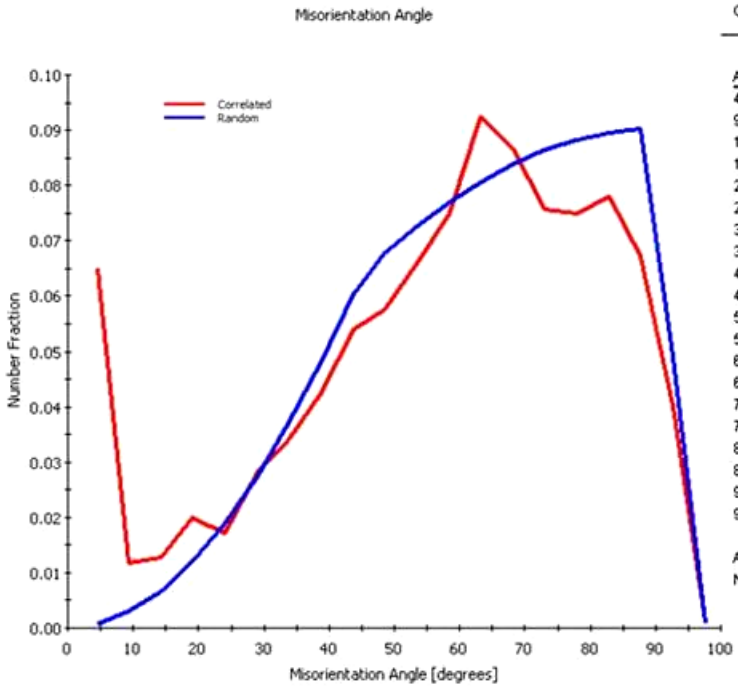

Chart: Misorientation Angle

Angle [degrees]	Correlated Number Fraction	Random Number Fraction
4.45	0.0650477	0.000712795
9.35	0.0116822	0.00295115
14.25	0.0127431	0.00676126
19.15	0.0200165	0.0121153
24.05	0.0170223	0.0189741
28.95	0.028174	0.0272875
33.85	0.0339031	0.0369948
38.75	0.0423317	0.048025
43.65	0.0540493	0.0602975
48.55	0.0576565	0.067715
53.45	0.066038	0.0725718
58.35	0.0749027	0.0768986
63.25	0.0926677	0.0806636
68.15	0.0866085	0.0838395
73.05	0.0756926	0.0864029
77.95	0.074891	0.0883352
82.85	0.0780384	0.0896222
87.75	0.067205	0.0902546
92.65	0.0402334	0.0489922
97.55	0.00109631	0.000677222
Average Number	57.2659	63.0123

b) Sn with 1.3% Au, Sample 268, 18 months at 50% RH / 50°C

Electroplated Sn with 1.3% Au
Grain Boundary Characterization Chart

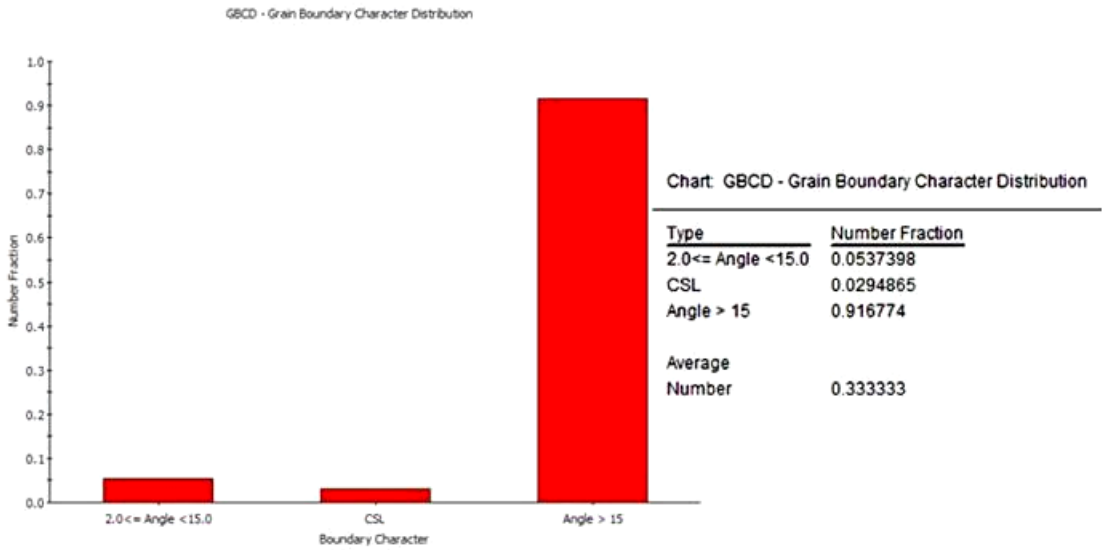

a) Sn with 1.3% Au, Sample 267, post plating

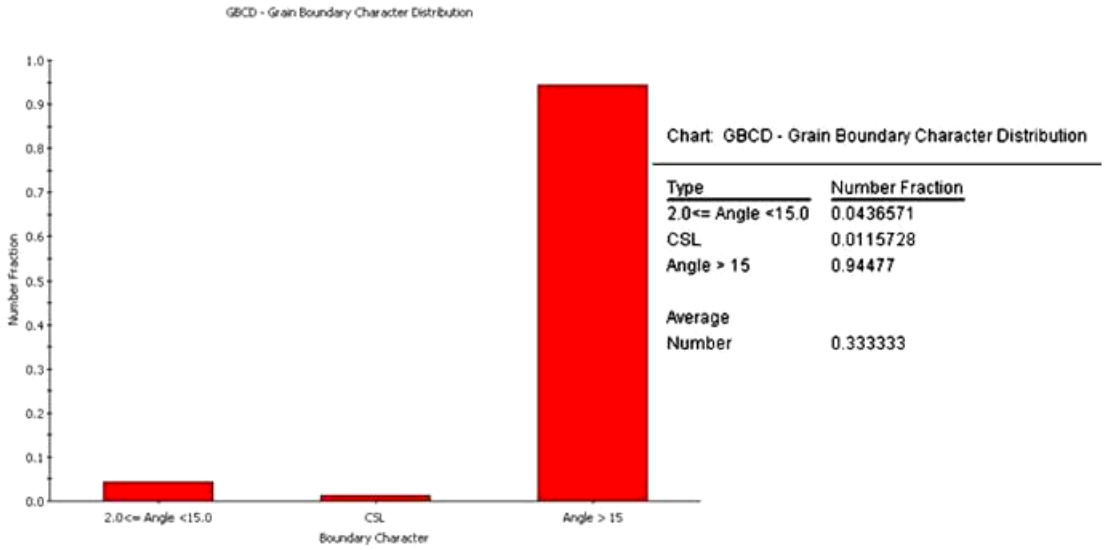

b) Sn with 1.3% Au, Sample 268, 18 months at 50% RH / 50°C

Electroplated Sn with 1.3% Au

Coincident Site Lattice Boundary Chart

The total fraction of CSL boundaries is approximately 2% of boundaries measured

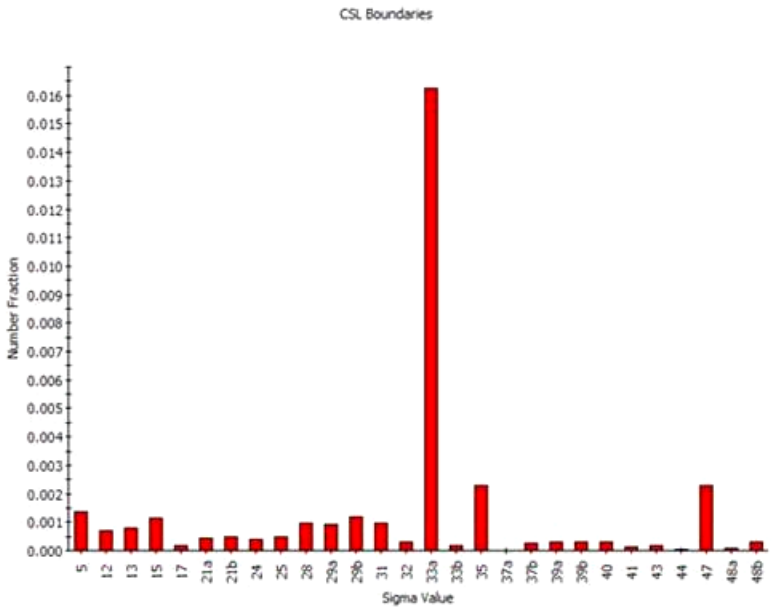

Overall fraction of CSL boundaries: 0.033

Sigma	Number Fraction
5	0.00134941
12	0.000692938
13	0.000773173
15	0.0011476
17	0.000172627
21a	0.000425488
21b	0.000474116
24	0.000406038
25	0.000471684
28	0.000989565
29a	0.000914192
29b	0.00120596
31	0.000953094
32	0.000316077
33a	0.0162707
33b	0.000162901
35	0.00229764
37a	1.94509e-005
37b	0.000272313
39a	0.00030392
39b	0.000325803
40	0.000289332
41	0.000136156
43	0.000172627
44	5.349e-005
47	0.00227332
48a	8.75291e-005
48b	0.000318509

a) Sn with 1.3% Au, Sample 267, post plating

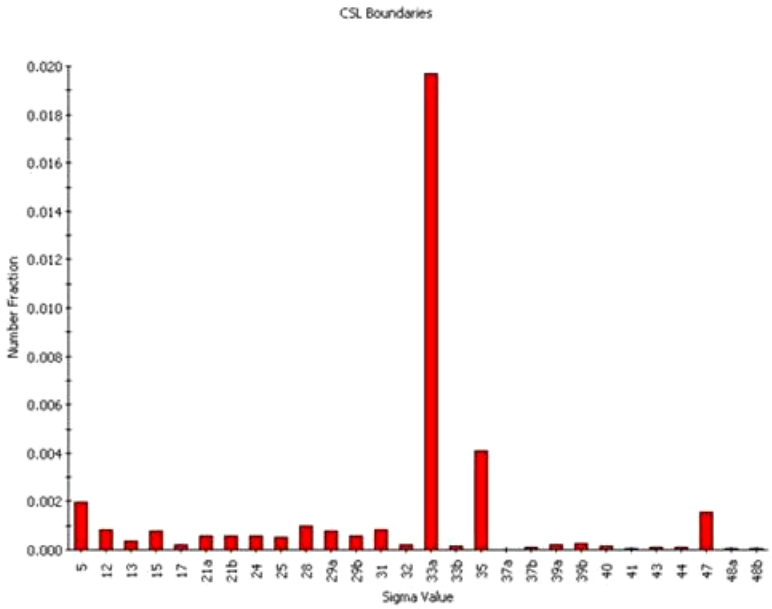

Overall fraction of CSL boundaries: 0.036

Sigma	Number Fraction
5	0.00198043
12	0.000836968
13	0.000365437
15	0.000801603
17	0.000200401
21a	0.000589414
21b	0.000554049
24	0.000577626
25	0.000518684
28	0.000966639
29a	0.000801603
29b	0.000589414
31	0.000836968
32	0.000188613
33a	0.0196864
33b	0.000153248
35	0.00407875
37a	2.35766e-005
37b	0.000117883
39a	0.000188613
39b	0.00027113
40	0.000141459
41	4.71531e-005
43	0.000106095
44	8.2518e-005
47	0.00156784
48a	3.53648e-005
48b	4.71531e-005

b) Sn with 1.3% Au, Sample 268, 18 months at 50% RH / 50°C

Electroplated Sn with 1.3% Au
Misorientation Distribution Function (MODF) Plot

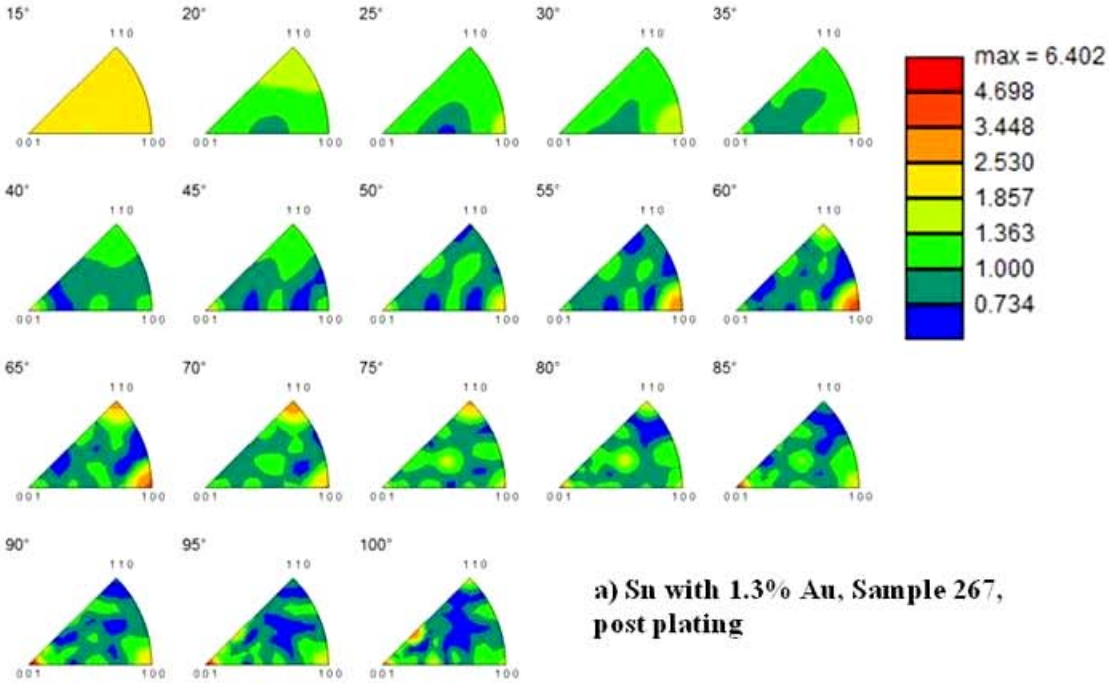

a) Sn with 1.3% Au, Sample 267, post plating

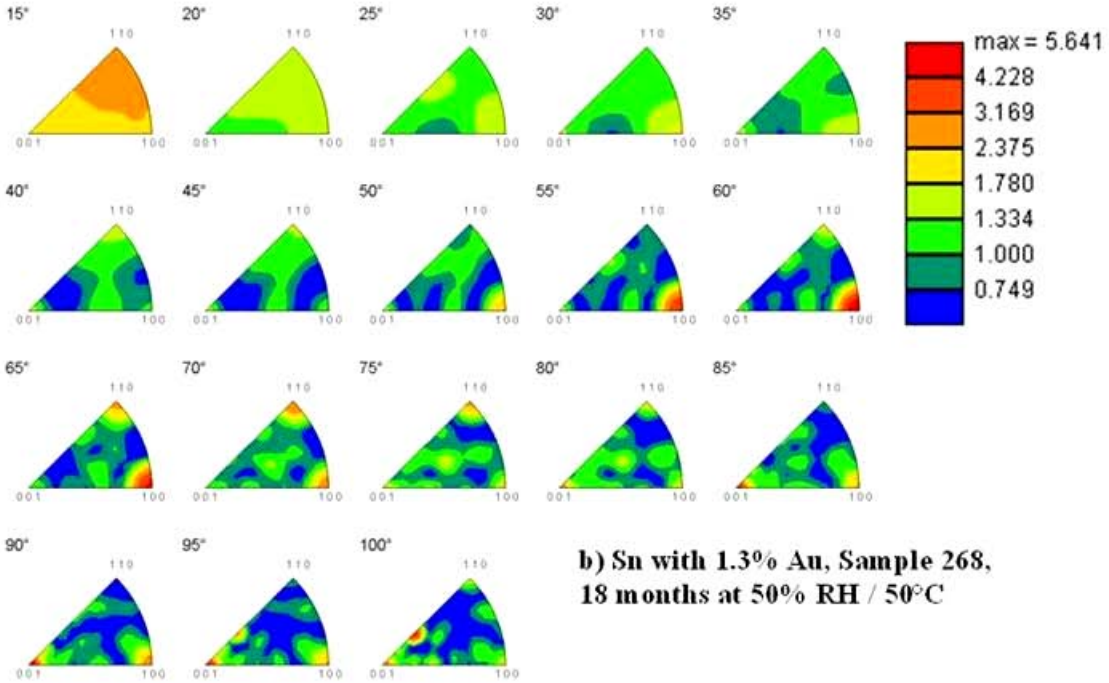

b) Sn with 1.3% Au, Sample 268, 18 months at 50% RH / 50°C

Electroplated Sn with 1.3% Au

Crystal Direction Map

Blue Indicates C-Direction in sample normal

Red indicates C-direction in sample plane 15º tolerance

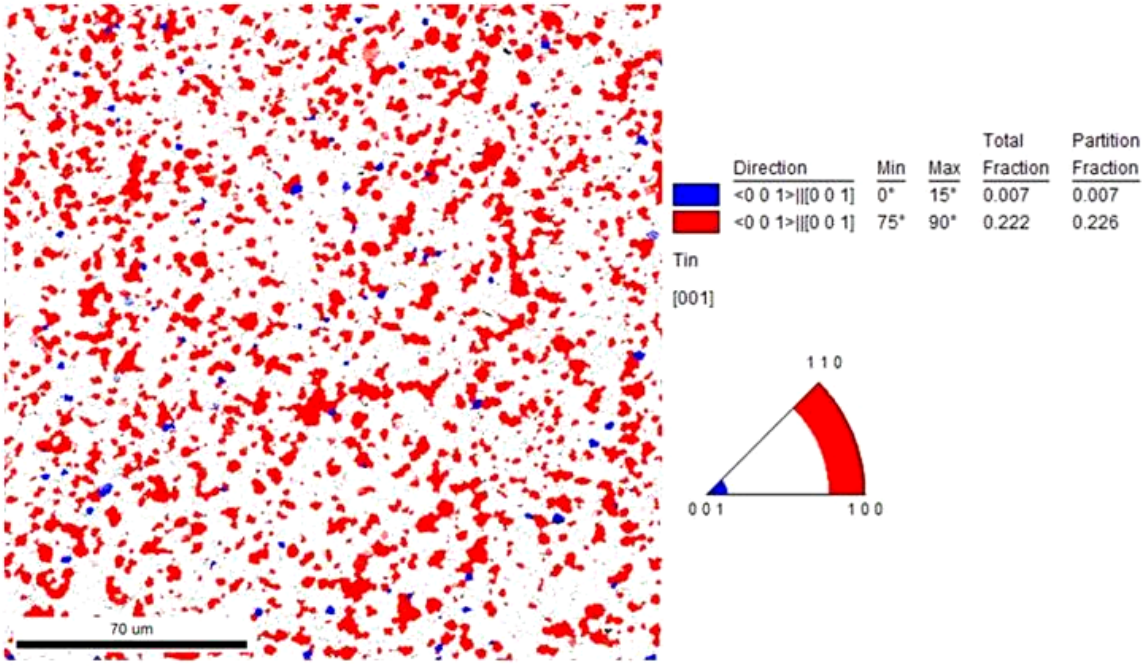

a) Sn with 1.3% Au, Sample 267, post plating

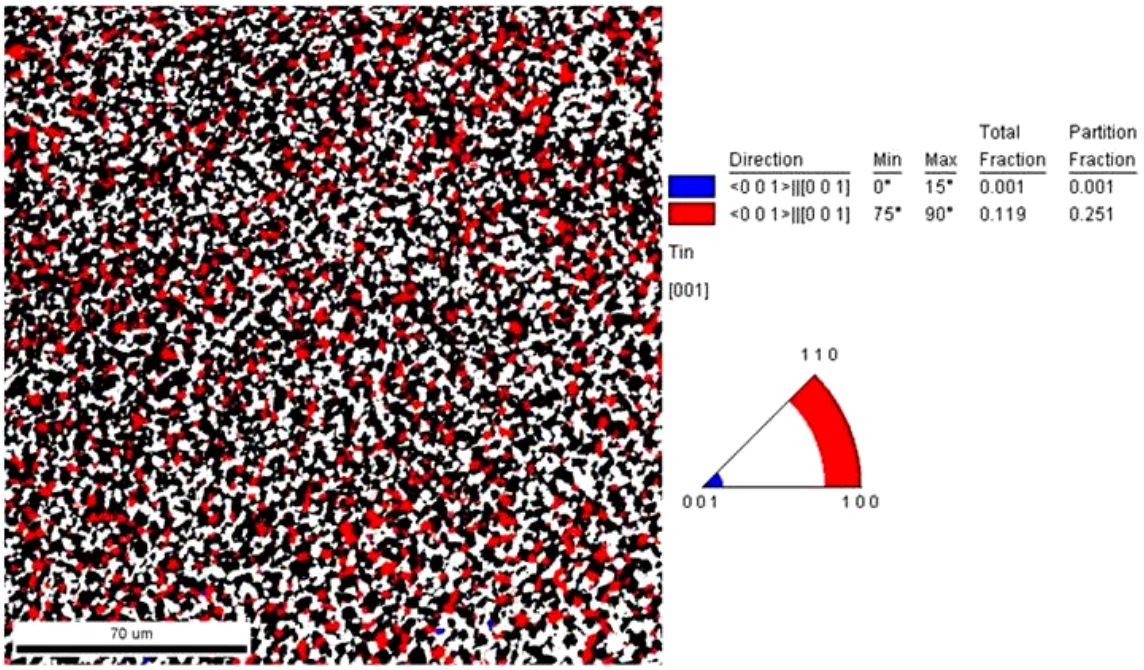

b) Sn with 1.3% Au, Sample 268, 18 months at 50% RH / 50°C

Appendix R: EBSD Data for Pure Tin prior to aging compared with Pure Tin with 53nm Au Cap Layer after aging

Pure Sn Post Plating / Pure Sn with 53nm Au Cap Post Plating
Image Quality Map

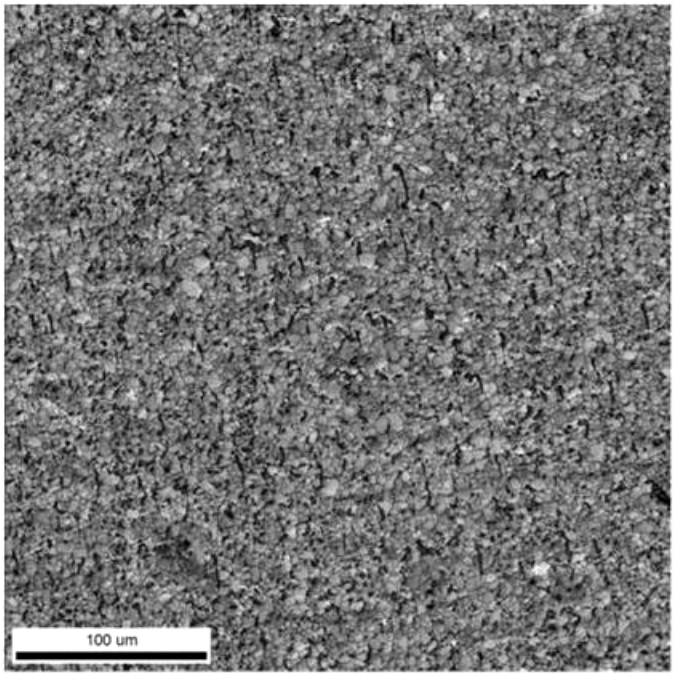

X = 350 microns
Y = 350 microns
Step size = 0.4 microns

a) Pure Tin, Sample 65, post plating

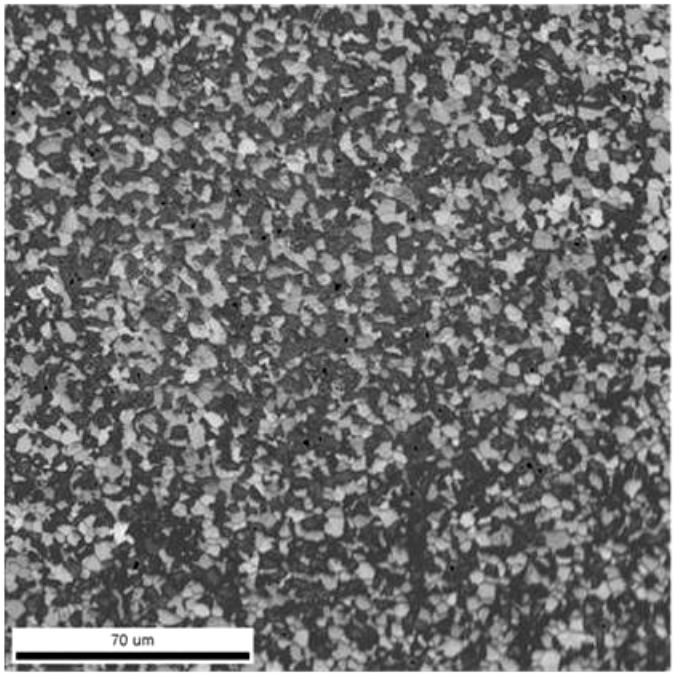

X = 200 microns
Y = 200 microns
Step size = 0.2 microns

b) Pure Tin with 53nm of Au sputtered on top, Sample 67, 18 months at 50% RH / 50°C

Pure Sn Post Plating / Pure Sn with 53nm Au Cap Post Plating
Color Coded Orientation Map

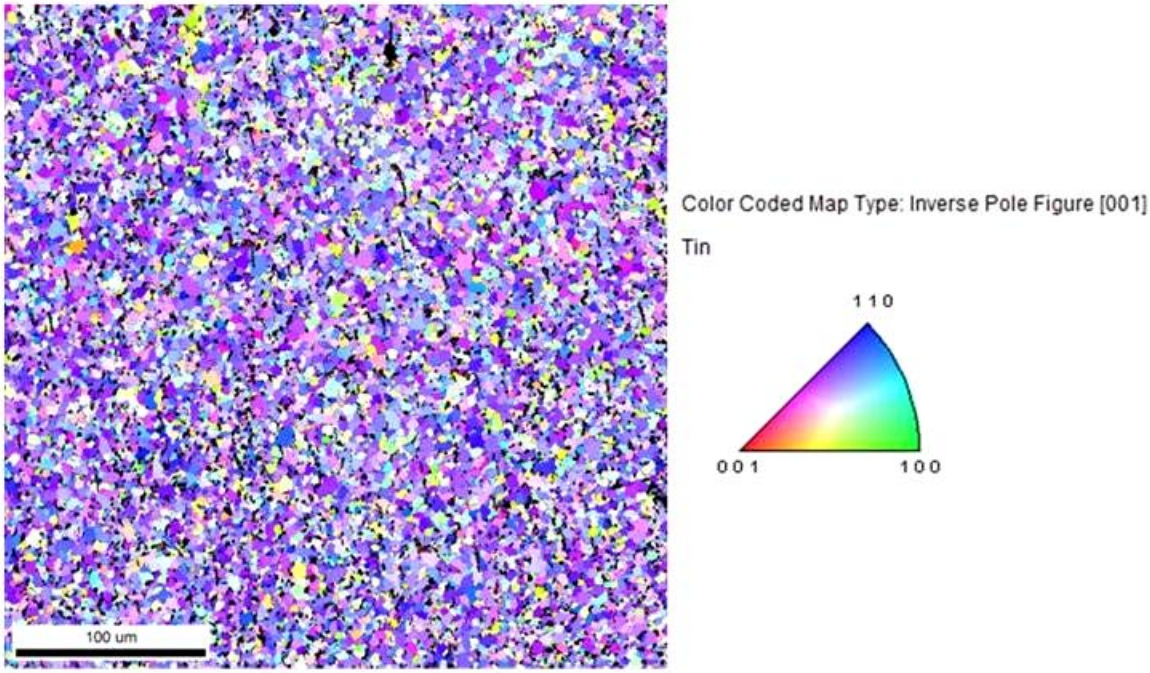

a) Pure Tin, Sample 65, post plating

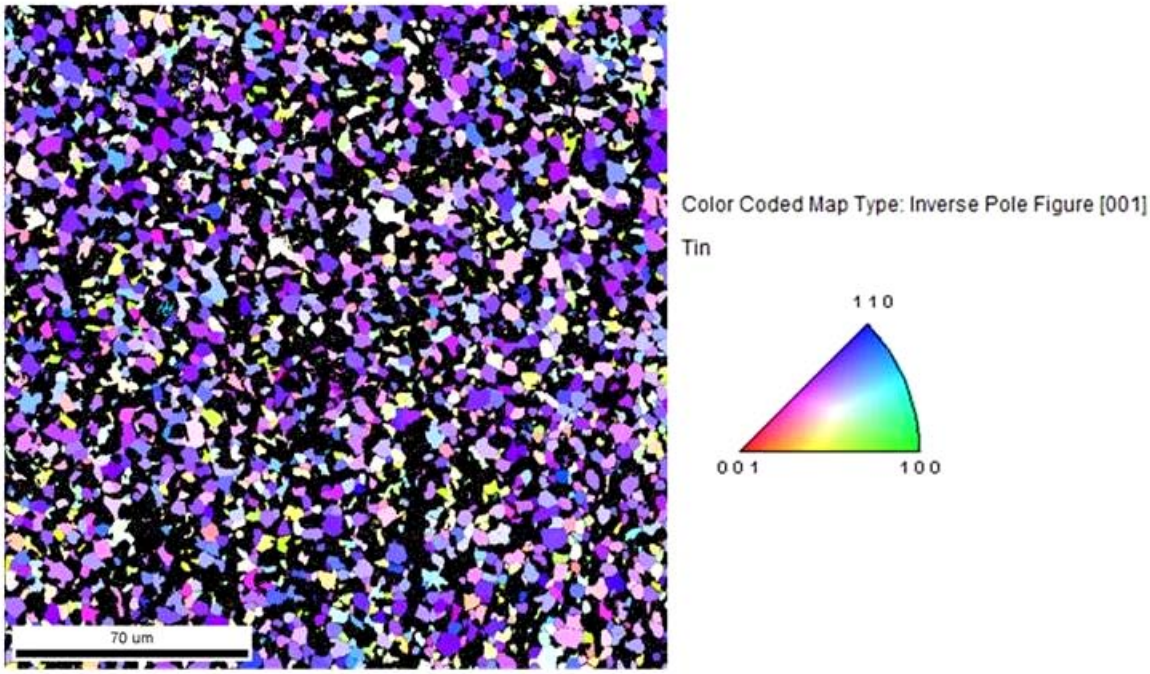

b) Pure Tin with 53nm of Au sputtered on top, Sample 67, 18 months at 50% RH / 50°C

Pure Sn Post Plating / Pure Sn with 53nm Au Cap Post Plating

Crystal Direction Map Showing <111> crystal direction in ND direction 15º Tolerance

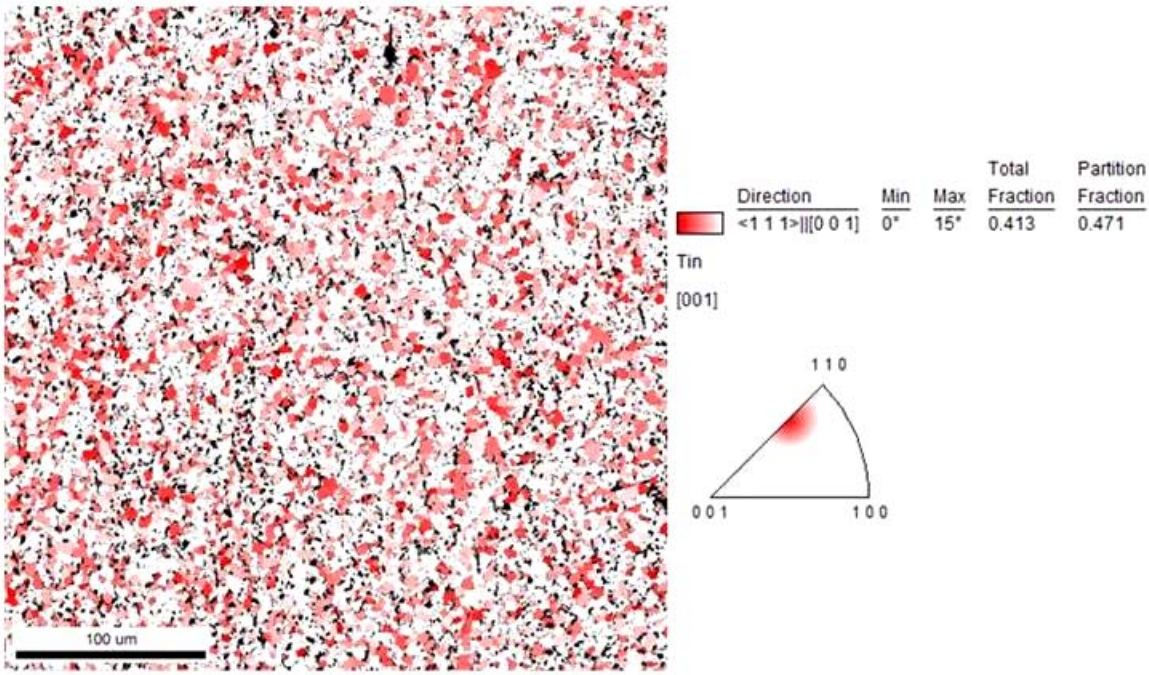

a) Pure Tin, Sample 65, post plating

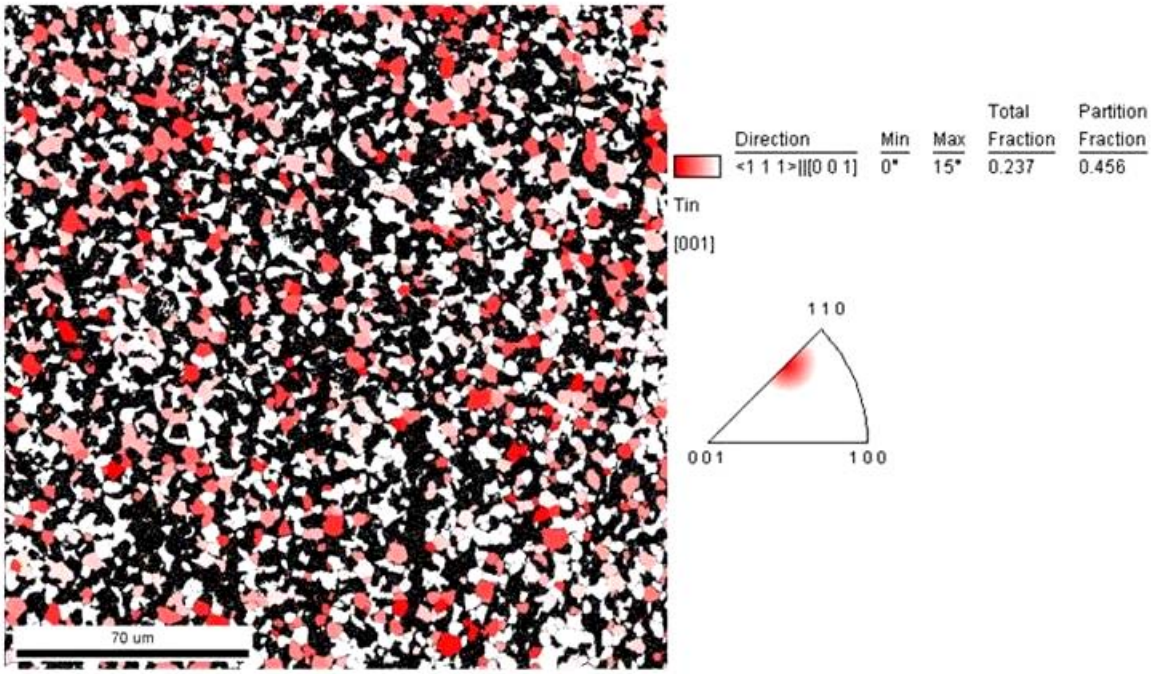

b) Pure Tin with 53nm of Au sputtered on top, Sample 67, 18 months at 50% RH / 50°C

Pure Sn Post Plating / Pure Sn with 53nm Au Cap Post Plating

Crystal Direction Map Showing <111> crystal direction in ND direction 20º Tolerance

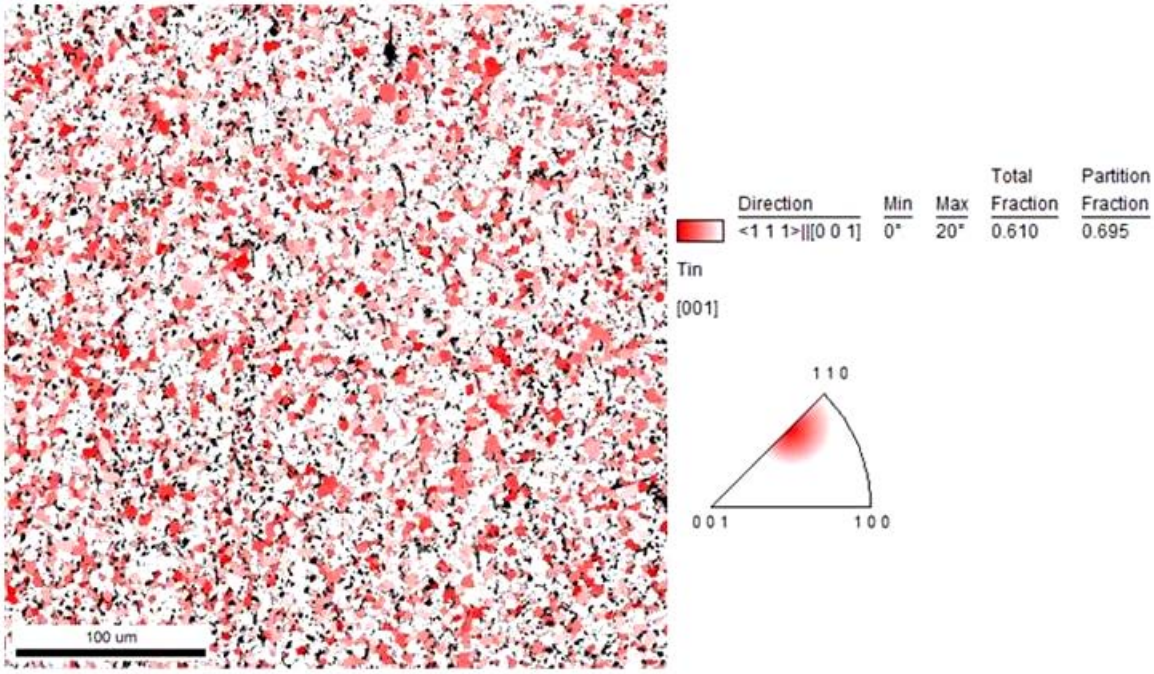

a) Pure Tin, Sample 65, post plating

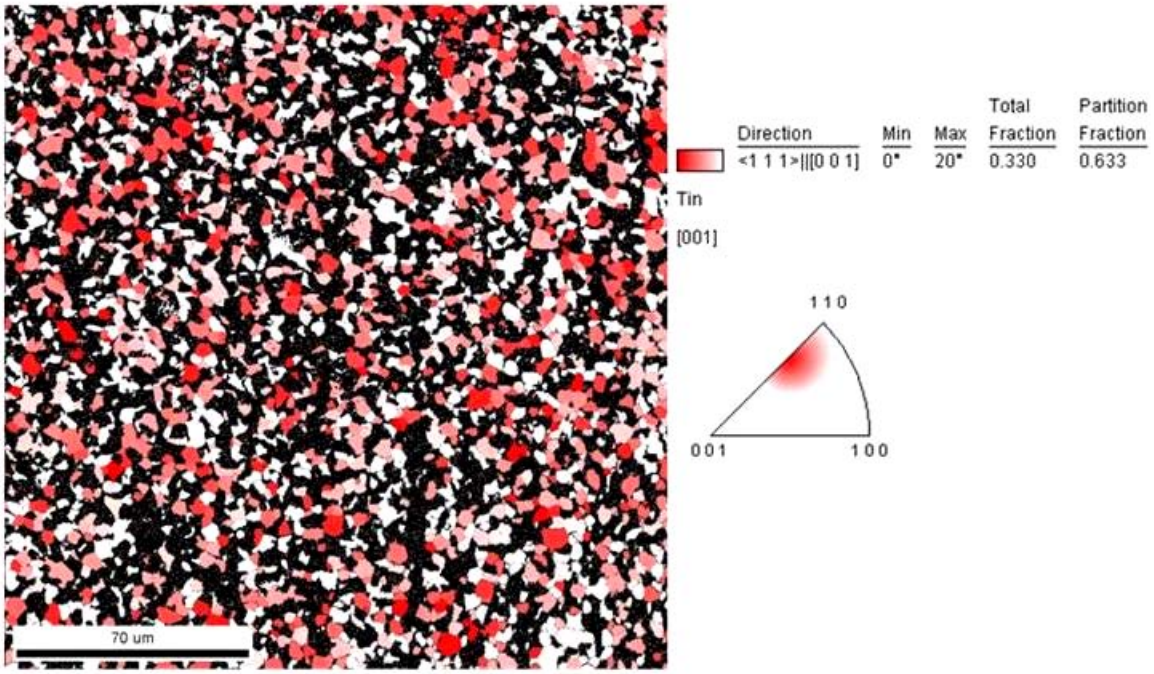

b) Pure Tin with 53nm of Au sputtered on top, Sample 67, 18 months at 50% RH / 50°C

Pure Sn Post Plating / Pure Sn with 53nm Au Cap Post Plating

Confidence Index (CI) Chart

Data points with a CI above 0.1 are generally considered to be indexed correctly.

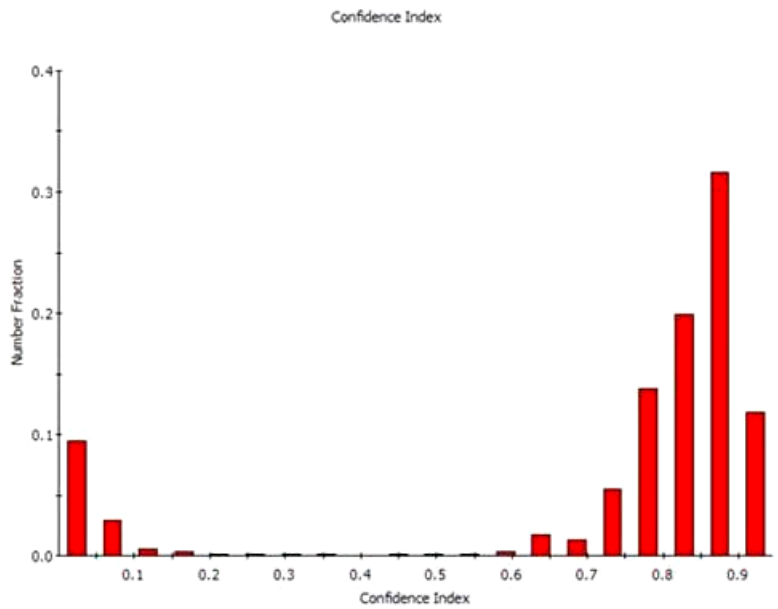

(a) Pure Tin, Sample 65, post plating. Indicates that about 12.3% of data points were not indexed with a high degree of confidence

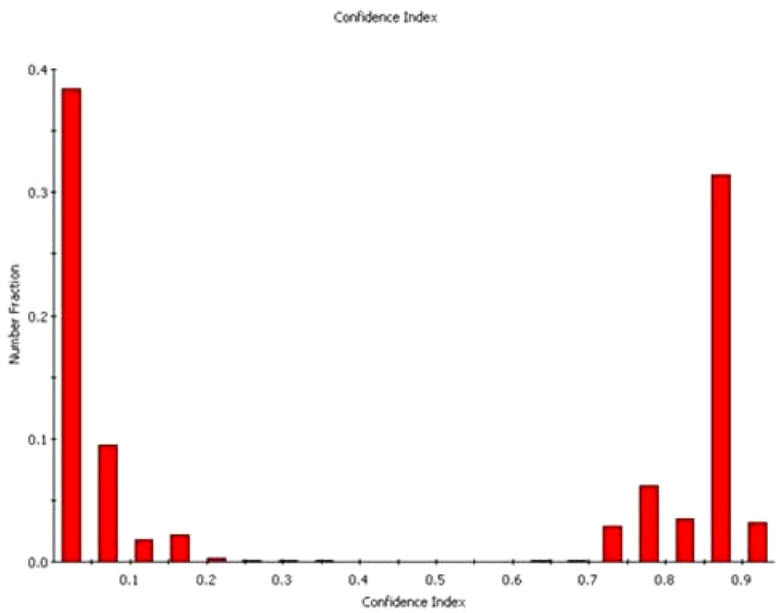

(b) Pure Tin with 53nm of Au sputtered on top, Sample 67, 18 months at 50% RH / 50°C. Indicates that about 48% of data points were not indexed with a high degree of confidence

Pure Sn Post Plating / Pure Sn with 53nm Au Cap Post Plating
Pole Figure and Inverse Pole Figure Plots

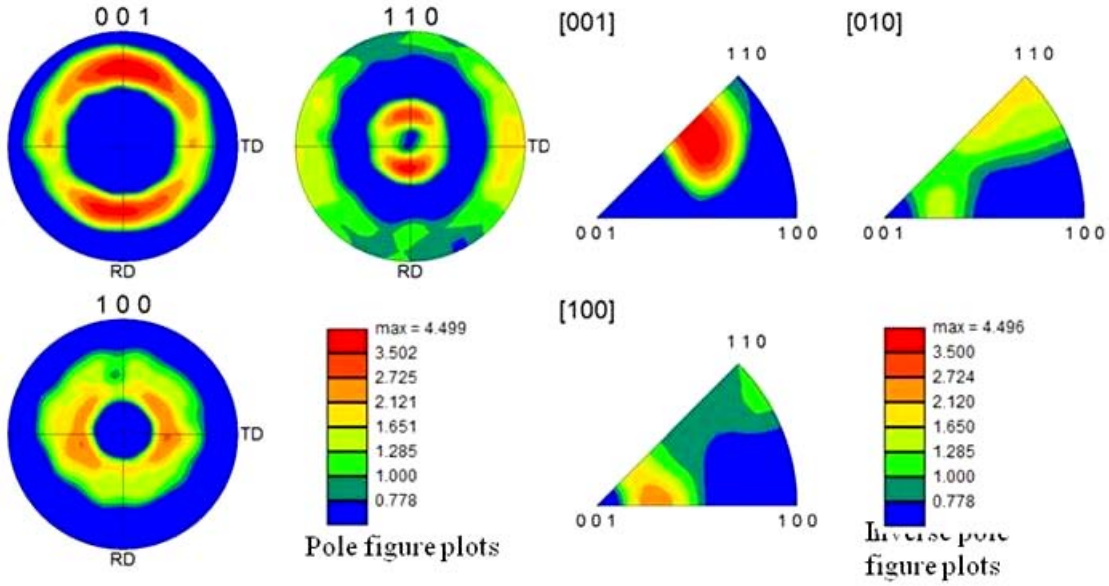

a) Pure Tin, Sample 65, post plating

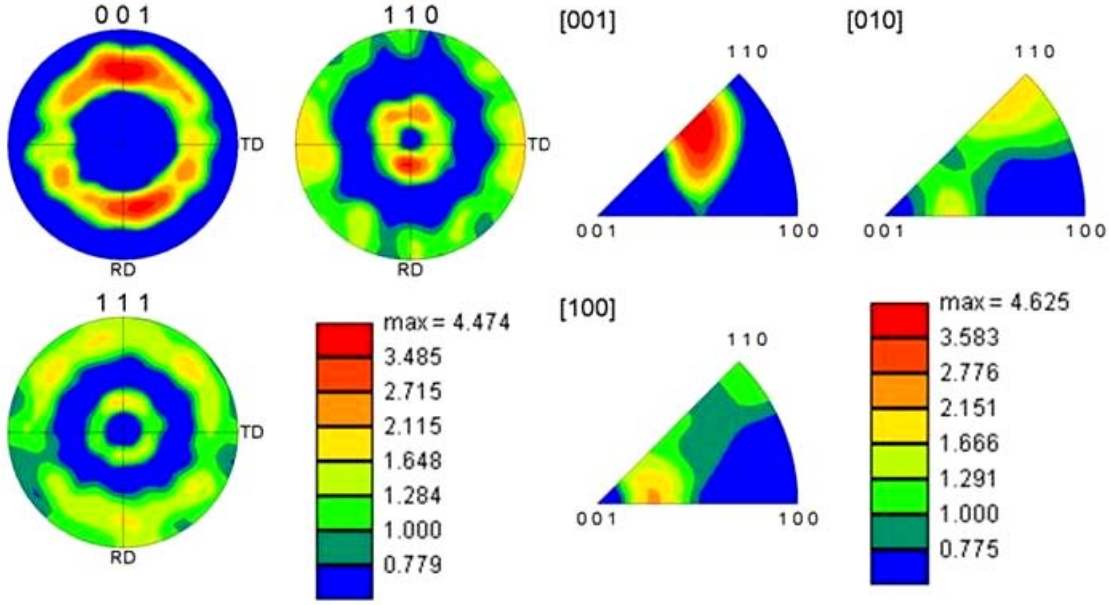

b) Pure Tin with 53nm of Au sputtered on top, Sample 67, 18 months at 50% RH / 50°C

Pure Sn Post Plating / Pure Sn with 53nm Au Cap Post Plating
Grain Size Histogram and Data

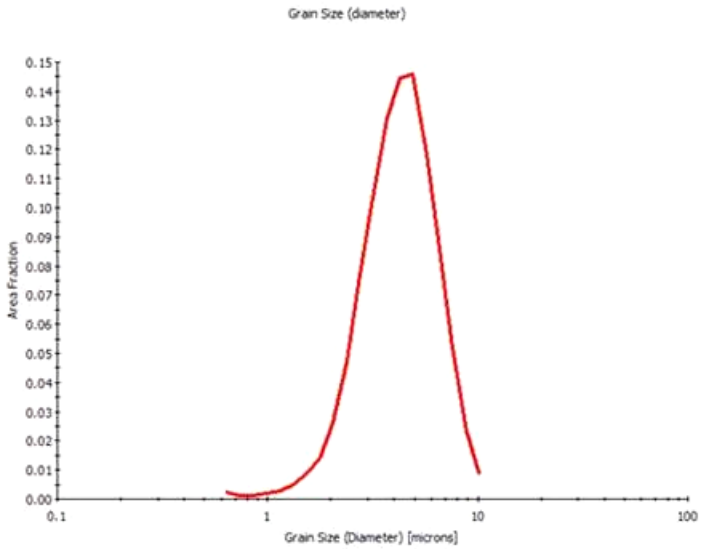

Edge grains included in analysis

Diameter [microns]	Area Fraction
0.638932	0.00253414
0.73922	0.00140641
0.855249	0.00118242
0.98949	0.0021643
1.1448	0.00275552
1.32449	0.00487555
1.53239	0.00874968
1.77291	0.0142047
2.05119	0.0260784
2.37315	0.0470756
2.74564	0.0771349
3.1766	0.10313
3.6752	0.130137
4.25207	0.14427
4.91948	0.145863
5.69164	0.118551
6.58501	0.0857153
7.61861	0.052123
8.81443	0.0233919
10.198	0.00865722

Average	
Number	2.87793
Standard Deviation	1.59386
Area	4.49422

a) Pure Tin, Sample 65, post plating

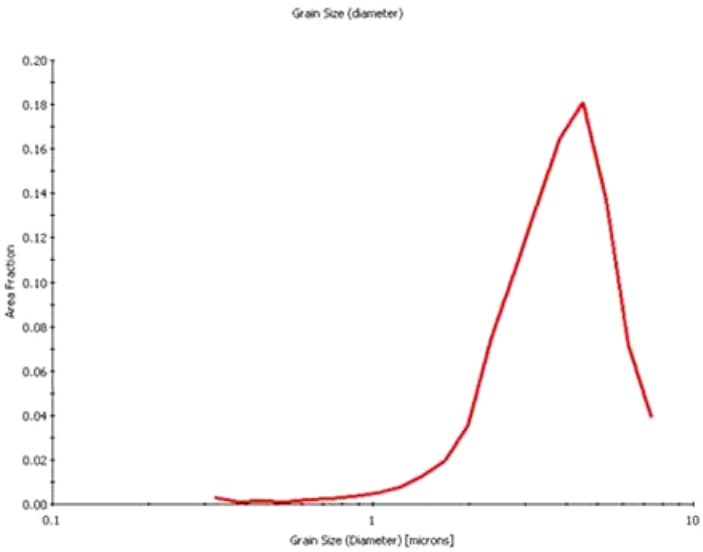

Edge grains included in analysis

Diameter [microns]	Area Fraction
0.322531	0.00295984
0.380351	0.00109228
0.448536	0.00137124
0.528944	0.001239
0.623768	0.00183133
0.73559	0.00243091
0.867458	0.00351775
1.02297	0.00512809
1.20635	0.00737424
1.42261	0.0126038
1.67764	0.0194038
1.97839	0.0352337
2.33306	0.0749343
2.7513	0.103263
3.24452	0.134031
3.82616	0.164673
4.51207	0.18115
5.32095	0.137305
6.27483	0.0717698
7.39971	0.038688

Average	
Number	1.89142
Standard Deviation	1.56148
Area	3.94511

b) Pure Tin with 53nm of Au sputtered on top, Sample 67, 18 months at 50% RH / 50°C

Pure Sn Post Plating / Pure Sn with 53nm Au Cap Post Plating
Misorientation Angle Histogram, 2º minimum misorientation

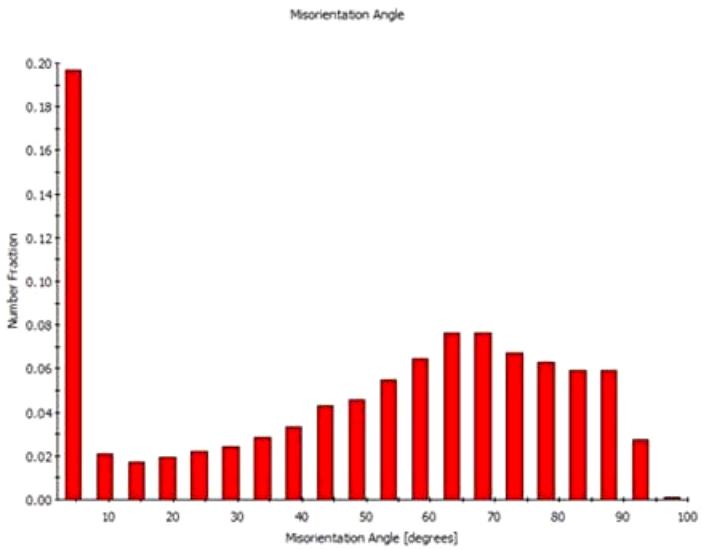

Angle [degrees]	Number Fraction
4.45	0.196949
9.35	0.0208752
14.25	0.0169873
19.15	0.0192069
24.05	0.0221032
28.95	0.024151
33.85	0.0286046
38.75	0.0333804
43.65	0.043247
48.55	0.0455847
53.45	0.0545885
58.35	0.0644981
63.25	0.0766094
68.15	0.0764125
73.05	0.0669648
77.95	0.0627439
82.85	0.0591101
87.75	0.0593214
92.65	0.0275234
97.55	0.00113845
Average Number	48.297

a) Pure Tin, Sample 65, post plating

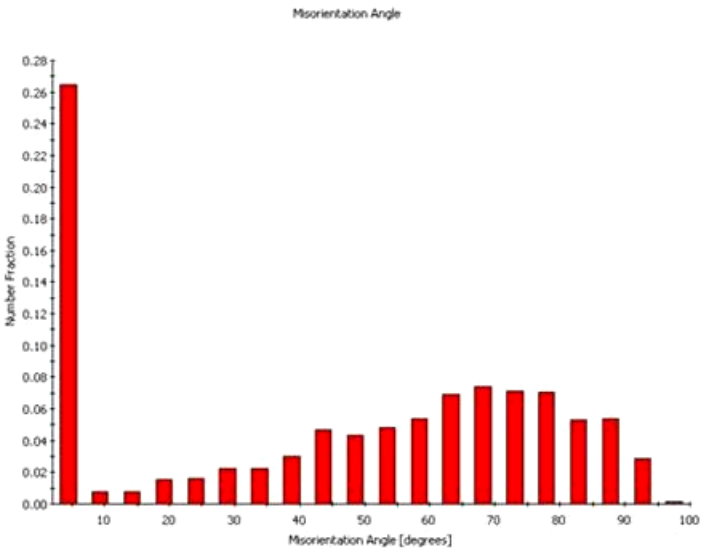

Angle [degrees]	Number Fraction
4.45	0.264825
9.35	0.00757666
14.25	0.0079452
19.15	0.0156303
24.05	0.0159988
28.95	0.0226541
33.85	0.0220146
38.75	0.0300899
43.65	0.0465439
48.55	0.0432162
53.45	0.0479638
58.35	0.0534919
63.25	0.0691004
68.15	0.0740974
73.05	0.0710515
77.95	0.0705529
82.85	0.0533835
87.75	0.0537303
92.65	0.0287675
97.55	0.00136575
Average Number	45.9969

b) Pure Tin with 53nm of Au sputtered on top, Sample 67, 18 months at 50% RH / 50°C

Pure Sn Post Plating / Pure Sn with 53nm Au Cap Post Plating
Misorientation Angle Histogram, 2º minimum misorientation

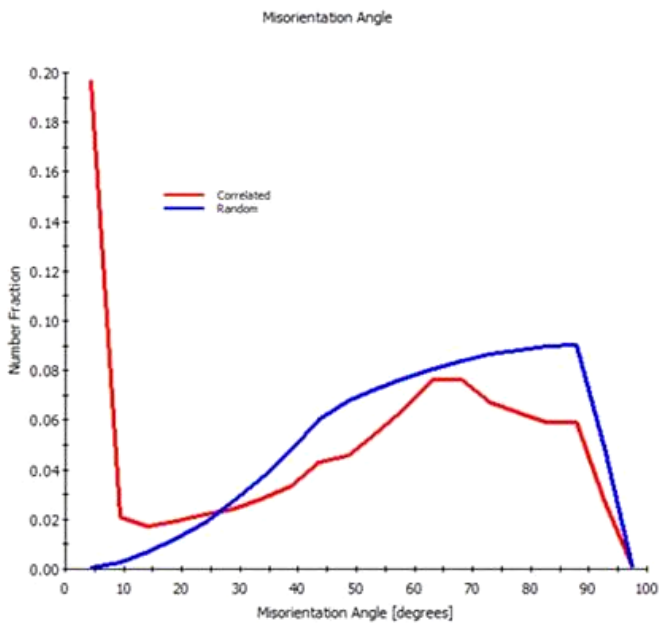

Chart: Misorientation Angle

Angle [degrees]	Correlated Number Fraction	Random Number Fraction
4.45	0.196949	0.000708709
9.35	0.0208752	0.00294711
14.25	0.0169873	0.00675729
19.15	0.0192069	0.0121114
24.05	0.0221032	0.0189703
28.95	0.024151	0.0272839
33.85	0.0286046	0.0369914
38.75	0.0333804	0.0480218
43.65	0.043247	0.0602946
48.55	0.0455847	0.0677123
53.45	0.0545885	0.0725691
58.35	0.0644981	0.076896
63.25	0.0766094	0.0806611
68.15	0.0764125	0.083837
73.05	0.0669648	0.0864005
77.95	0.0627439	0.0883329
82.85	0.0591101	0.0896199
87.75	0.0593214	0.0902523
92.65	0.0275234	0.0489891
97.55	0.00113845	0.000673135
Average Number	48.297	63.0123

a) Pure Tin, Sample 65, post plating

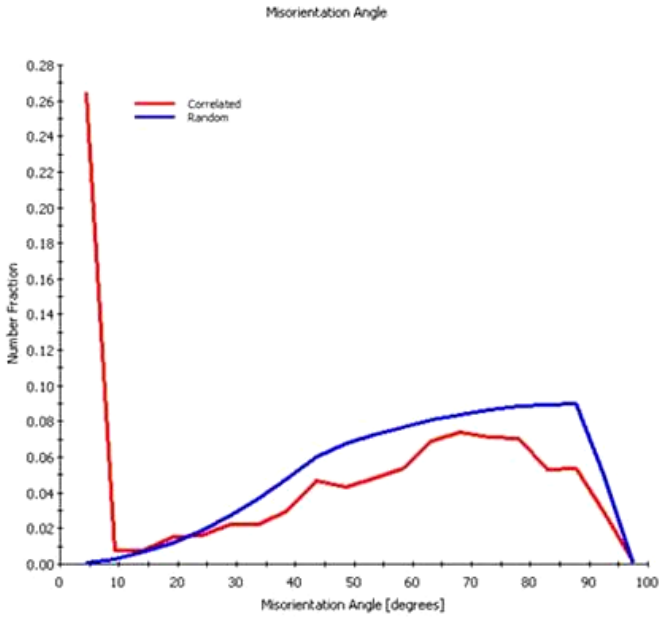

Chart: Misorientation Angle

Angle [degrees]	Correlated Number Fraction	Random Number Fraction
4.45	0.264825	0.000712341
9.35	0.00757666	0.00295076
14.25	0.0079452	0.00676098
19.15	0.0156303	0.0121151
24.05	0.0159988	0.0189741
28.95	0.0226541	0.0272878
33.85	0.0220146	0.0369954
38.75	0.0300899	0.0480259
43.65	0.0465439	0.0602987
48.55	0.0432162	0.0677165
53.45	0.0479638	0.0725734
58.35	0.0534919	0.0769003
63.25	0.0691004	0.0806654
68.15	0.0740974	0.0838414
73.05	0.0710515	0.0864049
77.95	0.0705529	0.0883373
82.85	0.0533835	0.0896243
87.75	0.0537303	0.0902567
92.65	0.0287675	0.0489931
97.55	0.00136575	0.000676767
Average Number	45.9969	63.0123

b) Pure Tin with 53nm of Au sputtered on top, Sample 67, 18 months at 50% RH / 50°C

Pure Sn Post Plating / Pure Sn with 53nm Au Cap Post Plating
Grain Boundary Characterization Chart

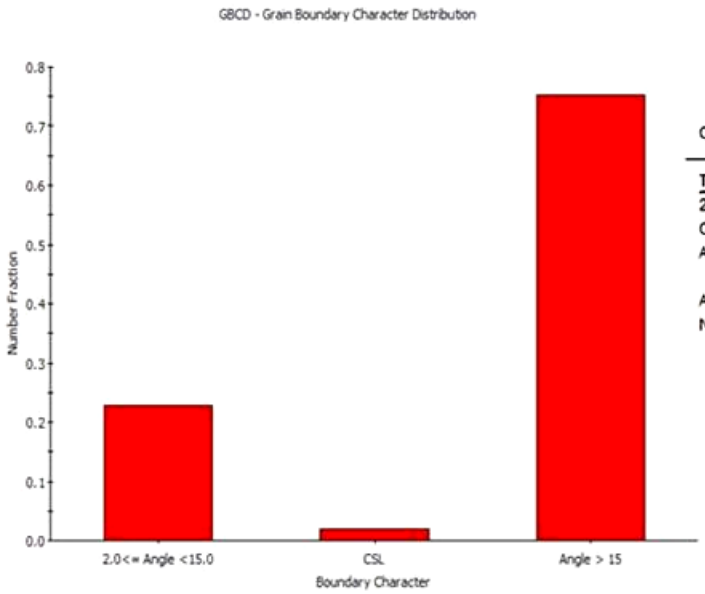

Chart: GBCD - Grain Boundary Character Distribution

Type	Number Fraction
2.0<= Angle <15.0	0.228862
CSL	0.0194755
Angle > 15	0.751663
Average Number	0.333333

a) Pure Tin, Sample 65, post plating

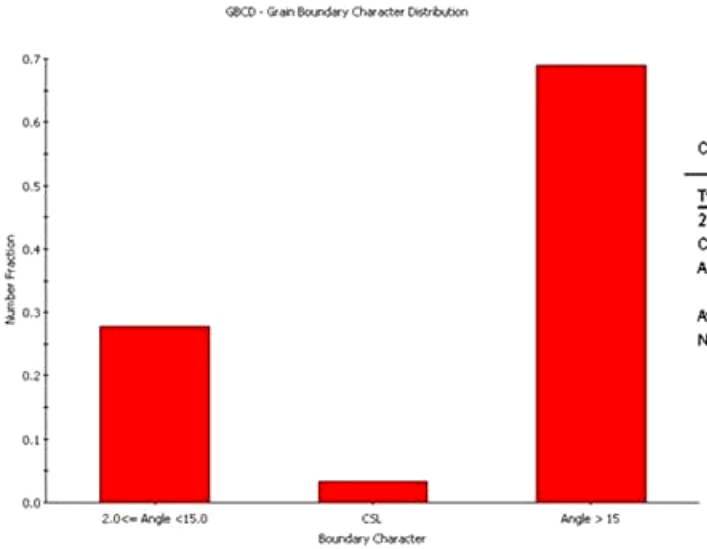

Chart: GBCD - Grain Boundary Character Distribution

Type	Number Fraction
2.0<= Angle <15.0	0.277648
CSL	0.0324095
Angle > 15	0.689942
Average Number	0.333333

b) Pure Tin with 53nm of Au sputtered on top, Sample 67, 18 months at 50% RH / 50°C

Pure Sn Post Plating / Pure Sn with 53nm Au Cap Post Plating

Coincident Site Lattice Boundary Chart

The total fraction of CSL boundaries is approximately 2% of boundaries measured

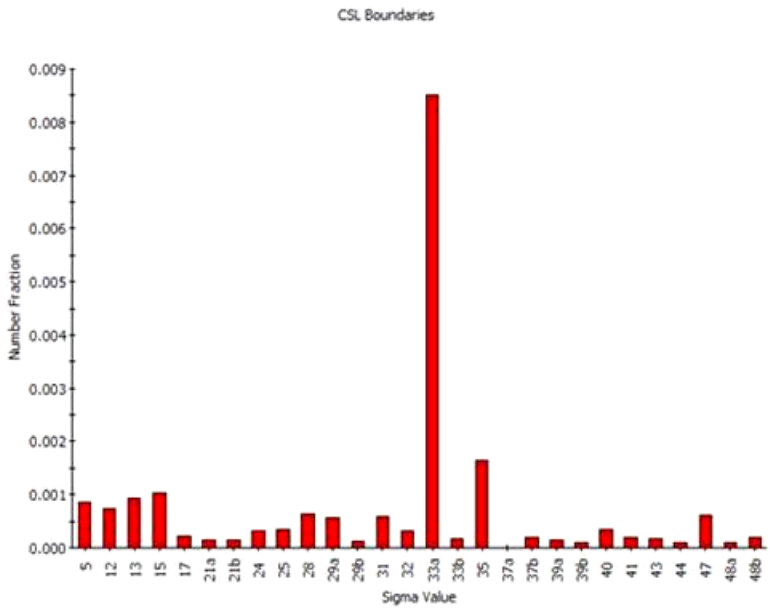

Overall fraction of CSL boundaries: 0.019

Sigma	Number Fraction
5	0.000866371
12	0.000730329
13	0.000930812
15	0.00103463
17	0.000211223
21a	0.000146782
21b	0.000146782
24	0.000311464
25	0.000336524
28	0.000640828
29a	0.000572807
29b	0.000132462
31	0.000583548
32	0.000325784
33a	0.00851335
33b	0.000179002
35	0.00165398
37a	1.07401e-005
37b	0.000196903
39a	0.000157522
39b	8.95012e-005
40	0.000350845
41	0.000186162
43	0.000179002
44	8.59211e-005
47	0.000612188
48a	8.95012e-005
48b	0.000200483

a) Pure Tin, Sample 65, post plating

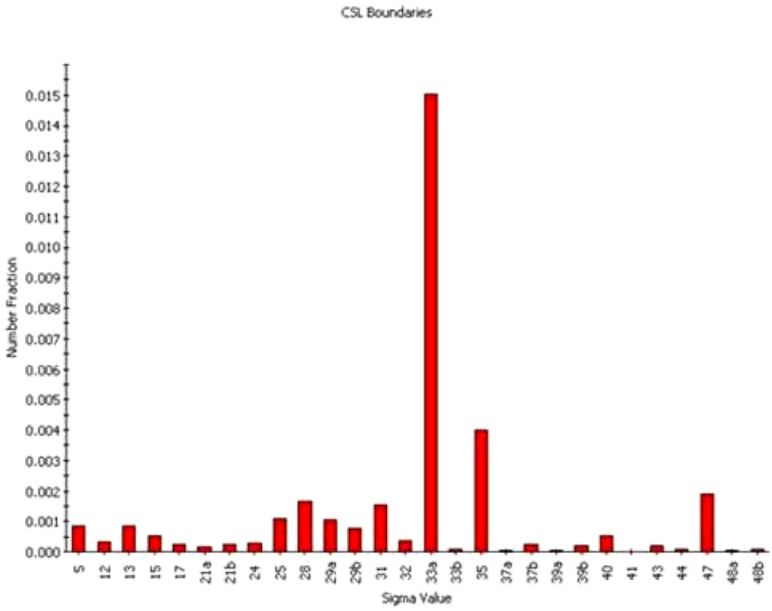

Overall fraction of CSL boundaries: 0.032

Sigma	Number Fraction
5	0.000834625
12	0.000325179
13	0.000834625
15	0.000541964
17	0.000249304
21a	0.000173429
21b	0.000238464
24	0.000292661
25	0.00108393
28	0.00166925
29a	0.00106225
29b	0.000780429
31	0.00155002
32	0.000357696
33a	0.0150341
33b	8.67143e-005
35	0.00398886
37a	4.33571e-005
37b	0.000249304
39a	3.25179e-005
39b	0.000184268
40	0.000509446
41	1.08393e-005
43	0.000184268
44	9.75536e-005
47	0.00188604
48a	2.16786e-005
48b	8.67143e-005

b) Pure Tin with 53nm of Au sputtered on top, Sample 67, 18 months at 50% RH / 50°C

Pure Sn Post Plating / Pure Sn with 53nm Au Cap Post Plating
Misorientation Distribution Function (MODF) Plot

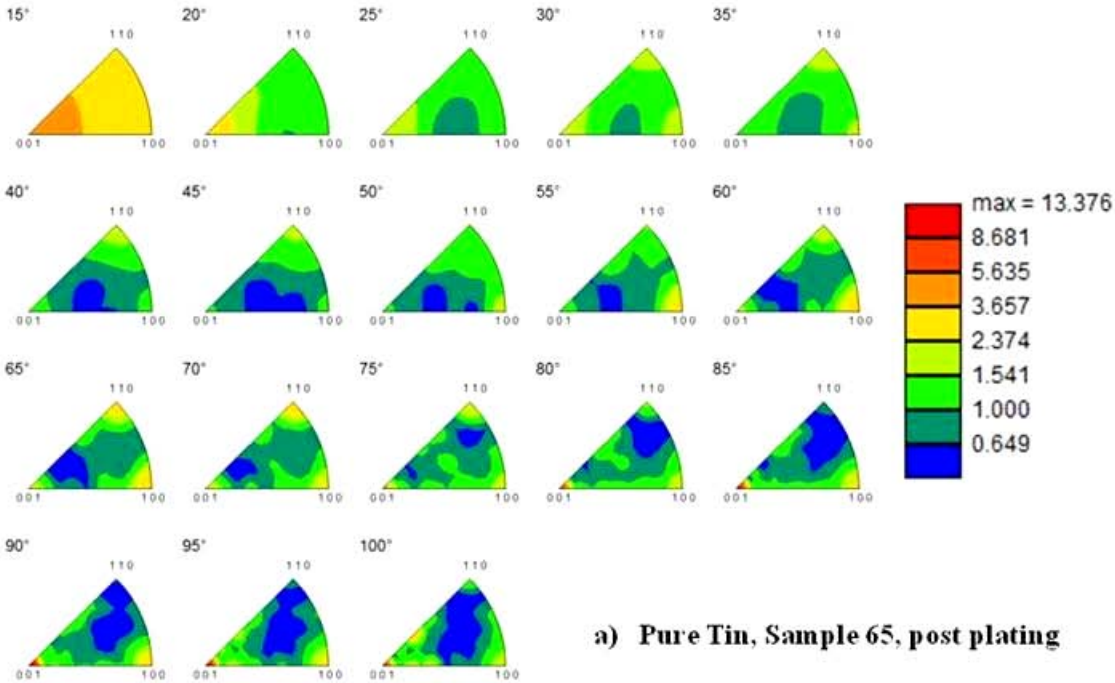

a) Pure Tin, Sample 65, post plating

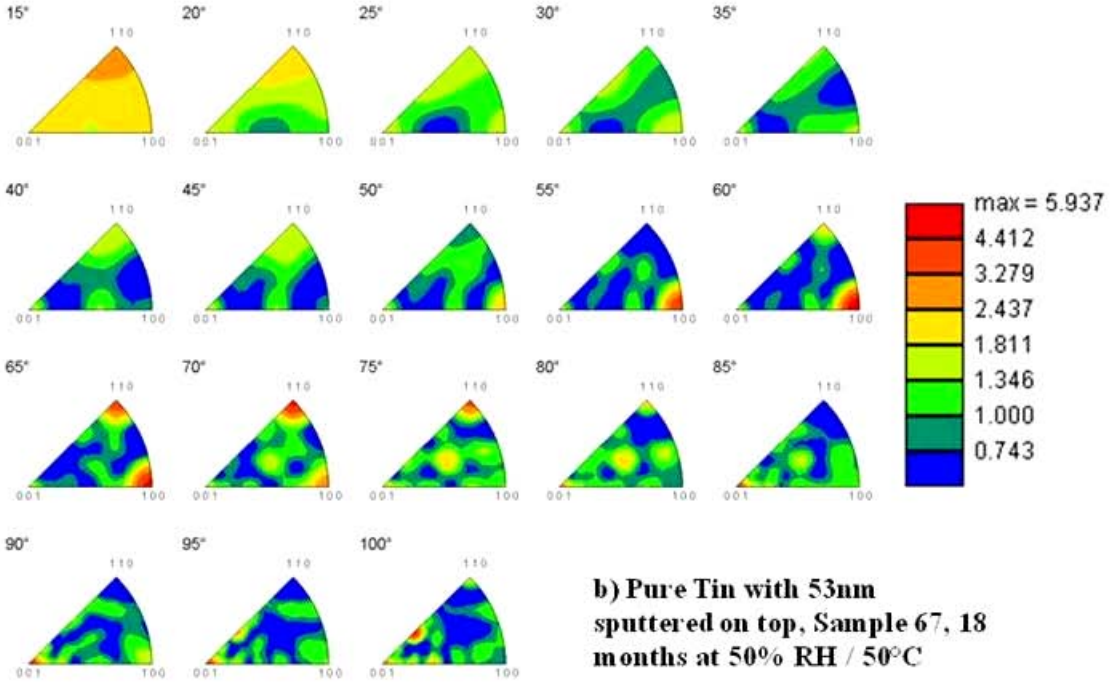

b) Pure Tin with 53nm sputtered on top, Sample 67, 18 months at 50% RH / 50°C

Pure Sn Post Plating / Pure Sn with 53nm Au Cap Post Plating

Crystal Direction Map

Blue Indicates C-Direction in sample normal

Red indicates C-direction in sample plane 15º tolerance

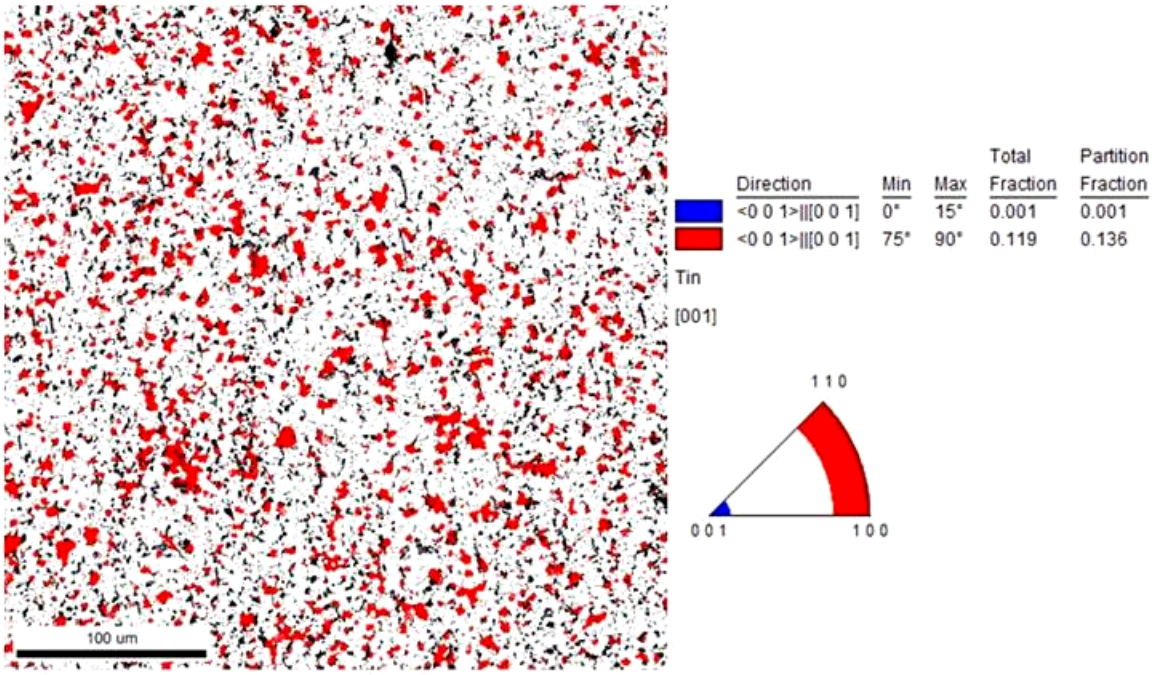

a) Pure Tin, Sample 65, post plating

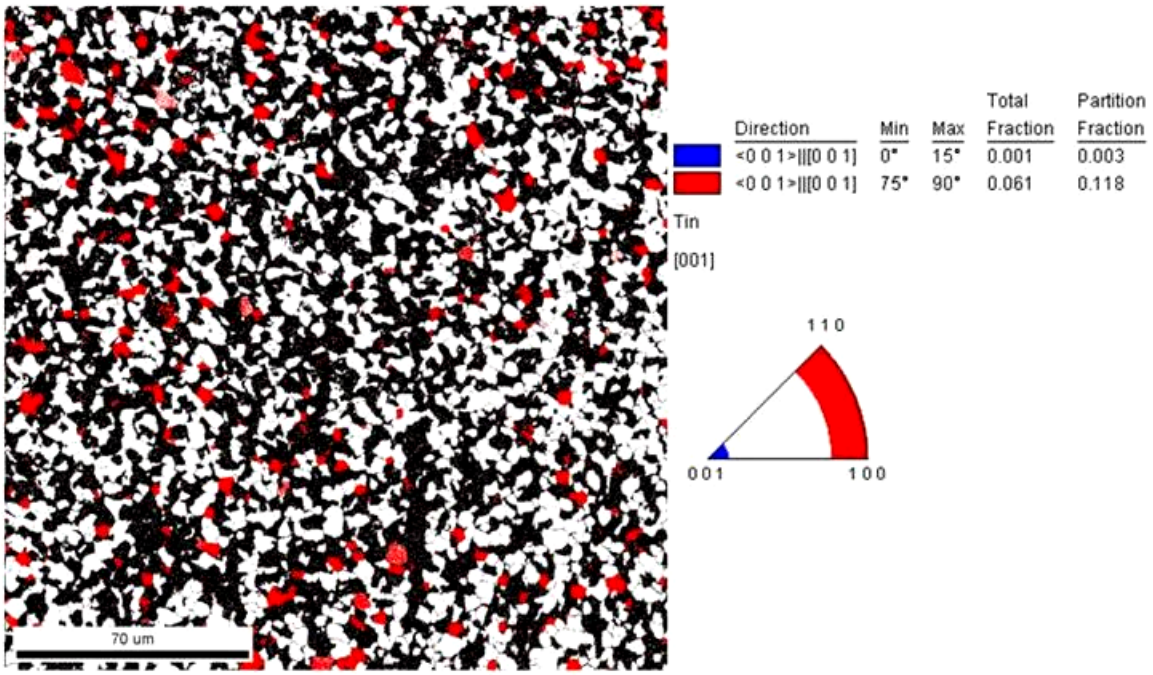

b) Pure Tin with 53nm of Au sputtered on top, Sample 57, 18 months at 50% RH / 50°C